EMERGING INFECTIOUS DISEASES®

U.S. CENTERS FOR DISEASE CONTROL AND PREVENTION

Mpox and Other Viral Diseases

August 2025

Jean-Antoine Houdon (1741–1828), *Terre cuite marble bust of Honoré-Gabriel Riqueti*, comte de Mirabeau (1749–1791) élu du Tiers-État aux États-Généraux de 1789, 1791. Height: 0.537 m, length: 0.385 m; width: 0.347 m. Total height including the polychrome marble pedestal: 0.67 m. Photograph by Andreas G. Nerlich.

EMERGING INFECTIOUS DISEASES®

Emerging Infectious Diseases is published monthly by the Centers for Disease Control and Prevention, 1600 Clifton Rd NE, Mailstop H16-2, Atlanta, GA 30329-4018, USA. Telephone 404-639-1960; email eideditor@cdc.gov

EMERGING INFECTIOUS DISEASES®

Mpox and Other Viral Diseases **August 2025**

On the Cover

Jean-Antoine Houdon (1741–1828), *Terre cuite marble bust of Honoré-Gabriel Riqueti,* comte de Mirabeau (1749–1791), élu du Tiers-État aux États-Généraux de 1789, 1791. Height, 0.537 m; length, 0.385 m; width, 0.347 m. Total height including polychrome marble pedestal, 0.67 m. Louvre-Lens, Galérie du Temps, Lens, France. Photograph by Andreas G. Nerlich.

About the Cover p. 1684

Perspective

Synopses

Research

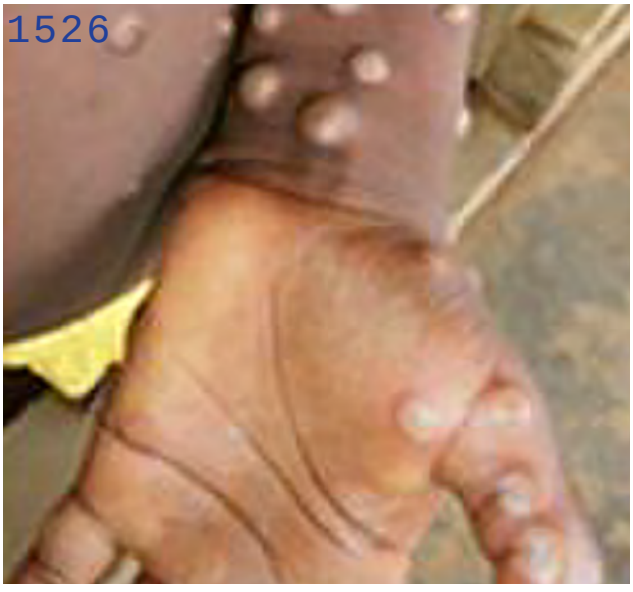

Dispatches

EMERGING INFECTIOUS DISEASES®
August 2025

Research Letters

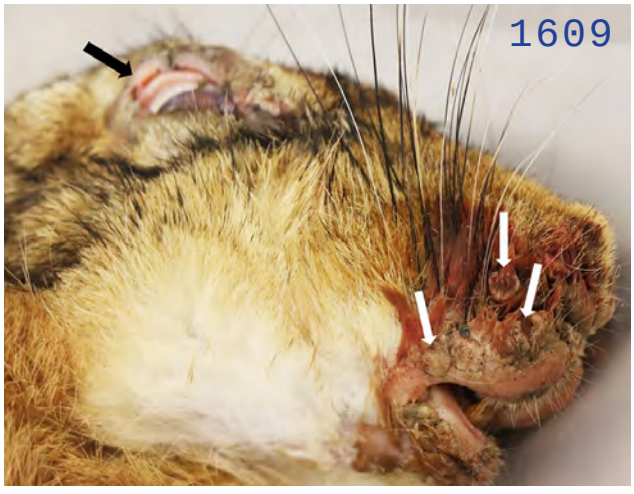

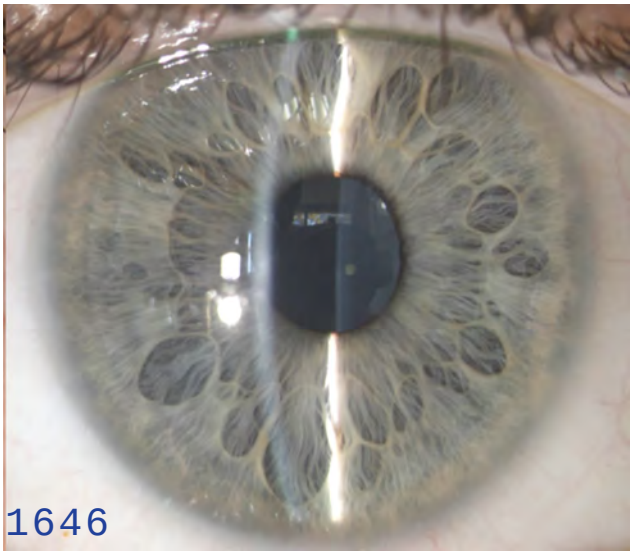

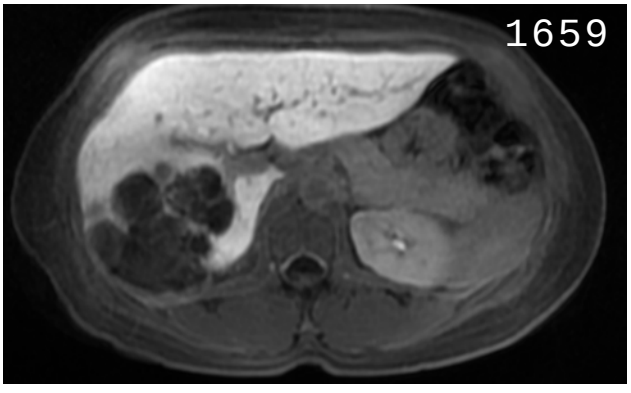

EMERGING INFECTIOUS DISEASES®
August 2025

Comment Letter

About the Cover

Online Report

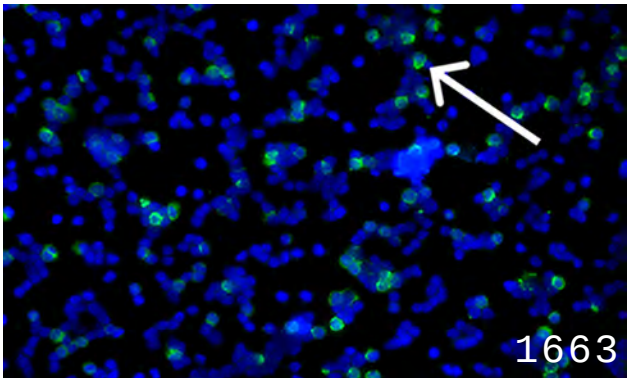

Etymologia

Corrections

Vol. 31, No. 2
The name of author Alexis M. Siegler was incorrect in Contribution of Limited Molecular Testing to Low Ehrlichiosis Diagnosis in High Incidence Area, North Carolina, USA **1682**

Vol. 31, No. 6
A category label was incorrect in Table 1 of High Prevalence of Artemisinin-Resistant *Plasmodium falciparum*, Southeastern Sudan **1682**

Vol. 31, No. 7
The name of author Evangelia Ouranou was incorrect in Spatiotemporal Distribution and Clinical Characteristics of Zoonotic Tuberculosis, Spain, 2018–2022 **1682**

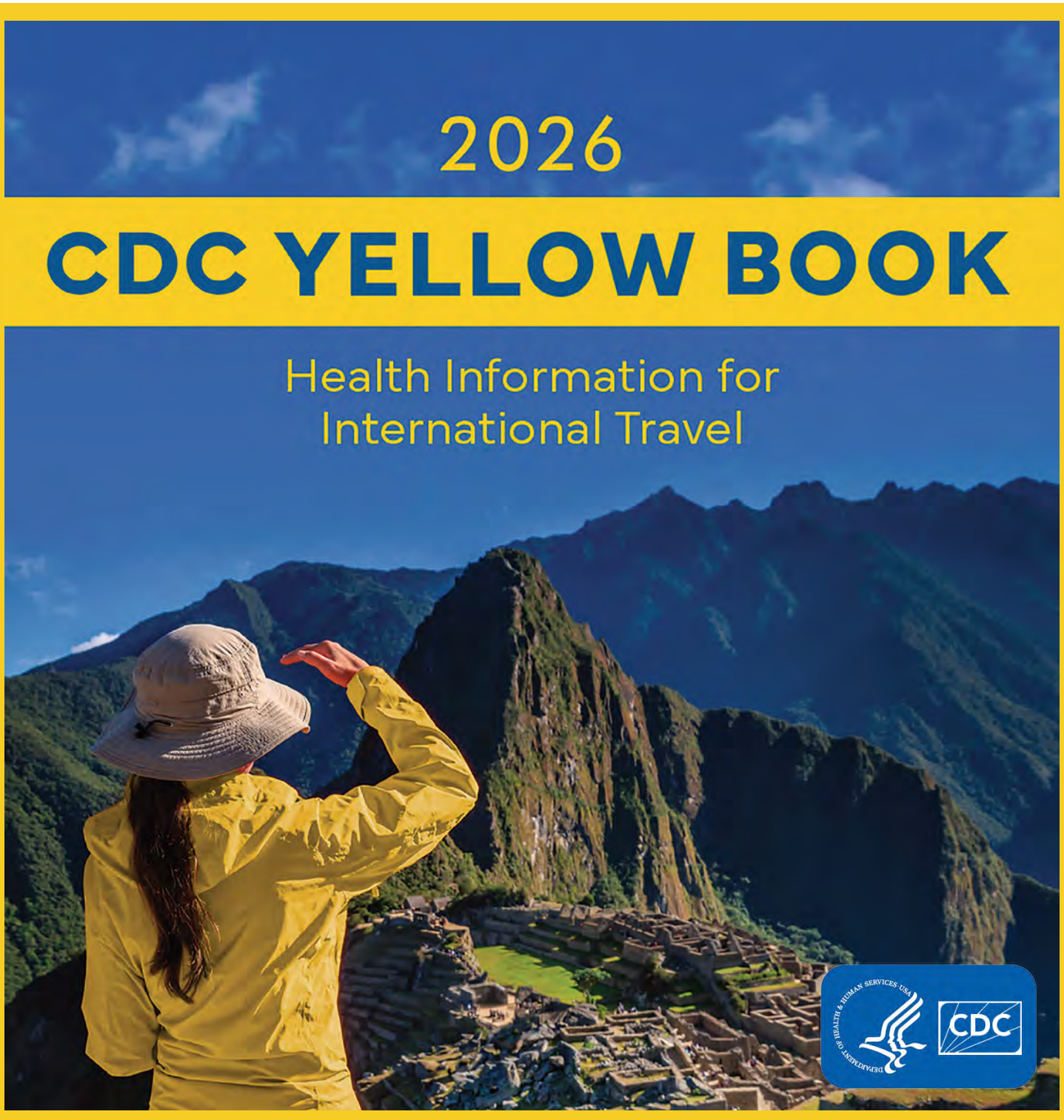

Launch of CDC Yellow Book 2026– A Trusted Travel Medicine Resource

CDC is pleased to announce the launch of the **CDC Yellow Book 2026**. The CDC Yellow Book is a resource containing the U.S. government's travel medicine recommendations and has been trusted by the travel medicine community for over 50 years. Healthcare professionals can use the print and digital versions to find the most up-to-date travel medicine information to better serve their patients' healthcare needs.

The CDC Yellow Book is available online now at www.cdc.gov/yellowbook and in print starting in June 2025 through Oxford University Press and other major online booksellers.

A Roadmap of Primary Pandemic Prevention Through Spillover Investigation

Emily S. Gurley, Raina K. Plowright

Since the COVID-19 pandemic, attention and investment in pandemic preparedness have increased. Although there are many valiant plans around pandemic preparedness, they typically involve slowing the spread or mitigating the effects of a pathogen after it has already entered the human population. The task of stopping the pathogen from entering the human population in the first place, spillover prevention, remains a neglected area in discussions and planning for pandemic risk mitigation. Every spillover offers an opportunity to learn about an emerging public health threat and the conditions that aligned to enable spillover occurrence. In this article, we outline One Health approaches for use in spillover investigations, drawing from our experience investigating Hendra and Nipah virus spillovers. We present a roadmap for how findings from those investigations can lead to the development of interventions for spillover and ultimately pandemic prevention.

Pandemics occur when a pathogen is transmitted across continents through human populations that lack prior immunity (*1*). Most pathogens that start pandemics are zoonotic, originating in wildlife or other animals (*1*). Typically, those animal pathogens are novel to humans, so most humans are susceptible, and if those pathogens have or gain the ability to transmit between humans, they pose a pandemic risk. In the wake of the COVID-19 pandemic, pandemic preparedness has been a focus of global engagement. Although such efforts include valiant plans, they largely focus on slowing the spread or mitigating the effects of a pathogen after it has already entered the human population. Initiatives of note include the Coalition for Epidemic Preparedness Innovation plans to deliver vaccines within 100 days of an emerging threat, the World Bank's investment in surveillance in low- and middle-income countries, and the World Health Organization's efforts to develop more rigorous global agreements on investigation and collective action. Although those strategies enhance our responses to emerging infection outbreaks, they primarily address scenarios after a pathogen has established transmission between humans. However, the task of stopping the pathogen from entering the human population in the first place, spillover prevention, remains a neglected area in discussions and plans for pandemic risk mitigation.

A spillover occurs when a pathogen infects a new host species (*2*,*3*). The vast majority of spillovers will not lead to an outbreak or pandemic. However, for pathogens with pandemic potential, each spillover into a human is an opportunity to launch a pandemic. Most pandemic prevention plans focus on finding outbreak events earlier, notifying neighboring countries, assembling effective outbreak response teams, and enhancing global surveillance for spillover and outbreak events. Those measures are all crucial. However, preventing the spillover in the first place should be a fundamental component of our global strategy for preventing pandemics.

Numerous initiatives have attempted to identify potential pandemic causing pathogens before they cause outbreaks. One approach is to model geographic areas at high risk for spillovers, correlating putative drivers with locations of past spillovers and overlap of humans and reservoir species (*4*–*6*). Those efforts aim to focus surveillance and resources on areas or species of high risk. Substantial investments have led to the discovery of new viruses infecting rodents, bats, and primates, including viruses that were phylogenetically related to outbreak causing pathogens, suggesting a potential risk for spillover (*7*–*19*). Although such efforts have produced findings of interest, they have not produced actionable public health data. Those approaches do not inform which pathogens are spilling over and the mechanisms driving these events.

Author affiliations: Johns Hopkins University, Baltimore, Maryland, USA (E.S. Gurley); Cornell University, Ithaca, New York, USA (R.K. Plowright).

DOI: https://doi.org/10.3201/eid3108.250442

Spillovers do provide actionable data. Once an emerging pathogen infects a human, a public health threat is actualized. Those events garner our attention and concern much more than hypothetical risk warnings. Particularly alarming is evidence of transmission of the pathogen from human to human, because this capability is necessary to cause a pandemic. For example, if there was evidence that persons infected with bovine strains of avian influenza H5 across the United States (*20*) were able to infect others, the risk of a pandemic from this virus would increase drastically.

Every spillover offers a critical opportunity to learn about an emerging public health threat and the conditions that aligned to enable the spillover occurrence. Investigating those events requires a transdisciplinary approach, often best conceptualized as a One Health investigation that integrates multiple fields of expertise (Figure 1). The investigation typically begins with medical experts who understand the clinical manifestations of the disease and natural history of infection because the spillover is detected when a sick person seeks care. Spillovers sometimes also occur first in other species, which become bridging hosts to humans. Laboratory analysis of the genetic sequence of the pathogen can provide more information about its origins and potential reservoir hosts. Concurrently, epidemiologic investigations can determine the exposures that led to infection and assess if transmission is ongoing through extensive contact tracing efforts. Next, veterinary and ecologic investigations of animals in the affected communities can identify potential reservoir species and bridging hosts. Social scientists contribute in-depth understanding of how local practices might have enabled exposure and transmission, including human–animal interactions and their drivers. Finally, environmental and ecologic investigations elucidate how changes in the reservoir host condition or distribution might have enabled spillover. The timing of those investigations is critical because the conditions for spillover can be fleeting, so rapid identification and investigation of spillovers is vital.

One Health spillover investigations represent a crucial step in a broader continuum of actions

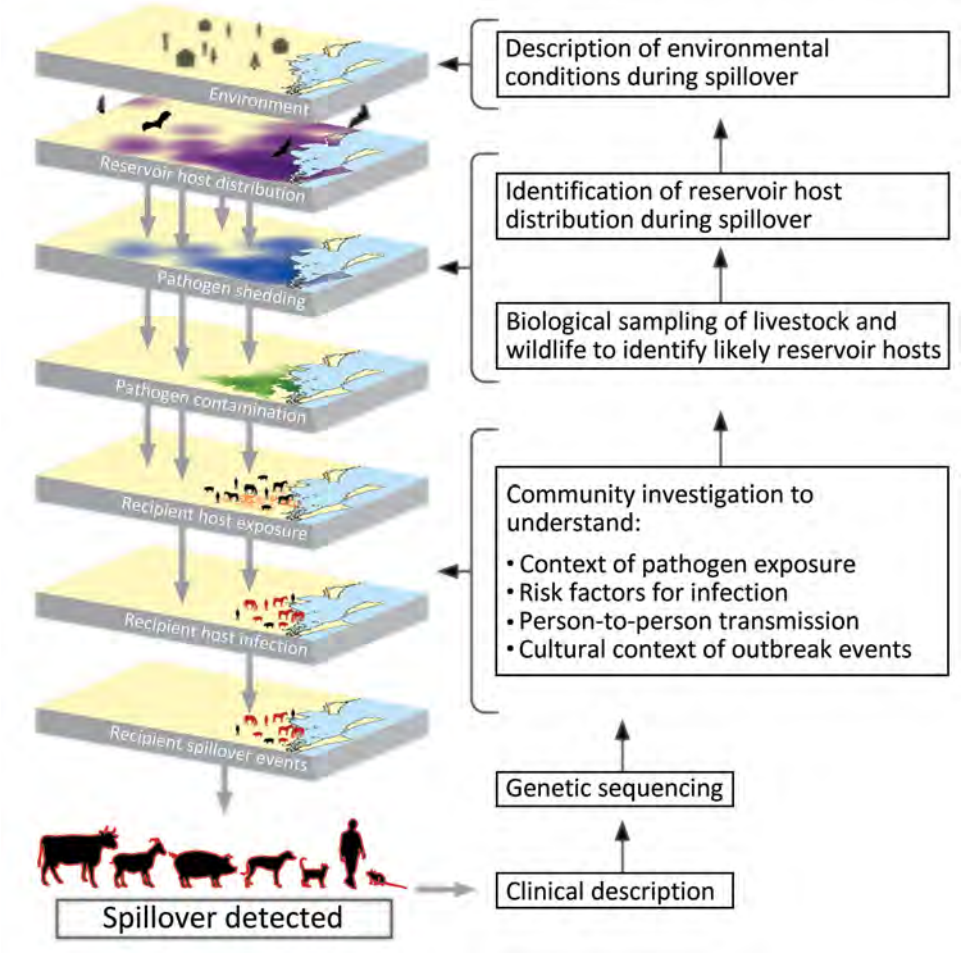

Figure 1. A visual guide to One Health investigations of spillovers to assist with primary pandemic prevention. One Health investigations trace spillover events backward from detection, systematically uncovering the causal chain that led to spillover. This process involves characterizing the pathogen, contexts, and risks for transmission and determining the reservoir hosts and environmental conditions that enabled the event.

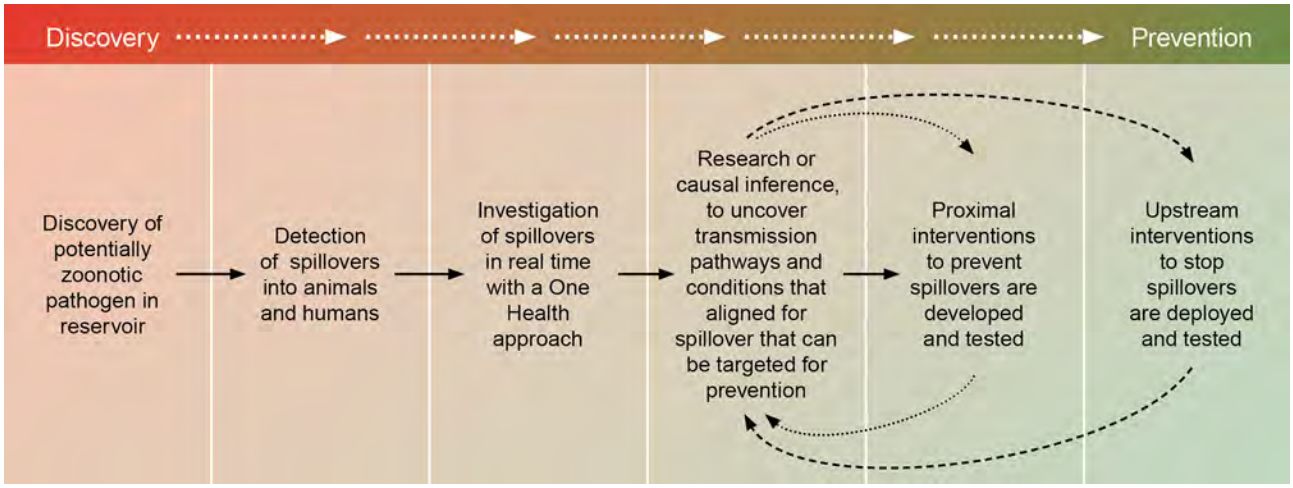

Figure 2. A roadmap of primary pandemic prevention through spillover investigation from discovery to the prevention of zoonotic spillover. The pathway from discovery of a zoonotic pathogen in reservoir hosts to the prevention of future spillovers often begins with the detection of spillovers in persons or domestic animals. If those detections prompt One Health investigations, followed by in-depth studies to identify the root causes of spillover, the resulting knowledge can inform the design, testing, and implementation of interventions to address both proximal and distal drivers of spillover risk.

designed to move from identifying mechanistic, proximal causes of spillover to designing and testing interventions to prevent them. This continuum from discovery to spillover prevention (Figure 2) encompasses multiple interconnected steps: discovery of the zoonotic pathogen in reservoir hosts, detection of spillover events, carrying out One Health spillover investigations, and identifying the transmission pathways and conditions that enabled spillover. The subsequent steps involve iterative research to develop, test, and deploy interventions to prevent spillovers by targeting both proximal and upstream causes. Each step informs the others, creating ongoing feedback essential for pandemic prevention.

Spillover investigations are crucial for pandemic prevention, and more effort is needed to identify and study spillovers. There are multiple barriers to identifying spillovers that span global, national, and local levels. Because of those barriers, many spillovers remain undetected or unreported. At the local level, there might be insufficient resources to diagnose common causes of disease, much less rare and emerging pathogens. Even if that barrier is overcome, communities might be apprehensive about uncovering emerging pathogens because that process can lead to blame, stigmatization, and negative economic impacts. At the national level, there are political, financial, and economic threats to navigate. The reality is that spillovers are almost always negative events for governments. Spillovers are politically sensitive and sometimes not reported out of fear. Reporting of emerging pathogen outbreaks has led to severe economic outcomes for reporting countries, including travel bans or trade embargoes (*21*–*23*). Once a spillover is identified, governments might be expected to expend considerable resources for investigation and response to reduce the global pandemic risk. For governments that have threadbare budgets for combating endemic public health problems, there might be little desire to take on those additional actions. Although the numerous disincentives to spillover detection are formidable, we have much to gain by overcoming them.

When investigations of spillovers, particularly those conducted through a One Health approach, have taken place, they have yielded critical insights and even solutions to prevent future spillovers (Figure 2). For example, Hendra virus is an often-fatal virus transmitted from bats to horses and subsequently to humans in Australia. Ecologists involved in the investigations of Hendra virus spillovers noted unusual bat activity in the paddocks of affected horses. Bats were feeding on unripe figs and other foods associated with starvation avoidance. This observation prompted the researchers to hypothesize that food shortages for bats were somehow associated with spillovers. Subsequent long-term studies revealed that climate fluctuations, interacting with habitat loss, led to acute food shortages that drove bats into agricultural areas and caused them to shed Hendra virus in proximity to horses (*24*). During those investigations, researchers noted that spillovers did not occur when remnant patches of critical habitat flowered, providing food for bats. This finding suggested a potential solution: restoring critical habitats to mitigate spillovers (*24*). This example illustrates the critical role of spillover

investigation and subsequent studies to understand the mechanisms underlying spillovers. When mechanisms are understood, interventions to prevent future occurrences become apparent. Restoration of critical habitat has begun, but it will take more than a decade to determine if that intervention decreases the risk for Hendra virus spillovers.

Nipah virus transmission in Bangladesh provides another excellent case study about how looking for spillovers and then conducting One Health investigations have led to major insights into proximal causes of spillover and possible targets for spillover prevention (Figure 2). The first outbreaks of Nipah virus were discovered in Bangladesh in 2001 (*25*), and after years of One Health investigations of spillovers, an understanding of the source began to form in 2005 (*26*). Epidemiologic studies identified date palm sap consumption as a key risk factor for Nipah virus infection, and social scientists studied how the sap was harvested and sold (*26*–*29*). Date palm sap is collected from trees and drunk fresh during the cool, winter months; it is a cultural delicacy (*29*). Wildlife investigations identified that bats shed virus in their urine and saliva (*30*), ecologic investigations revealed that bats drink and contaminate date palm sap as it drips into the pots (*31*), and virologic studies showed that Nipah virus is stable in date palm sap (*32*). Further studies then demonstrated that simple covers of the pots and sap stream on the tree, which were already being used by some sap collectors, would protect the sap from contact with bats (*33*,*34*).

Spillover dynamics are driven by the interaction of multiple complex systems, including infection dynamics in the reservoir hosts, their shifting population distributions, and emergent human behaviors and practices (Figure 1). Drivers span from local alterations in land use change to global climate. Investigating the underlying drivers of spillovers often requires sustained effort over years or decades (Figure 1), extending beyond the duration of individual grants, or any single person's tenure in a particular job. However, the example of Hendra virus spillover investigations in Australia exemplifies how a strong curiosity and a commitment to understanding the mechanisms underlying spillovers can lead to the potential for ecological solutions to prevent pandemics (*24*).

In summary, we have presented evidence about how a One Health approach to spillover investigation can lead to spillover prevention by using Hendra and Nipah virus as case studies. However, those approaches are applicable to any spillover pathogen, not just viruses, and any reservoir host, not just bats. Opportunities to learn more about and prevent spillovers are frequent but often missed. We know very little about the specific spillovers that led to most of the large outbreaks or pandemics in the past 100 years, mostly because by the time investigations began, the trail was cold. For example, the origin of the 2013–2016 Ebola epidemic in West Africa was not investigated until months after its onset, leaving the initial spillover that led to that outbreak uncertain, similar to most other Ebola outbreaks (*35*,*36*). The origins of several recent spillovers remain unresolved, including how Nipah virus first spilled over to humans in Kerala, India, in 2018, 2019, and 2023 (*37*,*38*), and how H5N1 spilled over into dairy cattle in the United States (*20*). The origins of the COVID-19 pandemic are likely to remain unsolved indefinitely, because of delays in investigations. Until we dedicate ourselves to the search for and One Health investigation of spillovers, we remain vulnerable to their devastating consequences.

This study was funded in part by the US National Science Foundation (grant no. EF-2133763/EF-2231624) and the Defense Advanced Research Projects Agency PREempt Emerging Pathogenic Threats program (cooperative agreement no. D18AC00031). The content of the information does not necessarily reflect the position or the policy of the US government, and no official endorsement should be inferred.

About the Authors

Dr. Gurley is an epidemiologist at the Johns Hopkins Bloomberg School of Public Health. Her research interests include the mechanisms of zoonotic spillover and prevention strategies for Nipah virus and other emerging infections in Bangladesh.

Dr. Plowright is a professor at Cornell University and a Cornell Atkinson Scholar at the Cornell Atkinson Center for Sustainability. Her research interests include transdisciplinary approaches to identify the mechanisms driving zoonotic spillover and informing strategies to prevent the emergence of novel pathogens and future pandemics.

References

1. Dias RA. Towards a comprehensive definition of pandemics and strategies for prevention: a historical review and future perspectives. Microorganisms. 2024;12:1802. https://doi.org/10.3390/microorganisms12091802
2. Plowright RK, Parrish CR, McCallum H, Hudson PJ, Ko AI, Graham AL, et al. Pathways to zoonotic spillover. Nat Rev Microbiol. 2017;15:502–10. https://doi.org/10.1038/nrmicro.2017.45

3. Lloyd-Smith JO, George D, Pepin KM, Pitzer VE, Pulliam JR, Dobson AP, et al. Epidemic dynamics at the human-animal interface. Science. 2009;326:1362–7. https://doi.org/10.1126/science.1177345
4. Pigott DM, Golding N, Mylne A, Huang Z, Henry AJ, Weiss DJ, et al. Mapping the zoonotic niche of Ebola virus disease in Africa. eLife. 2014;3:e04395. https://doi.org/10.7554/eLife.04395
5. Muylaert RL, Wilkinson DA, Kingston T, D'Odorico P, Rulli MC, Galli N, et al. Using drivers and transmission pathways to identify SARS-like coronavirus spillover risk hotspots. Nat Commun. 2023;14:6854. https://doi.org/10.1038/s41467-023-42627-2
6. Han BA, Schmidt JP, Bowden SE, Drake JM. Rodent reservoirs of future zoonotic diseases. Proc Natl Acad Sci U S A. 2015;112:7039–44. https://doi.org/10.1073/pnas.1501598112
7. Goldstein T, Anthony SJ, Gbakima A, Bird B, Bangura J, Tremeau-Bravard A, et al. The discovery of a new Ebolavirus, Bombali virus, adds further support for bats as hosts of Ebolaviruses. Int J Infect Dis. 2019;79:4–5. https://doi.org/10.1016/j.ijid.2018.11.030
8. Valitutto MT, Aung O, Tun KYN, Vodzak ME, Zimmerman D, Yu JH, et al. Detection of novel coronaviruses in bats in Myanmar. PLoS One. 2020;15:e0230802. https://doi.org/10.1371/journal.pone.0230802
9. Cameron K, Hayes B, Olson SH, Smith BR, Pante J, Laudisoit A, et al. Detection of first gammaherpesvirus sequences in Central African bats. New Microbes New Infect. 2020;36:100705. https://doi.org/10.1016/j.nmni.2020.100705
10. Amman BR, Bird BH, Bakarr IA, Bangura J, Schuh AJ, Johnny J, et al. Isolation of Angola-like Marburg virus from Egyptian rousette bats from West Africa. Nat Commun. 2020;11:510. https://doi.org/10.1038/s41467-020-14327-8
11. Nziza J, Goldstein T, Cranfield M, Webala P, Nsengimana O, Nyatanyi T, et al. Coronaviruses detected in bats in close contact with humans in Rwanda. EcoHealth. 2020;17:152–9. https://doi.org/10.1007/s10393-019-01458-8
12. Kumakamba C, N'Kawa F, Kingebeni PM, Losoma JA, Lukusa IN, Muyembe F, et al. Analysis of adenovirus DNA detected in rodent species from the Democratic Republic of the Congo indicates potentially novel adenovirus types. New Microbes New Infect. 2019;34:100640. https://doi.org/10.1016/j.nmni.2019.100640
13. Lange CE, Niama FR, Cameron K, Olson SH, Aime Nina R, Ondzie A, et al. First evidence of a new simian adenovirus clustering with human mastadenovirus F viruses. Virol J. 2019;16:147. https://doi.org/10.1186/s12985-019-1248-z
14. Diffo J, Ndze VN, Ntumvi NF, Takuo JM, Mouiche MMM, Tamoufe U, et al. DNA of diverse adenoviruses detected in Cameroonian rodent and shrew species. Arch Virol. 2019;164:2359–66. https://doi.org/10.1007/s00705-019-04323-9
15. Islam A, Islam S, Ferdous J, Rahman MK, Uddin MH, Akter S, et al. Diversity and prevalence of parasitic infestation with zoonotic potential in dromedary camel (*Camelus dromedarius*) and fat-tailed sheep (dhumba) in Bangladesh. J Adv Vet Anim Res. 2019;6:142–7. https://doi.org/10.5455/javar.2019.f324
16. Lacroix A, Duong V, Hul V, San S, Davun H, Omaliss K, et al. Genetic diversity of coronaviruses in bats in Lao PDR and Cambodia. Infect Genet Evol. 2017;48:10–8. https://doi.org/10.1016/j.meegid.2016.11.029
17. Epstein JH, Anthony SJ. Viral discovery as a tool for pandemic preparedness. Rev Sci Tech. 2017;36:499–512. https://doi.org/10.20506/rst.36.2.2669
18. Yang X-L, Zhang Y-Z, Jiang R-D, Guo H, Zhang W, Li B, et al. Genetically diverse filoviruses in *Rousettus* and *Eonycteris* spp. bats, China, 2009 and 2015. Emerg Infect Dis. 2017;23:482–6. https://doi.org/10.3201/eid2302.161119
19. Ge X-Y, Yang W-H, Pan H, Zhou JH, Han X, Zhu GJ, et al. Fugong virus, a novel hantavirus harbored by the small oriental vole (*Eothenomys eleusis*) in China. Virol J. 2016;13:27. https://doi.org/10.1186/s12985-016-0483-9
20. Centers for Disease Control and Prevention. H5 bird flu: current situation. Avian influenza (bird flu). 2025 [cited 2025 Feb 17]. https://www.cdc.gov/bird-flu/situation-summary/index.html
21. Pattani R. Unsanctioned travel restrictions related to Ebola unravel the global social contract. CMAJ. 2015;187:166–7. https://doi.org/10.1503/cmaj.141488
22. Meier BM, Bueno de Mesquita J, Burci GL, Chirwa D, Dagron S, Eccleston-Turner M, et al. Travel restrictions and variants of concern: global health laws need to reflect evidence. Bull World Health Organ. 2022;100:178–178A. https://doi.org/10.2471/BLT.21.287735
23. Worsnop CZ. Domestic politics and the WHO's international health regulations: explaining the use of trade and travel barriers during disease outbreaks. Rev Int Organ. 2017;12:365–95. https://doi.org/10.1007/s11558-016-9260-1
24. Eby P, Peel AJ, Hoegh A, Madden W, Giles JR, Hudson PJ, et al. Pathogen spillover driven by rapid changes in bat ecology. Nature. 2023;613:340–4. https://doi.org/10.1038/s41586-022-05506-2
25. Hsu VP, Hossain MJ, Parashar UD, Ali MM, Ksiazek TG, Kuzmin I, et al. Nipah virus encephalitis reemergence, Bangladesh. Emerg Infect Dis. 2004;10:2082–7. https://doi.org/10.3201/eid1012.040701
26. Luby SP, Rahman M, Hossain MJ, Blum LS, Husain MM, Gurley E, et al. Foodborne transmission of Nipah virus, Bangladesh. Emerg Infect Dis. 2006;12:1888–94. https://doi.org/10.3201/eid1212.060732
27. Hegde ST, Sazzad HMS, Hossain MJ, Alam MU, Kenah E, Daszak P, et al. Investigating rare risk factors for Nipah virus in Bangladesh: 2001–2012. EcoHealth. 2016;13:720–8. https://doi.org/10.1007/s10393-016-1166-0
28. Chakraborty A, Sazzad HMS, Hossain MJ, Islam MS, Parveen S, Husain M, et al. Evolving epidemiology of Nipah virus infection in Bangladesh: evidence from outbreaks during 2010–2011. Epidemiol Infect. 2016;144:371–80. https://doi.org/10.1017/S0950268815001314
29. Nahar N, Sultana R, Gurley ES, Hossain MJ, Luby SP. Date palm sap collection: exploring opportunities to prevent Nipah transmission. EcoHealth. 2010;7:196–203. https://doi.org/10.1007/s10393-010-0320-3
30. Anderson DE, Islam A, Crameri G, Todd S, Islam A, Khan SU, et al. Isolation and full-genome characterization of Nipah viruses from bats, Bangladesh. Emerg Infect Dis. 2019;25:166–70. https://doi.org/10.3201/eid2501.180267
31. Khan MSU, Hossain J, Gurley ES, Nahar N, Sultana R. Use of infrared camera to understand bats' access to date palm sap: implications for preventing Nipah virus transmission. *Ecohealth* 2010. https://link.springer.com/article/10.1007/s10393-010-0366-2.
32. Fogarty R, Halpin K, Hyatt AD, Daszak P, Mungall BA. Henipavirus susceptibility to environmental variables. Virus Res. 2008;132:140–4. https://doi.org/10.1016/j.virusres.2007.11.010
33. Nahar N, Mondal UK, Sultana R, Hossain MJ, Khan MS, Gurley ES, et al. Piloting the use of indigenous methods to prevent Nipah virus infection by interrupting bats'

access to date palm sap in Bangladesh. Health Promot Int. 2013;28:378–86. https://doi.org/10.1093/heapro/das020
34. Khan SU, Gurley ES, Hossain MJ, Nahar N, Sharker MAY, Luby SP. A randomized controlled trial of interventions to impede date palm sap contamination by bats to prevent Nipah virus transmission in Bangladesh. PLoS One. 2012; 7:e42689. https://doi.org/10.1371/journal.pone.0042689
35. Marí Saéz A, Weiss S, Nowak K, Lapeyre V, Zimmermann F, Düx A, et al. Investigating the zoonotic origin of the West African Ebola epidemic. EMBO Mol Med. 2015;7:17–23. https://doi.org/10.15252/emmm.201404792
36. Plowright RK, Hudson PJ. From protein to pandemic: the transdisciplinary approach needed to prevent spillover and the next pandemic. Viruses. 2021;13:1298. https://doi.org/10.3390/v13071298
37. Arunkumar G, Chandni R, Mourya DT, Singh SK, Sadanandan R, Sudan P, et al.; Nipah Investigators People and Health Study Group. Outbreak investigation of Nipah virus disease in Kerala, India, 2018. J Infect Dis. 2019;219:1867–78. https://doi.org/10.1093/infdis/jiy612
38. Rahim AA, Chandran P, Bindu V, Radhakrishnan C, Moorkoth AP, Ramakrishnan LV. Recurrent Nipah outbreaks in Kerala: implications for health policy and preparedness. Front Public Health. 2024;12:1356515. https://doi.org/10.3389/fpubh.2024.1356515

Address for correspondence: Emily S. Gurley, E6545, Johns Hopkins Bloomberg School of Public Health, 615 N Wolfe St, Baltimore, MD 21205, USA; email: egurley1@jhu.edu

Preparedness and Response Considerations for High-Consequence Infectious Disease

Justin Chan, Corri B. Levine, Jocelyn J. Herstein, Nicole Cloutier, Lauren Sauer, Aneesh K. Mehta, Jared Evans, on behalf of the Basic and Translational State of the Science Working Group of the National Emerging Special Pathogens Training and Education Center's Special Pathogens Research Network[1]

High-consequence infectious diseases (HCIDs) are acute human infectious diseases with high illness and case-fatality rates, few or no available effective treatment or prevention options, and the ability to spread in the community and within healthcare settings. Those characteristics lead to significant risks to patients and their close contacts, healthcare workers, laboratory personnel, and communities exposed to an outbreak. We describe aspects of healthcare system preparedness for and response to HCIDs, including the role of high-level isolation units, ensuring safe clinical laboratory capabilities and waste management, increasing availability of medical countermeasures, coordinating with stakeholders and systems of care, and communicating with the public. Finally, we discuss priority areas for further investment in HCID preparedness, care, and research. Effective and equitably disseminated medical countermeasures for HCIDs are urgently needed.

Pathogens that cause infectious diseases vary widely in virulence, infectiousness, and transmissibility. They are divided into different groups for ease of identification of threat to health and safety (Table) (*1*–*4*). The World Health Organization (WHO), the European Centre for Disease Prevention and Control (ECDC), the US Centers for Disease Control and Prevention (CDC), and US National Institutes of Health (NIH) play major roles in defining hazard classification and biosafety practices for a group of pathogens. NIH and WHO each defined 4 risk groups (RGs) for infectious agents and toxins on basis of the relative agent hazards involved when managed in a laboratory setting. Although slight differences exist between risk group definitions defined by NIH and WHO, RG1 (lowest risk) pertains to agents that are not associated with disease in healthy adult humans and RG4 (highest risk) contains agents that are likely to cause serious or lethal disease in persons and pose high community transmission risk (*4*). RGs are one consideration when conducting a biologic risk assessment to determine the Biosafety Level (BSL) in which the agent should be managed. CDC defines BSL-1–4 and describes laboratory design features, engineering controls, personal protective equipment (PPE), and biosafety practices that should be adhered to when handling a given biologic agent or toxin (*3*). BSL-4 practices and facility specifications apply to biologic agents that pose a high risk for life-threatening disease and for which there is often no available vaccine or therapy.

US federal agencies have designated specific infectious agents as requiring additional oversight of the possession and use of these pathogens. The Federal Select Agent Program (FSAP) is jointly managed by the Division of Regulatory Science and Compliance at CDC and the Division of Agricultural Select Agents and Toxins at the US Department of Agriculture (*1*). The program regulates the possession, use, and transfer of certain biologic agents and toxins, referred to as select agents, that could pose a severe threat to human, animal, or plant health. In addition, the US Department of Transportation (DOT) Pipeline and Hazardous Materials Safety Administration defines a classification system that outlines requirements for packaging and transporting certain infectious

Author affiliations: New York University Grossman School of Medicine, New York, New York, USA (J. Chan); The University of Texas Medical Branch at Galveston, Galveston, Texas, USA (C.B. Levine, N. Cloutier); University of Nebraska Medical Center, Omaha, Nebraska, USA (J.J. Herstein, L. Sauer, J. Evans); Emory University School of Medicine, Atlanta, Georgia, USA (A.K. Mehta)

DOI: https://doi.org/10.3201/eid3108.250313

[1]Group members are listed at the end of this article.

substances that can pose elevated risk to health, safety, and property during transport (*2*).

Those regulatory frameworks guide the safe handling of infectious pathogens in a laboratory setting, including waste management and transport. However, those classification systems do not specifically address risk posed when delivering care to patients in the clinical care setting. The National Emerging Special Pathogens Training and Education Center (NETEC) (*5*) describes a category of infectious agents and their associated diseases that pose elevated risk to staff, other patients, and the public and therefore generally merit management in a clinical setting with enhanced facility engineering controls and infection prevention and control processes. Several terms have been used to describe such pathogens, including highly infectious pathogen, highly hazardous pathogen, high-consequence pathogen, and special pathogen, among others. NETEC recommends using the term special pathogen to refer to the infectious agent (e.g., Ebola virus), and the term high-consequence infectious disease (HCID) to refer to the disease caused by that agent (e.g., Ebola disease). That terminology conveys the distinct nature of the infectious pathogens and concerns for the potential consequences to healthcare facilities, healthcare workers, and communities.

Clarifying terminology and describing characteristics of HCIDs can help focus appropriate resources to enhance clinical and public health responses during an outbreak and determine appropriate triage of individual patients to specialized facilities equipped for high-level isolation. Rather than providing a list of pathogens, we aim to describe defining characteristics of HCIDs, key aspects of HCID preparedness and response, and areas for advancement in HCID preparedness, care, and research. The list of specific pathogens that cause HCIDs will change over time because genetic evolution and medical advancements lead to changes in epidemiology, transmission, and clinical outcomes.

Characteristics of HCIDs and Special Pathogens

NETEC agrees with other international health authorities (*6*–*8*) that HCIDs are acute human infectious diseases with high illness and case-fatality rates, few or no available effective treatment or prevention options, and the ability to spread in the community and within healthcare settings. As such, the use of a high-level isolation unit (HLIU), also known as a biocontainment unit (*9*), may be warranted to provide safe clinical care and prevent transmission to healthcare workers and other patients. Effective management of HCIDs typically requires enhanced coordination between stakeholders, including health systems and public health authorities, along with clear communication to maintain public assuredness about how the situation is being handled. A special pathogen is highly infectious, highly contagious, and highly hazardous and is likely to cause an HCID (*10*). Many special pathogens are on the WHO and NIH lists of priority diseases for research and development (*11*,*12*).

An example of a special pathogen is Ebola virus, which causes an HCID, Ebola virus disease. The disease has a high case-fatality rate of 32%–100% in past outbreaks (*13*) and significant person-to-person transmission. Although the US Food and Drug Administration has approved 2 monoclonal antibodies and 1 vaccine for the species *Orthoebolavirus zairense* (*14*), no medical countermeasures have been approved for the species *O. sudanense*, the second most common cause of Ebola outbreaks. Marburg virus (*15*) and Nipah virus (*16*) also demonstrate characteristics of special pathogens that cause HCIDs. Some emerging pathogens may be considered special pathogens, such as SARS-CoV-2 before effective medical countermeasures were available (*17*). Others can reemerge as special pathogens; monkeypox virus evolved to efficiently transmit between humans with limited availability of medical countermeasures and concern for a high case-fatality rate (*18*,*19*).

Key Aspects of HCID Preparedness and Response

Outbreaks and cases of some HCIDs such as Ebola disease, Marburg virus disease, and Nipah virus infection have been more frequently detected and reported since the late 1990s (Figure). Those and other HCIDs demand purposeful preparedness and coordinated responses between frontline healthcare providers, health systems, public health agencies, the research community, and regulatory agencies. Together, the groups must develop a system of care that includes effective and efficient treatment facilities and protocols to safely manage infected patients, protect healthcare workers, and contain spread of the pathogen.

HLIUs

HLIUs constitute a key element of a response to HCIDs. Such specialized facilities offer advanced isolation and ongoing patient care to a small number of patients. They implement infection prevention and control protocols and standards that are beyond the usual capabilities of most hospital settings. Characteristics of HLIU design and function

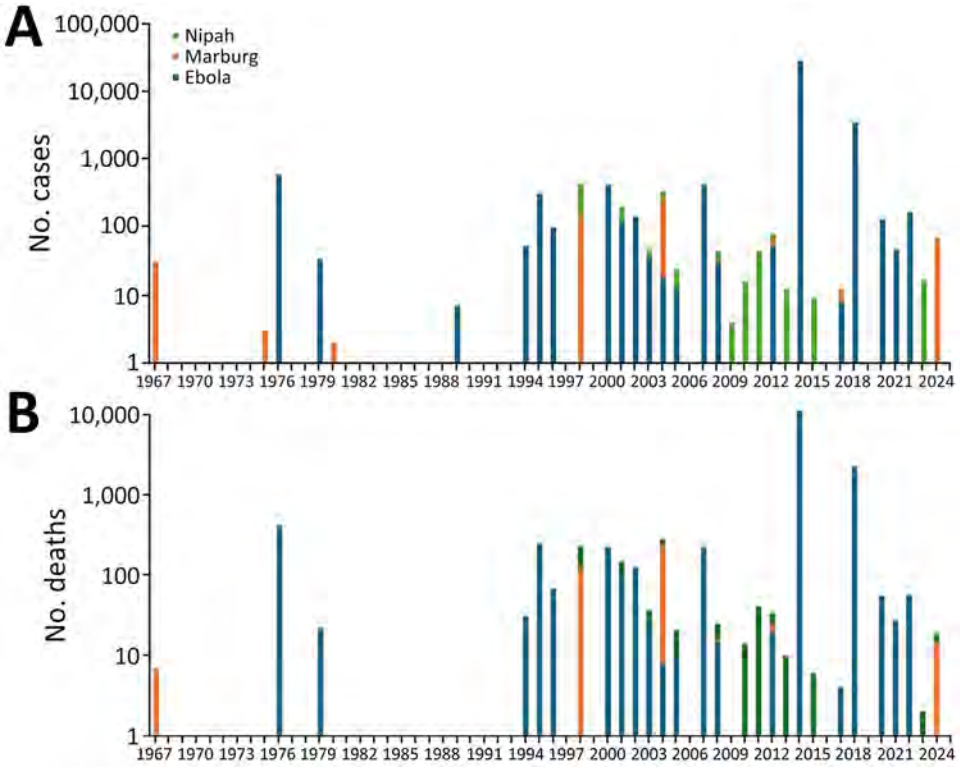

Figure. Global cases of infection with and deaths from Ebola, Marburg, and Nipah viruses, 1967–2024. A) No. cases; B) no. deaths.

have been described previously (*8*,*9*,*20*,*21*). The units must maintain regular education and training on infection prevention practices, use of PPE, and clinical care protocols for patients with HCIDs. Units involve multidisciplinary teams including nurses, physicians, advanced practice providers, laboratory technicians, respiratory therapists, infection preventionists, industrial hygienists, and waste management technicians, among others.

A total of 13 federally designated Regional Emerging Special Pathogen Treatment Centers in the United States operate HLIUs, funded by the Administration for Strategic Preparedness and Response. A limited number of additional Special Pathogen Treatment Centers (SPTCs) operate HLIUs (*22*); patient care capacity can be overwhelmed by a surge in cases of a novel pathogen, as we saw early on during the COVID-19 pandemic. During outbreaks, health systems may need to rapidly increase capacity to safely care for patients with contagious pathogens (*23*) and modify patient care space to increase isolation capacity (*24*). Moreover, frontline healthcare facilities are the likely setting where patients with HCIDs will initially seek care. It is critical to prepare those sites to identify suspected cases, implement prompt isolation, and inform public health officials while providing stabilizing treatment before possible transfer to an HLIU (*25*). In the United States, as of July 1, 2024, the Joint Commission regulatory agency requires specific elements of frontline preparedness for HCIDs at all hospitals (*26*).

HLIUs capacity is limited because associated costs are high (*9*,*27*,*28*), but they provide significant value in return. HLIU patient rooms can be used for routine patient care as well as isolation and care during an HCID outbreak. In addition to maintaining training for HLIU staff, HLIU programs can deliver training to frontline staff at other hospitals to improve regional preparedness (*20*). HLIUs also advance research in areas such as infection prevention, human factors engineering, environmental engineering, and PPE, regardless of whether there is a current HCID outbreak.

Clinical Laboratory Services

Laboratories associated with HLIUs require staff trained in safe handling and transport of specimens containing special pathogens (*29*,*30*); in addition, all frontline hospitals must maintain minimum routine laboratory capabilities critical for providing stabilizing care (*31*). Certain sample processing techniques may generate aerosols and risk staff exposure to a special pathogen if proper precautions are not implemented. Clinical laboratories should conduct risk assessments to identify potential hazards and mitigate risk through the use of engineering controls, such as

primary containment equipment (e.g., biosafety cabinets, sealed centrifuge rotors), and appropriate PPE (*32*). If those safety measures are not in place in the existing core laboratories, then point-of-care testing may be an alternative option.

Medical Countermeasures

The limited availability of medical countermeasures, including vaccines and therapeutics, is a key characteristic and challenge of HCIDs. For example, an expanded access investigational new drug protocol available to prescribe tecovirimat for nonvariola orthopoxvirus infections posed substantial regulatory and administrative burdens on patients and prescribers to access the drug during the 2022 multinational mpox outbreak (*33*). This experience highlighted the importance of fostering partnerships between academic medical centers and community hospitals to ensure prompt access to therapeutics that may be beneficial, but have not achieved full regulatory approval, while collecting appropriate data to determine the therapeutic efficacy and safety of such investigational therapies.

Management of Contaminated Materials and Waste

Management of waste and contaminated materials associated with HCIDs often requires enhanced protocols to ensure safe disposal. Many special pathogens, including Ebola and Marburg viruses, are considered category A infectious substances by the US DOT (*2*) and have stringent requirements for safe packaging and transport. Management of associated waste requires detailed protocols and training of staff to adhere to DOT requirements and to ensure staff and patient safety (*34*). Other processes may involve handling material contaminated with a special pathogen, including daily cleaning and disinfection while caring for a patient, terminal cleaning and disinfection, management of spills, management of the deceased, and discharge of successfully treated patients. In general, waste containing special pathogens should be segregated at the point of generation and contained in leakproof, puncture-resistant containers that are clearly labeled as biohazardous. That waste must be decontaminated using methods such as autoclaving, incineration, or chemical disinfection before disposal. Personnel handling this waste should wear appropriate PPE and be trained in proper waste handling procedures and emergency protocols to manage accidental exposures or spills. Finally, adherence to relevant local, state, and federal regulations related to category A waste handling is essential. Although the proper handling and disposal of category A infectious substances remains a challenge in HCID response plans (*35*), The Joint Commission mandates that all hospitals implement protocols for proper waste management and cleaning and disinfecting of patient care spaces, surfaces, and equipment contaminated with special pathogens (*26*).

Other Clinical Considerations

Other aspects of HCID preparedness and response require consideration of infection prevention and control, ability to provide standard of care, occupational health, and health equity. Those processes include developing and implementing protocols for performing invasive procedures when necessary, monitoring healthcare workers after caring for an HCID patient or handling infectious material, safely transporting patients within and outside of the hospital setting, visitor management, and preparing postexposure plans for staff and community members, including postexposure prophylaxis and quarantine. Protocols for special populations such as children and pregnant persons often require additional planning, expertise, and attention to providing equitable access to care.

Coordination with Other Stakeholders and the System of Care

Public health agencies on the federal, state, and local level play important roles in HCID response (*36*). They promote awareness of and surveillance for outbreaks of concern, coordinate patient triage to the most appropriate care setting, and develop guidelines and protocols for safe patient transport, contact tracing, and prevention of community transmission. The United States is engaging a national special pathogen system of care to improve national preparedness for HCIDs; it consists of a tiered system of healthcare facilities from frontline hospitals to regional treatment centers led by NETEC as coordinating body (*37*). NETEC has also identified gaps in HCID direct care delivery, communication and coordination, workforce capacity, training and education, research, data systems and technology, monitoring and evaluation, financial sustainability, and supply chain management (*38*). Improving equitable access to these aspects of HCID care is critical; NETEC's analysis indicates that minoritized groups currently have less access to special pathogens treatment centers.

Communication with the Public

Events involving HCIDs are likely to make news headlines, so it is important to proactively address the public's concerns regarding local or international outbreaks. During an outbreak, the public should be

informed about known risk factors for contracting the disease; the information can help mitigate transmission related to individual behavior and avoid stigmatizing vulnerable groups. When a patient is admitted to a facility with an HCID, the approach to communication is multifaceted regarding the information that should be shared and who should receive it. If a hospital incident command system is activated, it will likely be a unified command with a joint information center. A public information officer would be identified to coordinate regular updates to the public. Such updates may happen through the local public health official or the HLIU facility, or often both, with all communications coordinated through the command system. In addition, protected health information may need to be shared with response agencies and senior governmental leadership, which must be done cautiously, on a need-to-know basis, and only as permitted by the law.

Areas for Advancement in Preparedness, Care, and Research

Sustaining research on HCIDs is critical to advance the health and safety of the workforce and community. Research efforts should focus on better understanding of pathogenesis, including molecular mechanisms of disease, development and testing of therapeutics and vaccines, and development of diagnostics that can be used rapidly in various settings. Not all clinical facilities have the capabilities to collect or process research specimens; partnering with other organizations such as an academic institution or academic medical center can support or enable this effort.

Limited availability or access to medical countermeasures is a major gap in HCID preparedness efforts. Vaccines and therapeutics are under development in both in vitro and in vivo pipelines, but transition to clinical trials is difficult because of sporadic outbreaks and limited number of affected persons, which can be perceived as a lack of need for these medical countermeasures. The COVID-19 pandemic demonstrated the ability to rapidly develop effective medical countermeasures when sufficient investment is made (*39*). A similar proportionate scale of investment has not been made for many high-priority HCIDs, including Crimean-Congo hemorrhagic fever, Ebola virus disease, Marburg virus disease, Lassa fever, and Nipah virus infection (*11*,*12*). Although we do not suggest that all HCIDs merit the same scale of investment as was mobilized for COVID-19, the pandemic demonstrated the value of sustained, proactive funding for preparedness infrastructure and medical countermeasures. The epidemic and potential pandemic risk for HCIDs, increased by global interconnectedness, climate change (*40*), and frequency of spillover events (*41*), indicates that strategic investments could provide a global benefit.

To evaluate countermeasures properly, it is necessary to prepare trials before an outbreak occurs. Phase I/II safety and immunogenicity trials should occur when possible, and plans and protocols should be drafted for efficacy testing that can be implemented early in an outbreak. During the 2013–2016 Ebola virus outbreak in West Africa, clinical trials were initiated late, and clinical efficacy could not be determined because enrollment did not meet goals (*42*,*43*). Although placebo-controlled trials may not be ethically appropriate, randomized trials of multiple alternative therapeutics can be beneficial, such as the PALM trial initiated during the 2018 Democratic Republic of the Congo Ebola disease outbreak (*44*). When a clinical trial is not possible, WHO's monitored emergency use of unregistered and experimental interventions framework should be consulted to ensure it is ethically appropriate to administer specific therapeutics while data are collected to contribute to future decisions about efficacy (*45*). Facilities that are expected or preparing to care for HCID patients should include plans for safe and ethical participation in research trials and also understand the processes for obtaining investigational countermeasures (*33*).

Vaccines, and protocols for their study, should be prepared in advance to determine efficacy and potentially limit spread as new outbreaks occur. Ring vaccination refers to a strategy to vaccinate persons who have been in close contact with an infected person to prevent transmission. Trials that compare different ring vaccination arms can be effective tools, and the use of randomization to immediate or delayed vaccination groups mitigates concerns about inequitable access (*46*). As with other countermeasures, placebo-controlled vaccine trials are likely not ethical; possible treatment arms that can evaluate efficacy and implementation hurdles are randomization to receive different vaccines, vaccine combinations, or timing between doses. Longitudinal data collected from vaccine recipients can be used to monitor immunogenicity profiles over time and long-term effectiveness during subsequent outbreaks.

Developing and improving access to diagnostics must also be prioritized in countries both endemic and nonendemic for HCIDs. The ideal diagnostic test would be feasible to deploy at scale in low-resource settings where HCID outbreaks often start and would be able to detect a pathogen at the earliest sign of illness. It is appropriate to be judicious about testing in

nonendemic countries to prevent escalations resulting from false positives; however, we must be able to enhance laboratory capacity during active outbreaks.

The continual emergence and reemergence of HCID threats require preparation for future events. Immediate concerns include highly pathogenic avian influenza, which always has pandemic potential; other proximate threats include novel pathogens with relatively low human-to-human transmission, such as Middle East respiratory syndrome coronavirus (MERS-CoV) and Nipah virus. However, introduction of those types of pathogens into a highly populated area could increase the potential for sustained human transmission (*47*). Prioritization for developing

Table. Summary of major classification systems of infectious agents*

Term	Select agents and toxins	Category	Biosafety level	Risk group	Special pathogens and HCIDs (proposed)
Regulating or guiding organization(s)	CDC; USDA	US DOT Hazardous Materials Regulations	CDC; NIH	NIH	None
Levels of classification	SAT or Tier 1 SAT	A and B	1–4	1–4	NA
Scope of pathogens (animal vs. human vs. plant)	Pathogens and toxins posing a severe threat to animals, plants, and humans	Pathogens capable of infecting animals and humans	Pathogens capable of infecting animals and humans	Pathogens capable of infecting or causing harm to humans	Pathogens capable of infecting humans
Purpose of classification	Provide regulations on possession, use, and transfer of pathogens and toxins that have potential to pose a severe threat to the public, animal or plant health. The regulations allow laboratories to conduct important research on these materials in a safe and secure fashion.	Provide regulations on how to safely handle and transport infectious waste that may be capable of causing permanent disability or death in humans or animals upon exposure to the substance.	Provide guidance on the safe handling and containment of infectious microorganisms and hazardous biologic material to protect lab workers, the environment, and public from exposure to infectious microorganisms stored and handled in laboratories.	Describe relative hazard posed by infectious agents or toxins in the laboratory.	Provide guidance on human pathogens that require specialized clinical and public health response to prevent transmission in healthcare facilities and in the community.
Criteria related to classification	Pathogens and toxins that have the potential to pose a severe threat to public, animal or plant health, or to animal or plant products.	Category A classifies an infectious substance as in a form capable of causing permanent disability or life-threatening or fatal disease in otherwise healthy humans or animals when exposure to it occurs. Category B classifies an infectious substance as not in a form generally capable of causing permanent disability or life-threatening or fatal disease in otherwise healthy humans or animals when exposure to it occurs.	BSLs 1–4 are associated with specific guidance on how to prevent exposure to certain pathogens that could pose an infectious risk to persons working in a laboratory.	RG 1–4 are classified based on seriousness or lethality of human disease, whether preventive or therapeutic interventions are available, and risk posed to persons and the community.	Special pathogens cause HCIDs with high illness and death, have few available medical countermeasures, and can transmit from person to person.
List of pathogens	(*1*)	(*2*)	(*3*)	(*4*)	There is no universal list. Examples that meet criteria include Ebola, Marburg, and Nipah viruses.

*BSL, Biosafety Level; CDC, Centers for Disease Control and Prevention; DOT, Department of Transportation; HCID, high-consequence infectious disease; NA, not applicable; NIH, National Institutes of Health; RG, risk group; SAT, select agents and toxins; USDA, US Department of Agriculture; WHO, World Health Organization.

diagnostics and medical countermeasures can be guided by several factors: the pathogen's potential for sustained human-to-human transmission, disease severity, evidence of geographic spread, potential for spillover, lack of existing medical countermeasures, and historical response delays. Expanded surveillance and new artificial intelligence tools to inform risk-assessment can support prioritization (*48*). Strategic investment in novel approaches to clinical research and study design, investment in platform technologies (e.g., viral vector vaccines, monoclonal antibody platforms), and maintaining pathogen-specific research readiness, including validated animal models, early-stage product candidates, and regulatory protocols, can permit rapid escalation of countermeasure development if an outbreak emerges. The goal is not to predict every threat but to build flexible, proactive systems that reduce the time between pathogen emergence and intervention deployment.

We believe that public sector funding, particularly from national governments and multilateral partners, remains essential given the limited commercial incentive to invest in rare but severe pathogens that cause HCIDs. Funding decisions should also account for global interconnectedness with strategic investments to develop capacity where these pathogens are endemic or at highest risk of emerging. Supporting early detection, research, and containment efforts in disease-endemic regions serves both humanitarian and strategic national interests. Considering the COVID-19 pandemic resulted in $16 trillion in economic loss in the United States alone by one estimate (*49*), any increase in investment in improving prediction analytics would provide value.

Conclusions

The US federal government (Table) developed several classification systems to stratify risk of infectious agents in the context of laboratory research, specimen transport, and waste management. Through the lens of patient care delivery, we describe characteristics of a group of HCIDs that represent high threats to public health because of their high illness and case-fatality rates, limited availability of effective treatment or prevention options, and the ability to spread in the community and within healthcare settings.

Optimal preparedness and response require appropriate patient identification, isolation, treatment, and waste management, which might involve the use of HLIUs. Effective medical countermeasures must be developed and made accessible in an equitable fashion. In addition, clear communication and coordination across healthcare workers, health systems, and public health authorities is necessary to ensure public safety and assuredness. Priority areas for investment include research on new diagnostics and medical countermeasures, including clinical trials that should be planned before an outbreak. Because the evidence base to guide several aspects of preparedness and response we have described is limited, a modified Delphi method (*50*) could be used to establish consensus guidelines.

Basic and Translational State of the Science Working Group members: Julie Bulson, Corewell Health, Grand Rapids, Michigan, USA; Vicki Herrera, University of Nebraska Medical Center, Omaha, Nebraska, USA; Anthony Lo Piccolo, NYU Grossman School of Medicine, New York, New York, USA, and NYC Health + Hospitals/Bellevue, New York; Patricia McCabe, MedStar Washington Hospital Center, Washington, DC, USA; Rachel Miller, Denver Health and Hospital Authority, Denver, Colorado, USA; Margie Morgan, Cedars-Sinai Medical Center, Los Angeles, California, USA; Corrie Ntiforo, University of Texas Medical Branch at Galveston, Galveston, Texas, USA.

Acknowledgments

We thank Vikramjit Mukherjee for his critical review of this manuscript.

The National Emerging Special Pathogens Training and Education Center is funded by the US Administration for Strategic Preparedness and Response (grant no. U3REP150549).

About the Author

Dr. Chan is an associate professor of medicine in the Division of Infectious Disease & Immunology at the NYU Grossman School of Medicine in New York, NY, USA. He serves as Director of Infection Prevention and Control at NYC Health + Hospitals/Bellevue, and as the Enterprise Chief Healthcare Epidemiologist at NYC Health + Hospitals. His research interests include understanding the epidemiology, prevention, and control of high-consequence infectious disease outbreaks.

References

1. US Department of Transportation. Planning guidance for handling category A solid waste. 2024 [cited 2025 Feb 11]. https://www.phmsa.dot.gov/transporting-infectious-substances/planning-guidance-handling-category-solid-waste
2. Centers for Disease Control and Prevention. Select agents and toxins list. 2025 [cited 2025 Feb 11]. https://www.selectagents.gov/sat/list.htm
3. Administration for Strategic Preparedness and Response. Risk groups. 2024 [cited 2025 Feb 11]. https://aspr.hhs.gov/S3/Pages/Risk-Groups.aspx

4 Centers for Disease Control and Prevention. Biosafety in microbiological and biomedical laboratories (BMBL). 6th edition. 2020 [cited 2025 Feb 11]. https://www.cdc.gov/labs/bmbl/index.html
5. National Emerging Special Pathogens Training & Education Center. National Emerging Special Pathogens Training and Education Center. 2025 [cited 2025 May 11]. https://netec.org
6. UK Health Security Agency. High consequence infectious diseases (HCID). 2018 [cited 2024 July 5]. https://www.gov.uk/guidance/high-consequence-infectious-diseases-hcid
7. NSW Health. Early response to high consequence infectious diseases. 2024 [cited 2024 July 5]. https://www1.health.nsw.gov.au/pds/Pages/doc.aspx?dn=PD2024_005
8. Bannister B, Puro V, Fusco FM, Heptonstall J, Ippolito G; EUNID Working Group. Framework for the design and operation of high-level isolation units: consensus of the European Network of Infectious Diseases. Lancet Infect Dis. 2009;9:45–56. https://doi.org/10.1016/S1473-3099(08)70304-9
9. Garibaldi BT, Kelen GD, Brower RG, Bova G, Ernst N, Reimers M, et al. The creation of a biocontainment unit at a tertiary care hospital. The Johns Hopkins Medicine Experience. Ann Am Thorac Soc. 2016;13:600–8. https://doi.org/10.1513/AnnalsATS.201509-587PS
10. Cieslak TJ, Herstein JJ, Kortepeter MG, Hewlett AL. A methodology for determining which diseases warrant care in a high-level containment care unit. Viruses. 2019;11:773. https://doi.org/10.3390/v11090773
11. World Health Organization. Prioritizing diseases for research and development in emergency contexts. 2024 [cited 2024 Jul 5]. https://www.who.int/activities/prioritizing-diseases-for-research-and-development-in-emergency-contexts
12. National Institute of Allergy and Infectious Diseases. NIAID biodefense pathogens. 2024 [cited 2024 Jul 5]. https://www.niaid.nih.gov/research/emerging-infectious-diseases-pathogens
13. Letafati A, Salahi Ardekani O, Karami H, Soleimani M. Ebola virus disease: a narrative review. Microb Pathog. 2023;181:106213. https://doi.org/10.1016/j.micpath.2023.106213
14. Centers for Disease Control and Prevention. Clinical guidance for Ebola disease. 2025 [cited 2025 Apr 28]. https://www.cdc.gov/ebola/hcp/clinical-guidance/index.html
15. Kortepeter MG, Dierberg K, Shenoy ES, Cieslak TJ; Medical Countermeasures Working Group of the National Ebola Training and Education Center's (NETEC) Special Pathogens Research Network (SPRN). Marburg virus disease: a summary for clinicians. Int J Infect Dis. 2020;99:233–42. https://doi.org/10.1016/j.ijid.2020.07.042
16. Branda F, Ceccarelli G, Giovanetti M, Albanese M, Binetti E, Ciccozzi M, et al. Nipah virus: a zoonotic threat re-emerging in the wake of global public health challenges. Microorganisms. 2025;13:124. https://doi.org/10.3390/microorganisms13010124
17. Hu B, Guo H, Zhou P, Shi Z-L. Characteristics of SARS-CoV-2 and COVID-19. Nat Rev Microbiol. 2021;19:141–54. https://doi.org/10.1038/s41579-020-00459-7
18. O'Toole Á, Neher RA, Ndodo N, Borges V, Gannon B, Gomes JP, et al. APOBEC3 deaminase editing in mpox virus as evidence for sustained human transmission since at least 2016. Science. 2023;382:595–600. https://doi.org/10.1126/science.adg8116
19. Akingbola A, Adegbesan CA, Adewole O, Idahor C, Odukoya T, Nwaeze E, et al. Understanding the resurgence of mpox: key drivers and lessons from recent outbreaks in Africa. Trop Med Health. 2025;53:47. https://doi.org/10.1186/s41182-024-00678-1
20. Flinn JB, Hynes NA, Sauer LM, Maragakis LL, Garibaldi BT. The role of dedicated biocontainment patient care units in preparing for COVID-19 and other infectious disease outbreaks. Infect Control Hosp Epidemiol. 2021;42:208–11. https://doi.org/10.1017/ice.2020.451
21. Smith PW, Anderson AO, Christopher GW, Cieslak TJ, Devreede GJ, Fosdick GA, et al. Designing a biocontainment unit to care for patients with serious communicable diseases: a consensus statement. Biosecur Bioterror. 2006;4:351–65. https://doi.org/10.1089/bsp.2006.4.351
22. National Emerging Special Pathogens Training & Education Center. National Special Pathogen System (NSPS). 2025 [cited 2025 Apr 28]. https://netec.org/nsps/nsps-about-the-nsps
23. Mandel-Ricci J, Belfi K, Shapiro J, Wiener A, Cintron BS, Warshaw A, et al. Rethinking surge preparedness after COVID-19: effective patient load balancing within health systems and beyond. Health Secur. 2022;20:497–503. https://doi.org/10.1089/hs.2022.0059
24. Shadpour F, Johnson S. Makeshift negative pressure patient rooms in response to COVID-19. ASHRAE J. 2020;62:24–31.
25. Madad S. Preparing frontline hospitals for dangerous special pathogens beyond Ebola. Health Secur. 2021;19:209–13. https://doi.org/10.1089/hs.2020.0134
26. The Joint Commission. R3 report issue 41: new and revised requirements for infection prevention and control for critical access hospitals and hospitals. 2023 [cited 2024 Jul 5]. https://www.jointcommission.org/standards/r3-report/r3-report-issue-41-new-and-revised-requirements-for-infection-prevention-and-control-for
27. Herstein JJ, Biddinger PD, Kraft CS, Saiman L, Gibbs SG, Smith PW, et al. Initial costs of Ebola treatment centers in the United States. Emerg Infect Dis. 2016;22:350–2. https://doi.org/10.3201/eid2202.151431
28. Herstein JJ, Wolf T, Nicastri E, Leo YS, Lim PL, Jacobs M, et al. Capabilities of global high-level isolation units: a pre-workshop survey. Infect Control Hosp Epidemiol. 2022;43:1679–85. https://doi.org/10.1017/ice.2021.477
29. Pentella MA. Update on biosafety and emerging infections for the clinical microbiology laboratory. Clin Lab Med. 2020;40:473–82. https://doi.org/10.1016/j.cll.2020.08.005
30. Madad S, Jacobson JL, Caruso RR, Dunning J. High-consequence infectious diseases, bioterrorism, and the imperative for international and US biosecurity and biosafety frameworks for biocontainment clinical laboratories. Health Secur. 2024;22:455–60. https://doi.org/10.1089/hs.2023.0164
31. Centers for Disease Control and Prevention. Guidance on performing routine diagnostic testing for patients with suspected VHFs or other high-consequence disease. 2024 [cited 2024 Jul 5]. https://www.cdc.gov/viral-hemorrhagic-fevers/php/laboratories/guidance-on-performing-routine-diagnostic-testing-for-patients-with-suspected-vhfs-or-other.html
32. Turbett SE, Lazarus JE, Nardini MA, Braidt JE, Lane SA, Searle EF, et al. Enabling laboratory readiness and preparedness for the evaluation of suspected viral hemorrhagic fevers: development of a laboratory toolkit. Infect Control Hosp Epidemiol. 2024;45:1–7. https://doi.org/10.1017/ice.2024.143
33. Mgbako O, Chan J, Pitts RA, DiLorenzo MA, Knutsen D, Mazo D. Navigating the expanded access investigational new drug protocol for tecovirimat: lessons learned from a public-private hospital partnership during the 2022 NYC mpox outbreak. Antimicrob Steward

Healthc Epidemiol. 2023;3:e110. https://doi.org/10.1017/ash.2023.194
34. Jelden KC, Gibbs SG, Smith PW, Schwedhelm MM, Iwen PC, Beam EL, et al. Nebraska Biocontainment Unit patient discharge and environmental decontamination after Ebola care. Am J Infect Control. 2015;43:203–5. https://doi.org/10.1016/j.ajic.2014.12.005
35. Gibbs SG, Schwedhelm MM, Lowe JJ, Tennill P, Persson CC, Carrasco SV, et al. Category A waste processing and disposal is a critical weakness in the United States response plans for outbreaks of high consequence infectious diseases. Am J Infect Control. 2024;52:136–8. https://doi.org/10.1016/j.ajic.2023.08.022
36. Herstein JJ, Biddinger PD, Gibbs SG, Le AB, Jelden KC, Hewlett AL, et al. US state public health departments special pathogen planning. J Public Health Manag Pract. 2018;24:E28–33. https://doi.org/10.1097/PHH.0000000000000714
37. Mukherjee V, Sauer LM, Mehta AK, Shea SY, Biddinger PD, Carr BG, et al. The evolution of the National Special Pathogen System of Care. Health Secur. 2022;20(S1):S39–48. https://doi.org/10.1089/hs.2022.0026
38. National Emerging Special Pathogens Training & Education Center. National Special Pathogen System (NSPS) strategy. 2024 [cited 2024 Dec 12]. https://netec.org/wp-content/uploads/2024/02/NETEC_NSPS-Refreshed-Strategy_20240201.pdf
39. Toussi SS, Hammond JL, Gerstenberger BS, Anderson AS. Therapeutics for COVID-19. Nat Microbiol. 2023;8:771–86. https://doi.org/10.1038/s41564-023-01356-4
40. Mora C, McKenzie T, Gaw IM, Dean JM, von Hammerstein H, Knudson TA, et al. Over half of known human pathogenic diseases can be aggravated by climate change. Nat Clim Chang. 2022;12:869–75. https://doi.org/10.1038/s41558-022-01426-1
41. Baker RE, Mahmud AS, Miller IF, Rajeev M, Rasambainarivo F, Rice BL, et al. Infectious disease in an era of global change. Nat Rev Microbiol. 2022;20:193–205. https://doi.org/10.1038/s41579-021-00639-z
42. Davey RT Jr, Dodd L, Proschan MA, Neaton J, Neuhaus Nordwall J, Koopmeiners JS, et al.; Multi-National PREVAIL II Study Team. A randomized, controlled trial of ZMapp for Ebola virus infection. N Engl J Med. 2016;375:1448–56. https://doi.org/10.1056/NEJMoa1604330
43. Sissoko D, Laouenan C, Folkesson E, M'Lebing AB, Beavogui AH, Baize S, et al.; JIKI Study Group. Experimental treatment with favapiravir for Ebola virus disease (the JIKI trial): a historically controlled, single-arm proof-of-concept trial in Guinea. PLoS Med. 2016;13:e1001967. https://doi.org/10.1371/journal.pmed.1001967
44. Mulangu S, Dodd LE, Davey RT Jr, Tshiani Mbaya O, Proschan M, Mukadi D, et al.; PALM Writing Group; PALM Consortium Study Team. A randomized, controlled trial of Ebola virus disease therapeutics. N Engl J Med. 2019;381:2293–303. https://doi.org/10.1056/NEJMoa1910993
45. World Health Organization. Emergency use of unproven clinical interventions outside clinical trials: ethical considerations. 2022 [cited 2024 Jul 5]. https://www.who.int/publications/i/item/9789240041745
46. Dean NE, Longini IM. The ring vaccination trial design for the estimation of vaccine efficacy and effectiveness during infectious disease outbreaks. Clin Trials. 2022;19:402–6. https://doi.org/10.1177/17407745211073594
47. Cho SY, Kang JM, Ha YE, Park GE, Lee JY, Ko JH, et al. MERS-CoV outbreak following a single patient exposure in an emergency room in South Korea: an epidemiological outbreak study. Lancet. 2016;388:994–1001. https://doi.org/10.1016/S0140-6736(16)30623-7
48. Gawande MS, Zade N, Kumar P, Gundewar S, Weerarathna IN, Verma P. The role of artificial intelligence in pandemic responses: from epidemiological modeling to vaccine development. Mol Biomed. 2025;6:1. https://doi.org/10.1186/s43556-024-00238-3
49. Cutler DM, Summers LH. The COVID-19 pandemic and the $16 trillion virus. JAMA. 2020;324:1495–6. https://doi.org/10.1001/jama.2020.19759
50. Eubank BH, Mohtadi NG, Lafave MR, Wiley JP, Bois AJ, Boorman RS, et al. Using the modified Delphi method to establish clinical consensus for the diagnosis and treatment of patients with rotator cuff pathology. BMC Med Res Methodol. 2016;16:56. https://doi.org/10.1186/s12874-016-0165-8

Address for correspondence: Corri B. Levine, University of Texas Medical Branch, Department of Internal Medicine, Division of Infectious Diseases, 4.210 Marvin Graves, 120 11th St, Galveston, TX 77555-0435, USA; email: cblevine@utmb.edu

Emergence of Clade Ib Monkeypox Virus—Current State of Evidence

Panayampalli S. Satheshkumar,[1] Crystal M. Gigante,[1] Placide Mbala-Kingebeni, Yoshinori Nakazawa, Mark Anderson, Stephen Balinandi, Sophia Mulei, James Fuller, Jennifer H. McQuiston, Andrea M. McCollum, Christina L. Hutson

Medscape CME Activity

In support of improving patient care, this activity has been planned and implemented by Medscape, LLC and Emerging Infectious Diseases. Medscape, LLC is jointly accredited with commendation by the Accreditation Council for Continuing Medical Education (ACCME), the Accreditation Council for Pharmacy Education (ACPE), and the American Nurses Credentialing Center (ANCC), to provide continuing education for the healthcare team.

Medscape, LLC designates this Journal-based CME activity for a maximum of 1.00 ***AMA PRA Category 1 Credit(s)™***. Physicians should claim only the credit commensurate with the extent of their participation in the activity.

Successful completion of this CME activity, which includes participation in the evaluation component, enables the participant to earn up to 1.0 MOC points in the American Board of Internal Medicine's (ABIM) Maintenance of Certification (MOC) program. Participants will earn MOC points equivalent to the amount of CME credits claimed for the activity. It is the CME activity provider's responsibility to submit participant completion information to ACCME for the purpose of granting ABIM MOC credit.

All other clinicians completing this activity will be issued a certificate of participation. To participate in this journal CME activity: (1) review the learning objectives and author disclosures; (2) study the education content; (3) take the post-test with a 75% minimum passing score and complete the evaluation at https://www.medscape.org/qna/processor/74833?showStandAlone=true&src=prt_jcme_eid_mscpedu; and (4) view/print certificate. For CME questions, see page 1688.

NOTE: It is the policy of Medscape Education to avoid the mention of brand names or specific manufacturers in accredited educational activities. However, trade and manufacturer names in this activity are provided in an effort to provide clarity. The use of brand or manufacturer names should not be viewed as an endorsement by Medscape of any specific product or manufacturer.

Release date: July 23, 2025; Expiration date: July 23, 2026

Learning Objectives

Upon completion of this activity, participants will be able to:

- Distinguish the clade of monkeypox virus (MPXV) responsible for a global outbreak in 2022 and 2023
- Compare clinical characteristics of clade I and clade II MPXV
- Assess the application and efficacy of vaccines against MPXV
- Evaluate treatment options for mpox

CME Editor

Susan Zunino, PhD, Technical Writer/Editor, Emerging Infectious Diseases. *Disclosure: Susan Zunino, PhD, has no relevant financial relationships.*

CME Author

Charles P. Vega, MD, Health Sciences Clinical Professor of Family Medicine, University of California, Irvine School of Medicine, Irvine, California. *Disclosure: Charles P. Vega, MD, has the following relevant financial relationships: served as consultant or advisor for Boehringer Ingelheim; Exact Sciences.*

Authors

Panayampalli S. Satheshkumar, PhD; Crystal M. Gigante, PhD; Placide Mbala-Kingebeni, MD, MSPH, PhD; Yoshinori Nakazawa, PhD; Mark Anderson, MD, MPH; Stephen Balinandi, MSc, PhD; Sophia Mulei, BS; James Fuller, PhD; Jennifer H. McQuiston, MS, DVM; Andrea M. McCollum, PhD; Christina L. Hutson, MS, PhD.

Mpox was first identified against the backdrop of the smallpox eradication campaign. Monkeypox virus (MPXV), the causative agent of mpox, has been maintained in animal reservoirs in the forested regions of West and Central Africa as 2 distinct clades; clade I has historically caused more severe infection in Central Africa than clade II, historically found in West Africa. However, rapid reemergence and spread of both MPXV clades through novel routes of transmission have challenged the known characteristics of mpox. We summarize mpox demographic distribution, clinical severity, and case-fatality rates attributed to genetically distinct MPXV subclades and focus on MPXV clade Ib, the more recently identified subclade. Broad worldwide assistance will be necessary to halt the spread of both MPXV clades within mpox endemic and nonendemic regions to prevent future outbreaks.

Monkeypox virus (MPXV), the causative agent of mpox (formerly known as monkeypox), has reemerged as a major public health concern across the globe because of recent outbreaks. Accordingly, the World Health Organization declared public health emergencies of international concern, initially for the global mpox outbreak on July 22, 2022, and again on August 14, 2024, for ongoing mpox outbreaks in the Democratic Republic of the Congo and nearby countries (*1*,*2*). MPXV has circulated in endemic regions since the 1970s, primarily because of zoonotic spillover followed by limited household transmission (*3*). However, more efficient spread in humans via sexual contact led to ≈100,000 mpox cases during May 2022–August 2024, including in 115 previously nonendemic countries (*4*).

After eradication of smallpox (caused by variola virus) in 1980, MPXV has become the major orthopoxvirus infecting humans. The increased incidence of mpox has likely been caused by several factors, such as an increase in the proportion of immunologically naive populations after discontinuing routine smallpox vaccination and waning immunity in those persons previously vaccinated. Increased surveillance and diagnostic testing have also led to the detection of mpox in various countries after several decades with no reported cases (*5*,*6*).

Author affiliations: Centers for Disease Control and Prevention, Atlanta, Georgia, USA (P.S. Satheshkumar, C.M. Gigante, Y. Nakazawa, M. Anderson, J. Fuller, J.H. McQuiston, A.M. McCollum, C.L. Hutson); Institut National de Recherche Biomédicale, Kinshasa, Democratic Republic of the Congo (P. Mbala-Kingebeni); Uganda Virus Research Institute, Entebbe, Uganda (S. Balinandi, S. Mulei)

DOI: https://doi.org/10.3201/eid3108.241551

MPXV is classified into 2 distinct clades and further into subclades on the basis of genetic differences (*7*). Historically, mpox cases caused by clade I and clade II MPXV were segregated to countries in central (clade I) and western (clade II) Africa, presumably because of geographic barriers separating the reservoir host(s) populations (Figure 1) (*8*). Clade I and II MPXV genomes differ by ≈0.4%–0.5% in nonrepetitive regions conserved between the clades and by the presence of 4 large insertion/deletions (*7*); the clades are estimated to have evolved separately over hundreds of years.

Clade II MPXV

Clade II MPXV (previously known as West African MPXV) was first identified in the 1970s. According to sequence data, clade II MPXV is divided into subclades IIa and IIb. Before 2022, mpox cases caused by clades IIa and IIb were separated by the Dahomey Gap in West Africa (*9*), which might have been a geographic barrier for unknown MPXV reservoir hosts that enabled those 2 subclades to evolve separately (*8*,*9*). Clades IIa and IIb share ≈99.8% nucleotide identity in conserved nonrepetitive regions and can be differentiated by a large subclade-specific insertion/deletion. In 2017, Nigeria reported an mpox outbreak caused by MPXV clade IIb after decades of no reported cases (*10*). In 2022, clade IIb spread globally to many countries that had previously not reported mpox cases. Global mpox cases caused by clade IIb MPXV peaked for most countries during July–October 2022 (*11*), but the outbreak has been ongoing since then; low numbers of cases have been reported in many countries previously unaffected by mpox.

Since the 2017 outbreak in Nigeria, extensive human-to-human transmission of clade IIb MPXV has disproportionately impacted men who have sex with men through sexual activity (*10*,*12*,*13*), conflicting with the general understanding of mpox cases in endemic countries as being caused by zoonotic spillover followed by limited person-to-person spread. Moreover, starting with MPXV sequences from Nigeria in 2017 through the 2022 global outbreak, it became clear that clade IIb MPXV was accumulating mutations at a faster rate than previously reported for orthopoxviruses (*12*–*14*). Most single-nucleotide polymorphisms were GA to AA mutations, linked to the activity of host innate immunity proteins belonging to the apolipoprotein B mRNA editing catalytic polypeptide-like (APOBEC) 3 family (*12*–*14*). APOBEC3 family members exhibit diverse functions,

[1]These first authors contributed equally to the article.

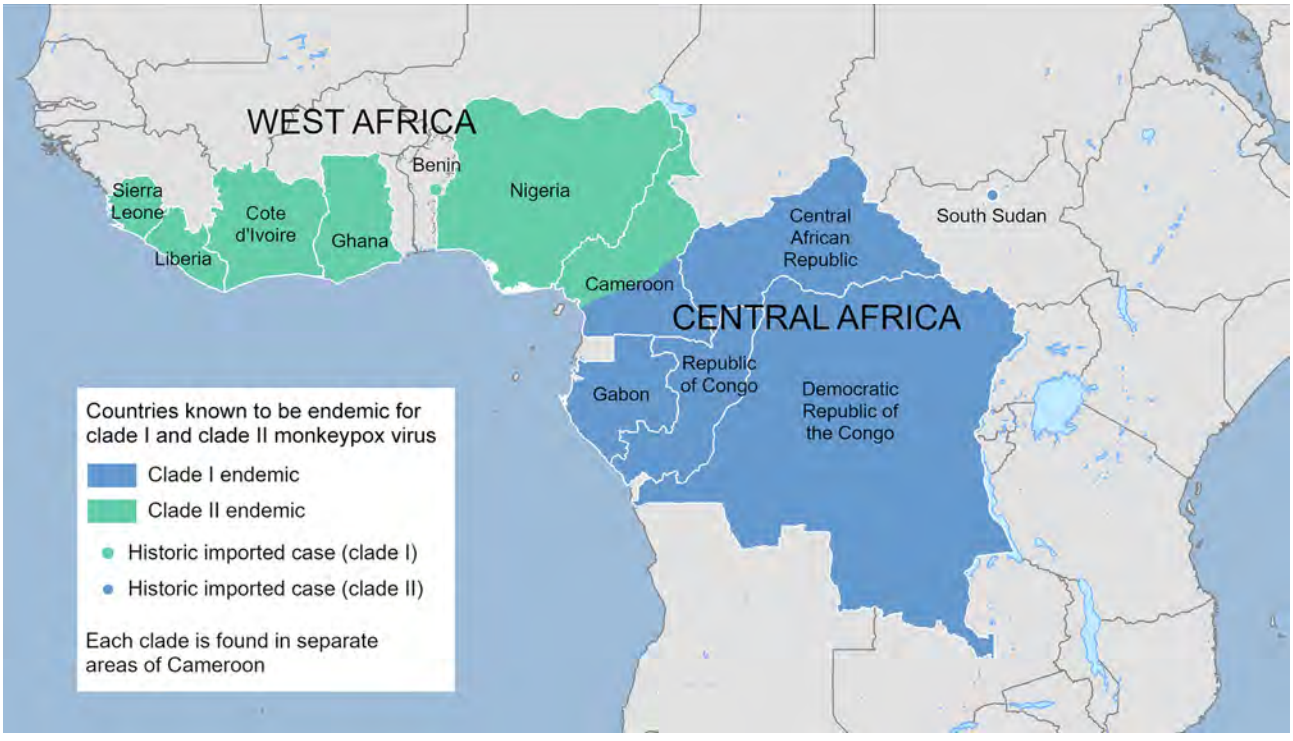

Figure 1. Geographic distribution of countries in Africa considered endemic for mpox caused by monkeypox virus clades I and II. Clade I (blue dot) and clade II (green dot) indicate historic imported mpox cases linked to mpox-endemic areas through known travel before 2022. Geographic separation of clades in Cameroon is approximate.

including cytidine deamidation leading to signature G-to-A point mutations. The human genome encodes 6 functional APOBEC3 proteins, including APOBEC3F, which has been shown to produce extensive G-to-A mutations in the MPXV genome in cultured cells (*15*). APOBEC3 signature mutations are not observed in MPXV lineages having documented zoonotic transmission but are limited to those lineages involved in human-to-human transmission (i.e., clades Ia and IIa) (*12*,*13*); accumulations of APOBEC3-mediated signature mutations in MPXV lineages are now considered an indicator of sustained human-to-human transmission. It is not clear how those host-induced mutations are affecting MPXV; however, no evidence exists suggesting they cause increased virulence. The mutations have been reported across the genome in both coding and noncoding regions. In animal models, clade IIb viruses have been associated with decreased virulence compared with clades Ia and IIa (*16*), but genetic differences between those clades are not limited to APOBEC3-mediated mutations.

Clade I MPXV

Whereas clade IIb MPXV spread globally in 2022 and 2023, mpox cases caused by clade I MPXV were reported only in known mpox-endemic countries: the Democratic Republic of the Congo (DRC), the Republic of Congo, Gabon, Cameroon, and Central African Republic. None of the clade I–endemic countries reported cases caused by clade IIb MPXV during the 2022 global clade II outbreak except for Cameroon (only country in which clades I and II were both endemic before 2022), although virus characterization and testing were limited. Since 2022, the number of suspected clade I–associated mpox cases and deaths in DRC has increased considerably, and the highest number of suspected mpox cases in DRC was recorded in 2024 (*17*). Epidemiologic and genetic investigations of mpox in DRC during 2023–2024 revealed multiple outbreaks occurred involving different transmission dynamics, geographic distribution, and affected populations.

Although mpox is endemic to DRC, in 2023 and 2024, mpox cases were being reported in previously disease-free areas in persons >15 years of age, whereas in other provinces those <15 years of age were most affected. Historically, children have been the most vulnerable to and affected by clade I–associated mpox in DRC; >80% of suspected cases and the highest case-fatality rates (CFRs) have been recorded in children <15 years of age (*3*). The historically high incidence of mpox in children was predominantly thought to be mediated by zoonotic spillover or occasional household transmissions (*18*).

In late 2023, South Kivu, a province with few mpox cases, reported an mpox outbreak that had sexual contact as a primary factor for virus transmission (*19*). The MPXV causing cases in South Kivu was genetically distinct from clade I MPXV sequences from other regions of DRC (*19*,*20*), indicating that 2 distinct subclades were causing outbreaks in that country; the subclades have officially been designated Ia (which includes historical clade I MPXV sequences) and Ib (Figure 2, panels A, B) (*19*,*20*). Since late 2023, clade Ib MPXV has spread beyond South Kivu into other provinces of DRC and internationally to countries that had not previously reported mpox (Figure 3). The mpox outbreak caused by clade IIb continues to be associated with person-to-person transmission through both sexual and nonsexual close contact.

Although clade Ib MPXV has been recently discovered and named, similar MPXV sequences were

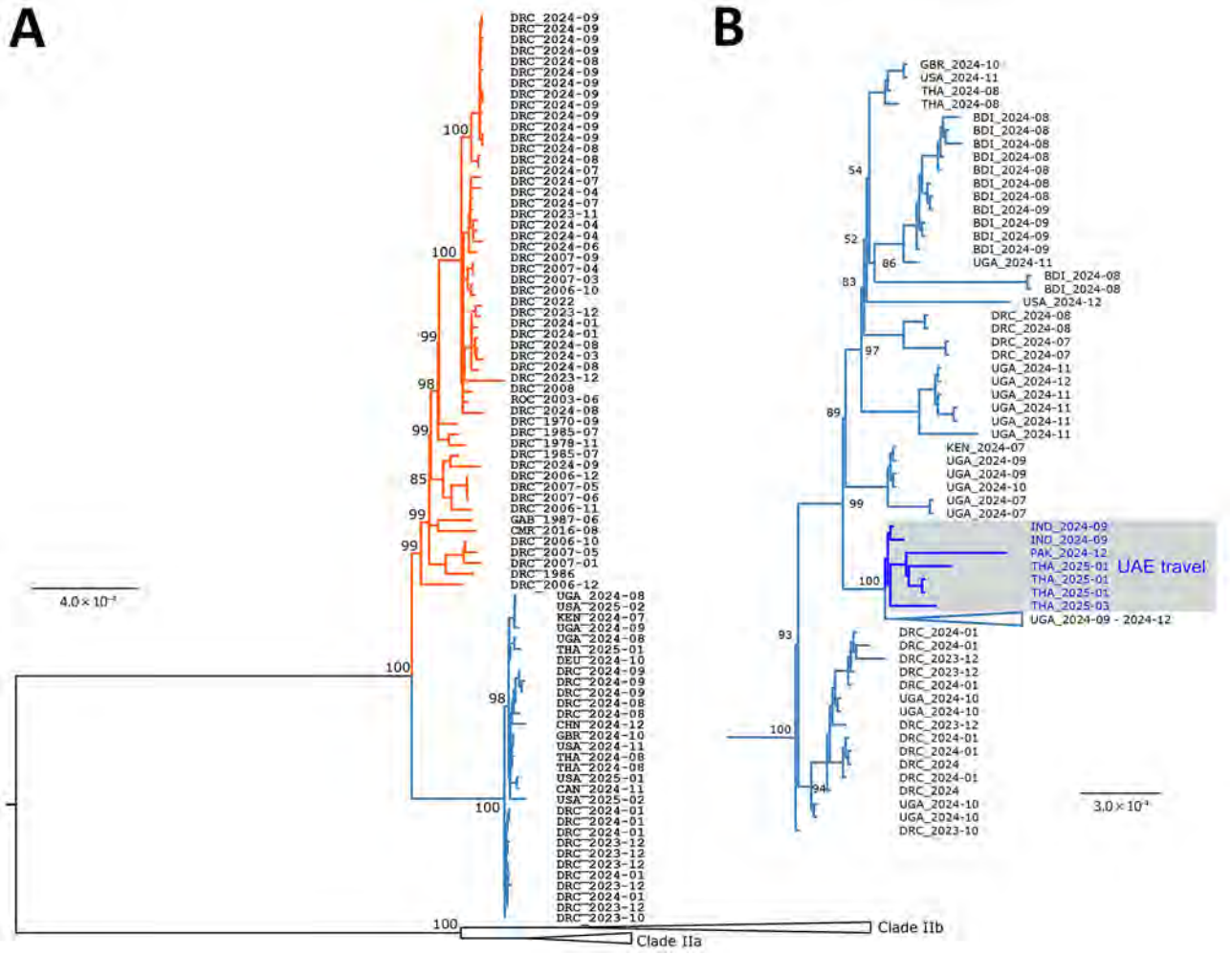

Figure 2. Phylogenetic analysis of clade I monkeypox virus (MPXV) sequences. A) Phylogenetic tree estimated for sequences from 1970–2024 according to core single-nucleotide differences among 103 clade I MPXV genomes. Sequences are identified by country (3-letter code) and collection date (year-month). Red branches indicate MPXV clade Ia; blue branches indicate clade Ib. Numbers at branch points indicate bootstrap support values (percentage of 1,000 replicates). B) Phylogenetic analysis of select clade Ib MPXV sequences. Blue text in gray box indicates sequences linked to persons who had traveled to UAE. Phylogenetic analyses were performed by using the maximum-likelihood method and the 3 substitution types model and equal base frequency plus empirical base frequencies plus proportion of invariable sites substitution model in ModelFinder (IQ-TREE version 2.2.6, https://iqtree.github.io). Whole-genome alignments of sequences downloaded from GISAID (https://www.gisaid.org) and GenBank (Appendix, https://wwwnc.cdc.gov/EID/article/31/8/24-1551-App1.xlsx; data contributor information, https://doi.org/10.55876/gis8.250505zb) databases were generated by using MAFFT version 7.490 (https://mafft.cbrc.jp/alignment/software). Trees were rooted by using clade II reference genomes: ON627808, ON585033, DQ011156, and DQ011153. Clade Ia sequences are not shown in the tree in panel B. Scale bars indicate nucleotide substitutions per site. BDI, Burundi; CAN, Canada; CHN, China; CMR, Cameroon; DEU, Germany; DRC, Democratic Republic of the Congo; GAB, Gabon; GBR, United Kingdom; IND, India; KEN, Kenya; PAK, Pakistan; ROC, Republic of Congo; THA, Thailand; UAE, United Arab Emirates; UGA, Uganda; USA, United States.

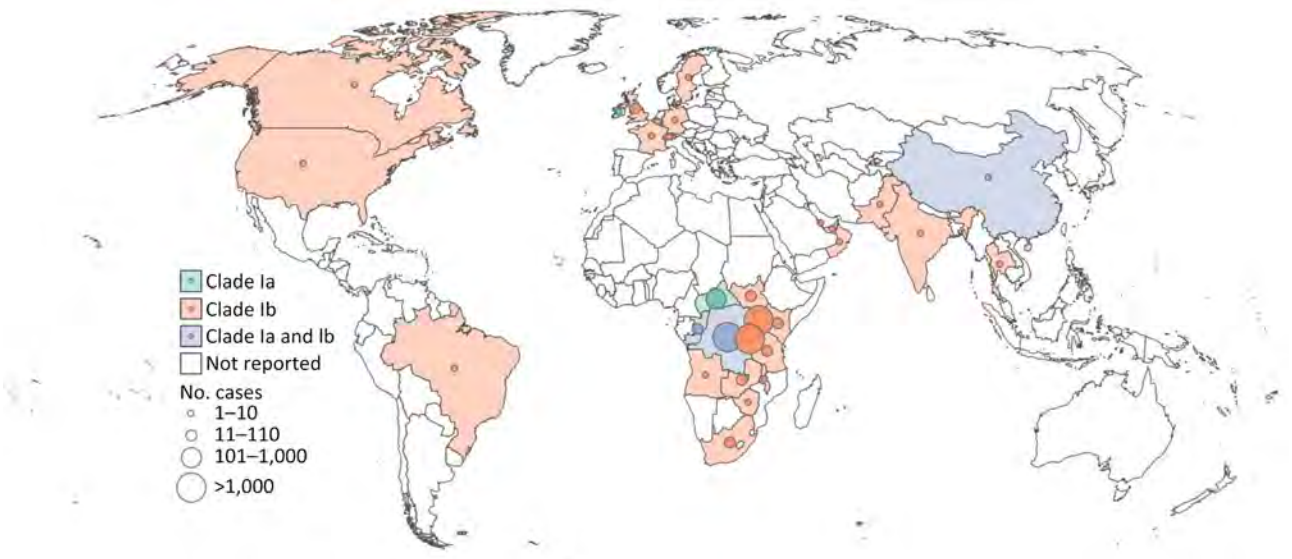

Figure 3. Global distribution of laboratory-confirmed cases of clade I monkeypox virus according to subclade during January 1, 2024–April 27, 2025 (*31*). Size of circles indicates estimated number of cases.

collected during 2011–2012 in North and South Kivu (*21*), suggesting a clade Ib ancestor of the virus causing the 2023–2024 outbreak might have been present in the same region years earlier (*21*). Clade Ib MPXV sequences from the 2023–2024 outbreak are characterized by low overall genetic diversity, the accumulation of APOBEC3-mediated signature mutations, and a large 1,142-bp genomic deletion relative to clade Ia (*19*), resulting in loss of the complement control protein (CCP) gene. Although low genetic diversity within the clade Ib outbreak lineage is indicative of a recent outbreak, the abundance of APOBEC3-induced mutations is an indicator of sustained human-to-human transmission. However, transmission and demographic data for clade Ib suggests that increased sexual transmission, including through female sex trade workers, was predominantly driving the initial outbreak and subsequent sustained transmission (*22*). Clade Ia MPXV sequences from across DRC had much higher overall genetic diversity (≈10-fold higher than clade Ib) and a lower proportion of APOBEC3-induced signature mutations, suggesting that, unlike the clade Ib outbreak lineage, sustained human-to-human spread of clade Ia has not been pervasive throughout DRC, according to sequence data from 2018 through early 2024. Epidemiologic and genetic data for clade Ia MPXV still largely support the modality of zoonotic spillover followed by occasional human-to-human transmission or small outbreaks, but how the virus is repeatedly introduced into the human population is poorly understood.

One exception to the association between MPXV clade subtypes and zoonotic (clade Ia) or human-to-human (clade Ib) transmission has been reported in Kinshasa, DRC, where mpox outbreaks caused by both clade Ia and Ib MPXV are ongoing (*23*; T. Wawina-Bokalanga et al., unpub. data, https://doi.org/10.1101/2024.11.15.24317404). MPXV sequences from the Kinshasa outbreaks have accumulated APOBEC3-induced mutations (T. Wawina-Bokalanga et al., unpub. data), regardless of the clade subtype, reinforcing the notion that accumulation of APOBEC3-induced mutations is a molecular indicator of sustained human-to-human transmission. Since 2022, many investigations have focused on genetic changes that might have occurred in clade IIb MPXV that led to a global outbreak. Current evidence has not identified any subclade-specific virus adaptations that can explain why clade Ia, Ib, and IIb lineages have led to large outbreaks, suggesting that environmental factors (i.e., the network of persons into which the virus is introduced) play a critical role. Clade Ia, Ib, and IIb lineages have each caused outbreaks with sustained human-to-human transmission; thus, it is clear that any MPXV clade or subclade has the potential to cause such outbreaks, if (or when) the virus is introduced into a permissive transmission network that supports sustained transmission (*23*; T. Wawina-Bokalanga et al., unpub. data). Continued genomic sequence surveillance is critical to monitor ongoing mpox outbreaks in DRC and beyond.

Comparisons of MPXV Clade Pathogenesis and Spread

Clinical studies of mpox in humans, as well as animal studies, have reported higher fatality rates for clade I

than clade II infections; a higher number of persons with severe disease and more nonsexual human-to-human spread have also been reported for clade I MPXV (before the current outbreaks) compared with clade II infections (*7*,*16*,*24*,*25*). However, the pathogenesis, CFRs, and standards of treatment for mpox have varied for clades I and II. From a review of historic literature published before 2020, CFRs were estimated to be 10.6% for clade Ia and 3.6% for clade II MPXV infections without any medical intervention, and those estimates were likely influenced by limited or biased testing (*26*). Even in 2023, the CFR for clade I–associated suspected and confirmed mpox cases in DRC was estimated at 4.5% (*27*). However, general medical interventions have been shown to decrease CFR for MPXV clade I–associated cases. For instance, a 1.38% CFR was observed in the town of Kole during a natural history observational clinical study that included standard medical care (*28*), and a 1.7% CFR was observed with similar care during a clinical trial testing tecovirimat (both presumably clade Ia studies) (*29*). The mpox CFRs in South Kivu (which has only reported clade Ib MPXV infections) have consistently stayed <1% for suspected cases (*27*,*30*,*31*), lower than for clade Ia infections elsewhere in DRC. In addition, Burundi, which has had a clade Ib–associated mpox outbreak because of cross-border spread from DRC, had 1,607 confirmed mpox cases but only 1 fatality reported during July 22–October 31, 2024; moreover, in 1 Burundi study, ≈50% of mpox infections were in children, with no reported deaths (*31*–*33*). Taken together, those preliminary data suggest a lower CFR for clade Ib than for clade Ia, but additional studies are needed to confirm that difference.

CFR estimates can be affected by differences in populations, demographics, and underlying health conditions (including food insecurity); access to healthcare; and testing biases. For example, the CFR (≈0.2% globally) for mpox caused by the clade IIb global outbreak lineage was considerably less than historical estimates for clade II, according to data from parts of the world with access to strong medical care systems. CFRs and clinical details from Kinshasa and other areas of DRC where clade Ia and Ib are co-circulating in comparable populations will provide a more reliable comparison of disease severity caused by those subclades (*4*).

Comparisons of MPXV genomic sequences revealed loss of the CCP gene (also known as monkeypox inhibitor of complement enzymes, encoded by *D14L*, a homologue of smallpox inhibitor of complement enzymes of vaccinia virus Copenhagen, encoded by *C4L*) in clades II and Ib compared with clade Ia. Researchers have hypothesized that deletion of the CCP gene might be the reason for decreased CFRs and disease severity historically reported for mpox caused by clades II and Ib compared with clade Ia viruses. However, animal studies investigating the effect of CCP gene loss have produced conflicting results. In 1 study, targeted deletion of the CCP gene from clade Ia MPXV (isolate ROC-2003-358) caused significantly decreased illness and death in infected prairie dogs, whereas addition of that gene to clade IIa MPXV caused slight changes in disease manifestation but had no apparent effect on disease-associated death (*34*). In another study, replacing large regions of the terminal genome of clade Ia with a corresponding sequence from clade IIa did not produce a difference in animal survival (*35*). A third study in nonhuman primates found differences in adaptive immune responses when the CCP gene was deleted from clade Ia MPXV (isolate Zaire-1979 005) (*36*). Investigators of all 3 studies concluded that the CCP deletion was not solely responsible for the differential pathogenicity between the clades (*34*–*36*). Additional animal studies with clade Ib isolates will help elucidate whether the genetic changes observed (CCP deletion and other mutations) do indeed result in a less virulent virus compared with clade Ia isolates. Other mutations (induced by APOBEC3 and non-APOBEC3 proteins) that distinguish clades Ia and Ib might also contribute to lower CFRs currently observed for clade Ib in South Kivu and Burundi compared with those of clade Ia cases elsewhere in DRC.

Even if clade Ib is confirmed to be less virulent than clade Ia, recent reports highlight the threat of that virus subclade, which appears to spread efficiently via sexual contact and within some household settings. Spread of clade Ib has occurred beyond South Kivu into neighboring and nonneighboring provinces of DRC, including the capital city Kinshasa, as well as internationally to multiple surrounding countries; >30 travel-associated cases have been reported outside of Africa. Because of privacy concerns, the country (or countries) to which patients had traveled was not released for most of those cases. However, only ≈17% had traveled to DRC; the remaining patients (≈80%) for which the US Centers for Disease Control and Prevention had received travel information had traveled to other countries in Africa that had sustained clade Ib outbreaks or to the United Arab Emirates (UAE). Eight mpox cases caused by clade Ib from 5 different countries (China, India, Oman, Pakistan, and Thailand) have been reported in persons who traveled to UAE. Sequences from 6 cases linked to UAE travel form a monophyletic cluster (Figure 2, panel B),

suggesting a common ancestor. Considering the common travel history, the simplest explanation for clustering of those cases is exposure of the travelers to MPXV in UAE. Data suggest the presence of a similar strain of MPXV in Uganda and UAE around September/October 2024. Infections with the same strain in travelers to UAE during January–March 2025 warrant investigation into the possibility of sustained person-to-person transmission in UAE. Travelers should be aware of the exposure risks for clade Ib mpox in countries with ongoing clade I transmission (*37*).

Mpox Diagnostics and Treatment

The genomic deletion characteristic of recent clade Ib sequences prevents detection by commonly used PCR developed for clade I (*38*). When performing clade-specific PCR that targets nonessential genes, laboratories should also use PCR targeting other genomic regions, including essential genes, such as the DNA polymerase gene (target of the Centers for Disease Control and Prevention nonvariola orthopoxvirus test) (*39*,*40*), to ensure mpox cases caused by clade Ib are not missed. In the United States, the recommended approach is to first (or concurrently) test by using a nonvariola orthopoxvirus or generic MPXV PCR targeting a conserved region. Then, after orthopoxvirus or MPXV is confirmed, additional clade-specific PCR or sequencing can be used (if needed) to determine the clade.

Irrespective of the differences in clades, the current smallpox and mpox vaccines are expected to be effective in controlling the spread and severity of disease because orthopoxviruses (e.g., MPXV [clades Ia, Ib, IIa, and IIb], vaccinia virus, variola virus) are >90% genetically related. Genetic relatedness was the premise and success behind smallpox eradication, which used vaccinia virus vaccine to cross-protect against smallpox. Live, replicating smallpox vaccines (e.g., ACAM2000; Emergent Bioservices, https://emergentbio.com) are contraindicated for immunocompromised persons and those with certain skin conditions. Hence, nonreplicating modified vaccinia Ankara vaccines, MVA-BN (Bavarian Nordic, https://www.bavarian-nordic.com) and JYNNEOS (https://jynneos.com), have been widely used in the United States and have been approved for use in adults ≥18 years of age. More than 1.2 million vaccine doses have been administered in the United States, and only very few vaccine breakthrough cases have been reported for most vaccinated persons after >2 years since completion of both doses (*41*). Those breakthrough case-patients also tended to exhibit milder disease course with no hospitalizations compared with unvaccinated patients (*42*). Multiple studies evaluating vaccine effectiveness for MVA-BN demonstrated >66%–86% protection against mpox (clade IIb); 2-dose vaccinations provided higher levels of protection than a single dose (*43*–*45*). To control clade I–associated mpox, several countries (DRC, Rwanda, Central African Republic, and Uganda) experiencing that outbreak have extended temporary or emergency use authorization of MVA-BN in adults, and vaccination of high-risk populations is ongoing. The European Medicines Agency approved MVA-BN for adolescents 12–17 years of age in late 2024, and the World Health Organization recently prequalified the vaccine for that same age group. In addition to MVA-BN, another smallpox vaccine, LC-16 (attenuated strain of vaccinia virus strain Lister; KM Biologics, https://www.kmbiologics.com), received emergency authorization in DRC. Unlike MVA-BN, LC-16 is a minimally replicating vaccine requiring 1 dose and approved for use in persons >1 year of age.

For many mpox patients in the United States, the smallpox antiviral drug tecovirimat (inhibits extracellular virus formation) has been administered as the primary therapeutic intervention through an expanded access investigational new drug protocol. For severe mpox cases or those patients at risk for severe disease (e.g., immunocompromised persons), combination therapy with tecovirimat and other antiviral drugs approved for smallpox treatment, such as cidofovir, brincidofovir (inhibits DNA replication), and vaccinia immune globulin, has been sometimes recommended on the basis of clinical needs of the patient (*46*). Prolonged treatment with tecovirimat has led to the development of resistant viruses; limited spread of resistant viruses among persons with no previous treatment has been observed, indicating the importance of containment and surveillance to detect those viruses (*47*,*48*). A randomized controlled study to determine the effectiveness of tecovirimat against clade I mpox in DRC reported no improvement in mpox resolution (*30*,*49*). A study on tecovirimat efficacy against clade IIb MPXV infections in the United States reported similar results (*50*). Additional studies assessing alternative drugs, earlier treatment with tecovirimat (i.e., before lesion onset), tecovirimat efficacy in immunocompromised persons, and combination treatment with other interventions are still needed. Because of the spread of mpox to many countries that historically did not see cases, including ongoing cases of clade IIb–associated mpox 2 years after the start of the outbreak, effective therapeutic agents for mpox are urgently needed.

Conclusion

Mpox is an old disease but is now reemerging and causing international concern because of decreasing population immunity and sustained human-to-human transmission mediated through global travel, increased animal–human interfaces, and expansive sexual networks, leading to spread from small geographic regions and establishment of the disease in various parts of the world. Renewed global attention to mpox has occurred yet again because of the surge in reported mpox cases caused by clade I MPXV in DRC and the spread of the newly recognized clade Ib virus. Although clade Ib is in the spotlight, the remote forested regions of DRC where zoonotic clade Ia MPXV continues to circulate should not be forgotten. Broad worldwide assistance is necessary to halt the spread of both clade Ia and Ib within Africa to prevent future outbreaks.

Acknowledgments

We thank all of the past and present members of the US Centers for Disease Control and Prevention clade I mpox response team, particularly Satish Pillai and Ermias Belay for their response leadership; the US Centers for Disease Control and Prevention Poxvirus and Rabies Branch (Division of High-Consequence Pathogens and Pathology, National Center for Emerging and Zoonotic Infectious Diseases); and domestic and internal partners for their dedicated work in this ongoing outbreak, including Namanya Dianah, Kaleebu Pontiano, and Lutwama Julius from Uganda Virus Research Institute; and the countries that have had clade Ib imported cases and have shared the travel, clinical, and epidemiologic information for those cases to inform our understanding of this newly recognized subclade. We gratefully acknowledge all data contributors, including the authors and their originating laboratories responsible for obtaining the specimens and the submitting laboratories for generating the genetic sequence and metadata and sharing via the GISAID Initiative or GenBank databases, on which this research is based (Appendix, https://wwwnc.cdc.gov/EID/article/31/8/24-1551-App1.xlsx).

All genome sequences and associated metadata in this dataset are published in GISAID's EpiPox database (https://www.gisaid.org; accession no. EPI_SET_250505zb). EPI_SET_250505zb is composed of 1,788 individual genome sequences collected in 27 countries and territories; collection dates range from 1996 to April 1, 2025. List of contributors of each individual sequence with details such as accession numbers, virus name, collection date, originating and submitting laboratories, and the list of authors is provided (https://doi.org/10.55876/gis8.250505zb).

About the Author

Dr. Satheshkumar is the team lead for the Immunodiagnostics and Proteomics Team, Poxvirus and Rabies Branch, National Center for Emerging and Zoonotic Infectious Diseases, Centers for Disease Control and Prevention, Atlanta, Georgia, USA. His research interests focus on diagnostics, assay development, and immunological studies of pox and rabies viruses.

References

1. World Health Organization. WHO Director-General's statement at the press conference following IHR Emergency Committee regarding the multi-country outbreak of monkeypox—23 July 2022. 2022 [cited 2025 May 9]. https://www.who.int/director-general/speeches/detail/who-director-general-s-statement-on-the-press-conference-following-IHR-emergency-committee-regarding-the-multi--country-outbreak-of-monkeypox--23-july-2022
2. World Health Organization. WHO Director-General declares mpox outbreak a public health emergency of international concern. 2024 [cited 2025 May 9]. https://www.who.int/news/item/14-08-2024-who-director-general-declares-mpox-outbreak-a-public-health-emergency-of-international-concern
3. Beer EM, Rao VB. A systematic review of the epidemiology of human monkeypox outbreaks and implications for outbreak strategy. PLoS Negl Trop Dis. 2019;13:e0007791. https://doi.org/10.1371/journal.pntd.0007791
4. Centers for Disease Control and Prevention. 2022–2023 Mpox outbreak global map [cited 2025 May 9]. https://archive.cdc.gov/#/details?url=https://www.cdc.gov/poxvirus/mpox/response/2022/world-map.html
5. Reynolds MG, Wauquier N, Li Y, Satheshkumar PS, Kanneh LD, Monroe B, et al. Human monkeypox in Sierra Leone after 44-year absence of reported cases. Emerg Infect Dis. 2019;25:1023–5. https://doi.org/10.3201/eid2505.180832
6. Durski KN, McCollum AM, Nakazawa Y, Petersen BW, Reynolds MG, Briand S, et al. Emergence of monkeypox—West and Central Africa, 1970–2017. MMWR Morb Mortal Wkly Rep. 2018;67:306–10. https://doi.org/10.15585/mmwr.mm6710a5
7. Likos AM, Sammons SA, Olson VA, Frace AM, Li Y, Olsen-Rasmussen M, et al. A tale of two clades: monkeypox viruses. J Gen Virol. 2005;86:2661–72. https://doi.org/10.1099/vir.0.81215-0
8. Curaudeau M, Besombes C, Nakouné E, Fontanet A, Gessain A, Hassanin A. Identifying the most probable mammal reservoir hosts for monkeypox virus based on ecological niche comparisons. Viruses. 2023;15:727. https://doi.org/10.3390/v15030727
9. Nakazawa Y, Mauldin MR, Emerson GL, Reynolds MG, Lash RR, Gao J, et al. A phylogeographic investigation of African monkeypox. Viruses. 2015;7:2168–84. https://doi.org/10.3390/v7042168
10. Yinka-Ogunleye A, Aruna O, Dalhat M, Ogoina D, McCollum A, Disu Y, et al.; CDC Monkeypox Outbreak Team. Outbreak of human monkeypox in Nigeria in 2017–18: a clinical and epidemiological report. Lancet Infect Dis. 2019;19:872–9. https://doi.org/10.1016/S1473-3099(19)30294-4
11. World Health Organization. 2022–24 Mpox (monkeypox) outbreak: global mpox trends. 2024 [cited 2025 May 9].

https://worldhealthorg.shinyapps.io/mpx_global/#21_Epidemic_curves
12. Gigante CM, Korber B, Seabolt MH, Wilkins K, Davidson W, Rao AK, et al. Multiple lineages of monkeypox virus detected in the United States, 2021–2022. Science. 2022;378:560–5. https://doi.org/10.1126/science.add4153
13. O'Toole Á, Neher RA, Ndodo N, Borges V, Gannon B, Gomes JP, et al. APOBEC3 deaminase editing in mpox virus as evidence for sustained human transmission since at least 2016. Science. 2023;382:595–600. https://doi.org/10.1126/science.adg8116
14. Isidro J, Borges V, Pinto M, Sobral D, Santos JD, Nunes A, et al. Phylogenomic characterization and signs of microevolution in the 2022 multi-country outbreak of monkeypox virus. Nat Med. 2022;28:1569–72. https://doi.org/10.1038/s41591-022-01907-y
15. Suspène R, Raymond KA, Boutin L, Guillier S, Lemoine F, Ferraris O, et al. APOBEC3F is a mutational driver of the human monkeypox virus identified in the 2022 outbreak. J Infect Dis. 2023;228:1421–9. https://doi.org/10.1093/infdis/jiad165
16. Americo JL, Earl PL, Moss B. Virulence differences of mpox (monkeypox) virus clades I, IIa, and IIb.1 in a small animal model. Proc Natl Acad Sci USA. 2023;120:e2220415120. https://doi.org/10.1073/pnas.2220415120
17. World Health Organization. Regional Office for Africa. Mpox in the WHO African Region. Weekly regional situation report #17. 2024 Dec 15 [cited 2025 May 9]. https://iris.who.int/handle/10665/379903/AFRO-Mpox%20bulletin-%2015%20December%202024.pdf
18. European Centre for Disease Prevention and Control. Outbreak of mpox caused by monkeypox virus clade I in the Democratic Republic of the Congo. 2024 [cited 2025 May 9]. https://www.ecdc.europa.eu/en/news-events/outbreak-mpox-caused-monkeypox-virus-clade-i-democratic-republic-congo
19. Vakaniaki EH, Kacita C, Kinganda-Lusamaki E, O'Toole Á, Wawina-Bokalanga T, Mukadi-Bamuleka D, et al. Sustained human outbreak of a new MPXV clade I lineage in eastern Democratic Republic of the Congo. Nat Med. 2024;30:2791–5. https://doi.org/10.1038/s41591-024-03130-3
20. Masirika LM, Udahemuka JC, Schuele L, Ndishimye P, Otani S, Mbiribindi JB, et al. Ongoing mpox outbreak in Kamituga, South Kivu province, associated with monkeypox virus of a novel clade I sub-lineage, Democratic Republic of the Congo, 2024. Euro Surveill. 2024;29:2400106. https://doi.org/10.2807/1560-7917.ES.2024.29.11.2400106
21. McCollum AM, Nakazawa Y, Ndongala GM, Pukuta E, Karhemere S, Lushima RS, et al. Human monkeypox in the Kivus, a conflict region of the Democratic Republic of the Congo. Am J Trop Med Hyg. 2015;93:718–21. https://doi.org/10.4269/ajtmh.15-0095
22. Masirika LM, Udahemuka JC, Schuele L, Nieuwenhuijse DF, Ndishimye P, Boter M, et al. Epidemiological and genomic evolution of the ongoing outbreak of clade Ib mpox virus in the eastern Democratic Republic of the Congo. Nat Med. 2025;31:1459–63. PubMed https://doi.org/10.1038/s41591-025-03582-1
23. Wawina-Bokalanga T, Akil-Bandali P, Kinganda-Lusamaki E, Lokilo E, Jansen D, Amuri-Aziza A, et al. Co-circulation of monkeypox virus subclades Ia and Ib in Kinshasa Province, Democratic Republic of the Congo, July to August 2024. Euro Surveill. 2024;29:2400592. https://doi.org/10.2807/1560-7917.ES.2024.29.38.2400592
24. Reed KD, Melski JW, Graham MB, Regnery RL, Sotir MJ, Wegner MV, et al. The detection of monkeypox in humans in the western hemisphere. N Engl J Med. 2004;350:342–50. https://doi.org/10.1056/NEJMoa032299
25. Moss B. Understanding the biology of monkeypox virus to prevent future outbreaks. Nat Microbiol. 2024;9:1408–16. https://doi.org/10.1038/s41564-024-01690-1
26. Bunge EM, Hoet B, Chen L, Lienert F, Weidenthaler H, Baer LR, et al. The changing epidemiology of human monkeypox—a potential threat? A systematic review. PLoS Negl Trop Dis. 2022;16:e0010141. https://doi.org/10.1371/journal.pntd.0010141
27. Government of the Democratic Republic of the Congo. Report on the epidemiological situation of monkeypox (Mpox) in the DRC—sitrep No 025 (29 August 2024) [cited 2025 May 9]. https://reliefweb.int/report/democratic-republic-congo/rapport-de-la-situation-epidemiologique-de-la-variole-simienne-mpox-en-rdc-sitrep-no-025-29-aout-2024
28. Pittman PR, Martin JW, Kingebeni PM, Tamfum JM, Mwema G, Wan Q, et al.; Kole Human Mpox Infection Study Group. Clinical characterization and placental pathology of mpox infection in hospitalized patients in the Democratic Republic of the Congo. PLoS Negl Trop Dis. 2023;17:e0010384. https://doi.org/10.1371/journal.pntd.0010384
29. National Institutes of Health. The antiviral tecovirimat is safe but did not improve clade I mpox resolution in Democratic Republic of the Congo. 2024 [cited 2025 May 9]. https://www.nih.gov/news-events/news-releases/antiviral-tecovirimat-safe-did-not-improve-clade-i-mpox-resolution-democratic-republic-congo
30. Brosius I, Vakaniaki EH, Mukari G, Munganga P, Tshomba JC, De Vos E, et al. Epidemiological and clinical features of mpox during the clade Ib outbreak in South Kivu, Democratic Republic of the Congo: a prospective cohort study. Lancet. 2025;405:547–59. https://doi.org/10.1016/S0140-6736(25)00047-9
31. World Health Organization. Global mpox trends. 2025 [cited 2025 May 9]. https://worldhealthorg.shinyapps.io/mpx_global/#severity
32. Nizigiyimana A, Ndikumwenayo F, Houben S, Manirakiza M, van Lettow M, Liesenborghs L, et al. Epidemiological analysis of confirmed mpox cases, Burundi, 3 July to 9 September 2024. Euro Surveill. 2024;29:2400647. https://doi.org/10.2807/1560-7917.ES.2024.29.42.2400647
33. Nzoyikorera N, Nduwimana C, Schuele L, Nieuwenhuijse DF, Koopmans M, Otani S, et al. Monkeypox clade Ib virus introduction into Burundi: first findings, July to mid-August 2024. Euro Surveill. 2024;29:2400666. https://doi.org/10.2807/1560-7917.ES.2024.29.42.2400666
34. Hudson PN, Self J, Weiss S, Braden Z, Xiao Y, Girgis NM, et al. Elucidating the role of the complement control protein in monkeypox pathogenicity. PLoS One. 2012;7:e35086. https://doi.org/10.1371/journal.pone.0035086
35. Earl PL, Americo JL, Reynolds S, Xiao W, Cotter C, Moss B. A functional approach to analyze the genetic basis for differences in virulence of monkeypox virus clades. Emerg Microbes Infect. 2025;14:2456144. https://doi.org/10.1080/22221751.2025.2456144
36. Estep RD, Messaoudi I, O'Connor MA, Li H, Sprague J, Barron A, et al. Deletion of the monkeypox virus inhibitor of complement enzymes locus impacts the adaptive immune response to monkeypox virus in a nonhuman primate model of infection. J Virol. 2011;85:9527–42. https://doi.org/10.1128/JVI.00199-11
37. Centers for Disease Control and Prevention. Prevention strategies for mpox, including vaccinating people at risk via sexual exposure, for U.S. travelers visiting countries with

clade I mpox outbreaks. 2024 [cited 2025 May 9]. https://www.cdc.gov/han/2024/han00516.html
38. Li Y, Zhao H, Wilkins K, Hughes C, Damon IK. Real-time PCR assays for the specific detection of monkeypox virus West African and Congo Basin strain DNA. J Virol Methods. 2010;169:223–7. https://doi.org/10.1016/j.jviromet.2010.07.012
39. Centers for Disease Control and Prevention. Non-variola orthopoxvirus generic real-time PCR test. 2022 [cited 2025 May 9]. https://www.cdc.gov/mpox/media/pdfs/2024/08/Non-variola-Orthopoxvirus-Generic-Real-Time-PCR-Test.pdf
40. Li Y, Olson VA, Laue T, Laker MT, Damon IK. Detection of monkeypox virus with real-time PCR assays. J Clin Virol. 2006;36:194–203. https://doi.org/10.1016/j.jcv.2006.03.012
41. Centers for Disease Control and Prevention. Mpox vaccine administration in the U.S. 2024 [cited 2025 May 9]. https://archive.cdc.gov/#/details?url=https://www.cdc.gov/poxvirus/mpox/response/2022/vaccines_data.html
42. Guagliardo SAJ, Kracalik I, Carter RJ, Braden C, Free R, Hamal M, et al. Monkeypox virus infections after 2 preexposure doses of JYNNEOS vaccine—United States, May 2022–May 2024. MMWR Morb Mortal Wkly Rep. 2024;73:460–6. https://doi.org/10.15585/mmwr.mm7320a3
43. Dalton AF, Diallo AO, Chard AN, Moulia DL, Deputy NP, Fothergill A, et al.; CDC Multijurisdictional Mpox Case Control Study Group. Estimated effectiveness of JYNNEOS vaccine in preventing mpox: a multijurisdictional case-control study—United States, August 19, 2022–March 31, 2023. MMWR Morb Mortal Wkly Rep. 2023;72:553–8. https://doi.org/10.15585/mmwr.mm7220a3
44. Deputy NP, Gerhart JL, Feldstein LR. Vaccine effectiveness against mpox in the United States. Reply. N Engl J Med. 2023;389:1440–1. https://doi.org/10.1056/NEJMc2309583
45. Wolff Sagy Y, Zucker R, Hammerman A, Markovits H, Arieh NG, Abu Ahmad W, et al. Real-world effectiveness of a single dose of mpox vaccine in males. Nat Med. 2023;29:748–52. https://doi.org/10.1038/s41591-023-02229-3
46. Rao AK, Schrodt CA, Minhaj FS, Waltenburg MA, Cash-Goldwasser S, Yu Y, et al. Interim clinical treatment considerations for severe manifestations of mpox—United States, February 2023. MMWR Morb Mortal Wkly Rep. 2023;72:232–43. https://doi.org/10.15585/mmwr.mm7209a4
47. Garrigues JM, Hemarajata P, Espinosa A, Hacker JK, Wynn NT, Smith TG, et al. Community spread of a human monkeypox virus variant with a tecovirimat resistance-associated mutation. Antimicrob Agents Chemother. 2023;67:e0097223. https://doi.org/10.1128/aac.00972-23
48. Smith TG, Gigante CM, Wynn NT, Matheny A, Davidson W, Yang Y, et al. Tecovirimat resistance in mpox patients, United States, 2022–2023. Emerg Infect Dis. 2023;29:2426–32. https://doi.org/10.3201/eid2912.231146
49. Ali R, Alonga J, Biampata JL, Kombozi Basika M, Maljkovic Berry I, Bisento N, et al.; PALM007 Writing Group. Tecovirimat for clade I MPXV infection in the Democratic Republic of Congo. N Engl J Med. 2025;392:1484–96. https://doi.org/10.1056/NEJMoa2412439
50. National Institutes of Health. NIH study finds tecovirimat was safe but did not improve mpox resolution or pain. 2024 [cited 2025 May 9]. https://www.nih.gov/news-events/news-releases/nih-study-finds-tecovirimat-was-safe-did-not-improve-mpox-resolution-or-pain

Address for correspondence: Panayampalli S. Satheshkumar, Centers for Disease Control and Prevention, 1600 Clifton Rd NE, Mailstop H23-4, Atlanta, GA 30329-4018, USA; email: xdv3@cdc.gov

Mpox and Monkeypox Virus [em′poks] and [muhng′kee poks′ vī-ruhs′]

Clyde Partin

Mpox, the infectious disease caused by monkeypox virus (MPXV), is characterized in humans by fever, lymphadenopathy, and a painful mucocutaneous rash. During 1958–1959, Danish virologist Preben von Magnus isolated the virus in macaque monkeys—hence, the name monkeypox. However, small mammals are likely the MPXV reservoir, not the aberrantly infected monkeys that received unwarranted blame as the host and created the misnomer monkeypox.

The derivation of the word monkey is shrouded in debate, antiquity, and complexity. The Oxford English Dictionary postulates Moneke referred to the son of Martin the Ape, a character in a collection of beloved European fables, Reynard the Fox, and the moniker might have accompanied continental showmen to England in the 1400s, but earlier variations of Moneke exist in other languages.

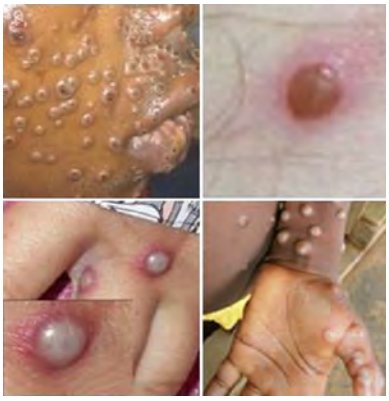

Figure 1. Examples of pustular eruptions from monkeypox virus. Image source: Centers for Disease Control and Prevention (https://www.cdc.gov/mpox/hcp/clinical-signs).

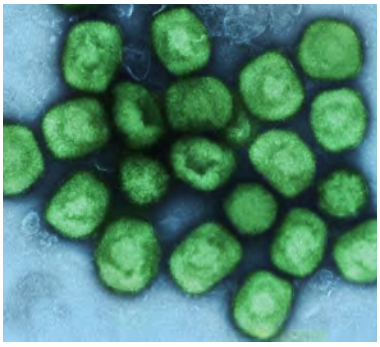

Figure 2. Colorized transmission electron microscopic image of monkeypox virus particles (green) that were cultivated and purified from cell culture. The image was captured at the National Institute of Allergy and Infectious Diseases Integrated Research Facility, Fort Detrick, Maryland, USA.

Pox, plural of pock, is Norman-French in origin from poque, meaning pouch. The diminutive form was poquet, or little pocket, describing the small scars remaining in the wake of various viral pustular eruptions, classically smallpox or syphilis. Plague and pox appear interchangeably in Shakespeare's 1597 play Romeo and Juliet, in which Mercutio utters the famous and pejorative phrase, "A pox on both your houses."

The first known human case of MPXV infection was reported in the Democratic Republic of the Congo in 1970. A global outbreak in 2022 was the first that involved widespread human-to-human MPXV transmission outside of Africa, prompting the World Health Organization to declare a Public Health Emergency. In November 2022, citing concerns of "racist and stigmatizing language" provoked by the original disease name, the World Health Organization renamed MPXV infection as mpox, but the virus name remains unchanged.

Sources

1. AP News. WHO renames monkeypox as mpox, citing racism concerns [cited 2024 Feb 4]. https://apnews.com/article/who-renames-monkeypox-to-mpox
2. BookBrowse. Well-known expressions: a plague on both your houses [cited 2024 Feb 4]. https://www.bookbrowse.com/expressions/detail/index.cfm/expression_number/666/a-plague-on-both-your-houses
3. Cho CT, Wenner HA. Monkeypox virus. Bacteriol Rev. 1973;37:1–18. https://doi.org/10.1128/br.37.1.1-18.1973
4. Haubrich WS. Medical meanings: a glossary of word options, 2nd edition. Philadelphia: American College of Physicians; 2003. p. 189.
5. OUPblog. Wrenching an etymology out of a monkey [cited 2024 Feb 4]. https://blog.oup.com/2013/01/monkey-word-origin-etymology
6. Rondle C. The natural history of smallpox. New Sci. 1978;20:680–2.
7. Weiner ESC, Simpson JA. Compact edition of the Oxford English Dictionary. Oxford: Oxford University Press; 1971. p. 1838.
8. World Health Organization. Mpox [cited 2024 Feb 4]. https://www.who.int/news-room/fact-sheets/detail/monkeypox
9. World Health Organization. WHO recommends new name for monkeypox disease [cited 2024 Feb 4] https://www.who.int/news/item/28-11-2022-who-recommends-new-name-for-monkeypox-disease

Author affiliation: Emory University, Atlanta, Georgia, USA

Address for correspondence: Clyde Partin, Emory University, 1365 Clifton Rd NE, Atlanta GA 30322-1007, USA; email: wpart01@emory.edu

DOI: https://doi.org/10.3201/eid3108.240211

Surveillance of Viral Respiratory Infections within Maximum-Security Prison, Australia

Nicolas M. Legrand, Rowena A. Bull, Behzad Hajarizadeh, Andrew R. Lloyd, Kirsty Johnston, Katya Issa, Christine Harvey, Alicia Arnott, Dominic E. Dwyer, Vitali Sintchenko, Luke Grant, Gregory J. Dore, John Kaldor, Marianne Martinello

Limited surveillance data have hindered understanding of SARS-CoV-2 transmission within prisons. We integrated routine surveillance data with viral sequencing to investigate transmission dynamics and associated factors during a Delta variant outbreak in a maximum-security prison in Sydney, New South Wales, Australia. Infection incidence and associated factors were determined by using person-time and Cox regression. We generated transmission chains by integrating epidemiologic and viral sequencing data. Of 1,562 patients, SARS-CoV-2 infection was diagnosed in 169 (11%), predominantly acquired in prison and asymptomatic. Prisonwide testing identified substantial unrecognized transmission, and 4 subvariants indicated multiple viral introductions. Infection was associated with housing location, having a cellmate (regardless of infection status), and vaccination status. Our findings underscore the inadequacy of symptom-based testing and the efficacy of entry-quarantine, strategic housing, extensive testing, and vaccination in reducing transmission. This integrated approach to surveillance and genomic sequencing offers a valuable model for enhancing infectious disease surveillance in correctional settings.

As the global health community transitions from a pandemic response to managing COVID-19 as an endemic disease, environments such as prisons and other congregate settings continue to demonstrate unique public health challenges. Implementing minimally restrictive preventive measures, such as physical distancing, is difficult because of inherent structural and organizational barriers, including close confinement, poor ventilation, and limited capacity for medical isolation (*1*,*2*). In addition, the continual cycle of custodial transfers, reception, and releases increases the likelihood of infection introduction and the potential for outbreaks of acute respiratory infection, including COVID-19, among incarcerated persons (*3*–*6*).

Substantial knowledge gaps remain regarding factors associated with transmission during acute respiratory infection outbreaks in prisons. Previous studies of COVID-19 outbreaks in prisons were limited by low SARS-CoV-2 testing coverage (*7*–*9*), inconsistent testing schedules (*10*–*12*), and minimal genomic data (*13*–*15*). In addition, the cycle of admissions and departures complicates data completeness, leading to uncertainty around the at-risk population size. Previous research often relied on approximating at-risk population size (*7*,*16*,*17*), which overlooks true variability over time, introduces potential bias because of residual confounding, and affects the quality of time-series analyses. Understanding transmission dynamics in prison is crucial for enhancing effective outbreak response strategies and enabling timely interventions to mitigate risk. Because of the higher prevalence of chronic diseases among incarcerated persons (*18*,*19*), improving systematic approaches to reducing acute respiratory infection (including SARS-CoV-2) outbreaks within prisons and other congregate settings remains a public health concern.

After several months of no local SARS-CoV-2 transmission in Australia, the first case of the Delta variant was confirmed on June 16, 2021, by whole-genome sequencing (WGS) in Sydney, New South

Author affiliations: University of New South Wales, Sydney, New South Wales, Australia (N.M. Legrand, R.A. Bull, B. Hajarizadeh, A.R. Lloyd, G.J. Dore, J. Kaldor, M. Martinello); St Vincent's Correctional Health, Sydney (K. Johnston, K. Issa); New South Wales Ministry of Health, Sydney (C. Harvey); New South Wales Health Pathology, Sydney (A. Arnott, D.E. Dwyer, V. Sintchenko); University of Sydney, Sydney (D.E. Dwyer, V. Sintchenko); Corrective Services New South Wales, Sydney (L. Grant).

DOI: https://doi.org/10.3201/eid3108.240571

Wales. Public health restrictions on movement were enacted on June 26, 2021, because of the evidence of increasing community infection. During this period of increasing community spread, an outbreak of the SARS-CoV-2 Delta variant occurred within a prison in Australia, spanning 48 days. The outbreak began 6 months after COVID vaccines were available in Australia (February 22, 2021) and precipitated a multijurisdictional public health response, building upon substantive existing control measures including quarantine on entry, isolation of recognized cases, and personal protective equipment for staff (Appendix Figure 1, https://wwwnc.cdc.gov/EID/article/31/8/24-0571-App1.pdf). The response to the outbreak included a total prison lockdown on day 13, continuous mass surveillance testing, genomic sequencing of SARS-CoV-2 with WGS, and ongoing vaccination. Our study objectives were to determine the incidence of SARS-CoV-2 infection and identify factors associated with transmission among incarcerated persons during a large-scale outbreak.

Methods

Study Design and Setting

This prospective cohort study, conducted in a prison in Sydney, followed the strengthening of reporting of observational studies in epidemiology reporting guidelines for observational cohort studies. The prison had a maximum operational capacity of 1,300 beds, housing men who were sentenced or on remand. The prison was divided into 6 housing units (blocks A–F) and a clinic (Figure 1). Operational housing capacity across blocks ranged from 118 to 500 persons, with 30 beds in the clinic (Figure 1). Housing arrangements were either single or 2-bed occupancy. The study period was 48 days, commencing with the identification of the first COVID-19 case and ending on the date of the last laboratory-confirmed case.

Participants and Data Sources

We included all persons housed in the prison during the study period (Appendix Figure 2). We used routinely collected person-day–level data gathered by local

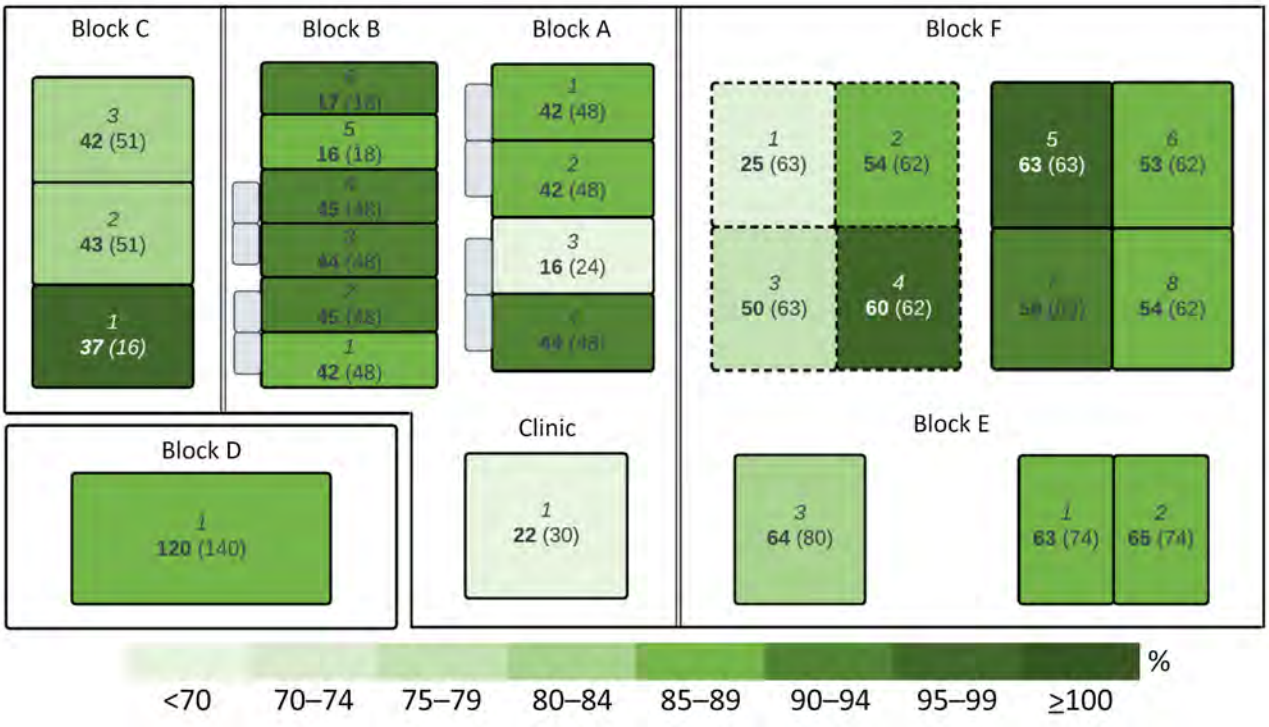

Figure 1. Stylized map of prison depicting housing capacity by wing on day of prison lockdown for SARS-CoV-2 outbreak in a maximum-security prison in Australia, 2021. Blocks A–E are general housing for incarcerated persons not in quarantine or isolation. Block F contained both general housing wings (wings 5–8) and 4 dedicated quarantine wings (wings 1–4) for persons undergoing a mandatory 14-day quarantine period before entry. Block D, the minimum-security wing, was located outside the main prison. Each wing is indicated in italics, the number of incarcerated persons is indicated in bold, and the reported maximum operational capacity is in brackets. The categorical color gradient of each unit indicates percentage of housing capacity. Quarantine zones in block F (1–4) are indicated by dashed outlines. Double lines represent internal walls. Gray shaded areas in blocks A and B represent external yard space, separated by chain-wire fencing. External yards are found in all areas but not displayed in each instance because they are contained within wings and are not considered a potential site of interwing transmission.

health authorities and corrective services (sociodemographic characteristics, prison entry and exit, SARS-CoV-2 nucleic acid testing [NAT], vaccination administration, housing location), and SARS-CoV-2 WGS data for analysis. We conducted NAT by using EasyScreen SARS-CoV-2 RT-PCR (Genetic Signatures, https://geneticsignatures.com) or the GeneXpert SARS-CoV-2 assay (Cepheid, https://www.cepheid.com). We conducted prisonwide surveillance SARS-CoV-2 testing, regardless of symptom or contact status, by living unit on a continuous 72-hour basis. All health and prison staff providing direct, in-person care of incarcerated persons were required to wear personal protective equipment appropriate for contact, droplet, and airborne precautions (P2/N95 mask, eye or face protection, gown, gloves) and to assess inmates in their cells.

Study Definitions and Outcomes

We defined the date of infection by symptom onset or positive NAT, whichever came first. We defined the infectious period of positive cases as starting 2 days before symptom onset or sample collection, whichever came first, and ending 14 days later. We assigned case definitions relative to their potential source of infection (community, prison, or unknown) and the confidence of the source of transmission (probable, possible, unknown) (Appendix). We defined clinical infection severity as asymptomatic, mild, moderate, or severe (*20*). We defined SARS-CoV-2 infection as a positive SARS-CoV-2 NAT result.

WGS

We sent samples with detectable SARS-CoV-2 RNA to the Institute of Clinical Pathology and Medical Research, New South Wales Health Pathology (Sydney), for WGS to support contact tracing and cluster analysis. We extracted viral genomes from upper respiratory tract swabs and PCR amplified by using the Illumina Midnight (Illumina, https://www.illumina.com) sequencing protocol and sequenced PCR products by using the Illumina platform. We generated a consensus sequence from each sample to conduct genomic sequence comparisons between suspected transmission clusters, as previously described (*21*).

We aligned the consensus genomes by using MAFFT v7.471 (FFT-NS-2, progressive method) (*22*). We manually inspected the consensus genomes and excluded any sequences missing >20% of the genome. We observed poor sequence read coverage across regions 21381 and 21683; therefore, we removed the region from all alignments. We constructed a phylogenetic tree visualizing sequence similarity between different samples by using the maximum-likelihood approach in IQTree v1.6.7 with the general time-reversible with unequal empirical base frequency and proportion of invariable sites substitution model and 1,000 bootstrap replicates (*23*). We defined transmission clusters genomically on the basis of shared mutational profiles and by clustering on the phylogenetic tree (Appendix Figure 3). We considered sequence pairs or clusters sharing <3 mutations genomic evidence in support of direct or recent transmission.

Statistical and Molecular Analyses

We calculated incidence by using person-time of observation and reported as the number of infections per 100 person-years. We calculated 95% CIs for rates by using a Poisson distribution. Time at-risk commenced on day 1 of the study period, or the date of prison entry for people received later, and was censored at day 48, or at the earliest occurrence of the incarcerated person testing NAT positive, being transferred out before lockdown, or being released.

We used Cox proportional hazards regression analysis to estimate hazard ratios (HRs) and 95% CIs to evaluate factors associated with SARS-CoV-2 transmission, by using person-level time-varying covariates for changes in factors related to exposure. This approach enabled evaluation of hazards on the basis of each person's status daily, capturing the transition in infection risk status. Those factors were determined a priori and included housing location, vaccination status, and cellmate exposure in the preceding 14 days. We determined the frequency of cellmate exposures over the course of the outbreak by using a moving 14-day window.

We mapped within-prison movement of case-patients and cellmates and generated chains of transmission including direction to the individual level (Appendix). Genomic sequencing was available for 128 (76%) cases, and we used the sequencing data to validate the hypothesized chains of transmission on the basis of epidemiologic data.

We performed statistical analyses by using Stata software version 17 (StataCorp, LLC, https://www.stata.com). We conducted the data visualization by using Microsoft Power Bi (Microsoft, https://www.microsoft.com) and Lucidchart (https://www.lucidchart.com).

Study Oversight

Because this investigation was a public health priority, it was conducted under the Public Health Act at the request of the NSW Ministry of Health and in collaboration with St Vincent's Correctional Health NSW, Justice Health and Forensic Mental Health

Network, the Institute of Clinical Pathology and Medical Research, and the Kirby Institute for Infection and Immunity in Society. This study received ethical approval from the University of NSW Human Research Ethics Committee (approval no. HC220683). A waiver of consent was granted as the research involved secondary analysis of existing deidentified data collected during routine public health activities.

Results

Demographic and Clinical Characteristics

During the 48-day study period, 1,562 persons were housed in the prison, and SARS-CoV-2 infection was diagnosed in 169 (11%) incarcerated persons (Appendix Figure 2). There was complete data capture for each person, covering SARS-CoV-2 NAT, vaccination status, and housing location. Total follow-up time was 131 person years (median follow-up 39 days [IQR 14–48 days]). With prisonwide surveillance testing, 9,575 SARS-CoV-2 NATs were conducted (249 positives, 9,326 negatives; median tests of incarcerated persons = 7 [IQR 3–11]). Of 169 persons with laboratory-confirmed COVID-19 (median age 34 years [IQR 18–78 years]), 62 (37%) were symptomatic at diagnosis, whereas in 122 (72%) patients, symptoms developed at some point during infection. Asymptomatic or mild infections accounted for 93% (n = 157) of cases (Table 1); 7 cases were moderate and 1 was severe.

COVID-19 vaccination coverage was low at the outbreak's onset, driven by high refusal rates. At the time of lockdown, 853 (70%) of incarcerated persons had not been vaccinated, 262 (21%) of incarcerated persons had received 1 vaccine dose, and 111 (9%) of incarcerated persons had received 2 doses. By the end of the study period, after the implementation of a vaccination campaign as part of the outbreak response, the percentages of persons vaccinated increased; 121 (13%) of incarcerated persons were not vaccinated, 247 (26%) of incarcerated persons received 1 vaccine dose, and 567 (61%) of incarcerated persons received 2 doses; only 14 incarcerated persons declined vaccination.

Location and Source of Acquisition

Evidence of SARS-CoV-2 transmission was found in 4 of the 6 housing blocks (A, B, E, and F), as well as in the clinic; 59% (n = 100) of cases occurred within quarantine units. Most SARS-CoV-2 infections were likely acquired in prison (91%, n = 153) and were diagnosed after 14 days of continuous incarceration (n = 144). SARS-CoV-2 was diagnosed in a smaller group (n = 9) within 14 days of prison entry; epidemiologic and genomic evidence, including exposure to a COVID-19 positive cellmate (n = 4) and genomic cluster membership (n = 5), suggested those persons also acquired the infection in prison. Among prison-acquired cases (n = 153), a probable or possible source of transmission was identified in 141 cases (92%) (probable, n = 77; possible, n = 64). Of sequenced cases (76%, n = 128), 4 Delta subvariants were identified: NSW130.0 (n = 35), NSW130.18 (n = 11), NSW130.34 (n = 65), and NSW130.74 (n = 17). The predominant circulating Delta subvariant in NSW at that time was NSW130.0.

Incidence of SARS-CoV-2 Infection and Factors Associated with Transmission in Prison

Infection incidence was 121 (95% CI 104–142)/100 person-years. SARS-CoV-2 infection was associated with housing type, vaccination status, and cellmate exposure (Table 2; Appendix Figure 4). Incidence was higher in quarantine units compared with general units (aHR 1.90 [95% CI 1.39–2.59]). Incidence was higher among unvaccinated persons, compared with those who received 2 doses (aHR 0.46 [95% CI 0.27–0.79]) of COVID-19 vaccine. Infection risk was highest for persons exposed to a SARS-CoV-2–positive cellmate in the 14 days before SARS-CoV-2 diagnosis (aHR 18.87 [95% CI 10.99–32.37]).

Time-Course of Outbreak Detection and Public Health Response

We plotted the prison transmission chains (Figure 2). SARS-CoV-2 infection was first detected in the prison by a routine entry screening test conducted on an asymptomatic person housed alone. Over the next 5 days, 2 more incarcerated persons (patients 3 and 5), also housed alone in the clinic area and within their 14-day entry quarantine period (negative SARS-CoV-2 NAT on entry), had SARS-CoV-2 diagnosed through routine NAT screening on day 11 of incarceration. Of note, there was no evidence of close contact between those patients, raising concerns about the role of cell proximity and structural drivers in transmission. Genomic sequencing and phylogenetic analysis revealed that those cases belonged to the NSW130.34 cluster, indicating a close genetic relationship and a common source of infection (Figure 2; Appendix Figure 5).

Independent of that cluster, a newly incarcerated person housed within 1 of the prison's dedicated entry quarantine wings (block F3) returned a day 4 SARS-CoV-2–positive NAT, 2 days into their mandatory 14-day entry quarantine period. Over the next 7 days, 11 additional persons housed in the entry quarantine wings (F1–F4) had SARS-CoV-2 infections

diagnosed. Patient 6, an unvaccinated, asymptomatic person whose SARS-CoV-2 infection was diagnosed by surveillance screening and was continuously incarcerated for >14 days, was housed alone in the quarantine wing F2, where they worked as a sweeper, a person whose job involves domestic tasks and has permission to move more freely within the designated area, for 6 weeks. Acquisition likely occurred while patient 6 was undertaking sweeper duties, with supportive evidence provided by WGS (Figure 2; Appendix Figure 5). The movements and interactions of patient 6 with other sweepers likely enabled transmission within F1 and the subsequent spread from quarantine wings F1–F2 to F5–F6 before the facility lockdown on day 13. Epidemiologic and genomic clustering analysis supported the probability that transmission had occurred among blocks F2, F5, and F6, with most sequences belonging to the NSW130.0 cluster (Appendix Figures 3 and 5).

By day 13, SARS-CoV-2 infection was confirmed in 28 persons. In response, the prison was placed into lockdown, confining incarcerated persons to their cells, limiting internal movements to interrupt further transmission, and a coordinated outbreak response was enacted. Key response measures included continual mass surveillance, SARS-CoV-2 testing, clinical isolation of those with SARS-CoV-2 diagnosis and their cellmates, rapid establishment of onsite healthcare provision for persons with COVID-19, contact tracing of incarcerated persons and staff, cessation of new receptions and prison transfers, and scaling up of voluntary vaccination. Healthcare workers underwent SARS-CoV-2 NAT every 3 days before facility entry, and prison staff were tested 3 times weekly. On day 26, the testing protocol transitioned from NAT to rapid antigen testing for all staff screening. Staff with positive or invalid rapid antigen testing results underwent onsite NAT.

Prisonwide SARS-CoV-2 NAT-based surveillance (regardless of symptom or contact status) was initiated the day after lockdown (day 14), and 80% of the total prison population was tested. After lockdown, a structured NAT testing schedule was implemented by living unit, testing all incarcerated persons every 72 hours. Daily 7-day-average testing coverage increased from 2% in the first week to 20% in the second week and thereafter maintained coverage of 19%–25% (Figure 3). The implementation of continual mass testing detected ongoing, previously unrecognized transmission with cases in blocks A, B, E, and F (Figure 3). The outbreak was considered resolved after 14 days had elapsed (1 maximum incubation period) with no new cases.

Discussion

An outbreak of COVID-19 occurred in a maximum-security prison in Australia, spanning 48 days, with 169 cases of SARS-CoV-2 infection diagnosed. Transmission occurred within wings dedicated to entry-quarantine and areas housing the general population. Infection severity among cases was predominantly asymptomatic or mild. The prison lockdown and mass testing schedule initiated as part of the outbreak response identified many asymptomatic and presymptomatic cases who were not detected through symptom-based testing or reported close contact. Genomic analysis identified distinct genomic clusters involving 4 Delta subvariants, indicating multiple independent viral incursions into the prison. Increased

Table 1. Demographic and clinical characteristics of incarcerated persons with SARS-CoV-2 in maximum-security prison, Australia, 2021*

Case characteristics	Value, n = 169
Age group	
18–29	65 (38)
30–39	62 (36)
40–49	26 (17)
50–59	13 (8)
≥60	3 (2)
Likely source of infection acquisition	
Prison	153 (92)
Community	16 (8)
Housing location	
General unit	69 (41)
Quarantine unit	100 (59)
Cellmate placement in 14 days before date of infection	
Housed alone	20 (12)
Housed with COVID-19 positive cellmate	47 (28)
Housed with COVID-19 negative cellmate	102 (60)
Duration of incarceration before diagnosis, d	
Median (IQR)	47 (19–100)
Range	0–804
SARS-CoV-2 vaccination status at time of diagnosis	
2 doses, >2 weeks after second dose	8 (5)
2 doses, <2 weeks after second dose	5 (3)
1 dose	45 (27)
0 doses	111 (66)
Disease severity	
Asymptomatic	43 (25)
Mild	114 (68)
Moderate	7 (4)
Severe	1 (1)
Unknown	4 (2)
Symptomatic at diagnosis	62 (37)
Symptomatic ever	122 (72)
Reason for testing	
Mass testing schedule	140 (83)
Entry screening	7 (4)
Quarantine screening	18 (11)
Symptom driven, close contact, or both	4 (2)
SARS-CoV-2 Delta subvariant	
130	35 (21)
130.18	11 (7)
130.34	65 (38)
130.74	17 (10)
Missing	41 (24)

*Values are no. (%) except as indicated. IQR, interquartile range.

Table 2. Incidence rate of and factors associated with SARS-CoV-2 infection in incarcerated persons in maximum-security prison, Australia, 2021*

Characteristics	No. infections	Follow-up time, person-years	Infection incidence/100 person-years (95% CI)†	Unadjusted hazard ratio (95% CI)	Adjusted hazard ratio (95% CI)
Overall	160†	131	121 (104–142)	0.98 (0.97–1.0)	0.99 (0.97–1.01)
Living unit					
General units	70	87	80 (63–102)	Referent	Referent
Quarantine units	90	44	202 (165–249)	2.43 (1.77–3.34)	1.90 (1.39–2.59)
Vaccination status					
Unvaccinated	102	56	183 (151–223)	Referent	Referent
First dose	45	47	95 (71–128)	0.67 (0.45–0.98)	0.84 (0.59–1.19)
Second dose	13	28	45 (26–78)	0.43 (0.24–0·77)	0.46 (0.27–0.79)
Cellmate exposure status					
No cellmate	18	35	51 (33–82)	Referent	Referent
NAT-negative cellmate	95	94	101 (83–124)	1.78 (1.07–2.95)	1.84 (1.11–3.05)
NAT-positive cellmate	47	2	1,888 (1,418–2,153)	21.74 (12.9–36.72)	18.87 (10.99–32.37)

*NAT, nucleic acid testing.
†Infection incidence analyses included 160 cases of SARS-CoV-2 infection among incarcerated persons; 9 cases were excluded because of positive test on prison entry (n = 4) or after transfer or release into the community (n = 5).

SARS-CoV-2 infection risk was associated with cellmate exposure, unvaccinated status, and housing in units dedicated to quarantine and isolation.

Global investigations of SARS-CoV-2 outbreaks in prisons have underscored the significance of systematic testing schedules and genomic sequencing (*24*,*25*). When implemented, mass testing frequently identifies widespread unrecognized infection and transmission (*26*,*27*). In this study, the most substantial peak in case detection occurred after the first round of mass surveillance testing, conducted the day after lockdown, which resulted in 80% of the prison population being tested, including many housed in blocks that were not previously subject to surveillance testing. That testing resulted in identification of unrecognized transmission outside of quarantine wings, highlighting the limitations of surveillance strategies relying on close-contact and symptom-based testing, which may prolong outbreak duration (*28*). In addition, the availability of genomic evidence identified the recurring external introduction of SARS-CoV-2. Although the origins and pathways of the repeated introductions were unclear, vulnerabilities in entry quarantine procedures were revealed, and the importance of timely and extensive testing was reinforced. Continual widespread testing offers the advantage of detecting mild or asymptomatic infection in areas where clinical suspicion is low and provides the opportunity to monitor the effect of containment strategies. Identifying those gaps provides a framework for developing more robust prevention measures for SARS-CoV-2 and other infectious respiratory pathogens within congregate settings.

Housing location was a key contributor to infection acquisition. Persons in quarantine units experienced ≈2 times the risk for infection compared with those in general units. The increased risk for SARS-CoV-2 infection in quarantine areas was attributed, in part, to the placement of undetected community acquired cases with uninfected cellmates during their mandatory 14-day entry quarantine. However, before lockdown, cellmate-to-cellmate transmission accounted for only 10% of prison-acquired cases undergoing entry quarantine, indicating that other factors were more influential in transmission within dedicated quarantine wings. Although entry quarantine measures aim to confine potential transmission to quarantine wings, inadvertent exposure might occur. Specifically, interactions with mobile persons, such as incarcerated persons with special roles who move between areas, might unintentionally introduce infections into previously unaffected areas.

Cellmate exposure was associated with increased risk for infection. Although direct person-to-person transmission through close contact, whether between persons sharing a cell or direct interaction between incarcerated persons, appeared to be the primary mode of spread before the lockdown, transmission persisted even after movement restrictions were implemented. Phylogenetic clustering was observed among persons who were continuously housed alone or with an infected person for 14 days before their date of infection, supporting a shared transmission pathway despite the absence of known close contact. That clustering suggests close contact alone was not a prerequisite for SARS-CoV-2 transmission within a high-density congregate living environment and that the transmission of SARS-CoV-2 might be assisted by the structural and environmental characteristics inherent in prisons. This finding is necessary for planning preparedness and response to outbreaks of known and emerging airborne respiratory infections in such settings, particularly development of tailored interventions to mitigate transmission risk.

Although recent evidence has demonstrated vaccination and prior infection are major factors in reducing the infectiousness of index cases within prisons settings (*29*), data are limited on the effectiveness of mass-timed vaccination during SARS-CoV-2 outbreaks (*29*,*30*). Over the study period, the ongoing vaccination campaign progressively increased first dose coverage from 17% to 90% and second dose coverage from 4% to 64%. The result was a marked reduction in infection incidence with each additional dose administered. By using a time-varying Cox model that accounted for changing vaccination status throughout the study period, we found that, compared with unvaccinated persons, infection incidence was approximately half that among those who had received 1 dose and one quarter among those who received a second dose. That trend suggests a stepwise protective effect of vaccination against infections. Mass-timed vaccination should be considered a viable strategy for managing outbreaks of SARS-CoV-2 in prisons and congregate settings where other containment strategies may not be feasible, a finding that is relevant to other vaccine-preventable respiratory diseases.

Strengths of this study include complete capture of high-resolution spatiotemporal and person-day level data of the at-risk population, coupled with SARS-CoV-2 viral genomic information. Comparatively, in previously published studies, the absence of person-day level data required incidence rates and risk factors to be determined on the basis of a surrogate of the at-risk population size, typically the prison's average population size or theoretical capacity (*3*,*4*,*7*). That limitation, combined with imprecise time-to-event data because of infrequent testing (*8*,*14*,*24*), can distort the accuracy and measurement of incidence and risk factor calculations. Although mass testing and symptom surveillance was conducted among

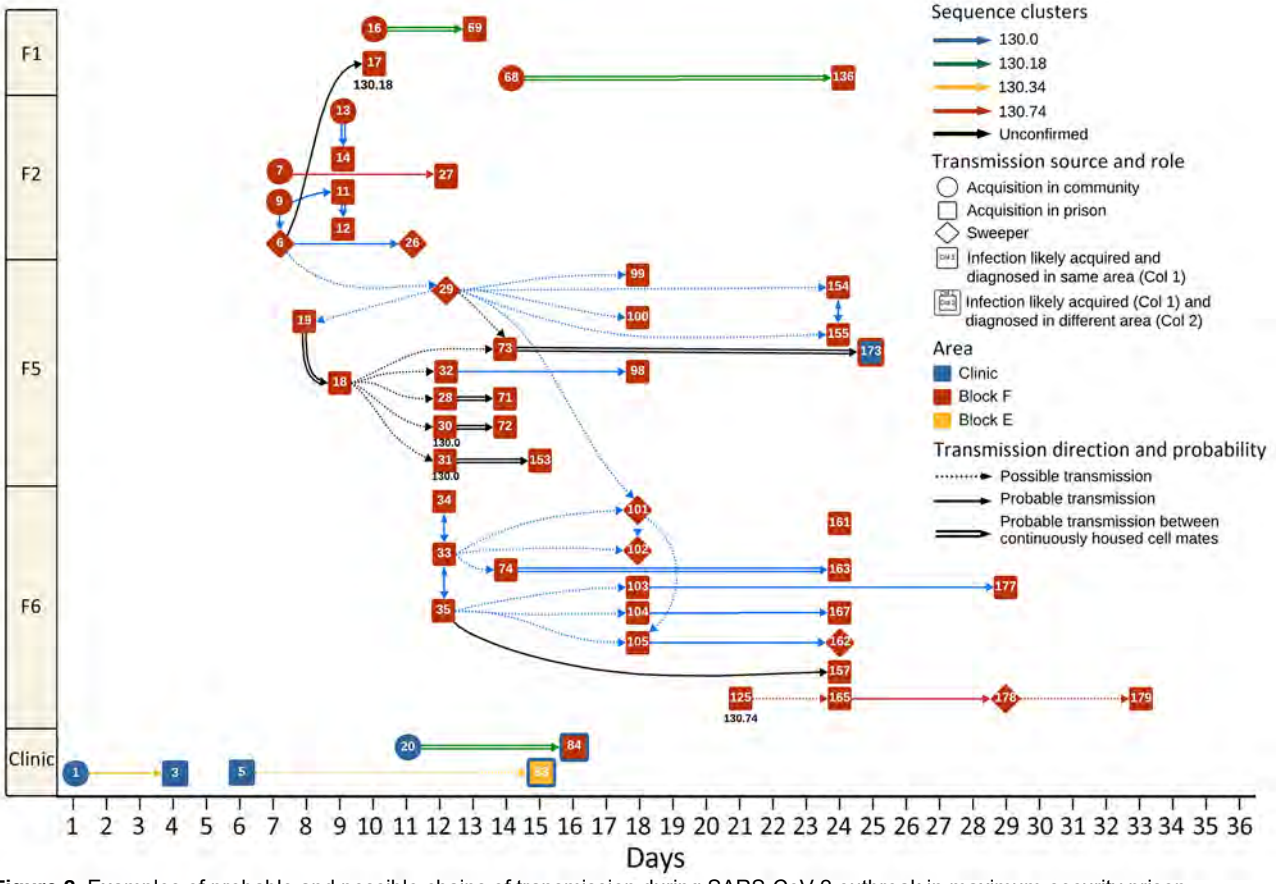

Figure 2. Examples of probable and possible chains of transmission during SARS-CoV-2 outbreak in maximum-security prison in Australia, 2021. Cases are plotted temporally on the basis of infection date and spatially according to both location of infection acquisition and location at the time of diagnosis. Diamonds denote incarcerated persons working as sweepers and circles indicate community-acquired cases. Transmission is visualized with solid lines for probable transmission, dotted lines for possible, and double solid black lines for transmission between cellmates consistently housed together before and after lockdown. Arrowheads mark the likely direction of transmission, and line colors represent genomic sequence clusters. For transmission pathways where only 1 genomic sequence was available, the sequence identification is displayed below the patient.

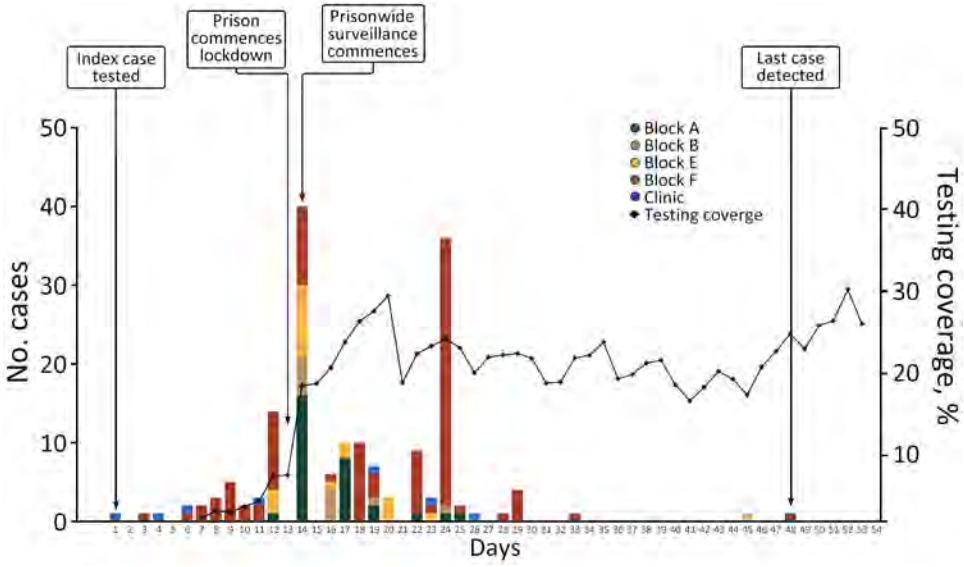

Figure 3. Timeline of SARS-CoV-2 infections during outbreak in maximum-security prison in Australia, 2021. Bars indicate numbers of cases by housing location and date of infection; line indicates 7-day moving average of testing coverage.

staff, the level of detail available regarding daily staff movements and intra-prison contacts was insufficient to determine exposure risks or integrate into detailed chain-of-transmission analyses. However, available clinical and molecular epidemiology did not support transmission from staff to inmates, highlighting the predominance of inmate-to-inmate transmission. In addition, the Delta variant is no longer the globally predominant strain of SARS-CoV-2. Of consequence, variations in transmissibility, severity, and immune escape potential between SARS-CoV-2 variants might limit the generalizability of our results in settings or time periods involving other circulating variants.

Beyond the epidemiologic findings, a critical lesson from this study was the demonstrated potential of integrating data sources to develop standardized reporting systems for infectious diseases in enclosed congregate settings. In collecting person-day-level data that encompassed demographic, clinical, geospatial, and genomic information, we gained a deep understanding of the outbreak dynamic. Those data-driven insights emphasize the need for prisons to establish enhanced surveillance systems by using routinely collected datasets from both health and corrective services. Leveraging those data can enable timely decision-making and tailored interventions. To be effective, collaboration between health and corrective services is critical to ensure epidemiologic data are not only interpreted and integrated appropriately but also adapted to the unique operational nuances and demands of the correctional setting.

Our findings provide robust data on the factors associated with transmission of SARS-CoV-2 within prison settings and the feasibility of enhancing surveillance of infectious respiratory pathogens by using routinely collected data. This approach can be applied more broadly to guide the management of future respiratory infection outbreaks with epidemic potential in enclosed settings. During the initial stages of an outbreak, a timely and coordinated response is critical in limiting further spread and interrupting chains of transmission. When implemented together, strategic housing assignments, continual mass testing with rapid NAT, genomic sequencing, and mass timed vaccination can substantially reduce the risk for SARS-CoV-2 transmission and mitigate the severity of outbreaks in high-density living environments.

Acknowledgments

We thank St Vincent's Correctional Health, Mark Tattersall, Michael Douglas, Jennie Musto, James Blogg, Colette McGrath, Shani Prosser, and Mailie Gall for their roles in the outbreak response and management. We also thank the COVID-19 Public Health Response Branch, contact tracing, operational, policy, epidemiology, surveillance, data quality, and data acquisition teams of the New South Wales Ministry of Health, as well as the pathology partner laboratories and the Institute of Medical Pathology and Research New South Wales Health Pathology for their support with case investigations, outbreak management, and for providing SARS-CoV-2 sequences.

This study was funded in part by St Vincent's Correctional Health and St Vincent's Health Network Sydney. R.A.B., A.R.L., G.J.D., J.K., and M.M. were supported by the Australian National Health and Medical Research Council.

Author contributions: data integrity and accuracy, N.M.L. and M.M.; study concept and design, N.M.L., M.M., and R.A.B.; data acquisition, analysis, and interpretation,

N.M.L., M.M., R.A.B, K.J., K.I., A.A., D.E.D., V.S., and C.H.; initial manuscript drafting, N.M.L., M.M., and R.A.B.; manuscript revision, all authors; statistical analysis, N.M.L. and M.M.; funding acquisition, N.M.L.; administrative, technical, and material support, L.G., K.I., K.J., and C.H.; and study supervision, M.M., J.K., G.J.D., and A.R.L.

About the Author

Mr. Legrand is an infectious diseases research epidemiologist at the Kirby Institute. His research interests include the use of laboratory testing data to improve national disease surveillance, testing coverage and representativeness, and infections of public health significance.

References

1. Duarte C, Cameron DB, Kwan AT, Bertozzi SM, Williams BA, McCoy SI. COVID-19 outbreak in a state prison: a case study on the implementation of key public health recommendations for containment and prevention. BMC Public Health. 2022;22:977. https://doi.org/10.1186/s12889-022-12997-1
2. Saloner B, Parish K, Ward JA, DiLaura G, Dolovich S. COVID-19 cases and deaths in federal and state prisons. JAMA. 2020;324:602–3. https://doi.org/10.1001/jama.2020.12528
3. Leibowitz AI, Siedner MJ, Tsai AC, Mohareb AM. Association between prison crowding and COVID-19 incidence rates in Massachusetts prisons, April 2020–January 2021. JAMA Intern Med. 2021;181:1315–21. https://doi.org/10.1001/jamainternmed.2021.4392
4. Marquez N, Ward JA, Parish K, Saloner B, Dolovich S. COVID-19 incidence and mortality in federal and state prisons compared with the US population, April 5, 2020, to April 3, 2021. JAMA. 2021;326:1865–7. https://doi.org/10.1001/jama.2021.17575
5. LeMasters K, Ranapurwala S, Maner M, Nowotny KM, Peterson M, Brinkley-Rubinstein L. COVID-19 community spread and consequences for prison case rates. PLoS One. 2022;17:e0266772. https://doi.org/10.1371/journal.pone.0266772
6. Parsons TL, Worden L. Assessing the risk of cascading COVID-19 outbreaks from prison-to-prison transfers. Epidemics. 2021;37:100532. https://doi.org/10.1016/j.epidem.2021.100532
7. Blair A, Parnia A, Siddiqi A. A time-series analysis of testing and COVID-19 outbreaks in Canadian federal prisons to inform prevention and surveillance efforts. Can Commun Dis Rep. 2021;47:66–76. https://doi.org/10.14745/ccdr.v47i01a10
8. Wilburn J, Blakey E, Trindall A, Burr H, Tanti V, Doolan S, et al. COVID-19 within a large UK prison with a high number of vulnerable adults, March to June 2020: an outbreak investigation and screening event. Int J Infect Dis. 2021;104:349–53. https://doi.org/10.1016/j.ijid.2021.01.027
9. Giuliani R, Cairone C, Tavoschi L, Ciaffi L, Sebastiani T, Bartolotti R, et al. COVID-19 outbreak investigation and response in a penitentiary setting: the experience of a prison in Italy, February to April 2020. Euro Surveill. 2021;26:2001385. https://doi.org/10.2807/1560-7917.ES.2021.26.38.2001385
10. Stufano A, Buonvino N, Cagnazzo F, Armenise N, Pontrelli D, Curzio G, et al. Efficacy of the measures adopted to prevent COVID-19 outbreaks in an Italian correctional facility for inmates affected by chronic diseases. Front Public Health. 2021;9:694795. https://doi.org/10.3389/fpubh.2021.694795
11. Lewis NM, Salmanson AP, Price A, Risk I, Guymon C, Wisner M, et al. Community-associated outbreak of COVID-19 in a correctional facility—Utah, September 2020–January 2021. MMWR Morb Mortal Wkly Rep. 2021;70:467–72. https://doi.org/10.15585/mmwr.mm7013a2
12. Kronfli N, Dussault C, Maheu-Giroux M, Halavrezos A, Chalifoux S, Sherman J, et al. Seroprevalence and risk factors for severe acute respiratory syndrome coronavirus 2 among incarcerated adult men in Quebec, Canada, 2021. Clin Infect Dis. 2022;75:e165–73. https://doi.org/10.1093/cid/ciac031
13. Hagan LM, McCormick DW, Lee C, Sleweon S, Nicolae L, Dixon T, et al. Outbreak of SARS-CoV-2 B.1.617.2 (Delta) variant infections among incarcerated persons in a federal prison—Texas, July–August 2021. MMWR Morb Mortal Wkly Rep. 2021;70:1349–54. https://doi.org/10.15585/mmwr.mm7038e3
14. Tan ST, Kwan AT, Rodríguez-Barraquer I, Singer BJ, Park HJ, Lewnard JA, et al. Infectiousness of SARS-CoV-2 breakthrough infections and reinfections during the Omicron wave. Nat Med. 2023;29:358–65. https://doi.org/10.1038/s41591-022-02138-x
15. Vusirikala A, Flannagan J, Czachorowski M, Zaidi A, Twohig KA, Plugge E, et al. Impact of SARS-CoV-2 Alpha variant (B.1.1.7) on prisons, England. Public Health. 2022;204:21–4. https://doi.org/10.1016/j.puhe.2021.12.018
16. Hershow RB, Segaloff HE, Shockey AC, Florek KR, Murphy SK, DuBose W, et al. Rapid spread of SARS-CoV-2 in a state prison after introduction by newly transferred incarcerated persons—Wisconsin, August 14–October 22, 2020. MMWR Morb Mortal Wkly Rep. 2021;70:478–82. https://doi.org/10.15585/mmwr.mm7013a4
17. Mazzilli S, Tavoschi L, Soria A, Fornili M, Cocca G, Sebastiani T, et al. COVID-19 infection among incarcerated individuals and prison staff in Lombardy, Italy, March 2020 to February 2021. JAMA Netw Open. 2022;5:e224862. https://doi.org/10.1001/jamanetworkopen.2022.4862
18. Australian Institute of Health and Welfare. The health of Australia's prisoners 2018. 2019 [cited 2024 Apr 20]. https://www.aihw.gov.au/reports/prisoners/health-australia-prisoners-2018/report-editions
19. Blogg J, McGrath C, Galouzis J, Grant L, Hoey W. Lessons learned from keeping NSW's prisons COVID-free. Int J Prison Health. 2021;17:398–405. https://doi.org/10.1108/IJPH-09-2020-0073
20. National Institutes of Health. Clinical spectrum of SARS-CoV-2 infection. 2023 [cited 2023 Nov 5]. https://www.covid19treatmentguidelines.nih.gov/overview/clinical-spectrum
21. Rockett R, Basile K, Maddocks S, Fong W, Agius JE, Johnson-Mackinnon J, et al. Resistance mutations in SARS-CoV-2 Delta variant after sotrovimab use. N Engl J Med. 2022;386:1477–9. https://doi.org/10.1056/NEJMc2120219
22. Katoh K, Standley DM. MAFFT multiple sequence alignment software version 7: improvements in performance and usability. Mol Biol Evol. 2013;30:772–80. https://doi.org/10.1093/molbev/mst010

23. Nguyen LT, Schmidt HA, von Haeseler A, Minh BQ. IQ-TREE: a fast and effective stochastic algorithm for estimating maximum-likelihood phylogenies. Mol Biol Evol. 2015;32:268–74. https://doi.org/10.1093/molbev/msu300
24. Blackmore C, Czachorowski M, Farrington E, O'Moore É, Plugge E. Testing for COVID-19 during an outbreak within a large UK prison: an evaluation of mass testing to inform outbreak control. Int J Infect Dis. 2022;125:138–44. https://doi.org/10.1016/j.ijid.2022.10.018
25. Adamson JP, Smith C, Pacchiarini N, Connor TR, Wallsgrove J, Coles I, et al. A large outbreak of COVID-19 in a UK prison, October 2020 to April 2021. Epidemiol Infect. 2022;150:e134. https://doi.org/10.1017/S0950268822000991
26. Hagan LM, Williams SP, Spaulding AC, Toblin RL, Figlenski J, Ocampo J, et al. Mass testing for SARS-CoV-2 in 16 prisons and jails—six jurisdictions, United States, April–May 2020. MMWR Morb Mortal Wkly Rep. 2020;69:1139–43. https://doi.org/10.15585/mmwr.mm6933a3
27. Tompkins LK, Gunn JKL, Cherney B, Ham JE, Horth R, Rossetti R, et al.; CDC COVID-19 Surge Diagnostic Testing Laboratory. Mass SARS-CoV-2 testing in a dormitory-style correctional facility in Arkansas. Am J Public Health. 2021;111:907–16. https://doi.org/10.2105/AJPH.2020.306117
28. Zawitz C, Welbel S, Ghinai I, Mennella C, Levin R, Samala U, et al. Outbreak of COVID-19 and interventions in a large jail—Cook County, IL, United States, 2020. Am J Infect Control. 2021;49:1129–35. https://doi.org/10.1016/j.ajic.2021.03.020
29. Esposito M, Salerno M, Di Nunno N, Ministeri F, Liberto A, Sessa F. The risk of COVID-19 infection in prisons and prevention strategies: a systematic review and a new strategic protocol of prevention. Healthcare (Basel). 2022;10:270. https://doi.org/10.3390/healthcare10020270
30. Salvatore PP, Lee CC, Sleweon S, McCormick DW, Nicolae L, Knipe K, et al. Transmission potential of vaccinated and unvaccinated persons infected with the SARS-CoV-2 Delta variant in a federal prison, July–August 2021. Vaccine. 2023;41:1808–18. https://doi.org/10.1016/j.vaccine.2022.11.045

Address for correspondence: Nicolas M. Legrand, Kirby Institute, Level 6, Wallace Wurth Building, UNSW, Sydney, NSW 2052, Australia; email: nlegrand@kirby.unsw.edu.au

etymologia revisited

Coronavirus

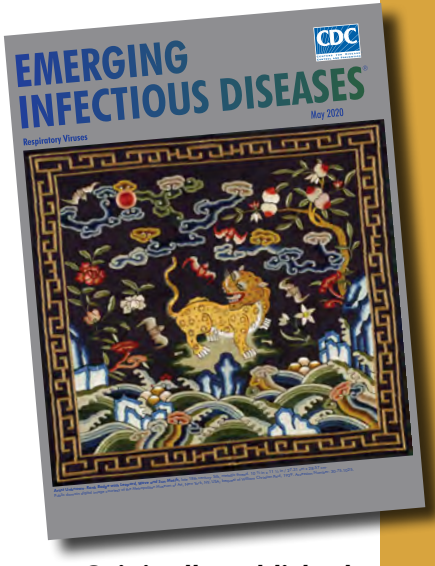

Originally published in May 2020

The first coronavirus, avian infectious bronchitis virus, was discovered in 1937 by Fred Beaudette and Charles Hudson. In 1967, June Almeida and David Tyrrell performed electron microscopy on specimens from cultures of viruses known to cause colds in humans and identified particles that resembled avian infectious bronchitis virus. Almeida coined the term "coronavirus," from the Latin *corona* ("crown"), because the glycoprotein spikes of these viruses created an image similar to a solar corona. Strains that infect humans generally cause mild symptoms. However, more recently, animal coronaviruses have caused outbreaks of severe respiratory disease in humans, including severe acute respiratory syndrome (SARS), Middle East respiratory syndrome (MERS), and 2019 novel coronavirus disease (COVID-19).

References

1. Almeida JD, Tyrrell DA. The morphology of three previously uncharacterized human respiratory viruses that grow in organ culture. J Gen Virol. 1967;1:175–8. https://doi.org/10.1099/0022-1317-1-2-175
2. Beaudette FR, Hudson CB. Cultivation of the virus of infectious bronchitis. J Am Vet Med Assoc. 1937;90:51–8.
3. Estola T. Coronaviruses, a new group of animal RNA viruses. Avian Dis. 1970;14:330–6. https://doi.org/10.2307/1588476
4. Groupe V. Demonstration of an interference phenomenon associated with infectious bronchitis virus of chickens. J Bacteriol. 1949;58:23–32. https://doi.org/10.1128/JB.58.1.23-32.1949

https://wwwnc.cdc.gov/eid/article/26/5/et-2605_article

Rapid Emergence and Evolution of SARS-CoV-2 Intrahost Variants among COVID-19 Patients with Prolonged Infections, Singapore

Yvonne C.F. Su, Michael A. Zeller, Peter Cronin, Rong Zhang, Yan Zhuang, Jordan Ma, Foong Ying Wong, Giselle G.K. Ng, Áine O'Toole, Andrew Rambaut, Jenny G. Low, Gavin J.D. Smith

The evolution and spread of SARS-CoV-2 variants have driven successive waves of global COVID-19 outbreaks, yet the longitudinal dynamics of intrahost variation within the same patient remain less clear. We conducted a longitudinal cohort study by deep sequencing 198 swab samples collected from COVID-19 patients with varying infection durations. Our analysis showed that prolonged infections enhanced viral genomic diversity, leading to emergence of co-occurring variants that maintained high (≥20%) frequency and became dominant in virus populations. We observed heterogeneous intrahost dynamics among individual patients, 2 of whom exhibited a minor variant of the spike D614G substitution over the course of infection. The increase in intrahost variants strongly correlated with prolonged infections, highlighting the complex interplay between viral diversity and host factors. This study revealed the intricate evolutionary mechanisms driving the emergence of de novo variants and lineage dominance, which could inform development of effective vaccine candidates and strategies to protect public health.

The COVID-19 pandemic, caused by the zoonotic SARS-CoV-2 virus, led to an unprecedented global crisis in the 21st Century. The application of advanced sequencing technologies enabled rapid identification of emerging de novo SARS-CoV-2 variants and helped elucidate how prevailing lineages were arising and spreading. Singapore was among the first countries outside China to implement rigorous COVID-19 surveillance. During the early period of the SARS-CoV-2 outbreak, from late January to early March 2020, viruses from multiple patients in Singapore exhibited a long, 382-nt deletion mutation in the open reading frame (ORF) regions ORF7b and ORF8 (*1*) that was later eliminated in the population, possibly because of the reduction in case counts resulting from the country's effective control measures (*2*). ORF8 deletions of varying lengths have repeatedly reemerged in subsequent major variants, including Alpha, Delta, and Omicron XBB.1 (*3*–*6*).

Studies investigating the intrahost dynamics of SARS-CoV-2 virus have demonstrated that intrahost single-nucleotide variants (iSNVs) are associated with virus shredding (*7*), transmission bottlenecks (*8*,*9*), purifying selection (*10*), immunosuppression (*11*), and vaccinations (*12*). Growing attention has been directed toward determining the complexity of viral evolution during persistent infections within hosts (*13*–*15*; M. Ghafari et al., unpub. data, https://doi.org/10.1101/2024.06.21.24309297; N. Rutsinsky et al., unpub. data, https://doi.org/10.1101/2024.11.23.624482). However, the intrahost evolutionary dynamics of SARS-CoV-2 in Singapore remain largely uncharacterized. We investigated the longitudinal intrahost variation of SARS-CoV-2 in patients with varying durations of infection during early 2020.

Materials and Methods

Sample Collection

During March–May 2020, we collected a total of 198 nasopharyngeal swab samples from 20 adult hospitalized COVID-19 patients at Singapore General Hospital (SGH). Epidemiologic and clinical data included

Author affiliations: Programme in Emerging Infectious Diseases, Duke-NUS Medical School, Singapore (Y.C.F. Su, M.A. Zeller, P. Cronin, R. Zhang, Y. Zhang, J. Ma, F.Y. Wong, G.G.K. Ng, J.G. Low, G.J.D. Smith); Institute of Evolutionary Biology, University of Edinburgh, Edinburgh, Scotland, UK (A. O'Toole, A. Rambaut); Singapore General Hospital, Singapore (J.G. Low)

DOI: https://doi.org/10.3201/eid3108.241419

age, sex, height, weight, body mass index, underlying conditions, intensive care unit (ICU) admission, infection duration, leukocyte count, C-reactive protein (CRP) count, and remdesivir treatment.

RNA Extraction and Next-Generation Sequencing

We extracted viral RNA from swab samples and tested for the SARS-CoV-2 RNA-dependent RNA polymerase gene, as previously described (*16*). We generated complete SARS-CoV-2 genomes via next-generation sequencing. We conducted library preparation by using the Illumina RNA Prep Enrichment Kit (https://www.illumina.com) and performed viral enrichment by using Respiratory Virus Oligo Panel (Illumina), following manufacturer protocols. We quantified libraries by using the Qubit dsDNA HS Assay Kit (Thermo Fisher Scientific, https://www.thermofisher.com) and quality-checked by using 2100 Bioanalyzer (Agilent Technologies, https://www.agilent.com). We ran pooled libraries on an Illumina MiSeq platform at 2 × 250 bp. We used Trimmomatic version 0.39 (*17*) to quality-trim reads using a minimum read quality of 20, leading/trailing quality of 10, and a minimum length of 50. For samples collected on the first day of swab sampling, we mapped trimmed paired reads to the wild-type SARS-CoV-2 reference genome (GenBank accession no. NC_045512.2) using Burrow-Wheeler Aligner–Maximal Exact Match (*18*) with UGENE version 42 (*19*). We used Pangolin version 4.3.1 (*20*) to assign Pango lineages to SARS-CoV-2 genomes from patients (GISAID accession nos. EPI_ISL_19591944–57).

iSNV Analyses

To investigate within-host evolutionary dynamics of SARS-CoV-2, we used daily nasopharyngeal swab specimens collected from the 20 participants hospitalized at SGH over the course of infection, spanning up to 40 days. We deep sequenced all 198 samples, yielding 92 complete genomes from serial timepoints (Table 1). We used SAMtools (*21*) to identified iSNVs and generate mpileup files, then performed variant calling by using VarScan version 2.3.4 (*22*).

We applied rigorous quality control steps to reduce sequencing errors. First, we trimmed and filtered reads with a minimum Phred score ≥30. We required variants to have sequencing depth of 200–60,000 reads, a p value of ≤0.01, variant read depth >10×, and genome coverage >95%. Then we used the strand-filter parameter to remove variants detected predominantly on either the forward or reverse strand but not both. To minimize false-positive results and exclude potentially fixed variants, we only retained variants with frequencies of 5%–95%, following widely used minor allele frequency cutoffs (*13*,*23*,*24*). That threshold is well above the reported error rates for next-generation sequencing platforms, ensuring reliable variant detection (*25*). For samples collected on the first day of hospitalization, we used SnpEff (*26*) to perform variant annotation on the basis of the wild-type reference genome (*7*,*8*,*27*,*28*). For longitudinal samples, we based annotations on

Table 1. Epidemiologic and clinical characteristics of hospitalized patients in a study of rapid emergence and evolution of SARS-CoV-2 intrahost variants among COVID-19 patients with prolonged infections, Singapore*

ID	Age,y/ sex	BMI	Underlying conditions†	ICU admission	No. days hospitalized	Remdesivir treatment	Median lymphocyte count‡	Median CRP, mg/L	Median leukocyte count‡	Long-term medication	Pangolin lineage
P1	29/F	23.3	N	N	5	N	0.71	0	3.95	N	B.6.6
P2	48/M	26.8	N	N	13	Y	2.28	18.5	5.93	N	B.6
P3	70/M	22.5	Y	Y	40	Y	0.79	236.5	10.89	Y	B.6.6
P4	65/M	NA	Y	N	30	N	1.22	51.2	6.89	Y	B.6.6
P5	67/F	30.9	N	N	14	Y	1.05	122	4.61	N	B.1.104
P6	28/M	NA	N	N	7	N	1.75	0	4.28	N	B.6.3
P7	64/M	31.5	Y	N	16	N	2.32	12.6	5.09	Y	B.6.6
P8	29/M	20.8	N	N	5	N	1.14	0	4.45	N	B.6.6
PP9	35/F	21.6	N	N	7	N	1.44	0.9	4.66	N	B.1.1
P10	25/M	21.7	N	N	11	N	1.45	0	3.80	N	B.6.6
P11	32/M	27.3	N	N	4	N	0.87	0	7.00	N	B.1.1
P12	41/M	NA	N	N	6	N	0.98	0	4.99	N	B.6.6
P13	37/M	28.7	N	N	6	N	0.92	0	2.48	N	B.6.6
P14	34/F	NA	N	N	5	N	1.82	0	5.29	N	B.6.6
P15	54/M	NA	N	N	12	N	1.18	0.3	8.83	N	B.6.6
P16	21/F	NA	N	N	8	N	1.31	31.9	4.98	N	B.1.1
P17	50/M	31.8	N	N	3	Y	1.61	73	4.65	N	B.6
P18	37/M	NA	N	N	5	N	3.31	0	6.89	N	ND
P19	39/M	14.7	N	N	5	N	0.74	0	3.73	N	B.1.1
P20	61/F	25.8	Y	Y	30	Y	1.47	158	9.06	Y	B.6

*BMI, body mass index; CRP, C-reactive protein; ICU, intensive care unit; ID, patient identification; ND, not determined; P, patient.
†Including hypertension or hyperlipidemia.
‡Value × 10^9 cells/L.

the reference genome of the first confirmed Singapore case (BetaCoV/Singapore/2/2020; GISAID accession no. EPI_ISL_406973) that differs from the wild-type reference genome by a single nucleotide. We used MAFFT (https://mafft.cbrc.jp) to conduct genome alignments in Geneious Prime version 2022.1.1 (https://www.geneious.com), then manually refined.

We identified iSNVs representing subconsensus genetic diversity on the basis of nucleotide composition at each genomic position (*27*,*29*) (Appendix 1 Table 1, https://wwwnc.cdc.gov/EID/article/31/8/24-1419-App1.xlsx). We found iSNV counts and frequencies were consistent when we used either the wild-type or BetaCoV/Singapore/2/2020 reference genomes. We visualized iSNV frequencies and distributions by using the ggplot2 package (https://github.com/tidyverse/ggplot2) and custom scripts in R (The R Project for Statistical Computing, https://www.r-project.org). We used the ComplexHeatmap package (*30*) in R to display high (>20%) frequency iSNVs as heatmaps. To assess variation of iSNV counts and frequencies over the course of infection, we stratified patients by illness duration into acute (≤7 days) and prolonged (≥8 days) groups. That cutoff reflects earlier studies indicating that mild or moderate COVID-19 cases typically resolve within a week, but severe cases exhibit extended viral shedding (*31*–*34*). For each patient, we quantified the number of synonymous, nonsynonymous, and nonsense (stop) variants. We normalized iSNV counts per gene by length (kb). We visualized normalized values across all sampling days per patient as bar plots, indicating relative proportions of synonymous and nonsynonymous variants.

Correlation and Linear Regression Analyses

We used the corrplot package version 0.92 in R (https://CRAN.R-project.org/package=corrplot) to calculate Pearson correlation coefficients (r) for assessing associations between iSNV counts and 11 clinical variables and considered $p<0.05$ statistically significant. We defined iSNV counts as the number of unique genomic positions with a variant detected in ≥1 sample per patient. We classified correlation strength as very strong ($r>0.7$), strong (r = 0.5–0.7), moderate (r = 0.3–0.5), or weak ($r<0.3$). We further tested associations between iSNV counts and clinical parameters by using a negative binomial regression model with a log-link function in the MASS package (*35*) in R. We performed Wilcoxon tests to compare factors between 2 groups. We used the Benjamini-Hochberg method to correct all p values for false discovery rate.

Table 2. Clinical features of patients in a study of rapid emergence and evolution of SARS-CoV-2 intrahost variants among COVID-19 patients with prolonged infections, Singapore*

Characteristics	All patients, n = 20
Median age, y (range)	38 (21–70)
Sex	
F	6 (30)
M	14 (70)
Healthcare worker	2 (10)
Median height, cm (range)	168 (151–185)
Median weight, kg (range)	69.2 (42.5–95.1)
Median body mass index (range)	25.8 (14.7–31.8)
Hypertension	4 (20)
Intensive care unit admission	2 (10)
Median length of hospitalization, d (range)	7 (4–40)
Median C-reactive protein, mg/L (IQR)	41.53 (14.1–109.7)
Median leukocyte count, × 10^9 cells/L (range)	4.99 (2.5–21.7)
Median lymphocyte count, × 10^9 cells/L (IQR)	1.27 (0.97–1.68)
Remdesivir treatment	5 (25)
Long-term medication	4 (20)
International travel	8 (40)

*Values are no. (%) except as indicated. IQR, interquartile range.

Ethics Considerations

This study was approved by the SingHealth Centralized Institutional Review Board (CIRB reference no. 2018/3045) and the National University of Singapore (NUS) Institutional Review Board (NUS-IRB reference code 2022-320). Written informed consent was obtained from all participants. All recruited COVID-19 patients were hospitalized during the early phase of the pandemic, isolated in negative pressure rooms, and discharged only after 2 consecutive negative quantitative PCR (qPCR) tests. All samples were de-identified and processed under Biosafety Level 3 conditions.

Results

Clinical Characteristics of Hospitalized COVID-19 Patients

The 20 enrolled patients ranged in age from 21 to 70 (median 38 ± 15.4) years, and body mass index ranged from 14.7 to 31.8 (median 25.8 ± 5.0) kg/m^2 (Tables 1, 2; Appendix 2 Figure 1, https://wwwnc.cdc.gov/EID/article/31/8/24.1419-App2.pdf). Hospital stays varied from 3 to 40 (median 7 ± 10.2) days. Five patients (P2, P3, P5, P17, and P20) received remdesivir treatment. Four patients (P3, P4, P7, and P20) had underlying conditions, including hypertension, and experienced SARS-CoV-2 infections lasting 16 to 40 days (Table 1).

iSNVs in Longitudinal SARS-CoV-2 Samples

We analyzed subconsensus de novo iSNVs in longitudinal samples from 16 COVID-19 patients. Of 198 sequenced samples, only 92 samples had sequencing

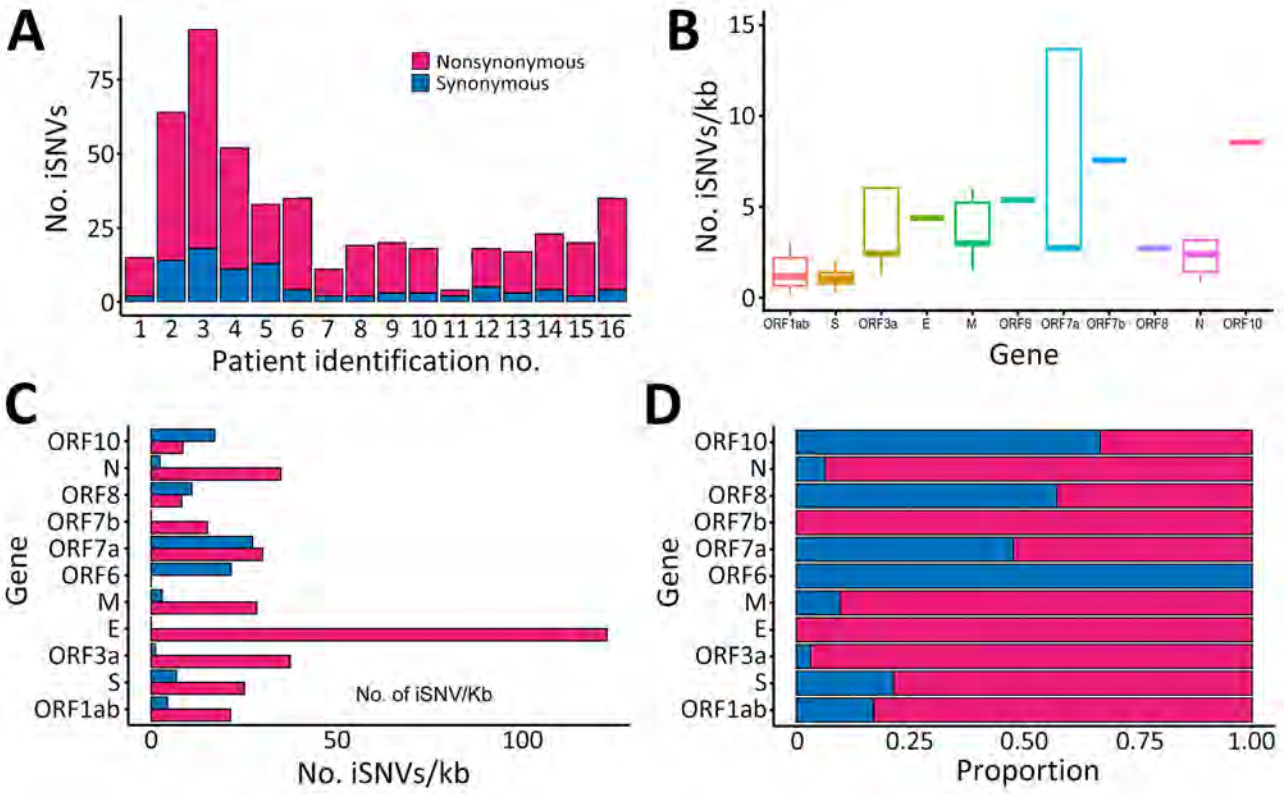

Figure 1. Distribution of iSNVs among patients in study of rapid emergence and evolution of SARS-CoV-2 intrahost variants among COVID-19 patients with prolonged infections, Singapore. A) Total number of iSNV detected in longitudinal samples from each patient, categorized as nonsynonymous or synonymous intrahost variants. B) Distribution plots of all iSNVs per kilobase among genes. Horizontal bars within boxes indicate medians; box tops and bottoms indicate upper and lower quartiles; vertical bars indicate minimum and maximum values. C) Overall iSNV counts across different genes with 5%–95% frequency from longitudinal samples of all patients. D) Overall proportions of iSNVs among genes. E, envelope; iSNV, intrahost single-nucleotide variant; kb, kilobase; M, membrane; N, nucleocapsid; ORF, open reading frame; S, spike.

depths of 200–62,000 reads, which we included for intrahost analysis. We excluded samples from 4 patients because reads were <200 or had inadequate coverage. Among the 16 included patients, we detected 4–108 iSNVs per patient at frequencies of 5%–95% (Appendix 1 Table 2) and more nonsynonymous than synonymous mutations (Figure 1, panel A). Two patients (P2, hospitalized for 30 days, and P3, hospitalized for 40 days) exhibited higher (≥70) variant counts than other patients (Table 1; Figure 1, panel A).

Unique iSNVs were unevenly distributed across the genome. ORF7b and ORF10 exhibited moderately higher iSNVs per kilobase (Figure 1, panel B), and ORF1ab harbored the highest (n = 360) number of iSNVs compared with other gene regions (n = 4–60) (Appendix 1 Table 3). Within ORF1ab, nonsynonymous (n = 261) mutations exceeded synonymous (n = 61) mutations (Appendix 1 Table 4). Nonsynonymous mutations represented >50% of all variants in most genes, except for ORF6, ORF8, and ORF10 (Figure 1, panels C, D, Appendix 1 Table 4).

Temporal Intrahost Dynamics of SARS-CoV-2 across Patients

To assess the prevalence and distribution of de novo variants across SARS-CoV-2 genomes, we combined iSNV data from all longitudinal samples of 16 patients (Appendix 1 Table 1). Frequency plots revealed numerous minor variants at both low (5%–10%) and mid (10%–50%) frequencies and a notable decrease in iSNV count at >50% frequency (Appendix 2 Figure 2). We detected 9 high-frequency (>70%) variants, none of which were shared between patients. Conversely, we observed shared iSNVs in more than half the patients, and ≥11 shared variants detected at frequencies of 40%–70% (Appendix 2 Figure 2, panels A, B). For lower-frequency (5%–10%) variants, most were unique to individual patients, but a few were shared among multiple patients, including A7507C (ORF1a: K2414N), G10481A (ORF1a: G3406S), T15071A (ORF1b: L535I), T17190C (ORF1b: V1241A), T18402A (ORF1b: L1645Q), A20079T (ORF1b: H2204L), A21949C (spike: K129N), T23652C (spike: M697T),

and A26433C (envelope: K63N) (Appendix 2 Figure 2, panel C). The K129N residues were in the N-terminal domain and the M697T residues were in the S2 subunit of the spike protein.

We observed a diverse array of iSNVs and substantial interpatient variability in both number and frequency (Figure 2; Appendix 2 Figures 3–6). Several patients, including P1, P8, P9, P13, P14, and P15, primarily harbored low-frequency (5%–20%) variants (Figure 2; Appendix 1 Table 1; Appendix 2 Figure 3). P1 exhibited more variants on day 1, most of which disappeared by day 2. That patient also harbored a unique spike substitution, A706S (Appendix 2 Figure 3), within the S2 subunit and had a short hospital stay of 5 days. By comparison, P5, who was older (>60 years of age) and hospitalized for 14 days, displayed a higher number of variants, particularly in the ORF1ab region, which appeared sporadically throughout infection (Figure 2; Appendix 2 Figure 3). That patient also carried a unique spike substitution at F823L. Patients with hospital stays >7 days, such as P2, P3, P4, P5, and P16, acquired more low-frequency variants (Figure 2; Appendix 2 Figures 3–6). Of note, P4 harbored a unique spike mutation at A397S within the receptor-binding domain of the spike protein as late as day 29 (Appendix 2 Figure 6), and P16 acquired a mutation, H1271Y, on day 8. In most patients, although some variants persisted, most either disappeared or appeared intermittently during infection.

During April–May 2020, we identified 76 variants with frequencies >20% in ≥1 sample (Figure 3). Because all patients were isolated, most variants likely emerged independently at specific time points. However, only 13 variants persisted during the early pandemic phase (Figure 3). Those variants included dual mutations at C6310A (nonstructural protein [NSP] 3: S1197R) and C6312A (NSP3: T1198K); co-occurrence in NSP3 has been associated with increased infection severity (*34*). Other persistent nonsynonymous variants included C8730T (NSP4: S59F), G11083T (NSP6: L37F), A12413C (NSP8: N108H), C19524T (NSP14: S495L), A23403G (spike: D614G), G25429T (ORF3a: V13L), and C28311T (N: P13L), suggesting those mutations were independently fixed. Among those mutations, the prominent spike D614G variant at nucleotide position 23403 might have emerged in multiple patients and coincided with S1197R (position 6310) and T1198K (position 6312), indicating a potential fitness advantage.

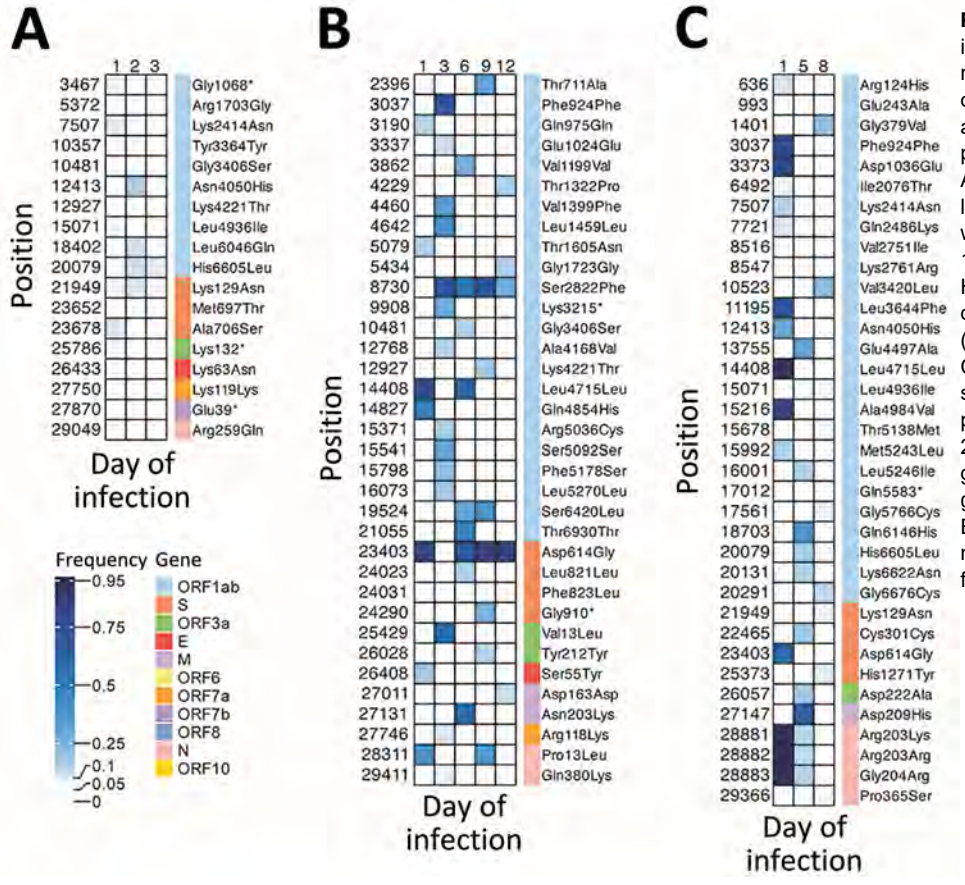

Figure 2. Variant heatmaps from individual patients in study of rapid emergence and evolution of SARS-CoV-2 intrahost variants among COVID-19 patients with prolonged infections, Singapore. A) Patient 1, infected with B6.6 lineage; B) patient 5, infected with B1.1 lineage; C) patient 16, infected with B1.1 lineage. Heatmaps show the frequency distribution of intrahost variants (5%–95%) identified in SARS-CoV-2 genomes from longitudinal samples collected in hospitalized patients during March–May 2020. Maps show corresponding genomic positions, associated genes, and amino acid changes. E, envelope; M, membrane; N, nucleocapsid; ORF, open reading frame; S, spike.

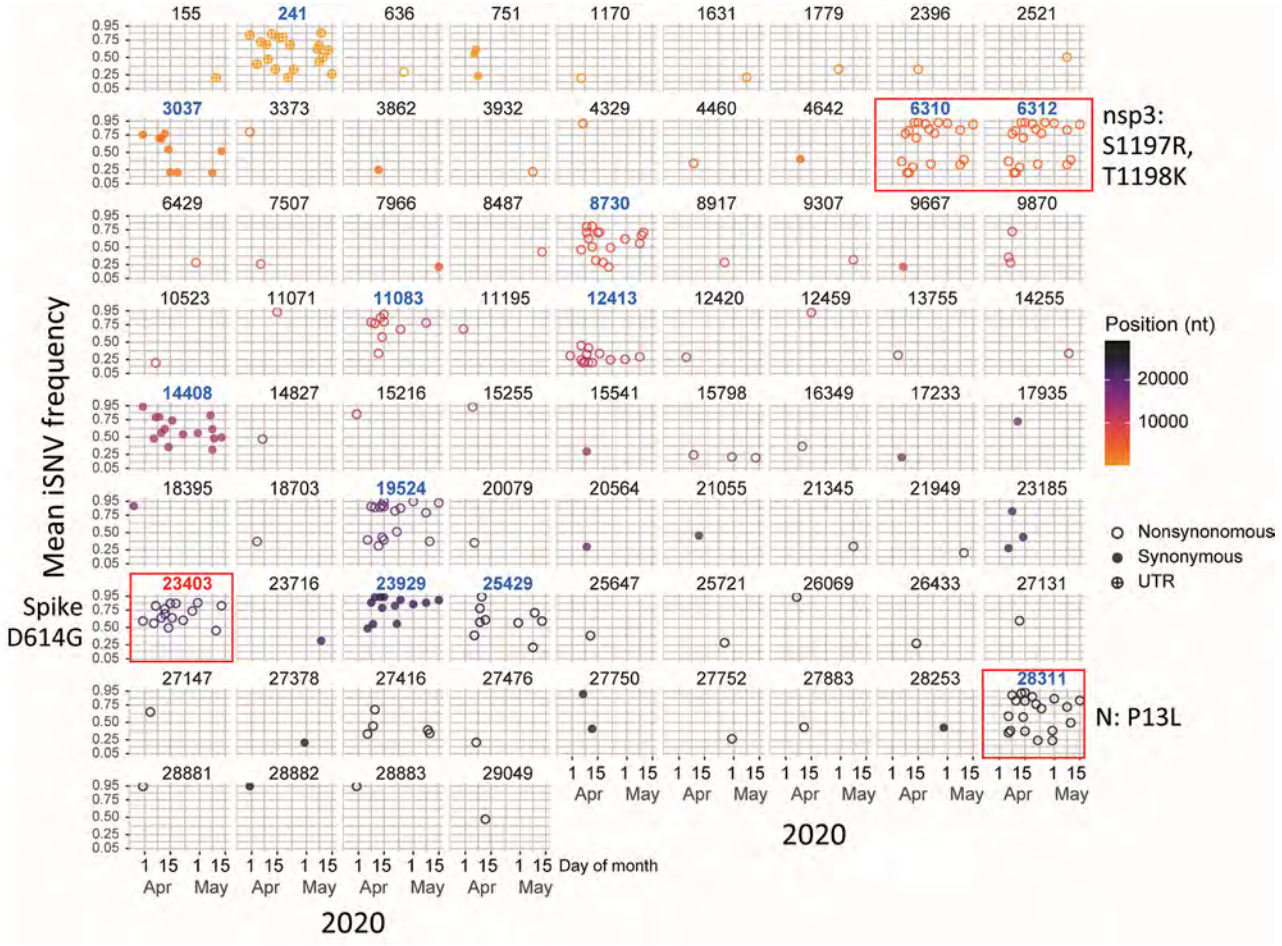

Figure 3. Temporal dynamics of 76 high-frequency iSNVs in study of rapid emergence and evolution of SARS-CoV-2 intrahost variants among COVID-19 patients with prolonged infections, Singapore. Colored closed circles represent synonymous variants; colored open circles represent nonsynonymous variants; crossed dots indicate variants at UTRs. Nucleotide positions of each iSNV are shown above the gray panels. The gradient of colored circles corresponds to iSNVs at respective nucleotide positions. Intrahost variants associated with persistent infections are highlighted in blue bold font, including the D614G intrahost variant (nucleotide position 23403), which marked is in red font above the corresponding open circles. Red rectangles indicate selected variants and their corresponding amino acid substitutions. iSNV, intrahost single-nucleotide variant; N, nucleocapsid; nsp, nonstructural protein; UTR, untranslated region.

The P13L mutation (position 28311) in the N gene has also been linked to reduced ICU admission and lower risk for death (*36*). Together, those findings highlight the emergence of diverse de novo synonymous and nonsynonymous variants in COVID-19 patients during the early phase of the pandemic.

To assess the local prevalence of the spike D614G mutation, we analyzed all available SARS-CoV-2 genomes from Singapore in 2020. The G variant of S614 was detected on March 5, 2020, and its prevalence increased substantially by mid-March (Figure 4, panel A). The 614G mutation was detected in several sublineages, predominantly in B.1 (42.3%) and B.1.1 (32.9%), and the 614D variant was predominant (73.4%) in the B.6.6 lineage (Figure 4, panels B, C; Appendix 1 Table 5).

Differential Landscape of Intrahost Evolution between SARS-CoV-2 B.1 and B.6 Lineages

To investigate differences in intrahost evolution, we compared iSNV distributions in patients infected with B.1 or B.6/B.6.6 lineage viruses. The B.1 lineage exhibited fewer minor variants (iSNVs = 71) at 5%–20% frequency (Figure 5, panel A), whereas B.6/B.6.6 showed a marked increase (iSNVs = 185) (Figure 5, panel B). B.1 lineage also had fewer mid- to high-frequency (>20%) variants (n = 31) compared with B.6 (n = 60), although each lineage displayed a diverse set of shared high-frequency iSNVs.

In the B.1 lineage, several variants were shared among patients, including those at nucleotide positions 3037 (NSP3: F106F), 5434 (NSP3: G905G), 7507 (NSP3: K1596N), 14408 (NSP12: L323L), 15071

(NSP12: L544I), 18703 (NSP14: Q222H), 23403 (S: D614G), 20079 (NSP15: H153L), 21949 (spike: K129N), and 27750 (ORF7a: K119K) (Figure 5, panel A). In contrast, B.6/B.6.6 exhibited more low- to high-frequency iSNVs (Figure 5, panel B). However, we found only a few unique high-frequency (>20%) variants in 5 patients infected with B.6/B.6.6, including mutations at 6310 (NSP3: S1197R), 6312 (NSP3: T1198K), 11083 (NSP6: L37F), 19524 (NSP14: S495L), and 28311 (N: P13L). Spike D614G was observed at lower frequencies in B.6 patients compared with B.1.1 patients. Of note, 3 patients (P2, P3, and P4) acquired the S:D614G mutation during acute or postacute infection: P2 on day 1, P3 on day 3, and P4 as late as day 18 (Appendix 2 Figures 4–6). That time to acquisition suggests high-frequency variants might emerge over the course of infection, as in P3 and P4, who had B.6.6 lineage (Appendix 2 Figures 5, 6), but other variants might appear early, as in P16, who had B.1.1 lineage (Figure 2; Appendix 2 Figure 3).

Prolonged SARS-CoV-2 Infection and Increasing Intrahost Genetic Variability

We next compared de novo iSNVs in patients with infections ≤7 days versus those with 8–40 days of active infection. Patients with prolonged infections yielded more (n = 223) iSNVs across the genome than those with shorter infections (n = 93 iSNVs) (Figure 5, panels C, D). That difference was more pronounced in variants with >20% frequency (69 vs. 15). Among patients with shorter infections, most variants were at low (5%–20%) frequencies, and certain sites, such as 4329 (NSP3: I537T), 7507 (NSP3: K1596N), 17190 (NSP13: V318A), and 27750 (ORF7a: K119K), occurred sporadically. In contrast, prolonged infections exhibited 69 high-frequency (20%–80%) variants, although the fluctuation among those variants should be interpreted with caution. Notable nonsynonymous substitutions included D614G (S), S1197R and T1198K (NSP3), L37F (NSP6), V13L (ORF3a), and P13L (nucleocapsid [N]). To explore intrahost diversity during prolonged (≥8 days) infection, we analyzed iSNVs during acute (≤7 days) and nonacute phases. Many (n = 133) iSNVs emerged within 7 days, and most persisted beyond day 8 of infection (Appendix 2 Figure 7). Of note, patients with prolonged infections exhibited more iSNVs during the first week than those with shorter illness durations (Figure 5, panel C; Appendix 2 Figure 7).

We further examined intrahost SARS-CoV-2 evolution in individual patients. Most patients had numerous low-frequency iSNVs on day 1 (Figure 6; Appendix 2 Figures 8–10). We observed distinct patterns across patients: P6 (7-day hospitalization) showed low-frequency variants on days 2 and 3 and had few nonsynonymous variants (e.g., at nt position 12413) that were >25% by day 5 (Figure 6, panel A). P2 (13-day hospitalization) exhibited more iSNVs, many of which disappeared by day

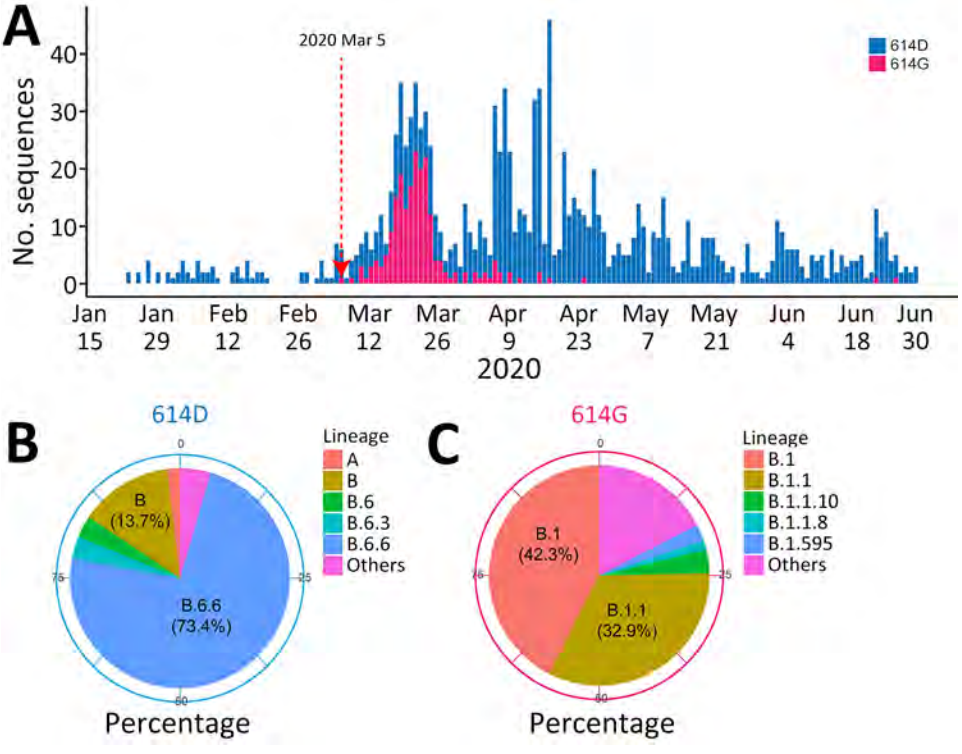

Figure 4. Evolutionary landscape in study of rapid emergence and evolution of SARS-CoV-2 intrahost variants among COVID-19 patients with prolonged infections, Singapore. A) Number of SARS-CoV-2 cases carrying the spike 614D or 614G mutations in all available SARS-CoV-2–positive samples. Dotted red line shows the first detection of the 614G mutation in Singapore. B, C) Percentages of different SARS-CoV-2 Pango lineages containing the 614D (B) or 614G (C) residues in the spike protein.

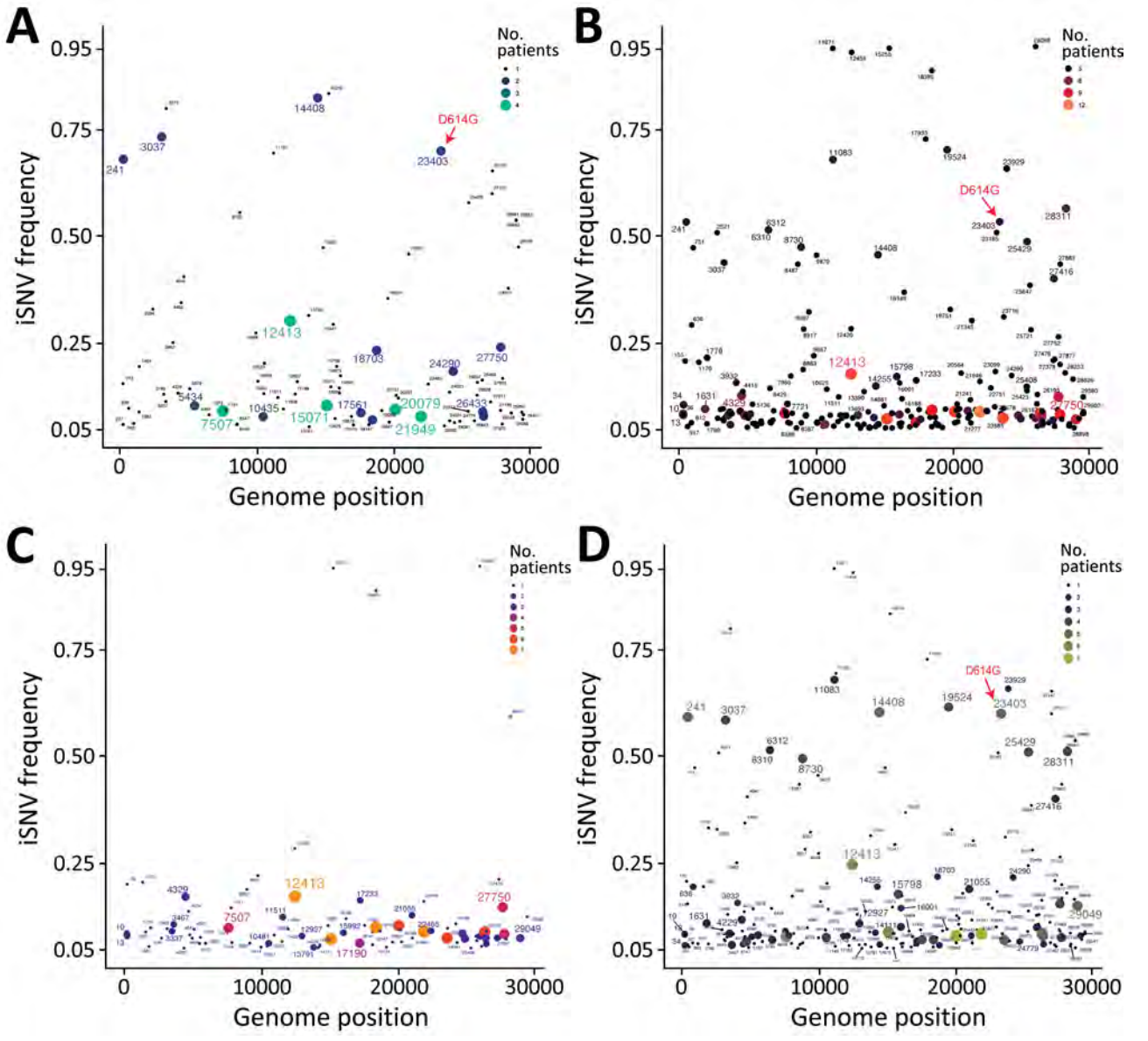

Figure 5. Comparative analysis of variants among lineages and infection durations in study of rapid emergence and evolution of SARS-CoV-2 iSNVs among COVID-19 patients with prolonged infections, Singapore. A, B) Variant frequency between B.1 lineages (A) and B.6 or B.6.6 lineages (B). Red arrows indicate the appearance of intrahost D614G spike variant at nucleotide position 23403. C, D) Variant frequency between COVID-19 patients with shorter infections (≤7 days) (C) and those with prolonged infections (8–40 days) (D). Colored circles represent the number of patients with co-occurring intrahost variants; circle size is proportional to patient count. iSNVs, intrahost single-nucleotide variants.

8 (Figure 6, panel B). Both patients were infected with B.6.6, but P2 was older (48 years of age) and treated with remdesivir and P6 (28 years of age) was not treated (Table 1).

Two patients experienced prolonged infections; P4 had a 30-day infection, and P3 had a 40-day infection. P4 displayed several high-frequency nonsynonymous variants at positions 11071 and 11083 as early as day 1 (Figure 6, panel C), suggesting founder variants were present. In contrast, P3 showed many low-frequency iSNVs throughout infection, and only a few persisted beyond 3 weeks (Figure 6, panel D). Both patients were infected with lineage B.6.6. Specifically, in P3, the spike D614G variant fluctuated in frequency (Figure 6, panel D). It first appeared at 7% on day 3 (April 10, 2020), remained <18.2% for over a week, and then rose to 60.4% by day 15 (April 22, 2020) (Appendix 2 Figure 4). In contrast, patients with shorter (≤7 days) infections (P1 and P7–P15) exhibited fewer iSNVs and limited frequency variation (Appendix 2, Figures 9,10). Those

findings highlight the variability in intrahost variant abundance and dynamics among patients.

Correlation between iSNV Counts and Clinical Variables

Finally, we assessed Pearson correlations between iSNV counts and 11 clinical variables. We observed strong positive correlations with underlying conditions (r = 0.55), ICU admission (r = 0.80), infection duration (r = 0.78), remdesivir treatment (r = 0.81), leukocyte count (r = 0.66), and CRP (r = 0.78) (Table 3; Figure 7). Those variables also demonstrated strong intercorrelations, suggesting collinearity. Regression analysis further confirmed a statistically significant association between iSNV count and infection duration (p = 0.004) (Appendix 1 Table 6; Appendix 2 Figure 11). We observed no statistically significant differences between B.1 and B.6 lineages when comparing patient age or iSNV counts (Appendix 2 Figure 12). Collectively, those findings suggest host factors and treatment interventions influence the emergence of intrahost variants and contribute to viral genomic diversity.

Discussion

As with most RNA viruses, SARS-CoV-2 undergoes rapid mutations and continuously generates de novo genetic variants, seeding sequential epidemics worldwide. In this study, we uncovered longitudinal intrahost dynamics of SARS-CoV-2 among hospitalized patients during the early months of the pandemic. Genomic analysis revealed a substantial number of intrahost variants emerged at varying frequencies from the first day of virus detection onwards. The

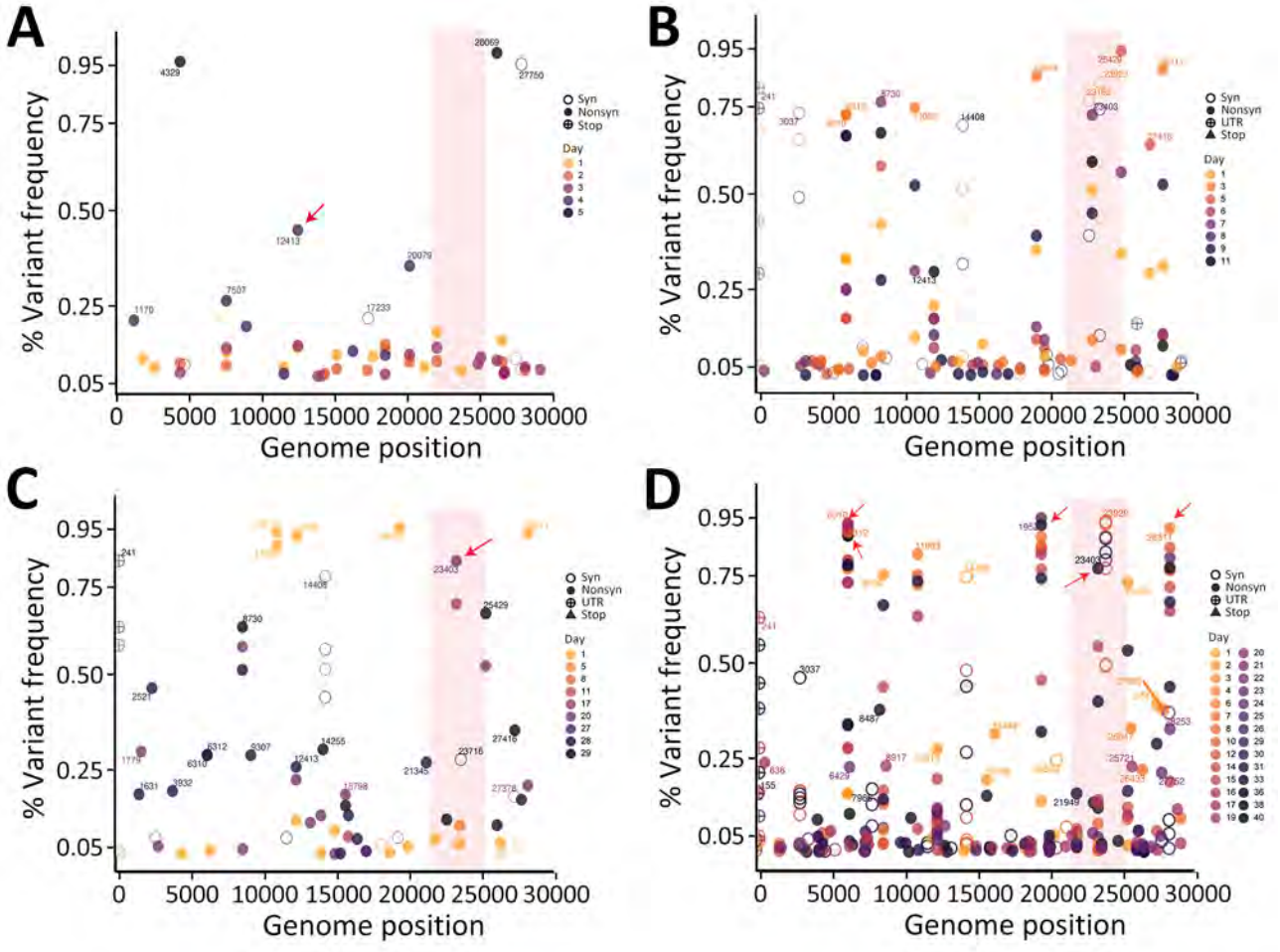

Figure 6. Temporal evolution of iSNVs in study of rapid emergence and evolution of SARS-CoV-2 intrahost variants among COVID-19 patients with prolonged infections, Singapore. The dot plots illustrate iSNVs detected over time and their fluctuations throughout the course of infection in 4 patients: A) patient 6, a 28-year-old man, who had a short infection and hospitalization lasting 7 days; B) patient 2, a 48-year-old man, who had a longer infection and hospitalization of 13 days; C) patient 4, a 65-year-old-man, who had a prolonged infection and hospitalization lasting 30 days; and D) patient 3, a 70-year-old man, who had a prolonged infection and hospitalization lasting 40 days. Colored gradient circles represent days of infections, and the shaded vertical bar indicates the spike region. Red arrows indicate nonsynonymous iSNVs that persisted at high frequency. iSNVs, intrahost single-nucleotide variants; nonsyn, nonsynonymous variants; U syn, synonymous variants; TR, untranslated region.

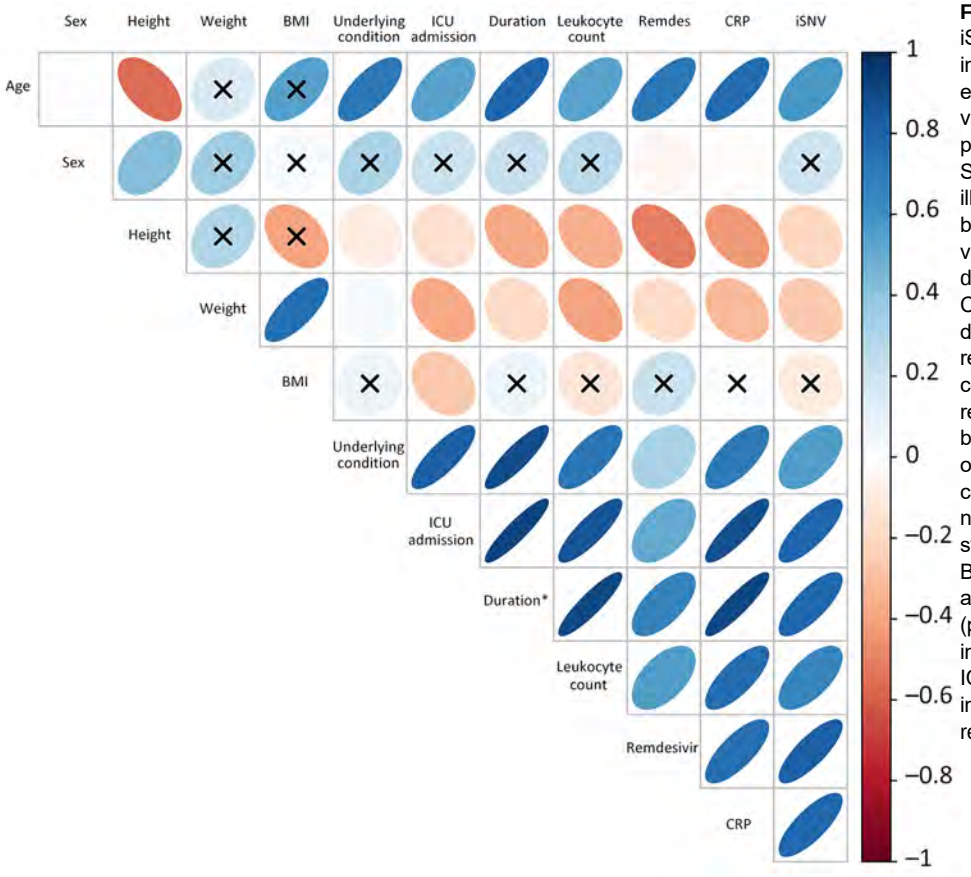

Figure 7. Correlation between iSNVs and clinical parameters in study of rapid emergence and evolution of SARS-CoV-2 intrahost variants among COVID-19 patients with prolonged infections, Singapore. Correlation matrix illustrates the relationships between the number of iSNVs and various clinical variables. Asterisk denotes duration of infection. Colored gradient indicates the degree of pairwise correlation with respect to Pearson correlation coefficient. Blue ellipsoids represent positive associations between any pairwise variables; orange ellipsoids denote negative correlations; the darker and narrower blue ellipsoids indicate stronger positive correlations. Black X denotes correlations that are not statistically significant (p>0.05). BMI, body mass index; CRP, C-reactive protein; ICU, intensive care unit; iSNVs, intrahost-single nucleotide variants; remdes, remdesivir.

low-frequency variants likely resulted from relaxed selection of a virus transmitting in an immunologically naive population or might be indicative of adaptation to the new human host. Relaxed selection on a virus population was previously observed in the first year of pandemic influenza A(H1N1) virus circulation in 2009, before the virus was subjected to immune-driven selection either from widespread infection or vaccination (*37*).

Intrahost population bottlenecks and natural selection play crucial roles in eliminating nonadvantageous variants (*24*). Several studies have indicated that intrahost variants show evidence of positive selection within persons who have persistent infections

Table 3. Pearson correlation matrix of iSNV counts and clinical characteristics patients in a study of rapid emergence and evolution of SARS-CoV-2 intrahost variants among COVID-19 patients with prolonged infections, Singapore*

Characteristic	Age	Sex	Height	Weight	BMI	Underlying conditions†	ICU admission	Infection duration	Leukocyte count	Remdesivir treatment	CRP	iSNV counts
Age	–	0.00	**−0.56**	0.16	0.54	**0.71**	**0.54**	**0.79**	**0.54**	**0.72**	**0.77**	**0.58**
Sex		–	**0.43**	0.35	0.04	0.32	0.22	0.22	0.26	**−0.05**	**−0.02**	0.21
Height			–	0.30	−0.39	**−0.09**	**−0.16**	**−0.38**	**−0.36**	**−0.50**	**−0.43**	**−0.21**
Weight				–	**0.75**	**0.04**	**−0.38**	**−0.18**	**−0.40**	**−0.18**	**−0.32**	**−0.26**
BMI					–	0.08	**−0.26**	0.08	−0.13	0.22	0.02	−0.10
Underlying conditions†						–	**0.81**	**0.88**	**0.73**	**0.32**	**0.70**	**0.55**
ICU admission							–	**0.92**	**0.85**	**0.51**	**0.88**	**0.80**
Infection duration								–	**0.90**	**0.66**	**0.91**	**0.78**
Leukocyte count									–	**0.55**	**0.76**	**0.66**
Remdesivir treatment										–	**0.76**	**0.81**
CRP											–	**0.78**
iSNV counts												–

*Bold text indicates p≤0.05. BMI, body mass index; CRP, C-reactive protein; ICU, intensive care unit; iSNV, intrahost single nucleotide variant.
†Including hypertension or hyperlipidemia.

or chronic diseases or who are immunocompromised (*13*,*38*–*41*). Therefore, persistent infections might serve as suitable reservoirs for harboring de novo variants that can spread into the broader community. We showed that prolonged infections played a role in contributing to the broader range of genomic diversity within hosts. We also observed differential patterns of intrahost dynamics among Pango lineages. Of note, the presence of spike D614G in 3 patients with B.6 and B.6.6 lineages suggest that mutation evolved independently. However, because of stringent quarantine controls, those COVID-19 patients remained hospitalized until they tested negative by qPCR for 2 consecutive days before being discharged, preventing further transmission of that variant.

We also demonstrated that the magnitude of intrahost diversity was positively correlated with host and clinical factors. Higher leukocyte counts and increased CRP levels also have been associated with COVID-19 severity (*42*,*43*). Persistent SARS-CoV-2 infections have been shown to lead to extended periods of ongoing replication, enabling the virus to remain infectious and evolve immune escape mechanisms within hosts (*44*). In addition, older populations, particularly persons >65 years of age, might have impaired immune response, which has also been shown to result in a higher risk for long COVID (*45*) and an increased risk for reinfection with Omicron variants (*46*). Antiviral treatment has been suggested to contribute to greater levels of viral intrahost diversity (*47*).

The ongoing evolution and transmission of SARS-CoV-2 have triggered periodic epidemic waves in many countries, driven by the sequential emergence of variants over time and geographic space. Intrahost investigations have captured the dynamic patterns of population shifts, both longitudinally and cross-sectionally. Here, we showed the role of single-nucleotide variants in contributing to the overall genetic diversity and adaptive evolution of SARS-CoV-2 lineages. Collectively, both viral and host factors play major roles in the emergence and persistence of variants, which can increase the virus's ability to evade immune-driven and vaccine-driven antibodies, displacing older lineages and potentially seeding future outbreaks.

In conclusion, we identified shared SARS-CoV-2 variants across multiple patients and found that only a limited subset of high-frequency variants predominated and persisted throughout the course of infections. We also found that prolonged infections are positively associated with increased genetic diversity, underscoring the significant role of virus–host interactions in shaping intrahost variation and evolution. Enhanced genomic sequencing and monitoring should be prioritized for vulnerable populations, such older adults, immunocompromised persons, and persons living with chronic diseases. The data generated from this study provide crucial insights into the emergence and transmission of de novo variants and can inform the development of effective vaccine candidates and strategies for protection.

Acknowledgments

We thank the anonymous reviewers and Haogao Gu for invaluable suggestions. We also thank the staff at Duke-NUS Biosafety Level 3 research facility for their support and assistance in facilitating high-containment experiments in Singapore.

This study was supported and funded by Singapore National Medical Research Council's (NMRC) Open-Fund Large Collaborative Research Grant OF-LCG/MOH-000505-05 and by contract 75N93021C00016 from the National Institute of Allergy and Infectious Diseases, US National Institutes of Health, and Duke-NUS Signature Research Programme by the Ministry of Health, Singapore.

Author contributions: Y.C.F.S., J.G.L., and G.J.D.S. conceived and designed research. J.G.L. collected clinical samples and data. Z.Y., W.F.Y., and N.G.K. performed experiments. M.A.Z. and P.C. wrote and designed in-house scripts for figures. Y.C.F.S., M.A.Z., P.C., R.Z., W.F.Y., and J.M. analysed data. Y.C.F.S., M.A.Z., P.C., and G.J.D.S drafted and wrote the manuscript, with input from A.O.T. and A.R. All authors contributed to reviewing and editing of the manuscript.

About the Author

Dr. Su is an associate professor at Duke-NUS Medical School in Singapore. Her research interests focus on the evolutionary and transmission dynamics of respiratory diseases in humans and animals, involving outbreak investigations particularly on influenza viruses and coronaviruses.

References

1. Su YCF, Anderson DE, Young BE, Linster M, Zhu F, Jayakumar J, et al. Discovery and genomic characterization of a 382-nucleotide deletion in ORF7b and ORF8 during the early evolution of SARS-CoV-2. MBio. 2020;11:e01610-20. https://doi.org/10.1128/mBio.01610-20
2. Lin RJ, Lee TH, Lye DC. From SARS to COVID-19: the Singapore journey. Med J Aust. 2020;212:497–502.e1. https://doi.org/10.5694/mja2.50623
3. Mazur-Panasiuk N, Rabalski L, Gromowski T, Nowicki G, Kowalski M, Wydmanski W, et al. Expansion of a SARS-CoV-2 Delta variant with an 872 nt deletion encompassing ORF7a,

ORF7b and ORF8, Poland, July to August 2021. Euro Surveill. 2021;26:22. https://doi.org/10.2807/1560-7917.ES.2021.26.39.2100902
4. Tang Z, Yu P, Guo Q, Chen M, Lei Y, Zhou L, et al. Clinical characteristics and host immunity responses of SARS-CoV-2 Omicron variant BA.2 with deletion of ORF7a, ORF7b and ORF8. Virol J. 2023;20:106. https://doi.org/10.1186/s12985-023-02066-3
5. Feng Y, Zhao X, Luo T, Chen Z, Yang H, Chen N, et al. Emergence of a SARS-CoV-2 Omicron subvariant BA.2.2 with a 454-nucleotide genomic deletion—Sichuan Province, China, May 10, 2022. China CDC Wkly. 2022;4:904–6. https://doi.org/10.46234/ccdcw2022.098
6. Niemeyer D, Stenzel S, Veith T, Schroeder S, Friedmann K, Weege F, et al. SARS-CoV-2 variant Alpha has a spike-dependent replication advantage over the ancestral B.1 strain in human cells with low ACE2 expression. PLoS Biol. 2022;20:e3001871. https://doi.org/10.1371/journal.pbio.3001871
7. Ke R, Martinez PP, Smith RL, Gibson LL, Mirza A, Conte M, et al. Daily longitudinal sampling of SARS-CoV-2 infection reveals substantial heterogeneity in infectiousness. Nature Microbiol. 2022;7:640–52. https://doi.org/ 10.1038/s41564-022-01105-z
8. Lythgoe KA, Hall M, Ferretti L, de Cesare M, MacIntyre-Cockett G, Trebes A, et al.; Oxford Virus Sequencing Analysis Group (OVSG); COVID-19 Genomics UK (COG-UK) Consortium. SARS-CoV-2 within-host diversity and transmission. Science. 2021;372:eabg0821. https://doi.org/10.1126/science.abg0821
9. Valesano AL, Rumfelt KE, Dimcheff DE, Blair CN, Fitzsimmons WJ, Petrie JG, et al. Temporal dynamics of SARS-CoV-2 mutation accumulation within and across infected hosts. PLoS Pathog. 2021;17:e1009499. https://doi.org/10.1371/journal.ppat.1009499
10. Tonkin-Hill G, Martincorena I, Amato R, Lawson ARJ, Gerstung M, Johnston I, et al. Patterns of within-host genetic diversity in SARS-CoV-2. eLife. 2021;10:e66857. https://doi.org/10.7554/eLife.66857
11. Weigang S, Fuchs J, Zimmer G, Schnepf D, Kern L, Beer J, et al. Within-host evolution of SARS-CoV-2 in an immunosuppressed COVID-19 patient as a source of immune escape variants. Nat Commun. 2021;12:6405. https://doi.org/10.1038/s41467-021-26602-3
12. Khateeb D, Gabrieli T, Sofer B, Hattar A, Cordela S, Chaouat A, et al. SARS-CoV-2 variants with reduced infectivity and varied sensitivity to the BNT162b2 vaccine are developed during the course of infection. PLoS Pathog. 2022;18:e1010242. https://doi.org/10.1371/journal.ppat.1010242
13. Li J, Du P, Yang L, Zhang J, Song C, Chen D, et al. Two-step fitness selection for intra-host variations in SARS-CoV-2. Cell Rep. 2022;38:110205. https://doi.org/10.1016/j.celrep.2021.110205
14. Kemp SA, Collier DA, Datir RP, Ferreira IATM, Gayed S, Jahun A, et al.; CITIID-NIHR BioResource COVID-19 Collaboration; COVID-19 Genomics UK (COG-UK) Consortium. SARS-CoV-2 evolution during treatment of chronic infection. Nature. 2021;592:277–82. https://doi.org/10.1038/s41586-021-03291-y
15. Voloch CM, da Silva Francisco R Jr, de Almeida LGP, Brustolini OJ, Cardoso CC, Gerber AL, et al. Intra-host evolution during SARS-CoV-2 prolonged infection. Virus Evol. 2021;7:veab078. https://doi.org/10.1093/ve/veab078
16. Corman VM, Landt O, Kaiser M, Molenkamp R, Meijer A, Chu DKW, et al. Detection of 2019 novel coronavirus (2019-nCoV) by real-time RT-PCR. Euro Surveill. 2020;25:2000045. https://doi.org/10.2807/1560-7917.ES.2020.25.3.2000045
17. Bolger AM, Lohse M, Usadel B. Trimmomatic: a flexible trimmer for Illumina sequence data. Bioinformatics. 2014;30:2114–20. https://doi.org/10.1093/bioinformatics/btu170
18. Li H, Durbin R. Fast and accurate short read alignment with Burrows-Wheeler transform. Bioinformatics. 2009;25:1754–60. https://doi.org/10.1093/bioinformatics/btp324
19. Okonechnikov K, Golosova O, Fursov M; UGENE team. Unipro UGENE: a unified bioinformatics toolkit. Bioinformatics. 2012;28:1166–7. https://doi.org/10.1093/bioinformatics/bts091
20. O'Toole Á, Scher E, Underwood A, Jackson B, Hill V, McCrone JT, et al. Assignment of epidemiological lineages in an emerging pandemic using the Pangolin tool. Virus Evol. 2021;7:veab064. https://doi.org/10.1093/ve/veab064
21. Li H, Handsaker B, Wysoker A, Fennell T, Ruan J, Homer N, et al.; 1000 Genome Project Data Processing Subgroup. The sequence alignment/map format and SAMtools. Bioinformatics. 2009;25:2078–9. https://doi.org/10.1093/bioinformatics/btp352
22. Koboldt DC, Zhang Q, Larson DE, Shen D, McLellan MD, Lin L, et al. VarScan 2: somatic mutation and copy number alteration discovery in cancer by exome sequencing. Genome Res. 2012;22:568–76. https://doi.org/10.1101/gr.129684.111
23. Raglow Z, Surie D, Chappell JD, Zhu Y, Martin ET, Kwon JH, et al.; Investigating Respiratory Viruses in the Acutely Ill (IVY) Network. SARS-CoV-2 shedding and evolution in patients who were immunocompromised during the Omicron period: a multicentre, prospective analysis. Lancet Microbe. 2024;5:e235–46. https://doi.org/10.1016/S2666-5247(23)00336-1
24. Wang Y, Wang D, Zhang L, Sun W, Zhang Z, Chen W, et al. Intra-host variation and evolutionary dynamics of SARS-CoV-2 populations in COVID-19 patients. Genome Med. 2021;13:30. https://doi.org/10.1186/s13073-021-00847-5
25. Schirmer M, D'Amore R, Ijaz UZ, Hall N, Quince C. Illumina error profiles: resolving fine-scale variation in metagenomic sequencing data. BMC Bioinformatics. 2016;17:125. https://doi.org/10.1186/s12859-016-0976-y
26. Cingolani P, Platts A, Wang L, Coon M, Nguyen T, Wang L, et al. A program for annotating and predicting the effects of single nucleotide polymorphisms, SnpEff: SNPs in the genome of *Drosophila melanogaster strain* w^{1118}; iso-2; iso-3. Fly (Austin). 2012;6:80–92. https://doi.org/10.4161/fly.19695
27. Gu H, Quadeer AA, Krishnan P, Ng DYM, Chang LDJ, Liu GYZ, et al. Within-host genetic diversity of SARS-CoV-2 lineages in unvaccinated and vaccinated individuals. Nat Commun. 2023;14:1793. https://doi.org/10.1038/s41467-023-37468-y
28. Gonzalez-Reiche AS, Alshammary H, Schaefer S, Patel G, Polanco J, Carreño JM, et al.; PARIS/PSP study group. Sequential intrahost evolution and onward transmission of SARS-CoV-2 variants. Nat Commun. 2023;14:3235. https://doi.org/10.1038/s41467-023-38867-x
29. Markov PV, Ghafari M, Beer M, Lythgoe K, Simmonds P, Stilianakis NI, et al. The evolution of SARS-CoV-2. Nat Rev Microbiol. 2023;21:361–79. https://doi.org/10.1038/s41579-023-00878-2
30. Gu Z, Gu L, Eils R, Schlesner M, Brors B. *circlize* implements and enhances circular visualization in R. Bioinformatics. 2014;30:2811–2. https://doi.org/10.1093/bioinformatics/btu393
31. Wölfel R, Corman VM, Guggemos W, Seilmaier M, Zange S, Müller MA, et al. Virological assessment of

hospitalized patients with COVID-2019. Nature. 2020;581:465–9. https://doi.org/10.1038/s41586-020-2196-x
32. Young BE, Ong SWX, Kalimuddin S, Low JG, Tan SY, Loh J, et al.; Singapore 2019 Novel Coronavirus Outbreak Research Team. Epidemiologic features and clinical course of patients infected with SARS-CoV-2 in Singapore. JAMA. 2020;323:1488–94. https://doi.org/10.1001/jama.2020.3204
33. Hu B, Guo H, Zhou P, Shi ZL. Characteristics of SARS-CoV-2 and COVID-19. Nat Rev Microbiol. 2021;19:141–54. https://doi.org/10.1038/s41579-020-00459-7
34. Lamers MM, Haagmans BL. SARS-CoV-2 pathogenesis. Nat Rev Microbiol. 2022;20:270–84. https://doi.org/10.1038/s41579-022-00713-0
35. Venables WNRB. Modern applied statistics with S. 4th ed. New York: Springer; 2002.
36. Alsuwairi FA, Alsaleh AN, Alsanea MS, Al-Qahtani AA, Obeid D, Almaghrabi RS, et al. Association of SARS-CoV-2 nucleocapsid protein mutations with patient demographic and clinical characteristics during the Delta and Omicron waves. Microorganisms. 2023;11:1288. https://doi.org/10.3390/microorganisms11051288
37. Su YCF, Bahl J, Joseph U, Butt KM, Peck HA, Koay ESC, et al. Phylodynamics of H1N1/2009 influenza reveals the transition from host adaptation to immune-driven selection. Nat Commun. 2015;6:7952. https://doi.org/10.1038/ncomms8952
38. Ghafari M, Hall M, Golubchik T, Ayoubkhani D, House T, MacIntyre-Cockett G, et al.; Wellcome Sanger Institute COVID-19 Surveillance Team; COVID-19 Infection Survey Group; COVID-19 Genomics UK (COG-UK) Consortium. Prevalence of persistent SARS-CoV-2 in a large community surveillance study. Nature. 2024;626:1094–101. https://doi.org/10.1038/s41586-024-07029-4
39. Choi B, Choudhary MC, Regan J, Sparks JA, Padera RF, Qiu X, et al. Persistence and evolution of SARS-CoV-2 in an immunocompromised host. N Engl J Med. 2020;383:2291–3. https://doi.org/10.1056/NEJMc2031364
40. Chaguza C, Hahn AM, Petrone ME, Zhou S, Ferguson D, Breban MI, et al.; Yale SARS-CoV-2 Genomic Surveillance Initiative. Accelerated SARS-CoV-2 intrahost evolution leading to distinct genotypes during chronic infection. Cell Rep Med. 2023;4:100943. https://doi.org/10.1016/j.xcrm.2023.100943
41. Wagner C, Kistler KE, Perchetti GA, Baker N, Frisbie LA, Torres LM, et al. Positive selection underlies repeated knockout of ORF8 in SARS-CoV-2 evolution. Nat Commun. 2024;15:3207. https://doi.org/10.1038/s41467-024-47599-5
42. Wang G, Wu C, Zhang Q, Wu F, Yu B, Lv J, et al. C-reactive protein level may predict the risk of COVID-19 aggravation. Open Forum Infect Dis. 2020;7:ofaa153. https://doi.org/10.1093/ofid/ofaa153
43. Bhargava A, Fukushima EA, Levine M, Zhao W, Tanveer F, Szpunar SM, et al. Predictors for severe COVID-19 infection. Clin Infect Dis. 2020;71:1962–8. https://doi.org/10.1093/cid/ciaa674
44. Hettle D, Hutchings S, Muir P, Moran E; COVID-19 Genomics UK (COG-UK) consortium. Persistent SARS-CoV-2 infection in immunocompromised patients facilitates rapid viral evolution: Retrospective cohort study and literature review. Clin Infect Pract. 2022;16:100210. https://doi.org/10.1016/j.clinpr.2022.100210
45. Mansell V, Hall Dykgraaf S, Kidd M, Goodyear-Smith F. Long COVID and older people. Lancet Healthy Longev. 2022;3:e849–54. https://doi.org/10.1016/S2666-7568(22)00245-8
46. Breznik JA, Rahim A, Zhang A, Ang J, Stacey HD, Bhakta H, et al. Early Omicron infection is associated with increased reinfection risk in older adults in long-term care and retirement facilities. EClinicalMedicine. 2023;63:102148. https://doi.org/10.1016/j.eclinm.2023.102148
47. Heyer A, Günther T, Robitaille A, Lütgehetmann M, Addo MM, Jarczak D, et al. Remdesivir-induced emergence of SARS-CoV2 variants in patients with prolonged infection. Cell Rep Med. 2022;3:100735. https://doi.org/10.1016/j.xcrm.2022.100735

Address for correspondence: Yvonne C.F. Su, Programme in Emerging Infectious Diseases, Duke-NUS Medical School, 8 College Rd, 169857, Singapore; email: yvonne.su@duke-nus.edu.sg

Scheffersomyces spartinae Fungemia among Pediatric Patients, Pakistan, 2020–2024

Kauser Jabeen, Joveria Farooqi, Lacy M. Simons, Judd F. Hultquist, Ramon Lorenzo-Redondo, Charlesnika T. Evans, Erica M. Hartmann, Mohammad Hanif, Zahra Hasan, Syed Faisal Mahmood, Javaria Ashraf, Hassan Ghayas, Sadaf Zaka, Noureen Saeed, Sayed Ali Raza Shah Bukhari, Mehreen Arshad, Larry K. Kociolek, Sameer J. Patel, Rumina Hasan, Egon A. Ozer

Medscape CME Activity

In support of improving patient care, this activity has been planned and implemented by Medscape, LLC and Emerging Infectious Diseases. Medscape, LLC is jointly accredited with commendation by the Accreditation Council for Continuing Medical Education (ACCME), the Accreditation Council for Pharmacy Education (ACPE), and the American Nurses Credentialing Center (ANCC), to provide continuing education for the healthcare team.

Medscape, LLC designates this Journal-based CME activity for a maximum of 1.00 ***AMA PRA Category 1 Credit(s)™***. Physicians should claim only the credit commensurate with the extent of their participation in the activity.

Successful completion of this CME activity, which includes participation in the evaluation component, enables the participant to earn up to 1.0 MOC points in the American Board of Internal Medicine's (ABIM) Maintenance of Certification (MOC) program. Participants will earn MOC points equivalent to the amount of CME credits claimed for the activity. It is the CME activity provider's responsibility to submit participant completion information to ACCME for the purpose of granting ABIM MOC credit.

All other clinicians completing this activity will be issued a certificate of participation. To participate in this journal CME activity: (1) review the learning objectives and author disclosures; (2) study the education content; (3) take the post-test with a 75% minimum passing score and complete the evaluation at https://www.medscape.org/qna/processor/74834?showStandAlone=true&src=prt_jcme_eid_mscpedu; and (4) view/print certificate. For CME questions, see page 1689.

NOTE: It is the policy of Medscape Education to avoid the mention of brand names or specific manufacturers in accredited educational activities. However, trade and manufacturer names in this activity are provided in an effort to provide clarity. The use of brand or manufacturer names should not be viewed as an endorsement by Medscape of any specific product or manufacturer.

Release date: July 24, 2025; Expiration date: July 24, 2026

Learning Objectives

Upon completion of this activity, participants will be able to:

- Assess characteristics of *S. spartinae*
- Distinguish the median age of patients with *S. spartinae* infection in the current study
- Analyze the antifungal sensitivity profile of *S. spartinae*
- Evaluate the genetic signature of *S. spartinae* isolates in the current study

CME Editor

Amy J. Guinn, BA, MA, Technical Writer/Editor, Emerging Infectious Diseases. *Disclosure: Amy J. Guinn, BA, MA, has no relevant financial relationships.*

CME Author

Charles P. Vega, MD, Health Sciences Clinical Professor of Family Medicine, University of California, Irvine School of Medicine, Irvine, California. *Disclosure: Charles P. Vega, MD, has the following relevant financial relationships: served as consultant or advisor for Boehringer Ingelheim Pharmaceuticals, Inc.; Exact Sciences Corporation.*

Authors

Kauser Jabeen, MBBS, MSc; Joveria Farooqi, MBBS, MSc; Lacy M. Simons, BS; Judd F. Hultquist, PhD; Ramon Lorenzo-Redondo, PhD ; Charlesnika T. Evans, PhD, MPH; Erica M. Hartmann, PhD; Mohammad Hanif, MBBS; Zahra Hasan, PhD; Syed Faisal Mahmood, MBBS; Javaria Ashraf, PhD; Hassan Ghayas, PhD; Sadaf Zaka, MPhil; Noureen Saeed, MSc; Sayed Ali Raza Shah Bukhari, PhD; Mehreen Arshad, MBBS; Larry K. Kociolek, MD, MSCI; Sameer J. Patel, MD; Rumina Hasan, MBBS, PhD; Egon A. Ozer, MD, PhD.

Prevalence of emerging fungal infections is increasing, particularly among immunocompromised persons, children, and older persons. We report 108 cases of *Scheffersomyces spartinae* infection in pediatric patients from Karachi and other cities in Pakistan, of which 107 were identified from blood cultures. Cultures were initially misidentified as *Clavispora lusitaniae* by a biochemical assay before speciation as *S. spartinae* by whole-genome sequencing. All isolates were from children ≤12 years of age, and >69% were from children <1 month of age. Isolates were genetically distinct across regions of Pakistan; however, genetic diversity was low in isolates from patients in Karachi and nearby Nawabshah and had median differences of just 9 pairwise nucleotide variants. This study demonstrates *S. spartinae* is a potentially emerging pathogen in neonates and young infants in Pakistan. The findings highlight the limitations of phenotypic identification for detecting emerging fungal infections and underscore the value of molecular identification approaches.

Globally, fungi continue to emerge as serious threats to human health, marked by an increase in incidence of invasive fungal infections and deaths, the growing burden of cutaneous and allergic fungal diseases, and the rapid emergence of antifungal resistance in fungi pathogenic to humans (*1*). The number of fungi associated with invasive disease is rising as new pathogenic fungi emerge and modern sequencing and analysis approaches drive insights into fungal taxonomy (*2*,*3*). Emergence of new pathogenic species and increased infections caused by previously rare or region-specific pathogens might be attributed in various cases to climate change (*4*–*7*), more frequent or severe natural disasters (*8*,*9*), expanding host populations (*10*–*12*), increased use of antifungal agents in clinical or industrial practice, or other unknown epidemiologic drivers.

Considering the immense diversity of fungi and the emergence of new pathogens, ongoing epidemiologic and molecular surveillance of fungal infections is essential. Current phenotypic and biochemical methods do not reliably identify rare or emerging fungal pathogens, and misclassification can occur (*13*–*15*). Molecular approaches, such as internal transcribed spacer (ITS) sequencing, and genomic approaches, such as whole-genome sequencing (WGS), can provide greater specificity for distinguishing new or uncommon fungal infections; however, those methods might not be available to clinical microbiology laboratories in some resource-limited settings (*16*).

In late 2022, the Aga Khan University Hospital (AKUH) clinical mycology laboratory in Karachi, Pakistan, noticed increased cases of yeast, biochemically identified as *Clavispora lusitaniae*, cultured from the blood of infants admitted to neonatal intensive care units. Most isolates were subsequently identified by WGS as *Scheffersomyces spartinae*, an environmental yeast with high tolerance to temperature, pH, and salinity changes (*17*,*18*). *S. spartinae* has been isolated from brackish waters, marshes, and oceans and can survive temperatures of 5°C–35°C, pH of 3–9, and salinity of 0–60 g/L NaCl (*19*,*20*). We conducted genomic analyses of available isolates to identify epidemiologic characteristics of *S. spartinae* infections in Pakistan.

Methods

Study Setting and Duration

The study was performed at AKUH during 2020–2024. The AKUH clinical microbiology laboratory received specimens from 315 satellite collection units in 99 cities and towns across all 4 provinces of Pakistan. Specimens were sent at the primary physician's request; the laboratory had no control over specimen ordering.

Isolate Collection

The AKUH clinical microbiology laboratory followed a standardized approach for processing fungal cultures and selecting specimens for archiving. The laboratory received and cultured blood samples in a BacT/ALERT continuous monitoring system (bioMérieux) for 5 days. If samples were flagged positive, results of Gram stain from the broth determined the choice of solid media for subculture. Specimens with yeast on Gram stain were inoculated on BD BBL sheep blood agar, BD BBL Saboraud's dextrose agar, and BD BBL CHROMagar chromogenic agar plates (all from Becton, Dickinson and Company) and

Author affiliations: Aga Khan University, Karachi, Pakistan (K. Jabeen, J. Farooqui, Z. Hasan, S.F. Mahmood, J. Ashraf, H. Ghayas, S. Zaka, N. Saeed, S.A.R. Shah Buhari, M. Arshad, R. Hasan); Northwestern University Feinberg School of Medicine, Chicago, Illinois, USA (L.M. Simons, J.F. Hultquist, R. Lorenzo-Redondo, C.T. Evans, E.M. Hartmann, E.A. Ozer); Northwestern University Havey Institute for Global Health, Chicago (L.M. Simons, J.F. Hultquist, R. Lorenzo-Redondo, E.A. Ozer); Edward Hines Jr. VA Hospital, Hines, Illinois, USA (C.T. Evans); Northwestern University McCormick School of Engineering, Evanston, Illinois, USA (E.M. Hartmann); National Institute of Child Health, Karachi (M. Hanif); Ann & Robert H. Lurie Children's Hospital of Chicago, Chicago (M. Arshad, L.K. Kociolek, S.J. Patel); London School of Hygiene and Tropical Medicine, London, UK (R. Hasan)

DOI: https://doi.org/10.3201/eid3108.241604

incubated at 35°C–37°C. In addition, the laboratory staff struck yeast on BiGGY agar and Corn Meal Agar with Tween 80 (all Oxoid) for morphological identification, then performed biochemical identification by using the VITEK 2 YST ID card system (bioMérieux).

Antifungal susceptibility was determined by using the Sensititre YeastONE system (Thermo Fisher Scientific). Laboratory staff regularly reviewed sample processing records and selected isolates resistant to fluconazole, echinocandins, or amphotericin B and uncommon or rare yeast isolates for banking. Selected isolates were recultured on potato dextrose agar and incubated at 37°C for 48 hours. Staff transferred colonies from pure cultures to vials of 50% glycerol phosphate broth and banked isolates at −80°C.

Retrospective Data Review

We reviewed the laboratory database to identify all cases of *C. lusitaniae* in blood cultures from 2015–2024. We retrieved patient age, sex, location of residence, and contact details from the clinical laboratory's integrated laboratory information system. For most cases, the contact details were for patients or their guardians and not for the treating physicians. We obtained informed consent from the patients or their guardians by telephone in the presence of a witness before obtaining medical histories. We recorded information in a database on REDCap. The AKUH ethical review committee provided ethical review and approval (study nos. 2022-6798-20372 and 2019-0438-2659).

Whole-Genome Sequencing

We inoculated banked isolates in sterile brain heart infusion broth for overnight incubation at 37°C and subcultured on Sabouraud's dextrose agar for DNA extraction. We performed cell lysis from colonies by using glass beads in lysis buffer and proteinase K and 2 cycles of vortexing at 3,000 rpm for 1 minute each. We then incubated cells at 56°C for 15 minutes. We used the QIAquick DNA Minikit (QIAGEN) to extract genomic DNA from the lysate using the default protocol, eluted in AE buffer, and either stored at −20°C for <2 weeks before sequencing or stored at −80°C if sequencing was not performed within 2 weeks. Sequencing was performed at Aga Khan University (AKU) or Northwestern University (NU; Chicago, Illinois, USA). We used the Speed Vac vacuum concentrator (Thermo Fisher Scientific) to dry extracted DNA specimens before shipping to NU at ambient temperature. NU performed WGS by using the NovaSeq X or MiSeq platforms (Illumina) after library preparation with the plexWell Library Prep Kit (SeqWell). AKU sequenced a subset of the specimens on the Illumina MiniSeq platform after library preparation using the Nextera XT Kit (Illumina).

We trimmed Illumina read sequences by using fastp version 0.23.2 and performed de novo assembly by using SPAdes version 3.9.1. We removed contigs <200 bp or that had <5× mean read coverage. We used BUSCO and the saccharomyces_odb10 database (*21*) to assess completeness of genome assembly. We performed species identification by extracting ITS sequences from draft assemblies by using in silico PCR and previously described primer sequences ITS5 and ITS4 (*22*). We compared resulting sequences against the National Center for Biotechnology Information (NCBI) Fungal ITS RNA sequence database (BioProject accession no. PRJNA177353) using BLAST (*23*). We generated ITS sequence alignments by using MAFFT (*24*) and generated neighbor-joining trees by using RapidNJ (*25*).

Long-Read Sequencing

We randomly selected 1 isolate, 128-CS, for long-read sequencing on the MinION sequencer at AKU by using a Flongle Flow Cell R10.4.1 after genomic DNA library preparation using the Ligation Sequencing Kit V14 (all Oxford Nanopore). We used the 400-bp super accuracy model for basecalling, then performed genome assembly by using Trycycler version 0.5.0 (*26*) as follows. We filtered raw nanopore reads by using Filtlong version 0.2.1 to remove reads of <1,000 bases and the 5% of reads with the lowest quality. We used Trycycler to subsample reads into 12 subsets, then separately reassembled read subsets by using Raven version 1.5.3 (*27*). We used Trycycler to perform clustering, reconciliation, circularization, multiple sequence alignment, and consensus sequence generation from the 12 assemblies. We polished the resulting consensus assembly with nanopore long reads and medaka version 1.4.3 using the r1041_e82_400bps_sup_v4.1.0 model. We aligned Illumina reads to the assembly by using BWA version 0.7.15 (*28*) and corrected assembly errors by using Polypolish version 0.5.0 (*29*) and the POLCA module of MaSuRCA version 4.0.9 (*30*,*31*). We deposited sequences in the NCBI BioProject database (accession no. PRJNA1164417) (Appendix Table 1, https://wwwnc.cdc.gov/EID/article/31/8/24-1604-App1.xlsx).

Single-Nucleotide Variant Identification and Phylogenetic Analysis

We aligned Illumina reads from each isolate to the genome sequence of strain 128-CS by using BWA version 0.7.15 (*28*). We used bcftools version 1.9 and a haploid model to identify single-nucleotide variants

(SNVs) and skipped bases with quality <25 or alignment quality <30. We further filtered SNVs by using the bcftools_filter software, as previously described (*32*), to remove variants with SNV quality scores of <200, read consensus <75%, read depth <5, read numbers of <1 in each direction, or locations within repetitive regions as defined by BLAST alignment of the reference genome sequence against itself. We generated a maximum-likelihood phylogenetic tree from the core genome alignment by using IQ-TREE version 2.2.0 and the ModelFinder function to estimate the best fit nucleotide substitution model by means of Bayesian information criterion (*33*,*34*). We used the ultrafast boostrap method (*35*) with 1,000 replicates to assess tree topology. We used phylo-treetime 0.11.4 to estimate time-scaled phylogeny by using the previously inferred maximum-likelihood phylogeny and incorporating specimen sampling dates using the covariation and stochastic-resolve options, an autocorrelated molecular clock with the relax 1.0 0.5 option, and then rerooted the tree by using the least-squares method (*36*). We visualized and annotated the tree in R version 4.2.2 (The R Project for Statistical Computing) by using the ggtree version 3.8.0 and ggtreeExtra version 1.8.1 packages (*37*,*38*).

Results

During 2015–2023, the AKUH clinical microbiology laboratory identified 432 presumed *Clavispora* (formerly *Candida*) *lusitaniae* fungemia cases. Presumed *C. lusitaniae* cases detected from blood cultures increased from 10–20 cases/year during 2015–2019 to 30 cases in 2020 and 56 cases in 2021. The number of cases detected from cultures from blood specimens further increased to 108 in 2022 and to 150 in 2023 (Figure 1, panel A), representing ≤0.11% of the total annual blood culture specimens processed by the laboratory (Appendix Table 2). Of the 432 *C. lusitaniae* cases, 415 patients (96.1%) were <13 years (4,745 days) of age and 365 (84.5%) were <1 year (365 days) of age: 326 (75.4%) <3 months of age, 274 (63.4%) <1 month of age, and 68 (15.7%) <7 days of age. Reflective of the primary referral base for the AKUH laboratory, most (n = 369; 85.4%) *C. lusitaniae* bloodstream cases were from Karachi, and 241 (55.8%) samples were from 1 tertiary care public sector pediatric hospital.

Using the laboratory practices for isolate banking described herein, 136 presumed *C. lusitaniae* isolates had been banked: 21 of 31 isolates cultured in 2020, 0 of 56 isolates cultured in 2021, 29 of 108 isolates cultured in 2022, 80 of 150 isolates cultured in 2023, and 6 of 15 isolates cultured in January of 2024. To investigate those cases, we performed WGS on banked isolates, 121 of which yielded high-quality assemblies. We excluded 15 isolates because total contig size exceeded 12.3 million bases (n = 8), total contig number exceeded 800 (n = 11), genome coverage was <95% as determined by BUSCO (n = 9), or a combination of those factors. BUSCO analyses showed equivalent rates of assembly completeness, fragmentation, and missingness between the isolates sequenced at either institution. Querying the internal ITS sequences from the whole-genome assemblies against the NCBI ITS database showed that just 13 (11%) of the 121

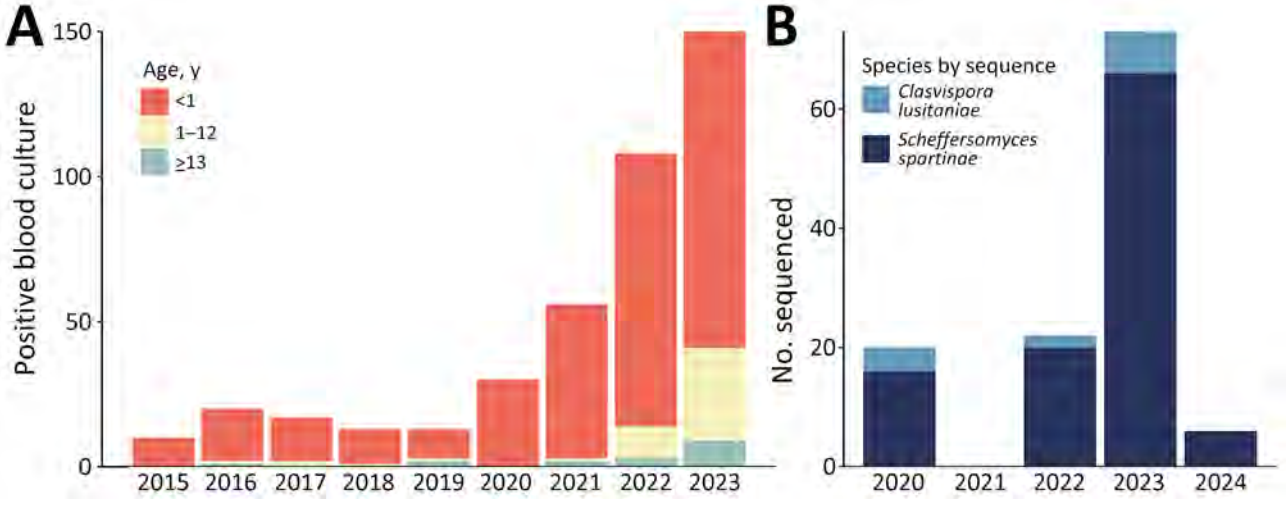

Figure 1. Characteristics of yeast biochemically identified as *Clavispora lusitaniae* during an outbreak of *Scheffersomyces spartinae* fungemia among pediatric patients, Pakistan, 2020–2024. A) Number of blood cultures with yeast identified as *C. lusitaniae* by patient age range and year, 2015–2023. Biochemical species identification performed by VITEK 2 YST ID card system (bioMérieux). B) Species designation by internal transcribed sequence among isolates initially identified as *C. lusitaniae* from blood or other sources that subsequently underwent whole-genome sequencing, 2020–2024.

high-quality genome sequences were true *C. lusitaniae*, whereas ITS sequences from the other 108 (89%) sequences had 99.3%–100% sequence identity with the ITS sequence of *Scheffersomyces spartinae* CBS 6059 (NCBI accession no. NR_111290.1) (Figure 1, panel B; Appendix Table 1).

The median age of *S. spartinae* patients was 19.5 days (range 2 days–12 years); 68.5% of cases were among infants <4 weeks of age (Table 1). For most cases, specimens were obtained in Karachi, reflective of catchment, but >8% of cases were identified in patients from other regions. Most (69.4%) cases were identified at a single hospital (hospital H) in Karachi specializing in neonatal and pediatric care. Blood cultures from that hospital constituted 1.4% of the total blood cultures processed by the AKUH clinical microbiology laboratory since 2020, and 2.9% of blood cultures from that hospital were *C. lusitaniae* positive by biochemical assay (Appendix Table 2).

We cultured *S. spartinae* from specimens received from 14 different institutions but could not determine the origin of 11% of specimens (Table 1). Of patients whose families or guardians could be contacted and consented to provide clinical information (92/108), all were hospitalized at the time of specimen collection. Treating physicians provided admitting diagnoses and brief clinical histories for 63 (58.3%) patients, 43 (68.2%) of whom were admitted for sepsis. MICs for amphotericin, azole, and echinocandin antifungal drugs were low among the 108 *S. spartinae* isolates tested, and MIC_{90} values were ≤1 μg/mL for all agents in those classes (Table 2).

Isolate 128-CS, which we selected for long-read sequencing, came from a sample collected in Karachi in December 2022. Assembly from long and short reads of 128-CS produced 8 linear chromosomes ranging in length from 1.19 to 2.05 Mbp and 1 circular mitochondrial genome, for a total genome size of 12.27 Mbp (Appendix Table 3). Comparison of the ITS sequence of isolate 128-CS to the NCBI ITS database reconfirmed *S. spartinae* (Figure 2).

Phylogenetic analysis of all 108 *S. spartinae* sequences aligned to 128-CS revealed that most sequences belonged to a clade consisting of nearly all specimens obtained from Karachi and 2 specimens from Nawabshah (Figure 3). That large clade (clade A) contained 2 subclades, clades A-1 and A-2 (Figure 4). We also identified 2 smaller clades: clade B, consisting of 1 isolate each from Karachi and Hafizabad and all 5 isolates from Lahore, and clade C, consisting of 1 genetically distant sequence isolated from a patient in Multan (Figure 3). Although the Multan isolate differed by >213,000 SNVs from 128-CS, the ITS regions of the 2 isolates were 100% identical. All isolates in clade B were collected from infants <1 month of age; the clade C isolate was collected from a 6-month-old child (Figure 3, panel A).

Table 1. Patient demographic and clinical characteristics from cases of *Scheffersomyces spartinae* fungemia among pediatric patients, Pakistan, 2020–2024

Characteristics	No. (%), n = 108
Age group	
<2 wk	40 (37.0)
2–3 wk	34 (31.5)
1–6 mo	5 (4.6)
7–11 mo	8 (7.4)
1–6 y	14 (13.0)
7–12 y	7 (6.5)
City of residence	
Karachi	99 (91.7)
Lahore	5 (4.6)
Nawabshah	2 (1.9)
Hafizabad	1 (0.9)
Multan	1 (0.9)
Isolation year	
2020	16 (14.8)
2021	0
2022	20 (18.5)
2023	66 (61.1)
2024	6 (5.6)
Hospital or institution	
Hospital B	5 (4.6)
Hospital H	75 (69.4)
Hospital N	5 (4.6)
Hospitals with only 1 case	11 (10.2)
Unknown hospital	12 (11.1)
Clinical details	
Patient family or guardian contacted	92 (85.2)
Hospitalization reported, n = 92	92 (100)
Clinical information available	63 (58.3)
Presumed sepsis, n = 63	43 (68.2)

Because most isolates cultured during 2020–2024 were closely related, we examined the characteristics of those 100 specimens. Within that clade, the median pairwise genetic distance across the 12.2 million base alignment was just 9 (range 0–22) SNVs. The time-scaled maximum-likelihood phylogenetic tree showed that, despite the small genetic distances between sequences, subclades A-1 and A-2 are separated with >80% bootstrap support (Figure 4). Isolates

Table 2. MICs of 108 isolates from *Scheffersomyces spartinae* fungemia among pediatric patients, Pakistan, 2020–2024*

Antifungal drug	MIC, μg/mL		
	Detected range	MIC_{50}	MIC_{90}
Fluconazole	0.06–16	0.5	1
Itraconazole	0.015–2	0.06	0.12
Voriconazole	0.008–1	0.03	0.03
Posaconazole	0.008–1	0.03	0.06
Flucytosine	0.06–64	32	64
Amphotericin	0.03–0.5	0.12	0.25
Caspofungin	0.015–0.5	0.06	0.12
Anidulafungin	0.015–0.5	0.12	0.12
Micafungin	0.015–0.25	0.06	0.12

*MIC_{50}, concentration required to inhibit 50% of strains; MIC_{90}, concentration required to inhibit 90% of strains.

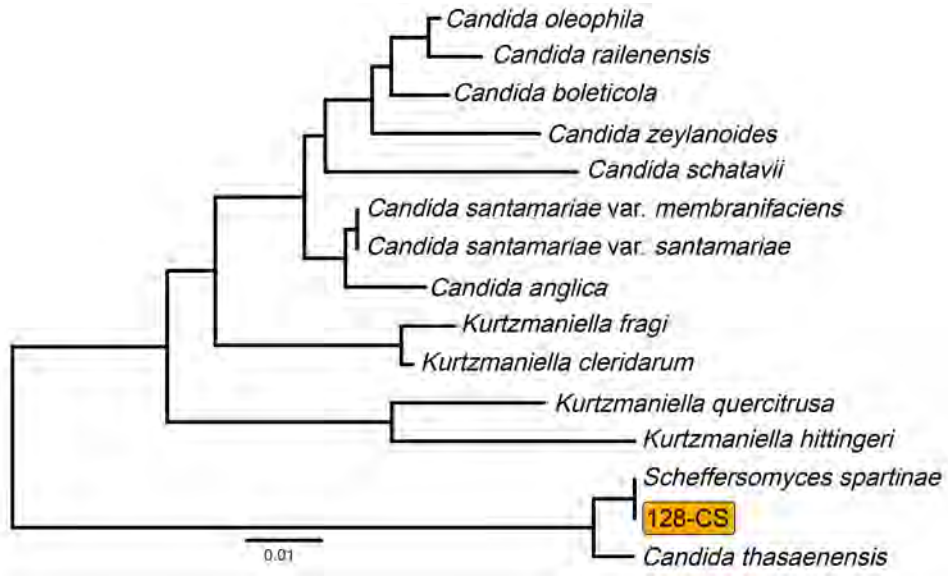

Figure 2. Internal transcribed spacer (ITS) sequence phylogeny of *Scheffersomyces spartinae* isolate 128-CS from fungemia among pediatric patients, Pakistan, 2020–2024. Midpoint-rooted neighbor-joining tree from alignment of ITS sequence of strain 128-CS and the 14 most closely related ITS sequences in the National Center for Biotechnology Information Fungal Internal Transcribed Spacer RNA database (BioProject accession no. PRJNA177353). Scale bar indicates nucleotide substitutions per site.

from 2020 were all in clade A-2 and clustered more closely with each other than with most later isolates; we excluded 1 isolate, 2020-498, which did not follow the fitted molecular clock. All 5 isolates from hospital B were in the same subclade; otherwise, we noted no apparent association between sampling location and either isolation date or genetic similarity.

Isolates from patients <1 month of age predominated in subclade A-2, comprising 93.6% of that clade compared with 38.5% of clade A-1 ($p<0.001$ by Fisher exact test) (Table 3). No association between patient age and genetic similarity was noted among isolates in either subclade. Only isolates from hospital H were represented in both subclades and were equally distributed (Table 3). Those results suggest that genetic distances are small among *S. spartinae* in that group; that isolates were diverse across time, geography, and patient ages; and that closely related but independent lineages were cocirculating within the same region and institution, potentially indicating separate sources of infection.

Discussion

We describe *S. spartinae* as a cause of fungemia in pediatric patients in Pakistan. *S. spartinae* has been previously described as an environmental organism

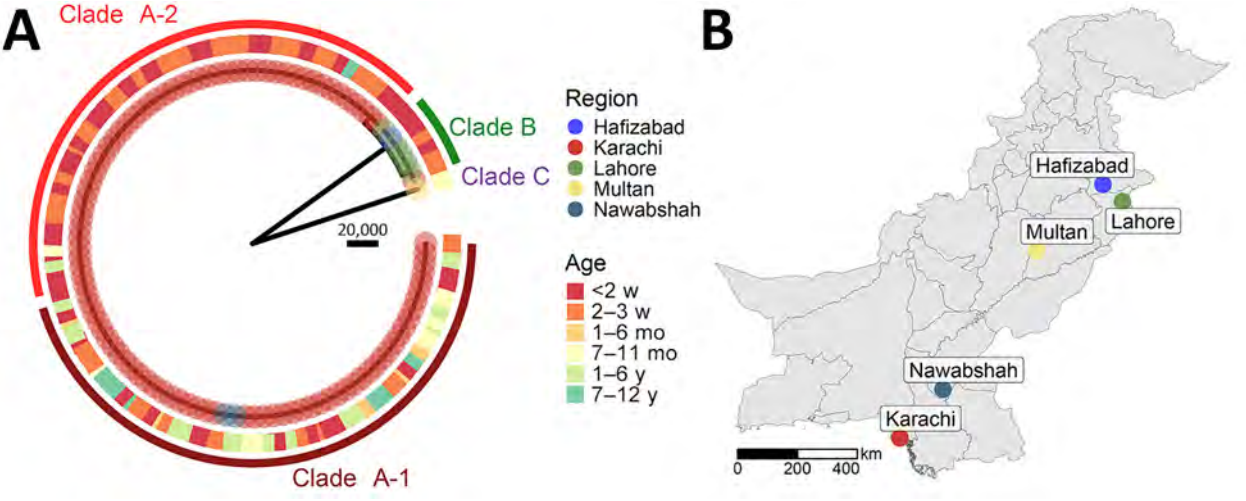

Figure 3. Whole-genome phylogeny and locations of *Scheffersomyces spartinae* fungemia isolates among pediatric patients, Pakistan, 2020–2024. A) Midpoint-rooted maximum-likelihood phylogenetic tree from whole-genome sequence alignment of 108 *S. spartinae* isolates from human blood cultures. Tip circles indicate the patient's city of residence. Outer squares indicate the age of the patient. Arcs indicate observed major phylogenetic clades or subclades. Scale bar indicates number of single-nucleotide variant differences corresponding to branch lengths. B) Cities of residence for all patients with *S. spartinae*–positive blood cultures detected by whole-genome sequencing.

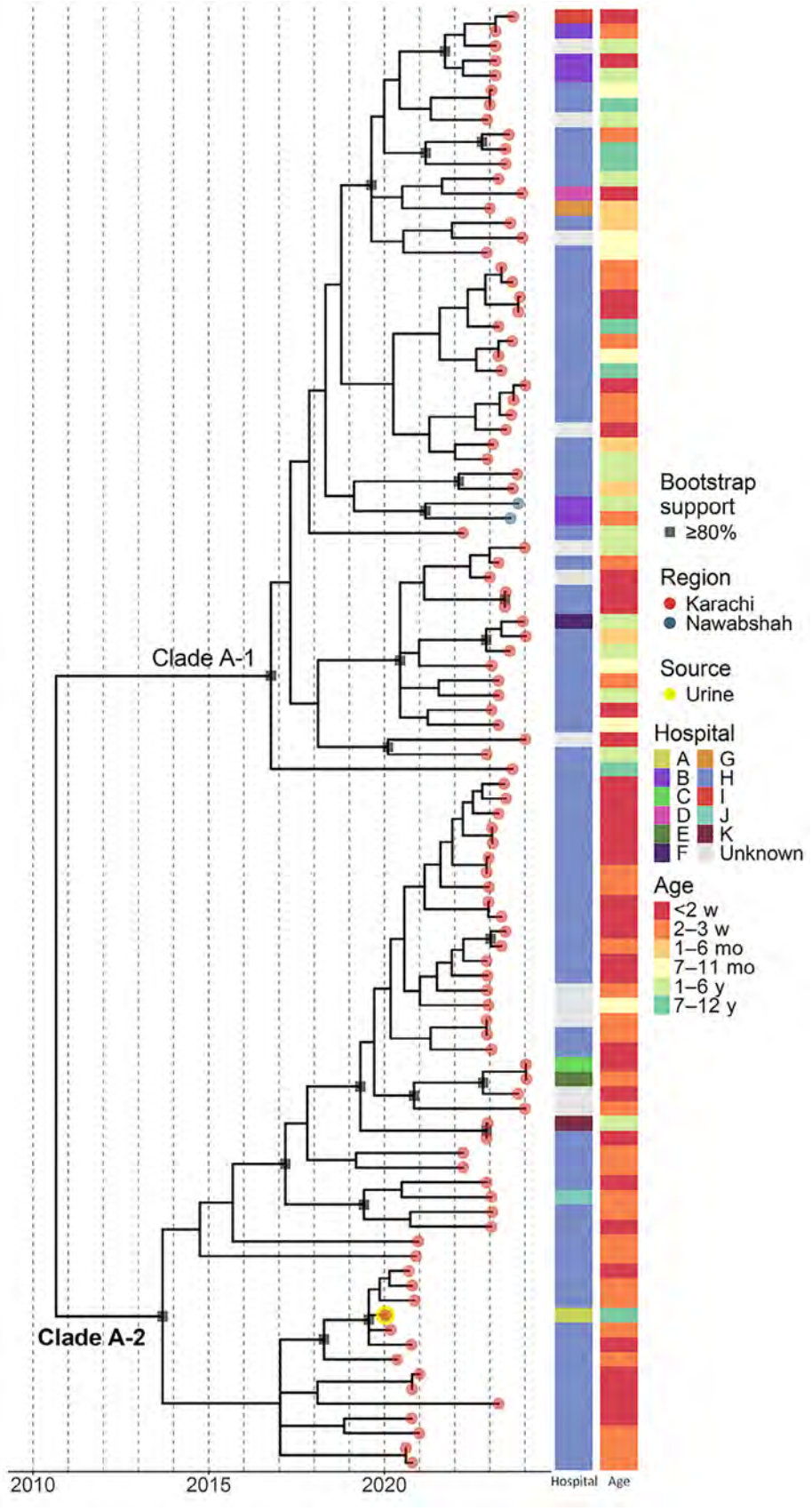

Figure 4. Time-scaled maximum-likelihood phylogenetic tree of *Scheffersomyces spartinae* major clade A in cases of fungemia among pediatric patients, Pakistan, 2020–2024. Nodes marked by gray squares indicate branches with ≥80% bootstrap support based on 1,000 resamplings. Tree tips correspond to the sampling date. Tip colors indicate patient's city of residence. All specimens isolated from blood cultures other than the specimen from urine highlighted in yellow. Heatmaps show the anonymized hospital or institution at which the specimen was collected and age group of the patient. Dotted vertical lines represent individual years.

capable of surviving extreme conditions, but isolation from clinical specimens represents emergence as a human pathogen. The genus *Scheffersomyces* was proposed by Kurtzman and Suzuki on the basis of D1-D2 large subunit rRNA and small subunit rRNA sequencing; species assigned to the *Scheffersomyces* genus were originally included in the genus *Pichia* (*39*). Most *Scheffersomyces* species ferment xylose and are used in industrial applications (*39*–*41*). The assignment of *S. spartinae* to the genus was originally considered uncertain because of weak bootstrap support in the D1–D2 small subunit tree and because *S. spartinae* does not ferment xylose. According to our literature review, *S. spartinae* has not previously been reported as a cause of human infections nor cultured in healthcare facilities. We speculate *S. spartinae* might be emerging in humans because of introduction from environmental sources into healthcare environments. However, given the broad distribution of healthcare facilities from which we cultured *S. spartinae* in Pakistan, we cannot rule out nonhealthcare community sources of infection.

The reasons for the emergence of some fungi as agents of human infection have been multifactorial. Fungi often survive extreme conditions, adapt to selection pressures, and develop enhanced thermotolerance, virulence, and antifungal drug resistance. Emergence of *Candida auris* in human infections has been attributed to global warming (*6*,*7*); some researchers postulate that *C. auris* inhabits an environmental niche and has only recently become a human pathogen (*4*). Low virulence fungi such as *Saccharomyces cerevisiae*, *Saprochaeta clavate*, and *Rhodotorula* spp. can contaminate food, medical products, and healthcare environments and cause infections in susceptible hosts (*10*–*12*). Alterations in the geographic range of *Cryptococcus deuterogattii* from tropical regions to temperate climates have led to human infections in nonendemic areas, attributed to human activity, thermal adaptation, and climate change (*5*).

Another reason for increased emergence of fungal infections is environmental disruption caused by natural disasters, which can lead to a wider distribution of fungi (*9*). An example is increased human *Coccidioides immitis* infections after earthquake-related landslides and sandstorms in previously low-prevalence areas (*8*). Whether similar or other factors contributed to the emergence of *S. spartinae* as a human pathogen is unclear.

Cases of *C. lusitaniae* fungemia identified by the AKUH laboratory began increasing in 2020, and a further substantial rise in cases began in 2022. Most *C. lusitaniae* patients were children <1 year of age who were admitted to hospitals in the city of Karachi. During 2015–2019, rare *Candida* species were reported as causes of invasive infections in neonatal and pediatric populations in Pakistan (*42*). Isolation of *C. lusitaniae* was infrequent, however, so rising case numbers from 2022 onward were flagged by the laboratory, which more frequently banked cultured isolates. Biochemical identification of *Candida* by the VITEK 2 YST ID card system inaccurately identified the organism, and most of the isolates were ultimately identified as *S. spartinae* by whole-genome and ITS sequencing. The high percentage of isolates subsequently identified as *S. spartinae* suggests that at least some of the isolates identified as *C. lusitaniae* from before 2020 also might have been *S. spartinae*, but we cannot verify that hypothesis because earlier specimens were not banked.

Table 3. Subclade characteristics from *Scheffersomyces spartinae* fungemia among pediatric patients, Pakistan, 2020–2024*

Characteristics	Clade, no. (%)		p value
	A-1, n = 52	A-2, n = 47	
Age group			
<2 wk	12 (23.1)	23 (48.9)	**0.011**
2–3 wk	10 (19.2)	21 (44.7)	**0.0090**
1–6 mo	5 (9.6)	0	0.058
7–11 mo	6 (11.5)	1 (2.1)	0.11
1–6 y	13 (25)	1 (2.1)	**0.001**
7–12 y	6 (11.5)	1 (2.1)	0.11
Hospital			
A	0	1 (2.1)	0.47
B	5 (9.6)	0	0.058
C	0	1 (2.1)	0.47
D	1 (1.9)	0	1
E	0	1 (2.1)	0.47
F	1 (1.9)	0	1
G	1 (1.9)	0	1
H	36 (69.2)	37 (78.7)	0.36
I	1 (1.9)	0	1
J	0	1 (2.1)	0.47
K	0	1 (2.1)	0.47
Unknown	7 (13.5)	5 (10.6)	0.76

*All p values from Fisher exact test comparing values for each age group or hospital to values from all other age groups or hospitals. Bold font indicates statistical significance.

Species misidentification is concerning and implies that phenotypic identification systems cannot reliably identify emerging pathogens. Misidentification underscores the need for using molecular approaches, such as ITS sequencing, for species identification. Decreasing costs and increasing availability of WGS promise improved species identification as well as strain typing and genomic epidemiology, but the technology remains difficult to access in many low-resource areas.

Although evidence implies that cases of *S. spartinae* infection represent the emergence of a new pathogen, the possibility of a pseudo-outbreak (i.e., clustering of positive cultures because of contamination of clinical specimens incorrectly attributed to infections) must also be considered. Compared with

bacterial pseudo-outbreaks, fungal pseudo-outbreaks have rarely been reported. Documented pseudo-outbreaks involving *Candida guilliermondii* were related to inadequate sterile technique during blood culture collection (*43*), contamination of heparin solution used to flush needles before blood draws (*44*), and an anaerobic holding chamber in the clinical microbiology laboratory (*45*). Pseudo-outbreaks reported with other *Candida* species include *C. versatilis* contamination in olive oil used for culture media supplementation (*46*) and *C. parapsilosis* contamination of a salt solution used for grinding tissues (*47*).

Unlike prior pseudo-outbreak reports that involved temporally clustered samples from single institutions, we report isolates collected over the course of 4 years from >14 healthcare institutions across Pakistan. Furthermore, we noted considerable demographic similarity between patients from which the positive specimens were collected: >68% were <1 month of age, and >80% were <1 year of age (Table 1). Although all the isolates were cultured and identified by a single clinical microbiology laboratory at AKUH, all processes and equipment used for processing clinical specimens in the laboratory were independent of the age of the patient from which the specimen was collected. If contamination in the laboratory explained most or all observed cases, we would expect detection in cultures from patients across all age ranges and a larger number of specimens. Even when *C. lusitaniae* cases increased during 2022 and 2023, those cases constituted only 0.57% of 16,505 blood cultures processed from children <1 year of age in 2022 and only 0.60% of 18,051 cultures from children in that age group in 2023 (Appendix Table 2).

The genetic diversity of specimens across and within geographic locations (Figures 3, 4) reduces the likelihood of a single infection or contamination source. Although genetic diversity between isolates within a geographic area of sampling was low, that diversity was not inconsistent with the degree of genetic variation among geographically clustered infections caused by other yeast species, such as *C. auris* (*48*,*49*). Until we learn more about the genomic variability and evolution of *S. spartinae*, the degree of expected genetic difference among epidemiologically linked or unlinked specimens will remain unclear; however, cocirculation of at least 2 lineages in Karachi over the course of ≥4 years suggests multiple introductions into the region.

One limitation of this study is that, before 2022, AKUH prioritized its finite laboratory resources for investigating and banking invasive antimicrobial-resistant isolates and isolates from known pathogens of epidemiologic concern. As a result, isolates identified as *C. lusitaniae* were not consistently banked, and few isolates from before 2022 were available for species verification and genomic analysis. Another limitation is that detailed patient clinical and demographic information was either unavailable or difficult to obtain because of variability in record-keeping and data availability across the many institutions that provided specimens to AKUH. Many treating physicians could not be contacted because in Pakistan laboratory tests are paid out of pocket by the patients or their guardians, who often provide their own contact details rather than their physicians' contact information at sample collection. That practice greatly hinders epidemiologic investigations and transmission reconstructions to determine common exposures or shared risk factors among affected persons, to establish patients' clinical manifestations, and to assess responses to treatments or outcomes. Efforts are ongoing to establish cooperative agreements and study protocols for the most affected institutions in Pakistan for standardized data collection and sharing for *S. spartinae* fungemia cases or other unusual yeasts.

In summary, our findings underscore the value of epidemiologic monitoring for identifying infection clusters and of genomic and molecular surveillance for identifying rare and emerging pathogens. Future studies will be directed at characterizing mediators of pathogenicity and virulence factors that could contribute to *S. spartinae* emergence as a human pathogen, as well as exploring potential environmental reservoirs or other sources of infection. Nonetheless, this study demonstrates that building capacity for specimen identification and banking, WGS, and bioinformatic analysis in low- and middle-income countries like Pakistan is imperative for early detection and study of emerging infectious disease threats.

Acknowledgments

We thank Safia Bibi for her contribution.

This study was supported by the US Centers for Disease Control and Prevention (award no. NU3HCK000007) and by the US National Institutes of Health (award no. S10OD032243). Support was also provided by the Antimicrobial Resistance Working Group in the Northwestern University Buffett Institute for Global Affairs. This work was supported in part through the computational resources and staff contributions provided by Genomics Compute Cluster, which is jointly supported by the Feinberg School of Medicine, the Center for Genetic Medicine, and Feinberg's Department of Biochemistry and Molecular Genetics, the Office of the Provost, the Office for Research, and Northwestern Information Technology.

The Genomics Compute Cluster is part of Quest, Northwestern University's high-performance computing facility, with the purpose to advance research in genomics. The funding sources had no role in the study design, data collection, analysis, interpretation, or writing of the report.

Author contributions: conceptualization: K.J., J.F., R.H., E.A.O.; methodology: K.J., J.F., L.M.S., R.L.R., J.A., H.G., S.A.R.S.B., R.H., E.A.O.; software: R.L.R., E.A.O.; validation: K.J., J.F., L.M.S., N.S., E.A.O.; formal analysis: K.J., J.F., R.L.R., E.A.O.; investigation: K.J., J.F., L.M.S., J.F.H., R.L.R., C.T.E., E.M.H., M.H., S.F.M., J.A., H.G., S.Z., N.S., S.A.R.S.B., M.A., L.K.K., S.J.P., R.H., E.A.O.; resources: K.J., J.F., J.F.H., M.H., Z.H., R.H., E.A.O.; data curation: K.J., L.M.S., N.S., R.H., E.A.O.; writing original draft: K.J., E.A.O.; writing, review, and editing: K.J., J.F., L.M.S., J.F.H., R.L.R., C.T.E., E.M.H., Z.H., S.F.M., N.S., S.A.R.S.B., M.A., L.K.K., S.J.P., R.H., E.A.O.; visualization: K.J., E.A.O.; supervision: K.J., J.F., J.F.H., Z.H., L.K.K., R.H., E.A.O.; project administration: L.M.S., J.F.H., Z.H., R.H., E.A.O.; funding acquisition: J.F.H., R.H., E.A.O.

About the Author

Dr. Jabeen is a medical microbiologist at the Aga Khan University in Karachi, Pakistan. She is the Global Action Fund for Fungal Infections Country Ambassador for Pakistan. Her primary research interests include fungal diseases and antimicrobial resistance.

References

1. Fisher MC, Gurr SJ, Cuomo CA, Blehert DS, Jin H, Stukenbrock EH, et al. Threats posed by the fungal kingdom to humans, wildlife, and agriculture. MBio. 2020;11:e00449-20. https://doi.org/10.1128/mBio.00449-20
2. Wiederhold NP. Emerging fungal infections: new species, new names, and antifungal resistance. Clin Chem. 2021;68:83–90. https://doi.org/10.1093/clinchem/hvab217
3. World Health Organization. WHO fungal priority pathogens list to guide research, development and public health action. Geneva: The Organization; 2022.
4. Casadevall A, Kontoyiannis DP, Robert V. On the emergence of *Candida auris*: climate change, azoles, swamps, and birds. MBio. 2019;10:e01397-19. https://doi.org/10.1128/mBio.01397-19
5. Bartlett KH, Kidd SE, Kronstad JW. The emergence of *Cryptococcus gattii* in British Columbia and the Pacific Northwest. Curr Infect Dis Rep. 2008;10:58–65. https://doi.org/10.1007/s11908-008-0011-1
6. Chakrabarti A, Sood P. On the emergence, spread and resistance of *Candida auris*: host, pathogen and environmental tipping points. J Med Microbiol. 2021;70:001318. https://doi.org/10.1099/jmm.0.001318
7. Du H, Bing J, Hu T, Ennis CL, Nobile CJ, Huang G. *Candida auris*: epidemiology, biology, antifungal resistance, and virulence. PLoS Pathog. 2020;16:e1008921. https://doi.org/10.1371/journal.ppat.1008921
8. Schneider E, Hajjeh RA, Spiegel RA, Jibson RW, Harp EL, Marshall GA, et al. A coccidioidomycosis outbreak following the Northridge, Calif, earthquake. JAMA. 1997;277:904–8. https://doi.org/10.1001/jama.1997.03540350054033
9. Seidel D, Wurster S, Jenks JD, Sati H, Gangneux JP, Egger M, et al. Impact of climate change and natural disasters on fungal infections. Lancet Microbe. 2024;5:e594–605. https://doi.org/10.1016/S2666-5247(24)00039-9
10. Vaux S, Criscuolo A, Desnos-Ollivier M, Diancourt L, Tarnaud C, Vandenbogaert M, et al.; Geotrichum Investigation Group. Multicenter outbreak of infections by *Saprochaete clavata*, an unrecognized opportunistic fungal pathogen. MBio. 2014;5:e02309-14. https://doi.org/10.1128/mBio.02309-14
11. Wirth F, Goldani LZ. Epidemiology of *Rhodotorula*: an emerging pathogen. Interdiscip Perspect Infect Dis. 2012;2012:465717. https://doi.org/10.1155/2012/465717
12. Muñoz P, Bouza E, Cuenca-Estrella M, Eiros JM, Pérez MJ, Sánchez-Somolinos M, et al. *Saccharomyces cerevisiae* fungemia: an emerging infectious disease. Clin Infect Dis. 2005;40:1625–34. https://doi.org/10.1086/429916
13. Wickes BL, Wiederhold NP. Molecular diagnostics in medical mycology. Nat Commun. 2018;9:5135. https://doi.org/10.1038/s41467-018-07556-5
14. Lücking R, Aime MC, Robbertse B, Miller AN, Ariyawansa HA, Aoki T, et al. Unambiguous identification of fungi: where do we stand and how accurate and precise is fungal DNA barcoding? IMA Fungus. 2020;11:14. https://doi.org/10.1186/s43008-020-00033-z
15. Steenwyk JL, Balamurugan C, Raja HA, Gonçalves C, Li N, Martin F, et al. Phylogenomics reveals extensive misidentification of fungal strains from the genus *Aspergillus*. Microbiol Spectr. 2024;12:e0398023. https://doi.org/10.1128/spectrum.03980-23
16. Chen SC, Perfect J, Colombo AL, Cornely OA, Groll AH, Seidel D, et al. Global guideline for the diagnosis and management of rare yeast infections: an initiative of the ECMM in cooperation with ISHAM and ASM. Lancet Infect Dis. 2021;21:e375–86. https://doi.org/10.1016/S1473-3099(21)00203-6
17. Breyer E, Espada-Hinojosa S, Reitbauer M, Karunarathna SC, Baltar F. Physiological properties of three pelagic fungi isolated from the Atlantic Ocean. J Fungi (Basel). 2023;9:439. https://doi.org/10.3390/jof9040439
18. Urano N, Shirao A, Naito Y, Okai M, Ishida M, Takashio M. Molecular phylogeny and phenotypic characterization of yeasts with a broad range of pH tolerance isolated from natural aquatic environments. Adv Microbiol. 2019;9:56–73. https://doi.org/10.4236/aim.2019.91005
19. Hagler AN, Mendonça-Hagler LC, Pagnocca FC. Yeasts in aquatic ecotone habitats. In: Buzzini P, Lachance M-A, Yurkov A, editors. Yeasts in natural ecosystems: diversity. Cham: Springer International Publishing; 2017. p. 63–85.
20. Frigon MD, Liu D. Effect of high salinity on yeast activated sludge reactor operation. Water Sci Technol. 2016;74:2124–34. https://doi.org/10.2166/wst.2016.391
21. Manni M, Berkeley MR, Seppey M, Simão FA, Zdobnov EM. BUSCO update: novel and streamlined workflows along with broader and deeper phylogenetic coverage for scoring of eukaryotic, prokaryotic, and viral genomes. Mol Biol Evol. 2021;38:4647–54. https://doi.org/10.1093/molbev/msab199
22. White T, Bruns T, Lee S, Taylor J, Innis M, Gelfand D, et al. Amplification and direct sequencing of fungal ribosomal RNA genes for phylogenetics. In: Innis MA, Gelfand DH, Sninsky JJ, White TJ, editors. PCR protocols: a guide to methods and applications, volume 18. San Diego: Academic Press; 1990. p. 315–22.

23. Altschul SF, Gish W, Miller W, Myers EW, Lipman DJ. Basic local alignment search tool. J Mol Biol. 1990;215:403–10. https://doi.org/10.1016/S0022-2836(05)80360-2
24. Katoh K, Standley DM. MAFFT multiple sequence alignment software version 7: improvements in performance and usability. Mol Biol Evol. 2013;30:772–80. https://doi.org/10.1093/molbev/mst010
25. Simonsen M, Mailund T, Pedersen CNS. Rapid neighbour-joining. In: Cradall KA, Lagergren J, editors. WABI '08: Proceedings of the 8th international workshop on algorithms in bioinformatics. Berlin: Springer Berlin Heidelberg; 2008. p. 113–22.
26. Wick RR, Judd LM, Cerdeira LT, Hawkey J, Méric G, Vezina B, et al. Trycycler: consensus long-read assemblies for bacterial genomes. Genome Biol. 2021;22:266. https://doi.org/10.1186/s13059-021-02483-z
27. Vaser R, Šikić M. Time- and memory-efficient genome assembly with Raven. Nat Comput Sci. 2021;1:332–6. https://doi.org/10.1038/s43588-021-00073-4
28. Li H, Durbin R. Fast and accurate short read alignment with Burrows-Wheeler transform. Bioinformatics. 2009;25:1754–60. https://doi.org/10.1093/bioinformatics/btp324
29. Wick RR, Holt KE. Polypolish: Short-read polishing of long-read bacterial genome assemblies. PLOS Comput Biol. 2022;18:e1009802. https://doi.org/10.1371/journal.pcbi.1009802
30. Zimin AV, Salzberg SL. The genome polishing tool POLCA makes fast and accurate corrections in genome assemblies. PLOS Comput Biol. 2020;16:e1007981. https://doi.org/10.1371/journal.pcbi.1007981
31. Zimin AV, Marçais G, Puiu D, Roberts M, Salzberg SL, Yorke JA. The MaSuRCA genome assembler. Bioinformatics. 2013;29:2669–77. https://doi.org/10.1093/bioinformatics/btt476
32. Bulman ZP, Krapp F, Pincus NB, Wenzler E, Murphy KR, Qi C, et al. Genomic features associated with the degree of phenotypic resistance to carbapenems in carbapenem-resistant *Klebsiella pneumoniae*. mSystems. 2021;6:e0019421. https://doi.org/10.1128/msystems.00194-21
33. Kalyaanamoorthy S, Minh BQ, Wong TKF, von Haeseler A, Jermiin LS. ModelFinder: fast model selection for accurate phylogenetic estimates. Nat Methods. 2017;14:587–9. https://doi.org/10.1038/nmeth.4285
34. Minh BQ, Schmidt HA, Chernomor O, Schrempf D, Woodhams MD, von Haeseler A, et al. IQ-TREE 2: new models and efficient methods for phylogenetic inference in the genomic era. Mol Biol Evol. 2020;37:1530–4. https://doi.org/10.1093/molbev/msaa015
35. Hoang DT, Chernomor O, von Haeseler A, Minh BQ, Vinh LS. UFBoot2: improving the ultrafast bootstrap approximation. Mol Biol Evol. 2018;35:518–22. https://doi.org/10.1093/molbev/msx281
36. Sagulenko P, Puller V, Neher RA. TreeTime: maximum-likelihood phylodynamic analysis. Virus Evol. 2018;4:vex042. https://doi.org/10.1093/ve/vex042
37. Yu G. Using ggtree to visualize data on tree-like structures. Curr Protoc Bioinformatics. 2020;69:e96. https://doi.org/10.1002/cpbi.96
38. Xu S, Dai Z, Guo P, Fu X, Liu S, Zhou L, et al. ggtreeExtra: compact visualization of richly annotated phylogenetic data. Mol Biol Evol. 2021;38:4039–42. https://doi.org/10.1093/molbev/msab166
39. Kurtzman CP, Suzuki M. Phylogenetic analysis of ascomycete yeasts that form coenzyme Q-9 and the proposal of the new genera *Babjeviella*, *Meyerozyma*, *Millerozyma*, *Priceomyces*, and *Scheffersomyces*. Mycoscience. 2010;51:2–14. https://doi.org/10.1007/S10267-009-0011-5
40. Kurtzman CP, Suzuki M. Chapter 65: *Scheffersomyces*. In: Kurtzman CP, Fell JW, Boekhout T, editors. The yeasts, fifth edition. London: Elsevier; 2011. p. 773–7.
41. Tan L, He M, Song L, Fu X, Shi S. Aerobic decolorization, degradation and detoxification of azo dyes by a newly isolated salt-tolerant yeast *Scheffersomyces spartinae* TLHS-SF1. Bioresour Technol. 2016;203:287–94. https://doi.org/10.1016/j.biortech.2015.12.058
42. Rattani S, Memon S, Jabeen K, Farooqi J. Spectrum of invasive yeast infections in neonates, children and adults in Pakistan over five years: 2015–2019. Infect Dis J Pakistan. 2021;30:14–8.
43. Medeiros EA, Lott TJ, Colombo AL, Godoy P, Coutinho AP, Braga MS, et al. Evidence for a pseudo-outbreak of *Candida guilliermondii* fungemia in a university hospital in Brazil. J Clin Microbiol. 2007;45:942–7. https://doi.org/10.1128/JCM.01878-06
44. Yagupsky P, Dagan R, Chipman M, Goldschmied-Reouven A, Zmora E, Karplus M. Pseudooutbreak of *Candida guilliermondii* fungemia in a neonatal intensive care unit. Pediatr Infect Dis J. 1991;10:928–32.
45. Kirby JE, Branch-Elliman W, LaSalvia MT, Longhi L, MacKechnie M, Urman G, et al. Investigation of a *Candida guilliermondii* pseudo-outbreak reveals a novel source of laboratory contamination. J Clin Microbiol. 2017;55:1080–9. https://doi.org/10.1128/JCM.02336-16
46. Brandt ME, Benjamin LE, Steinkraus GE. Pseudooutbreak of *Candida versatilitis* fungemia in a microbiology laboratory. Diagn Microbiol Infect Dis. 2003;46:73–5. https://doi.org/10.1016/S0732-8893(02)00573-4
47. Deresinski SC, Clemons KV, Kemper CA, Roesch K, Walton B, Stevens DA. Genotypic analysis of pseudoepidemic due to contamination of Hanks' balanced salt solution with *Candida parapsilosis*. J Clin Microbiol. 1995;33:2224–6. https://doi.org/10.1128/jcm.33.8.2224-2226.1995
48. Gorzalski A, Ambrosio FJ III, Massic L, Scribner MR, Siao DD, Hua C, et al. The use of whole-genome sequencing and development of bioinformatics to monitor overlapping outbreaks of *Candida auris* in southern Nevada. Front Public Health. 2023;11:1198189. https://doi.org/10.3389/fpubh.2023.1198189
49. Roberts SC, Zembower TR, Ozer EA, Qi C. Genetic evaluation of nosocomial *Candida auris* transmission. J Clin Microbiol. 2021;59:e02252-20. https://doi.org/10.1128/JCM.02252-20

Address for correspondence: Egon A. Ozer, Northwestern University Feinberg School of Medicine, 303 E Superior St, Ste 900, Chicago, IL 60611, USA; email: e-ozer@northwestern.edu

Transmission Dynamics of Highly Pathogenic Avian Influenza A(H5N1) and A(H5N6) Viruses in Wild Birds, South Korea, 2023–2024

Ye-Ram Seo,[1] Andrew Y. Cho,[1] Dong-Ju Kim,[1] Young-Jae Si, Hye-sung Jeong, Su-woong Lee, Chang-Seon Song, Dong-Hun Lee

We analyzed 15 cases of highly pathogenic avian influenza (HPAI) clade 2.3.4.4b virus infections detected in wild birds in South Korea during September 2023–March 2024. We isolated and sequenced 8 H5N1 and 7 H5N6 viruses. We investigated spatiotemporal transmission dynamics by using a Bayesian discrete trait phylodynamic model that incorporated geographic and host species information. Our source–sink dynamics support introductions of H5N1 viruses from northern Japan to South Korea and subsequent spread through multiple regions in South Korea. The H5N6 viruses were most likely introduced into southwestern South Korea and spread northeastward. Wild waterfowl, especially wild ducks, played a key role in transmission of both H5N1 and H5N6 viruses. Our data showed multiple introductions and extensive spread of HPAI clade 2.3.4.4b viruses and bidirectional transmission between Japan and South Korea. Our results highlight the value of enhanced active surveillance for monitoring HPAI viruses, which can provide insight into preventing future outbreaks.

Highly pathogenic avian influenza viruses (HPAIVs) cause severe clinical signs and high mortality rates in gallinaceous birds, leading to substantial economic losses in the poultry industry (*1*). Among HPAIVs, the A/Goose/Guangdong/1/1996 (gs/GD) lineage of H5Nx, which emerged in China in 1996, has caused outbreaks and diverged into 10 primary clades (nos. 0–9) and multiple subclades (*2*–*4*). Wild waterfowl play a crucial role in the wide and rapid geographic spread of gs/GD lineage highly pathogenic avian influenza (HPAI) H5Nx virus (*5*). Of note, HPAI H5Nx clade 2.3.4.4b viruses have caused widespread outbreaks across diverse geographic regions, including Asia, Europe, North America, South America, Africa, and even Antarctica (*6*–*10*). Increasing reports of HPAI clade 2.3.4.4b virus infections in diverse mammalian hosts, including dairy cows in North America, raise substantial public health concerns (*11*,*12*).

In South Korea, 6 major HPAI clade 2.3.4.4b outbreaks occurred during 2017–2024 (*13*–*16*). During the 2022–2023 HPAI outbreak, 174 cases of HPAI H5N1 clade 2.3.4.4b virus infection in various wild bird species were reported throughout South Korea (*17*). Spatiotemporal analysis of HPAI H5N1 clade 2.3.4.4b viruses revealed multiple hot spots in the Korean Peninsula that were responsible for the maintenance and spread of the viruses during the outbreak (*18*,*19*). Phylodynamic analysis integrating host trait information revealed a complex intertwined relationship between different regions inside and outside the Korean Peninsula and cross-species transmission of viruses among susceptible wild bird hosts (*17*,*20*). Whole-genome sequencing (WGS) of isolates from that outbreak also revealed emergence of diverse genotypes resulting from extensive reassortment (*21*).

During September 2023–March 2024, two different HPAI clade 2.3.4.4b virus subtypes, H5N1 and H5N6, caused influenza outbreaks in wild birds and poultry farms in South Korea (*22*–*24*). In particular,

Author affiliations: Konkuk University, Seoul, South Korea (Y.-R. Seo, A.Y. Cho, C.-S. Song, D.-H. Lee); National Institute of Wildlife Disease Control and Prevention, Gwangju, South Korea (D.-J. Kim, Y.-J. Si, H.-S. Jeong, S.-W Lee)

DOI: https://doi.org/10.3201/eid3108.250373

[1]These first authors contributed equally to this article.

the index case in poultry was identified as a co-infection of H5N1 and H5N6 on a chicken farm (*24*). However, the evolutionary history and spread pattern of H5N1 and H5N6 viruses have not been clearly identified. To clarify the spatiotemporal diffusion and transmission dynamics between host species, we performed WGS on HPAIV isolates collected from wild birds during the 2023–2024 outbreak and performed a Bayesian phylodynamic analysis incorporating host species and sampling locations.

Materials and Methods

Virus Detection and Isolation

During September 2023–March 2024, the National Institute of Wildlife Disease Control and Prevention (NIWDC) of the Ministry of Environment of South Korea collected samples from wild birds as part of the national HPAI surveillance program. Samples were collected from wild bird feces (n = 11,294), carcasses (n = 555), and captured birds (n = 1,058) from 87 major migratory bird habitats across all provinces of South Korea.

Oropharyngeal and cloacal swab samples from captured birds and carcasses and bird fecal samples were placed in phosphate-buffered saline with 0.1% volume of 400 mg/mL gentamicin and homogenized. We then filtered the supernatant by using a 0.45-μm Minisart Syringe Filter (Sartorius, https://www.sartorius.com) and inoculated into the allantoic cavity of 10-day-old specific pathogen–free embryonated chicken eggs. After 72 hours of incubation at 37°C, we harvested the allantoic fluids from eggs and tested for hemagglutination activity by using 10% chicken red blood cells. We extracted RNA from allantoic fluid samples positive for hemagglutination activity by using the Maxwell RSC Simply RNA Tissue Kit (Promega, https://www.promega.com) and screened for the avian influenza virus matrix (M) gene and H5 gene using real-time reverse transcription PCR (rRT-PCR) (*25*–*27*).

WGS and Assembly

We sequenced 8 H5N1 and 7 H5N6 viruses in this study. We synthesized complementary DNA for M gene and H5 rRT-PCR–positive samples by using the SuperScript III First-Strand Synthesis System (ThermoFisherScientific, https://www.thermofisher.com). For samples confirmed as HPAIV via hemagglutinin (HA) gene sequencing, we amplified all 8 gene segments (HA, M, neuraminidase [NA], nucleoprotein [NP], nonstructural [NS], polymerase acidic [PA], and polymerase basic [PB] 1 and 2) by using AccuPrime Pfx DNA Polymerase (Invitrogen), according to methods described in a previous study (*28*). We constructed DNA libraries by using the Nextera DNA Flex Library Prep Kit (Illumina, https://www.illumina.com) and 96 dual-index barcodes, according to the manufacturer's instruction. We conducted WGS on the MiSeq platform (Illumina) with 150 bp paired-end reads. We used CLC Genomics Workbench 24.0.1 software (QIAGEN, https://www.qiagen.com) to trim and assemble reads and identified HPAIV-positive samples (Table).

Phylogenetic Analysis

To determine the genotypes and temporal signal of datasets for molecular clock analysis, we conducted maximum-likelihood analysis. We conducted BLAST searches (https://blast.ncbi.nlm.nih.gov) of all viral

Table. Detailed information on highly pathogenic avian influenza A(H5N1) and A(H5N6) virus isolates from wild birds during 2023–2024 outbreak, in chronological order, South Korea*

No.†	Collection date	Sample ID	Region	Sample type	Host species	Subtype	Isolate ID
1	2023 Nov 27	23WS022-22	Jeollabuk-do	Captured	Eurasian wigeon	H5N1	EPI_ISL_18717640
2	2023 Dec 1	23WC066	Gyeongsangbuk-do	Carcass	Whooper swan	H5N1	EPI_ISL_20051148
3	2023 Dec 2	23WC068	Gyeongsangbuk-do	Carcass	Whooper swan	H5N1	EPI_ISL_20051147
4	2023 Dec 4	23WC069	Gyeongsangbuk-do	Carcass	Whooper swan	H5N1	EPI_ISL_20051146
7	2023 Dec 8	23WC075	Gyeongsangbuk-do	Carcass	Whooper swan	H5N6	EPI_ISL_18853568
9	2023 Dec 19	23WF435	Jeollabuk-do	Feces	Mandarin duck	H5N6	EPI_ISL_18853569
10	2023 Dec 21	23WC111	Gyeongsangbuk-do	Carcass	Bean goose	H5N6	EPI_ISL_18853650
11	2023 Dec 22	23WC116	Gyeongsangbuk-do	Carcass	Whooper swan	H5N6	EPI_ISL_18853651
12	2023 Dec 22	23WC117	Gyeongsangbuk-do	Carcass	Whooper swan	H5N1	EPI_ISL_20051145
13	2024 Jan 10	23WC160	Gyeongsangnam-do	Carcass	Bean goose	H5N6	EPI_ISL_20051144
14	2024 Jan 10	23WS033-1	Gwang-ju	Feces	Mandarin duck	H5N6	EPI_ISL_20051143
16	2024 Jan 26	23WC195	Jeju island	Carcass	Northern shoveler	H5N1	EPI_ISL_20051142
17	2024 Jan 30	23WC215	Jeju island	Carcass	Gadwall	H5N1	EPI_ISL_20051141
18	2024 Feb 4	23WC224	Gyeongsangbuk-do	Carcass	Peregrine falcon	H5N1	EPI_ISL_20051140
19	2024 Feb 6	23WC229	Gyeongsangnam-do	Carcass	Great cormorant	H5N6	EPI_ISL_20051139

*ID, identification.
†Indicates the order of occurrence among the 19 confirmed cases of highly pathogenic avian influenza A(H5N1) clade 2.3.4.4b identified in wild birds during November 2023–February 2024, of which 15 viruses were detected and isolated by National Institute of Wildlife Disease Control and Prevention.

genomes sequenced in this study against the GISAID database (https://www.gisaid.org). We used the retrieved results as reference sequences for phylogenetic analysis. We used ElimDupes software (https://www.hiv.lanl.gov/content/sequence/elimdupesv2/elimdupes.html) to remove identical sequences. We aligned nucleotide sequences of each gene segment by using MAFFT version 7.490 (https://mafft.cbrc.jp). We constructed maximum-likelihood trees for each gene (PB2, PB1, PA, HA, NP, NA, M, and NS) by using RAxML version 8.0 (https://github.com/stamatak/standard-RAxML) and the general time-reversible model with 1,000 bootstrap iterations. We used iTOL (https://itol.embl.de) to visualize the trees and considered a cluster monophyletic only when it had a bootstrap support value >70 and a nucleotide sequence identity >97% (*29*).

We focused the phylodynamic analysis on the HA gene because of its variability and role as a key antigen. We extracted HA gene sequences belonging to same clade of our sequences from the maximum-likelihood phylogenetic tree. We used TempEst version 1.5.3 (http://tree.bio.ed.ac.uk/software/tempest) to conduct root-to-tip regression analysis and assess the temporal signal. Upon confirming a significant temporal signal (R^2 >0.5), we used datasets to investigate transmission dynamics across geographic regions and host species. We conducted Bayesian discrete trait phylodynamic analyses of the HA gene by using BEAST version 1.10.4 (https://beast.community). We broadly categorized traits into host and region, and to reduce bias among traits, we performed subsampling, resulting in 6 major datasets (Appendix Table 1, https://wwwnc.cdc.gov/EID/article/31/8/25-0373-App1.pdf). For H5N1, we constructed 2 datasets for phylogeography. The discrete categories for estimation of international virus spread consisted of South Korea (n = 10), northern Japan (n = 10), central Japan (n = 6), southern Japan (n = 12), and outside of Korean Peninsula (i.e., Russia and China, n = 10). The discrete categories for estimation of virus spread between provinces within South Korea included Gyeong-buk (southeast province of South Korea, n = 5), Jeonbuk (southwest province of South Korea, n = 1), Jeonnam (south-southwest province of South Korea, n = 2), Jeju (southern island of South Korea, n = 3), and Japan (n = 10). Similarly, the regional dataset for H5N6 viruses included Gyeong-buk (n = 3), Gyeong-nam (south-southeast province of South Korea, n = 2), Jeonbuk (n = 1), Jeonnam (n = 3), and Japan (n = 1).

For datasets analyzing transmission among hosts, we categorized H5N1 sequences into raptors (n = 1), domestic ducks (n = 2), and wild waterfowl (n = 8) from South Korea and wild waterfowl (n = 4) and crows (n = 6) from Japan. The H5N6 sequence dataset included domestic ducks (n = 2) and wild waterfowl (n = 7) from South Korea, 1 raptor from Japan, and H5N1 sequences from East Asia collected during 2022–2023 (n = 36). We categorized the viruses identified from East Asia during 2022–2023 as a discrete nominal category regardless of animal species and sampling location because the viruses from wild birds and poultry across that region during the 2022–2023 epidemic were the most probable ancestral origins inferred from the ML phylogenetic analysis. To elucidate the role of wild waterfowl in transmission, we combined H5N1 and H5N6 data to form datasets comprising wild ducks (n = 8), geese (n = 9), swans (n = 8), and other hosts (n = 10).

For Bayesian inferences, we applied a Hasegawa-Kishino-Yano substitution model plus gamma, an uncorrelated log-normal distribution, and a Gaussian Markov random field Bayesian skyride coalescent prior (*30*). We executed Markov chain Monte Carlo runs of the configuration in parallel across 3 separate chains, each consisting of 100 million steps. We combined samples from those chains after a 10% burn-in period. We used Tracer version 1.5 (https://beast.community/tracer) to analyze parameters with adequate effective sample sizes (>200). We generated a maximum clade credibility tree by using TreeAnnotator (https://beast.community/treeannotator) and visualized the tree by using FigTree version 1.4.4 (http://tree.bio.ed.ac.uk/software/Figtree). To quantify the support for transmission routes, we used SpreaD3 version 1.0.7 (https://beast.community/spread3) and interpreted results as positive support when the Bayes factor (BF) was $\geq$3 and the posterior probability (PP) was $\geq$0.5 and strong support when the BF was >20, and the PP was >0.9 (*31*). We also used FluMutGUI 3.1.1 (https://github.com/izsvenezie-virology/FluMutGUI) to identify molecular markers for mammalian adaptation across the 8 viral genes.

Results

Overview of 2023–2024 HPAI viruses from Wild Birds in South Korea

During November 27, 2023–February 6, 2024, a total of 8 cases of H5N1 and 11 cases of H5N6 were reported from wild birds in South Korea (*22*,*23*) (Appendix Figure 1). Among those cases, we isolated 8 H5N1 and 7 H5N6 viruses (Table). Next-generation sequencing yielded total read counts ranging from 21,507 to

756,810 and average coverage depths ranging from 240.80 to 8,442.09. During the 2023–2024 winter season, HPAI H5N1 was detected in a Eurasian wigeon (*Mareca penelope*) on November 27, 2023, six days before the initial H5N1 and H5N6 outbreak in poultry. The index H5N6 was detected in a Mandarin duck (*Aix galericulata*) on December 4, 2023. The number of cases gradually increased over time, reaching a peak in December 2023 (Figure 1).

Origin and Genotypes of H5N1 and H5N6 HPAI Viruses

Maximum-likelihood phylogenetic analysis of the 8 genes revealed that the HA and M genes of H5N1 and H5N6 shared >97% nucleotide sequence identity and formed a monophyletic cluster. The other 5 internal genes of isolates from South Korea formed distinct monophyletic clades within their respective subtypes (Appendix Figures 2–9). The phylogenies showed that the H5N1 viruses consisted of genes derived from HPAI H5N1 strains previously circulating in East Asia. In contrast, the H5N6 viruses were reassortants between PB2, PA, NP, and NS genes from low pathogenicity avian influenza viruses from Eurasia and the NA gene from H5N6 viruses identified in China. Those findings were consistent with findings observed in genetic analysis of index cases (*22*,*23*), suggesting no further reassortment occurred in wild birds during that outbreak.

According to recommendations from the European Food Safety Authority (*32*), we screened 14 selections of molecular markers associated with the pandemic potential of avian influenza viruses (HA, 222L; PB2, 271A, 292V, 526R, 588V, 591K, 627K, 627V, 631L, and 701N; PA, 356R; NP, 52N; and MP, 95K) by using the deduced amino acid sequences of all 15 isolates. We analyzed mammalian adaptation markers, but did not detect major markers (PB2: E627K, D701N), and we identified only a few minor markers (Appendix Table 2). Among other minor mutations, we observed 156A in HA, which is associated with increased binding to α2,6-sialic acid, and N66S in PB1-F2, which is associated with increased virulence and replication in mice.

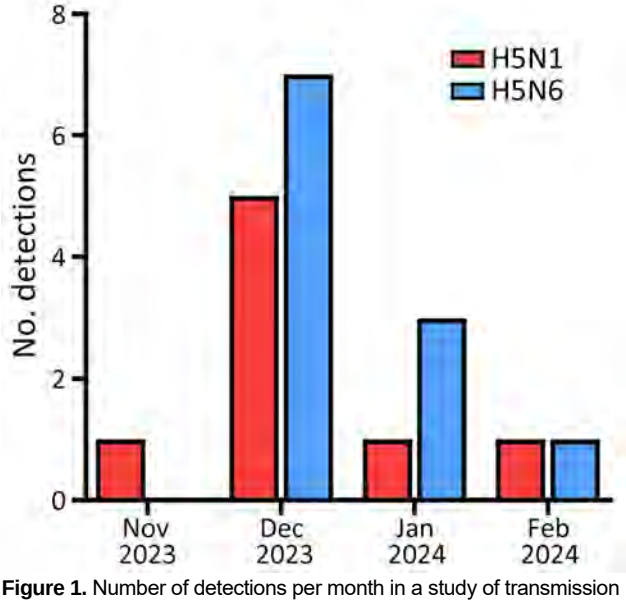

Figure 1. Number of detections per month in a study of transmission dynamics of highly pathogenic avian influenza A(H5N1) and A(H5N6) viruses in wild birds, South Korea, 2023–2024.

Transmission Dynamics of HPAI H5N1 Viruses in South Korea during 2023–2024

The maximum clade credibility phylogeny constructed from the HA gene of HPAI H5N1 viruses suggested that the virus initially entered northern Japan from China or Russia, then subsequently spread to central Japan and South Korea. Within Japan, the virus spread southward from the northern region to the southern region (Figure 2). In South Korea, we identified at least 2 separate H5N1 virus introductions, which most likely entered through the east-central region (Gyeong-buk province) and the southwest region (Jeon-nam province). The virus subsequently spread southwestward (Jeon-buk) and, finally, to Jeju Island in southern South Korea (Figure 3). Of note, within South Korea, virus dissemination from northern Japan to South Korea (BF 33.57, PP 0.91), from Japan to Gyeong-buk (BF 41.24, PP 0.926), and from Gyeong-buk to Jeon-buk (BF 31.701, PP 0.906) were among the most probable H5N1 transmission routes (BF >30 and high support values) (Appendix Tables 3, 4). Our findings suggest the virus was transmitted from Japan to South Korea through migratory wild waterfowl (Figure 4, panels A, B; Appendix Table 5). In particular, H5N1 virus was transmitted from wild waterfowl to raptors (BF 4.725, PP 0.591) and domestic ducks (BF 13.376, PP 0.803) in South Korea, as well as to crows in Japan (BF 46.186, PP 0.934) (Figure 4, panel A). We also estimated source–sink dynamics between wild waterfowl, including wild ducks, geese, swans, and other wild waterfowl. Our data suggest that wild ducks played a major role in transmitting the virus to other hosts (Figure 4, panel C).

Transmission Dynamics of HPAI H5N6 Viruses in South Korea during 2023–2024

The HA gene of HPAI H5N6 isolated during 2023–2024 was highly similar to that of the HPAI H5N1 viruses circulating in northeast Asia during the 2022–23 winter season (*23*). Phylogenetic analysis suggested that, after reassortment with the N6 gene originating

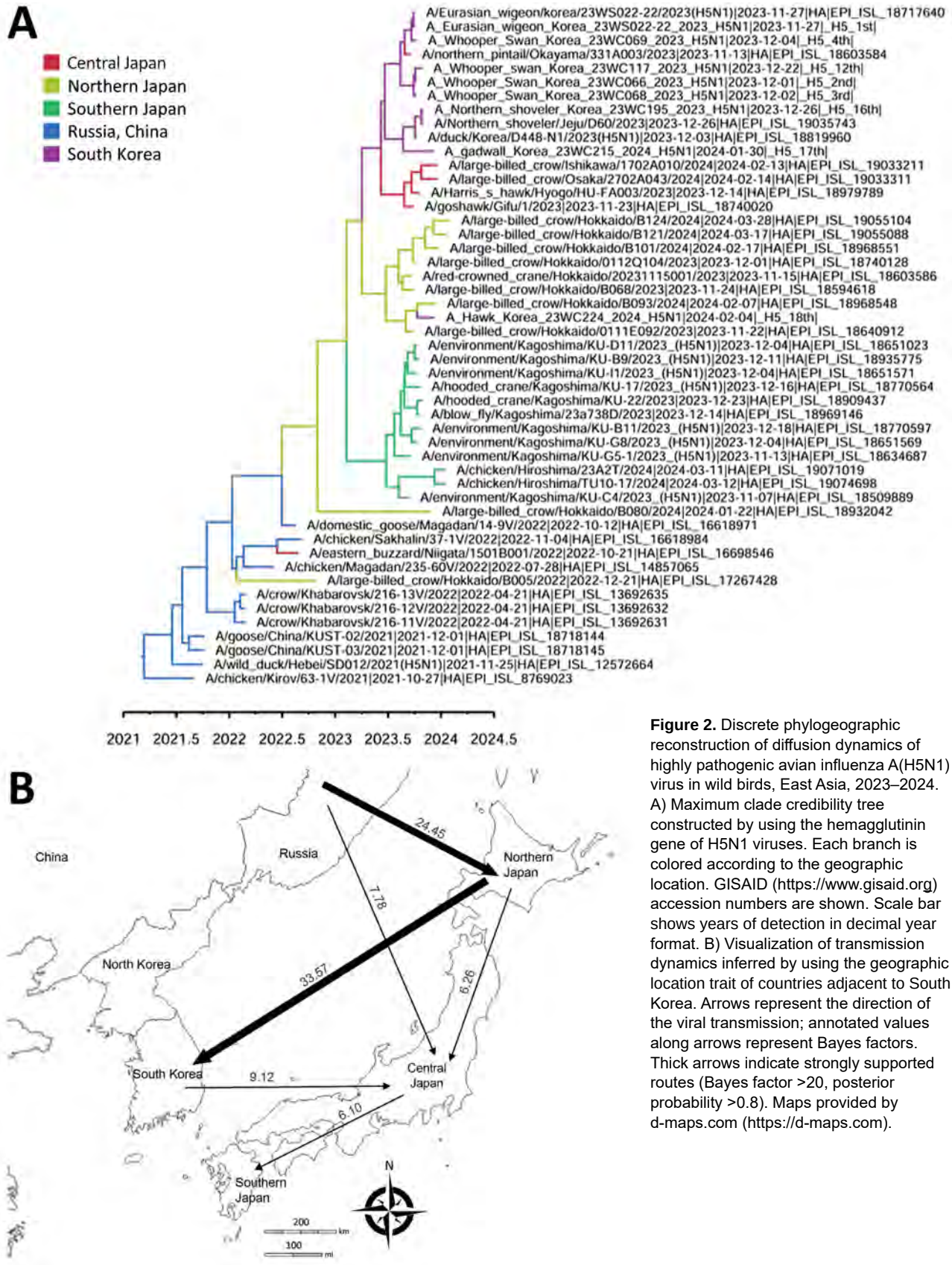

Figure 2. Discrete phylogeographic reconstruction of diffusion dynamics of highly pathogenic avian influenza A(H5N1) virus in wild birds, East Asia, 2023–2024. A) Maximum clade credibility tree constructed by using the hemagglutinin gene of H5N1 viruses. Each branch is colored according to the geographic location. GISAID (https://www.gisaid.org) accession numbers are shown. Scale bar shows years of detection in decimal year format. B) Visualization of transmission dynamics inferred by using the geographic location trait of countries adjacent to South Korea. Arrows represent the direction of the viral transmission; annotated values along arrows represent Bayes factors. Thick arrows indicate strongly supported routes (Bayes factor >20, posterior probability >0.8). Maps provided by d-maps.com (https://d-maps.com).

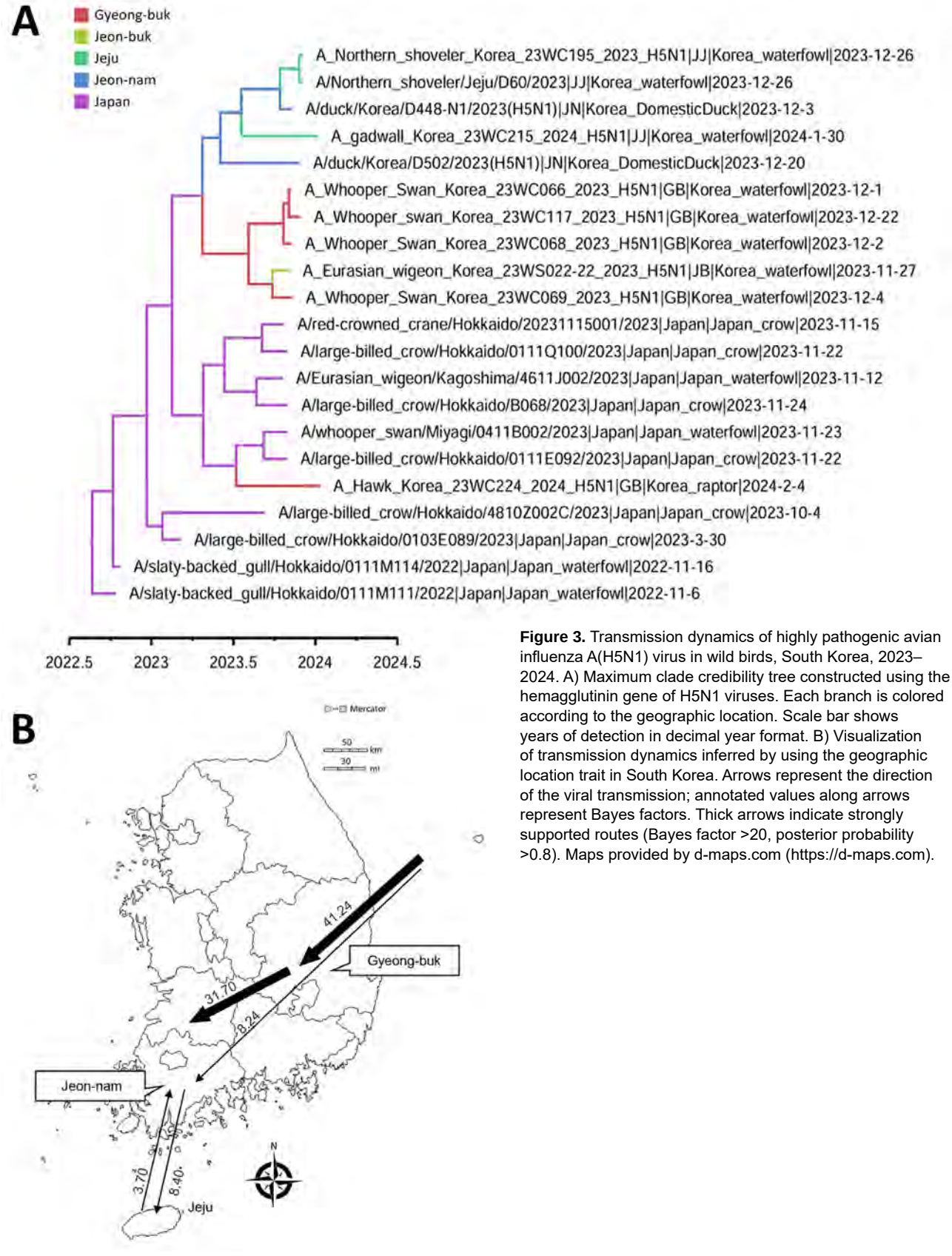

Figure 3. Transmission dynamics of highly pathogenic avian influenza A(H5N1) virus in wild birds, South Korea, 2023–2024. A) Maximum clade credibility tree constructed using the hemagglutinin gene of H5N1 viruses. Each branch is colored according to the geographic location. Scale bar shows years of detection in decimal year format. B) Visualization of transmission dynamics inferred by using the geographic location trait in South Korea. Arrows represent the direction of the viral transmission; annotated values along arrows represent Bayes factors. Thick arrows indicate strongly supported routes (Bayes factor >20, posterior probability >0.8). Maps provided by d-maps.com (https://d-maps.com).

in China, H5N6 likely entered the southwestern region of the Korean Peninsula (Jeonnam) and subsequently spread northeastward (Gyeong-buk and Gyeong-nam). Our findings also supported transmission from southern South Korea (Jeon-nam and Gyeong-nam) to southern Japan (Figure 5). Among the various HPAI H5N6 transmission routes, our findings supported movement from Jeonnam to Gyeong-nam (BF 24.176, PP 0.850) and Gyeong-buk (BF 10.022, PP 0.701) (Appendix Table 6). For virus transmission between host species, H5N6 most likely was transmitted from South Korea to Japan via wild waterfowl (Figure 4, panel C). Our findings supported virus spread from wild waterfowl to raptors in Japan (BF 18.752, PP 0.893) and to domestic ducks in South Korea (BF 14.932, PP 0.869). Consistent with the H5N1 viruses, wild ducks played the most prominent role in transmission to other species (Figure 4; Appendix Table 7).

Discussion

Over the past decade, molecular epidemiologic studies in South Korea have helped clarify the genetic diversity and transmission dynamics of HPAI clade 2.3.4.4 viruses (*16*,*33*). Genomic sequencing and phylodynamic analysis have shown that, since 2014, multiple introductions of reassortant HPAI H5Nx clade 2.3.4.4 viruses by wild waterfowl have occurred

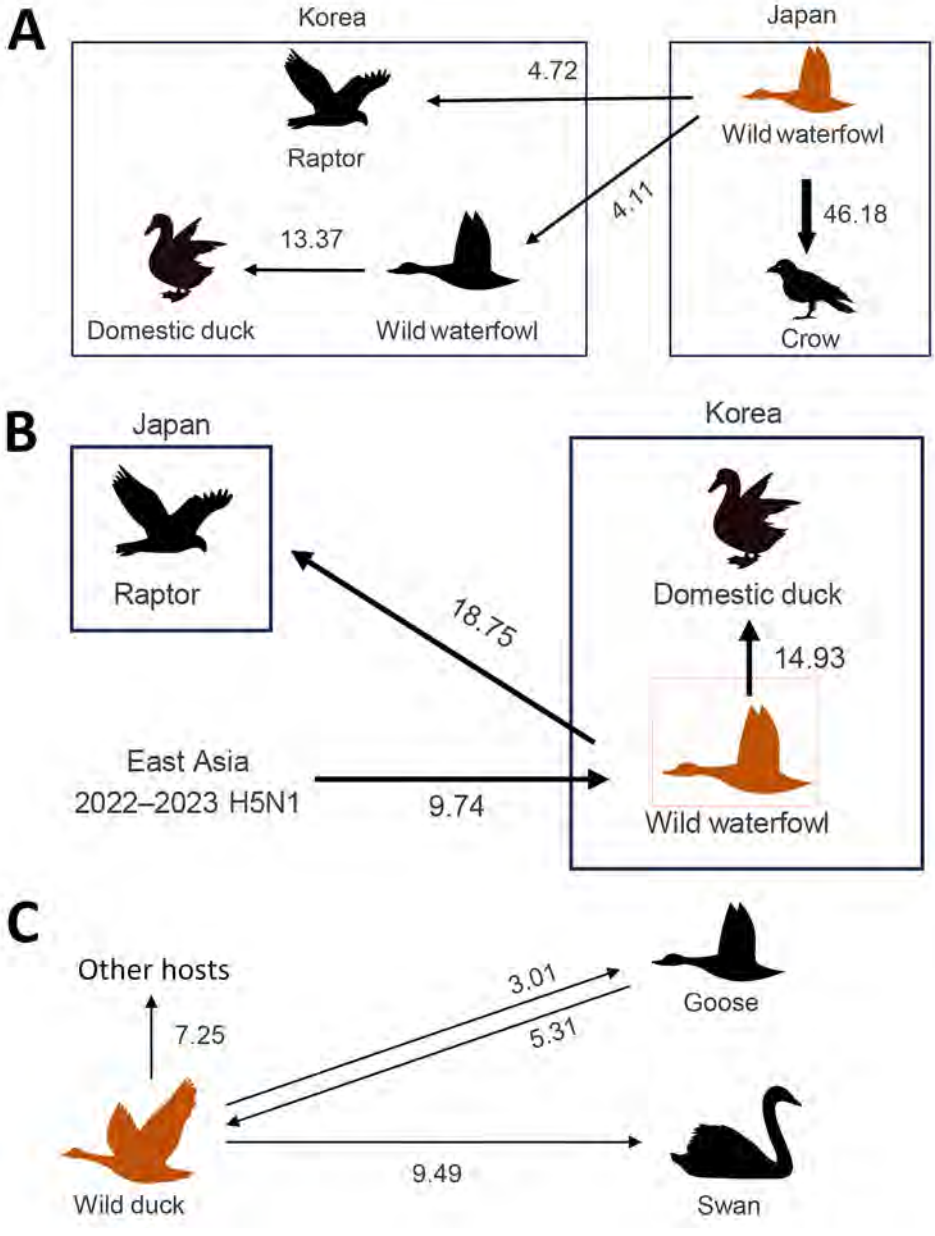

Figure 4. Transmission dynamics of highly pathogenic avian influenza (HPAI) A(H5N1) and A(H5N6) viruses in wild birds, South Korea and Asia, 2023–2024. A, B) Transmission dynamics inferred using the hemagglutinin gene of H5N1 (A) and H5N6 (B) viruses, incorporating the host trait. C) Transmission dynamics inferred using the hemagglutinin genes of both HPAI H5N1) clade 2.3.4.4b and H5N6 viruses. Arrows represent the direction of the viral transmission; annotated values represent Bayes factors. Thick arrow indicates a strongly supported route (Bayes factor >20, posterior probability >0.8). Orange indicates the largest source trait.

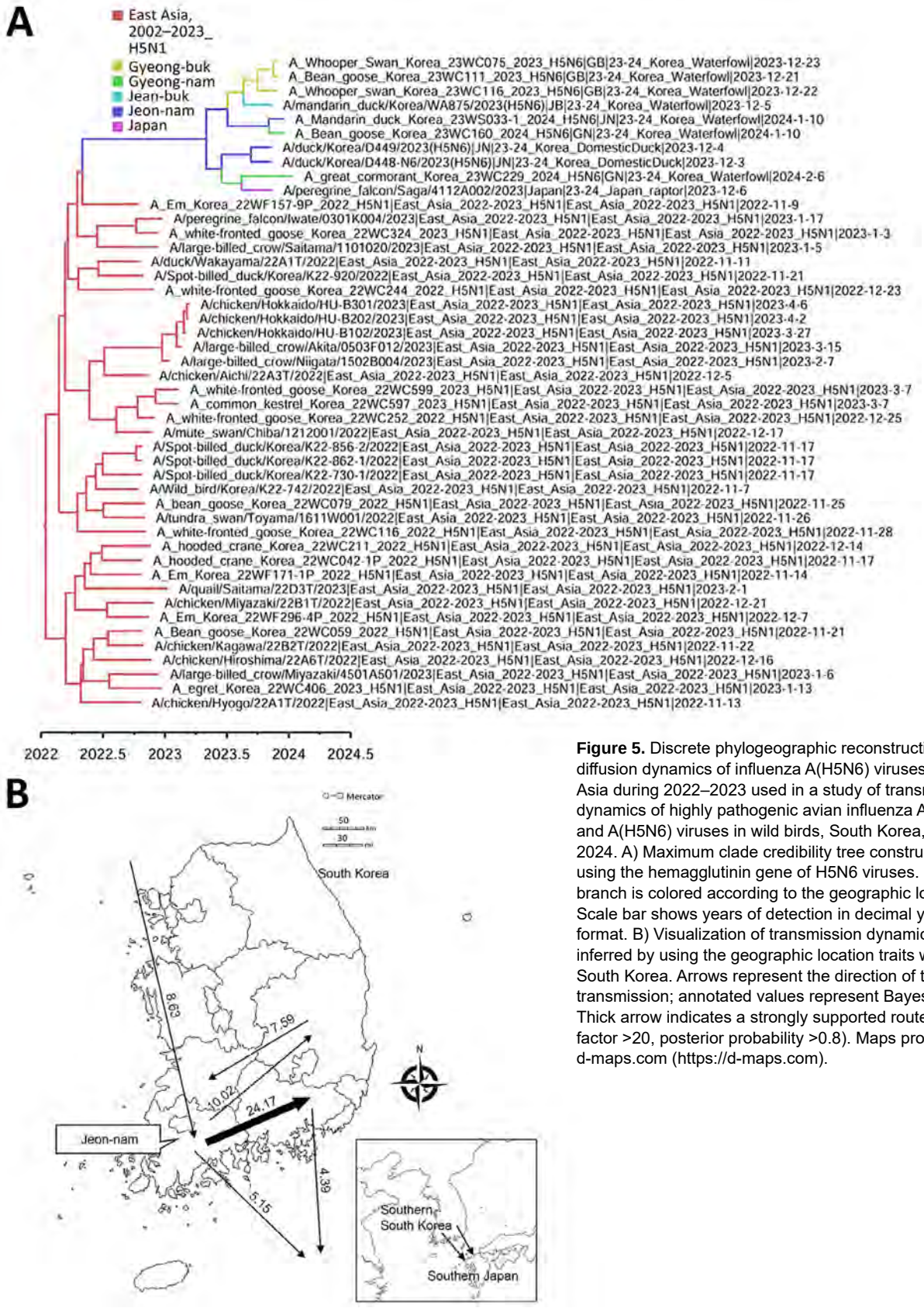

Figure 5. Discrete phylogeographic reconstruction of diffusion dynamics of influenza A(H5N6) viruses in East Asia during 2022–2023 used in a study of transmission dynamics of highly pathogenic avian influenza A(H5N1) and A(H5N6) viruses in wild birds, South Korea, 2023–2024. A) Maximum clade credibility tree constructed using the hemagglutinin gene of H5N6 viruses. Each branch is colored according to the geographic location. Scale bar shows years of detection in decimal year format. B) Visualization of transmission dynamics inferred by using the geographic location traits within South Korea. Arrows represent the direction of the viral transmission; annotated values represent Bayes factors. Thick arrow indicates a strongly supported route (Bayes factor >20, posterior probability >0.8). Maps provided by d-maps.com (https://d-maps.com).

almost every fall migration season in South Korea, and then viral detections gradually decrease or disappear within ≈5 months, around the end of waterfowl migration season (*13*–*15*,*34*,*35*). Previous phylogeography studies on HPAIV outbreaks in South Korea and Japan during 2022–2023 and 2023–2024 revealed bidirectional virus exchange between those countries (*17*,*22*,*23*). Consistent with those findings, our data also highlight the bidirectional virus exchange between South Korea and Japan. In November 2023, HPAI H5N1 viruses initially entered South Korea's Gyeongbuk and Jeonnam regions from northern Japan and subsequently spread southwestward. Given that H5N1 virus was dominant early in the season, that spread likely was associated with the southward movement of migratory birds in both South Korea and Japan during the early phase of the season. In addition, movement of H5N1 from the mid-latitude regions of South Korea to central Japan follows a pattern observed in previous seasons, suggesting that transmission might have occurred between regions at similar latitudes (*17*).

In December 2023, HPAI H5N6 appears to have entered the Jeonnam region and displayed a more irregular transmission pattern than H5N1, likely influenced by movement of wild birds within their wintering sites. Furthermore, given its introduction into the Jeonnam region, H5N6, unlike H5N1, likely was not introduced from Japan but rather from proximal countries to the west, such as China or Russia. We also observed a notable transmission link between southern Japan and southern South Korea, resembling patterns of viral movements from previous seasons where transmission occurred through hooded cranes (*Grus monacha*) in southern Japan and southern South Korea (*17*,*36*).

Migratory waterfowl disseminate HPAIVs during fall migration through north-to-south migration routes (*33*,*37*–*39*), including wild ducks (*40*), geese (*41*), and swans (*37*) that migrate from Siberia to South Korea and Japan. Those species share stopover and wintering habitats around inland water bodies and play a crucial role in the maintenance and transmission of HPAIVs. In this study, we largely attributed the diffusion of H5N1 and H5N6 viruses to wild waterfowl. Our findings indicate that wild ducks played a major role in virus transmission not only to other wild waterfowl species, including geese and swans, but also to crows, raptors, and domestic ducks. During the outbreak, whooper swans (*Cygnus cygnus*) accounted for the highest (44.45%) percentage of H5N1 cases among wild birds in South Korea, which might be because of their high susceptibility to HPAIVs and distinctive morphology (*37*). During outbreaks in South Korea, we also detected HPAIVs from raptors that likely were infected by hunting infected birds or scavenging virus-contaminated carcasses (*17*,*42*). Of note, we detected H5N6 virus from a great cormorant (*Phalacrocorax carbo*) found dead. The great cormorant used to breed in Primorsky Krai and Sakhalin, Russia, and descend to South Korea and Japan every winter but is now an invasive species in South Korea, where it has been endemic since the 2000s because of the effects of climate change; the current population is estimated to be 23,000–30,000 (*43*). HPAI virus infection in this new waterfowl population is a concern because it can substantially affect the epidemiology and ecology of the virus.

Since 2014, HPAI clade 2.3.4.4 viruses have evolved through reassortment with prevailing local low pathogenicity avian influenza viruses (*44*). A wide range of avian species, including wild and domestic waterfowl, appear to be permissive for infection and transmission of clade 2.3.4.4 viruses. Among those species, domestic ducks play a key role in the maintenance, amplification, and spread of HPAIVs of wild bird origin to terrestrial poultry (*45*). In this study, estimation of the host transmission dynamics supports that H5N1 and H5N6 viruses are transmitted from wild waterfowl to domestic ducks in South Korea. Because domestic ducks can host a variety of avian influenza viruses as a natural reservoir species, that population can accelerate the genetic and antigenic evolution of viruses, potentially giving rise to new strains with altered antigenicity, pathogenicity, or increased zoonotic potential. To prevent dissemination of HPAI from wild birds to poultry, biosecurity measures should be enhanced at poultry farms, especially those located near wild bird habitats, to block contact with wild birds or their excreta.

To minimize the impact of HPAIV in wild and domestic animals, effective information sharing among countries along migratory bird flyways and timely reporting of genomic surveillance data are essential. Next-generation sequencing–based genomic surveillance activities enable rapid and accurate characterization of complete viral genome and evolutionary history of viruses (*46*–*48*). Despite those advances and the high number of HPAIV cases reported in Eurasia in recent years, the amount of complete genome sequence data available in public databases was limited in terms of representativeness across different countries and species. In particular, the limited availability of recent genomic sequence data from poultry outbreaks could hinder the accurate reconstruction of transmission dynamics at the wildlife–domestic poultry

interface in South Korea. The limited sample sizes for certain discrete traits in this study might have introduced unrecognized biases in the inferred transmission dynamics. Nonetheless, our findings underscore the need for enhanced genomic sequencing and rapid sharing of poultry-derived viral sequences to better track viral evolution and spread.

In conclusion, public sharing of genome sequence data varies substantially between different countries and laboratories (*49*,*50*). In the last few years, we have tried to rapidly provide updated information on HPAIVs identified in wild birds in South Korea by generating and sharing HPAIV sequence data from extensive genomic surveillance efforts conducted by NIWDC (*16*,*17*,*22*,*23*). Enhanced genomic surveillance in both wild and domestic animals are needed to monitor evolution and spread of HPAIVs, which can provide insights into preventing future outbreaks and assessing zoonotic potential.

Acknowledgments

We gratefully acknowledge all data contributors, i.e., the authors and their originating laboratories responsible for obtaining the specimens and submitting laboratories for generating the genetic sequence and metadata and sharing via the GISAID Initiative, on which this research is based.

This research was financially supported by a grant from the National Institute of Wildlife Disease Control and Prevention (grant no. 2023-007) and the Ministry of Environment, South Korea. The project was supported in part by funds from the National Research Foundation of Korea grant funded by the Korean Government (no. RS-2024-00358211).

About the Author

Ms. Ye-Ram Seo is a veterinary and graduate student at the College of Veterinary Medicine, Konkuk University. Her research interests focus on the molecular epidemiology of animal diseases. Dr. Cho is a postdoctoral researcher at the College of Veterinary Medicine, Konkuk University. His research interests are molecular epidemiology and vaccine development of avian diseases.

References

1. Swayne DE. Epidemiology of avian influenza in agricultural and other man-made systems. In: Swayne DE, editor. Avian influenza. Ames (IA): Blackwell Publishing; 2008. p. 59–85.
2. Lee DH, Criado MF, Swayne DE. Pathobiological origins and evolutionary history of highly pathogenic avian influenza viruses. Cold Spring Harb Perspect Med. 2021;11:a038679. https://doi.org/10.1101/cshperspect.a038679
3. WHO/OIE/FAO H5N1 Evolution Working Group. Toward a unified nomenclature system for highly pathogenic avian influenza virus (H5N1). Emerg Infect Dis. 2008;14:e1. https://doi.org/10.3201/eid1407.071681
4. Sonnberg S, Webby RJ, Webster RG. Natural history of highly pathogenic avian influenza H5N1. Virus Res. 2013; 178:63–77. https://doi.org/10.1016/j.virusres.2013.05.009
5. Wan XF. Lessons from emergence of A/goose/Guangdong/1996-like H5N1 highly pathogenic avian influenza viruses and recent influenza surveillance efforts in southern China. Zoonoses Public Health. 2012;59:32–42. https://doi.org/10.1111/j.1863-2378.2012.01497.x
6. Bennett-Laso B, Berazay B, Muñoz G, Ariyama N, Enciso N, Braun C, et al. Confirmation of highly pathogenic avian influenza H5N1 in skuas, Antarctica 2024. Front Vet Sci. 2024;11:1423404. https://doi.org/10.3389/fvets.2024.1423404
7. Wille M, Atkinson R, Barr IG, Burgoyne C, Bond AL, Boyle D, et al. Long-distance avian migrants fail to bring 2.3.4.4b HPAI H5N1 into Australia for a second year in a row. Influenza Other Respir Viruses. 2024;18:e13281. https://doi.org/10.1111/irv.13281
8. Bevins SN, Shriner SA, Cumbee JC Jr, Dilione KE, Douglass KE, Ellis JW, et al. Intercontinental movement of highly pathogenic avian influenza A(H5N1) clade 2.3.4.4 virus to the United States, 2021. Emerg Infect Dis. 2022;28:1006–11. https://doi.org/10.3201/eid2805.220318
9. Fusaro A, Zecchin B, Giussani E, Palumbo E, Agüero-García M, Bachofen C, et al. High pathogenic avian influenza A(H5) viruses of clade 2.3.4.4b in Europe—why trends of virus evolution are more difficult to predict. Virus Evol. 2024;10:veae027. https://doi.org/10.1093/ve/veae027
10. Sanogo IN, Djegui F, Akpo Y, Gnanvi C, Dupré G, Rubrum A, et al. Highly pathogenic avian influenza A(H5N1) clade 2.3.4.4b virus in poultry, Benin, 2021. Emerg Infect Dis. 2022;28:2534–7. https://doi.org/10.3201/eid2812.221020
11. Plaza PI, Gamarra-Toledo V, Euguí JR, Lambertucci SA. Recent changes in patterns of mammal infection with highly pathogenic avian influenza A(H5N1) virus worldwide. Emerg Infect Dis. 2024;30:444–52. https://doi.org/10.3201/eid3003.231098
12. Leguia M, Garcia-Glaessner A, Muñoz-Saavedra B, Juarez D, Barrera P, Calvo-Mac C, et al. Highly pathogenic avian influenza A (H5N1) in marine mammals and seabirds in Peru. Nat Commun. 2023;14:5489. https://doi.org/10.1038/s41467-023-41182-0
13. Sagong M, Lee YN, Song S, Cha RM, Lee EK, Kang YM, et al. Emergence of clade 2.3.4.4b novel reassortant H5N1 high pathogenicity avian influenza virus in South Korea during late 2021. Transbound Emerg Dis. 2022;69:e3255–60. https://doi.org/10.1111/tbed.14551
14. Jeong S, Lee DH, Kwon JH, Kim YJ, Lee SH, Cho AY, et al. Highly pathogenic avian influenza clade 2.3.4.4b subtype H5N8 virus isolated from Mandarin duck in South Korea, 2020. Viruses. 2020;12:1389. https://doi.org/10.3390/v12121389
15. Baek YG, Lee YN, Lee DH, Shin JI, Lee JH, Chung DH, et al. Multiple reassortants of H5N8 clade 2.3.4.4b highly pathogenic avian influenza viruses detected in South Korea during the winter of 2020–2021. Viruses. 2021;13:490. https://doi.org/10.3390/v13030490
16. Lee SH, Cho AY, Kim TH, Ahn SJ, Song JH, Lee H, et al. Novel highly pathogenic avian influenza A(H5N1) clade 2.3.4.4b virus in wild birds, South Korea. Emerg Infect Dis. 2023;29:1475–8. https://doi.org/10.3201/eid2907.221893
17. Seo YR, Cho AY, Si YJ, Lee SI, Kim DJ, Jeong H, et al. Evolution and spread of highly pathogenic avian influenza A(H5N1) clade 2.3.4.4b virus in wild birds, South Korea, 2022–

2023. Emerg Infect Dis. 2024;30:299–309. https://doi.org/10.3201/eid3002.231274
18. Ahmad S, Koh KY, Yoo DS, Lee JI. Spatial variation in risk for highly pathogenic avian influenza subtype H5N6 viral infections in South Korea: poultry population–based case-control study. Vet Sci. 2022;9:135. https://doi.org/10.3390/vetsci9030135
19. Shin J, Kang S, Byeon H, Cho SM, Kim SY, Chung YJ, et al. Highly pathogenic H5N6 avian influenza virus subtype clade 2.3.4.4 indigenous in South Korea. Sci Rep. 2020;10:7241. https://doi.org/10.1038/s41598-020-64125-x
20. Kim JY, Jeong S, Kim DW, Lee DW, Lee DH, Kim D, et al. Genomic epidemiology of highly pathogenic avian influenza A (H5N1) virus in wild birds in South Korea during 2021–2022: changes in viral epidemic patterns. Virus Evol. 2024;10:veae014. https://doi.org/10.1093/ve/veae014
21. Lee SH, Kwon JH, Youk S, Lee SW, Lee DH, Song CS. Epidemiology and pathobiology of H5Nx highly pathogenic avian influenza in South Korea (2003–2024): a comprehensive review. Vet Q. 2025;45:23–38. https://doi.org/10.1080/01652176.2025.2498918
22. Cho AY, Si Y-J, Lee D-Y, Kim D-J, Kim D, Jeong H, et al. Index case of H5N1 clade 2.3.4.4b highly pathogenic avian influenza virus in wild birds, South Korea, November 2023. Front Vet Sci. 2024;11:1366082. https://doi.org/10.3389/fvets.2024.1366082
23. Cho AY, Si YJ, Kim DJ, Seo YR, Lee DY, Kim D, et al. Novel avian influenza A(H5N6) virus in wild birds, South Korea, 2023. Emerg Infect Dis. 2024;30:1285–8. https://doi.org/10.3201/eid3006.240192
24. Heo GB, Kang YM, An SH, Kim Y, Cha RM, Jang Y, et al. Concurrent infection with clade 2.3.4.4b highly pathogenic avian influenza H5N6 and H5N1 viruses, South Korea, 2023. Emerg Infect Dis. 2024;30:1223–7. https://doi.org/10.3201/eid3006.240194
25. Spackman E. Avian influenza virus detection and quantitation by real-time RT-PCR. In: Spackman E, editor. Animal influenza virus. New York: Springer New York; 2014. p. 105–18.
26. Spackman E, Senne DA, Bulaga LL, Myers TJ, Perdue ML, Garber LP, et al. Development of real-Time RT-PCR for the detection of avian influenza virus. Avian Dis. 2003;47:1079–82. https://doi.org/10.1637/0005-2086-47.s3.1079
27. Spackman E, Senne DA, Myers TJ, Bulaga LL, Garber LP, Perdue ML, et al. Development of a real-time reverse transcriptase PCR assay for type A influenza virus and the avian H5 and H7 hemagglutinin subtypes. J Clin Microbiol. 2002;40:3256–60. https://doi.org/10.1128/JCM.40.9.3256-3260.2002
28. Lee DH. Complete genome sequencing of influenza A viruses using next-generation sequencing. Methods Mol Biol. 2020;2123:69–79. https://doi.org/10.1007/978-1-0716-0346-8_6
29. Hillis DM, Bull JJ. An empirical test of bootstrapping as a method for assessing confidence in phylogenetic analysis. Syst Biol. 1993;42:182–92. https://doi.org/10.1093/sysbio/42.2.182
30. Minin VN, Bloomquist EW, Suchard MA. Smooth skyride through a rough skyline: Bayesian coalescent-based inference of population dynamics. Mol Biol Evol. 2008;25:1459–71. https://doi.org/10.1093/molbev/msn090
31. Kass RE, Raftery AE. Bayes factors. J Am Stat Assoc. 1995;90:773–95. https://doi.org/10.1080/01621459.1995.10476572
32. Alvarez J, Boklund A, Dippel S, Dórea F, Figuerola J, Herskin MS, et al.; EFSA Panel on Animal Health and Animal Welfare (AHAW); ECDC. Preparedness, prevention and control related to zoonotic avian influenza. EFSA J. 2025;23:e9191.
33. Kwon J, Youk S, Lee D-h. Role of wild birds in the spread of clade 2.3.4.4e H5N6 highly pathogenic avian influenza virus into South Korea and Japan. Infect Genet Evol. 2022;101:105281. https://doi.org/10.1016/j.meegid.2022.105281
34. Lee YJ, Kang HM, Lee EK, Song BM, Jeong J, Kwon YK, et al. Novel reassortant influenza A(H5N8) viruses, South Korea, 2014. Emerg Infect Dis. 2014;20:1087–9. https://doi.org/10.3201/eid2006.140233
35. Kwon JH, Lee DH, Swayne DE, Noh JY, Yuk SS, Erdene-Ochir TO, et al. Reassortant clade 2.3.4.4 avian influenza A(H5N6) virus in a wild Mandarin duck, South Korea, 2016. Emerg Infect Dis. 2017;23:822–6. https://doi.org/10.3201/eid2305.161905
36. Seo Y-R, Lee S-H, Jeong S, Cho H, Kim D, Kim D-J, et al. Genetic and pathological analysis of hooded cranes (*Grus monacha*) naturally infected with clade 2.3.4.4b highly pathogenic avian influenza H5N1 virus in South Korea in the winter of 2022. Front Vet Sci. 2024;11:1499440. https://doi.org/10.3389/fvets.2024.1499440
37. Newman SH, Iverson SA, Takekawa JY, Gilbert M, Prosser DJ, Batbayar N, et al. Migration of whooper swans and outbreaks of highly pathogenic avian influenza H5N1 virus in eastern Asia. PLoS One. 2009;4:e5729. https://doi.org/10.1371/journal.pone.0005729
38. Lee K, Yu D, Martínez-López B, Yoon H, Kang S-I, Hong S-K, et al. Fine-scale tracking of wild waterfowl and their impact on highly pathogenic avian influenza outbreaks in the Republic of Korea, 2014–2015. Sci Rep. 2020;10:18631. https://doi.org/10.1038/s41598-020-75698-y
39. Takekawa JY, Prosser DJ, Sullivan JD, Yin S, Wang X, Zhang G, et al. Potential effects of habitat change on migratory bird movements and avian influenza transmission in the East Asian–Australasian Flyway. Diversity (Basel). 2023;15:601. https://doi.org/10.3390/d15050601
40. Doko T, Chen W, Hijikata N, Yamaguchi N, Hiraoka E, Fujita M, et al. Migration patterns and characteristics of Eurasian wigeons (*Mareca penelope*) wintering in southwestern Japan based on satellite tracking. Zool Sci. 2019;36:490–503. https://doi.org/10.2108/zs180207
41. Meng F, Zhang J, Li C, Zhao Q, Solovyeva D, Lee H, et al. Differing migration patterns and year-round habitat-use of allopatric nesting eastern tundra bean geese (*Anser fabalis serrirostris*) in East Asia. Avian Res. 2022;13:100062. https://doi.org/10.1016/j.avrs.2022.100062
42. Lee S-H, Jeong S, Cho AY, Kim T-H, Choi Y-J, Lee H, et al. Caught right on the spot: isolation and characterization of clade 2.3.4.4b H5N8 high pathogenicity avian influenza virus from a common pochard (*Aythya ferina*) being attacked by a peregrine falcon (*Falco peregrinus*). Avian Dis. 2024;68:72–9. https://doi.org/10.1637/aviandiseases-D-23-00062
43. Cormorant sweep-up operation will fail at this rate. The Kyunghyang Newspaper. 2024 June 3 [cited 2025 Feb 16]. https://news.nate.com/view/20240603n33538
44. Lee D-H, Bertran K, Kwon J-H, Swayne DE. Evolution, global spread, and pathogenicity of highly pathogenic avian influenza H5Nx clade 2.3.4.4. J Vet Sci. 2017;18(S1):269–80. https://doi.org/10.4142/jvs.2017.18.S1.269
45. Kwon JH, Bahl J, Swayne DE, Lee YN, Lee YJ, Song CS, et al. Domestic ducks play a major role in the maintenance and spread of H5N8 highly pathogenic avian influenza viruses in South Korea. Transbound Emerg Dis. 2020;67:844–51. https://doi.org/10.1111/tbed.13406
46. Maljkovic Berry I, Melendrez MC, Bishop-Lilly KA, Rutvisuttinunt W, Pollett S, Talundzic E, et al. Next

generation sequencing and bioinformatics methodologies for infectious disease research and public health: approaches, applications, and considerations for development of laboratory capacity. J Infect Dis. 2020;221:S292–307. https://doi.org/10.1093/infdis/jiz286
47. Attwood SW, Hill SC, Aanensen DM, Connor TR, Pybus OG. Phylogenetic and phylodynamic approaches to understanding and combating the early SARS-CoV-2 pandemic. Nat Rev Genet. 2022;23:547–62. https://doi.org/10.1038/s41576-022-00483-8
48. Carnegie L, Raghwani J, Fournié G, Hill SC. Phylodynamic approaches to studying avian influenza virus. Avian Pathol. 2023;52:289–308. https://doi.org/10.1080/03079457.2023.2236568
49. Chen Z, Azman AS, Chen X, Zou J, Tian Y, Sun R, et al. Global landscape of SARS-CoV-2 genomic surveillance and data sharing. Nat Genet. 2022;54:499–507. https://doi.org/10.1038/s41588-022-01033-y
50. Khare S, Gurry C, Freitas L, Schultz MB, Bach G, Diallo A, et al. GISAID's role in pandemic response. China CDC Wkly. 2021;3:1049–51. https://doi.org/10.46234/ccdcw2021.255

Address for correspondence: Dong-Hun Lee, Wildlife Health Laboratory, College of Veterinary Medicine, Konkuk University, 120 Neungdong-ro, Gwangjin-gu, Seoul 05029, South Korea; email: donghunlee@konkuk.ac.kr

Estimated COVID-19 Periodicity and Correlation with SARS-CoV-2 Spike Protein S1 Antigenic Diversity, United States

Erica Billig Rose, Clinton R. Paden, Peter W. Cook, Kevin C. Ma, Amber Winn, Juan Castro, Lakshmi Panagiotakopoulos, Benjamin J. Silk

Emergence of antigenically diverse SARS-CoV-2 variants may be correlated with temporal circulation patterns. We analyzed positive SARS-CoV-2 tests in the United States reported to a national, laboratory-based surveillance network and unique amino acid sequences of the S1 region of the spike protein reported to national genomic surveillance during October 2020–September 2024. We estimated SARS-CoV-2 dominant periodicities using a discrete Fourier transform, described S1 variation using the Simpson diversity index (SDI), and estimated Spearman cross-correlation coefficients between percentage change in SDI and percentage positivity. SARS-CoV-2 activity consistently peaked during July–September and December–February, and dominant periodicities were at weeks 52.2 and 26.1. Percentage positivity and percentage change in SDI were negatively correlated ($\rho = -0.30$; $p<0.001$). SARS-CoV-2 peaks occurred in late summer and winter, a pattern likely related to rapid SARS-CoV-2 evolution and cyclical diversity. Monitoring associations between percentage positivity and SDI can help forecast expected surges and optimize prevention and preparedness.

Determining the expected temporal patterns of SARS-CoV-2 circulation has important public health implications, including the timing of vaccine recommendations and health systems preparedness. A single winter peak annually is characteristic of several respiratory viruses, including seasonal influenza, respiratory syncytial virus, and seasonal human coronaviruses (*1*,*2*). Conversely, other respiratory viruses, including parainfluenza and rhinoviruses/enteroviruses, typically peak twice a year (*3*,*4*). Respiratory viruses also have subtype diversity that adds variation into their temporal patterns of circulation (*2*,*4*).

To date, however, few studies that describe SARS-CoV-2 circulation patterns in the United States have been published. One study found the number of reported COVID-19 cases consistently peaked from late fall through spring (*5*). Another study found both an annual winter peak in the number of reported COVID-19 cases and additional periodicity that suggested ≈3 peaks per year (*6*). Such studies confront the challenge of characterizing seasonality relatively soon after emergence of a novel virus and rapid changes in population-level immunity and vaccine introduction that substantially affect virus transmission.

The frequent emergence of new variants, designated phylogenetically, has been characteristic of SARS-CoV-2 evolution, and its antigenic diversity could affect COVID-19 seasonal trends. In the United States, variants of concern detected by genomic surveillance have been temporally associated with increasing COVID-19 incidence to varying degrees. Some variants were temporally associated with mid-year surges observed in late summer 2021 (Delta [B.1.617.2]), late summer 2022 (Omicron BA.5), and late summer 2023 (Omicron EG.5) (*7*–*9*). Other variants were associated with winter surges in 2021–22 (Omicron BA.1), 2022–23 (Omicron XBB.1.5), and 2023–24 (Omicron JN.1), when peaks in respiratory virus activity are expected.

In this study, we sought to determine national and regional SARS-CoV-2 periodicity using the percentage of laboratory detections (percentage positivity) in the United States, which is robust to changes in testing and reporting practices, and thus useful for analyzing temporal patterns of circulation. We also describe SARS-CoV-2 antigenic diversity using the proportion of unique S1 spike genotypes reported each week and

Authors affiliation: Centers for Disease Control and Prevention, Atlanta, Georgia, USA

DOI: https://doi.org/10.3201/eid3108.250451

the correlation with percentage positivity as a hypothesized driver of COVID-19 seasonality.

Methods

To determine the percentage of positive SARS-CoV-2 tests reported nationally and by US Department of Health and Human Services (HHS) Region (https://www.hhs.gov/about/agencies/iea/regional-offices), we used data from the National Respiratory and Enteric Virus Surveillance System (NREVSS) during October 2020–September 2024. NREVSS is a voluntary, laboratory-based system to which participating clinical, commercial, and public health laboratories reported the weekly total numbers of aggregate tests performed and SARS-CoV-2 detections. We estimated the proportion of detections that occurred during late summer (July–September) and winter (December–February) and determined the maximum percentage positivity nationally and by HHS Region. We used a discrete Fourier transform (DFT) for spectral decomposition to identify dominant frequencies nationally and regionally; we calculated DFT by using a fast Fourier transform (*10*). We defined dominant periodicities as the reciprocal of the frequencies with the highest magnitude. We then fit those dominant frequencies using linear regression with harmonic functions to model the smoothed, 3-week moving average of the weekly percent positivity data (*6*) (Appendix, https://wwwnc.cdc.gov/EID/article/31/8/25-0451-App1.pdf).

We then determined the weekly predominant SARS-CoV-2 lineages and number of unique amino acid sequences of the S1 region of the spike protein (genotypes) among high-quality sequences submitted publicly for national genomic surveillance during October 2020–September 2024. All sequences included in this analysis are publicly available (https://data.cdc.gov). We estimated variation in the S1 region of the spike protein by using the Simpson diversity index (SDI). SDI is a metric typically used in ecology that incorporates the number and proportion of each species (*11*). Values range from 0 to 1; larger numbers represent more unique sequences with relatively more even distribution (i.e., higher diversity) (Appendix).

We estimated the Spearman cross-correlation coefficient between the percentage change in SDI and smoothed percentage positivity. We selected the lag with the highest mean correlation over 26-week moving windows and estimated the coefficient across both the entire study period and the most recent 2 years, October 2022–September 2024. We computed p values by using the asymptotic *t* approximation ($\alpha = 0.05$).

Results

Nationally, SARS-CoV-2 circulated year-round but had peaks in the late summer (July–September) and winter (December–February) months during the entire study period. The only exception occurred during the first winter of the pandemic in 2020–21, when the national peak occurred in late November; during that winter, percentage positivity remained elevated (within 1% of peak positivity) through early January (Figure 1). All HHS regions had peaks 2 times a year, except HHS Region 8, where only 1 peak occurred between summer 2023 and winter 2023–2024. Nearly two thirds (65%; 396,688,638/605,632,990) of detections were reported nationally during the 6 combined months of the late summer and winter periods (i.e., 50% of the year), but the percentages of detections varied by region. HHS Region 4 (the Southeast) had the highest percentage (77%; 60,115,750/78,506,974) reported during late summer and winter, and HHS Region 8 (the Mountain West) had the lowest percentage (54%; 35,198,192/65,255,668). The maximum 3-week smoothed percentage positivity averaged across seasonal peaks varied by region from 13.8% (Region 1) to 22.2% (Region 7). During the most recent 2 years (October 2022–September 2024), the percentage of detections reported nationally during the 6 combined months of late summer and winter was similar to the overall percentage (64%) but showed less regional variation (range 56%–72%).

The spectral decomposition of periodicity revealed 2 nationally dominant periodicities at 52.2 and 26.1 weeks, followed by 3 smaller but notable periodicities at 104.5, 20.9, and 17.4 weeks (Figure 2, panel A). The 2 dominant periodicities fit with observed national trends ($R^2 = 0.43$) (Figure 2, panel B), and including the top 5 periodicities improved fit ($R^2 = 0.66$), suggesting an overall bimodal seasonality (Figure 2, panel C). Across the 10 HHS Regions, the periodogram varied to include 2–4 of the 7 regionally dominant periodicities; we noted considerable overlap with the nationally dominant periodicities (Appendix Table 1).

We observed periods during which a single S1 sequence predominated among the circulating viruses, often coinciding with seasonal surges and increasing percentage positivity. The volume of sequence data varied from >40,000 high-quality spike sequences per week in 2021 to <1,000 per week in 2023. A single S1 sequence represented >30% of isolates for 46 weeks during 2021 and 43 weeks during 2022; in 2023, we observed only 22 weeks. The predominant S1 sequence consistently had a maximum proportion in the range of 0.5 to 0.7 (Figure 3, panel A).

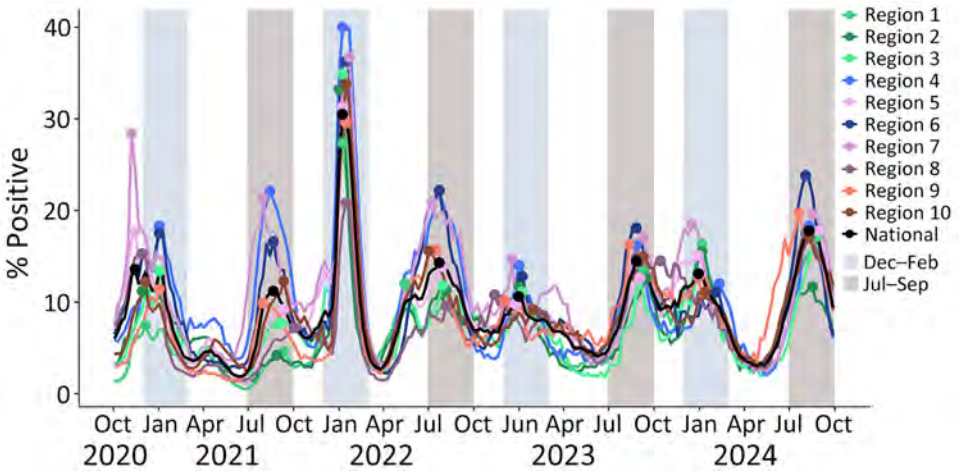

Figure 1. Weekly smoothed (3-week) percentages of positive SARS-CoV-2 tests reported to the National Respiratory and Enteric Surveillance System (NREVSS), nationally and by Health and Human Services (HHS) Region, United States, October 2020–September 2024. The data represent SARS-CoV-2 nucleic acid amplification test results, which include reverse transcription PCR tests from the NREVSS sentinel network of laboratories in the United States, including clinical, public health, and commercial laboratories. These data exclude antigen, antibody, and at-home test results. Blue (December–February) and gray (July–September) vertical bands indicate time periods with increased percentage positivity. Seasonal peaks are indicated by dots at the week when smoothed percent positivity peaked. Regional colors are grouped by geography (e.g., Regions 1, 2, and 3 are shades of green and comprise the Northeast). All HHS Regions had 2 seasonal peaks a year, except HHS Region 8, which only had 1 peak between summer 2023 and winter 2023–2024. HHS Region 1: Connecticut, Maine, Massachusetts, New Hampshire, Rhode Island, and Vermont; HHS Region 2: New Jersey, New York, Puerto Rico, and the Virgin Islands; HHS Region 3: Delaware, District of Columbia, Maryland, Pennsylvania, Virginia, and West Virginia; HHS Region 4: Alabama, Florida, Georgia, Kentucky, Mississippi, North Carolina, South Carolina, and Tennessee; HHS Region 5: Illinois, Indiana, Michigan, Minnesota, Ohio, and Wisconsin; HHS Region 6: Arkansas, Louisiana, New Mexico, Oklahoma, and Texas; HHS Region 7: Iowa, Kansas, Missouri, and Nebraska; HHS Region 8: Colorado, Montana, North Dakota, South Dakota, Utah, and Wyoming; HHS Region 9: Arizona, California, Hawaii, Nevada, American Samoa, Commonwealth of the Northern Mariana Islands, Federated States of Micronesia, Guam, Marshall Islands, and Republic of Palau; HHS Region 10: Alaska, Idaho, Oregon, and Washington. Data from US-affiliated Pacific Islands are not included in NREVSS.

Periods with a large decrease in SDI, which often represented predominance (>50% prevalence) of a new lineage, typically preceded peaks in percentage positivity, particularly in July 2021 (Delta [B.1.617.2]), December 2021 (Omicron BA.1), July 2022 (BA.4/BA.5), December 2022 (XBB.1.5), and December 2023 (JN.1) (Figure 3, panel B). Percentage positivity and weekly percentage change in SDI had a significant negative correlation maximized at a 2-week lag throughout the entire study period ($\rho = -0.30$; $p<0.001$); we observed a stronger correlation during the later part of the study period, starting in October 2022 ($\rho = -0.60$; $p<0.001$). The lag suggests that, typically 2 weeks before a peak in percentage positivity, SDI rate of change begins to decrease. However, during the late summer 2023 and 2024 surges, we saw no substantial change in SDI diversity. Instead, several spike S1 sequences with proportions <0.42 circulated; no single predominant variant emerged.

Discussion

Our analysis revealed biannual COVID-19 peaks in late summer and winter, a pattern that is expected to persist as long as the rapid evolution of SARS-CoV-2 and cyclical S1 diversity continues. The spectral decomposition of periodicity revealed 2 dominant frequencies each year at 52.2 and 26.1 weeks, consistent with a biannual peak approximately every 6 months, and 3 additional notable frequencies at 104.5, 20.9, and 17.4 weeks. Based on the timing of the percentage positivity data, the interval after the winter peak is a longer, 6–9-month period, compared with a 4–5-month interval after the late summer peak. However, our analysis using the DFT approach cannot distinguish whether the periodicity at 20.9 and 17.4 weeks captures an additional, but less apparent, regular seasonality or variation in the timing of the peaks throughout the study period. The periodicity at 104.5 weeks is a harmonic (multiple) of the dominant periodicities that might have been driven by the sharp Omicron BA.1 surge in winter 2021–22, which occurred ≈2 years into the 4-year study period.

A single, dominant S1 sequence genotype was associated with both winter and late summer surges until November 2022. Since winter 2022–23, a dominant genotype was also associated with a surge in virus activity during the winter season, but co-circulating variants with similar spike substitutions have been associated with late summer surges (*12*). Like other betacoronaviruses, SARS-CoV-2 has shown the capacity to undergo both gradual, stepwise evolution and large, periodic changes (*13*,*14*); since 2022,

the large shifts in circulating lineages in the United States have occurred during late fall and winter (*12*). The spike protein, and particularly the S1 region, is the major viral protein under selective pressure by population immunity; changes in the spike protein can result in changes in virus fitness or transmission efficiency (*15*). The negative correlation observed between S1 diversity and percentage positivity supports a hypothesis that trends in viral diversity might be a predictor of expected COVID-19 seasonal activity. After surges featuring a predominant spike S1 sequence and associated increasing percentage positivity, the seasonal cycle seems to reset and renewed selective pressure and greater viral evolution subsequently are observed as S1 diversity. Those findings indicate that sustained genomic surveillance sampling during periods of low SARS-CoV-2 activity, when spike diversity is high, is critical for monitoring viral evolution and predicting seasonal increases in SARS-CoV-2 activity, rather than augmenting sequencing when activity is high and antigenic diversity is low. Continued monitoring will be useful for determining whether this cyclical pattern of a predominant spike S1 sequence followed by increased diversity can anticipate future surges in COVID-19 activity.

Transmission of SARS-CoV-2 variants is driven by a combination of intrinsic viral fitness, including cyclical patterns of spike S1 mutations, interacting with a changing landscape of population immunity. After implementation of the national COVID-19

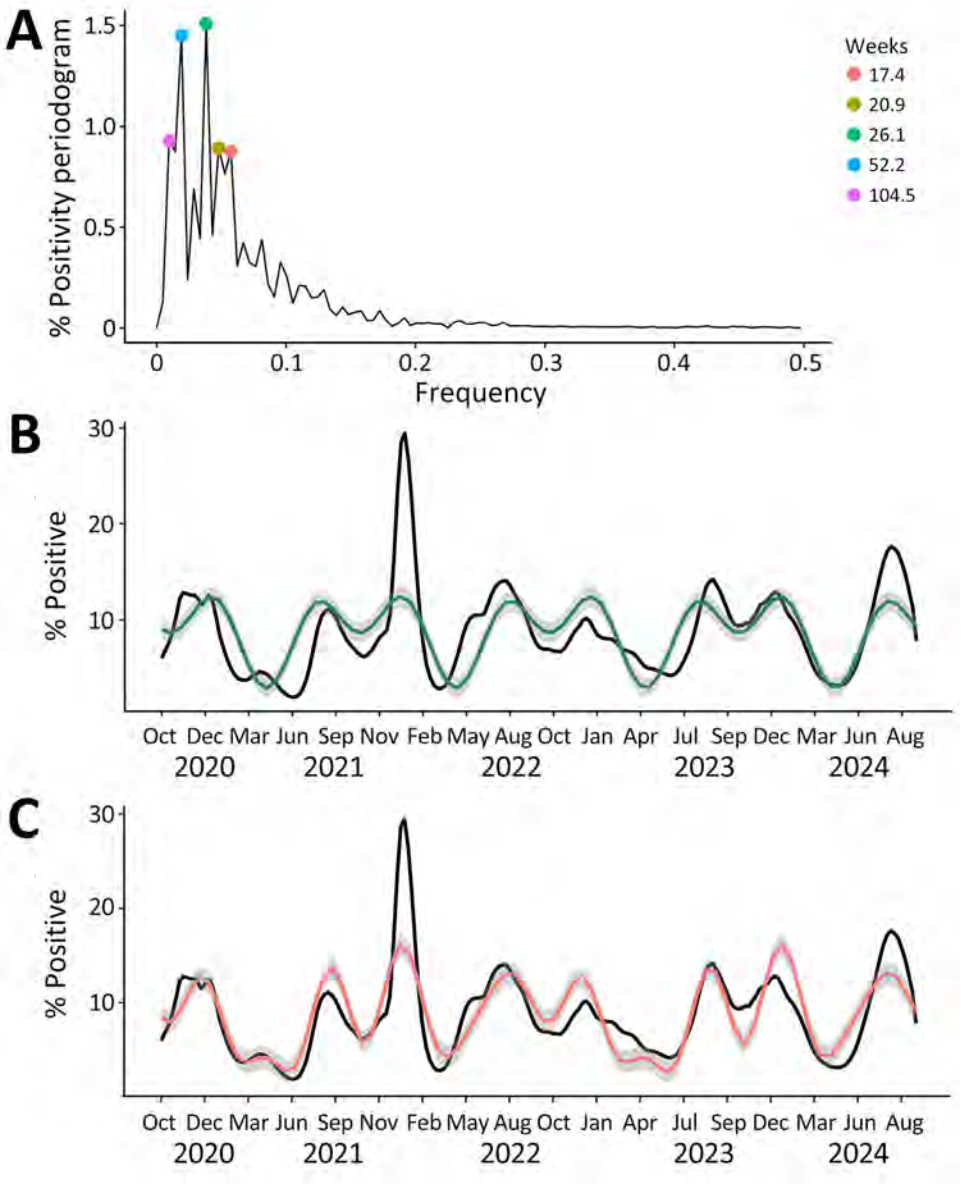

Figure 2. National smoothed (3-week) percentages of positive SARS-CoV-2 tests reported to the National Respiratory and Enteric Surveillance System (NREVSS), United States, October 2020–September 2024. Data represent SARS-CoV-2 nucleic acid amplification test results, which include reverse transcription PCR tests from the NREVSS sentinel network of laboratories in the United States, including clinical, public health, and commercial laboratories. These data exclude antigen, antibody, and at-home test results. A) Periodogram, in which the height of each point indicates strength of the periodicity at the corresponding frequency. Dots indicate 5 dominant periodicities, at frequencies corresponding to surges every 104.5, 52.2, 26.1, 20.9, and 17.4 weeks. Weeks represent time intervals (i.e., weeks do not represent a year of calendar time in the context of this analysis). B) Fitted harmonic function using the 52.2- and 26.1-week periodicities determined by discrete Fourier transform (green line). C) Fitted harmonic function using the 104.5-, 52.2-, 26.1-, 20.9-, and 17.4-week periodicities determined by discrete Fourier transform (pink line).

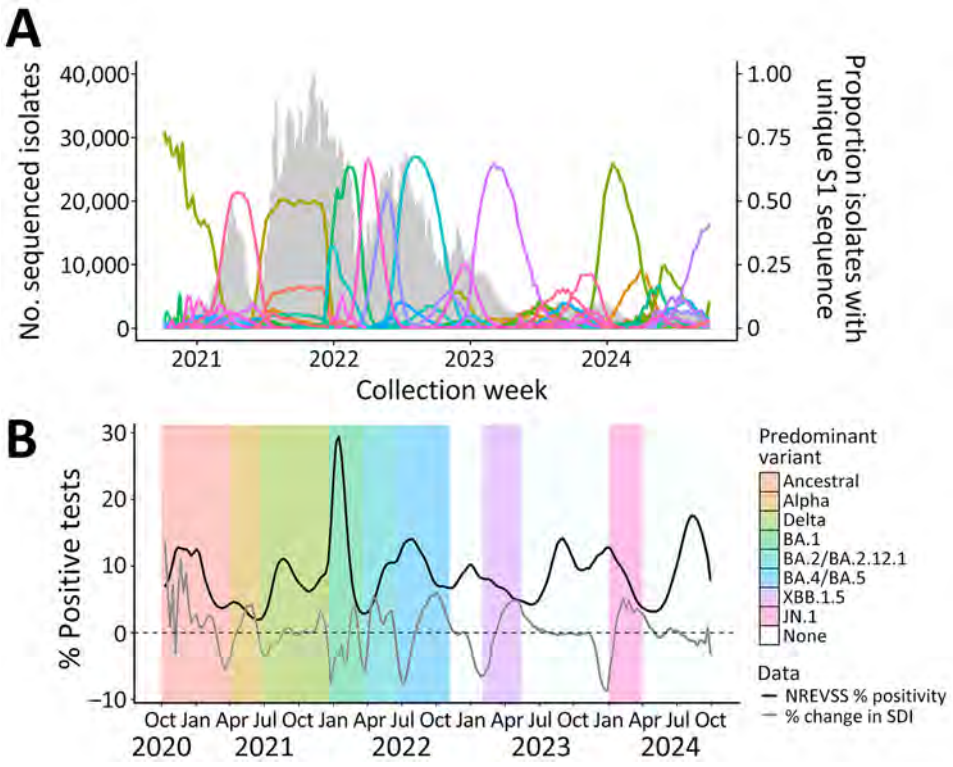

Figure 3. Weekly numbers of sequenced SARS-CoV-2 isolates, proportions with unique S1 spike sequences, and national percentages of positive SARS-CoV-2 tests and percentage changes in SDI, United States, October 2020–September 2024. A) Numbers of sequenced isolates (gray bars) and proportions of isolates with each unique S1 sequence (colored lines). Unique S1 sequences with a maximum proportion of <0.02 during the study period are included in the total number of isolates but not shown as proportion lines to improve visibility of patterns. B) National smoothed (3-week) percentages of positive SARS-CoV-2 tests reported to the NREVSS and percentage changes in SDI of S1 spike proteins. NREVSS, National Respiratory and Enteric Surveillance System; SDI, Simpson diversity index.

vaccination program in the United States during 2020–2021, natural immunity from infection during the Omicron surge in the winter of 2021–22 further augmented population immunity. SARS-CoV-2 sterilizing immunity after infection typically wanes, although the duration and extent vary after infection with different variants (*16*,*17*). Because vaccine-induced neutralizing antibodies typically wane within 3–6 months, the biannual COVID-19 seasonality highlights the importance of a 2-dose vaccine schedule for older adults and persons with moderate or severe immunocompromise, who are at elevated risk for severe infection (*18*–*20*). In 2025, most of the US population has immune memory from prior infection, vaccination, or both. Studies have shown that a higher number of cumulative SARS-CoV-2 infections and COVID-19 vaccinations leads to higher antibody levels; however, smaller incremental increases in antibody occur with each exposure to the virus or vaccination (*21*,*22*). A study in rhesus macaques determined that high concentrations of neutralizing antibodies alone prevented infection, and those authors calculated an estimated threshold of protection (*23*). In that same study, the authors determined that, near the threshold of immunity after recovery from infection, T cells contributed to viral clearance. In humans, one study estimated that neutralizing antibodies mediated a portion of protection against infection and that the protection is variant specific (*24*). However, those authors hypothesized that nonneutralizing antibodies, likely in the form of cellular immunity, contribute the remaining protection, indicating both humoral and cellular arms of the immune system are important.

The seasonality of many respiratory infections is partly the result of weather and climate; increases in COVID-19 cases have been associated with low temperatures and low humidity (*5*,*25*,*26*). Seasonal patterns of behavior, including school terms, holiday gatherings, and travel, also influence respiratory virus transmission (*27*–*30*). During periods when seasonal surges occur, the risk for exposure increases for persons at higher risk for severe disease.

The first limitation of this analysis is that the DFT cannot determine why certain frequencies are dominant or whether variations in periodicity throughout the study period occurred; including additional frequencies in the linear regression will continue to improve model fit. Second, different laboratory methods used throughout the study period could have different sensitivities and specificities, causing variation in the reported results of laboratory testing and percent positivity. Third, NREVSS is a passive, voluntary reporting system. Participating laboratories vary from season to season, and SARS-CoV-2 percentage positivity data might not be representative of all geographic areas. Several additional limitations are associated

with the changing epidemiologic and clinical features of COVID-19. The proportion of infections causing severe disease has decreased since 2020, which could reduce the number of tests conducted and reported to NREVSS. In addition, the use of screening tests has decreased, and at-home test use peaked in January 2022 (*31*,*32*); those changes can affect how COVID-19 trends are observed and reported. Genomic sampling methods also changed during the study period, and the volume of sequences reported to surveillance decreased. Finally, we described national and regional COVID-19 trends, but local variability in transmission is not represented in our analysis.

In conclusion, SARS-CoV-2 circulation in the United States has been meaningful year-round, but consistent peaks have occurred in late summer and winter since 2020. We observed decreases in antigenic diversity, representing predominance of a new SARS-CoV-2 lineage, before late summer and winter COVID-19 surges during 2021 and 2022. In 2023 and 2024, antigenic diversity increased and remained stable during late-summer surges, indicating sustained co-circulation of multiple lineages. Given the complexity of the interacting factors, additional data and modeling studies are needed to understand the effects of predominant S1 sequences and other drivers of COVID-19 seasonality. Continuing to monitor the associations between percentage positivity and SDI can help to forecast expected surges, describe changing seasonality over time, and optimize prevention and health system preparedness. In particular, the timing of COVID-19 vaccination recommendations could be further optimized to maximize protection according to expected surges in COVID-19 activity.

Acknowledgments

We thank Marc Lipsitch for expert advice provided in conceptualizing this report and Natalie Thornburg for contributing SARS-CoV-2 immunology expertise.

About the Author

Dr. Rose is an epidemiologist in the Predict Division of CDC's Center for Forecasting and Outbreak Analytics. Her research interests include the surveillance and analytics of respiratory viruses and foodborne illnesses.

References

1. Shaman J, Goldstein E, Lipsitch M. Absolute humidity and pandemic versus epidemic influenza. Am J Epidemiol. 2011;173:127–35. https://doi.org/10.1093/aje/kwq347
2. Shah MM, Winn A, Dahl RM, Kniss KL, Silk BJ, Killerby ME. Seasonality of common human coronaviruses, United States, 2014–2021. Emerg Infect Dis. 2022;28:1970–6. https://doi.org/10.3201/eid2810.220396
3. Ma KC, Winn A, Moline HL, Scobie HM, Midgley CM, Kirking HL, et al.; New Vaccine Surveillance Network Collaborators. Increase in acute respiratory illnesses among children and adolescents associated with rhinoviruses and enteroviruses, including enterovirus D68—United States, July–September 2022. MMWR Morb Mortal Wkly Rep. 2022;71:1265–70. https://doi.org/10.15585/mmwr.mm7140e1
4. Fry AM, Curns AT, Harbour K, Hutwagner L, Holman RC, Anderson LJ. Seasonal trends of human parainfluenza viral infections: United States, 1990–2004. Clin Infect Dis. 2006;43:1016–22. https://doi.org/10.1086/507638
5. Wiemken TL, Khan F, Puzniak L, Yang W, Simmering J, Polgreen P, et al. Seasonal trends in COVID-19 cases, hospitalizations, and mortality in the United States and Europe. Sci Rep. 2023;13:3886. https://doi.org/10.1038/s41598-023-31057-1
6. Shamsa EH, Shamsa A, Zhang K. Seasonality of COVID-19 incidence in the United States. Front Public Health. 2023;11:1298593. https://doi.org/10.3389/fpubh.2023.1298593
7. Truelove S, Smith CP, Qin M, Mullany LC, Borchering RK, Lessler J, et al. Projected resurgence of COVID-19 in the United States in July–December 2021 resulting from the increased transmissibility of the Delta variant and faltering vaccination. eLife. 2022;11:e73584. https://doi.org/10.7554/eLife.73584
8. Ma KC, Shirk P, Lambrou AS, Hassell N, Zheng XY, Payne AB, et al. Genomic surveillance for SARS-CoV-2 variants: circulation of Omicron lineages—United States, January 2022–May 2023. MMWR Morb Mortal Wkly Rep. 2023;72:651–6. https://doi.org/10.15585/mmwr.mm7224a2
9. Centers for Disease Control and Prevention. Update on SARS-CoV-2 variant BA.2.86 being tracked by CDC [cited 2024 Jan 13]. https://www.cdc.gov/ncird/whats-new/covid-19-variant-update-2023-11-27.html
10. Cooley JW, Tukey JW. An algorithm for the machine calculation of complex Fourier series. Math Comput. 1965;19:297–301. https://doi.org/10.1090/S0025-5718-1965-0178586-1
11. Simpson EH. Measurement of diversity. Nature. 1949;163:688–9. https://doi.org/10.1038/163688a0
12. Ma KC, Castro J, Lambrou AS, Rose EB, Cook PW, Batra D, et al. Genomic surveillance for SARS-CoV-2 variants: circulation of Omicron XBB and JN.1 lineages—United States, May 2023–September 2024. MMWR Morb Mortal Wkly Rep. 2024;73:938–45. https://doi.org/10.15585/mmwr.mm7342a1
13. Carabelli AM, Peacock TP, Thorne LG, Harvey WT, Hughes J, Peacock SJ, et al.; COVID-19 Genomics UK Consortium. SARS-CoV-2 variant biology: immune escape, transmission and fitness. Nat Rev Microbiol. 2023;21:162–77. https://doi.org/10.1038/s41579-022-00841-7
14. Hodcroft EB, Zuber M, Nadeau S, Vaughan TG, Crawford KHD, Althaus CL, et al.; SeqCOVID-SPAIN consortium. Spread of a SARS-CoV-2 variant through Europe in the summer of 2020. Nature. 2021;595:707–12. https://doi.org/10.1038/s41586-021-03677-y
15. Kistler KE, Huddleston J, Bedford T. Rapid and parallel adaptive mutations in spike S1 drive clade success in SARS-CoV-2. Cell Host Microbe. 2022;30:545–555.e4. https://doi.org/10.1016/j.chom.2022.03.018
16. Stein C, Nassereldine H, Sorensen RJD, Amlag JO, Bisignano C, Byrne S, et al.; COVID-19 Forecasting Team. Past SARS-CoV-2 infection protection against re-infection: a

systematic review and meta-analysis. Lancet. 2023;401:833–42. https://doi.org/10.1016/S0140-6736(22)02465-5
17. Chemaitelly H, Ayoub HH, Coyle P, Tang P, Hasan MR, Yassine HM, et al. Differential protection against SARS-CoV-2 reinfection pre- and post-Omicron. Nature. 2025;639:1024–31. https://doi.org/10.1038/s41586-024-08511-9
18. Ma KC, Surie D, Lauring AS, Martin ET, Leis AM, Papalambros L, et al. Effectiveness of updated 2023–2024 (monovalent XBB.1.5) COVID-19 vaccination against SARS-CoV-2 Omicron XBB and BA.2.86/JN.1 lineage hospitalization and a comparison of clinical severity–IVY network, 26 hospitals, 18 October 2023–9 March 2024. Clin Infect Dis. 2024;6:ciae405. https://doi.org/10.1093/cid/ciae405
19. DeCuir J, Payne AB, Self WH, Rowley EAK, Dascomb K, DeSilva MB, et al.; CDC COVID-19 Vaccine Effectiveness Collaborators. Interim effectiveness of updated 2023–2024 (monovalent XBB.1.5) COVID-19 vaccines against COVID-19–associated emergency department and urgent care encounters and hospitalization among immunocompetent adults aged ≥18 years—VISION and IVY networks, September 2023–January 2024. MMWR Morb Mortal Wkly Rep. 2024;73:180–8. https://doi.org/10.15585/mmwr.mm7308a5
20. Goldberg Y, Mandel M, Bar-On YM, Bodenheimer O, Freedman LS, Ash N, et al. Protection and waning of natural and hybrid immunity to SARS-CoV-2. N Engl J Med. 2022;386:2201–12. https://doi.org/10.1056/NEJMoa2118946
21. Srivastava K, Carreño JM, Gleason C, Monahan B, Singh G, Abbad A, et al.; PARIS Study Group. SARS-CoV-2-infection- and vaccine-induced antibody responses are long lasting with an initial waning phase followed by a stabilization phase. Immunity. 2024;57:587–599.e4. https://doi.org/10.1016/j.immuni.2024.01.017
22. Barateau V, Peyrot L, Saade C, Pozzetto B, Brengel-Pesce K, Elsensohn M-H, et al. Prior SARS-CoV-2 infection enhances and reshapes spike protein-specific memory induced by vaccination. Sci Transl Med. 2023;15:eade0550. https://doi.org/10.1126/scitranslmed.ade0550
23. McMahan K, Yu J, Mercado NB, Loos C, Tostanoski LH, Chandrashekar A, et al. Correlates of protection against SARS-CoV-2 in rhesus macaques. Nature. 2021;590:630–4. https://doi.org/10.1038/s41586-020-03041-6
24. Sun K, Bhiman JN, Tempia S, Kleynhans J, Madzorera VS, Mkhize Q, et al.; PHIRST-C group. SARS-CoV-2 correlates of protection from infection against variants of concern. Nat Med. 2024;30:2805–12. https://doi.org/10.1038/s41591-024-03131-2
25. D'Amico F, Marmiere M, Righetti B, Scquizzato T, Zangrillo A, Puglisi R, et al. COVID-19 seasonality in temperate countries. Environ Res. 2022;206:112614. https://doi.org/10.1016/j.envres.2021.112614
26. Huang Z, Huang J, Gu Q, Du P, Liang H, Dong Q. Optimal temperature zone for the dispersal of COVID-19. Sci Total Environ. 2020;736:139487. https://doi.org/10.1016/j.scitotenv.2020.139487
27. Klinkenberg D, Hahné SJM, Woudenberg T, Wallinga J. The reduction of measles transmission during school vacations. Epidemiology. 2018;29:562–70. https://doi.org/10.1097/EDE.0000000000000841
28. Chao DL, Halloran ME, Longini IM Jr. School opening dates predict pandemic influenza A(H1N1) outbreaks in the United States. J Infect Dis. 2010;202:877–80. https://doi.org/10.1086/655810
29. Huang KE, Lipsitch M, Shaman J, Goldstein E. The US 2009 A(H1N1) influenza epidemic: quantifying the impact of school openings on the reproductive number. Epidemiology. 2014;25:203–6. https://doi.org/10.1097/EDE.0000000000000055
30. Walter ND, Taylor TH Jr, Dowell SF, Mathis S, Moore MR; Active Bacterial Core Surveillance System Team. Holiday spikes in pneumococcal disease among older adults. N Engl J Med. 2009;361:2584–5. https://doi.org/10.1056/NEJMc0904844
31. Ritchey MD, Rosenblum HG, Del Guercio K, Humbard M, Santos S, Hall J, et al. COVID-19 self-test data: challenges and opportunities—United States, October 31, 2021–June 11, 2022. MMWR Morb Mortal Wkly Rep. 2022;71:1005–10. https://doi.org/10.15585/mmwr.mm7132a1
32. Rader B, Gertz A, Iuliano AD, Gilmer M, Wronski L, Astley CM, et al. Use of at-home COVID-19 tests—United States, August 23, 2021–March 12, 2022. MMWR Morb Mortal Wkly Rep. 2022;71:489–94. https://doi.org/10.15585/mmwr.mm7113e1

Address for correspondence: Erica Billig Rose, Centers for Disease Control and Prevention, 1600 Clifton Rd NE, Mailstop H20-3, Atlanta, GA 30329-4018, USA; email: nqx4@cdc.gov

Group A *Streptococcus* among American Indian Persons, White Mountain Apache Tribal Lands, United States, 2016–2019[1]

Catherine G. Sutcliffe,[2] Ryan Close,[2] Laura B. Brown, Dennie Parker, Jayshree Patel, Eugene Romancito, Robert Weatherholtz, James McAuley,[3] Laura L. Hammitt[3]

American Indian populations have higher rates of invasive disease because of group A *Streptococcus* (GAS). This study describes the rates of severe and invasive GAS (siGAS) infections and the distribution of circulating *emm* types among nonsevere and siGAS cases in the White Mountain Apache Tribal lands in Arizona, USA, during 2016–2019. Isolates underwent whole-genome sequencing to determine *emm* type. Among siGAS cases, 36% of patients were female, the median age was 40.7 years, and 47.2% of patients were co-infected with *Staphylococcus aureus*. The age-standardized incidence rate during 2018–2019 was 554.2/100,000 persons. Among the pharyngitis isolates from 2017–2018, the most common *emm* types were 82 (36.3%), 6 (22.2%), and 60 (16.3%). Among the siGAS cases in 2017–2019, the most common *emm* type was 82 (65.5%) in the first year and 91 (36.2%) in the second year. Interventions are needed to address the high rates of GAS disease in this population.

Streptococcus pyogenes (group A *Streptococcus* [GAS]) causes multiple clinical conditions, from noninvasive pharyngitis and impetigo to more invasive streptococcal toxic shock syndrome and necrotizing fasciitis (*1*). Globally, invasive GAS (iGAS) infections are estimated to cause >160,000 deaths annually, and poststreptococcal conditions, primarily rheumatic heart disease, are estimated to cause an additional 476,000 deaths annually (*2*,*3*). In the United States, the increased severity of GAS infections and rising rates of iGAS were first described in the 1980s (*4*). After several decades of stable incidence rates, rates increased from <4.0 cases to 7.6 cases/100,000 persons in 2019 (*5*–*7*; Bact Facts Interactive Data Dashboard, https://www.cdc.gov/abcs/bact-facts/data-dashboard.html). After decreasing during the COVID-19 pandemic, rates continued to increase to 8.2 cases/100,000 persons in 2022 (Bact Facts Interactive Data Dashboard).

American Indian populations have disproportionately high rates of infectious disease related death compared with the general US population (*8*,*9*). However, American Indian populations are underrepresented in national surveillance systems for iGAS, such as the Active Bacterial Core (ABC) surveillance program of the Centers for Disease Control and Prevention. This underrepresentation limits understanding of the epidemiology and rates of iGAS in the United States. A more complete understanding is critical to inform disease prevention strategies, including the development of vaccines against GAS (*10*,*11*).

Studies from the 1980s in Arizona and New Mexico suggested rates of iGAS among American Indian persons are 8–10 times higher than for other ethnic groups (*4*,*12*). A more recent study in Alaska during 2001–2013 found Alaska Native persons accounted for nearly half of Alaska's reported iGAS cases and had a rate >3 times higher than non–Alaska Native persons, despite comprising only 20% of the state's population (*13*).

Author affiliations: Johns Hopkins Bloomberg School of Public Health, Baltimore, Maryland, USA (C.G. Sutcliffe, L.B. Brown, D. Parker, R. Weatherholtz, L.L. Hammitt); Indian Health Service Hospital, Whiteriver, Arizona, USA (R. Close, J. Patel, E. Romancito, J. McAuley); MaineHealth, Portland, Maine, USA (R. Close)

DOI: https://doi.org/10.3201/eid3108.240765

[1]Preliminary results from this study were presented at IDWeek, October 2–6, 2019, Washington, DC, USA.

[2]These first authors contributed equally to this article.

[3]These senior authors contributed equally to this article.

In the fall of 2016, the Indian Health Service (IHS) hospital in Whiteriver, Arizona, USA, which serves the White Mountain Apache (WMA) community, experienced several GAS-related hospitalizations, including 2 invasive cases. To better understand the rate of disease and epidemiology of iGAS in this vulnerable community, we conducted a series of studies, including active laboratory-based surveillance of all hospitalizations secondary to GAS infection. The objectives of this analysis were to describe the rates of severe and invasive GAS infections, the clinical manifestation and underlying medical conditions of severe and invasive cases, and the distribution of circulating M protein gene (*emm*) types among nonsevere, severe, and invasive cases during 2016–2019.

Methods

Study Setting and Overview

We conducted study activities during August 2016–February 2019 in the WMA Tribal lands, which cover an area of 2600 square miles (2) in eastern Arizona and have a population of ≈17,000 Tribal members. The population is served by 1 main IHS facility that provides inpatient and outpatient care and a smaller IHS outpatient clinic. A private health facility, with inpatient and outpatient services, also serves Tribal members and is located 15 miles from the WMA Tribal lands.

We undertook 3 activities in response to an apparent increase in GAS cases at the IHS hospital. First, we collected samples from 19 GAS positive cultures during August–October 2016, irrespective of infection site, clinical syndrome, or severity. We collected a limited set of demographic and clinical information and sequenced the isolates to determine *emm* types. Second, we performed active, laboratory-based surveillance for GAS pharyngitis during May 2017–August 2018, including all patients with a clinical manifestation consistent with pharyngitis who had 2 swabs collected for testing (1 for rapid antigen testing and 1 for traditional culture in the event the rapid antigen test was negative). We monitored the cultures for GAS and collected positive isolates. We collected the patient's age and sequenced the isolates to determine *emm* types. Finally, we conducted active, laboratory-based surveillance for severe and invasive GAS infections during March 2017–February 2019. We included all cases that met eligibility criteria and conducted a chart review. We collected and sequenced isolates to determine *emm* types.

Active, Laboratory-Based Surveillance for Invasive and Severe GAS

We conducted active, laboratory-based surveillance for severe and invasive GAS infections over a 2-year period; year 1 was March 1, 2017–February 28, 2018, and year 2 was March 1, 2018–February 28, 2019. At the IHS hospital, patient specimens were collected at the discretion of the clinical provider; we then sent isolates to the Johns Hopkins Center for Indigenous Health (CIH) laboratory in Whiteriver for processing and storage. We initiated surveillance at the private facility in August 2018. We retrospectively identified all cases of severe and invasive GAS infection that occurred during March 1, 2017–July 31, 2018, through review of microbiology reports and medical charts. During August 1, 2018–February 28, 2019, we identified cases prospectively and sent isolates to the CIH laboratory. At both facilities, we obtained information on case demographics (age, sex, race), underlying medical conditions, clinical syndrome (on the basis of physician report), co-infections (identified on the hospital laboratory report), and health outcomes (amputation or death within 30 days of the initial culture) by using chart review.

We defined a case of iGAS as an American Indian patient living in a community in or near the WMA Tribal lands who had GAS isolated from a normally sterile body site (e.g., blood, cerebrospinal fluid) or from a wound with a diagnosis of streptococcal toxic shock syndrome or necrotizing soft tissue infection, including necrotizing fasciitis. We defined a case of severe GAS infection as an American Indian patient living in a community in or near the WMA Tribal lands who had GAS isolated from a nonsterile site (e.g., wound, ear) and who required hospitalization that otherwise did not meet invasive criteria. We considered patients with multiple isolates collected within 7 days of the initial culture the same case. We defined a reoccurring case as a patient with a new case event, which was GAS isolated from specimens collected $\geq$8 days after the initial date of culture.

Laboratory Methods

At the IHS laboratory, positive blood cultures were identified by using the BACTEC FX automated blood culture system (Becton, Dickinson and Company, https://www.bd.com) for samples collected in BACTEC (Becton, Dickinson and Company) aerobic and anaerobic blood culture bottles. When growth was detected, the positive blood cultures were subcultured to MacConkey, chocolate, and sheep's blood agar plates. Wound and throat samples were

collected by using liquid double swabs (Becton Dickinson) and plated onto sheep's blood agar with a bacitracin disc.

At the private facility, positive blood cultures were identified by using the VITEK 2 automated blood culture system (bioMérieux, https://www.biomerieux.com). When growth was detected, GAS was confirmed by using a latex agglutination test.

As part of the surveillance for invasive and severe GAS infections, we subcultured eligible isolates in the CIH laboratory on sheep's blood agar plates with a bacitracin disc to confirm the presence of GAS. After 24 hours of incubation, we stored the cultured colonies in skim milk at −80°C.

We sent all the recovered isolates to the Musser laboratory at Houston Methodist Research Institute (Houston, TX, USA) for whole-genome sequencing to determine *emm* types. Strain growth, isolation of chromosomal DNA, generation of paired-end libraries, and multiplexed sequencing by using an Illumina NextSeq 550 (Illumina, https://www.illumina.com) were performed as previously described (*14*–*16*). Reads were preprocessed by using Trimmomatic and Musket (*17*,*18*) and then assembled de novo by using SPAdes (*19*). Gene content data were generated by using short-read sequence typer 2 (*20*) and custom databases as previously described (*21*).

Statistical Analysis

We compared the characteristics and outcomes of invasive and severe cases from year 1 and year 2 by using χ^2 or Fisher exact tests for categorical variables and Wilcoxon rank-sum tests for continuous variables. We calculated incidence rates of invasive and severe GAS infections (overall and separately) by using the IHS user population during 2017–2018 as the denominator for years 1 and 2. IHS defines users as any American Indian patient receiving services at the IHS facility in the preceding 3 years (*22*). We included all cases identified from the surveillance system from communities included in the IHS user population for the IHS facility in the numerator, regardless of whether an isolate was collected. For each year and type of infection, we calculated incidence overall and by age by using Poisson regression with robust variance estimation to account for recurrent infections. For comparison with the general US population (Bact Facts Interactive Data Dashboard), we calculated age-standardized incidence rates for each year by using direct standardization methods by using US census data from 2017 as the reference (*23*).

We summarized the distribution of *emm* types by sample type (clinical, pharyngitis, severe or invasive isolates), year, and patient characteristics (age, sex, clinical manifestation). We separately estimated the proportion of *emm* types targeted by an experimental 30-valent type-specific vaccine for pharyngitis and severe or invasive isolates (*24*,*25*). We conducted analyses by using SAS software version 9.4 (SAS Institute, https://www.sas.com) and Stata software version 14.2 (StataCorp, LLC, https://www.stata.com).

Ethics Statement

This study was approved by the WMA Tribe and by the Institutional Review Boards of the Phoenix Area IHS (approval no. PXR 18.06) and the Johns Hopkins Bloomberg School of Public Health (approval no. 8510). A Health Insurance Portability and Accountability Act waiver was obtained to conduct medical chart reviews.

Results

Effect of Severe and Invasive GAS

During the surveillance period, 48 invasive cases (23 cases in year 1 and 25 in year 2) and 113 severe cases (56 cases in year 1 and 57 in year 2) were detected. The 161 cases occurred among 146 persons: 9 persons had 1 recurrent infection, and 3 persons had 2 recurrent infections.

Among the 48 invasive cases, 52 isolates were identified: 32 (61.5%) from blood, 1 (1.9%) from synovial fluid, and 19 (36.5%) from wounds. Among the 113 severe cases, 113 isolates were identified: 106 (93.8%) from wounds, 5 (4.2%) from abscesses, 1 (0.9%) from a peritonsillar abscess, and 1 (0.9%) from an ear culture in a patient with mastoiditis.

Among the GAS cases (Table 1, http://wwwnc.cdc.gov/EID/article/31/8/24-0765-T1.htm), compared with those with severe cases, patients with invasive cases were older, were more likely to have underlying conditions of hypertension and heart failure, were more likely to have pneumonia and sepsis, and had much longer hospitalization lengths. Patients with severe cases were much more likely to have alcoholism as an underlying condition and to have cellulitis as a disease syndrome. The clinical syndromes associated with severe and invasive infections differed by age: skin infections (e.g., eczema, impetigo) were dominant among children <5 years of age; trauma (e.g., falls and self-inflicted wounds) and skin infections (e.g., insect bites, sores, blisters) were dominant among older children and adolescents; trauma (e.g., lacerations, burns, injuries) was dominant among adults 18–49 years of age; and trauma (e.g., burns and falls) and complications of underlying conditions (e.g., prior amputation or diabetic foot

ulcers) were dominant among older adults (Appendix 1 Table 1, http://wwwnc.cdc.gov/EID/article/31/8/24-0765-App1.pdf).

Almost half of patients were co-infected with *Staphylococcus aureus* (47.2%). Those with severe cases were significantly more likely to be co-infected with *S. aureus* than were those with invasive cases (59.3% vs. 18.8%; p<0.0001). Among patients co-infected with *S. aureus*, 44.7% were co-infected with methicillin-resistant *S. aureus*, at similar rates for severe (44.8%) and invasive (44.4%; p = 0.99) cases. Similar results were found when restricting the data to cases with GAS isolated from a wound: those with severe cases (61.3%) were more likely to be co-infected than were those with invasive cases (35.0%), and a similar proportion of co-infections were methicillin-resistant *S. aureus* (45.8%; severe, 46.2%; invasive, 42.9%; p = 0.87).

Overall, 6 (3.7%) patients had an amputation because of the GAS infection, 3 (6.7%) of those with invasive cases and 3 (2.6%) of those with severe cases (p = 0.22). Three (1.9%) patients died within 30 days of the initial culture; all had invasive infections (6.3%; p = 0.002).

Antimicrobial resistance testing at the clinical laboratories was only performed on the 32 invasive isolates identified from blood. No resistance was identified to the cephalosporins, penicillins, or fluoroquinolones tested (Appendix 1 Table 2). Only 6 (18.8%) isolates demonstrated resistance; all were resistant to tetracycline, and 3 (9.4%) were also resistant to clindamycin.

The overall incidence of severe and invasive GAS infections during the surveillance period was 472.7 (95% confidence interval [CI] 405.2–551.4)/100,000 persons (Table 2). The incidence of invasive infections was 140.9 (95% CI 106.2–187.0)/100,000 persons and the incidence of severe infections was 331.8 (95% CI 276.0–398.8)/100,000 persons. Rates did not vary significantly by year (Table 3). For both severe and invasive infections, rates were higher for adults than children; the highest rates of severe infections were observed among adults 18–49 years of age and invasive infections were observed among adults ≥65 years of age. The overall age-standardized incidence of severe and invasive infections was 554.2/100,000 persons. Separately, the age-standardized incidence of severe infections was 359.6/100,000 persons and of invasive infections was 194.6/100,000 persons.

Molecular Characteristics of GAS Isolates

Whole-genome sequencing was completed on all 19 clinical isolates from 2016, as well as 135 of 149 pharyngitis isolates and 131 of 165 severe and invasive GAS isolates (Appendix 1 Tables 3–7; Appendix 2 Table, http://wwwnc.cdc.gov/EID/article/31/8/24-0765-App2.xlsx). Four isolates were from a second source from the same invasive case and yielded the same *emm* type and were excluded from

Table 2. Incidence rates of severe and invasive group A *Streptococcus* infection among American Indian persons in the White Mountain Apache Tribal lands, Arizona, USA, 2017–2019

Characteristic	Total no.	Severe and invasive infections		Invasive infections		Severe infections	
		No.	Incidence* (95% CI)	No.	Incidence* (95% CI)	No.	Incidence* (95% CI)
Overall	34,061	161	472.7 (405.2–551.4)	48	140.9 (106.2–187.0)	113	331.8 (276.0–398.8)
By age, y							
0–4	3,391	7	206.4 (98.5–432.7)	1	29.5 (4.2–209.4)	6	176.9 (79.5–393.6)
5–17	8,791	11	125.1 (69.3–225.9)	0	0	11	125.1 (69.3–225.9)
18–49	14,514	90	620.1 (504.7–761.9)	22	151.6 (99.8–230.1)	68	468.5 (369.6–593.9)
50–64	4,845	32	660.5 (467.6–932.9)	12	247.7 (140.8–435.9)	20	412.8 (266.6–639.3)
≥65	2,520	21	833.3 (544.3–1,275.8)	13	516.0 (300.0–887.3)	8	317.5 (158.9–634.1)
Year 1†	16,948	79	466.1 (374.1–580.8)	23	135.7 (90.2–204.2)	56	330.4 (254.4–429.2)
By age, y							
0–4	1,693	5	295.3 (123.1–708.8)	1	59.1 (8.3–419.3)	4	236.3 (88.8–629.0)
5–17	4,366	5	114.5 (47.7–275.0)	0	0	5	114.5 (47.7–275.0)
18–49	7,260	42	578.5 (427.9–782.1)	8	110.2 (55.1–220.3)	34	468.3 (334.9–654.9)
50–64	2,383	14	587.5 (348.5–990.5)	6	251.9 (113.3–560.0)	8	335.7 (168.1–670.5)
≥65	1,246	13	1043.3 (607.5–1,791.8)	8	642.1 (321.8–1,281.0)	5	401.3 (167.3–962.4)
Year 2†	17,113	82	479.2 (386.1–594.7)	25	146.1 (98.7–216.1)	57	333.1 (257.0–431.6)
By age, y							
0–4	1,698	2	117.8 (29.5–470.8)	0	0	2	117.8 (29.5–470.8)
5–17	4,425	6	135.6 (61.0–301.7)	0	0	6	135.6 (61.0–301.7)
18–49	7,254	48	66.2 (499.1–877.2)	14	193.0 (114.4–325.7)	34	468.7 (335.2–655.5)
50–64	2,462	18	731.1 (461.4–1,158.5)	6	243.7 (109.5–541.9)	12	487.4 (277.2–857.1)
≥65	1,274	8	627.9 (314.7–1,252.9)	5	392.4 (163.6–941.3)	3	235.5 (76.1–729.2)

*Cases/100,000 persons.
†No significant difference was observed between years 1 (March 2017–February 2018) and 2 (March 2018–February 2019) for all group A *Streptococcus* (incidence rate ratio: 1.03; 95% confidence interval: 0.76–1.40), invasive group A *Streptococcus* (incidence rate ratio: 1.08; 95% confidence interval: 0.61–1.90) or severe group A *Streptococcus* (incidence rate ratio: 1.01; 95% confidence interval: 0.70–1.46).

the analysis. The distribution of *emm* types varied by year and sample type (Appendix 1 Table 4; Figures 1, 2). In 2016, out of 19 clinical isolates collected, 13 (68%) were *emm*59. Among 135 pharyngitis isolates collected during 2017–2018, the most common *emm* types were 82, 60, and 6, with little variation by year (Appendix 1 Figure 2); 80% were *emm* types targeted by an experimental 30-valent type-specific vaccine (*24*). In year 1 (2017–2018) of active surveillance, *emm*82 caused most (65.5%) severe and invasive GAS infections. In year 2 (2018–2019), more *emm* types were present; 91 (36.2%), 82 (21.7%), and 49 (18.8%) were the most common. Of the 127 severe and invasive GAS isolates in this study, 66% were *emm* types targeted by the 30-valent type-specific vaccine (*24*).

Discussion

This study, conducted in an American Indian community in Arizona during 2016–2019, revealed high rates of severe and invasive GAS infections, particularly among older adults. Co-infection with *S. aureus* was common among persons with severe skin and soft tissue infections. Although most outcomes were favorable, a small proportion of infections resulted in amputation or death. Molecular characterization of isolates found a shift in dominant *emm* types over time with overlapping distributions between pharyngitis and severe and invasive isolates.

By using a population-based, laboratory-based surveillance system, we documented a rate of iGAS of 194.6/100,000 persons for the WMA community, which was >25 times that found in the general US population and among the highest reported in the world. In 2019, the rate of iGAS in the United States was 7.6/100,000 persons (Bact Facts Interactive Data Dashboard). Similar to our study, that study found the highest rates were observed among older adults (7.5/100,000 persons among adults 35–49 of age, 10.6/100,000 persons among adults 50–64 of age, and 16.1/100,000 persons among adults ≥65 years of age) (Bact Facts Interactive Data Dashboard). The rate in our study was also substantially higher than that reported among American Indian persons throughout Arizona in 2017 (21.6/100,000 persons) (*26*) and among Alaska Native persons during 2001–2013 (13.7/100,000 persons) (*13*). Globally, indigenous populations are found to have disproportionately high rates of iGAS, including those in Australia (23.8–82.5/100,000 persons) (*27*–*29*), New Zealand (20.4/100,000 persons) (*30*), Fiji (17.8/100,000 persons) (*31*), and Canada (10.0–52.2/100,000 persons) (*32*).

Host characteristics, host–pathogen dynamics, and pathogen virulence all likely contribute to the disparate rates of iGAS among American Indian communities, but the proportion of disease attributable to each factor is poorly understood. Many host characteristics associated with GAS infections in North America are driven by socioeconomic differences. In Canada and the United States, outbreaks of iGAS have been associated with substance use and homelessness (*33*–*36*). Whereas homelessness was uncommon in this study, alcohol misuse was common, reported in more than half the cases. Alcohol misuse was more common among persons with severe GAS infections, which were documented predominantly among younger men. All patients reported ≥1 underlying condition, and diabetes and hypertension, known risk factors for iGAS (*37*,*38*), were reported in approximately one third of cases. In addition, poor household conditions, household crowding, and exposure to children with sore throats have been found to be associated with iGAS in other studies

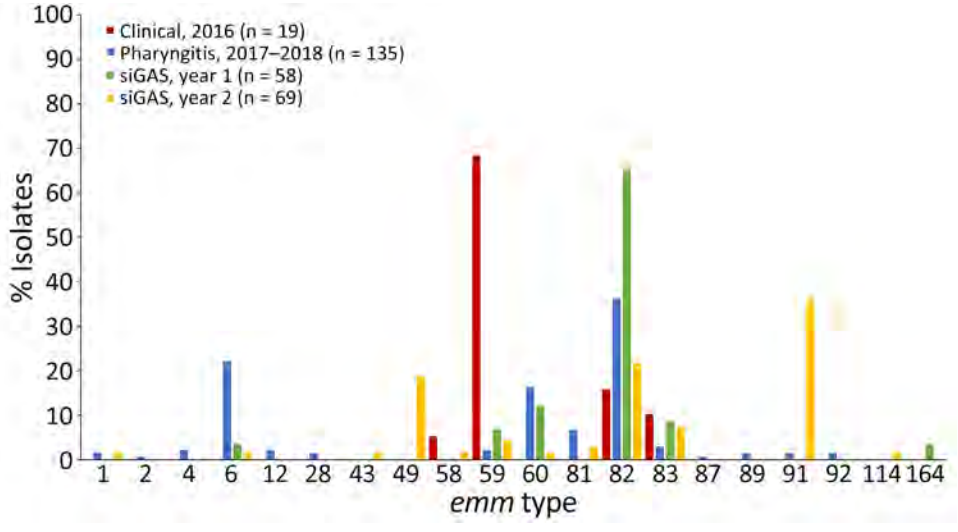

Figure 1. Distribution of *emm* types among cases of group A *Streptococcus* from American Indian persons in the White Mountain Apache Tribal Lands, Arizona, USA, 2016–2019. Clinical isolates were convenience samples; all other samples were collected as part of active, laboratory-based surveillance. Year 1 indicates active surveillance for siGAS during March 1, 2017–February 28, 2018, and year 2 indicates active surveillance for siGAS during March 1, 2018–February 28, 2019. siGAS, severe or invasive cases of group A *Streptococcus*.

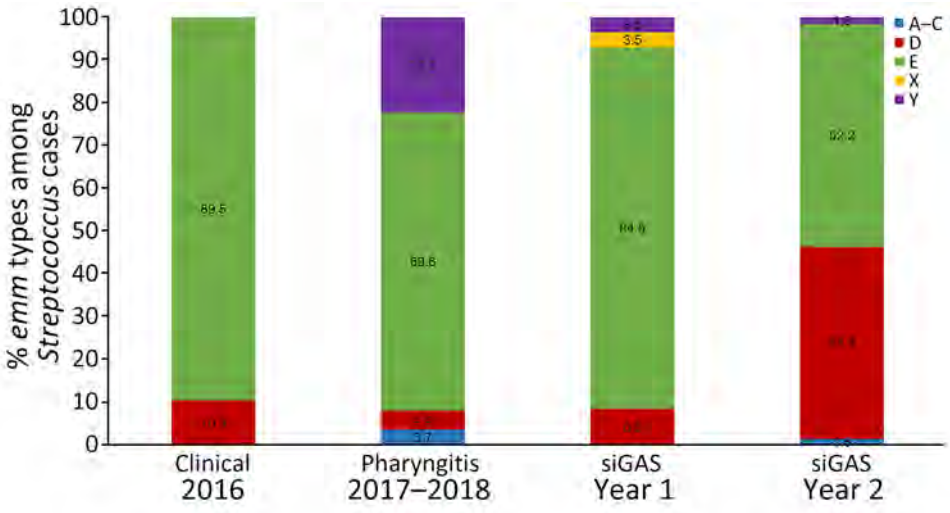

Figure 2. Distribution of *emm* type clusters by sample type among cases of group A *Streptococcus* from American Indian persons in the White Mountain Apache Tribal Lands, Arizona, USA, 2016–2019. Clinical isolates were convenience samples; all other samples were collected as part of active, laboratory-based surveillance. Year 1 indicates active surveillance for siGAS during March 1, 2017–February 28, 2018, and year 2 indicates active surveillance for siGAS during March 1, 2018–February 28, 2019. siGAS, severe or invasive cases of group A *Streptococcus*.

(*37*). Although those factors were not directly assessed in this study, 15% of patients had a severe GAS infection in the previous 5 years, including several persons with recurrent infections during the 2-year study period, indicating relatively common and repeated exposure to GAS in the household or community. In addition, the large proportion of *emm* types belonging to the D cluster (skin specialists) and small proportion belonging to the A–C cluster (throat specialists) among severe and invasive cases (*39*) suggest that skin and soft tissue infections, which are affected by household conditions and crowding, are a major driver of serious GAS disease. In the WMA community, families tend to be larger (4.2 vs. 3.1 in the general US population) and multigenerational (22.2% vs. 4.9% in Arizona), and a higher proportion live below the federal poverty line (40.4% vs. 12.6% in the United States) (*40*,*41*). Additional studies are needed of both GAS disease and carriage to further understand the contribution of those factors in this community.

There is an increased interest in the role of virulent *emm* types among vulnerable populations in recent years. Canada experienced an outbreak of iGAS driven by the hypervirulent *emm*59 clone beginning in 2006 (*33*), and First Nations persons were disproportionately represented among cases (*42*). Later studies revealed that clone migrated to the United States, mutated, and caused outbreaks in Wyoming, Montana, and Oregon (*43*,*44*). In the ABCs program, *emm*59 was reported almost exclusively from New Mexico in 2015, with a few isolates also identified from Oregon (*45*). In 2015, an outbreak of iGAS occurred in northern Arizona, and most cases were in American Indian persons. Most isolates (62%) were *emm*59 and genetically related to the Canada strain (*46*). Of interest, *emm*59 was the dominant type found in the clinical isolates in our study in 2016. However, the dominant type shifted to *emm*82 during 2017–2018 among both GAS pharyngitis and invasive cases and then to *emm*91 in 2018 and 2019 among invasive cases, potentially suggesting introduction and rapid circulation of different types into the community. Although other studies, particularly from Canada, have found rapid shifts in dominant types in indigenous populations (*32*), many report a variety of types with none clearly dominant (*13*,*27*,*28*,*30*,*47*). Of note, the common *emm* types identified from severe and invasive cases in this study (e.g., 49, 59, 60, 82) overlapped with those commonly identified from disadvantaged communities (e.g., persons experiencing homelessness or who inject drugs) in the ABCs program during the same period (2015–2018) (*48*). Persons experiencing homelessness or who inject drugs were also found to have higher rates of disease (≈14–80-fold higher) and were more likely to have acute skin breakdown than persons without those risks (*36*), highlighting the shared social drivers of health with indigenous communities and the potential for shared learnings from further research in these communities.

The high rates of disease observed in the WMA Tribal lands and other indigenous and vulnerable communities illustrates the need for effective interventions to decrease illness and death and address health differences. Eight GAS vaccine candidates are in development; the furthest along is an M protein–based vaccine candidate targeting 30 *emm* types that was found to be immunogenic and well tolerated in a phase 1 clinical trial (*24*,*49*). In this study, 66% of severe and invasive *emm* types and 80% of pharyngitis *emm* types would have been targeted by the vaccine, similar to the 53% coverage reported for invasive cases among First Nations populations in Alberta, Canada, during

2003–2017 (*32*). That study also observed a difference in coverage between First Nations and non–First Nations populations, with a higher coverage of 77% for the non–First Nations population (*32*). The authors also observed a major difference in *emm* cluster types between First Nations and non–First Nations populations, with a larger proportion in cluster D and smaller proportion in cluster A–C among First Nations cases (*32*). Although our study did not include a nonindigenous comparison population, the estimated coverage with the 30-valent vaccine was lower than that reported for invasive cases included in the ABCs program in 2015 (88%) in the United States (*45*). Few samples from ABCs were identified with *emm* types belonging to cluster D, and those are not well represented among *emm* types included in the vaccine (*24*,*45*). The larger proportion of *emm* types from cluster D identified from indigenous cases may explain the lower *emm* type coverage observed for Indigenous populations and between cases of severe and invasive disease and pharyngitis. Potential cross-reactivity with nonvaccine *emm* types could decrease differences between populations and increase the effectiveness of the vaccine (*24*,*25*,*50*).

In conclusion, we found high rates of severe and invasive GAS disease in this American Indian community in Arizona, USA, highlighting the need to increase representation of reservation-based American Indian populations in current laboratory and genomic surveillance systems. Vaccines to prevent GAS disease are under development but are still years from licensure. Until then, interventions that are culturally informed and promote early recognition and treatment are needed to reduce the illness and death associated with GAS infections.

Acknowledgments

We thank the Center for Indigenous Health staff involved in conducting the study, the White Mountain Apache Tribe, clinical and laboratory partners at the Indian Health Service, Tribally operated and private health facilities, the institutional review boards of the Phoenix area Indian Health Service and the Johns Hopkins Bloomberg School of Public Health, and Randall J. Olsen, Stephen B. Beres, and James M. Musser for conducting sequencing and analysis.

J.M.M. was funded by the Fondren Foundation.

About the Author

Dr. Sutcliffe identifies as a White woman who lives in the northeast of the USA. She is a research professor at the Johns Hopkins Bloomberg School of Public Health and member of the Infectious Disease Program at the Center for Indigenous Health. Her interests include the epidemiology of infectious diseases in underserved populations and working with Indigenous communities in the southwest United States.

References

1. Levinson W. Review of medical microbiology and immunology. 14th ed. New York: McGraw-Hill Education; 2016.
2. Carapetis JR, Steer AC, Mulholland EK, Weber M. The global burden of group A streptococcal diseases. Lancet Infect Dis. 2005;5:685–94. https://doi.org/10.1016/S1473-3099(05)70267-X
3. Hand RM, Snelling TL. JR C. Group A *Streptococcus*. In: Ryan ET HD, Solomon T, Aronson NE, Endy TP, editor. Hunter's Tropical Medicine and Emerging Infectious Diseases. 10th ed. London: Elsevier; 2020. p. 429–438.
4. Hoge CW, Schwartz B, Talkington DF, Breiman RF, MacNeill EM, Englender SJ. The changing epidemiology of invasive group A streptococcal infections and the emergence of streptococcal toxic shock-like syndrome. A retrospective population-based study. JAMA. 1993;269:384–9. https://doi.org/10.1001/jama.1993.03500030082037
5. O'Brien KL, Beall B, Barrett NL, Cieslak PR, Reingold A, Farley MM, et al. Epidemiology of invasive group a *streptococcus* disease in the United States, 1995–1999. Clin Infect Dis. 2002;35:268–76. https://doi.org/10.1086/341409
6. O'Loughlin RE, Roberson A, Cieslak PR, Lynfield R, Gershman K, Craig A, et al.; Active Bacterial Core Surveillance Team. The epidemiology of invasive group A streptococcal infection and potential vaccine implications: United States, 2000–2004. Clin Infect Dis. 2007;45:853–62. https://doi.org/10.1086/521264
7. Nelson GE, Pondo T, Toews KA, Farley MM, Lindegren ML, Lynfield R, et al. Epidemiology of invasive group A streptococcal infections in the United States, 2005–2012. Clin Infect Dis. 2016;63:478–86. https://doi.org/10.1093/cid/ciw248
8. Cheek JE, Holman RC, Redd JT, Haberling D, Hennessy TW. Infectious disease mortality among American Indians and Alaska Natives, 1999–2009. Am J Public Health. 2014;104 (Suppl 3):S446–52. https://doi.org/10.2105/AJPH.2013.301721
9. Lee NR, King A, Vigil D, Mullaney D, Sanderson PR, Ametepee T, et al. Infectious diseases in Indigenous populations in North America: learning from the past to create a more equitable future. Lancet Infect Dis. 2023; 23:e431–44. https://doi.org/10.1016/S1473-3099(23)00190-1
10. Moore HC, Cannon JW, Kaslow DC, Lamagni T, Bowen AC, Miller KM, et al. A systematic framework for prioritizing burden of disease data required for vaccine development and implementation: the case for group A streptococcal diseases. Clin Infect Dis. 2022;75:1245–54. https://doi.org/10.1093/cid/ciac291
11. Vekemans J, Gouvea-Reis F, Kim JH, Excler JL, Smeesters PR, O'Brien KL, et al. The path to group A *Streptococcus* vaccines: World Health Organization research and development technology roadmap and preferred product characteristics. Clin Infect Dis. 2019;69:877–83. https://doi.org/10.1093/cid/ciy1143
12. Benjamin EM, Gershman M, Goldberg BW. Community-acquired invasive group A beta-hemolytic streptococcal infections in Zuni Indians. Arch Intern Med. 1992;152:1881–4. https://doi.org/10.1001/archinte.1992.00400210103017

13. Rudolph K, Bruce MG, Bruden D, Zulz T, Reasonover A, Hurlburt D, et al. Epidemiology of invasive group A streptococcal disease in Alaska, 2001 to 2013. J Clin Microbiol. 2016;54:134–41. https://doi.org/10.1128/JCM.02122-15
14. Beres SB, Kachroo P, Nasser W, Olsen RJ, Zhu L, Flores AR, et al. Transcriptome remodeling contributes to epidemic disease caused by the human pathogen *Streptococcus pyogenes*. MBio. 2016;7:e00403-16. https://doi.org/10.1128/mBio.00403-16
15. Beres SB, Olsen RJ, Ojeda Saavedra M, Ure R, Reynolds A, Lindsay DSJ, et al. Genome sequence analysis of emm89 *Streptococcus pyogenes* strains causing infections in Scotland, 2010–2016. J Med Microbiol. 2017;66:1765–73. https://doi.org/10.1099/jmm.0.000622
16. Nasser W, Beres SB, Olsen RJ, Dean MA, Rice KA, Long SW, et al. Evolutionary pathway to increased virulence and epidemic group A *Streptococcus* disease derived from 3,615 genome sequences. Proc Natl Acad Sci U S A. 2014;111:E1768–76. https://doi.org/10.1073/pnas.1403138111
17. Bolger AM, Lohse M, Usadel B. Trimmomatic: a flexible trimmer for Illumina sequence data. Bioinformatics. 2014;30:2114–20. https://doi.org/10.1093/bioinformatics/btu170
18. Liu Y, Schröder J, Schmidt B. Musket: a multistage k-mer spectrum-based error corrector for Illumina sequence data. Bioinformatics. 2013;29:308–15. https://doi.org/10.1093/bioinformatics/bts690
19. Bankevich A, Nurk S, Antipov D, Gurevich AA, Dvorkin M, Kulikov AS, et al. SPAdes: a new genome assembly algorithm and its applications to single-cell sequencing. J Comput Biol. 2012;19:455–77. https://doi.org/10.1089/cmb.2012.0021
20. Inouye M, Dashnow H, Raven LA, Schultz MB, Pope BJ, Tomita T, et al. SRST2: Rapid genomic surveillance for public health and hospital microbiology labs. Genome Med. 2014;6:90. https://doi.org/10.1186/s13073-014-0090-6
21. Long SW, Olsen RJ, Eagar TN, Beres SB, Zhao P, Davis JJ, et al. Population genomic analysis of 1,777 extended-spectrum beta-lactamase-producing *Klebsiella pneumoniae* isolates, Houston, Texas: unexpected abundance of clonal group 307. MBio. 2017;8:e00489-17. https://doi.org/10.1128/mBio.00489-17
22. Indian Health Service. National data warehouse, user population/workload frequently asked questions: U. S. Department of Health and Human Services. 2019 [cited 2019 January 8]. https://www.ihs.gov/NDW/index.cfm?module=dsp_dqw_mq5-1&Answer=2
23. United States Census Bureau. 2015 American community survey 1-year estimates. 2015 [cited 2017 October 12]. https://factfinder.census.gov/faces/nav/jsf/pages/index.xhtml
24. Pastural É, McNeil SA, MacKinnon-Cameron D, Ye L, Langley JM, Stewart R, et al. Safety and immunogenicity of a 30-valent M protein-based group a streptococcal vaccine in healthy adult volunteers: a randomized, controlled phase I study. Vaccine. 2020;38:1384–92. https://doi.org/10.1016/j.vaccine.2019.12.005
25. Courtney HS, Niedermeyer SE, Penfound TA, Hohn CM, Greeley A, Dale JB. Trivalent M-related protein as a c omponent of next generation group A streptococcal vaccines. Clin Exp Vaccine Res. 2017;6:45–9. https://doi.org/10.7774/cevr.2017.6.1.45
26. Arizona Department of Health Services. Rates of reported confirmed and probable cases of selected notifiable diseases by race/ethnicity, per 100,000 population, Arizona, 2017. 2017 [cited 2025 Jul 10]. https://www.azdhs.gov/documents/preparedness/epidemiology-disease-control/disease-data-statistics-reports/data-statistics-archive/2017/raceethnicity2017.pdf
27. Boyd R, Patel M, Currie BJ, Holt DC, Harris T, Krause V. High burden of invasive group A streptococcal disease in the northern territory of Australia. Epidemiol Infect. 2016;144:1018–27. https://doi.org/10.1017/S0950268815002010
28. Carapetis JR, Walker AM, Hibble M, Sriprakash KS, Currie BJ. Clinical and epidemiological features of group A streptococcal bacteraemia in a region with hyperendemic superficial streptococcal infection. Epidemiol Infect. 1999;122:59–65. https://doi.org/10.1017/S0950268898001952
29. Norton R, Smith HV, Wood N, Siegbrecht E, Ross A, Ketheesan N. Invasive group A streptococcal disease in North Queensland (1996–2001). Indian J Med Res. 2004;119(Suppl):148–51.
30. Safar A, Lennon D, Stewart J, Trenholme A, Drinkovic D, Peat B, et al. Invasive group A streptococcal infection and vaccine implications, Auckland, New Zealand. Emerg Infect Dis. 2011;17:983–9. https://doi.org/10.3201/eid/1706.100804
31. Thean LJ, Jenney A, Engelman D, Romani L, Wand H, Mani J, et al. Prospective surveillance for invasive *Staphylococcus aureus* and group A *Streptococcus* infections in a setting with high community burden of scabies and impetigo. Int J Infect Dis. 2021;108:333–9. https://doi.org/10.1016/j.ijid.2021.05.041
32. Tyrrell GJ, Bell C, Bill L, Fathima S. Increasing incidence of invasive group A *Streptococcus* disease in First Nations population, Alberta, Canada, 2003–2017. Emerg Infect Dis. 2021;27:443–51. https://doi.org/10.3201/eid2702.201945
33. Tyrrell GJ, Lovgren M, St Jean T, Hoang L, Patrick DM, Horsman G, et al. Epidemic of group A *Streptococcus* M/emm59 causing invasive disease in Canada. Clin Infect Dis. 2010;51:1290–7. https://doi.org/10.1086/657068
34. Teatero S, McGeer A, Tyrrell GJ, Hoang L, Smadi H, Domingo MC, et al. Canada-wide epidemic of *emm74* group A *Streptococcus* invasive disease. Open Forum Infect Dis. 2018;5:ofy085. https://doi.org/10.1093/ofid/ofy085
35. Tyrrell GJ, Fathima S, Kakulphimp J, Bell C. Increasing rates of invasive group A streptococcal disease in Alberta, Canada; 2003–2017. Open Forum Infect Dis. 2018;5:ofy177. https://doi.org/10.1093/ofid/ofy177
36. Valenciano SJ, Onukwube J, Spiller MW, Thomas A, Como-Sabetti K, Schaffner W, et al. Invasive group A streptococcal infections among people who inject drugs and people experiencing homelessness in the United States, 2010–2017. Clin Infect Dis. 2021;73:e3718–26. https://doi.org/10.1093/cid/ciaa787
37. Factor SH, Levine OS, Schwartz B, Harrison LH, Farley MM, McGeer A, et al. Invasive group A streptococcal disease: risk factors for adults. Emerg Infect Dis. 2003;9:970–7. https://doi.org/10.3201/eid0908.020745
38. Davies HD, McGeer A, Schwartz B, Green K, Cann D, Simor AE, et al.; Ontario Group A Streptococcal Study Group. Invasive group A streptococcal infections in Ontario, Canada. N Engl J Med. 1996;335:547–54. https://doi.org/10.1056/NEJM199608223350803
39. Bessen DE. Tissue tropisms in group A *Streptococcus*: what virulence factors distinguish pharyngitis from impetigo strains? Curr Opin Infect Dis. 2016;29:295–303. https://doi.org/10.1097/QCO.0000000000000262
40. United States Census Bureau. Fort Apache Reservation, AZ. Families and living arrangements. 2022 [cited 2024 February

1]. https://data.census.gov/profile/Fort_Apache_Reservation,_AZ?g=2500000US1140#families-and-living-arrangements
41. Arizona Rural Policy Institute, Northern Arizona University. Demographic analysis of the White Mountain Apache Tribe using 2010 census and 2010 American community survey estimates. 2010 [cited 2025 Jul 10]. https://in.nau.edu/wp-content/uploads/sites/212/White-Mountain-Apache-2011-2015-Demographic-Analysis.pdf
42. Athey TB, Teatero S, Sieswerda LE, Gubbay JB, Marchand-Austin A, Li A, et al. High incidence of invasive group A *Streptococcus* disease caused by strains of uncommon *emm* types in Thunder Bay, Ontario, Canada. J Clin Microbiol. 2016;54:83–92. https://doi.org/10.1128/JCM.02201-15
43. Fittipaldi N, Olsen RJ, Beres SB, Van Beneden C, Musser JM. Genomic analysis of *emm59* group A *Streptococcus* invasive strains, United States. Emerg Infect Dis. 2012;18:650–2. https://doi.org/10.3201/eid1804.111803
44 Brown CC, Olsen RJ, Fittipaldi N, Morman ML, Fort PL, Neuwirth R, et al. Spread of virulent group A *Streptococcus* type *emm59* from Montana to Wyoming, USA. Emerg Infect Dis. 2014;20:679–81. https://doi.org/10.3201/eid2004.130564
45. Chochua S, Metcalf BJ, Li Z, Rivers J, Mathis S, Jackson D, et al. Population and whole genome sequence based characterization of invasive group A *Streptococci* recovered in the United States during 2015. MBio. 2017;8:e01422-17. https://doi.org/10.1128/mBio.01422-17
46. Engelthaler DM, Valentine M, Bowers J, Pistole J, Driebe EM, Terriquez J, et al. Hypervirulent *emm59* clone in invasive group A *Streptococcus* outbreak, southwestern United States. Emerg Infect Dis. 2016;22:734–8. https://doi.org/10.3201/eid2204.151582
47. Bocking N, Matsumoto CL, Loewen K, Teatero S, Marchand-Austin A, Gordon J, et al. High incidence of invasive group A streptococcal infections in remote indigenous communities in northwestern Ontario, Canada. Open Forum Infect Dis. 2016;4:ofw243. https://doi.org/10.1093/ofid/ofw243
48. Metcalf B, Nanduri S, Chochua S, Li Y, Fleming-Dutra K, McGee L, et al. Cluster transmission drives invasive group A *Streptococcus* disease within the United States and is focused on communities experiencing disadvantage. J Infect Dis. 2022;226:546–53. https://doi.org/10.1093/infdis/jiac162
49. Walkinshaw DR, Wright MEE, Mullin AE, Excler JL, Kim JH, Steer AC. The *Streptococcus pyogenes* vaccine landscape. NPJ Vaccines. 2023;8:16. https://doi.org/10.1038/s41541-023-00609-x
50. Frost HR, Laho D, Sanderson-Smith ML, Licciardi P, Donath S, Curtis N, et al. Immune cross-opsonization within *emm* clusters following group A *Streptococcus* skin infection: broadening the scope of type-specific immunity. Clin Infect Dis. 2017;65:1523–31. https://doi.org/10.1093/cid/cix599

Address for correspondence: Catherine G. Sutcliffe, Johns Hopkins Bloomberg School of Public Health, 415 N. Washington St, Baltimore, MD 21231 USA; email: csutcli1@jhu.edu

Multidisciplinary Tracking of Highly Pathogenic Avian Influenza A(H5N1) Outbreak in Griffon Vultures, Southern Europe, 2022

Julien Hirschinger, Ursula Höfle, Alberto Sánchez-Cano, Claire Guinat, Guillaume Croville, Marta Barral, José Antonio Donázar, Chloé Le Gall Ladevèze, Mathilda Walch, Vega Alvarez, Xeider Gerrikagoitia, Louis Du Plessis, Simon Dellicour, Eneko Arrondo, José Antonio Sánchez-Zapata, Ainara Cortés-Avizanda, Sara Minayo Martín, Jérémy Tornos, Samuel Perret, Thierry Boulinier, Pascal Orabi, Anne Van De Wiele, Jean-Luc Guerin, Olivier Duriez, Guillaume Le Loc'h

Since 2021, highly pathogenic avian influenza (HPAI) A(H5N1) clade 2.3.4.4b virus has affected wild bird populations globally. Griffon vultures (*Gyps fulvus*), a species hitherto considered unexposed, experienced an HPAI H5N1 outbreak in 2022 in southern Europe, leading to moderate mortality and reduced breeding success. The integration of virological, serologic, phylogenetic, and ecologic data revealed a short yet intense viral circulation and a probable common source of infection. The dissemination across Spain and France was likely caused by frequent interpopulation movements of birds. This integrated overview of the 2022 HPAI outbreak in vultures provides novel insights into the role of large-scale movements of wild birds in the spread of such disease. Understanding the epidemiologic dynamics of HPAI H5N1 in these scavenger species is crucial because the birds play vital roles in ecosystem functioning. Their susceptibility to this virus highlights potential broader ecologic effects of the ongoing outbreaks.

Since 2021, highly pathogenic avian influenza (HPAI) A(H5N1) clade 2.3.4.4b virus has emerged as a devastating pathogen in terms of bird species diversity, abundance, geographic extent, and economic losses (*1*). Although the effects on domestic birds have been staggering at >500 million reported deaths, the full extent of the toll on wild birds is unknown (*2*). Approximately 420,000 wild bird deaths have been reported, likely a considerable underestimate (*3*), and the diversity and number of affected species imply a profound threat to biodiversity (*4*).

This ongoing panzootic represents a paradigm shift in H5Nx avian influenza. HPAI H5N1 infections have now been reported on all continents except Oceania and in ≥50 mammal species (*5*,*6*). Most mammal infections have been reported in predators

Author affiliations: IHAP, ENVT, INRAE, Université de Toulouse, Toulouse, France (J. Hirschinger, C. Guinat, G. Croville, C. Le Gall Ladevèze, M. Walch, J.-L. Guerin, G. Le Loc'h); Grupo SaBio, Instituto de Investigación en Recursos Cinegéticos (CSIC-UCLM-JCCM), Ciudad Real, Spain (U. Höfle, A. Sánchez-Cano, S. Minayo Martín); NEIKER–Basque Institute for Agricultural Research and Development, Basque Research and Technology Alliance (BRTA), Derio, Spain (M. Barral, V. Alvarez, X. Gerrikagoitia); Estación Biológica de Doñana, CSIC, Sevilla, Spain (J.A. Donázar, A. Cortés-Avizanda); ETH Zurich, Basel, Switzerland (L. Du Plessis); Swiss Institute of Bioinformatics, Lausanne, Switzerland (L. Du Plessis); Spatial Epidemiology Lab, Université Libre de Bruxelles, Brussels, Belgium (S. Dellicour); Rega Institute, KU Leuven, Leuven, Belgium (S. Dellicour); Universidad Miguel Hernández, Elche, Spain (J.A. Sánchez-Zapata); Centre d'Ecologie Fonctionnelle et Evolutive, Univ Montpellier, CNRS, EPHE, IRD, Montpellier, France (J. Tornos, S. Perret, T. Boulinier, O. Duriez); Ligue pour la Protection des Oiseaux, Rochefort, France (P. Orabi); Office Français de la Biodiversité, Vincennes, France (A. Van De Wiele); University of Granada, Granada, Spain (E. Arrondo)

DOI: https://doi.org/10.3201/eid3108.241456

and scavengers, but livestock have also been affected, notably cattle in the United States (*7*). Furthermore, the loss of traditional seasonality, evidenced by outbreaks now persisting year-round, also represents a profound shift in HPAI virus ecology (*8*,*9*). Evidence for sustained mammal-to-mammal transmission is inconclusive, but the unprecedented geographic spread of the virus, coupled with the number of species infected, has raised concerns about the ability of the virus to expand its host range and gain pandemic potential (*10*).

Among wild birds, gregarious species, particularly those with colonial nesting behavior, have shown heightened vulnerability (*11*). Colonies of seabirds have experienced exceptionally high mortality rates worldwide (*12*–*16*). This susceptibility is likely because of enhanced virus transmission within densely aggregated avian populations, where the proximity of birds contributes to the rapid spread of the virus.

Vultures have been considered relatively resilient to pathogens, including HPAI virus, because of their scavenging diet and their associated physiologic adaptations to cope with pathogens (*17*). Before the current panzootic, only a local outbreak of HPAI had been reported in hooded vultures (*Necrosyrtes monachus*) in Burkina Faso in 2006 (*18*). Similarly, although ornitophagous raptors and scavengers have previously been only sporadically affected by HPAI H5Nx, they have been unexpectedly affected during the ongoing panzootic; birds affected have included obligate or occasional scavengers such as bald eagles (*Haliaaetus leucocephalus*), black vultures (*Coragyps atratus*), and California condors (*Gymnogyps californianus*) in North America and griffon vultures (*Gyps fulvus*) in Europe (*19*,*20*).

In spring 2022, abnormal deaths of nestling and adult griffon vultures were detected in Spain and France; HPAI H5N1 infection was confirmed by quantitative reverse transcription PCR (qRT-PCR) (Appendix Figure 1, https://wwwnc.cdc.gov/EID/article/31/8/24-1456-App1.pdf). This occurrence prompted an investigation into the epidemiology of HPAI in this vulture population. Leveraging ongoing ecologic studies, we investigated the origin of infection and assessed the nature and magnitude of viral spread through an integrated analysis of virological, serologic, genomic, and ecologic data obtained from field sampling in France and Spain. In addition to seroepidemiology and viral phylogenetic approaches, we further used long-term global positioning system (GPS) tracking data to evaluate potential sources of exposure, to study population connectivity pathways, and to investigate the potential of long-range contamination by movements of infected animals.

Methods

We collated and jointly analyzed information from griffon vultures collected from Spain and France in the framework of several research and surveillance programs dedicated to the study of vulture ecology, population dynamics, or HPAI outbreak follow-up (Appendix). In addition, the sampling included birds from national and local surveillance programs or those submitted for diagnosis to the institutions of the authors. In Spain, griffon vulture captures were performed in numerous colonies across the Iberian Peninsula during 2020–2022. Adult griffon vultures were captured with net traps or walk-in traps at vulture feeding stations, and nestlings were captured at nests. In France, 3 capture sessions were performed in 2022 and 2023 using walk-in traps at 5 sites.

All birds were ringed and a subset of vultures were fitted with GPS satellite transmitters. Blood samples, as well as oropharyngeal and cloacal swab samples, were collected from live birds. From dead birds, vascular feathers and tissues from the main organs (spleen, pancreas, heart, brain, trachea, intestine, lungs, and liver) were collected.

We extracted nucleic acids and submitted them to generic matrix gene qRT-PCR. We then submitted positive samples for nanopore sequencing (Oxford Nanopore Technologies, https://nanoporetech.com) and used consensus genomes in molecular marker and phylogeographic analysis.

We separated serum from the cell pellet by centrifugation in blood samples and stored at −20°C until analysis. We inactivated and tested serum samples with commercial ELISA and submitted positive samples to a hemagglutination inhibition (HI) test. We categorized HI samples as positive for an antigen if the titer was >16. We then estimated true seroprevalence by using the epidemiologic calculator Epitools (https://epitools.ausvet.com.au/prevalence).

We examined movement patterns of GPS-tagged griffon vultures during the 4-month period from March 1–June 29 during 2022 (outbreak year) and 2023 (control year), characterizing tracks as local or transit movements or immobility. We calculated daily distances traveled (DDT) and used generalized linear mixed models to identify factors affecting DDT. We first examined the movement patterns of a large sample of 114 birds, then examined the spatial and temporal dimensions of the movements of a subsample of 16 birds that remained in Europe during the study period.

Results

HPAI H5N1 Outbreak Dynamics

During April–August 2022, a total of 5 griffon vultures in Spain and 11 in France were confirmed to have died from HPAI H5N1 infection (Figure 1; Appendix). Despite the advanced state of decomposition, severe generalized congestion was detected on postmortem examination.

Apparently healthy live vultures sampled in both countries during March 2020–August 2023 tested negative for avian influenza virus (AIV) in oropharyngeal and cloacal swab samples (France, n = 393; Spain, n = 216). However, 2 birds admitted to a rehabilitation center in northern Spain (Figure 1, site 6) tested positive for HPAI H5 on May 5, 2022, and May 11, 2022. Both birds displayed weakness and severe central nervous system symptoms, including torticollis and inability to fly (Appendix). Only 1 of 87 live griffon vulture nestlings from Spain for which vascular feathers were available tested positive for HPAI H5 on May 24, 2022. The nestling, from southern Spain (site 14), lacked clinical signs at the time of ringing but was found dead on June 10, 2022; the remains tested positive for HPAI H5 (Appendix).

Exposure to H5 AIV in flying vultures was confirmed by the detection of H5-specific antibodies by HI tests after ELISA screening in 58 of 392 birds in France and 7 of 51 birds in Spain captured after the outbreak (summer 2022, autumn 2022, and summer 2023) (Table 1; Appendix Table 1). However, only 3 of 51 nestlings tested in Spain after the outbreak (summer 2022 and summer 2023) had H5-specific antibodies. Of 17 flying birds captured in Spain before the

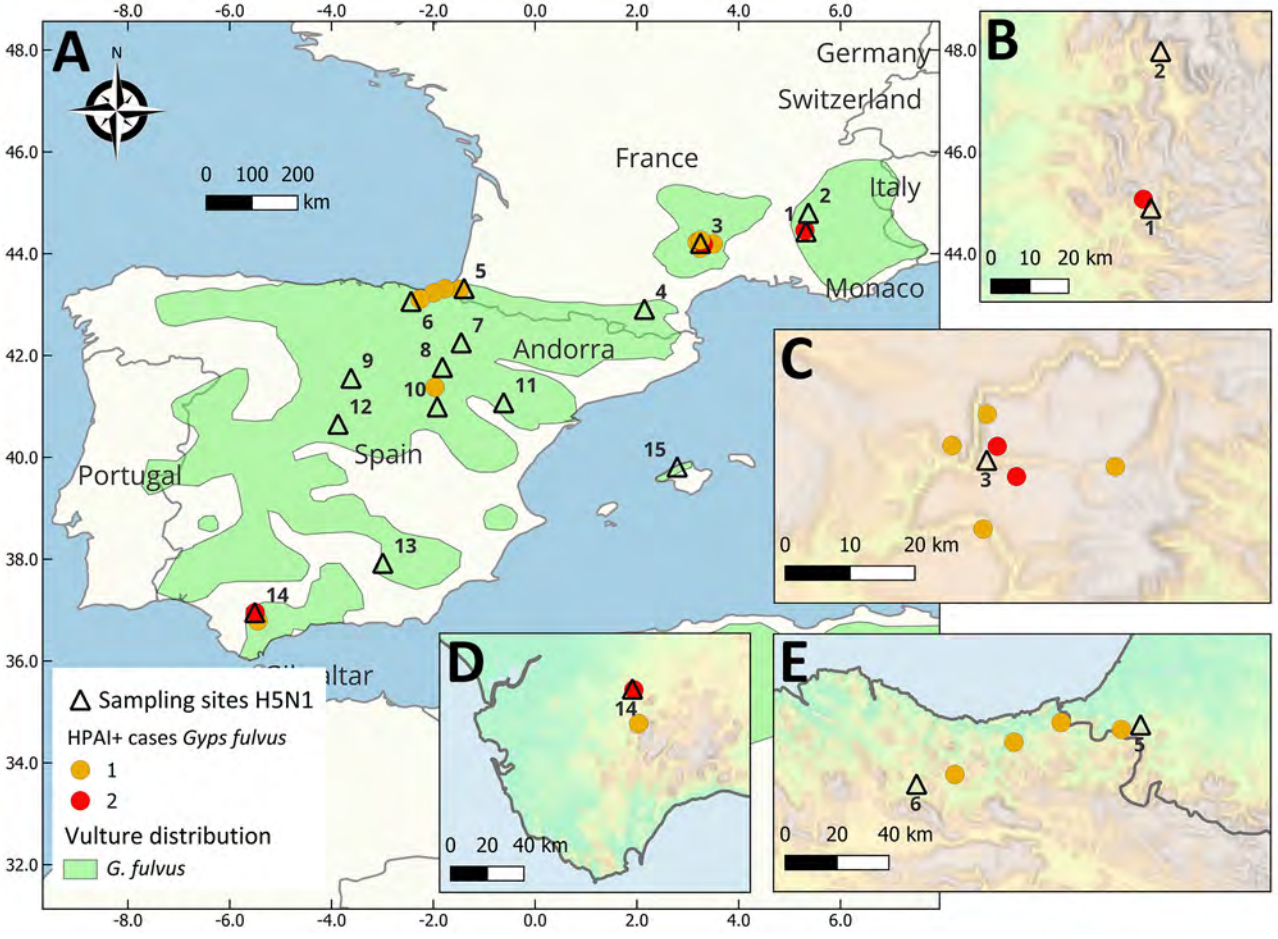

Figure 1. Sampling sites of live vultures (black triangles) and collection sites of carcasses of confirmed HPAI-positive vultures (dots) during March 2020–August 2023 in study of multidisciplinary tracking of highly pathogenic avian influenza A(H5N1) outbreak in griffon vultures (*Gyps fulvus*), southern Europe, 2022. The correspondence between site identification and the details of site names, region, or province area are given in the Appendix (https://wwwnc.cdc.gov/EID/article/31/8/24-1456-App1.pdf). The color of collection sites indicates the number of cases in each site. A) Sampling sites in France and Spain; light green shaded areas show the breeding range of Griffon vultures. Insets provide details of specific sites: B) Alps, C) Massif Central, D) South Spain, and E) Pyrenees and North Spain.

Table. Results of ELISA tests and H5-HI test of ELISA-positive serum samples in study of multidisciplinary tracking of highly pathogenic avian influenza A(H5N1) outbreak in griffon vultures, southern Europe, 2022*

		ELISA test		H5-HI test
Country	Date	Type	Estimated prevalence, % (95% CI)	Estimated prevalence, % (95% CI)
France	2020	NA	NA	NA
	2021	NA	NA	NA
	2022	Anti H5	28 (22–36)	82 (69–92)
	2023	Anti H5	20 (12–28)	20 (9–37)
Spain	2020	Anti AIV	47 (25–71)	0 (0–37)
	2021	Anti AIV	0 (0–5)	NA
	2022	Anti AIV	16 (9–26)	38 (17–68)
	2023	Anti AIV	31 (13–56)	100 (66–100)

*For details see Appendix Table 1 (https://wwwnc.cdc.gov/EID/article/31/8/24-1456-App1.pdf). AIV, avian influenza virus; H5-HI, H5 hemagglutination inhibition; NA, not applicable.

outbreak in spring 2020, a total of 8 were seropositive against strains of AIV other than H5 or H7, whereas none of the 50 nestlings tested before the outbreak (summer 2021) were seropositive against AIV. Of 128 H5 ELISA-positive vultures in France, 70 could not be confirmed by H5-specific HI tests.

Origin and Spatial Spread of Infection

We performed phylogenetic analysis on a dataset of 12 hemagglutinin genetic sequences retrieved from HPAI H5N1–infected griffon vultures (8 generated in this study), together with a background dataset of sequences from poultry and wild birds that were sampled in Europe during November 8, 2021–September 1, 2022 (n = 571) (Appendix). The analysis confirmed that the sequences obtained in this study belong to clade 2.3.4.4b and showed that most vulture sequences were grouped into a distinct clade (n = 32) in a maximum-likelihood tree (bootstrap support = 0.83) (Appendix), with vulture sequences already identified as genotype AB (*21*). Mutation analysis of the vulture sequences showed that several variable sites were identified in the hemagglutinin segment, some of which have been previously associated with specific phenotypes, such as increased virus binding to α2–3 and α2–6 receptors (Appendix).

We conducted continuous phylogeographic analysis on this vulture-associated clade and revealed that nearly all (11 of 12) griffon vulture sequences clustered together in a distinct clade (Figure 2, panel A, node A). That clade is supported (posterior probability = 0.84) and contains vulture sequences from both Spain and France. Of note, the only other sequences in this clade originated from bearded vultures (*Gypaetus barbatus*) and a peregrine falcon (*Falco peregrinus*). This pattern suggests that the birds might have shared a common source of infection because of their scavenging feeding behaviors or that some birds could have been initially infected and subsequently transmitted the virus to others. The median time of the most recent common ancestor of the clade (Figure 3, panel A, node A) was estimated to be March 8, 2022 (95% highest posterior density [HPD] February 10, 2022–April 4, 2022). This clade was nested within a larger clade predominantly composed of wild bird sequences from Spain, including greylag geese (*Anser anser*), white storks (*Ciconia ciconia*), and grey herons (*Ardea cinerea*), but that also includes some poultry sequences, suggesting a likely wild bird origin with spillover events to both poultry and vultures (Figure 2, panel A).

Our continuous phylogeographic reconstruction indicated that the vulture viral lineages likely originated from central Spain (Figure 2, panel B) and substantial spatial dispersal was observed across 4 regions (Figure 2, panel C). That dispersal likely originated from wild birds in central Spain, as suggested by the predominance of wild bird sequences in the parent clade, with subsequent spillover events to both poultry and vultures (Figure 2, panel A) and ≥1 dispersal event toward Massif Central in early March (median date March 3, 2022; 95% HPD February 7, 2022–April 4, 2022; posterior probability = 0.92). Subsequently, lineages spread to the Pyrenees by the end of March (median date March 29, 2022 [95% HPD March 4, 2022–April 20, 2022]; posterior probability = 0.73) and to southern Spain by the end of April (median date April 21, 2022 [95% HPD March 28, 2022–May 4, 2022]; posterior probability = 0.44).

One griffon vulture sequence originating from a rehabilitation center in northern Spain (PP150341; site 6 in Figure 1) fell in a distinct position within the phylogenetic tree (Appendix Figure 2) within a clade of predominantly seabird sequences originating from France. This particular PP150341 sequence is positioned near the BB genotype (H5N1-A/Herring_gull/France/22P015977/2022-like), which has been rapidly expanding across Europe since 2022 (*22*).

Dispersal of HPAI by Griffon Vulture Movements

To examine changes in the movement patterns of griffon vultures during the HPAI outbreak, we focused on the 4-month period of March–June and compared

the movements of flying birds during 2022 compared with 2023. From 114 vultures tagged before the start of the outbreak in Spain and France (94 adult and 20 immature birds, none of which were sampled for viral and serologic monitoring), the percentage of immature birds displaying long-range transit movements was significantly larger than the percentage of adult birds (88% immature vs. 24% adult when both years were pooled; $\chi^2 = 37.01$, degrees of freedom [d.f.] = 1; $p<0.001$). The proportion of long-range transit movements did not differ significantly between years ($\chi^2 = 0.76$, d.f. = 1, $p = 0.268$ for adults; $\chi^2 = 0.09$, $p = 0.610$ for immature birds).

We chose 16 vultures (4 immature and 4 adult birds in both 2022 and 2023) that best visually represent long-range transit movements to further

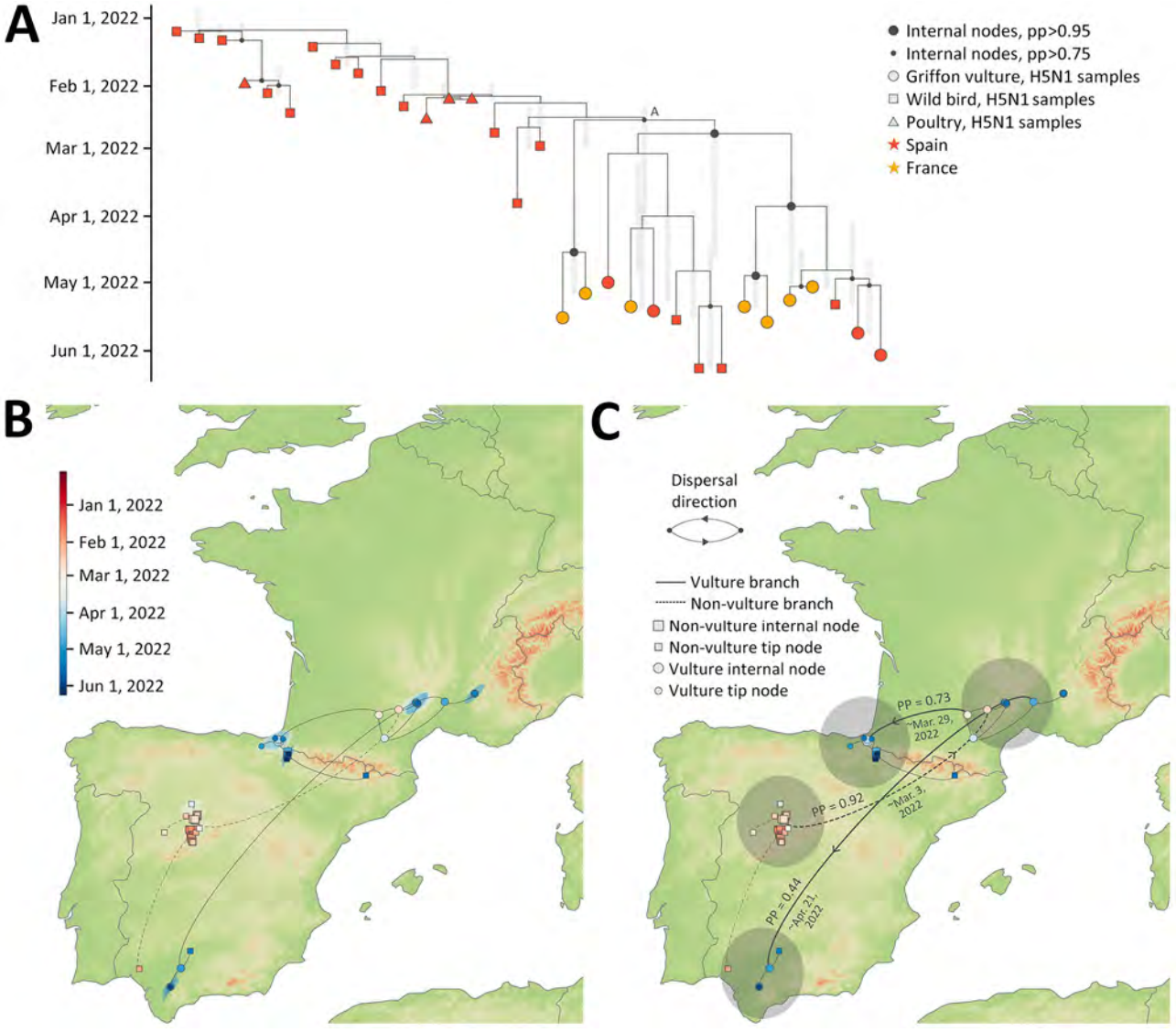

Figure 2. Phylogenetic and phylogeographic analysis conducted in study of multidisciplinary tracking of highly pathogenic avian influenza A(H5N1) outbreak in griffon vultures (*Gyps fulvus*), southern Europe, 2022. A) Maximum clade credibility (MCC) tree obtained from the time-scaled phylogenetic analysis based on genetic sequences of the hemagglutinin gene segment collected from H5N1 virus–infected birds during November 8, 2021–September 1, 2022, in Spain and France. Vertical light gray bars reflect 95% highest posterior density (HPD) intervals associated with the inferred age of internal nodes. B) Continuous phylogeographic reconstruction of the dispersal history of viral lineages. Specifically, we first report the mapped MCC tree and 80% HPD regions reflecting the uncertainty related to the Bayesian continuous phylogeographic inference; both the MCC tree and HPD regions are based on 1,000 trees sampled from the posterior distribution and colored according to their time of occurrence. Phylogenetic branches associated with the vulture subclade (node A) are displayed as solid lines, whereas dashed lines represent other branches in the clade. C) MCC tree as reported in panels A and B, but this time along the PPs and mean estimates associated with lineage dispersal events that occurred between the 4 main regions involved in the continuous phylogeographic reconstruction. PP, posterior probability.

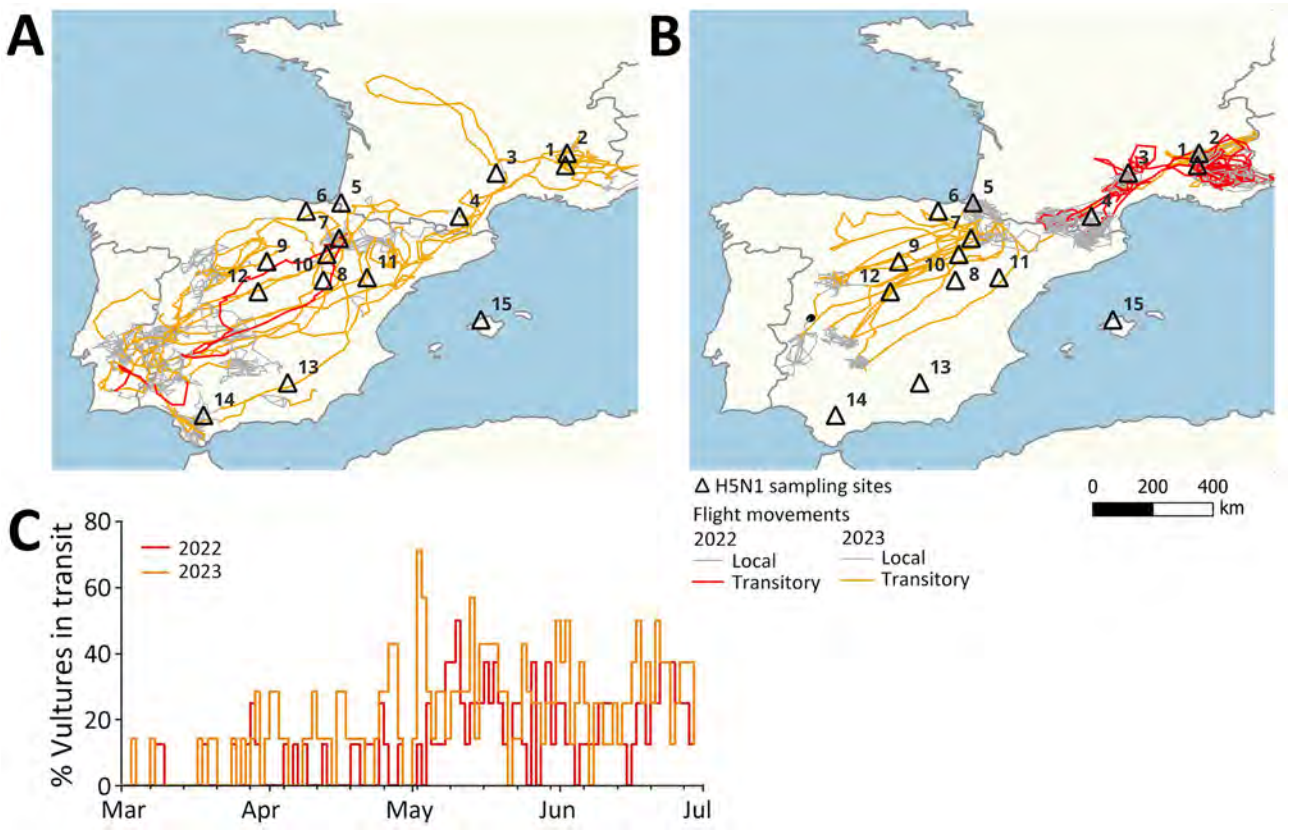

Figure 3. Movements of 16 individual birds during March 1–June 30, 2022, and March 1–June 30, 2023, in study of multidisciplinary tracking of highly pathogenic avian influenza A(H5N1) outbreak in griffon vultures (*Gyps fulvus*), southern Europe, 2022. Immature birds (A) and adult birds (B) show long-range transit movements (rectilinear movements with nocturnal roosts spaced >50 km apart) in red for 2022 and orange for 2023; local movements are shown in gray for both years. C) Timeline of the proportion of individual birds (all ages pooled) in transit every day in 2022 and 2023.

investigate the spatial and temporal dimensions of those movements (Figure 3). The DDT were significantly longer for days of transit compared with days of local movements (181.8 ± 77.4 km [max 438.2 km] for days of transit compared with 69.0 ± 47.5 km [max 272.1 km] for days of local movement) (Appendix Table 8). Regardless of the type of movement, DDT increased significantly ($p<0.001$) and progressively over the course of the period (shortest in March and longest in June) (Figure 3, panel C). We observed no qualitative differences in transit movement patterns between 2022 and 2023. In transit movements, adults and immature birds traveled at similar speed, but in general adults took more direct trajectories (Figure 3, panel B). Overall, griffon vultures were able to travel between southern Spain and the Pyrenees or between the Pyrenees and the Alps in 1–2 days.

Discussion

HPAI H5N1 infections were first detected in griffon vultures in southern Europe in spring 2022 in Spain and France. Infection led to central nervous clinical signs as well as reduced activity, immobility at the roost or nest, and death in some adults. Deaths were also recorded in nestlings, either from direct effects of infection or lack of parental care (*19*).

We investigated the origin of infection and assessed the nature and magnitude of viral spread through an integrated analysis of virologic, serologic, genomic, and ecologic data obtained from field sampling in France and Spain. In addition, we evaluated potential sources of exposure, studied population connectivity pathways, and investigated the potential of long-range contamination by movements of infected birds using long-term GPS tracking data.

Serologic results reflected the circulation of H5 HPAI among flying birds of all sampled colonies of griffon vultures. The high ELISA seroprevalence observed in flying birds seems to indicate widespread transmission but high survival within the meta-population, as opposed to the dramatic mortality rates observed in Sandwich terns, northern gannets, and bald eagles (*20*,*23*,*24*). In contrast, ELISA seroprevalence was considerably lower in

nestlings; seropositivity was detected in just 1 colony (Appendix Table 1). That lower seroprevalence could be because of a reduced exposure of nestlings or the result of a high mortality rate. Those seropositive nestlings, detected at the same time as H5N1 AIV–mediated deaths of nestlings in neighboring nests, fledged successfully, demonstrating that infected nestlings, as well as infected adults, were able to survive the infection.

The spread of the virus through the griffon vulture populations in Spain and France was very fast; most H5 HPAI PCR–positive dead birds were collected during April–June 2022, and almost all live and dead birds sampled in both countries after that period tested negative for H5 HPAI virus by qRT-PCR. None of the antibody-positive vultures from our sample set tested positive by PCR, suggesting the absence of active HPAI H5N1 circulation after June 2022, which might relate to the clearance of infection by surviving vultures (*25*,*26*). Sandwich terns sampled in 2022 and 2023 showed a similar pattern; seropositivity was detected in adults in the absence of viral shedding (*24*). However, the lack of data regarding persistence of AIV immunity in griffon vultures, which is known to be highly dependent on the species and age of the host, as well as the subtype of virus, does not preclude circulation at a low prevalence or in the absence of clinical signs (*27*,*28*). Presence of H5-specific AIV antibodies as much as a year after the outbreak, albeit at low titers (Appendix Table 2), might be from antibody persistence or reexposure or from exposure to a different H5 AIV. In fact, AIV seropositivity of vultures in Spain to AIV other than H5 before 2022 provides circumstantial evidence that exposure of vultures to AIV could occur occasionally, which contrasts with the common assumption before the H5N1 outbreak that vultures were either not exposed or not susceptible to AIV infection.

Of note, HPAIV-related deaths of bearded vultures (*G. barbatus*) were reported concurrently to the griffon vulture outbreak (SM17). In contrast, no evidence of infection was found in 2 other cooccurring species of vultures, namely cinereous vultures (*Aegypius monachus*) and Egyptian vultures (*Neophron percnopterus*), which also regularly feed alongside griffon vultures (data not shown).

Phylogenetic and phylogeographic analyses of H5 genetic sequences obtained during the HPAI H5N1 outbreak offered key insights into the potential origins and transmission dynamics of viral lineages among griffon vultures. Of note, the inclusion of almost all griffon vultures within the same genetic cluster, despite having been sampled from geographically distant locations in Spain and France, suggests that they could have shared a common source of infection because of their scavenging feeding behavior, or that some could have been initially infected and subsequently transmitted the virus to others.

Those analyses enable us to draw hypotheses regarding the origin of the virus that infected vultures. This virus was genetically close to strains found in greylag geese and other wetland species, such as grey herons and white storks. Griffon vultures rarely forage in wetlands in France, but they do more often in southern Spain, where they can feed on livestock or wild mammal carcasses in marshes (i.e., potentially close to waterbirds) (Appendix Figure 5). Interactions with waterbirds might also have occurred at small waterbodies in southern Spain, where griffon vultures regularly bathe. Contacts could also have occurred in open urban landfills in northern Spain, where griffon vultures regularly feed alongside other wild bird species that are highly susceptible to the virus, such as gulls and white storks (*29*–*32*). Previous studies have shown potential transmission of low pathogenic avian influenza viruses between species frequenting the same landfills (*33*,*34*). Finally, contacts might involve opportunistic carnivorous mammals, such as red foxes (*Vulpes vulpes*), in which deaths from HPAI H5N1 virus have been reported throughout Europe (*35*). Uncertainties remain regarding the specific mechanisms of the griffon vultures' contamination.

Our phylogenetic and phylogeographic analyses further suggest that the introduction of HPAI in griffon vultures from poultry farms seems unlikely. This conclusion is also supported by the behavior of griffon vultures, which do not typically visit poultry farm premises. Moreover, culled poultry from affected farms are discarded under strict biosecurity regulations, making the contact of griffon vultures with infected dead poultry unlikely. However, we cannot rule out that griffon vultures might have accessed inadequately discarded undiagnosed dead backyard poultry in some regions of Spain that could also have been consumed by gulls and storks, leading to the further spread and detection of the strain in both wild waterbirds and vultures (*31*,*32*).

The limited genetic diversity of the virus observed in griffon vulture populations, contrasting with the wide geographic distribution of infected birds, suggests that the virus spread in the southwestern Europe metapopulation through intraspecific contamination. The ecology of griffon vultures, especially their feeding behavior and their colonial nature, could

explain this finding. Dense short-term aggregations during feeding on carcasses or at vulture feeding stations and dumpsites, where hundreds of individual birds congregate, make griffon vultures particularly vulnerable to airborne pathogen transmission (*36*,*37*). Subsequently, movements of infected birds over long distances could easily have contributed to virus dissemination to the whole population (*38*).

Phylogeographic reconstructions reveal a spatial dissemination pattern across 4 distinct regions, originating from central Spain, spreading to France in the Massif central and the Alps, and subsequently disseminating to the western part of the Pyrenees and southern Spain. This finding is coherent with the analysis of telemetric data, which show an overlap in the distributions of several GPS-tagged birds in Spain and France and long-range movements occurring between populations, particularly in spring, concurrent with the 2022 outbreak (Appendix). Such movements were also observed in other years (*39*), and it thus seems unlikely for them to have been triggered by the outbreak, as observed with northern gannets (*23*,*40*,*41*).

The nestling that was found seronegative and without clinical signs but tested positive for HPAI H5 in the vascular feather provides circumstantial evidence for shedding during the presymptomatic period, because shedding from feather follicles has recently been described as an efficient route of HPAI transmission (*42*). Experimental infection of red-legged partridges (*Alectoris rufa*) with an HPAI H7N1 virus evidenced an incubation period of 3 days with shedding from day 1 (*43*), whereas a similar approach evidenced a 5-day incubation period in falcons (*Falco* spp.) experimentally infected with HPAI H5N1 (*44*). Thus, under the hypothesis of viral incubation lasting >3 days, a griffon vulture infected in the Pyrenees would have enough time to reach southern Spain or the French Alps before showing clinical signs and reduced mobility (*19*). As an example, an immature vulture (Imm_FR_JOR) traveled from southern Portugal to the French Alps in 6 full days (Appendix).

The outbreak described in this study appeared to have had only a mild effect in terms of the conservation of griffon vultures. Compared with long-lived seabird populations in which a large proportion of adults died, mortality in griffon vultures mostly affected nestlings and only few adult birds; adult survival is the most sensitive demographic parameter in such a long-lived species (*45*). In addition, the outbreak struck the world's largest population of griffon vultures, which could withstand such an ephemeral reduction in breeding success. However, even if griffon vulture populations seem able to overcome this HPAI outbreak, they face multiple threats on a global scale, particularly poisoning and persecution (*46*–*48*). The introduction and circulation of a new infectious pathogen could add additional pressure on the population. Unfortunately, the consequences of a population collapse of necrophagous birds could be catastrophic, especially from a sanitary point of view, in that longer persistence of the carcasses they eliminate would increase risk for pathogen persistence and spread in the environment (*17*,*49*).

Despite a likely limited epidemiologic role of griffon vultures in the circulation of HPAI in Spain and France, with very low permeability between griffon vulture populations and poultry farms, the infection of this new compartment raises multiple questions. In particular, this outbreak demonstrates the ability of this virus (and potentially other highly contagious pathogens) to spread rapidly through a population after a single introduction and shows that even a rare event has the potential for devastating effects.

In conclusion, the recent evolution of HPAI H5N1 has led to this pathogen being considered a severe concern for endangered bird species, especially those with colonial and scavenging behavior. Integrating the epidemiology of the virus with the ecology of the host species is key to a better understanding of outbreak dynamics and possible effects on wildlife conservation. More generally, implementing a multidisciplinary approach will be necessary to overcome these new challenges.

Acknowledgments

We thank the staff from LPO Grands Causses and LPO Occitanie for providing access to demographic data on griffon vulture populations in Grands Causses and helping in capturing vultures for tagging and collecting samples; particularly Lea Giraud, Thierry David, Robert Straughan, Matthieu Vaslin, Yves Roullaud, and Anna Terras. We thank the staff from Parc National des Cévennes et Parc National des Pyrénées, Parc Naturel Regional du Vercors, and the members of associations Vautours en Baronnies and Saiak for helping in capturing vultures for tagging and collecting samples, particularly Jocelyn Fonderflick, Jérôme Lafitte, Michel Clouet, Isabelle Rebours, Didier Peyrusqué, Nicolas Renous, Christian Tessier, Gael Foilleret, and Julien Traversier. We thank the staff from ENVT and CEFE for helping in collecting samples in the field and analyzing data, particularly Cécile Caubet, Laetitia Lebre, and Christophe de Franceschi. We acknowledge the Fundación para la Conservación del Quebrantahuesos FCQ, the regional government of Aragon and all organisms partaking in the LIFE PRO

Quebrantahuesos for access to griffon vulture samples collected in 2022 and 2023. We thank all the stakeholders who made possible the epidemiological monitoring of these birds (including SAGIR network and OFB and "Diputaciones Forales" of the Spanish Basque Country). We thank the "Diputación Foral de Gipuzkoa" for the video of the vulture with symptoms. We also thank all submitting laboratories for sharing H5N1 genome sequences in the GISAID database (https://www.gisaid.org), and especially Azucena Sanchez from Spanish "Laboratorio Central de Veterinaria" for helping us with tracing the geographical origin of some sequences.

Telemetry study of Griffon vultures was authorized in the Programme Personnel 961, coordinated by O. Duriez, under the supervision of the French ringing centre, CRBPO, Paris. Viral and serologic samples collected benefitted from special permission 2022-s-11 signed by the Prefecture de Lozère and DREAL Occitanie on July 19, 2022. Tracking and monitoring of vultures in France is supported by OSU-OREME (SO Ecopop) and the long-term Studies in Ecology and Evolution (SEE-Life) program of the CNR, and with technical assistance of PLT staff from CEFE (Christophe de Franceschi). E.N.V.T. participated in the framework of the "Chaire de Biosécurité et Santé Aviaires," funded by the Direction Générale de l'Alimentation, Ministère de l'Agriculture et de la Souveraineté Alimentaire, France. S.D. acknowledges support from the *Fonds National de la Recherche Scientifique* (F.R.S.-FNRS, Belgium; grant no. F.4515.22), from the Research Foundation–Flanders (*Fonds voor Wetenschappelijk Onderzoek – Vlaanderen*, FWO, Belgium; grant no. G098321N), and from the European Union Horizon 2020 projects MOOD (grant agreement no. 874850) and LEAPS (grant agreement no. 101094685). E.A. was supported by MCIN/AEI/10.13039/501100011033 grant nos. FJC2021-047885-I. The sampling and analyses carried out at NEIKER have been financed by MCIN/AEI/10.13039/501100011033 (grant no. PID2020-114060RR-C31) and by Basque Government (grant no. VIGIA-2200003). Analysis carried out at IREC was supported byMCIN/AEI/10.13039/501100011033 (grant no. PID2020-114060RR-C32). Monitoring of the GPS-tagged birds in Spain was funded by the Comunidad de Bardenas Reales de Navarra and the Projects RNM-1925 and P18-RT-1321 (Junta de Andalucía), and Ecotone Telemetry 2017-12-026.

U.H., J.L.G., O.D., and G.L.L. conceptualized the study. J.H., U.H., A.S., M.B., J.A.D., C.L.G.L., V.A., X.G., E.A., J.A.S.Z., A.C.A., S.M.M., J.T., S.P., P.O., A.V.D.W., and O.D. provided resources. J.H., U.H., A.S., C.G., G.C., M.B., J.A.D., C.L.G.L., M.W., V.A., X.G., L.D.P., S.D., S.M.M., and O.D. conducted the formal analysis. J.H., U.H., C.G., G.C., O.D., and G.L.L. wrote the original draft. J.H., U.H., C.G., M.B., J.A.D., L.D.P., S.D., E.A., J.A.S.Z., A.C.A., J.T., T.B., O.D., and G.L.L. reviewed and edited the manuscript. U.H., O.D., and G.L.L. supervised the research. U.H., M.B., J.A.D., J.A.S.Z., T.B., J.L.G., and O.D. acquired the funding.

About the Author

Dr. Hirschinger is a researcher at the National Veterinary School of Toulouse within the IHAP research unit. His work focuses on wildlife conservation, with a particular interest in the ecology and epidemiology of wildlife diseases and their effects on population dynamics and ecosystem health.

References

1. Graziosi G, Lupini C, Catelli E, Carnaccini S. Highly pathogenic avian influenza (HPAI) H5 clade 2.3.4.4b virus infection in birds and mammals. Animals (Basel). 2024;14:1372. https://doi.org/10.3390/ani14091372
2. Ramey AM, Hill NJ, DeLiberto TJ, Gibbs SEJ, Camille Hopkins M, Lang AS, et al. Highly pathogenic avian influenza is an emerging disease threat to wild birds in North America. J Wildl Manage. 2022;86:e22171. https://doi.org/10.1002/jwmg.22171
3. Clough C. Underestimating wild bird deaths from avian influenza. Vet Rec. 2022;191:221–2. https://doi.org/10.1002/vetr.2214
4. Klaassen M, Wille M. The plight and role of wild birds in the current bird flu panzootic. Nat Ecol Evol. 2023;7:1541–2. https://doi.org/10.1038/s41559-023-02182-x
5. Plaza PI, Gamarra-Toledo V, Euguí JR, Lambertucci SA. Recent changes in patterns of mammal infection with highly pathogenic avian influenza A(H5N1) virus worldwide. Emerg Infect Dis. 2024;30:444–52. https://doi.org/10.3201/eid3003.231098
6. Wille M, Klaassen M. No evidence for HPAI H5N1 2.3.4.4b incursion into Australia in 2022. Influenza Other Respir Viruses. 2023;17:e13118. https://doi.org/10.1111/irv.13118
7. Garg S, Reed C, Davis CT, Uyeki TM, Behravesh CB, Kniss K, et al. Outbreak of highly pathogenic avian influenza A(H5N1) viruses in U.S. dairy cattle and detection of two human cases — United States, 2024. MMWR Morb Mortal Wkly Rep. 2024;73:501–5. https://doi.org/10.15585/mmwr.mm7321e1
8. Pohlmann A, King J, Fusaro A, Zecchin B, Banyard AC, Brown IH, et al. Has epizootic become enzootic? Evidence for a fundamental change in the infection dynamics of highly pathogenic avian influenza in Europe, 2021. mBio. 2022;13:e0060922.
9. Scoizec A, Niqueux E, Schmitz A, Grasland B, Palumbo L, Huneau-Salaün A, et al. New patterns for highly pathogenic avian influenza and adjustment of prevention, control and surveillance strategies: the example of France. Viruses. 2024;16:101. https://doi.org/10.3390/v16010101
10. World Health Organization. Joint FAO/WHO/WOAH preliminary assessment of recent influenza A(H5N1) viruses [cited 2025 Mar 12]. https://cdn.who.int/media/docs/default-source/global-influenza-programme/2024_04_23_fao-woah-who_h5n1_assessment.pdf
11. European Food Safety Authority; Aznar I, Baldinelli F, Stoicescu A, Kohnle L. Annual report on surveillance for

avian influenza in poultry and wild birds in Member States of the European Union in 2021. EFSA J. 2022;20:e07554.
12. Molini U, Yabe J, Meki IK, Ouled Ahmed Ben Ali H, Settypalli TBK, Datta S, et al. Highly pathogenic avian influenza H5N1 virus outbreak among Cape cormorants (*Phalacrocorax capensis*) in Namibia, 2022. Emerg Microbes Infect. 2023;12:2167610. https://doi.org/10.1080/22221751.2023.2167610
13. Alexandrou O, Malakou M, Catsadorakis G. The impact of avian influenza 2022 on Dalmatian pelicans was the worst ever wildlife disaster in Greece. Oryx. 2022;56:813–813. https://doi.org/10.1017/S0030605322001041
14. Banyard AC, Lean FZX, Robinson C, Howie F, Tyler G, Nisbet C, et al. Detection of highly pathogenic avian influenza virus H5N1 clade 2.3.4.4b in great skuas: a species of conservation concern in Great Britain. Viruses. 2022;14:212. https://doi.org/10.3390/v14020212
15. Camphuysen K, Gear S. Great skuas and northern gannets on Foula, summer 2022—an unprecedented, H5N1 related massacre [cited 2023 Jan 27]. https://dataverse.nioz.nl/citation?persistentId=doi:10.25850/nioz/7b.b.gd
16. Pohlmann A, Stejskal O, King J, Bouwhuis S, Packmor F, Ballstaedt E, et al. Mass mortality among colony-breeding seabirds in the German Wadden Sea in 2022 due to distinct genotypes of HPAIV H5N1 clade 2.3.4.4b. J Gen Virol. 2023;104. https://doi.org/10.1099/jgv.0.001834
17. Plaza PI, Blanco G, Lambertucci SA. Implications of bacterial, viral and mycotic microorganisms in vultures for wildlife conservation, ecosystem services and public health. Ibis. 2020;162:1109–24. https://doi.org/10.1111/ibi.12865
18. Ducatez MF, Tarnagda Z, Tahita MC, Sow A, de Landtsheer S, Londt BZ, et al. Genetic characterization of HPAI (H5N1) viruses from poultry and wild vultures, Burkina Faso. Emerg Infect Dis. 2007;13:611–3. https://doi.org/10.3201/eid1304.061356
19. Duriez O, Sassi Y, Le Gall-Ladevèze C, Giraud L, Straughan R, Dauverné L, et al. Highly pathogenic avian influenza affects vultures' movements and breeding output. Curr Biol. 2023;33:3766–3774.e3. https://doi.org/10.1016/j.cub.2023.07.061
20. Nemeth NM, Ruder MG, Poulson RL, Sargent R, Breeding S, Evans MN, et al. Bald eagle mortality and nest failure due to clade 2.3.4.4 highly pathogenic H5N1 influenza A virus. Sci Rep. 2023;13:191. https://doi.org/10.1038/s41598-023-27446-1
21. Fusaro A, Zecchin B, Giussani E, Palumbo E, Agüero-García M, Bachofen C, et al. High pathogenic avian influenza A(H5) viruses of clade 2.3.4.4b in Europe—why trends of virus evolution are more difficult to predict. Virus Evol. 2024;10:veae027. https://doi.org/10.1093/ve/veae027
22. European Food Safety Authority; Adlhoch C, Fusaro A, Gonzales JL, Kuiken T, Mirinaviciute G, et al. Avian influenza overview March–April 2023. EFSA J. 2023;21:e08039.
23. Jeglinski JWE, Lane JV, Votier SC, Furness RW, Hamer KC, McCafferty DJ, et al. HPAIV outbreak triggers short-term colony connectivity in a seabird metapopulation. Sci Rep. 2024;14:3126. https://doi.org/10.1038/s41598-024-53550-x
24. Knief U, Bregnballe T, Alfarwi I, Ballmann MZ, Brenninkmeijer A, Bzoma S, et al. Highly pathogenic avian influenza causes mass mortality in Sandwich Tern *Thalasseus sandvicensis* breeding colonies across north-western Europe. Bird Conserv Int. 2024;34:e6. https://doi.org/10.1017/S0959270923000400
25. Root JJ, Bosco-Lauth AM, Marlenee NL, Bowen RA. Viral shedding of clade 2.3.4.4 H5 highly pathogenic avian influenza A viruses by American robins. Transbound Emerg Dis. 2018;65:1823–7. https://doi.org/10.1111/tbed.12959
26. Bosco-Lauth AM, Marlenee NL, Hartwig AE, Bowen RA, Root JJ. Shedding of clade 2.3.4.4 H5N8 and H5N2 highly pathogenic avian influenza viruses in peridomestic wild birds in the U.S. Transbound Emerg Dis. 2019;66:1301–5. https://doi.org/10.1111/tbed.13147
27. Ellis JW, Root JJ, McCurdy LM, Bentler KT, Barrett NL, VanDalen KK, et al. Avian influenza A virus susceptibility, infection, transmission, and antibody kinetics in European starlings. PLoS Pathog. 2021;17:e1009879. https://doi.org/10.1371/journal.ppat.1009879
28. Tolf C, Latorre-Margalef N, Wille M, Bengtsson D, Gunnarsson G, Grosbois V, et al. Individual variation in influenza A virus infection histories and long-term immune responses in mallards. PLoS One. 2013;8:e61201. https://doi.org/10.1371/journal.pone.0061201
29. Arévalo-Ayala DJ, Real J, Durà C, Aymerich J, Hernández-Matías A. Reduction of organic waste in a landfill lowers the visitation probability but not the local abundance of a long-lived scavenger species. Bird Conserv Int. 2023;33:e15. https://doi.org/10.1017/S0959270922000107
30. Rasmussen EA, Czaja A, Cuthbert FJ, Tan GS, Lemey P, Nelson MI, et al. Influenza A viruses in gulls in landfills and freshwater habitats in Minnesota, United States. Front Genet. 2023;14:1172048. https://doi.org/10.3389/fgene.2023.1172048
31. Arrondo E, Sebastián-González E, Moleón M, Morales-Reyes Z, María Gil-Sánchez J, Cortés-Avizanda A, et al. Vulture culture: dietary specialization of an obligate scavenger. Proc Biol Sci. 2023;290:20221951.
32. Fernández-Gómez L, Cortés-Avizanda A, Arrondo E, García-Alfonso M, Ceballos O, Montelío E, et al. Vultures feeding on the dark side: current sanitary regulations may not be enough. Bird Conserv Int. 2022;32:590–608. https://doi.org/10.1017/S0959270921000575
33. Bárbara A, Torrontegi O, Camacho MC, Barral M, Hernández JM, Höfle U. Avian influenza virus surveillance in south-central Spain using fecal samples of aquatic birds foraging at landfills. Front Vet Sci. 2017;4:178. https://doi.org/10.3389/fvets.2017.00178
34. López-Calderón C, Martín-Vélez V, Blas J, Höfle U, Sánchez MI, Flack A, et al. White stork movements reveal the ecological connectivity between landfills and different habitats. Mov Ecol. 2023;11:18. https://doi.org/10.1186/s40462-023-00380-7
35. Lagan P, McKenna R, Baleed S, Hanna B, Barley J, McConnell S, et al. Highly pathogenic avian influenza A(H5N1) virus infection in foxes with PB2-M535I identified as a novel mammalian adaptation, Northern Ireland, July 2023. Euro Surveill. 2023;28:2300526 https://doi.org/10.2807/1560-7917.ES.2023.28.42.2300526
36. Ellis J, Shriner S, McLean H, Petersen L, Root JJ. Inventory of wildlife use of mortality pits as feeding sites: implications of pathogen exposure [cited 2023 Jan 31]. https://digitalcommons.usu.edu/hwi/vol11/iss1/4/
37. Bosè M, Duriez O, Sarrazin F. Intra-specific competition in foraging Griffon Vultures *Gyps fulvus*: 1. Dynamics of group feeding. Bird Study. 2012;59:182–92. https://doi.org/10.1080/00063657.2012.658639
38. Fluhr J, Benhamou S, Peyrusque D, Duriez O. Space use and time budget in two populations of griffon vultures in contrasting landscapes. J Raptor Res. 2021;55:425–37. https://doi.org/10.3356/JRR-20-14
39. Delgado-González A, Cortés-Avizanda A, Serrano D, Arrondo E, Duriez O, Margalida A, et al. Apex scavengers

from different European populations converge at threatened savannah landscapes. Sci Rep. 2022;12:2500. https://doi.org/10.1038/s41598-022-06436-9
40. Boulinier T. Avian influenza spread and seabird movements between colonies. Trends Ecol Evol. 2023;38:391–5. https://doi.org/10.1016/j.tree.2023.02.002
41. Careen NG, Collins SM, D'Entremont KJN, Wight J, Rahman I, Hargan KE, et al. Highly pathogenic avian influenza virus resulted in unprecedented reproductive failure and movement behaviour by northern gannets. Marine Ornithology. 2024;52:121–8.
42. Gaide N, Filaire F, Bertran K, Crispo M, Dirat M, Secula A, et al. The feather epithelium contributes to the dissemination and ecology of clade 2.3.4.4b H5 high pathogenicity avian influenza viruses in ducks. Emerg Microbes Infect. 2023;12:2272644. https://doi.org/10.1080/22221751.2023.2272644
43. Bertran K, Pérez-Ramírez E, Busquets N, Dolz R, Ramis A, Darji A, et al. Pathogenesis and transmissibility of highly (H7N1) and low (H7N9) pathogenic avian influenza virus infection in red-legged partridge (*Alectoris rufa*). Vet Res. 2011;42:24. https://doi.org/10.1186/1297-9716-42-24
44. Bertran K, Busquets N, Abad FX, García de la Fuente J, Solanes D, Cordón I, et al. Highly (H5N1) and low (H7N2) pathogenic avian influenza virus infection in falcons via nasochoanal route and ingestion of experimentally infected prey. PLoS One. 2012;7:e32107. https://doi.org/10.1371/journal.pone.0032107
45. Robert A, Sarrazin F, Couvet D, Legendre S. Releasing adults versus young in reintroductions: interactions between demography and genetics. Conserv Biol. 2004;18:1078–87. https://doi.org/10.1111/j.1523-1739.2004.00218.x
46. Ogada DL, Keesing F, Virani MZ. Dropping dead: causes and consequences of vulture population declines worldwide. Ann N Y Acad Sci. 2012;1249:57–71. https://doi.org/10.1111/j.1749-6632.2011.06293.x
47. Buechley ER, Şekercioğlu ÇH. The avian scavenger crisis: looming extinctions, trophic cascades, and loss of critical ecosystem functions. Biol Conserv. 2016;198:220–8. https://doi.org/10.1016/j.biocon.2016.04.001
48. Posillico M, Costanzo A, Bottoni S, Altea T, Opramolla G, Pascazi A, et al. Reported mortality of griffon vulture *Gyps fulvus* in central Italy and indications for conservation and management. Bird Conserv Int. 2023;33:e68. https://doi.org/10.1017/S0959270923000199
49. Ogada DL, Torchin ME, Kinnaird MF, Ezenwa VO. Effects of vulture declines on facultative scavengers and potential implications for mammalian disease transmission. Conserv Biol. 2012;26:453–60. https://doi.org/10.1111/j.1523-1739.2012.01827.x

Address for correspondence: Guillaume Le Loc'h, UMR 1225 IHAP, École Nationale Vétérinaire de Toulouse, 23 Chemin des Capelles, 31300 Toulouse, France; email: guillaume.leloch@envt.fr

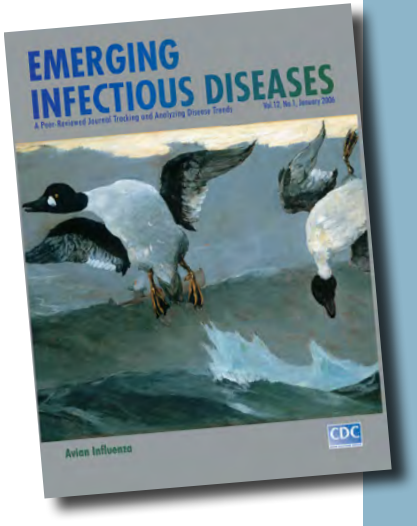

Originally published in January 2006

etymologia revisited

Influenza

[in''floo-en'zə]

An acute viral infection of the respiratory tract. From Latin influentia, "to flow into"; in medieval times, intangible fluid given off by stars was believed to affect humans. The Italian influenza referred to any disease outbreak thought to be influenced by stars. In 1743, what Italians called an influenza di catarro ("epidemic of catarrh") spread across Europe, and the disease came to be known in English as simply "influenza."

References

1. Dorland's illustrated medical dictionary. 30th ed. Philadelphia: Saunders; 2003
2. Quinion M. World wide words. 1998 Jan 3 [cited 2005 Dec 5]. http://www.worldwidewords.org/topicalwords/tw-inf1.htm

https://wwwnc.cdc.gov/eid/article/12/1/et-1201_article

Case Report of Clade Ib Monkeypox Virus Infection Linked to Travel to Democratic Republic of the Congo, Thailand, 2024

Drunphob Srithammavong, Chanunya Srihawan,[1] Rossaphorn Kittiyaowamarn,[1] Rapeepong Suphanchaimat,[1] Thitipong Yingyong,[1] Wichan Bunyakitikorn[1]

We report clade Ib monkeypox virus infection in a patient who returned to Thailand from the Democratic Republic of the Congo, the subclade epicenter. Improved diagnostic testing, public health response, and surveillance systems for mpox are needed in Thailand, and preexposure mpox vaccination should be considered, especially for high-risk persons.

Mpox is an infectious disease caused by monkeypox virus (MPXV), which is primarily transmitted through close contact with infected persons (*1*). In late 2023, a novel clade Ib MPXV was identified in the Democratic Republic of the Congo (DRC) after earlier mpox outbreaks in the United States in 2003 and the global outbreak in 2022 (*2*,*3*). Because of the rise in clade I–associated mpox cases, the World Health Organization (WHO) declared the outbreak in Africa a Public Health Emergency of International Concern in May 2024 (*4*). We report a case of clade Ib MPXV–associated mpox in Thailand and highlight the challenges in mpox public health responses. The case investigation was conducted by authorized public health officers according to the Communicable Disease Act of Thailand. Patient information remains confidential.

The Study

A 66-year-old man of German nationality who resides in eastern Thailand traveled to Germany on June 18, 2024. On July 30, he departed for Rwanda and then traveled to Bukavu, South Kivu, DRC, on August 1. He stayed with 2 friends in an apartment and denied participating in any sexual activity or having contact with infected persons during his visit. His friends reported no abnormal symptoms. He reported that he rarely wore a mask or washed his hands with soap or sanitizer during his stay. On August 10, genital itching developed. On August 13, his co-worker drove him to the border, and he took a taxi to the airport in Rwanda, where he departed and transited through Qatar, arriving in Thailand on August 14. On that same day, his symptoms progressed to fever, muscle aches, sore throat, fatigue, and rash, which primarily affected his genitalia, trunk, extremities, and face. His wife picked him up from Suvarnabhumi Airport (Thailand); they had dinner together in Bangkok before checking into a hotel. On August 15, he visited a private hospital and was admitted. On examination, he had multiple discrete erythematous maculopapular lesions and a few vesicular lesions distributed across his face, trunk, and extremities and had some necrotic papules with overlying scabs on his penis and right thigh (Figure).

We collected clinical samples on August 16, 21, and 29 and September 2. A private laboratory conducted real-time PCR and detected MPXV in the samples by amplifying the *F3L* gene; however, the result for clade I MPXV *D14L* gene amplification was inconclusive. The Thai Red Cross Emerging Infectious Disease Clinical Center also detected MPXV but did not specify the clade. We sent a swab sample from August 21 to the Bamrasnaradura Infectious Disease Institute, where clade II MPXV was

Author affiliations: Ministry of Public Health, Bangkok, Thailand (D. Srithammavong, R. Kittiyaowamarn, R. Suphanchaimat, T. Yingyong, W. Bunyakitikorn); Samitivej Sukhumvit Hospital, Bangkok (C. Srihawan)

DOI: https://doi.org/10.3201/eid3108.250255

[1]These senior authors contributed equally to this article.

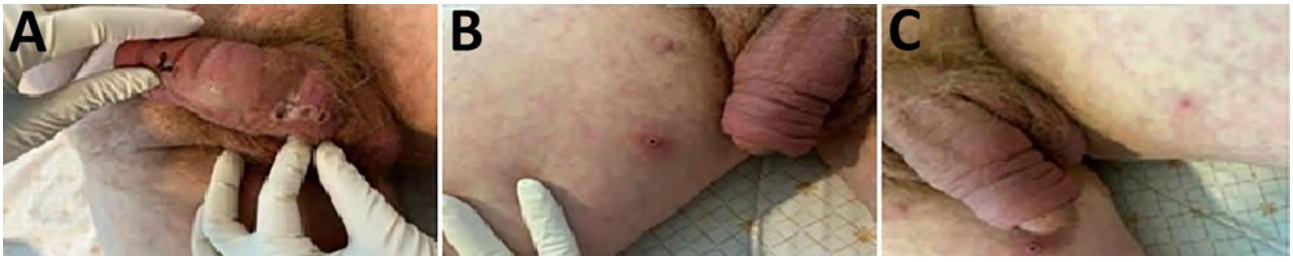

Figure. Lesions on patient who had clade Ib monkeypox virus infection linked to travel to the Democratic Republic of the Congo, Thailand, 2024. A, B) Necrotic papules with overlying scabs on the patient's penis (A) and right thigh (B). C) Maculopapular rash and a pustule on left thigh.

identified by using the QIAstat-Dx Viral Vesicular Panel (QIAGEN, https://www.qiagen.com). Because of conflicting results, we sent a swab sample from August 16 to Thailand's national reference laboratory at the National Institute of Health (NIH) for confirmation by whole-genome sequencing. The Thailand NIH confirmed the sample was clade Ib MPXV and deposited the sequence in the GISAID database (https://www.gisaid.org; accession no. EPI_ISL_19350788).

The lowest cycle threshold (Ct) value of 13.73 was obtained from a sample of combined vesicles and pustules collected from the patient's genitalia 6 days after symptom onset. The patient began treatment with tecovirimat on August 20. A subsequent swab sample from a scab lesion on the left leg showed the highest PCR Ct value 23 days after symptom onset (Ct 38.48). Cultures from all swab samples tested at NIH showed no virus growth (Table 1). The patient was discharged on September 5 without complications.

Contact tracing identified 89 persons who had direct contact with the patient's skin, bodily fluids, or contaminated objects (fomites) or who were within 1 meter of the patient during potential aerosol-generating activities. Among those 89 contacts, 33 were classified as high-risk because of exposure without proper personal protective equipment: the patient's wife, 13 flight passengers, 12 healthcare personnel, 6 hotel staff, and 2 restaurant staff (Table 2). Symptoms did not develop in any high-risk contacts during the monitoring period; no secondary cases were observed. Because of the close contact, a regional public health officer collected nasopharyngeal swab samples from the patient's wife on days 7, 14, and 23 after her last exposure to the patient. All samples were negative for MPXV by PCR.

Before the WHO public health emergency declaration, Thailand did not have specific mpox screening measures at points of entry. Mpox cases could potentially be identified through existing yellow fever screening by the Port and Quarantine Office,

Table 1. Diagnostic laboratory results for swab samples from index patient who had clade Ib monkeypox virus infection linked to travel to the Democratic Republic of the Congo, Thailand, 2024*

Sample no.	Laboratory	Collection point, lesion type	No. days†	Laboratory results according to method		
				Real-time PCR (Ct)	WGS	Culture
1	Private laboratory	Genitalia, combined vesicle and pustule	6	MPXV *F3L* gene detected (13.73); *D14L* gene, inconclusive signal for clade I, not detected for clade II	NA	NA
	TRC-EIDCC			MPXV detected (15.03)	NA	NA
	Thailand NIH			NA	MPXV clade Ib‡	NA
2	BIDI	Genitalia and extremities, combined vesicle, pustule, and ulcerated lesion	11	MPXV clade II detected (21.4)	NA	NA
3	Thailand NIH	Left arm, fallen-off scab	19	ND	NA	NA
		Trunk, fallen-off scab		ND		
		Right leg, beneath scab		MPXV detected (25.17)		
		Left toes, beneath scab		MPXV detected (26.07)		
		Genitalia, ulcerated lesion		MPXV detected (34.16)		
4	Thailand NIH	Left leg, fallen-off scab	23	MPXV detected (38.48)	NA	ND
		Right leg, fallen-off scab		MPXV detected (30.88)		
		Genitalia, fallen-off scab		MPXV detected (31.12)		
		Left toes, fallen-off scab, fully formed new skin layer		MPXV detected (33.37)		

*BIDI, Bamrasnaradura Infectious Disease Institute; Ct, cycle threshold; MPXV, monkeypox virus; NA, not applicable; ND, not detected; NIH, National Institute of Health; TRC-EIDCC, Thai Red Cross Emerging Infectious Disease Center.
†Number of days after onset of symptoms.
‡GISAID accession no. EPI_ISL_19350788 (https://www.gisaid.org).

Table 2. Characteristics of contacts of index patient who had clade Ib monkeypox virus infection linked to travel to the Democratic Republic of the Congo, Thailand, 2024*

Contacts, n = 89	No. contacts	Symptoms†	Contact level‡	Remark
Wife	1	No	High	Close contact with no PPE
Aircraft and airport				
Passenger of 2nd airline	13	No	High	Could not obtain
Aircrew of 2nd airline	25	No	Low	information for first airline
Airport officer	2	No	Low	
Private hospital				
Physician	3	No	High, n = 2; low, n = 1	No proper PPE
Nurse and nurse aide at ward A	16	No	Low	No proper PPE
Nurse and nurse aide at ward B	9	No	High	
Assistant officer	3	No	Low	
Hotel R				
Hotel officers, including housekeeper, bellboy, receptionist	6	No	High	No PPE
Elevator passenger	3	No	Low	Cannot contact
Other hotel guests in same room	6	Unknown	Unknown	Cannot contact
Restaurant A	2	No	High	No PPE

*PPE, personal protective equipment.
†Symptoms as of September 5, 2024.
‡Contact risk levels: low, proper PPE; high, without proper PPE.

which focuses on travelers from 42 yellow fever–risk countries (*5*). Screening procedures conducted by public health officers include taking travel history, checking body temperature, and verifying the International Certificate of Vaccination for yellow fever and Thailand Health Pass registration. At the time of the WHO declaration, 5 ongoing mpox outbreaks in DRC, Burundi, Kenya, Cote d'Ivoire, and Uganda overlapped with the yellow fever list. However, Rwanda was not among those. Nonetheless, on the day of arrival in Thailand, the patient voluntarily walked to the screening area wearing a long-sleeved shirt and hat and did not report any illness. Thus, the officer did not observe any visible rashes on his face.

At hotel R, public health officers from the Health Department of the Bangkok Metropolitan Administration collected environmental samples from suspected contact surfaces in the hotel room 9 days after the patient had left. All samples tested positive for MPXV except those taken from the light switch and the doorknobs of the bedroom and living room. The positive samples had Ct values ranging from 28 to 38; the lowest Ct value was detected on the curtain knob (Table 3). The hotel staff used 3 types of cleaning products containing active ingredients, such as citric acid, alkyl alcohol ethoxylate, didecyldimethylammonium chloride, alkyldimethylbenzylammonium chloride, and ethanol. At restaurant A, ethyl alcohol spray was used for table cleaning. All of those chemicals are considered effective against MPXV (*6*).

Conclusions

We report a travel-associated case of imported clade Ib mpox infection in Thailand with a mild clinical course, consistent with other clade Ib mpox infections reported outside of Africa (*7*). The likely source of infection was human-to-human transmission during community activities in DRC, differing from reports of predominantly sexual transmission among adults in the country (*8*,*9*). Inconsistent PCR results were attributed to the use of different detection methods across laboratory centers. Clade Ib MPXV contains a large deletion of ≈1,000 nt in the *D14L* gene region (*8*,*9*), which was the target sequence used in the

Table 3. Real-time PCR results of environmental samples from hotel room of index patient who had clade Ib monkeypox virus infection linked to travel to the Democratic Republic of the Congo, Thailand, 2024*

Sample no.	Collection site	MPXV PCR result	Cycle threshold value
1	Refrigerator handle	Detected	35.48
2	Curtain knob	Detected	28.64
3	Sofa	Detected	38.84
4	Bed edge	Detected	37.64
5	Air conditioner and television remote, pooled sample	Detected	35.23
6	Bathroom faucet	Detected	38.70
7	Handrail in bathroom	Detected	36.69
8	Bathtub drain	Detected	36.95
9	Light switch in bedroom	Not detected	NA
10	Doorknob in bedroom	Not detected	NA
11	Doorknob in living room	Not detected	NA

*Samples were taken 9 days after patient checked out of hotel room. MPXV, monkeypox virus; NA, not applicable.

private laboratory's real-time PCR and resulted in an inconclusive signal for clade I MPXV. Furthermore, the multiplex PCR kit used by the Bamrasnaradura Infectious Disease Institute exhibited cross-reactivity between MPXV clades I and II, leading to sample misidentification as clade II MPXV. The assay provider (QIAGEN) has since corrected this issue. For more accurate and timely diagnosis of clade Ib mpox, newly developed PCR methods are recommended (*10*). Swab samples taken from scab lesions still had detectable MPXV by real-time PCR; Ct values ranged from 30.88 to 38.48. Patient isolation duration and the contact monitoring period for clade Ib mpox should align with the US Centers for Disease Control and Prevention's recommendations (*11*).

Strengthening Thailand's public health response is crucial to prevent future travel-associated and imported clade I mpox cases. Point-of-entry screening should include visual inspection of travelers arriving from countries facing ongoing mpox outbreaks to detect rashes on the face and extremities. Healthcare providers should consistently use appropriate personal protective equipment and obtain detailed travel history from patients manifesting clinical symptoms compatible with mpox. In 2024, mpox vaccines were not publicly available in Thailand; thus, preexposure vaccination should be considered, especially for high-risk persons.

Acknowledgments

We thank the patient's admitting hospital, the Institute of Urban Disease and Control, Health Department of the Bangkok Metropolitan Administration, Suvarnabhumi Port and Quarantine Office, Thailand National Institute of Health, and Bamrasnaradura Infectious Disease Institute.

About the Author

Dr. Srithammavong is a medical doctor in the epidemiology training program in the Division of Epidemiology, Department of Disease Control, Ministry of Public Health, Thailand. His research interests focus on field epidemiology and disease control.

References

1. World Health Organization. Mpox. 2024 [cited 2024 Nov 20]. https://www.who.int/news-room/fact-sheets/detail/mpox
2. Ligon BL. Monkeypox: a review of the history and emergence in the Western hemisphere. Semin Pediatr Infect Dis. 2004;15:280–7. https://doi.org/10.1053/j.spid.2004.09.001
3. Centers for Disease Control and Prevention. Ongoing clade II mpox global outbreak. 2025 [cited 2025 Mar 31]. https://www.cdc.gov/mpox/outbreaks/2022/index-1.html
4. World Health Organization. Disease outbreak news. Mpox—Democratic Republic of the Congo. 2024 [cited 2024 Nov 21]. https://www.who.int/emergencies/disease-outbreak-news/item/2024-DON522
5. Royal Thai Embassy, Athens. List of countries which are declared yellow fever infected areas [cited 2025 Jun 18]. https://athens.thaiembassy.org/en/publicservice/17708-list-of-countries-which-are-declared-yellow-fever-infected-areas
6. United States Environmental Protection Agency. Disinfectants for emerging viral pathogens (EVPs): list Q. 2024 [cited 2024 Nov 21]. https://www.epa.gov/pesticide-registration/disinfectants-emerging-viral-pathogens-evps-list-q
7. World Health Organization. Mpox multi-country external situation report no. 45. January 2025 [cited 2025 Jan 11]. https://cdn.who.int/media/docs/default-source/documents/emergencies/mpox-sitrep_-45.pdf
8. Masirika LM, Udahemuka JC, Schuele L, Ndishimye P, Otani S, Mbiribindi JB, et al. Ongoing mpox outbreak in Kamituga, South Kivu province, associated with monkeypox virus of a novel clade I sub-lineage, Democratic Republic of the Congo, 2024. Euro Surveill. 2024;29:2400106. https://doi.org/10.2807/1560-7917.ES.2024.29.11.2400106
9. Vakaniaki EH, Kacita C, Kinganda-Lusamaki E, O'Toole Á, Wawina-Bokalanga T, Mukadi-Bamuleka D, et al. Sustained human outbreak of a new MPXV clade I lineage in eastern Democratic Republic of the Congo. Nat Med. 2024;30:2791–5. https://doi.org/10.1038/s41591-024-03130-3
10. Schuele L, Masirika LM, Udahemuka JC, Siangoli FB, Mbiribindi JB, Ndishimye P, et al.; GREATLIFE MPOX group; Collaborators. Real-time PCR assay to detect the novel clade Ib monkeypox virus, September 2023 to May 2024. Euro Surveill. 2024;29:2400486. https://doi.org/10.2807/1560-7917.ES.2024.29.32.2400486
11. Centers for Disease Control and Prevention. Mpox infection prevention and control in healthcare settings. 2024 [cited 2024 Oct 24]. https://www.cdc.gov/mpox/hcp/infection-control/healthcare-settings.html

Address for correspondence: Drunphob Srithammavong, 88/21, Division of Epidemiology, Department of Disease Control, Ministry of Public Health, Tiwanon Rd, Taladkwan, Muang, Nonthaburi, 11000, Thailand; email: darunphobfirst@gmail.com

Variance among Public Health Agencies' Boil Water Guidance

Megan Dorris, Shanna Miko, Jasen M. Kunz, Vincent R. Hill

We reviewed boil water guidance from 5 public health agencies and noted differences in boil definition, duration, and elevation adjustment. Publishing evidence-based models could clarify the scientific rationale, promote consensus, and minimize likelihood of incomplete water treatment or excess use of limited fuel resources during emergencies and in backcountry settings.

On September 27, 2024, Hurricane Helene brought strong winds and historic rainfall to the southeastern United States. Powerful flood waters, falling trees, and landslides left millions with limited access to electricity and fuel (*1*). Damage to hundreds of miles of distribution pipes risked contaminating the drinking water supply with disease-causing microorganisms. In response, drinking water utilities issued boil water advisories, affecting >1.8 million persons for days to weeks (*2*).

Boiling is an identifiable target that does not require a thermometer and occurs at 100°C (212°F) at sea level. Although boiling cannot remove suspended particulate matter, disease-causing microbes begin to die or deactivate as water temperature rises, losing their ability to cause illness (*3*). Consequently, boiling is a simple and effective way to disinfect drinking water in emergency situations, during water main breaks or low pressure events in drinking water distribution systems, or in backcountry settings (*4*–*10*). At higher elevations, where water boils at a lower temperature, some guidance recommends longer boil times (*5*,*7*,*8*). However, boiling water requires fuel, a resource often limited in emergency situations and backcountry settings. Variance in boil water guidance from public health agencies might leave the public weighing thorough water treatment against conserving limited fuel supplies.

Author affiliations: Epidemic Intelligence Service, Atlanta, Georgia, USA (M. Dorris); Centers for Disease Control and Prevention, Atlanta (M. Dorris, S. Miko, J. Kunz, V. Hill)

DOI: http://doi.org/10.3201/eid3108.250208

The Study

We compared boil water guidance from the US Centers for Disease Control and Prevention drinking water advisories webpage (*5*) and Yellow Book (*6*), US Environmental Protection Agency (EPA) (*7*), Health Canada (*8*), US Department of Homeland Security Ready.gov (*9*), and World Health Organization (WHO) (*10*,*11*) (Table). Our goal was to identify variances in boil water guidance, explore potential reasons for differences, and describe opportunities for future research to support the development of universally consistent guidelines.

Each guidance document includes boiling as an endpoint, with most guidance further specifying rolling boil (Table). Health Canada provides a definition to identify rolling boil, and Yellow Book recommends a full minute of boiling to "account for user variability in identifying boiling points." We speculated that issuing conservative recommendations out of caution might contribute to differences in guidance. Clearly and consistently defining the target endpoint could decrease user variability and enable agencies to recommend less cautious boil times. A concerted effort among public health organizations to set microbial-based targets and a universal health metric, reinforcing the scientific rationale behind water-boiling safety measures, would lay critical groundwork for a unified boil water guidance framework, as would conducting meta-analyses of time–temperature microbial inactivation. Study results from such investigations could inform recommendations for heat time, potential elevation affects, and how the cooling period factors into guidance.

During pasteurization, thermal inactivation of bacteria, viruses, and protozoa begins slowly at temperatures well below boiling point and accelerates as temperatures rise (*3*). Safety specialists perform pasteurization studies at 60°C–85°C (140°F–185°F) in a variety of foods and beverages and measure pathogen inactivation in log reductions. Such studies typically report a ≥3 log (≥99.9%) reduction of most

enteric pathogens in times ranging from 1 second to 30 minutes (*3*,*11*). However, few studies document log reductions achieved at or near boiling point or the corresponding timing. Data from pasteurization studies therefore inform estimates of how long water should boil before it is considered potable.

After boiling, cooling time also can contribute to thermal inactivation of pathogens. The EPA, Ready.gov, and WHO recommend letting water cool naturally (Table). During this cooling time, the water would be above pasteurization temperatures longer than other cooling methods, such as refrigerating or adding ice, which could cause recontamination. WHO advises that water may be removed from the heat source immediately after reaching a rolling boil, whereas other agencies recommend maintaining a rolling boil for 1 minute. No guidance specifies whether cooling is included in heat-time estimates of pathogen inactivation.

During pasteurization, minimum pathogen reduction requirements called log-reduction targets (LRTs) are based on initial quantity of pathogen present and the risk the pathogen poses to human health. As for pasteurization standards, boil water guidance aims to make water safe for drinking and cooking (i.e., potable), not sterile (*6*–*8*,*10*). Setting pathogen-specific LRTs for drinking water is difficult because the level of source water contamination is often unknown. In emergency situations and backcountry settings, available water sources may be visibly turbid, requiring higher LRTs to make the water potable. Higher temperatures, longer thermal time, or water filters may be required to achieve greater LRTs, highlighting the importance of achieving a true rolling boil. The use of different LRTs may contribute to variation across boil water guidance. Estimating minimum, pathogen-specific LRTs for potable water could increase transparency of boil water guidance and foster discussion among agencies.

Pathogens require different minimum exposure levels to cause disease and have distinct illness and death rates (*10*). From a microbial perspective, health officials generally consider water potable when pathogens are reduced below the disease-causing threshold. For instance, whereas bacterial spores are highly heat resistant and may survive boiling, they rarely cause human disease and are considered a tolerable risk in drinking water (*6*).

Health outcome metrics help estimate tolerable risk levels. The EPA estimates a tolerable risk as a level of exposure causing <1 illness/10,000 persons/year (*12*). WHO uses disability-adjusted life-years and defines tolerable burden of disease as 10^{-6} disability-adjusted life-years/person/year (*10*). Adopting a universal health metric for water safety standards could assist in establishing consistent LRTs for waterborne pathogens.

Researchers have used time-temperature models based on pasteurization data to illustrate pathogen inactivation time to specific LRTs. Although data >85°C (185°F) is often lacking, those models could be adapted to estimate pathogen-specific LRTs at boiling or near-boiling temperatures (Figure) and highlight pathogens lacking data points. Quantifying reductions for certain pathogens, such as norovirus and rotavirus, is challenging because of the lack of reliable methods for measuring viable units, but pathogens with equal or greater thermal resistance can be used as proxies to estimate inactivation (*10*).

Table. Comparison of guidance from 5 public health agencies for study of variance among public health agencies' boil water guidance*

Agency	Target endpoint	Endpoint definition	Duration at endpoint	Elevation adjustment	Cooling guidance
CDC drinking water advisories webpage (*5*)	Full rolling boil	Not defined	1 min	3 min at elevations above 1,981 m (6,500 ft)	Allow boiled water to cool before you use it
Yellow Book (*6*)	Boiling	Not defined	1 min, if fuel supplies are adequate	No adjustment needed at common terrestrial travel elevations.	Not addressed
EPA (*7*)	Rolling boil	Not defined	1 min	3 min at elevations 1,524 m (5,000 feet)	Let water cool naturally
Health Canada (*8*)	Rolling boil	A vigorous boil, where bubbles appear at the center and do not disappear when the water is stirred	1 min	2 min at elevations above 2,000 m (6,562 ft)	The water should then be cooled
Ready.gov (*9*)	Rolling boil	Not defined	1 min	Not addressed	Let the water cool before drinking
WHO (*11*)	Rolling boil	Not defined	No additional time after reaching rolling boil	No adjustment at high elevation	Cool naturally, without the addition of ice

*CDC, US Centers for Disease Control and Prevention; EPA, US Environmental Protection Agency; WHO, World Health Organization.

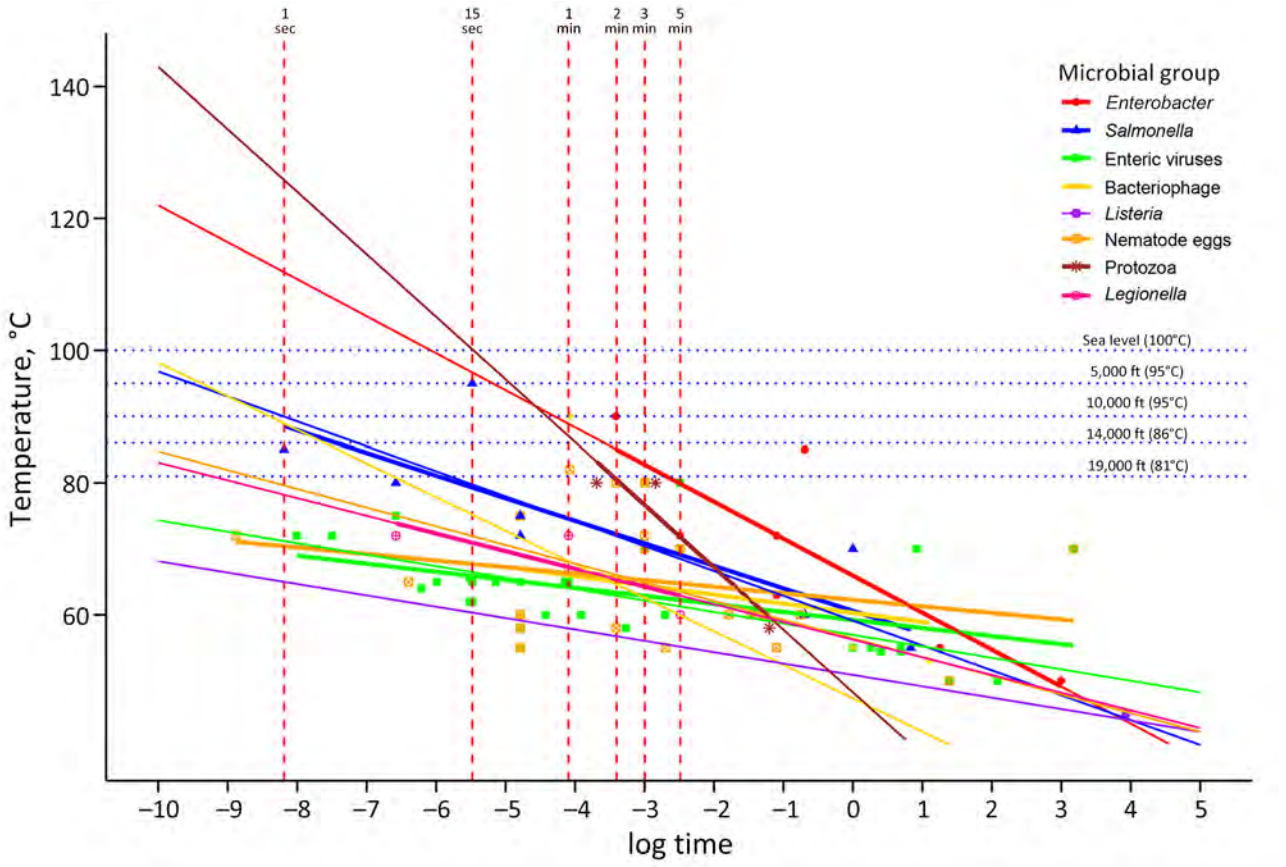

Figure. Linear model of boiling time required to reduce pathogen levels, by elevation, for study of variance among public health agencies' boil water guidance. Model estimates time to achieve 3–5 log reductions of specified microbial groups (*3*,*11*). At boiling point temperatures, all listed pathogens achieve the reductions in ≤1 minute, from sea level to 10,000 feet. Incorporating more data points at boiling or near-boiling temperatures could enhance accuracy. Models using pathogen-specific log reduction targets may provide more precise time estimates.

Existing time–temperature models could also help evaluate how elevation affects boil water recommendations. For every 150-m (492-ft) increase in elevation, the boiling point of water decreases by ≈0.5°C (0.9°F). In Asheville, North Carolina, USA, at 640 m (2,100 ft) elevation, water boils at 98°C (207.6°F), whereas in Denver, Colorado, USA, at 1,585 m (5,200 ft) elevation, water boils at ≈94°C (201°F). This inverse relationship between elevation and boiling point contributes to differences in boil water guidance at high elevations. Heat inactivation models could estimate when pathogen-specific LRTs are achieved at these lower boiling points, potentially incorporating cooling time to account for additional inactivation—and possibly providing support for discounting boil time adjustment for higher elevations.

Yellow Book and WHO guidance state that all disease-causing pathogens, except bacterial spores, are inactivated at boiling temperatures. Developing and publishing models to illustrate this guidance could clarify the scientific basis for decisions across agencies, identify gaps in pathogen inactivation data, and encourage informed discussion.

Conclusions

Extreme weather events can damage water systems, utilities, and roadways, limiting access to safe drinking water and fuel. To address this concern, public health agencies have published boil water guidance to educate the public on preparing safe drinking water during emergencies. Variances in boiling time and elevation adjustment across these guidelines may cause confusion, however, potentially hindering efforts to ensure water safety or leading to extra fuel use.

Although the concept of boiling water to ensure potability is straightforward, developing evidence-based guidance is complex. Adopting a consistent definition of a rolling boil, publishing analyses or models based on pathogen-specific LRTs supported by health outcome metrics, and incorporating cooling time into models could enhance clarity. This approach could illustrate the scientific rationale

behind current guidance, encourage informed multi-agency discussion, and create opportunities to build consensus on boil water recommendations.

About the Author

Ms. Dorris is an Epidemic Intelligence Service officer assigned to the Waterborne Disease Prevention Branch, Division of Foodborne, Waterborne, and Environmental Diseases. National Center for Emerging and Zoonotic Infectious Diseases, CDC. Her areas of clinical interest include prevention and treatment of waterborne infections, primarily cholera and typhoid, and strengthening surveillance systems for waterborne diseases.

References

1. State of North Carolina Office of State and Budget Management. Hurricane Helene damage needs assessment: Hurricane Helene recovery recommendations. December 13, 2024. [cited 2024 Dec 11]. https://www.osbm.nc.gov/hurricane-helene-dna/open
2. Phillis MAJ, Peterson B. A week after Helene hit, thousands still without water struggle to find enough [cited 2024 Dec 11]. https://apnews.com/article/hurricane-helene-asheville-north-carolina-water-737bd51b1351315dc28522e36c425f18
3. Espinosa MF, Sancho AN, Mendoza LM, Mota CR, Verbyla ME. Systematic review and meta-analysis of time-temperature pathogen inactivation. Int J Hyg Environ Health. 2020;230:113595. https://doi.org/10.1016/j.ijheh.2020.113595
4. Centers for Disease Control and Prevention, US Environmental Protection Agency, American Water Works Association, Association of State and Territorial Health Officials, Association of State Drinking Water Administrators, National Environmental Health Association. Drinking water advisory communication toolbox. Updated 2016 [cited 2024 Dec 9] https://www.cdc.gov/water-emergency/media/pdfs/2024/08/dwact-2016.pdf
5. Centers for Disease Control and Prevention. Drinking water advisories: an overview. [cited 2024 Dec 9]. https://www.cdc.gov/water-emergency/about/drinking-water-advisories-an-overview.html
6. Backer H, Hill V. Water disinfection. 2023. In: CDC Yellow Book 2024: health information for international travel [cited 2024 Dec 9]. https://wwwnc.cdc.gov/travel/yellowbook/2024/preparing/water-disinfection
7. US Environmental Protection Agency. Emergency disinfection of drinking water [cited 2024 Dec 9]. https://www.epa.gov/ground-water-and-drinking-water/emergency-disinfection-drinking-water
8. Health Canada. Guidance for issuing and rescinding boil water advisories in Canadian drinking water supplies. 2015 [cited 2024 Dec 9]. https://www.canada.ca/en/health-canada/services/publications/healthy-living/guidance-issuing-rescinding-boil-water-advisories-canadian-drinking-water-supplies.html
9. US Department of Homeland Security. Water [cited 2024 Dec 9]. https://www.ready.gov/water
10. World Health Organization. Guidelines for drinking-water quality: 4th edition, incorporating the 1st addendum. 2017 [cited 2024 Dec 9]. https://www.who.int/publications/i/item/9789241549950
11. World Health Organization. Boil water. 2015 [cited 2024 Dec 11]. https://iris.who.int/handle/10665/155821
12. Sharvelle S, Ashbolt N, Clerico E, Holquist R, Levernz H, Olivieri A. Risk-based framework for the development of public health guidance for decentralized non-potable water systems. Proc Water Environ Fed. 2017;8:3799–809. https://doi.org/10.2175/193864717822158189

Address for correspondence: Megan Dorris, Centers for Disease Control and Prevention, 1600 Clifton Rd NE, Mailstop H24-11, Atlanta, GA 30329-4018, USA; email: uqt4@cdc.gov

Recombinant Myxoma Virus in European Brown Hares, 2023–2024

Luisa Fischer, Erwin de Bruin, Evelien Jongepier, Erik Koffeman, Patricia König, Florian Pfaff, Martin Peters, Judith M.A. van den Brand, Marin Bussi, Dominik Fischer, Valentina Caliendo, Erik Weerts, Jooske IJzer, Janina Müller, Ann-Katrin Kühling, Maren Kummerfeld, Jana Müller, Henning Petersen, Sabine Merbach, Martin Beer, Mathilde Uiterwijk, Karst de Boer, Jolianne M. Rijks

Recombinant myxoma virus has emerged in European brown hares (*Lepus europaeus*), causing increased deaths associated with swollen eyelids, head edema, and dermatitis at face, legs, and perineum. Introduction may date back as far as September 2020. As of August 2024, the disease is spreading radially from the Germany–Netherlands border area.

In August 2024, reports of sick and dead European brown hares (*Lepus europaeus*) showing swollen eyelids, edema of head and ears, and dermatitis of face, legs, and perineum increased in the Germany–Netherlands border area of the federal state of North Rhine-Westphalia, Germany, and the provinces of Overijssel and Gelderland, the Netherlands (Figure 1, panel A). The clinical picture resembled myxomatosis, a disease caused by myxoma virus (MYXV; *Leporipoxvirus myxoma*, family *Poxviridae*). In 2023, a total of 4 European brown hares with similar lesions had been submitted for pathologic investigation in 2 adjacent North-Rhine Westphalia municipalities, but those cases were then thought to be sporadic MYXV cases, as reported elsewhere (*1*,*2*).

In Europe, MYXV was intentionally released in the 1950s as biological control for the European rabbit (*Oryctolagus cuniculi*), causing massive disease (*3*). Although outbreaks were less frequent and severe by time because virulence decreased and immunity increased in the rabbit population (*4*), a hare-adapted natural recombinant MYXV (ha-MYXV) emerged in 2018 in Iberian hares (*Lepus granatensis*) on the Iberian Peninsula (*5*,*6*) (Figure 1, panel B). Before then, mass deaths associated with MYXV were not known to occur in European brown hares. We investigated the 2024 outbreak in the Germany–Netherlands border area.

The Study

Wild lagomorphs were submitted from Germany and the Netherlands for investigation during August 1–October 20, 2024. Lagomorphs in this study were shot or found dead with myxomatosis-suspected lesions and submitted for postmortem examination; no animal was killed for the study. We performed pathological examination on 193 myxomatosis-like hares (159 from Germany, 26 from the Netherlands) and wild rabbits (6 from Germany, 2 from the Netherlands), mostly adult animals of both sexes. Body condition varied; 41 (21.2%) animals were cachectic, and of those, 39 (30 from Germany, 9 from the Netherlands) were hares and 2 (1 from each country) were rabbits.

Author affiliations: Research Center for Hunting Science and Wildlife Management, State Agency for Consumer Protection and Nutrition North Rhine-Westphalia, Bonn, Germany (L. Fischer); Dutch Wildlife Health Centre, Utrecht University, Utrecht, the Netherlands (E. de Bruin, J.M.A. van den Brand, M. Bussi, V. Caliendo, E. Weerts, J. IJzer, J.M. Rijks); Royal Dutch Hunters' Association, Amersfoort, the Netherlands (E. Jongepier); Fauna Management Unit Gelderland, Arnhem, the Netherlands (E. Koffeman); Friedrich-Loeffler-Institut, Greifswald-Insel Riems, Germany (P. König, F. Pfaff, M. Beer); Chemical and Veterinary Investigation Office Westphalia, Arnsberg, Germany (M. Peters, S. Merbach); Der Grüne Zoo Wuppertal, Wuppertal, Germany (D. Fischer); Chemical and Veterinary Investigation Office Rhein-Ruhr-Wupper, Krefeld, Germany (Janina Müller, A.-K. Kühling); Chemical and Veterinary Investigation Office Münsterland-Emscher-Lippe, Münster, Germany (M. Kummerfeld); Chemical and Veterinary Investigation Office Ostwestfalen-Lippe, Detmold, Germany (Jana Müller, H. Petersen); Centre for Monitoring of Vectors, Netherlands Food and Consumer Product Safety Authority, Wageningen, the Netherlands (M. Uiterwijk, K. de Boer)

DOI: https://doi.org/10.3201/eid3108.241969

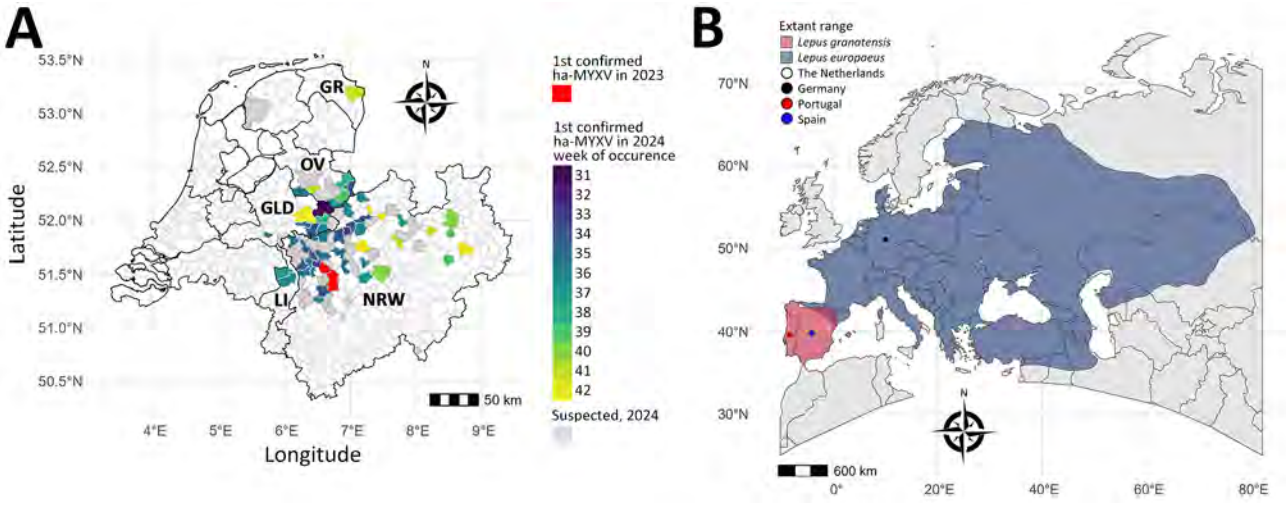

Figure 1. Location of an outbreak of ha-MYXV during 2024 in European brown hares (*Lepus europaeus*) in the border area of the Netherlands and Germany compared with ranges of the hares and the Iberian hare (*Lepus granatensis*). A) Municipalities and provinces in the Netherlands and the Germany federal state of North-Rhine Westphalia, showing the presumed epicenter of the outbreak (municipalities in which ha-MYXV occurred in 2023), as well as the spatiotemporal development of the outbreak in European brown hares during August 1–October 20, 2024. Confirmed ha-MYXV cases occurred in the Netherlands provinces Limburg, Gelderland, Overijssel, and Groningen and in North-Rhine Westphalia. Municipalities without laboratory-confirmed ha-MYXV cases during the study period, but where ha-MYXV-infection in hares was suspected on the basis of pathology, electron microscopy, or photographs of affected hares provide an indication of the probable area of virus presence, are indicated. Map created in R version 4.4.1 (The R Project for Statistical Computing, https://www.r-project.org). B) Extant ranges of both hare species. The outbreak area in northwest Europe is in the western part of the extant range of the European brown hare and far from the extant range of the Iberian hare, in which ha-MYXV was discovered in 2018, causing disease in both Spain and Portugal. Source of extant range shapes: International Union for Conservation of Nature. ha-MYXV, hare-adapted natural recombinant myxoma virus.

The conjunctivae and skin surrounding the eyes, nose, ears, perineum, and legs were thickened with secondary inflammation (Figure 2, panels A, B), orthokeratotic hyperkeratosis, acanthosis, intracorneal pustules, ulceration, and crust formation. Vacuolated keratinocytes, often with regular intracytoplasmic eosinophilic inclusion bodies, exocytosis by heterophilic granulocytes, and apoptosis were prominent in the intact epithelium, including that of the adnexa. Proliferation of pleomorphic mesenchymal cells (myxoma cells) with moderate anisocytosis and anisokaryosis, embedded in myxoid stroma (Appendix 1 Figure 1, panel A, https://wwwnc.cdc.gov/EID/article/31/8/24-1969-App1.pdf), was visible in the surrounding stroma, often accompanied by extensive infiltration of heterophilic granulocytes. Myxoma cells inconsistently contained prominent intracytoplasmic inclusion bodies and fewer amphophilic intranuclear inclusion bodies. The lesions were consistent with myxomatosis; electron microscopic findings further supported that determination (Appendix 1 Figure 1, panel B). In some cases, we diagnosed secondary bacterial infections of the lesions, as well as

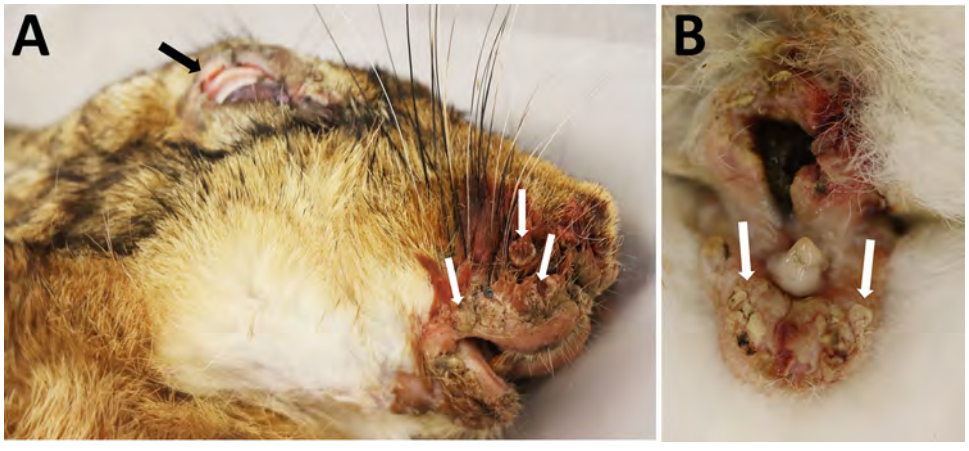

Figure 2. European brown hare (*Lepus europaeus*) with myxomatosis caused by a hare-adapted natural recombinant myxoma virus during a 2024 outbreak in the border area of the Netherlands and Germany. A) Conjunctivitis (black arrow) and nodular skin proliferations at the lips and nose (white arrows). B) Inflammatory swelling of male genital mucous membranes with ulcerations (white arrows).

co-infections (Appendix 2 Table 1, https://wwwnc.cdc.gov/EID/article/31/8/24-1969-App2.xlsx).

We confirmed myxomatosis by MYXV-specific real-time quantitative PCR (qPCR) analyses of eyelid, skin, or lung samples in 104 hares (78 from Germany, 26 from the Netherlands) and 8 rabbits (6 from Germany, 2 from the Netherlands) (Appendix 2 Table 2). We further categorized MYXV-positive samples into classical and ha-MYXV by a second strain-specific qPCR test (7). In total, all 104 hares and half (4/8) of the wild rabbits tested positive for the recombinant ha-MYXV; the remaining rabbits tested positive for classical MYXV. No case of double infection was detected. We performed full-genome sequencing on virus cultured from eyelid samples of 9 hares (4 from Germany, 5 from the Netherlands, all ha-MYXV) and 1 wild rabbit (classical MYXV) to confirm PCR results, enable comparisons with other MYXV, and give insight into the

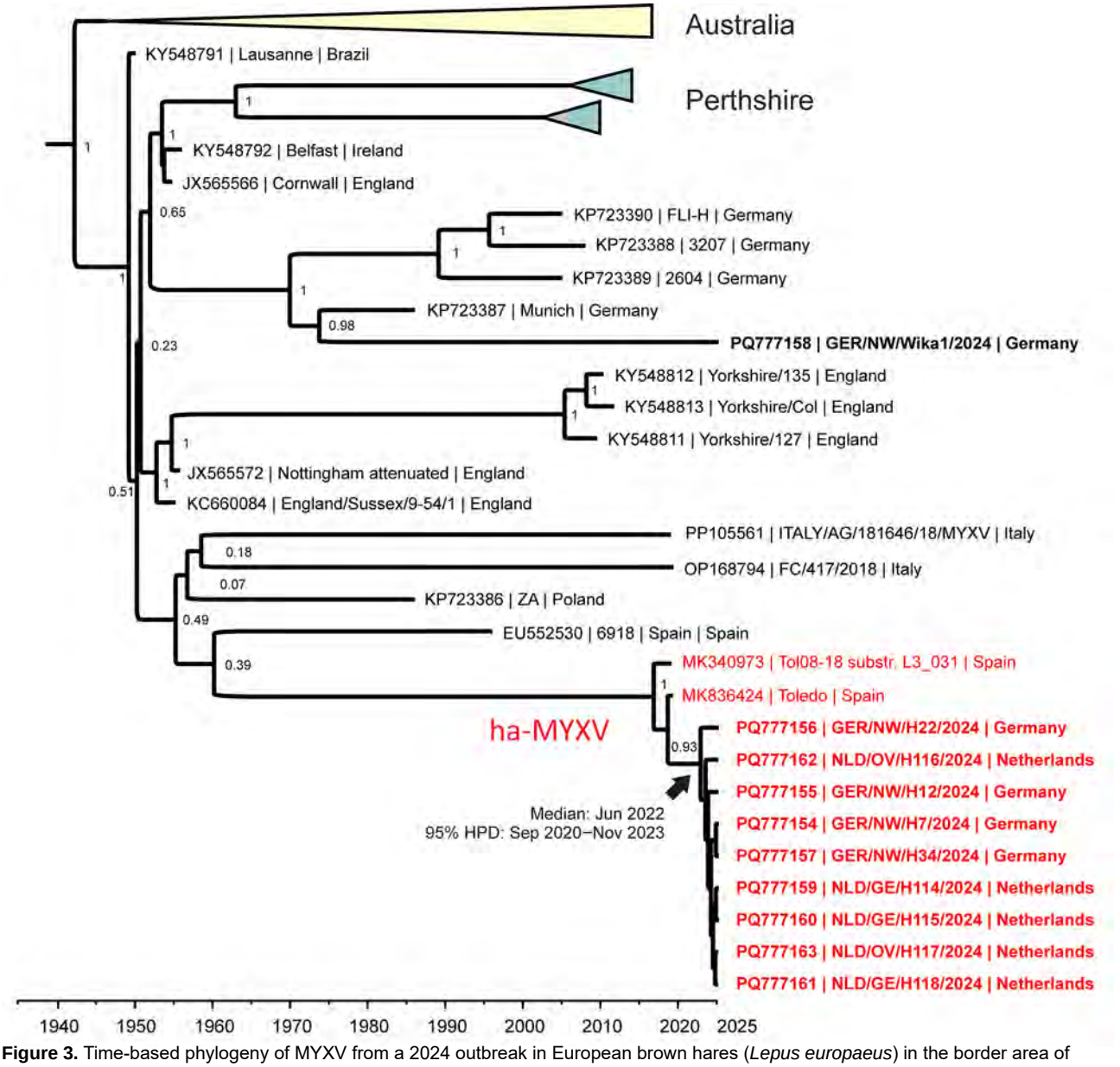

Figure 3. Time-based phylogeny of MYXV from a 2024 outbreak in European brown hares (*Lepus europaeus*) in the border area of the Netherlands and Germany and reference sequences. Ten full-length MYXV sequences from the outbreak were aligned to 114 available full-length MYXV reference genome sequences from GenBank and used for time-based phylogenetic analyses with BEAST version 1.10.4 (https://github.com/beast-dev/beast-mcmc/releases/tag/v1.10.4). Red indicates isolates belonging to ha-MYXV; bold text indicates sequences from this study. Branch labels represent statistical support values; values closer to 1 indicate stronger support. GenBank accession numbers are shown. ha-MYXV, hare-adapted natural recombinant MYXV; HPD, highest posterior density; MYXV, myxoma virus.

evolutionary history of the virus. We prepared DNA libraries and sequenced on the long-read sequencing platform PromethION (Oxford Nanopore Technologies, https://www.nanoporetech.com) (Appendix 1). We trimmed and de novo assembled the raw reads and aligned the resulting MYXV genome sequences with all available MYXV references. We submitted annotated MYXV genome sequences to the International Nucleotide Sequence Database Collaboration (https://www.insdc.org; accession nos. PQ777154–63). A time-structured phylogenetic analysis indicated that the MYXV genomes from hares from the 2024 outbreak have evolved from the same lineage of ha-MYXV that caused mass deaths in Iberian hares (Figure 3). Consistent with the qPCR results, the sequence from the wild rabbit clustered with classical MYXV strains from Germany. Time-aware phylogenetic analysis estimated that the most recent common ancestor of the sequenced ha-MYXV genomes could have emerged as early as September 2020; mean estimated date was June 2022 (95% highest posterior density September 2020–November 2023) (Figure 3).

We retrieved formalin-fixed paraffin-embedded (FFPE) samples from 5 hares found dead during October 2023–April 2024 in the municipalities of Rheinberg, Germany (n = 4) and Duisburg, Germany (n = 1) for retrospective virological examination. PCR results confirmed ha-MYXV infection, demonstrating the presence of pathogen in 2023 (Figure 1, panel A; Appendix 2 Tables 1, 2).

For further insight into the outbreak's probable epicenter and the pattern of spread, we identified municipalities with qPCR-confirmed ha-MYXV cases in 2024 and plotted them by week of first detection. For an overview of the probable area affected, we identified municipalities without confirmed but with suspected cases. We classified hares as suspected cases if pathology results suggested myxomatosis or, for reported hares not submitted for examination, if photographs showed myxomatosis-like lesions (Appendix 2 Table 1). The map suggested a radial and northward spread (Figure 1, panel A). The increased occurrence of ha-MYXV in hares was assumed to be associated with abundance of biting insects such as mosquitoes (Appendix 1 Figure 2), similar to transmission of classical MYXV and as assumed in previous studies (*8*). However, ha-MYXV was not detected via qPCR in 28 mosquitoes collected at 3 different locations in Germany that had confirmed ha-MYXV cases (Appendix 1 Figure 3).

To assess the immediate effect on the hare population, we used autumn hare counts conducted by hunters using thermal imaging from the Province of Gelderland, Netherlands. We compared the number of hares counted in October 2024 with the average count in the 3 preceding years. The results showed a population decline in municipalities with confirmed and suspected cases of ha-MYXV, compared with municipalities without reports of the pathogen ($W = 61$, $p<0.001$ by Wilcoxon signed-rank test) (Appendix 1 Figure 4; Appendix 2 Table 3).

Conclusions

This study demonstrated that ha-MYXV infection caused death in European brown hares. This hare species has a much wider distribution than the Iberian hare; its extant range overlaps with other native hare species in Europe, such as the mountain hare (*Lepus timidus*) and the vulnerable Corsican hare (*Lepus corsicanus*). Our findings also confirm previous results of ha-MYXV infection and death in European rabbits (*9*); however, the effect of this additional hare-adapted variant on the rabbit population is yet unknown. The pattern of disease spread in hares seems to be radial and northward. The outbreak occurrence in late summer suggests transmission by arthropods (*10*). Collectively, those results indicate that ha-MYXV could spread widely in lagomorphs in Europe and possibly beyond. The appearance of ha-MYXV in a central location in northwest Europe with a radial spread, far away from its origin at the Iberian Peninsula, is most likely the result of pathogen introduction via anthropogenic transport of contaminated fomites, vectors, or infected live or dead leporids. Our results indicated that ha-MYXV was already present in the outbreak area in 2023, and time-aware phylogenetic analyses suggest that introduction may date back as far as September 2020. Despite variation, municipalities with diseased hares showed on average a stronger decline in hare counts than those in which no ha-MYXV was reported. Those findings suggest that, at least in the short term, ha-MYXV affects the hare population in this region, and the disease is spreading.

Acknowledgments

We thank the Hunters Federation of North Rhine-Westphalia and the Game Management Units in Gelderland for collecting count data. We thank the involved hunting and nature protection authorities as well as hunters, game managers, and the public for submitting carcasses, reports, and photographs and for giving access to the hunting districts. We thank the pathologists and the technical assistance at the state laboratories and the pathology institutions for technical assistance.

About the Author

Dr. Fischer is a veterinarian with a board certification as Diplomate of the European College of Zoological Medicine and EVBS Veterinary Specialist in Wildlife Population Health and head of the Research Center for Hunting Science and Wildlife Management, State Agency for Consumer Protection and Nutrition North Rhine-Westphalia, Germany. Her research focuses on diseases and threats in wildlife, including emerging and infectious diseases.

References

1. Saari SA, Rudbäck E, Niskanen M, Syrjälä P, Nylund M, Anttila M. Contagious mucocutaneous dermatitis of the mountain hare (*Lepus timidus*): pathology and cause. J Wildl Dis. 2005;41:775–82. https://doi.org/10.7589/0090-3558-41.4.775
2. Barlow A, Lawrence K, Everest D, Dastjerdi A, Finnegan C, Steinbach F. Confirmation of myxomatosis in a European brown hare in Great Britain. Vet Rec. 2014;175:75–6. https://doi.org/10.1136/vr.g4621
3. Fenner F, Marshall ID. Occurrence of attenuated strains of myxoma virus in Europe. Nature. 1955;176:782–3. https://doi.org/10.1038/176782a0
4. Fenner F, Marshall ID. Passive immunity in myxomatosis of the European rabbit (*Oryctolagus cuniculus*): the protection conferred on kittens born by immune does. J Hyg (Lond). 1954;52:321–36. https://doi.org/10.1017/S0022172400027534
5. García-Bocanegra I, Camacho-Sillero L, Risalde MA, Dalton KP, Caballero-Gómez J, Agüero M, et al. First outbreak of myxomatosis in Iberian hares (*Lepus granatensis*). Transbound Emerg Dis. 2019;66:2204–8. https://doi.org/10.1111/tbed.13289
6. Carvalho CL, Abade dos Santos FA, Monteiro M, Carvalho P, Mendonça P, Duarte MD. First cases of myxomatosis in Iberian hares (*Lepus granatensis*) in Portugal. Vet Rec Case Rep. 2020;8:e001044. https://doi.org/10.1136/vetreccr- 2019-001044
7. Abade dos Santos FA, Carvalho CL, Parra F, Dalton KP, Peleteiro MC, Duarte MD. A quadruplex qPCR for detection and differentiation of classic and natural recombinant myxoma virus strains of leporids. International Journal of Molecular Sciences. 2021;22:12052.
8. García-Bocanegra I, Camacho-Sillero L, Caballero-Gómez J, Agüero M, Gómez-Guillamón F, Manuel Ruiz-Casas J, et al. Monitoring of emerging myxoma virus epidemics in Iberian hares (*Lepus granatensis*) in Spain, 2018–2020. Transbound Emerg Dis. 2021;68:1275–82. https://doi.org/10.1111/tbed.13781
9. Abade dos Santos FA, Carvalho CL, Pinto A, Rai R, Monteiro M, Carvalho P, et al. Detection of recombinant hare myxoma virus in wild rabbits (*Oryctolagus cuniculus algirus*). Viruses. 2020;12:1127. https://doi.org/10.3390/v12101127
10. Águeda-Pinto A, Lemos de Matos A, Abrantes M, García-Bocanegra I, Camacho-Sillero L, Caballero-Gómez J, et al. Monitoring of emerging myxoma virus epidemics in Iberian hares (*Lepus granatensis*) in Spain, 2018–2020. Transbound Emerg Dis. 2021;68:1275–82.

Address for correspondence: Luisa Fischer, Research Center for Hunting Science and Wildlife Management, State Agency for Consumer Protection and Nutrition North Rhine-Westphalia, Puetzchens Chaussee 228, D-53229 Bonn, Germany; email: luisa.fischer@lave.nrw.de

Progression from *Candida auris* Colonization Screening to Clinical Case Status, United States, 2016–2023

Anna D. Baker, Jeremy A.W. Gold, Kaitlin Forsberg, Sophie Jones, Meghan M. Lyman

During 2016–2023, among 21,195 US patients who tested positive for *Candida auris* colonization, 6.9% were subsequently found to have a positive clinical specimen (2.8% from blood). Strategies are needed to prevent invasive *C. auris* infections among patients with colonization (e.g., through patient decolonization).

Candida auris, an emerging, frequently antifungal-resistant yeast, can colonize patients asymptomatically and persist on skin for months to years without causing infection (*1*–*3*). Patients colonized with *C. auris* can progress to having invasive infections, which are associated with crude mortality rates of 30%–72% (*4*,*5*). Because *C. auris* spreads easily in healthcare settings, the Centers for Disease Control and Prevention (CDC) recommends colonization screening for patients with high-risk healthcare exposures (e.g., recent stay in a long-term acute-care hospital [LTACH] or ventilator-capable skilled nursing facility [SNF]) and those with an epidemiologic link to a patient with *C. auris* (*2*,*6*) (https://www.cdc.gov/candida-auris/hcp/screening-hcp).

Data characterizing the progression from *C. auris* colonization to invasive disease are limited but might help guide public health surveillance, prevention, and treatment efforts. We analyzed US national case-based surveillance data to characterize patients with positive *C. auris* screening results who were subsequently found to have a positive clinical specimen.

The Study

C. auris is a nationally notifiable condition, but reporting mandates vary across states and jurisdictions. State and jurisdictional health departments report *C. auris* screening and clinical cases to CDC. Screening cases were defined as a positive *C. auris* laboratory result from a swab sample (usually composite axilla/groin) collected to test for colonization. Clinical cases were defined as a positive *C. auris* laboratory result from a clinical specimen collected to determine the cause and treatment for infection in a patient. Clinical cases might involve body sites typically associated with invasive infection (e.g., blood) or those that potentially reflect colonization (e.g., urine) (https://ndc.services.cdc.gov/case-definitions/candida-auris-2023). Screening and clinical case data included information on patient age and sex, as well as date and facility type of specimen collection. Facility location was grouped by Antimicrobial Resistance Laboratory Network region (n = 7) (https://www.cdc.gov/antimicrobial-resistance-laboratory-networks/php/about/domestic.html). We used a patient-level identifier to link each patient's screening case with the corresponsing clinical case, if one occurred. We considered patients with a clinical case ≥1 calendar day after a screening case to have a screening-to-clinical (StC) event.

The analysis includes each patient's screening case on the basis of their first positive screening result (StC and non-StC events) and clinical case on the basis of first positive clinical specimen (StC events only) during 2016–2023. We calculated total and annual percentages of patients with screening cases who had StC events and described available data on non-StC events and StC events, stratifying by StC event status and examining StC events by body site involved. We analyzed categorical data using χ^2 tests and continuous data using Kruskal-Wallis rank-sum tests ($\alpha = 0.05$).

During 2016–2023, a total of 36 of 40 reporting jurisdictions reported 21,195 patients who had a positive screening result; of those, 1,458 (6.9%) patients across 22 jurisdictions had an StC event (2.8% blood, 4.1% nonblood) (Table 1). The number of patients

Author affiliation: Centers for Disease Control and Prevention, Atlanta, Georgia, USA

DOI: https://doi.org/10.3201/eid3108.250315

Table 1. Characteristics of patients with *Candida auris* screening cases with and without progression to clinical case status, United States, 2016–2023*

Characteristic	All, N = 21,195	With clinical case, n = 1,458	Without clinical case, n = 19,737	p value†
Median age at collection of screening case specimen, y (IQR), n = 17,928	68 (58–76)	67 (59–76)	68 (58–77)	0.650
Age group at collection of screening case specimen, y, n = 17,928				0.113
<45	1,738	118 (6.8)	1,620 (93.2)	
45–54	1,778	105 (5.9)	1,673 (94.1)	
55–64	3,725	279 (7.5)	3,446 (92.5)	
65–74	5,239	368 (7.0)	4,871 (93.0)	
75–84	3,808	274 (7.2)	3,534 (92.8)	
≥85	1,640	94 (5.7)	1,546 (94.3)	
Sex, n = 16,446				0.478
M	9,448	668 (7.1)	8,780 (92.9)	
F	6,998	515 (7.4)	6,483 (92.6)	
Antimicrobial Resistance Laboratory Network region of the facility of collection for screening case specimen‡				<0.001
West	6,617	898 (13.6)	5,719 (86.4)	
Midwest	4,264	96 (2.3)	4,168 (97.7)	
Southeast	4,235	56 (1.3)	4,179 (98.7)	
Northeast	3,570	302 (8.5)	3,268 (91.5)	
Mid-Atlantic	1,484	64 (4.3)	1,420 (95.7)	
Mountain	977	42 (4.3)	935 (95.7)	
Central	48	0	48 (100.0)	
Facility type of screening case specimen collection, n = 17,357				<0.001
Long-term acute care hospital	8,716	907 (10.4)	7,809 (89.6)	
Acute care hospital	5,033	299 (5.9)	4,734 (94.1)	
Ventilator-equipped skilled nursing facility	2,912	150 (5.2)	2,762 (94.8)	
Skilled nursing facility	490	13 (2.7)	477 (97.3)	
Other¶	206	4 (1.9)	202 (98.1)	

*Values are no. (%) except as indicated.
†p values were calculated using χ^2 tests to compare characteristics of patients with a *C. auris* screening case who had (vs. did not have) progression to a *C. auris* clinical case.
‡From https://www.cdc.gov/antimicrobial-resistance-laboratory-networks/php/about/domestic.html. Data from 2023 were unavailable from 1 state in the Central region.
¶Includes those listed as other (n = 193), inpatient rehabilitation (n = 12), and outpatient (n = 1).

with screening cases increased each year, and the percentage of those with an StC event increased from 0.0% (0/13) in 2016 to 9.9% (129/1,299) in 2020, then decreased to 4.9% (365/7,493) in 2023 (Figure 1).

Among patients with screening cases (n = 21,195), the median age was 68 (interquartile range [IQR] 58–76) years; of those with known sex (n = 16,446), 9,448 (57.4%) were men and 6,998 (42.6%) were women (Table 1). The most common regions of screening case specimen collection were the West (31.2%, n = 6,617), Midwest (20.1%, n = 4,264), and Southeast (20.0%, n = 4,235) and the most common

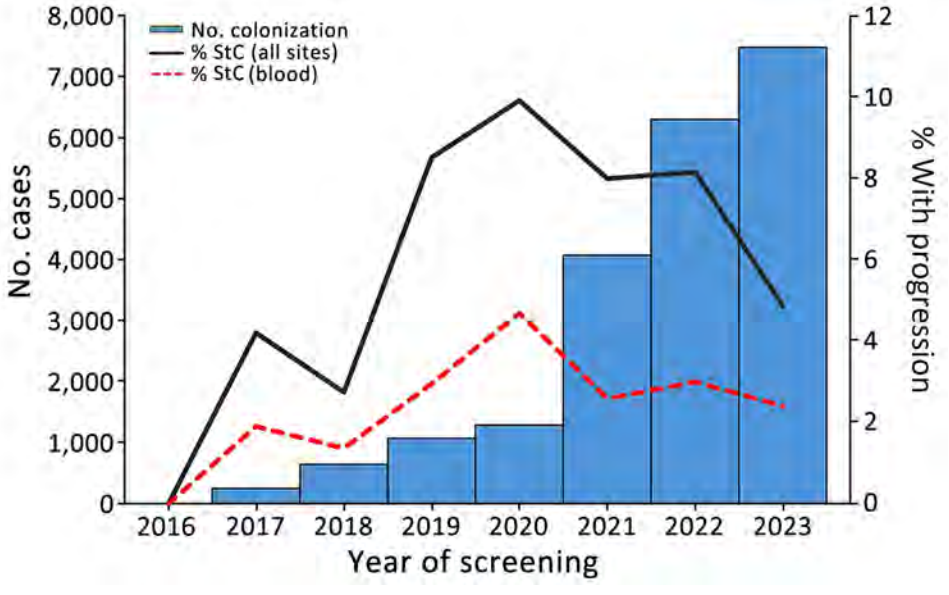

Figure 1. Number of patients with a *Candida auris* screening case and percentage who had progression to a clinical case, United States, 2016–2023. StC, screening-to-clinical.

Table 2. Patients with *Candida auris* screening cases with progression to clinical case status, by body site of clinical case detection, United States, 2016–2023*

Characteristic	All, N = 1,458	Blood, n = 584	Urine, n = 391	Respiratory, n = 233	Wound, n = 168	Other, n = 82†	p value‡
Median age at collection of screening case specimen, y (IQR), n = 1,238	67 (59–76)	68 (60–76)	68 (58–77)	68 (60–77)	67 (61–75)	64 (50–71)	0.023
Age group at collection of screening case specimen, y, n = 1,238							0.027
<45	118	42 (35.6)	40 (33.9)	8 (6.8)	15 (12.7)	13 (11.0)	
45–54	105	35 (33.3)	27 (25.7)	21 (20.0)	11 (10.5)	11 (10.5)	
55–64	279	106 (38.0)	69 (24.7)	55 (19.7)	38 (13.6)	11 (3.9)	
65–74	368	134 (36.4)	97 (26.4)	68 (18.5)	48 (13.0)	21 (5.7)	
75–84	274	106 (38.7)	83 (30.3)	43 (15.7)	31 (11.3)	11 (4.0)	
≥85	94	33 (35.1)	26 (27.7)	22 (23.4)	12 (12.8)	1 (1.1)	
Sex, n = 1,183							<0.001
M	671	215 (32.0)	216 (32.2)	124 (18.5)	76 (11.3)	40 (6.0)	
F	512	218 (42.6)	110 (21.5)	84 (16.4)	73 (14.3)	27 (5.3)	
Antimicrobial Resistance Laboratory Network region of the facility of specimen collection for clinical case§							<0.001
West	898	306 (34.1)	252 (28.1)	173 (19.3)	124 (13.8)	43 (4.8)	
Midwest	96	24 (25.0)	36 (37.5)	22 (22.9)	8 (8.3)	6 (6.3)	
Southeast	56	33 (58.9)	10 (17.9)	7 (12.5)	3 (5.4)	3 (5.4)	
Northeast	302	177 (58.6)	68 (22.5)	25 (8.3)	20 (6.6)	12 (4.0)	
Mid-Atlantic	64	37 (57.8)	11 (17.2)	3 (4.7)	4 (6.3)	9 (14.1)	
Mountain	42	7 (16.7)	14 (33.3)	3 (7.1)	9 (21.4)	9 (21.4)	
Central¶	0	0 (NA)	0 (NA)	0 (NA)	0 (NA)	0 (NA)	
No. days from collection date of first positive screening to first clinical case specimen#							0.001
Median (IQR)	46 (19–108)	58 (22–130)	44 (20–120)	33 (17–74)	44 (17–91)	28 (14–77)	
Minimum–maximum	1–1,597	1–1,309	1–1,597	1–1,240	1–666	1–745	

*Values are no. (%) except as indicated. IQR, interquartile range; NA, not applicable.
†Other specimen type included device (n = 14), fluid/drainage (n = 5), intraabdominal (n = 2), other (n = 60), and unknown (n = 1).
‡p values were calculated using χ^2 tests (categorical variables) or Kruskal-Wallis rank-sum test (continuous variables) to compare features of interest by body site.
§https://www.cdc.gov/antimicrobial-resistance-laboratory-networks/php/about/domestic.html. Data from 2023 were unavailable from 1 state in the Central region.
¶Row excluded from p value calculations because no screening-to-clinical cases were reported in the Central region.
#Data missing for 1 patient with a clinical case involving a wound.

facility types among those with known facility type (n = 17,357) were LTACH (50.2%, n = 8,716), acute care hospital (ACH) (29.0%, n = 5,033), and ventilator-capable SNF (16.8%, n = 2,912). StC event frequency was similar by age (p = 0.650) and sex (p = 0.478) and varied by region (p<0.001), and facility type (p<0.001). StC event frequency was similar between women (7.4%) and men (7.1%) and was greatest among patients with screening specimens collected in the West (13.6%), Northeast (8.5%), Mid-Atlantic (4.3%), or Mountain (4.3%) regions. StC events were most frequent for patients with screening specimens collected in LTACHs (10.4%), then ACHs (5.9%), ventilator-capable SNFs (5.2%), non–ventilator-equipped SNFs (2.7%), and other facility types (1.9%).

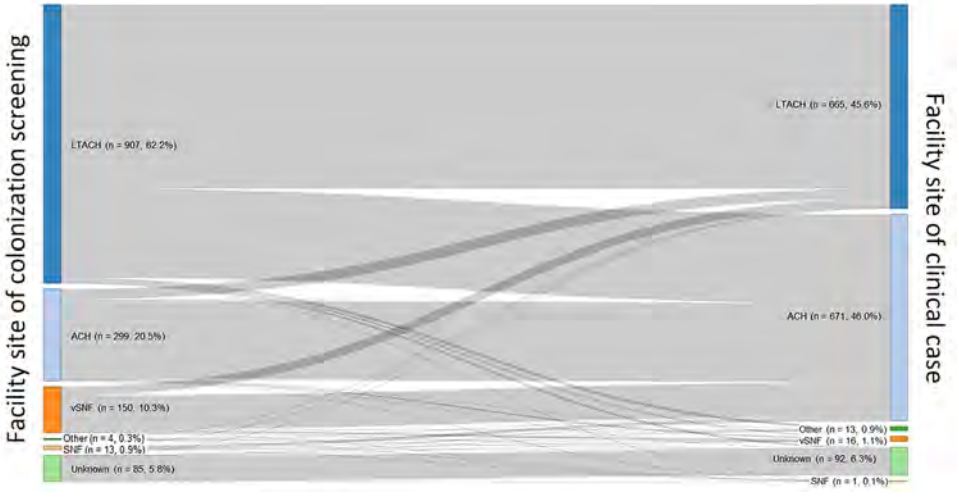

Figure 2. Facility type of specimen collection for patients with *Candida auris* screening cases in whom clinical *C. auris* cases occurred, United States, 2016–2023. Sankey diagram made in RStudio (https://www.rstudio.com). ACH, acute care hospital; LTACH, long-term acute-care hospital; SNF, skilled nursing facility (non–ventilator-equipped); vSNF, ventilator-equipped skilled nursing facility.

Among StC events (n = 1,458), blood (40.1%, n = 584) and urine (26.8%, n = 391) were most common (Table 2); the distribution of affected body sites was generally similar across years (Appendix Figure, https://wwwnc.cdc.gov/EID/article/31/8/25-0315-App1.pdf). Body sites of clinical cases varied by age (p = 0.023), sex (p<0.001), region (p<0.001), and time from screening case to clinical case specimen collection (p = 0.001) (Table 2). Among women, blood specimens were approximately twice as common as urine (42.6% vs. 21.5%), whereas among men, the percentage was similar (32.0% vs. 32.2%). Blood specimens constituted most StC events in the Southeast (58.9%), Northeast (58.6%), and Mid-Atlantic (57.8%) regions but less than half of specimens in other regions. The median number of days from initial screening case specimen to clinical specimen was longest for blood (58, IQR 22–130, range 1–1,309 days) and shortest for respiratory (33, IQR 17–74, range 1–1,240 days) and other (28, IQR 14–77, range 1–745 days) specimen types. The most common facility types of initial screening case detection were LTACHs (62.2%) and ACHs (20.5%) (Figure 2). Regardless of the facility type where the screening case was detected, most StC events were detected in an LTACH (45.6%) or ACH (46.0%).

Conclusions

This analysis of national *C. auris* case data revealed that, among 21,195 patients who tested positive for *C. auris* on a colonization screening swab during 2016–2023, a clinical case subsequently occurred in 6.9% (2.8% involving blood); more than half of clinical cases involving blood were detected 2 months after screening case detection. This finding is comparable with a smaller New York state study in which a *C. auris* bloodstream infection occurred in 7/187 (3.7%) colonized patients (median time from screening case testing to infection 86 days) (*7*).

The percentage of patients with an StC event peaked in 2020 then declined, potentially because of improved infection prevention and control efforts or increased screening after COVID-19–related resource strains resolved. The volume of screening cases and frequency of clinical cases was greatest in the West, but the region had a relatively low percentage of clinical cases involving blood; that finding might reflect regional differences in case reporting and in testing practices for *C. auris* in noninvasive body sites (*8*). Most StC events were identified in LTACHs and ACHs, underscoring the continued need for focused screening, enhanced surveillance, and efforts to improve infection prevention and control implementation in these settings.

For several reasons, we suspect that our study underestimates the actual percentage of patients with *C. auris* colonization who progress to having a clinical case. StC events could have been missed because of missed screening opportunities, the insensitivity of culture (*9*), treating clinical laboratories that might not routinely distinguish *C. auris* from other *Candida* species for nonsterile specimen types (*10*), and the fact that US *C. auris* data from 2024 are not finalized, meaning some patients might not have had sufficient lead time for clinical cases to occur. In addition, for clinical cases, we lacked data on previous negative screening results, the differentiation between infection and colonization, and underlying patient conditions.

Overall, our study highlights the potential for *C. auris* infections, particularly candidemia, among patients colonized with *C. auris*. Rigorous infection prevention and control remain necessary to prevent the spread of *C. auris* and subsequent clinical infections. Further studies could investigate risk factors and strategies to prevent invasive *C. auris* infections among patients with colonization (e.g., through patient decolonization).

Acknowledgments

We thank Malavika Rajeev for providing guidance on data management and informatics and the CDC Antimicrobial Resistance Laboratory Network in providing testing for *C. auris* detection and drug susceptibility.

This activity was reviewed by the CDC Institutional Review Board, deemed not research, and was conducted consistent with applicable federal law and CDC policy (see e.g., 45 C.F.R. part 46.102(l)(2), 21 C.F.R. part 56; 42 U.S.C. §241(d); 5 U.S.C. §552a; 44 U.S.C. §3501 et seq.).

About the Author

Ms. Baker is an epidemiologist with the Mycotic Diseases Branch, Division of Foodborne, Waterborne, and Environmental Diseases, National Center for Emerging and Zoonotic Infectious Diseases, Centers for Disease Control and Prevention, Atlanta, Georgia, USA. Her research interests include the epidemiology and prevention of fungal infections.

References

1. Lyman M, Forsberg K, Sexton DJ, Chow NA, Lockhart SR, Jackson BR, et al. Worsening spread of *Candida auris* in the United States, 2019 to 2021. Ann Intern Med. 2023;176:489–95. https://doi.org/10.7326/M22-3469
2. Pacilli M, Kerins JL, Clegg WJ, Walblay KA, Adil H, Kemble SK, et al. Regional emergence of *Candida auris* in Chicago and lessons learned from intensive follow-up at 1 ventilator-

capable skilled nursing facility. Clin Infect Dis. 2020;71:e718–25. https://doi.org/10.1093/cid/ciaa435
3. Arenas SP, Persad PJ, Patel S, Parekh DJ, Ferreira TBD, Farinas M, et al. Persistent colonization of *Candida auris* among inpatients rescreened as part of a weekly surveillance program. Infect Control Hosp Epidemiol. 2024;45:762–5. https://doi.org/10.1017/ice.2023.251
4. Lockhart SR, Etienne KA, Vallabhaneni S, Farooqi J, Chowdhary A, Govender NP, et al. Simultaneous emergence of multidrug-resistant *Candida auris* on 3 continents confirmed by whole-genome sequencing and epidemiological analyses. Clin Infect Dis. 2017;64:134–40. https://doi.org/10.1093/cid/ciw691
5. Chakrabarti A, Sood P, Rudramurthy SM, Chen S, Kaur H, Capoor M, et al. Incidence, characteristics and outcome of ICU-acquired candidemia in India. Intensive Care Med. 2015;41:285–95. https://doi.org/10.1007/s00134-014-3603-2
6. McKinnell JA, Singh RD, Miller LG, Kleinman K, Gussin G, He J, et al. The SHIELD Orange County Project: multidrug-resistant organism prevalence in 21 nursing homes and long-term acute care facilities in southern California. Clin Infect Dis. 2019;69:1566–73. https://doi.org/10.1093/cid/ciz119
7. Southwick K, Adams EH, Greenko J, Ostrowsky B, Fernandez R, Patel R, et al. New York state 2016–2018: progression from *Candida auris* colonization to bloodstream infection. Open Forum Infect Dis. 2018;5(suppl_1):S594–5. https://doi.org/10.1093/ofid/ofy210.1695
8. Lockhart SR, Jackson BR, Vallabhaneni S, Ostrosky-Zeichner L, Pappas PG, Chiller T. Thinking beyond the common *Candida* species: need for species-level identification of *Candida* due to the emergence of multidrug-resistant *Candida auris*. J Clin Microbiol. 2017;55:3324–7. https://doi.org/10.1128/JCM.01355-17
9. Clancy CJ, Nguyen MH. Finding the "missing 50%" of invasive candidiasis: how nonculture diagnostics will improve understanding of disease spectrum and transform patient care. Clin Infect Dis. 2013;56:1284–92. https://doi.org/10.1093/cid/cit006
10. Keighley C, Garnham K, Harch SAJ, Robertson M, Chaw K, Teng JC, et al. *Candida auris*: diagnostic challenges and emerging opportunities for the clinical microbiology laboratory. Curr Fungal Infect Rep. 2021;15:116–26. https://doi.org/10.1007/s12281-021-00420-y

Address for correspondence: Anna Baker, Centers for Disease Control and Prevention, 1600 Clifton Rd NE, Mailstop 17-02, Atlanta, GA 30329-4018, USA; email: ucd4@cdc.gov

etymologia revisited

Petri Dish
[pe'tre 'dish]

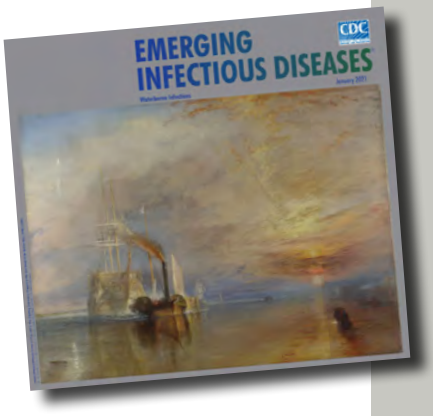

The Petri dish is named after the German inventor and bacteriologist Julius Richard Petri (1852–1921). In 1887, as an assistant to fellow German physician and pioneering microbiologist Robert Koch (1843–1910), Petri published a paper titled "A minor modification of the plating technique of Koch." This seemingly modest improvement (a slightly larger glass lid), Petri explained, reduced contamination from airborne germs in comparison with Koch's bell jar.

References
1 Central Sheet for Bacteriology and Parasite Science [in German]. Biodiversity Heritage Library. Volume 1, 1887 [cited 2020 Aug 25]. https://www.biodiversitylibrary.org/item/210666#page/313/mode/1up
2. Petri JR. A minor modification of the plating technique of Koch [in German]. Cent für Bacteriol und Parasitenkd. 1887;1:279–80.
3. Shama G. The "Petri" dish: a case of simultaneous invention in bacteriology. Endeavour. 2019;43:11–6. DOIExternal
4. The big story: the Petri dish. The Biomedical Scientist. Institute of Biomedical Science [cited 2020 Aug 25]. https://thebiomedicalscientist.net/science/big-story-petri-dish

Originally published in January 2021

https://wwwnc.cdc.gov/eid/article/27/1/et-2701_article

Genetic Characterization of Highly Pathogenic Avian Influenza A(H5N1) Clade 2.3.4.4b, Antarctica, 2024

Victor Neira, Naomi Ariyama, Pablo N. Castillo-Torres, Barbara Brito, Gabriela Muñoz, Karla B. Díaz Morales, Leonardo I. Almonacid, Benjamín Bennett-Laso, Barbara Berazay, Miloš Barták, Rafael Medina, Marcelo González-Aravena, Catalina Pardo-Roa

In 2024, we sequenced highly pathogenic avian influenza virus A(H5N1) clade 2.3.4.4b genomes isolated from 5 brown skuas from James Ross Island, Antarctica. Phylogenetic analysis suggested the virus reached Antarctica through South America. Continued genetic surveillance will be critical to elucidate H5N1 virus transmission dynamics within Antarctica and surrounding areas.

Highly pathogenic avian influenza (HPAI) A(H5N1) has been causing a panzootic since its resurgence in 2021 (*1*). H5N1 clade 2.3.4.4b virus has spread among domestic and wild animals; multiple spillovers into distinct mammal species have occurred (*2*). This virus reached South America in late 2022, causing numerous mortality events in wild birds and mammals along the coasts of Peru, Chile, Argentina, Uruguay, and Brazil (*2*,*3*). By late 2023, the virus had extended its range to the South Atlantic and Antarctic Oceans; virus was detected on the Malvinas/Falkland Islands and Bird Island, South Georgia (*4*,*5*). Bird Island is a subantarctic island located near the Antarctic Peninsula, raising concerns about potential virus spread to previously unaffected ecosystems.

In early 2024, H5N1 virus reached Antarctica; 11 cases were reported during the 2023–24 summer season (*6*). The virus primarily affected skuas seabirds but has also been detected in Adélie penguins, Antarctic fur seals, snowy sheathbills, kelp gulls, and southern elephant seals, according to the Scientific Committee on Antarctic Research (SCAR, https://scar.org/library-data/avian-flu#cases). We genetically characterized HPAI H5N1 virus samples collected on March 3, 2024, from brown skuas (*Stercorarius antarcticus*) on James Ross Island, located near the eastern side of the Antarctic Peninsula (latitude –63.7989S, longitude –57.8105W). The Faculty of Veterinary Sciences Ethics Committee, Universidad de Chile, approved the study (code no. 13–2022), which we registered with the Institutional Animal Care and Use Committee (code no. 22603-VET-UCH).

The Study

We collected 6 pooled swab samples from dead brown skuas during a mass mortality event and confirmed the presence of H5N1 clade 2.3.4.4 virus in 5 birds by using a US National Veterinary Services Laboratories protocol (*6*). Those were the only positive samples from a Chilean Antarctic Institute/University of Chile surveillance program conducted during the Southern Hemisphere summer of 2023–24 (*6*). We performed full virus genome sequencing by using multisegment PCR and MinION nanopore sequencing (Oxford Nanopore Technologies, https://www.nanoporetech.com), as previously described (*7*). After obtaining consensus genomes, we checked sequences for quality and annotated them by using the Influenza Virus Sequence Annotation Tool (https://www.ncbi.nlm.nih.gov/genomes/FLU/annotation). We performed H5 clade classification by using the Subspecies Classification tool (Bacterial and Viral Bioinformatics Resource Center, https://www.

Author affiliations: Universidad de Chile, Santiago, Chile (V. Neira, N. Ariyama, G. Muñoz, B. Bennett-Laso, B. Berazay); Pontificia Universidad Católica de Chile, Santiago (P.N. Castillo-Torres, K.B. Díaz Morales, L.I. Almonacid, C. Pardo-Roa); University of Technology Sydney, Sydney, New South Wales, Australia (B. Brito); Masaryk University, Brno, Czech Republic (M. Barták); Emory University Center of Excellence for Influenza Research and Response, Atlanta, Georgia, USA (R. Medina); Instituto Antártico Chileno, Punta Arenas, Chile (M. González-Aravena)

DOI: https://doi.org/10.3201/eid3108.250186

bv-brc.org). We deposited sequences in GenBank (Appendix 1 Table, https://wwwnc.cdc.gov/EID/article/ 31/8/25-0186-App1.pdf).

We aligned sequences from the H5N1 samples with sequences from GISAID (https://www.gisaid.org) and GenBank by using MAFFT (*8*). We aligned 245 neuraminidase (NA), 259 hemagglutinin (HA), 229 polymerase basic 2, 256 nucleoprotein, 231 polymerase basic 1, 233 polymerase acidic, 254 nonstructural (NS), and 249 matrix gene sequences. We inferred time-divergent phylogenetic trees by using BEAST version 1.10.4 (*9*) and the Hasegawa-Kishino-Yano plus gamma distribution 4 substitution model, an uncorrelated relaxed clock with a lognormal distribution, and an exponential growth tree prior. We ran a Markov Chain Monte Carlo chain for 500 million generations, logging parameters every 50,000 iterations. We assessed the convergence of parameters by using Tracer version 1.7.2 (http://beast.community/tracer). The final trees had an effective sample size (ESS) of >200, except the trees for NS and polymerase acidic segments, which each had an ESS of <200; no trees had an ESS of <100. We visualized the trees and annotations by using iTol (*10*).

We obtained 6 influenza A virus genomes, all classified as HPAI H5N1 clade 2.3.4.4b, displaying minimal variation; we observed >99.9% identity in the HA genes and consistent results across other genomic segments. The closest HA sequence identified via BLAST (https://blast.ncbi.nlm.nih.gov) was A/Kelp Gull/South Georgia and the South Sandwich Islands/32/2023 (H5N1) virus (GenBank accession no. PQ113961.1), along with related sequences from the same outbreak. Similar findings were observed for all other segments.

Phylogenetic analysis of HA grouped the 6 sequences into a monophyletic cluster (Appendix 1 Figure 1), which was part of a larger clade of sequences previously reported from South Georgia and the South Sandwich Islands and derived directly from South America (*5*). Another subcluster contained sequences from King George Island (Antarctica), detected on December 25, 2024, suggesting a different introduction; however, those viruses were still related to the viruses from South America and subantarctic regions. We observed similar patterns across all other H5N1 segments (Appendix 1 Figures 2–8), indicating the virus reached Antarctica through local migrations and progressively spread across the region. The timeline suggests an initial introduction into southern South America, followed by spread across the South Atlantic Ocean to South Georgia and finally to the Antarctic Peninsula and the islands on its western and eastern coasts.

To identify key mutations, we analyzed all available H5N1 sequences from Antarctica and subantarctic regions, along with sequences from humans, dairy cows, seals, and chickens, by using FluSurver (http://flusurver.bii.a-star.edu.sg) and compared those against genome segments from the reference strain A/goose/Guangdong/1/96 (GenBank accession nos. AF144300–7). The polymerase basic 2 D701N mutation, associated with mammal adaptation, was detected in a virus from a subantarctic kelp gull, South Georgia A/Kelp_Gull/Harpon_Bay/133943/2023 (GISAID accession no. EPI_ISL_18592427). Mutations associated with mammal adaptations were absent in virus sequences obtained from skuas. However, we detected mutations associated with high-level resistance to amantadine (matrix, V27A) (*11*), antigenic drift (NA, I396M and N366I) (*12*), and virulence (NS, S48X and I205X) in the 5 sequences from skuas (*13*) (Appendix 2 Table, https://wwwnc.cdc.gov/EID/article/31/8/25-0186-App2.xlsx).

The first limitation of our study is that it was based solely on sequences from 1 outbreak detected in 2024. However, other sequences from this region are not available, suggesting potential limitations in sequencing capacity or research efforts. To address those limitations, increased collaboration among research teams will be crucial to expand sequencing and elucidate virus spread in the region. Cost-effective technologies, such as nanopore sequencing, which enables whole-genome influenza A virus sequencing by using affordable equipment, should be prioritized to strengthen sequencing capabilities and data availability. Second, we only have sequences from brown skuas, which have been proposed to be the same species as south polar skuas (*Stercorarius maccormicki*) (*14*). Obtaining more H5N1 sequences from other species is essential to determine potential transmission pathways or virus adaptations that might occur across different hosts. Furthermore, SCAR data indicate the virus remained in Antarctica during the 2024–25 season, making it critical to study its dynamics and persistence in the region.

Antarctica has a plausible risk for H5N1 virus reassortment events, particularly those involving gene segments from strains from South America. The region's animal populations, including penguins, skuas, gulls, and marine mammals, can act as mixing vessels for virus strains with distinct genetic backgrounds, promoting genetic exchange between viruses circulating in South America and other global regions. Reassortment in HA and NA genes, key determinants of virus fitness, host tropism, and transmissibility, is of particular concern. Those segments might undergo selective pressure from local host species, leading to adaptations that influence virus infectivity. For example, a H5N5 strain isolated from a chinstrap penguin, A/chinstrap_penguin/Antarctica/B04/2015 (H5N5) low pathogenicity

avian influenza virus (AIV), showed phylogenetic links to AIVs from both North America and South America, suggesting potential reassortment events (*15*). In addition, the overlap of migratory bird routes with penguin breeding colonies creates a dynamic interface for AIV spillover and interspecies transmission, further supporting a role for Antarctica as a critical site for AIV reassortment and emergence of novel virus strains.

Conclusions

We genetically characterized HPAI A(H5N1) clade 2.3.4.4b viruses found in skuas in Antarctica. That clade has also been detected farther south on the Antarctic Peninsula (according to SCAR); however, those sequences are not yet publicly available for analysis. Our findings indicate that continued genetic surveillance and collaborative efforts to expand sequencing across diverse species in Antarctica will be critical to elucidate transmission dynamics, host adaptation, and spread of HPAI H5N1 in Antarctica and surrounding areas.

Acknowledgments

We thank the staff of the Animal Virology Lab at the University of Chile and the staff of the Molecular Virology Lab at Pontificia Universidad Católica de Chile for their invaluable assistance with fieldwork and laboratory analyses; all the staff of the Chilean Antarctic Institute, Armada de Chile, and the Czech Antarctic Research Program for administrative and logistic support in the Antarctic territory; and the GISAID EpiFlu Database, laboratories, and sources of original data for influenza A virus sequences.

This work was funded by the Instituto Antártico Chileno (grant no. RT-08-21 to V.N.; no. RT-30-22 to C.P.R.) and partially funded by the National Institute of Allergy and Infectious Diseases, National Institutes of Health, Department of Health and Human Services, Centers of Excellence for Influenza Research and Response (contract no. 75N93021C00017, Option 18A to C.P.R., V.N., and R.A.M.).

About the Author

Dr. Neira is an associate professor at the University of Chile. His primary research interests focus on emerging viral zoonotic pathogens.

References

1. Webby RJ, Uyeki TM. An update on highly pathogenic avian influenza A(H5N1) virus, clade 2.3.4.4b. J Infect Dis. 2024;230:533–42. https://doi.org/10.1093/infdis/jiae379
2. Peacock TP, Moncla L, Dudas G, VanInsberghe D, Sukhova K, Lloyd-Smith JO, et al. The global H5N1 influenza panzootic in mammals. Nature. 2025;637:304–13. https://doi.org/10.1038/s41586-024-08054-z
3. Pardo-Roa C, Nelson MI, Ariyama N, Aguayo C, Almonacid LI, Gonzalez-Reiche AS, et al. Cross-species and mammal-to-mammal transmission of clade 2.3.4.4b highly pathogenic avian influenza A/H5N1 with PB2 adaptations. Nat Commun. 2025;16:2232. https://doi.org/10.1038/s41467-025-57338-z
4. Bennison A, Adlard S, Banyard AC, Blockley F, Blyth M, Browne E, et al. A case study of highly pathogenic avian influenza (HPAI) H5N1 at Bird Island, South Georgia: the first documented outbreak in the subantarctic region. Bird Study. 2024;71:380–91. https://doi.org/10.1080/00063657.2024.2396563
5. Banyard AC, Bennison A, Byrne AMP, Reid SM, Lynton-Jenkins JG, Mollett B, et al. Detection and spread of high pathogenicity avian influenza virus H5N1 in the Antarctic Region. Nat Commun. 2024;15:7433. https://doi.org/10.1038/s41467-024-51490-8
6. Bennett-Laso B, Berazay B, Muñoz G, Ariyama N, Enciso N, Braun C, et al. Confirmation of highly pathogenic avian influenza H5N1 in skuas, Antarctica 2024. Front Vet Sci. 2024;11:1423404. https://doi.org/10.3389/fvets.2024.1423404
7. Ariyama N, Pardo-Roa C, Muñoz G, Aguayo C, Ávila C, Mathieu C, et al. Highly pathogenic avian influenza A(H5N1) clade 2.3.4.4b virus in wild birds, Chile. Emerg Infect Dis. 2023;29:1842–5. https://doi.org/10.3201/eid2909.230067
8. Katoh K, Rozewicki J, Yamada KD. MAFFT online service: multiple sequence alignment, interactive sequence choice and visualization. Brief Bioinform. 2019;20:1160–6. https://doi.org/10.1093/bib/bbx108
9. Drummond AJ, Suchard MA, Xie D, Rambaut A. Bayesian phylogenetics with BEAUti and the BEAST 1.7. Mol Biol Evol. 2012;29:1969–73. https://doi.org/10.1093/molbev/mss075
10. Letunic I, Bork P. Interactive Tree Of Life (iTOL) v5: an online tool for phylogenetic tree display and annotation. Nucleic Acids Res. 2021;49:W293–6. https://doi.org/10.1093/nar/gkab301
11. Ilyushina NA, Govorkova EA, Webster RG. Detection of amantadine-resistant variants among avian influenza viruses isolated in North America and Asia. Virology. 2005;341:102–6. https://doi.org/10.1016/j.virol.2005.07.003
12. Webster RG, Air GM, Metzger DW, Colman PM, Varghese JN, Baker AT, et al. Antigenic structure and variation in an influenza virus N9 neuraminidase. J Virol. 1987;61:2910–6. https://doi.org/10.1128/jvi.61.9.2910-2916.1987
13. Imai H, Shinya K, Takano R, Kiso M, Muramoto Y, Sakabe S, et al. The HA and NS genes of human H5N1 influenza A virus contribute to high virulence in ferrets. PLoS Pathog. 2010;6:e1001106. https://doi.org/10.1371/journal.ppat.1001106
14. Mota ACM, Costa ES, Torres JPM, de Araujo J, Tormena LC, Pires de Mendonça Dantas G. Brown skua and south polar skua (Aves: Stercorariidae) a hybridization case or same species? Polar Biol. 2023;46:1191–201. https://doi.org/10.1007/s00300-023-03193-x
15. Barriga GP, Boric-Bargetto D, San Martin MC, Neira V, van Bakel H, Thompsom M, et al. Avian influenza virus H5 strain with North American and Eurasian lineage genes in an Antarctic penguin. Emerg Infect Dis. 2016;22:2221–3. https://doi.org/10.3201/eid2212.161076

Address for correspondence: Victor Neira, Departamento de Medicina Preventiva Animal, Facultad de Ciencias Veterinarias y Pecuarias, Universidad de Chile, 11735 Santa Rosa, La Pintana, Santiago, Chile; email: vneiraram@gmail.com

Neurologic Manifestations Associated with Parvovirus B19 Epidemic, Madrid, Spain, 2024

Cristina Veintimilla, Pilar Catalán, Agustín Estévez, Roberto Alonso, Maricela Valerio, Patricia Muñoz

A reemergence of parvovirus B19 infections in Spain in early 2024 prompted a 10-year review of the virus at a tertiary center. We identified 8 case-patients with neurologic manifestations who had parvovirus B19 in cerebrospinal fluid. Early recognition and management of parvovirus B19–associated neurologic conditions will help yield favorable outcomes.

Parvovirus B19 is a small, nonenveloped DNA virus that belongs to the Parvoviridae family. Parvovirus B19 infection generally manifests in paucisymptomatic or mild forms (*1*,*2*). However, severe symptoms, including chronic anemia, pancytopenia, and transient aplastic crisis, have been observed in at-risk populations, such as pregnant women, immunocompromised patients, and persons with chronic hematologic diseases. Neurologic manifestations of parvovirus B19 are rarely documented, underscoring the necessity for further epidemiologic and clinical investigation (*2*,*3*).

Community parvovirus B19 outbreaks typically peak in winter and spring and last an average of 3–6 months (*4*). Because parvovirus B19 is a nonnotifiable disease, testing practices vary between countries. Pregnant women and immunocompromised patients represent special cases for which testing is common (*1*).

Author affiliations: Clinical Microbiology and Infectious Diseases, Hospital General Universitario Gregorio Marañón, Madrid, Spain (C. Veintimilla, P. Catalán, A. Estévez, R. Alonso, M. Valerio, P. Muñoz); Instituto de Investigación Sanitaria Gregorio Marañón, Madrid (C. Veintimilla, P. Catalán, A. Estévez, R. Alonso, M. Valerio, P. Muñoz); School of Medicine, Universidad Complutense de Madrid, Madrid (P. Catalán, R. Alonso, M. Valerio, P. Muñoz); Centro de Investigación Biomédica en Red de Enfermedades Respiratorias, Madrid (P. Muñoz)

DOI: https://doi.org/10.3201/eid3108.250278

Since March 2024, many countries in Europe, including Spain, have reported increased detection of parvovirus B19 (*1*). We observed a similar trend at Hospital Gregorio Marañón in Madrid, Spain, and we saw a larger peak of cases in the 2024 outbreak compared with the previous 10 years (Figure 1). After the reemergence of parvovirus B19, we observed the virus in cerebrospinal fluid (CSF) in some patients from our center. We investigated the clinical features and microbiological findings from case-patients with neurologic symptoms treated at Hospital Gregorio Marañón during 2014–2024.

The Study

We conducted a retrospective data extraction on CSF samples submitted to our laboratory for diagnostic workup of meningoencephalitis during January 2014–October 2024. We excluded bacterial and other viral causes of meningoencephalitis by using bacterial culture and molecular tests. We performed a review of demographic and clinical features on patients with CSF samples positive for parvovirus B19. We included serologic data when available by using an Alinity i System chemiluminescence assay (Abbott Laboratories, https://www.abbott.com). We performed molecular testing on CSF by using Allplex Meningitis V1-V2 Panel Assays multiplex PCR (Seegene, http://www.seegene.com) (Appendix, https://wwwnc.cdc.gov/EID/article/31/8/25-0278-App1.pdf). To ensure accuracy, we performed a second parvovirus B19–specific PCR on case-patients with virus detected in the central nervous system during 2024. For plasma samples, we used a specific target PCR (RealStar Parvovirus B19 PCR Kit; Altona Diagnostics, https://www.altona-diagnostics.com) and performed diagnostic testing procedures using the manufacturer's specifications. Since 2019, our laboratory has been equipped with multiplex PCR for CSF; before 2019, we outsourced that test to the national reference laboratory in Madrid.

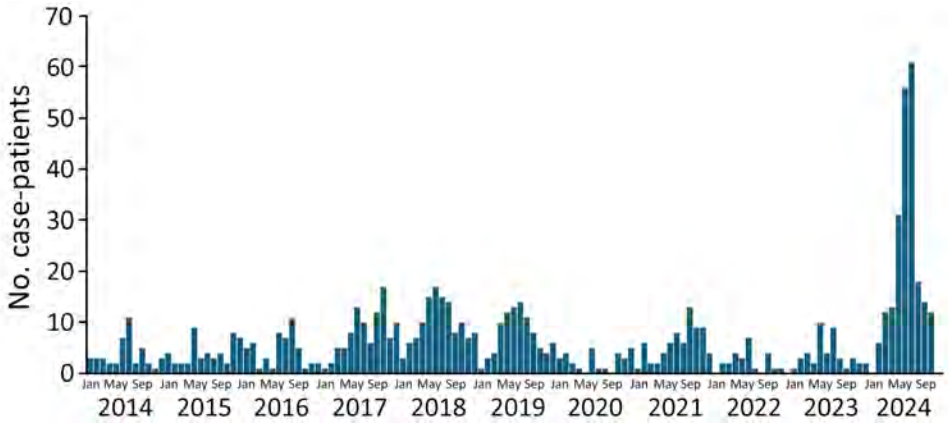

Figure 1. Parvovirus B19 case-patients confirmed by IgM during study of neurologic manifestations associated with parvovirus B19 outbreaks, Madrid, Spain, January 2014–October 2024. Numbers of case-patients are shown by month.

During the January–October 2024 outbreak, we found 6 of 223 CSF samples tested were positive for parvovirus B19. An archival review of meningoencephalitis cases tested during 2014–2023 revealed 2 of 801 additional hospital patients with parvovirus B19 in CSF. The overall CSF parvovirus B19 positivity rate for the entire 10-year period was 0.8% (8 patients): 6 patients had no underlying immunosuppression, but the other 2 had a history of hematologic disease (Table; Figure 2). No cutaneous manifestations were observed. Central nervous system manifestations exhibited variability, and mental status changes were the most common. CSF analysis showed protein levels greater than the upper reference limit (i.e., >30 mg/dL) in all samples. Three patients received a 5-day course of intravenous immunoglobulin (IVIg), but no clinical benefit was observed between treated and untreated patients. All patients recovered completely

Table. Clinical and epidemiologic characteristics of parvovirus B19 in CSF of case-patients with neurologic manifestations associated with parvovirus B19 epidemic, Madrid, Spain, 2014–2024*

Characteristic	Case-patient no.							
	1	2	3	4	5	6	7	8
Age, y/sex	17/M	77/M	10/F	42/F	65/M	46/M	78/M	<1/M†
Diagnosis date	2014 Jan	2022 Aug	2024 May	2024 May	2024 May	2024 May	2024 Jun	2024 Aug 2
Location	IP	IP	IP	IP	IP	OP	IP	IP
Relevant medical history	Acute lymphocytic leukemia	Hepatic steatosis	Migraine with aura	Schizophrenia, migraine	Prostate cancer	BPDCN	COPD, hypertension	Premature birth
Neurologic symptoms	Mental status change	Mental status change, encephalopathy and delirium	Stroke	Visual hallucinations	Memory loss episodes	Persistent headache	Encephalopathy, mental status change	Poorly responsive and central seizures
Other symptoms and signs	Fever	None	Fever	Fever and arthralgias	None	None	Fever	None
Initial IgM/IgG, serum	−/−	NA/−	−/−‡	+/+	−/NA	−/+	+/NA	NA/NA
Hematologic findings	Anemia (8.6 g/dL), TCP (10,000/μL)	Anemia (7.7 g/dL), TCP (42,000/μL)	UN	Lymphopenia (300 cells/μL)	Anemia (8.6 g/dL)	UN	TCP (69,000/μL), leukopenia (2,600 cells/μL)	Anemia (9.5 g/dL), TCP (67,000/μL)
CSF								
Leukocytes	0	0	0	0	70	0	0	NA; RBCs in CSF
Protein level, mg/dL	87	42	40	39	129	36	49	136
Viral DNA	Positive	Positive	Positive	Positive	Positive	Positive	Positive	Positive
Plasma viral DNA	Positive	Positive	Positive	Positive	Negative	Negative	Positive	Positive
Treatment	IVIg	IVIg	2 doses acyclovir	1 dose acyclovir	No	IVIg	10 d acyclovir	No

*BPDCN, blastic plasmacytoid dendritic cell neoplasm; COPD, chronic obstructive pulmonary disease; CSF, cerebrospinal fluid; IP, inpatient; IVIg, intravenous immunoglobulin; NA, not available; OP, outpatient; RBCs, red blood cells (erythrocytes); TCP, thrombocytopenia.
†Three-day-old infant.
‡Initial parvovirus B19 IgM and IgG were negative but seroconverted to 3 weeks later.
§Upper normal limit 30 mg/dL.

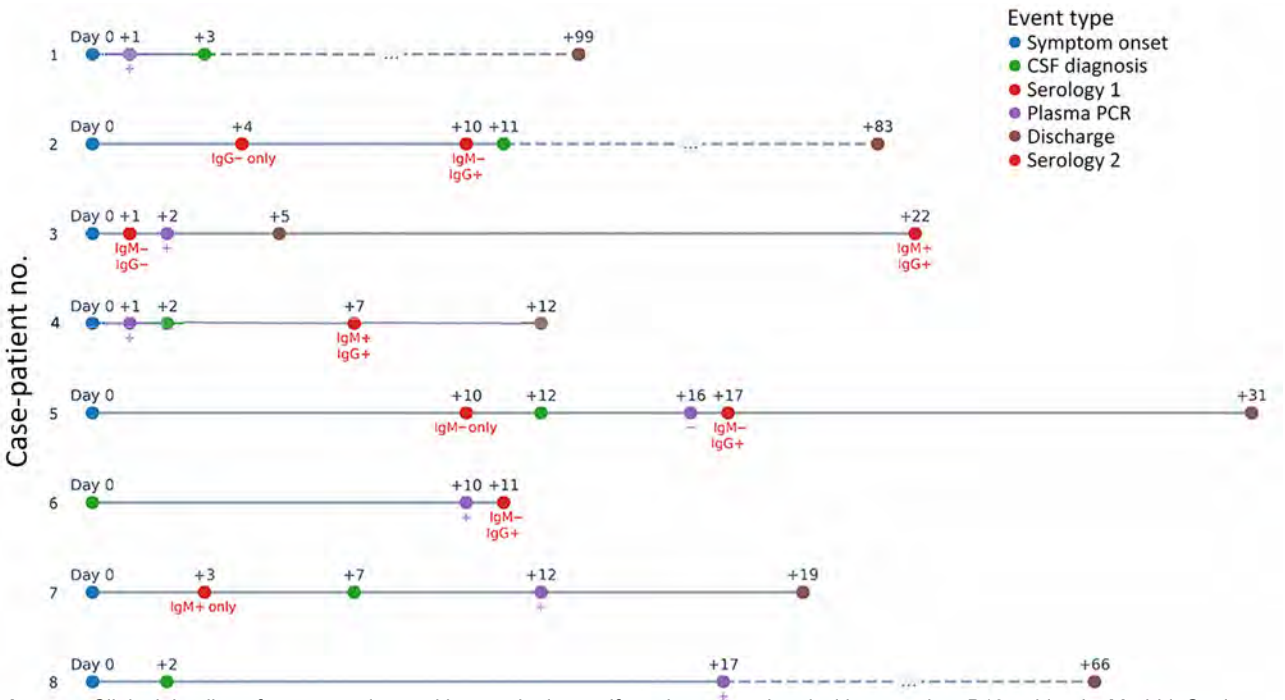

Figure 2. Clinical timelines for case-patients with neurologic manifestations associated with parvovirus B19 epidemic, Madrid, Spain, 2014–2024. CSF, cerebrospinal fluid.

without neurologic sequelae (range 3–21 days). Brain magnetic resonance imaging and computed tomography scans were unremarkable; the exception was case-patient 5, in whom a parenchymal lesion observed on the brain computed tomography scan was consistent with a high-grade lymphoproliferative disease. We performed cytology and confirmed lymphoproliferative disease (Appendix).

This study lends support to the numerous reports indicating a rise of parvovirus B19 infection during the 2024 outbreak compared with previous years (*1*,*5*,*6*). However, the precise causes of the increase in case numbers remain unclear. Although a multitude of factors are likely implicated, reduced host immune response attributable to restrictions during the COVID-19 pandemic period warrants consideration. Moreover, the absolute increase in case numbers could result in a proportional rise of symptomatic cases, and some cases might have more severe clinical manifestations.

The association between parvovirus B19 infection and neurologic symptoms is poorly documented. Cases of parvovirus B19 infection in persons exhibiting neurologic manifestations are not distinguishable from cases of encephalitis caused by other viral agents. The proposed physio-pathologic mechanisms contributing to the development of neurologic manifestations during parvovirus B19 infection are complex and variable. Those mechanisms include direct viral toxicity, dysregulated immune responses with the release of cytokines in the CSF, immune complex deposition on endothelial cells, and intracellular accumulation of the toxic nonstructural 1 protein (*5*,*7*).

Some studies reported findings that support parvovirus B19 infection as a cause of neurologic manifestations. A comprehensive review identified 129 cases related to parvovirus B19 infection and neurologic symptoms; one third of the patients had a previous history of altered immunity (*2*). Another study found the most common parvovirus B19–associated neurologic manifestation was encephalitic syndromes (39%) (*8*). Rash was observed more frequently among immunocompetent patients than in those with altered immunity; in some cases, rash preceded the onset of other clinical findings (*2*,*8*). Arthralgia or arthritis symptoms were infrequent. CSF alterations did not show a clear pattern; the median leukocyte count was 9 cells/mL, and a slight increase in protein levels (51%) was the most notable finding. Up to 42% of cases had hematologic disturbances (*2*,*8*).

In our case series, parvovirus B19 infection manifested in the absence of typical cutaneous manifestations. Among patients in our study, thrombocytopenia was the most prevalent hematologic disorder, and analysis of CSF samples revealed protein levels greater than the established threshold in all cases. In addition, most cases in our study were among adults without underlying immunocompromising diseases.

Parvovirus B19 is frequently underestimated in differential diagnosis schemes of meningoencephalitis. To accurately diagnose parvovirus B19 infection when neurologic involvement is observed, use of additional microbiological investigations is recommended, including serologic markers and virus DNA analysis in plasma and CSF.

In terms of management, steroids and IVIg have been identified as treatment options for clinical syndromes linked to parvovirus B19 infection. The choice to use IVIg is based on the assumption that it contains a substantial quantity of antibodies capable of neutralizing the virus. However, the precise mechanism of IVIg action remains uncertain (*2*,*8*). We did not observe any clinical differences between the patients who received IVIg and those who did not. The prognosis for neurologic manifestations associated with parvovirus B19 seems favorable; we saw a high rate of spontaneous recovery and an absence of sequelae. Nevertheless, long-term neurologic effects have been documented, including bradyphemia (slow speech), learning difficulties, and slurred speech, as well as more severe outcomes, such as mental and motor impairment and death (*2*,*8*). In this particular context, our findings are consistent with the available literature on parvovirus B19 infections with neurologic manifestations.

This study is limited by its retrospective design, single institution data collection, and small sample size of neurologic parvovirus B19 infections, which might bias the ability to draw definitive conclusions. Nevertheless, this study furnishes valuable information regarding viral determination in the CSF, thereby enabling the formulation of subsequent hypotheses and research initiatives.

Conclusions

Our findings underscore the importance of incorporating parvovirus B19 into differential diagnoses of encephalitis, given its capacity to affect both immunocompetent and immunocompromised persons. Research is needed to elucidate the underlying mechanisms of parvovirus B19 to develop targeted treatments. Early recognition and appropriate management of parvovirus B19–associated neurologic conditions have the potential to yield favorable outcomes.

Acknowledgments

We thank Lara Mesones Guerra and Sandra Rodrigo for contributing to the processing of samples for the B19V diagnostics.

C.V. and M.V. conceptualized the study. C.V., P.C., A.E., and R.A. provided data and performed data analyses. C.V. drafted the original manuscript. P.C., R.A., M.V., and P.M. supervised the data interpretation and revised the first draft. P.C., A.E., R.A., M.V., and P.M. contributed to critical reviewing and editing the manuscript. All authors have read and approved the final manuscript for publication.

About the Author

Dr. Veintimilla is a clinical microbiologist in the Department of Clinical Microbiology and Infectious Diseases at the Gregorio Marañón Hospital in Madrid, Spain. Her research interests include molecular diagnostics and infections in immunosuppressed hosts.

References

1. European Centre for Disease Prevention and Control. Risks posed by reported increased circulation of human parvovirus B19 in the EU/EEA–5 June 2024. Stockholm: The Centre; 2024.
2. Douvoyiannis M, Litman N, Goldman DL. Neurologic manifestations associated with parvovirus B19 infection. Clin Infect Dis. 2009;48:1713–23. https://doi.org/10.1086/599042
3. Eid AJ, Ardura MI; AST Infectious Diseases Community of Practice. Human parvovirus B19 in solid organ transplantation: guidelines from the American Society of Transplantation Infectious Diseases Community of Practice. Clin Transplant. 2019;33:e13535. https://doi.org/10.1111/ctr.13535
4. Cherry J, Demmler-Harrison GJ, Kaplan SL, Steinbach WJ, Hotez P. Feigin and Cherry's textbook of pediatric infectious diseases, 8th edition. New York: Elsevier; 2017.
5. Russcher A, van Boven M, Benincà E, Verweij EJTJ, Molenaar-de Backer MWA, Zaaijer HL, et al. Changing epidemiology of parvovirus B19 in the Netherlands since 1990, including its re-emergence after the COVID-19 pandemic. Sci Rep. 2024;14:9630. https://doi.org/10.1038/s41598-024-59582-7
6. Barah F, Vallely PJ, Cleator GM, Kerr JR. Neurological manifestations of human parvovirus B19 infection. Rev Med Virol. 2003;13:185–99. https://doi.org/10.1002/rmv.388
7. Nordholm AC, Trier Møller F, Fischer Ravn S, Sørensen LF, Moltke-Prehn A, Mollerup JE, et al. Epidemic of parvovirus B19 and disease severity in pregnant people, Denmark, January to March 2024. Euro Surveill. 2024;29:2400299. https://doi.org/10.2807/1560-7917.ES.2024.29.24.2400299
8. Barah F, Whiteside S, Batista S, Morris J. Neurological aspects of human parvovirus B19 infection: a systematic review. Rev Med Virol. 2014;24:154–68. https://doi.org/10.1002/rmv.1782

Address for correspondence: Cristina Veintimilla, Hospital General Universitario Gregorio Marañón, 46 C/Doctor Esquerdo, 28007 Madrid, Spain; email: cristina.veintimilla@gmail.com

Community-Scale Surveillance of SARS-CoV-2 and Influenza A Viruses in Wild Mammals, United States, 2022–2023

Grete Wilson-Henjum, J. Jeffrey Root, Alex Worgo, Jeffrey Chandler, Robin Dyer, Jeff Flores, Jesse Morris, Ian Plummer, John Paul Seman, Kyle Van Why, Caleb Wellman, H. Bryant White, John Wilt, Diego Diel, Jon Heale, David L. Bergman, Josh Hewitt, Derek Collins, Ryan S. Miller, Steven Rekant, Kim M. Pepin

Sampling of mammal communities across the United States during 2022–2023 detected evidence of SARS-CoV-2 antibodies in 3 new species and 2 previously described species and evidence of influenza A antibodies in 2 previously described species. Our analysis provides surveillance and sampling guidance for detection of rare exposure events.

Wildlife can transmit pathogens that threaten health of humans, domestic animals, and other wildlife (*1*). Wildlife disease surveillance can provide early warning of the changing epidemiology of rapidly evolving pathogens (*2*). In the United States, 2 rapidly evolving viruses with a broad host range have been detected in wildlife species: SARS-CoV-2 (*3*) and influenza A(H5N1) clade 2.3.4.4b (*4*). Coronaviruses and influenza A virus (IAV) both have a history of cross-species transmission and evolutionary events leading to strains that are highly virulent in multiple species and pandemic in humans (*5*,*6*).

Since January 2021, human-derived SARS-CoV-2 emerged and has been transmitting widely in wild cervids across North America (*7*) with evidence of spillback to humans (*8*). The virus has also emerged in domestic mink (*Neogale vison*) with transmission to sympatric free-roaming animals (*9*). Widespread distribution in animals and humans that are sympatric to wildlife species suggests risk for spillover and persistence in other wildlife. In addition, the host range of IAV has expanded to include marine mammals and seabirds (*10*) as well as cattle (*11*), which underscores the importance of understanding the changing host range of both SARS-CoV-2 and IAV in nature. We examined exposure to and co-infection of the 2 pathogens in wild mammal communities across different ecologic contexts.

The Study

We collected 1,172 samples from wildlife communities across the United States during September

Author affiliations: Utah State University S.J. and Jessie E. Quinney College of Natural Resources, Logan, Utah, USA (G. Wilson-Henjum, J. Hewitt); US Department of Agriculture Animal and Plant Health Inspection Service (APHIS) Wildlife Services, National Wildlife Research Center, Fort Collins, Colorado, USA (J.J. Root, A. Worgo, K.M. Pepin); US Department of Agriculture APHIS, Wildlife Disease Diagnostic Laboratory, Fort Collins (J. Chandler); US Department of Agriculture APHIS Wildlife Services, Augusta, Maine, USA (R. Dyer, J. Morris); US Department of Agriculture APHIS Wildlife Services, Sacramento, California, USA (J. Flores); US Department of Agriculture APHIS Wildlife Services, Portland, Oregon, USA (I. Plummer); US Department of Agriculture APHIS Wildlife Services, Sandusky, Ohio, USA (J.P. Seman, C. Wellman); Association of Fish and Wildlife Agencies, Phoenix, Arizona, USA (H.B. White); US Department of Agriculture APHIS Wildlife Services, Harrisburg, Pennsylvania, USA (K. Van Why, J. Wilt); Cornell University, Ithaca, New York, USA (D. Diel); US Department of Agriculture APHIS Wildlife Services, San Tan Valley, Arizona, USA (J. Heale); US Department of Agriculture APHIS Wildlife Services, Phoenix, Arizona, USA (D.L. Bergman); US Department of Agriculture APHIS Wildlife Services, National Wildlife Disease Program, Fort Collins (D. Collins); Centers for Epidemiology and Animal Health, Fort Collins (R.S. Miller); US Department of Agriculture Veterinary Services, Riverdale, Maryland, USA (S. Rekant)

DOI: https://doi.org/10.3201/eid3108.241671

Figure 1. Locations of intensive sampling for SARS-CoV-2 samples collected across 28 species in 8 states during community-scale surveillance of SARS-CoV-2 and influenza A viruses in wild mammals, United States, October 2022–June 2023. The number of samples collected varied across each state and by species within each state.

2022–November 2023. Postmortem samples were collected opportunistically from 36 species in 20 states and Puerto Rico (Appendix 1 Table 1, https://wwwnc.cdc.gov/EID/article/31/8/24-1671-App1.xlsx) by US Department of Agriculture Wildlife Services personnel during ongoing permitted management activity (Figure 1) and by the Association of Fish and Wildlife Agencies during Best Management Practices Trap Training (Figure 2); samples were taken from a variety of sympatric mammals in disparate locations. Where possible, we used continuous intensive sampling at the same location for ≥1 month to improve detection within a given mammal community.

Personnel collected swab samples and Nobuto strip blood samples from each animal (S. Bevins et al., unpub. data, https://doi.org/10.1101/2023.04.14.533542); we performed SARS-CoV-2 RNA preparation and subsequent detection using quantitative reverse transcription RT PCR (qRT-PCR) as previously described (*8*). US Department of Agriculture Animal and Plant Health Inspection Service National Veterinary Services Laboratories subjected nonnegative samples from novel hosts to confirmatory testing. We prepared SARS-CoV-2–specific neutralizing antibodies (NAbs) from Nobuto strips and detected using the Genscript cPass SARS-CoV-2 neutralization antibody detection kit (Thermo Fisher Scientific, https://www.thermofisher.com) as described (S. Bevins et al., unpub. data). We further investigated nonnegative samples from novel hosts by conventional viral neutralization testing (cVNT). We screened Nobuto eluates from intensively sampled sites (n = 747) (Figure 1) for IAV antibodies using a commercial blocking ELISA Influenza A MultiS-Screen Ab test (IDEXX Laboratories,

Figure 2. Locations of opportunistic sampling for SARS-CoV-2 samples collected across 17 species in 13 states and Puerto Rico during community-scale surveillance of SARS-CoV-2 and influenza A viruses in wild mammals, United States, September 2022–November 2023. The number of samples collected varied across each state.

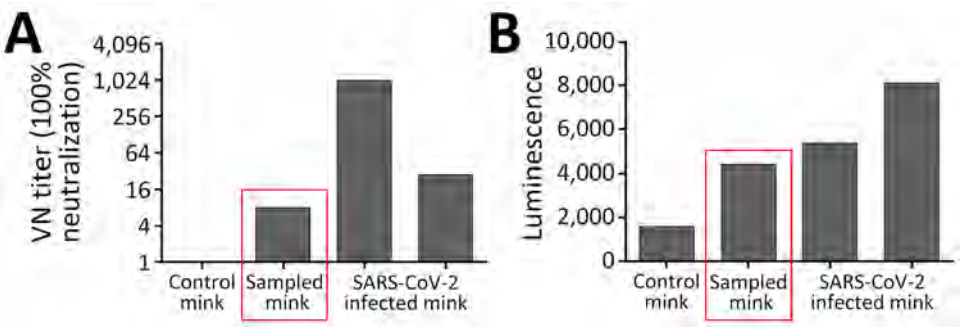

Figure 3. Results for testing conducted on a seropositive mink sample collected in Pennsylvania during community-scale surveillance of SARS-CoV-2 and influenza A viruses in wild mammals, United States, October 2022. A) Conventional VN testing; B) luciferase immunoprecipitation assay for nucleoprotein. The results from the 2 assays confirm previous exposure to the SARS-CoV-2 virus and rule out the likelihood that the immune response was generated in response to prior vaccination. Control mink data indicate results for a known negative-status mink, sampled mink data (red boxed) indicate results for our collected sample, and data for SARS-CoV-2–infected mink indicate results for known infected mink from samples collected outside of this study. VN, virus neutralization.

https://www.IDEXX.com) (*12*) as described previously (*13*). We used the manufacturer's recommended sample-to-negative ratio threshold of <0.5 to determine detection of IAV antibodies in serum (Appendix 2, https://wwwnc.cdc.gov/EID/article/31/8/24-1671-App2.pdf).

qRT-PCR testing detected SARS-CoV-2 RNA in 1 white-tailed deer (*Odocoileus virginianus*) sample (n = 45) and 2 nutria (*Myocastor coypus*) samples (n = 41) (Appendix 1 Table 2; Appendix 2 Figure 1). SARS-CoV-2 was not previously documented in nutria; because cycle threshold values were high, we used Sanger sequencing to verify the samples contained nutria host nucleic acid and were not contaminated by a sample from another species. After retesting, we did not have sufficient material for confirmatory

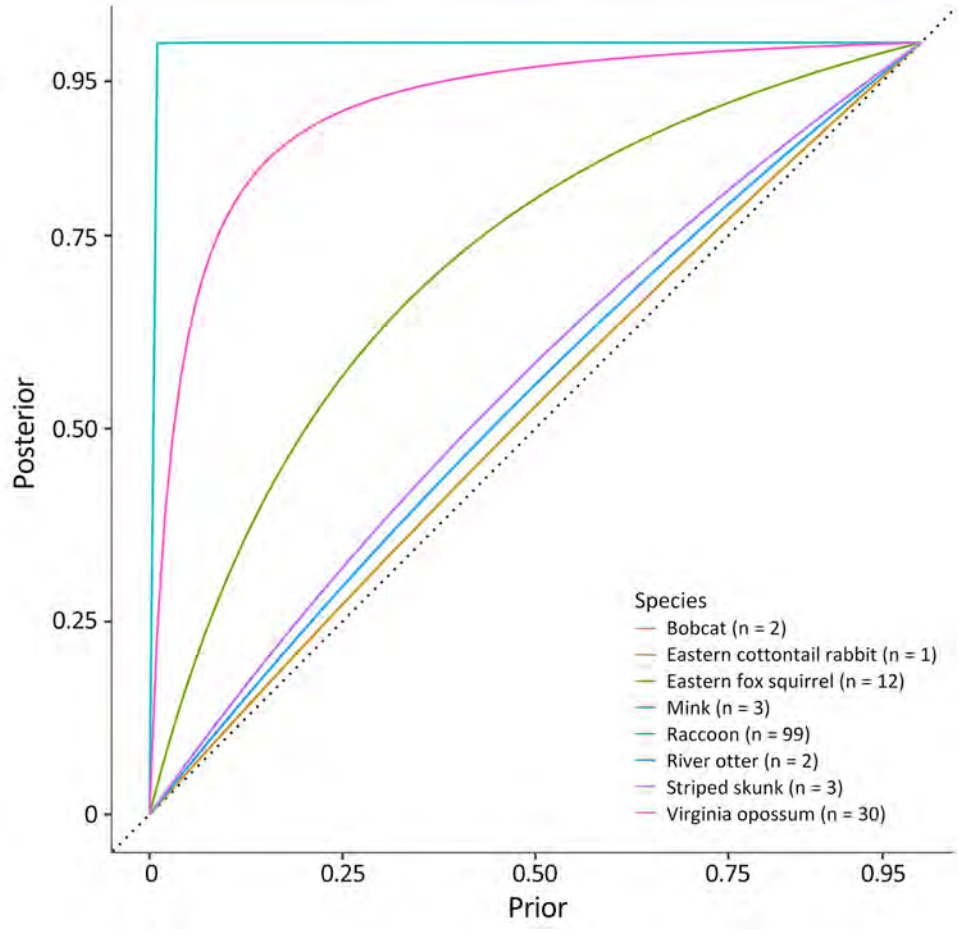

Figure 4. Posterior estimates of disease freedom varied based on prior input and the number of samples collected from each species in March 2023 in study of SARS-CoV-2 and influenza A viruses in wild mammals, United States. Collecting larger sample sizes enabled posterior estimates to depend less on prior inputs. The probability of disease freedom was analyzed for SARS-CoV-2–negative swabs from each species within each site. Probabilities for 8 species at a site in Iowa, United States, are shown.

testing. Additional sampling and testing are required to confirm nutria susceptibility to or SARS-CoV-2 presence in nutria populations.

We found serologic evidence of SARS-CoV-2 exposure in 14 samples from 5 species (Appendix 1 Table 3): 1 coyote (*Canis latrans*; n = 25) (Appendix 2 Figure 2), 1 muskrat (*Ondatra zibethicus*; n = 41) (Appendix 2 Figure 1), 1 woodchuck (*Marmota monax*; n = 18) (Appendix 2 Figure 1), 1 domestic American mink (n = 13) (Appendix 2 Figure 1), and 10 white-tailed deer (n = 45) Appendix 2 Figure 1). Sample quality issues prevented the coyote Nobuto sample from cVNT testing. cVNT testing of other Nobuto eluates detected SARS-CoV-2 NAbs at dilution factors of 1:32 for muskrat and 1:8 for woodchuck (Appendix 1 Table 3). Because the mink sample was an escaped domestic mink from a farm that vaccinated its mink, we tested the sample for the Omicron BA.1 and B1 (variant D614G) strains of SARS-CoV-2. We detected NAbs for the B1 (variant D614G) strain at a dilution factor of 1:8 from the mink Nobuto eluate (Figure 3, panel A) but no response to Omicron BA.1 strain. Finally, N luciferase immunoprecipitation assay screening showed reactivity against the N protein (Figure 3, panel B; Appendix 1 Table 4), which indicates the animal was likely exposed to a pre-Omicron variant instead of or in addition to being vaccinated.

ELISA screening for IAV antibodies detected positive results in 7 raccoons (*Procyon lotor*; n = 270 across sites) (Appendix 2 Figure 3) and 1 Virginia opossum (*Didelphis virginiana*; n = 112 across sites) (Appendix 1 Table 5; Appendix 2). All positive animals were from the same site in Iowa within the Mississippi Flyway during 2 time periods (October 2022 and March 2023). Samples collected during October 2022 included 3 raccoon detections (n = 88; seroprevalence 3.4%) and the Virginia opossum detection (n = 40; seroprevalence 2.5%), whereas samples collected during March 2023 included 4 raccoon detections (n = 98; seroprevalence 4.1%). Previous opportunistic surveillance of avian IAVs in raccoons reported a similar seroprevalence in Maryland during 2004 (2.4%) but a higher seroprevalence in some western states: 25% in Wyoming during 2004 and 12.8% in Colorado during 2006 (*14*).

In sites where no detections occurred, predictions of disease freedom were strongly influenced by the prior probability of disease freedom (i.e., site-level disease risk), but that influence was weakened by the sample size collected from each species within a site (Appendix 1 Table 6). We analyzed and illustrated the dependence between disease freedom estimates, sample size, and site-level disease risk at 1 site sampled in Iowa (Figure 4). Assumptions about site-level disease risk strongly determined disease freedom probability for species with ≤3 samples, such the eastern cottontail rabbit (*Sylvilagus floridanus*) with 1 sample. By comparison, disease freedom probability did not depend as greatly on site-level disease risk when ≥30 samples for a single species per site were collected, such as for raccoons or Virginia opossum.

Conclusions

We did not find widespread SARS-CoV-2 occurrence in the wildlife communities, even for wildlife species sympatric with deer. We found evidence for infrequent incidence of SARS-CoV-2 exposure in novel species, highlighting the importance of appropriate site-level sample sizes for detection of rare exposure events. Our disease freedom analysis provides sampling guidance for detection of rare events in future surveillance programs. We did not find evidence of co-circulation of SARS-CoV-2 and IAVs in the same animals or species but did find sympatric exposure to IAVs in raccoons and Virginia opossum in the Mississippi Flyway. Community-scale wildlife disease surveillance is important for monitoring changing host ranges that can be realized given local ecologic contexts for rapidly evolving viruses and for refining risk-based surveillance designs.

Acknowledgments

We thank the Wildlife Services employees, including Micah Bell, Nat Bornsen, Angela DeSimone, Wade Jones, Frank Klinger, Kirk Michaud, Jeff Pelc, Rod Perkins, Brandon Robinson, Nick Searfus, Arthur Young, and Micah Wellman, and Alaska Fish and Game employees, particularly Kimberlee Beckmen, for contributing to the wildlife sampling expertise. We thank all cooperating landowners and managers for granting access to lands for wildlife sampling. Finally, we thank the staff at the US Department of Agriculture Wildlife Disease and Diagnostic Laboratory and National Veterinary Service Laboratories for providing diagnostic expertise to this study.

This study was supported by American Rescue Plan Act and by the National Wildlife Disease Program of Wildlife Services from the US Department of Agriculture Animal and Plant Health Inspection Service. The findings and conclusions in this article are those of the authors and should not be construed to represent any official US Department of Agriculture or US Government determination or policy.

About the Author

Ms. Wilson-Henjum is a research assistant in the Department of Wildland Resources at Utah State University and at the National Wildlife Research Center in Fort Collins, Colorado, USA. Her research interests include the ecology of emerging diseases in wildlife.

References

1. Taylor LH, Latham SM, Woolhouse ME. Risk factors for human disease emergence. Philos Trans R Soc Lond B Biol Sci. 2001;356:983–9. https://doi.org/10.1098/rstb.2001.0888
2. Mörner T, Obendorf DL, Artois M, Woodford MH. Surveillance and monitoring of wildlife diseases. Rev Sci Tech. 2002;21:67–76. https://doi.org/10.20506/rst.21.1.1321
3. Chandler JC, Bevins SN, Ellis JW, Linder TJ, Tell RM, Jenkins-Moore M, et al. SARS-CoV-2 exposure in wild white-tailed deer (*Odocoileus virginianus*). Proc Natl Acad Sci U S A. 2021;118:e2114828118. https://doi.org/10.1073/pnas.2114828118
4. Elsmo EJ, Wünschmann A, Beckmen KB, Broughton-Neiswanger LE, Buckles EL, Ellis J, et al. Highly pathogenic avian influenza A (H5N1) virus clade 2.3. 4.4b infections in wild terrestrial mammals, United States, 2022. Emerg Infect Dis. 2023;29:2451–60. https://doi.org/10.3201/eid2912.230464
5. Peiris JSM. Coronaviruses. In: Greenwood D, Barer M, Slack R, Irving W, editors. Medical microbiology, 18th edition. London: Churchill Livingstone; 2012. p. 587–93.
6. Martin BE, Sun H, Carrel M, Cunningham FL, Baroch JA, Hanson-Dorr KC, et al. Feral swine in the United States have been exposed to both avian and swine influenza A viruses. Appl Environ Microbiol. 2017;83:e01346–17. https://doi.org/10.1128/AEM.01346-17
7. Hewitt J, Wilson-Henjum G, Collins DT, Linder TJ, Lenoch JB, Heale JD, et al. Landscape-scale epidemiological dynamics of SARS-CoV-2 in white-tailed deer. Transbound Emerg Dis. 2024;2024:7589509. https://doi.org/10.1155/2024/7589509
8. Feng A, Bevins S, Chandler J, DeLiberto TJ, Ghai R, Lantz K, et al. Transmission of SARS-CoV-2 in free-ranging white-tailed deer in the United States. Nat Commun. 2023;14:4078. https://doi.org/10.1038/s41467-023-39782-x
9. van Aart AE, Velkers FC, Fischer EAJ, Broens EM, Egberink H, Zhao S, et al. SARS-CoV-2 infection in cats and dogs in infected mink farms. Transbound Emerg Dis. 2022;69:3001–7. https://doi.org/10.1111/tbed.14173
10. Leguia M, Garcia-Glaessner A, Muñoz-Saavedra B, Juarez D, Barrera P, Calvo-Mac C, et al. Highly pathogenic avian influenza A (H5N1) in marine mammals and seabirds in Peru. Nat Commun. 2023;14:5489. https://doi.org/10.1038/s41467-023-41182-0
11. Burrough ER, Magstadt DR, Petersen B, Timmermans SJ, Gauger PC, Zhang J, et al. Highly pathogenic avian influenza A (H5N1) clade 2.3. 4.4 b virus infection in domestic dairy cattle and cats, United States, 2024. Emerg Infect Dis. 2024;30:1335–43. https://doi.org/10.3201/eid3007.240508
12. Brown JD, Stallknecht DE, Berghaus RD, Luttrell MP, Velek K, Kistler W, et al. Evaluation of a commercial blocking enzyme-linked immunosorbent assay to detect avian influenza virus antibodies in multiple experimentally infected avian species. Clin Vaccine Immunol. 2009;16:824–9. https://doi.org/10.1128/CVI.00084-09
13. Shriner SA, VanDalen KK, Root JJ, Sullivan HJ. Evaluation and optimization of a commercial blocking ELISA for detecting antibodies to influenza A virus for research and surveillance of mallards. J Virol Methods. 2016;228:130–4. https://doi.org/10.1016/j.jviromet.2015.11.021
14. Hall JS, Bentler KT, Landolt G, Elmore SA, Minnis RB, Campbell TA, et al. Influenza infection in wild raccoons. Emerg Infect Dis. 2008;14:1842–8. https://doi.org/10.3201/eid1412.071371

Address for correspondence: Grete Wilson-Henjum, Utah State University S.J. and Jessie E. Quinney College of Natural Resources, Department of Wildland Resources, 5200 Old Main Hill, Logan, UT 84322-5200, USA; email: grete.wilson-henjum@usda.gov

COVID-19 Predeparture Test Results and Vaccination Coverage among US-Bound Refugees, 2020–2022

Ashley S. Judge, Tarissa Mitchell, Alexander Klosovsky, Michelle Weinberg, Christina R. Phares

We describe predeparture COVID-19 test positivity and vaccination coverage for US-bound refugees. During November 24, 2020–June 11, 2022, a total of 23,972 refugees received 28,465 tests (87% reverse transcription PCR); 2.6% of refugees tested positive. During November 24, 2020–December 31, 2022, vaccination coverage rose from 0% to 71% among 24,831 adult refugees.

The COVID-19 pandemic disrupted global refugee resettlement, an international process offering permanent resettlement to a third country for persons who cannot return to their home country because of persecution on the basis of race, religion, nationality, social group, or political opinion and who can no longer remain in the country in which they reside. The United States suspended resettlement during March 20–July 29, 2020 (*1*,*2*). Upon resumption, the United States mandated pretravel COVID-19 testing for refugees, delaying travel for those who tested positive and their close contacts. During January 26, 2021–June 12, 2022, all travelers, including refugees, were required to show documentation of a negative test or recent recovery from COVID-19 before boarding a US-bound flight (*3*). This requirement was lifted on June 12, 2022 (*4*). US-bound refugees were not required to receive COVID-19 vaccinations but were referred to national programs for vaccination in their country of examination where possible. We assessed the prevalence of positive predeparture COVID-19 tests for all refugees and COVID-19 vaccination coverage for adult refugees. This activity was reviewed by Centers for Disease Control and Prevention's (CDC)'s National Center for Emerging and Zoonotic Infectious Diseases, Information Collection and Human Studies Team, was deemed not research, and was conducted consistent with applicable federal law and CDC policy (e.g., 45 C.F.R. part 46, 21 C.F.R. part 56; 42 U.S.C. §241(d); 5 U.S.C. §552a; 44 U.S.C. §3501 et seq.).

The Study

The International Organization for Migration coordinates US travel for refugees and manages many predeparture health assessments. To describe COVID-19 predeparture test results, we analyzed International Organization for Migration testing data for all refugees who entered the United States during November 24, 2020–June 11, 2022 (the last day for which predeparture testing was required for US-bound flights). To determine COVID-19 vaccination coverage, we queried the CDC Electronic Disease Notification system (*5*) for adult refugees (≥18 years of age) who entered the United States during November 24, 2020–December 31, 2022. During that period, most COVID-19 vaccinations were administered through national programs; analyses were limited to adults because most countries had not yet extended vaccination programs to minors. Testing and vaccination data were not linked.

We recorded test type as reverse transcription PCR, rapid antigen test, or other. Refugees could receive >1 test. Persons were considered to have tested positive if ≥1 test was positive, negative when ≥1 test was negative and no tests were positive, and unknown when all tests were indeterminate

Author affiliations: Oak Ridge Institute for Science and Education, Oak Ridge, Tennessee, USA (A.S. Judge); Centers for Disease Control and Prevention, Atlanta, Georgia, USA (A.S. Judge, T. Mitchell, M. Weinberg, C.R. Phares); International Organization for Migration, Washington, DC, USA (A. Klosovsky)

DOI: https://doi.org/10.3201/eid3108.250088

or missing. We calculated the percentage of persons who tested positive by dividing the number of persons with ≥1 positive result by the number of persons with known results. For the percentage positive over time, we only included persons in calculations for the first period in which they tested positive. We defined completion of a primary vaccine series as receipt of 1 dose of a single-dose vaccine or 2 doses (regardless of time interval) of a 2-dose series authorized in the United States or listed for emergency use by the World Health Organization (WHO).

Among 24,361 refugees who arrived in the United States during November 2020–June 2022, a total of 29,025 predeparture COVID-19 tests were documented. We excluded 560 missing or indeterminate test results (including results from 389 persons for whom all tests were indeterminate or missing), leaving 23,972 persons receiving 28,465 tests (Appendix, https://wwwnc.cdc.gov/EID/article/31/8/25-0088-App1.pdf). Most (85.0%) persons had 1 test, 12.0% had 2 tests, 2.2% had 3 tests, 0.6% had 4 tests, and 0.2% had 5–10 tests. Among all tests, 2.6% were positive for COVID-19. By type, positivity was 2.7% among 24,853 reverse transcription PCR tests, 2.0% among 3,590 rapid antigen tests, and 9.0% among 22 unspecified tests. Among 23,972 persons, 2.6% had ≥1 positive test.

The percentage positive was highest in Asia (4.1%), followed by Sub-Saharan Africa (2.9%) and the Americas (2.9%), and lowest in the Middle East/North Africa (1.9%) and Europe (1.8%) (Table 1). Within each region, percentage positive varied by country (Table 1). Over time, the percentage positive ranged from 0% in April 2021 to 21.7% in October 2021 (Figure 1). Across age groups, results were similar, ranging from 2.3% among children <5 years of age to 2.8% among adults ≥55 years of age.

During November 2020–December 2022, a total of 24,831 adult refugees arrived in the United

Table 1. Predeparture COVID-19 positivity among US-bound refugees by region and country of overseas medical examination, November 24, 2020–June 11, 2022*

Region and country	No. persons positive	No. persons tested	% Persons with positive test
Total	622	23,972	2.6
Europe	37	2,069	1.8
Moldova	20	312	6.4
Other†	4	201	2.0
Ukraine	13	1,556	0.8
Middle East/North Africa	153	8,228	1.9
Jordan	80	2,922	2.7
Turkey	46	2,032	2.3
Other‡	2	114	1.8
Egypt	24	2,007	1.2
Iraq	1	311	0.3
Lebanon	0	433	0.0
Qatar	0	409	0.0
Sub-Saharan Africa	274	9,318	2.9
Uganda	113	1,177	9.6
Ethiopia	14	397	3.5
Kenya	17	616	2.8
Tanzania	56	2,501	2.2
Zambia	16	725	2.2
Burundi	20	974	2.1
Rwanda	30	1,940	1.5
Malawi	4	362	1.1
Other§	4	626	0.6
Americas	49	1,674	2.9
El Salvador	27	506	5.3
Guatemala	17	702	2.4
Other¶	5	466	1.1
Asia	109	2,683	4.1
Thailand	46	916	5.0
Malaysia	43	911	4.7
Other#	20	856	2.3

*Persons were considered positive if ≥1 result was positive, negative when ≥1 result was negative and no tests were positive, and unknown when all results were indeterminate or missing. Number tested excludes persons classified as unknown. Most (88.8%) were tested by reverse transcription PCR, 11.2% by rapid antigen detection, and <0.1% had an unspecified test type.
†Albania, Armenia, Austria, Belarus, Germany, Israel, Kazakhstan, Malta, Uzbekistan.
‡Algeria, Bahrain, Kuwait, Oman, Saudi Arabia, United Arab Emirates.
§Angola, Botswana, Cameroon, Chad, Côte d'Ivoire, Democratic Republic of the Congo, Djibouti, Ghana, Guinea, Namibia, Niger, South Africa, Sudan, Togo, Zimbabwe.
¶Colombia, Costa Rica, Curaçao, Ecuador, Honduras.
#Afghanistan, Australia, Bangladesh, Myanmar, China, Hong Kong, India, Indonesia, Mongolia, Nauru, Nepal, Pakistan, Papua New Guinea, Sri Lanka,

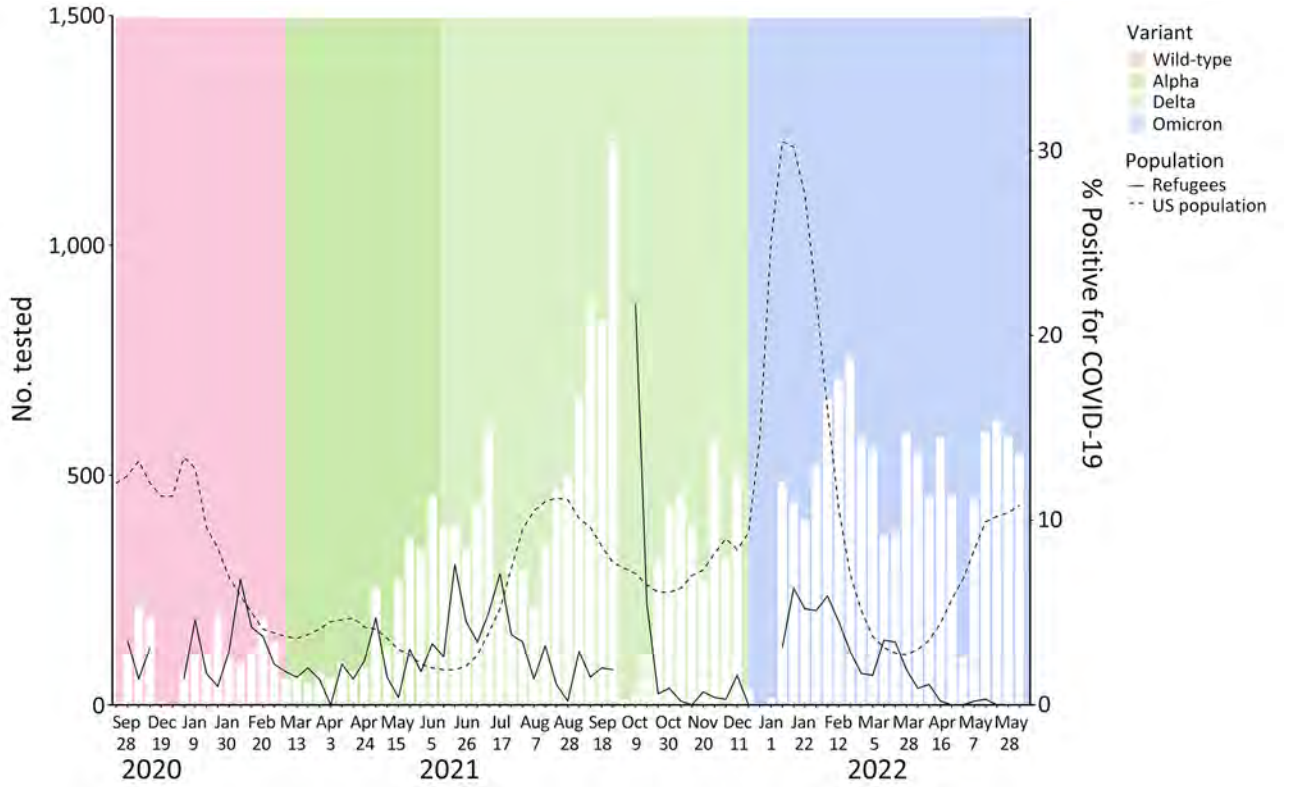

Figure 1. Predeparture COVID-19 test positivity among refugees by week of arrival in the United States (November 24, 2020–June 11, 2022) in study of test results and vaccination coverage among US-bound refugees, 2020–2022. Among refugees, weeks with <20 persons tested were suppressed. White bars indicate number of persons tested; dotted and solid lines indicate percentage positivity. Data for US population COVID-19 test positivity from National Respiratory and Enteric Virus Surveillance System (https://data.cdc.gov/Laboratory-Surveillance/Percent-Positivity-of-COVID-19-Nucleic-Acid-Amplif/gvsb-yw6g/about_data).

States (Appendix). Of those, 2,509 (10.1%) received a single-dose COVID-19 vaccine series, 1,030 (4.1%) received only 1 dose of a 2-dose vaccine series, and 7,878 (31.7%) received 2 doses of a 2-dose vaccine series (Table 2). In total, 41.8% of refugees completed a primary series before arrival in the United States. Coverage increased over time (Figure 2); by December 2022, a total of 71.3% had completed a primary series. The Americas had the highest percentage of persons who completed a primary series (63.4%), followed by Asia (51.0%), Middle East/North Africa (49.4%), Sub-Saharan Africa (34.8%), and Europe (15.7%) (Table 2).

Conclusions

The COVID-19 pandemic severely disrupted refugee resettlement. Such disruptions can prolong uncertainty and vulnerability for refugees, delay family reunification, and strain resources for host countries and humanitarian agencies (*6*). Even short disruptions can lead to a cascading derailment of administrative processes. Strategies to minimize disruption while preventing pathogen importation were needed.

Universal testing for US-bound refugees represented one such strategy. Despite concerns of heightened infection risk among refugees, predeparture testing showed low prevalence. For 23,972 US-bound refugees, just 2.6% of tests were positive, below the WHO 5% threshold for countries to reopen (*7*) and the 10.1% test positivity found in the general US population during the same period (*8*).

COVID-19 vaccines represented an additional tool to minimize resettlement disruptions while protecting refugees from severe disease; however, vaccine rollout to refugee populations was hampered by variable global distribution of vaccines, resulting in reduced initial access in low- and middle-income countries (*9*). Among US-bound refugees, those who had an overseas health assessment in Middle East/North Africa, Asia, and the Americas had higher COVID-19 vaccination coverage than those assessed in Sub-Saharan Africa or Europe, suggesting greater barriers to vaccination in those regions. In Sub-Saharan Africa, barriers included insufficient vaccine supply and cold chain issues in remote areas. In Eastern Europe, some

refugees received vaccines not approved for use in the United States or listed by WHO and thus were not counted in our calculations, and vaccine hesitancy was widespread (*10*). Other challenges included administrative difficulties, requirements for identity documents, and language barriers.

Despite challenges, COVID-19 vaccination coverage among US-bound refugees steadily increased over time, approaching coverage observed for the general US adult population. Within 1 month of US vaccination programs expanding to include adults ≤65 years of age on April 19, 2021, a total of 57.0% of the general US adult population had received ≥1 dose (*11*); by December 2022, that figure was 88.4% (*12*). For US-bound adult refugees, 54% had received 1 dose by April 2022 and 71.3% by December 2022, exceeding WHO's strategic objective for all countries to reach 70% (*13*). Although no vaccinations are mandatory for US-bound refugees, refugees were successfully referred to national vaccination programs in their country of examination for voluntary vaccination.

In conclusion, positivity for COVID-19 among US-bound refugees, which was monitored in real time, remained modest throughout the study period. A predeparture testing strategy further reduced risk by identifying persons who required travel postponement while permitting safe travel for others. Vaccination coverage among US-bound refugees improved over time, drawing near to that of the general US population. Our findings highlight the importance of including refugees in public health initiatives during global health emergencies, demonstrating that such approaches can protect the safety and continuity of resettlement efforts.

Table 2. Predeparture COVID-19 vaccination coverage among adult refugees by region and country of overseas health assessment, November 24, 2020–December 31, 2022

Region and country	No. (%) refugees				
	Single-dose series	Two-dose series		Completed primary series	Total population
		First dose only	First and second dose		
Total	2,509 (10.1)	1,030 (4.1)	7,878 (31.7)	10,387 (41.8)	24,831
Sub-Saharan Africa	2,059 (21.5)	343 (3.6)	1,275 (13.3)	3,334 (34.8)	9,594
Burundi	395 (46.4)	0	0	395 (46.4)	851
Ethiopia	240 (42.7)	9 (1.6)	29 (5.2)	269 (47.9)	562
Kenya	410 (47.6)	10 (1.1)	149 (17.3)	559 (64.9)	862
Malawi	47 (12.3)	8 (2.1)	72 (18.9)	119 (31.2)	381
Rwanda	49 (2.4)	157 (7.5)	742 (35.7)	791 (38.1)	2,079
Tanzania	489 (20.8)	7 (0.3)	17 (0.7)	506 (21.5)	2,352
Uganda	174 (16.4)	112 (10.5)	164 (15.5)	338 (31.9)	1,061
Zambia	94 (12.3)	12 (1.5)	9 (1.2)	103 (13.5)	764
Other*	161 (23.6)	28 (4.1)	93 (13.6)	254 (37.2)	682
Americas	17 (0.7)	239 (10.1)	1,474 (62.7)	1,491 (63.4)	2,352
Ecuador	15 (3.7)	21 (5.2)	299 (74.6)	314 (78.3)	401
El Salvador	0	45 (7.5)	412 (68.8)	412 (68.8)	599
Guatemala	1 (0.1)	134 (13.5)	579 (58.2)	580 (58.3)	994
Honduras	0	23 (7.4)	156 (50.5)	156 (50.5)	309
Other†	1 (2)	16 (32.7)	28 (57.1)	29 (59.1)	49
Asia	16 (0.5)	196 (6.3)	1,579 (50.5)	1,595 (51.0)	3,125
Malaysia	0	107 (7.5)	1,068 (75.3)	1,068 (75.3)	1,419
Thailand	0	63 (7.9)	168 (20.8)	168 (20.8)	806
Other‡	16 (1.8)	26 (2.9)	343 (38.1)	359 (39.9)	900
Europe	63 (2.5)	36 (1.5)	336 (13.2)	399 (15.7)	2,537
Moldova	15 (2.3)	6 (0.9)	78 (11.9)	93 (14.2)	655
Ukraine	1 (0.1)	0	76 (6)	77 (6.1)	1,269
Other§	47 (7.7)	30 (4.9)	182 (29.7)	229 (37.4)	613
Middle East/North Africa	354 (4.9)	216 (3)	3,214 (44.5)	3,568 (49.4)	7,223
Egypt	30 (1.9)	37 (2.3)	264 (16.8)	294 (18.7)	1,573
Jordan	0	77 (3.8)	1,428 (70.4)	1,428 (70.4)	2,027
Lebanon	3 (0.7)	25 (6)	64 (15.5)	67 (16.2)	413
Qatar	273 (30.8)	30 (3.4)	563 (63.5)	836 (94.3)	886
Turkey	0	21 (1.2)	612 (35.8)	612 (35.8)	1,710
Other¶	48 (7.8)	26 (4.2)	283 (46.1)	331 (53.9)	614

*Angola, Botswana, Cameroon, Chad, Côte d'Ivoire, Democratic Republic of the Congo, Djibouti, Ghana, Guinea, Madagascar, Mauritania, Mozambique, Namibia, Niger, South Africa, Sudan, Togo, Zimbabwe.
†Colombia, Costa Rica, Curaçao, Peru.
‡Afghanistan, Australia, Bangladesh, Myanmar, China, Hong Kong, India, Indonesia, Mongolia, Nepal, Nauru, Pakistan, Papua New Guinea, Sri Lanka, Vietnam.
§Albania, Armenia, Austria, Belarus, Belgium, Czech Republic, Germany, Israel, Italy, Kazakhstan, Kosovo, Kyrgyzstan, Malta, Poland, Russia, Slovak Republic, Slovenia, Tajikistan, Uzbekistan.
¶Algeria, Bahrain, Iraq, Kuwait, Morocco, Oman, Saudi Arabia, United Arab Emirates.

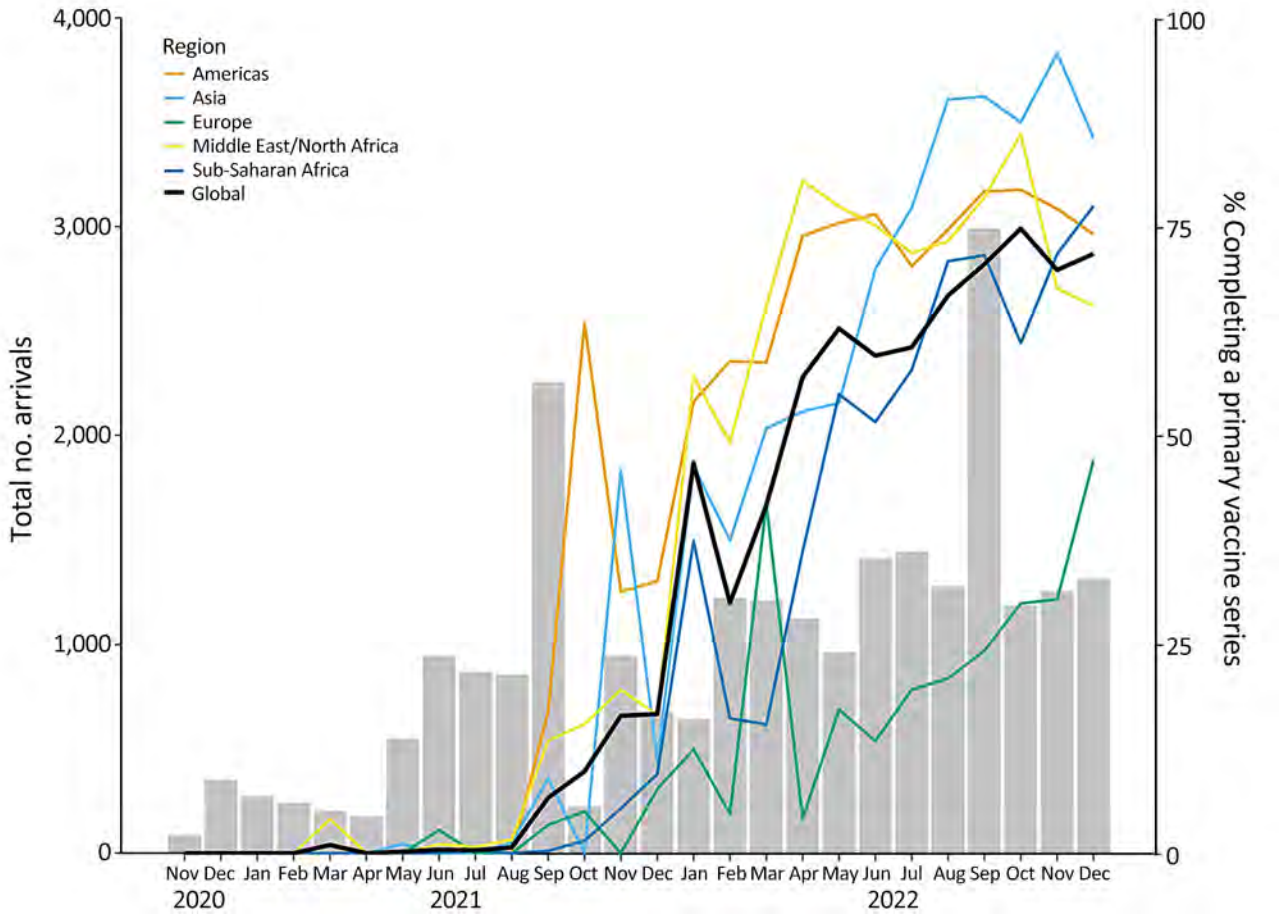

Figure 2. Predeparture completion of a primary COVID-19 vaccine series among adult refugees by month of arrival in the United States (November 24, 2020–December 31, 2022) in study of test results and vaccination coverage among US-bound refugees, 2020–2022. November 2020 represents November 24–30, 2020. Gray bars indicate number of arrivals; colored lines indicate percentage of persons completing primary vaccine series.

Acknowledgments

We thank the International Organization for Migration clinicians, support staff, laboratorians, data scientists, logisticians, and coordinators for their role in successfully navigating refugee resettlement in the midst of a global health crisis. We also thank Maria Litvinova, Mary Ann Bautista, and Sweetmavourneen Pernitez-Agan for their insightful comments to improve this manuscript.

About the Author

Ms. Judge conducted this analysis as an Oak Ridge Institute for Science and Education Fellow under the mentorship of Christina Phares in the CDC's Immigrant and Refugee Health Branch, Division of Global Migration and Quarantine, National Center for Emerging and Zoonotic Infectious Disease, during 2022–2023. She is an epidemiology PhD student at Indiana University in Bloomington, Indiana, USA.

References

1. Centers for Disease Control and Prevention. Control of communicable diseases; foreign quarantine: suspension of introduction of persons into United States from designated foreign countries or places for public health purposes [cited 2023 Feb 1]. https://www.federalregister.gov/documents/2020/03/24/2020-06238/control-of-communicable-diseases-foreign-quarantine-suspension-of-introduction-of-persons-into
2. US Department of State Bureau of Population Refugees and Migration. Report to Congress on proposed refugee admissions for fiscal year 2021 [cited 2023 Feb 1]. https://www.state.gov/reports/report-to-congress-on-proposed-refugee-admissions-for-fy-2021
3. Centers for Disease Control and Prevention. Requirement for negative pre-departure COVID-19 test result or documentation of recovery from COVID-19 for all airline or other aircraft passengers arriving into the United States from any foreign country [cited 2023 Feb 1]. https://www.federalregister.gov/documents/2021/11/05/2021-24388/requirement-for-negative-pre-departure-covid-19-test-result-or-documentation-of-recovery-from

4. Centers for Disease Control and Prevention. Rescinding requirement for negative pre-departure COVID-19 test result or documentation of recovery from COVID-19 for all airline or other aircraft passengers arriving into the United States from any foreign country [cited 2023 Feb 1]. https://www.federalregister.gov/documents/2022/06/15/2022-13022/rescinding-requirement-for-negative-pre-departure-covid-19-test-result-or-documentation-of-recovery
5. Phares CR, Liu Y, Wang Z, Posey DL, Lee D, Jentes ES, et al. Disease surveillance among U.S.-bound immigrants and refugees—electronic disease notification system, United States, 2014–2019. MMWR Surveill Summ. 2022;71:1–21. https://doi.org/10.15585/mmwr.ss7102a1
6. Brickhill-Atkinson M, Hauck FR. Impact of COVID-19 on resettled refugees. Prim Care. 2021;48:57–66. https://doi.org/10.1016/j.pop.2020.10.001
7. World Health Organization. Public health criteria to adjust public health and social measures in the context of COVID-19 [cited 2024 Jul 23]. https://iris.who.int/bitstream/handle/10665/332073/WHO-2019-nCoV-Adjusting_PH_measures-Criteria-2020.1-eng.pdf
8. Centers for Disease Control and Prevention. Percent positivity of COVID-19 nucleic acid amplification tests by HHS region, National Respiratory and Enteric Virus Surveillance System [cited 2023 Jun 2]. https://data.cdc.gov/Laboratory-Surveillance/Percent-Positivity-of-COVID-19-Nucleic-Acid-Amplif/gvsb-yw6g/about_data
9. Yoo KJ, Mehta A, Mak J, Bishai D, Chansa C, Patenaude B. COVAX and equitable access to COVID-19 vaccines. Bull World Health Organ. 2022;100:315–28. https://doi.org/10.2471/BLT.21.287516
10. Popa AD, Enache AI, Popa IV, Antoniu SA, Dragomir RA, Burlacu A. Determinants of the hesitancy toward COVID-19 vaccination in Eastern European countries and the relationship with health and vaccine literacy: a literature review. Vaccines (Basel). 2022;10:672. https://doi.org/10.3390/vaccines10050672
11. Diesel J, Sterrett N, Dasgupta S, Kriss JL, Barry V, Vanden Esschert K, et al. COVID-19 vaccination coverage among adults—United States, December 14, 2020–May 22, 2021. MMWR Morb Mortal Wkly Rep. 2021;70:922–7. https://doi.org/10.15585/mmwr.mm7025e1
12. Centers for Disease Control and Prevention. National immunization survey adult COVID module (NIS-ACM): COVIDVaxViews [cited 2023 Feb 1]. https://data.cdc.gov/Vaccinations/National-Immunization-Survey-Adult-COVID-Module-NI/udsf-9v7b/about_data
13. World Health Organization. Strategy to Achieve Global Covid-19 Vaccination by mid-2022 [cited 2024 Jul 23]. https://cdn.who.int/media/docs/default-source/immunization/covid-19/strategy-to-achieve-global-covid-19-vaccination-by-mid-2022.pdf

Address for correspondence: Christina Phares, Centers for Disease Control and Prevention, 1600 Clifton Rd NE, Mailstop H16-4, Atlanta, GA 30329-4018, USA; email: cphares@cdc.gov

Isolation of Highly Pathogenic Avian Influenza A(H5N1) Virus from Cat Urine after Raw Milk Ingestion, United States

Elisha A. Frye, Mohammed Nooruzzaman, Brittany Cronk, Melissa Laverack, Pablo Sebastian Britto de Oliveira, Leonardo C. Caserta, Manigandan Lejeune, Diego G. Diel

In 2024, 3 domestic cats in California, USA consumed raw milk contaminated with highly pathogenic avian influenza A(H5N1) virus. Fever and neurologic signs developed; 2 cats died. The surviving cat's urine tested positive for H5N1 virus by reverse transcription PCR. Raw dairy products pose a risk to both animal and human health.

Highly pathogenic avian influenza (HPAI) H5N1 virus infects felids, causing neurologic signs and death (*1*–*6*). In March 2024, H5N1 clade 2.3.4.4b genotype B3.13 was first detected in milk from dairy cattle, and large numbers of farm cats were reported dead or disappearing from affected farms (*1*,*2*). Urine has been reported as a suitable sample for detecting H5N1 in live cats (*7*). Here, we describe infection of domestic cats with HPAI H5N1 virus after ingesting commercial raw milk, including clinical signs and outcome of infection in affected animals, and report isolation of H5N1 virus from the urine of a surviving cat.

The Cases

An owner of 4 indoor-only cats living in southern California, USA, purchased 3 individual gallons of raw milk from 2 health food stores on November 17, 20, and 23, 2024; he fed the milk to his cats. Three of the cats consumed the raw milk through November 25. The milk lot numbers were included in a recall by the California Department of Public Health after multiple products tested positive for HPAI H5N1 virus (*8*). All cats were current on rabies vaccination.

On November 25, two of the cats, a 14-year-old male neutered brown tabby domestic short hair cat (cat 1) and a 4-year-old male neutered black and white domestic short hair cat (cat 2), had lethargy, anorexia, and fever develop. Cat 1 died on November 28 while hospitalized at an emergency veterinary clinic, and cat 2 died on November 30. No testing for H5N1 virus was performed on either cat.

Cat 3, a 5-year-old male neutered 5.9-kg tabby cat, displayed similar clinical signs and was hospitalized on December 1. His fever was 40.1°C (104.2°F). He received supportive care, including intravenous fluids, antibiotics (doxycycline and ampicillin/sulbactam), antinausea medication (maropitant citrate), an appetite stimulant (mirtazapine), and a nonsteroidal anti-inflammatory drug (robenacoxib). He was discharged on December 2 but was then admitted to a second emergency veterinary clinic on December 3.

At admission to the second clinic, the cat was anorexic and dull and had hind limb ataxia and paresis. His temperature was 39.7°C (103.5°F) during the night of December 3. A complete blood count, chemistry panel, abdominal ultrasound, and 3 view thoracic radiographs were performed. The only abnormal finding was consolidation of the left ventral lung field. A urinalysis was not performed. The cat was administered similar supportive care with the addition of oseltamivir phosphate (12 mg/12 h for 8 d). The cat also received pradofloxacin and gabapentin orally, as well as nasogastric tube feeding.

While cat 3 was at the second clinic, the cat owner contacted the San Bernardino County Department

Author affiliation: Cornell University College of Veterinary Medicine, Animal Health Diagnostic Center, Ithaca, New York, USA

DOI: https://doi.org/10.3201/eid3108.250309

of Public Health (SBCDPH) regarding concerns for HPAI virus infection and was advised to seek medical or veterinary care if he or his cats had clinical signs develop. The owner's fourth cat, a 5-year-old female spayed domestic shorthair, did not drink raw milk and did not develop clinical signs. The emergency clinic gave the owner no recommendations regarding cat 4. SBCDPH was not aware of cat 4 and did not recommend further testing or monitoring based on lack of clinical signs in any human contacts.

On December 4, cat 3 progressed to recumbency and lacked a menace response in the left eye. Passive range-of-motion exercises were initiated. Urine and nasal swab specimens in sterile containers and heparinized whole blood were collected and sent to the Cornell University College of Veterinary Medicine Animal Health Diagnostic Center (AHDC) (Ithaca, NY, USA). On December 5, the cat lacked a menace response in both eyes, but pupillary light and dazzle reflexes were intact bilaterally. He was more alert and was able to stand on the forelimbs but dragged the hind limbs (Video, https://wwwnc.cdc.gov/EID/article/31/8/25-0309-V1.htm). On December 7, he was discharged to the owner. Over the next few weeks, he used a wheelchair to ambulate and regained the ability to walk and jump on the hind limbs normally. On December 23, he was examined by a veterinary ophthalmologist and had present but weak menace response, pupillary light reflex, and dazzle reflex in the right eye.

At the AHDC, we tested the nasal swab and urine samples for HPAI virus by reverse transcription PCR (RT-PCR) (*9*). Results for the nasal swab sample were negative, but the urine was positive for influenza A (cycle threshold [Ct] of 35.4405) and for avian influenza H5 (Ct 36.706) virus. We froze the urine sample at −80°C (−112°F) and had results confirmed at the National Veterinary Services Laboratory (Ames, Iowa, USA). On December 6, we informed the attending veterinarian, the California State Animal Health Official, and the California Department of Public Health of the RT-PCR results.

On December 21, we performed virus isolation in 10-day old embryonated chicken eggs (ECEs) on the urine sample from cat 3. We inoculated a 1:10 dilution of the urine sample into 10 ECEs via the allantoic cavity route. Four embryos died at 24–48 hours after inoculation. Testing of the allantoic fluids from ECEs that died revealed hemagglutination on turkey red blood cells. The allantoic fluids tested positive for influenza A virus matrix protein by RT-PCR (*9*). In addition, targeted influenza A sequencing confirmed infection with HPAI H5N1 virus genotype B3.13 (Figure 1). We deposited the complete virus sequences into GenBank (accession nos. PV576479–86).

We further performed virus neutralization to detect H5N1 antibodies. We prepared the heparinized whole blood by centrifuging to isolate the plasma fraction and then tested the plasma. An endpoint neutralizing titer of 1:512 was determined, indicating seroconversion to H5N1 virus after exposure.

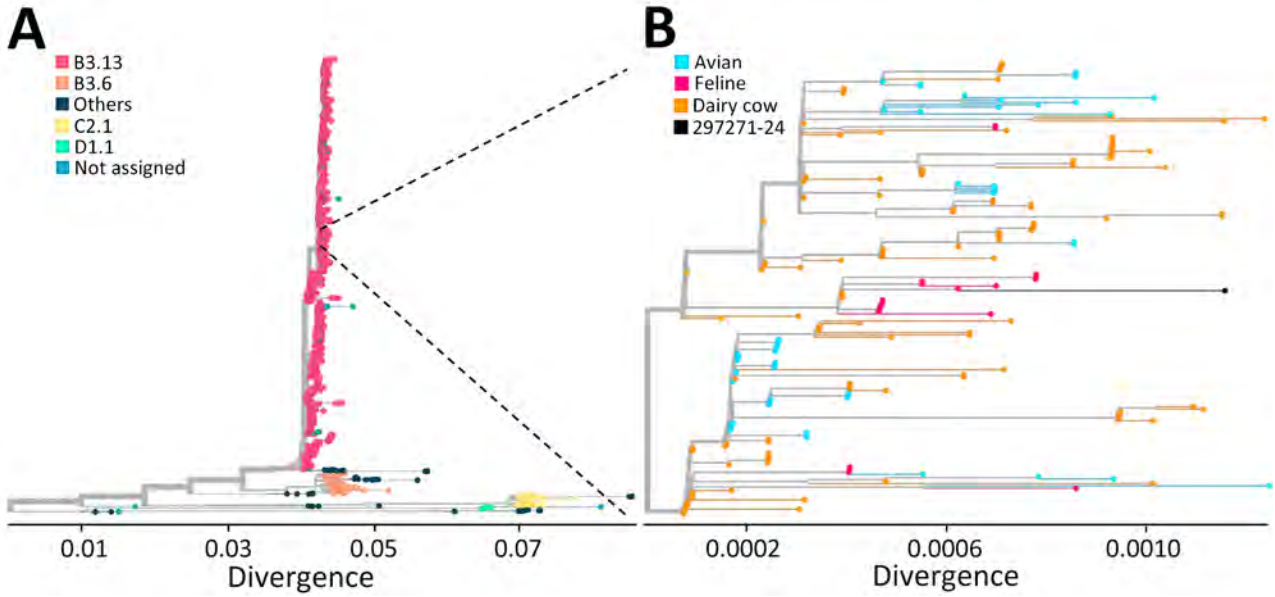

Figure 1. Phylogenetic analysis of complete genome sequences confirming highly pathogenic avian influenza A(H5N1) virus genotype B3.13 isolated from cat urine after raw milk ingestion, United States. A) Tree showing broader phylogeny of H5N1 virus genotypes; B) tree showing closer examination of the virus from the cat urine (sample no. 297271-24) and closely related virus sequences.

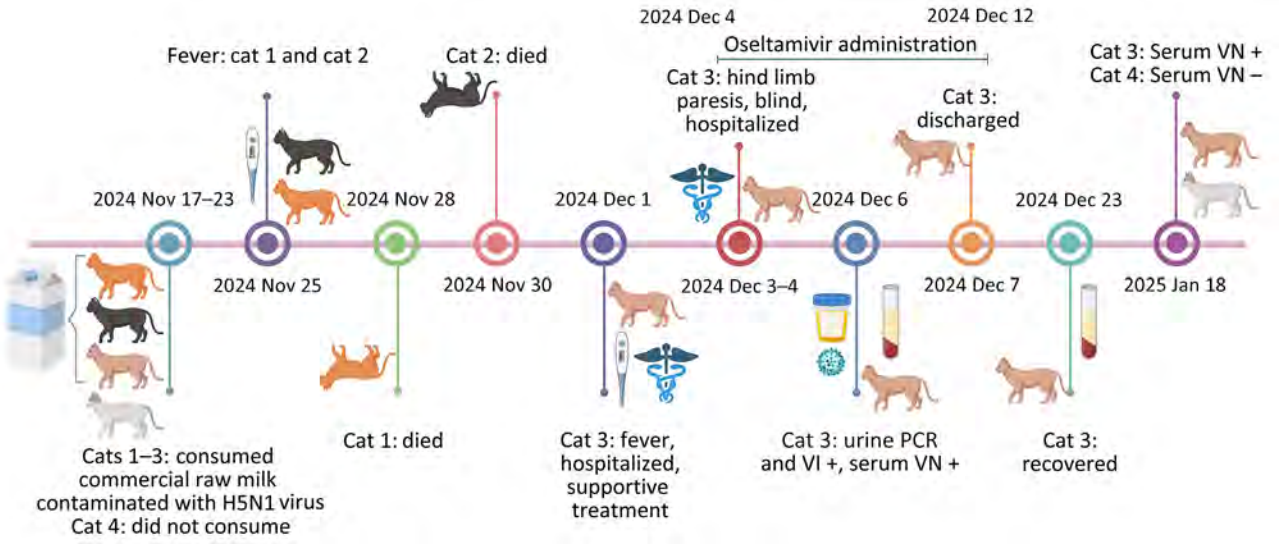

Figure 2. Timeline of events in domestic cats after exposure to highly pathogenic avian influenza A(H5N1) virus through consuming commercial raw milk contaminated with the virus, United States. Cats 1 and 2 died 10–12 days after initial exposure. Cat 3 showed characteristic clinical signs of H5N1 virus infection, was hospitalized and received supportive care including antiviral treatment (oseltamivir), and recovered from infection. Cat 4 did not consume milk and remained healthy throughout the outbreak. Figure created using BioRender (https://www.biorender.com). VI, virus isolation; VN, virus neutralization.

Seven weeks after cat 3 had symptoms develop, the original empty raw milk jugs and serum from cat 3 and cat 4 collected on January 18, 2025, were submitted to the AHDC. Milk residue from 1 of the jugs was positive for H5N1 virus by RT-PCR (Ct 35). However, attempts to isolate virus or sequence from the milk sample were unsuccessful. Cat 3 (clinically affected cat that recovered) had a virus neutralization titer of 1:1,024. Cat 4 was negative for H5N1 antibodies, confirming a lack of exposure (Figure 2).

Conclusions

This report provides evidence of HPAI H5N1 virus infection in domestic cats after consuming raw milk contaminated with the virus. Two cats died after a disease course characteristic of H5N1 virus infection in felids; however, no diagnostic test confirmed H5N1 virus infection. A third cat had hind limb paresis and blindness develop but recovered after hospitalization and supportive care, which included administration of the antiviral drug oseltamivir. Cat 3 tested positive for H5N1 virus, and a robust H5N1-specific neutralizing antibody titer developed. The raw milk consumed by the cats that had clinical signs of H5N1 virus infection was confirmed positive for HPAI H5N1 virus RNA by RT-PCR. The cat in the household that did not consume raw milk remained seronegative.

Given the broad circulation of H5N1 virus in dairy cattle in the United States, our results highlight the risk posed by raw dairy products to both animal and human health. Veterinarians examining cats with a history of exposure to wild birds or ingestion of raw poultry or dairy products and acute neurologic signs should have H5N1 infection on their differential diagnosis list.

Acknowledgments

We thank the California Department of Public Health and the San Bernardino County Public Health Department for their epidemiologic investigation efforts in this case.

About the Author

Dr. Frye is an associate professor of practice in the Department of Population Medicine and Diagnostic Sciences, College of Veterinary Medicine, Cornell University, Ithaca, NY. She is a veterinarian at the Animal Health Diagnostic Center, housed at the Cornell University College of Veterinary Medicine campus.

References

1. Burrough ER, Magstadt DR, Petersen B, Timmermans SJ, Gauger PC, Zhang J, et al. Highly pathogenic avian influenza A(H5N1) clade 2.3.4.4b virus infection in domestic dairy cattle and cats, United States, 2024. Emerg Infect Dis. 2024;30:1335–43. https://doi.org/10.3201/eid3007.240508
2. Caserta LC, Frye EA, Butt SL, Laverack M, Nooruzzaman M, Covaleda LM, et al. Spillover of highly pathogenic avian influenza H5N1 virus to dairy cattle. Nature. 2024;634:669–76. https://doi.org/10.1038/s41586-024-07849-4
3. Chothe SK, Srinivas S, Misra S, Nallipogu NC, Gilbride E, LaBella L, et al. Marked neurotropism and potential

adaptation of H5N1 clade 2.3.4.4.b virus in naturally infected domestic cats. Emerg Microbes Infect. 2025;14:2440498. https://doi.org/10.1080/22221751.2024.2440498
4. Cornell Wildlife Health Lab. Highly pathogenic avian influenza [cited 2025 Feb 16]. https://cwhl.vet.cornell.edu/article/highly-pathogenic-avian-influenza
5. Sillman SJ, Drozd M, Loy D, Harris SP. Naturally occurring highly pathogenic avian influenza virus H5N1 clade 2.3.4.4b infection in three domestic cats in North America during 2023. J Comp Pathol. 2023;205:17–23. https://doi.org/10.1016/j.jcpa.2023.07.001
6. Elsmo EJ, Wünschmann A, Beckmen KB, Broughton-Neiswanger LE, Buckles EL, Ellis J, et al. Highly pathogenic avian influenza A(H5N1) virus clade 2.3.4.4b infections in wild terrestrial mammals, United States, 2022. Emerg Infect Dis. 2023;29:2451–60. https://doi.org/10.3201/eid2912.230464
7. Mainenti M, Siepker C, Magstadt DR, Gauger P, Baum D, Petersen B, et al. Distribution of lesions and detection of influenza A(H5N1) virus, clade 2.3.4.4b, in ante- and postmortem samples from naturally infected domestic cats on U.S. dairy farms. J Vet Diagn Invest. 2025;37:27–35. https://doi.org/10.1177/10406387241300464
8. California Department of Public Health. State secures broad voluntary recall of raw milk and cream to protect consumers. 2024 Dec 3 [cited 2025 Jan 13]. https://www.cdph.ca.gov/Programs/OPA/Pages/NR24-044.aspx
9. National Animal Health Laboratory Network. Standard operating procedure for real-time RT-PCR detection of influenza A and avian paramyxovirus type-1 (NVSL-SOP-0068) [cited 2025 Feb 20]. https://www.aphis.usda.gov/media/document/15399/file
10. Peña-Mosca F, Frye EA, MacLachlan MJ, Rebelo AR, de Oliveira PSB, Nooruzzaman M, et al. The impact of highly pathogenic avian influenza H5N1 virus infection on dairy cows. Nat Commun. 2025;16:6520.

Address for correspondences: Elisha Frye or Diego Diel, Cornell University College of Veterinary Medicine, 240 Farrier Rd, Ithaca, NY 14850, USA; email: eab73@cornell.edu or dgdiel@cornell.edu

ACE2 Receptor Usage across Animal Species by SARS-CoV-2 Variants

Masato Hatta,[1] Gloria P. Larson,[1] Yasuko Hatta,[1] Wei Wang, Nannan Jiang, Yu-Jin Jung, Li Wang, Xiaoyu Fan, Brenda M. Calderon, Gaston Bonenfant, Xudong Lin, Chenchen Feng, Dan Cui, Ginger Atteberry, Michael Currier, John Steel, David E. Wentworth, Bin Zhou

We analyzed the receptor-binding activity and infectivity of 6 representative SARS-CoV-2 lineages in cell lines expressing angiotensin-converting enzyme 2 proteins from 54 different animal species. All viruses demonstrated infectivity in a broad range of species. Susceptible animal species could serve as natural reservoirs or intermediate hosts for SARS-CoV-2.

SARS-CoV-2, the causative agent of COVID-19, has resulted in >775 million cases and 7 million deaths worldwide (*1*). Although the origin and the intermediate host(s) of this virus remain unclear, the virus has infected dozens of animal species presumably through reverse zoonosis, including wild animals such as white-tailed deer and companion animals such as cats and dogs (*2*–*5*). During 2020–2025, the virus has evolved rapidly, giving rise to thousands of variants; hundreds spread and were replaced by newer lineages. During that process, mutations accumulated in the SARS-CoV-2 genome, especially in the spike gene. For example, Omicron XBB.1.5 has acquired >40 nonsynonymous mutations in the spike gene compared with the wild-type index virus. Because the spike–receptor interaction is the initial and decisive step in coronavirus infection, amino acid changes in the spike protein can enhance or reduce infectivity in humans and other animal species, potentially altering the virus's species specificity. Investigating spike interaction with a broad range of angiotensin-converting enzyme 2 (ACE2) receptors from different species is therefore crucial for understanding potential reservoirs before and after the virus's emergence in humans and for enabling risk assessment of viruses that have crossed into new hosts through reverse zoonosis.

Author affiliations: Centers for Disease Control and Prevention, Atlanta, Georgia, USA (M. Hatta, Y. Hatta, N. Jiang, L. Wang, X. Fan, B.M. Calderon, X. Lin, D. Cui, G. Atteberry, M. Currier, J. Steel, D.E. Wentworth, B. Zhou); Oak Ridge Institute for Science and Education, Oak Ridge, Tennessee, USA (G.P. Larson, G. Bonenfant, C. Feng); General Dynamics Information Technology, Inc., Falls Church, Virginia, USA (W. Wang, Y.-J. Jung)

DOI: https://doi.org/10.3201/eid3108.241844

The Study

We analyzed the ACE2 receptor activity of 54 animal species (36 mammals, 8 birds, 5 reptiles, 1 amphibian, and 4 fish) against various SARS-CoV-2 lineages that evolved over time (Figure 1; Appendix Table 1, https://wwwnc.cdc.gov/EID/article/31/8/24-1844-App1.pdf). Those animal species were selected to represent the broad diversity of ACE2 sequences and for other factors such as their potential role as reservoir of the SARS-CoV-2 progenitor (e.g., bats), potential role as intermediate host (e.g., pangolin, raccoon dog), close contact with humans (e.g., dog and cat), and indication of a large-scale reverse zoonotic event that appears to have led to enzootic disease (e.g., white-tailed deer). Compared with the human ACE2, the amino acid identity of the other 53 species ranged from 56% (wild turkey and western clawed frog) to 99% (chimpanzee) (Figure 1). We compared the sequences of the 20 ACE2 residues previously reported as critical in the spike–ACE2 binding interface across all 54 species (*6*,*7*).

To understand spike-ACE2 binding characteristics during the viral entry process, we developed 54 cell lines expressing different species of ACE2 proteins exogenously. We transfected a human ACE2 knockout HEK293T cell line (293T-ACE2-KO) with ACE2 expression plasmids. At 22–24 hours after

[1]These authors contributed equally to this article.

transfection, we incubated the recombinant trimeric spike proteins of the SARS-CoV-2 index virus, the Delta variant, or the Omicron BA.1 variant with the ACE2-expressing cells. We analyzed spike protein binding by flow cytometry. Generally, increased binding was detected when the spike protein concentration increased from 2 μg/mL to 20 μg/mL (Appendix Figure 1). To compare the binding of the 3 spikes across ACE2 receptors, we normalized the flow cytometry signals to the index virus spike versus human ACE2 receptor reference group at each spike concentration (2 μg/mL and 20 μg/mL) (Figure 2,

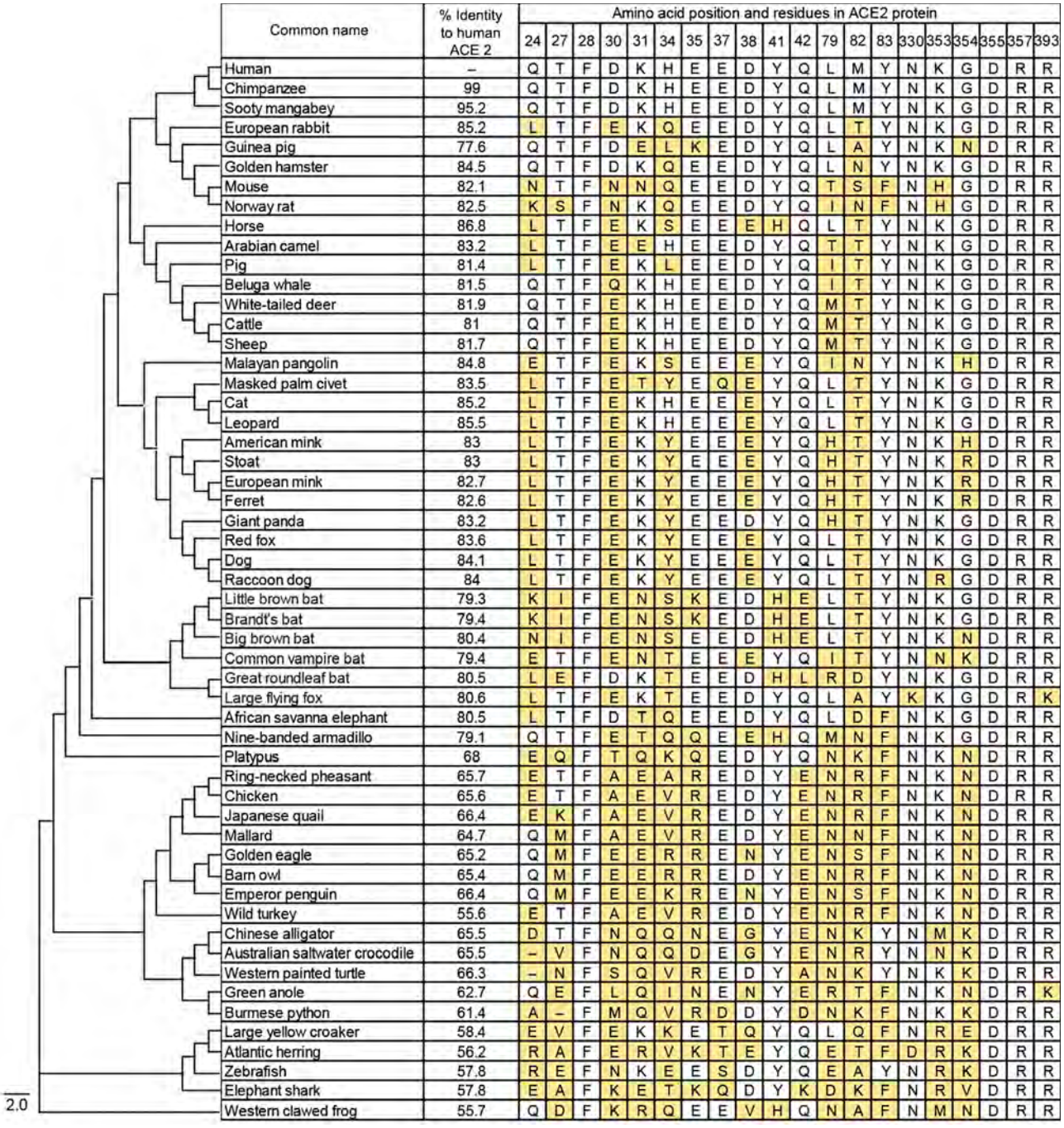

Common name	% Identity to human ACE 2	Amino acid position and residues in ACE2 protein																			
		24	27	28	30	31	34	35	37	38	41	42	79	82	83	330	353	354	355	357	393
Human	–	Q	T	F	D	K	H	E	E	D	Y	Q	L	M	Y	N	K	G	D	R	R
Chimpanzee	99	Q	T	F	D	K	H	E	E	D	Y	Q	L	M	Y	N	K	G	D	R	R
Sooty mangabey	95.2	Q	T	F	D	K	H	E	E	D	Y	Q	L	M	Y	N	K	G	D	R	R
European rabbit	85.2	L	T	F	E	K	Q	E	E	D	Y	Q	L	T	Y	N	K	G	D	R	R
Guinea pig	77.6	Q	T	F	D	E	L	K	E	D	Y	Q	L	A	Y	N	K	N	D	R	R
Golden hamster	84.5	Q	T	F	D	K	Q	E	E	D	Y	Q	L	N	Y	N	K	G	D	R	R
Mouse	82.1	N	T	F	N	N	Q	E	E	D	Y	Q	T	S	F	N	H	G	D	R	R
Norway rat	82.5	K	S	F	N	K	Q	E	E	D	Y	Q	I	N	F	N	H	G	D	R	R
Horse	86.8	L	T	F	E	K	S	E	E	E	H	Q	L	T	Y	N	K	G	D	R	R
Arabian camel	83.2	L	T	F	E	E	H	E	E	D	Y	Q	T	T	Y	N	K	G	D	R	R
Pig	81.4	L	T	F	E	K	L	E	E	D	Y	Q	I	T	Y	N	K	G	D	R	R
Beluga whale	81.5	Q	T	F	Q	K	H	E	E	D	Y	Q	I	T	Y	N	K	G	D	R	R
White-tailed deer	81.9	Q	T	F	E	K	H	E	E	D	Y	Q	M	T	Y	N	K	G	D	R	R
Cattle	81	Q	T	F	E	K	H	E	E	D	Y	Q	M	T	Y	N	K	G	D	R	R
Sheep	81.7	Q	T	F	E	K	H	E	E	D	Y	Q	M	T	Y	N	K	G	D	R	R
Malayan pangolin	84.8	E	T	F	E	K	S	E	E	E	Y	Q	I	N	Y	N	K	H	D	R	R
Masked palm civet	83.5	L	T	F	E	T	Y	E	Q	E	Y	Q	L	T	Y	N	K	G	D	R	R
Cat	85.2	L	T	F	E	K	H	E	E	E	Y	Q	L	T	Y	N	K	G	D	R	R
Leopard	85.5	L	T	F	E	K	H	E	E	E	Y	Q	L	T	Y	N	K	G	D	R	R
American mink	83	L	T	F	E	K	Y	E	E	E	Y	Q	H	T	Y	N	K	H	D	R	R
Stoat	83	L	T	F	E	K	Y	E	E	E	Y	Q	H	T	Y	N	K	R	D	R	R
European mink	82.7	L	T	F	E	K	Y	E	E	E	Y	Q	H	T	Y	N	K	R	D	R	R
Ferret	82.6	L	T	F	E	K	Y	E	E	E	Y	Q	H	T	Y	N	K	R	D	R	R
Giant panda	83.2	L	T	F	E	K	Y	E	E	D	Y	Q	H	T	Y	N	K	G	D	R	R
Red fox	83.6	L	T	F	E	K	Y	E	E	E	Y	Q	L	T	Y	N	K	G	D	R	R
Dog	84.1	L	T	F	E	K	Y	E	E	E	Y	Q	L	T	Y	N	K	G	D	R	R
Raccoon dog	84	L	T	F	E	K	Y	E	E	E	Y	Q	L	T	Y	N	R	G	D	R	R
Little brown bat	79.3	K	I	F	E	N	S	K	E	D	H	E	L	T	Y	N	K	G	D	R	R
Brandt's bat	79.4	K	I	F	E	N	S	K	E	D	H	E	L	T	Y	N	K	G	D	R	R
Big brown bat	80.4	N	I	F	E	N	S	E	E	D	H	E	L	T	Y	N	K	N	D	R	R
Common vampire bat	79.4	E	T	F	E	N	T	E	E	E	Y	Q	I	T	Y	N	N	K	D	R	R
Great roundleaf bat	80.5	L	E	F	D	K	T	E	E	D	H	L	R	D	Y	N	K	G	D	R	R
Large flying fox	80.6	L	T	F	E	K	T	E	E	D	Y	Q	L	A	Y	K	K	G	D	R	K
African savanna elephant	80.5	L	T	F	D	T	Q	E	E	D	Y	Q	L	D	F	N	K	G	D	R	R
Nine-banded armadillo	79.1	Q	T	F	E	T	Q	Q	E	E	H	Q	M	N	F	N	K	G	D	R	R
Platypus	68	E	Q	F	T	Q	K	Q	E	D	Y	Q	N	K	F	N	K	N	D	R	R
Ring-necked pheasant	65.7	E	T	F	A	E	A	R	E	D	Y	E	N	R	F	N	K	N	D	R	R
Chicken	65.6	E	T	F	A	E	V	R	E	D	Y	E	N	R	F	N	K	N	D	R	R
Japanese quail	66.4	E	K	F	A	E	V	R	E	D	Y	E	N	R	F	N	K	N	D	R	R
Mallard	64.7	Q	M	F	A	E	V	R	E	D	Y	E	N	N	F	N	K	N	D	R	R
Golden eagle	65.2	Q	M	F	E	E	R	R	E	N	Y	E	N	S	F	N	K	N	D	R	R
Barn owl	65.4	Q	M	F	E	E	R	R	E	D	Y	E	N	R	F	N	K	N	D	R	R
Emperor penguin	66.4	Q	M	F	E	E	K	R	E	N	Y	E	N	S	F	N	K	N	D	R	R
Wild turkey	55.6	E	T	F	A	E	V	R	E	D	Y	E	N	R	F	N	K	N	D	R	R
Chinese alligator	65.5	D	T	F	N	Q	Q	N	E	G	Y	E	N	K	Y	N	M	K	D	R	R
Australian saltwater crocodile	65.5	–	V	F	N	Q	Q	D	E	G	Y	E	N	R	Y	N	N	K	D	R	R
Western painted turtle	66.3	–	N	F	S	Q	V	R	E	D	Y	A	N	K	Y	N	K	K	D	R	R
Green anole	62.7	Q	E	F	L	Q	I	N	E	N	Y	E	R	T	F	N	K	N	D	R	K
Burmese python	61.4	A	–	F	M	Q	V	R	D	D	Y	D	N	K	F	N	K	K	D	R	R
Large yellow croaker	58.4	E	V	F	E	K	K	E	T	Q	Y	Q	L	Q	F	N	R	E	D	R	R
Atlantic herring	56.2	R	A	F	E	R	V	K	T	E	Y	Q	E	T	F	D	R	K	D	R	R
Zebrafish	57.8	R	E	F	N	K	E	E	S	D	Y	Q	E	A	Y	N	R	K	D	R	R
Elephant shark	57.8	E	A	F	K	E	T	K	Q	D	Y	K	D	K	F	N	R	V	D	R	R
Western clawed frog	55.7	Q	D	F	K	R	Q	E	E	V	H	Q	N	A	F	N	M	N	D	R	R

Figure 1. Sequence comparison of ACE2 proteins among 54 animal species with phylogenetic tree of ACE2 proteins in study of ACE2 receptor usage across animal species by SARS-CoV-2 variants. Protein sequence of ACE2 from various species are aligned at residues in the SARS-CoV-2 spike protein binding interface. Percent identity to human ACE2 was calculated by pairwise alignment of individual ACE2s to human ACE2. Residues differing from human ACE2 residues are highlighted in yellow. Scale bar indicates the number of amino acid substitutions based on ACE2 protein sequences. ACE2, angiotensin-converting enzyme 2.

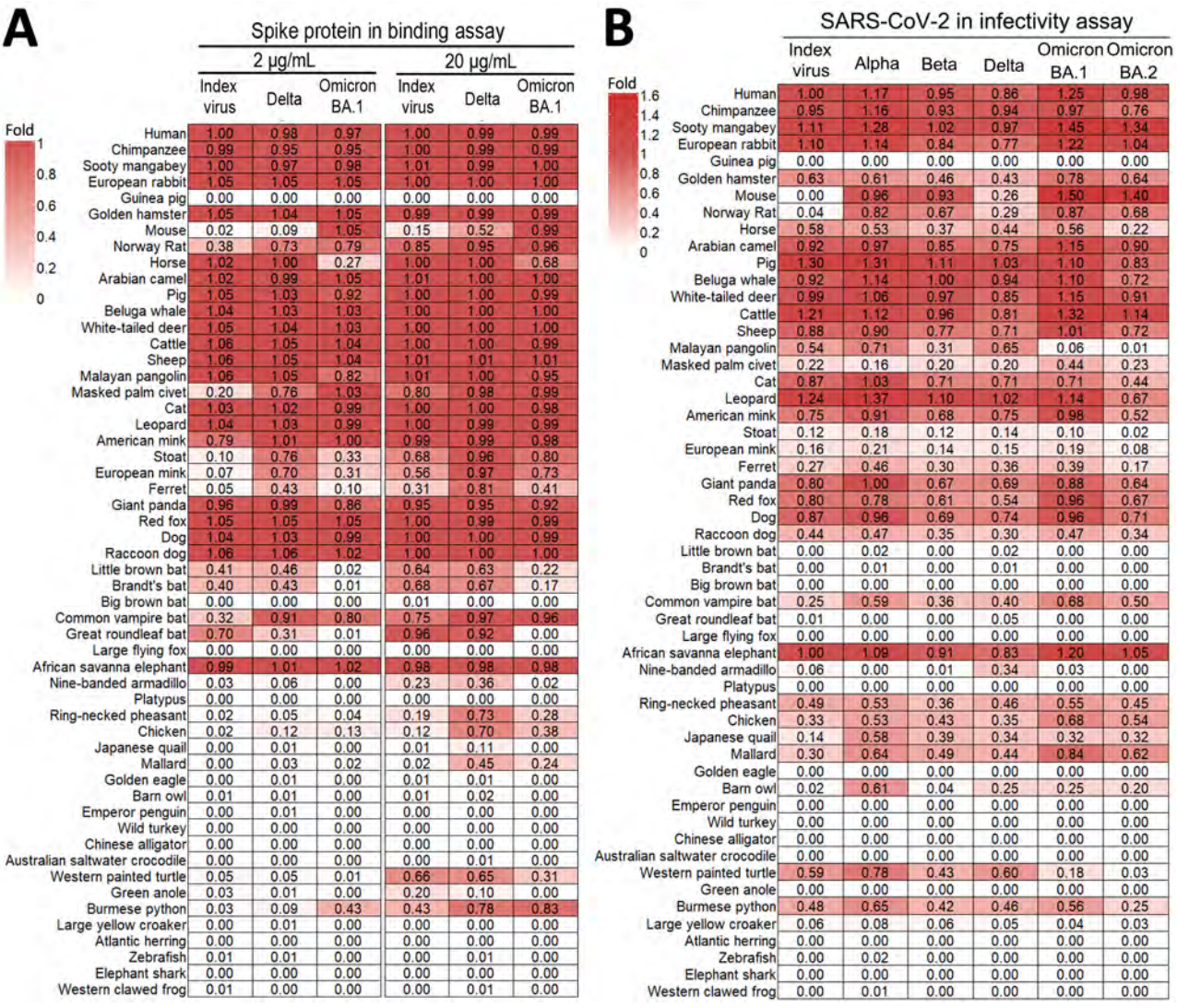

Figure 2. Heatmaps showing the binding strength of spike proteins (A) and infectivity of SARS-CoV-2 variants (B) to cells expressing ACE2 proteins from 54 animal species in study of ACE2 receptor usage across animal species by SARS-CoV-2 variants. The binding of the spike proteins to ACE2 was normalized to the reference group of index (wild-type) virus spike protein and human ACE2 cells (defined as 1) for both 2 μg/mL and 20 μg/mL spike protein concentrations. The representative data from 3 independent experiments are shown. The infectivity of SARS-CoV-2 reporter viruses was also normalized to the reference group of index virus and human ACE2 cells (defined as 1). The ratios, relative to the index virus and human ACE2 cells, are displayed as colors ranging from white to red. The experiment was performed in triplicate and the average was used in the heatmap. ACE2, angiotensin-converting enzyme 2.

panel A). Overall, spike proteins bound efficiently to most of the mammalian ACE2s but showed little to no binding to ACE2s from birds, reptiles, amphibians, or fish. Specifically, none of the spike proteins bound to guinea pig ACE2, suggesting guinea pig is unlikely to be a susceptible animal model for SARS-CoV-2, which was recently confirmed (*8*). In contrast, all spike proteins bound efficiently to the ACE2 of golden hamster, which is widely used in SARS-CoV-2 studies. Although the spike protein from the index virus does not bind to mouse ACE2, the Delta spike protein gained ability to bind to mouse ACE2 at high concentration, and the Omicron spike protein bound to mouse ACE2 with efficiency comparable to human ACE2. In addition to those laboratory model animals, this assay illustrates that spike proteins can also bind to ACE2s of domesticated animals (such as rabbit, camel, pig, cattle, sheep, cat, and dog) and wild animals (such as whale, pangolin, leopard, panda, fox, raccoon dog, and elephant). Of note, compared with the index virus spike, the Delta and Omicron spikes showed increased binding to ACE2s of rat, palm civet, American mink, stoat, European mink, ferret, pheasant, chicken, mallard, and python but showed decreased binding

to horse and turtle ACE2. The binding to bat ACE2s was variable depending on species. Those results indicate that the spike proteins of the index virus, Delta, and Omicron BA.1 have broad species specificity; however, differences in ACE2 binding specificity have emerged among SARS-CoV-2 variants.

Because viral entry goes beyond the spike–ACE2 binding step, we further explored ACE2 species specificity using infectious SARS-CoV-2 viruses, which require the ACE2 to be functional in mediating subsequent steps (e.g., fusion) of viral entry. We inoculated ACE2-transfected 293T-ACE2-KO cells with 10^4 focus-forming units of GFP-expressing SARS-CoV-2 viruses possessing the spike gene from the wild-type virus or the Alpha, Beta, Delta, or Omicron BA.1 and BA.2 lineages (*9*). We counted GFP-positive cells at 20–24 hours after inoculation and expressed results as ratio to the wild-type virus spike protein versus human ACE2 reference group. All tested viruses exhibited broad species specificity for ACE2 proteins; variants demonstrated differential infectivity against certain ACE2 receptors, largely consistent with the results of the spike protein–ACE2 binding assay (Figure 2). Of note, Omicron lineage variants lost the ability to infect pangolin ACE2-expressing cells, and BA.2 showed lower infectivity for horse ACE2-expressing cells. The common vampire bat is the only species that showed susceptibility among the 6 bat species analyzed, both in the spike–ACE2 binding assay and the live-virus infectivity assay. Little brown bat and Brandt's bat were moderately positive in the binding assay but not in the infectivity assay, supporting the value of performing the infectivity assay. The successful infection of cells expressing turtle and python ACE2 is also intriguing. Chicken and quail have been demonstrated to be nonsusceptible to SARS-CoV-2 infection (*10*). However, in this study, the cells expressing ACE2 of those species were susceptible to SARS-CoV-2 infection, although the infectivity was not high. Additional host factors, such as the distribution and amount of ACE2 proteins in tissues, cellular proteins involved in viral replication, or innate immunity, would affect the establishment of infection in animals exposed to SARS-CoV-2. For species of particular interest, further investigation through animal infection experiments is necessary to confirm susceptibility.

Conclusions

The susceptibility of animal species to SARS-CoV-2 has been diligently studied in various in silico, in vitro, in vivo, and epidemiologic analyses since the pandemic began (Appendix Table 2). However, the differences in ACE2 specificity among SARS-CoV-2 variants, especially Omicron lineages, have not been comprehensively studied. In this study, we demonstrated the wide range of species specificity of SARS-CoV-2 variants and the differences in their ability to use various ACE2 proteins as receptors. The dozens of amino acid differences in the spike proteins could affect the variants' pathogenicity, antigenicity, transmissibility, infectivity, and host species specificity. Further structural or mutagenesis analysis of the spike proteins and the ACE2 proteins could identify the key interacting amino acids (Figure 1) responsible for species specificity. This study suggests that susceptible animal species could evolutionarily serve as natural reservoirs or intermediate hosts, transmitting SARS-CoV-2 to other species or back to humans, potentially leading to future outbreaks or a new pandemic driven by novel SARS-CoV-2 variants with animal-adapted mutations.

This study was funded by the Centers for Disease Control and Prevention COVID-19 Emergency Response.

About the Author

Dr. Hatta is a senior service fellow in the Influenza Division, National Center for Immunization and Respiratory Diseases, Centers for Disease Control and Prevention, and was deployed to the Centers for Disease Control and Prevention COVID-19 Emergency Response. He primarily works on the evaluation and development of candidate vaccines for influenza viruses with pandemic potential.

References

1. World Health Organization. WHO coronavirus (COVID-19) dashboard [cited 2024 Aug 6]. https://covid19.who.int
2. Doliff R, Martens P. Cats and SARS-CoV-2: a scoping review. Animals (Basel). 2022;12:1413. https://doi.org/10.3390/ani12111413
3. Liew AY, Carpenter A, Moore TA, Wallace RM, Hamer SA, Hamer GL, et al.; Companion Animals Working Group. Clinical and epidemiologic features of SARS-CoV-2 in dogs and cats compiled through national surveillance in the United States. J Am Vet Med Assoc. 2023;261:480–9. https://doi.org/10.2460/javma.22.08.0375
4. Goldberg AR, Langwig KE, Brown KL, Marano JM, Rai P, King KM, et al. Widespread exposure to SARS-CoV-2 in wildlife communities. Nat Commun. 2024;15:6210. https://doi.org/10.1038/s41467-024-49891-w
5. Pandit R, Matthews QLA. A SARS-CoV-2: companion animal transmission and variants classification. Pathogens. 2023;12:775. https://doi.org/10.3390/pathogens12060775
6. Lan J, Ge J, Yu J, Shan S, Zhou H, Fan S, et al. Structure of the SARS-CoV-2 spike receptor-binding domain bound to the ACE2 receptor. Nature. 2020;581:215–20. https://doi.org/10.1038/s41586-020-2180-5
7. Shang J, Ye G, Shi K, Wan Y, Luo C, Aihara H, et al. Structural basis of receptor recognition by SARS-CoV-2.

Nature. 2020;581:221–4. https://doi.org/10.1038/s41586-020-2179-y
8. Iwatsuki-Horimoto K, Kiso M, Ito M, Yamayoshi S, Kawaoka Y. Sensitivity of rodents to SARS-CoV-2: gerbils are susceptible to SARS-CoV-2, but guinea pigs are not. Npj Viruses. 2024;2:59. https://doi.org/10.1038/s44298-024-00068-8
9. Wang L, Kainulainen MH, Jiang N, Di H, Bonenfant G, Mills L, et al.; SSEV Bioinformatics Working Group. Differential neutralization and inhibition of SARS-CoV-2 variants by antibodies elicited by COVID-19 mRNA vaccines. Nat Commun. 2022;13:4350. https://doi.org/10.1038/s41467-022-31929-6
10. Suarez DL, Pantin-Jackwood MJ, Swayne DE, Lee SA, DeBlois SM, Spackman E. Lack of susceptibility to SARS-CoV-2 and MERS-CoV in poultry. Emerg Infect Dis. 2020;26:3074–6. https://doi.org/10.3201/eid2612.202989

Address for correspondence: Bin Zhou, Centers for Disease Control and Prevention, 1600 Clifton Rd NE, Mailstop H17-5, Atlanta, GA 30329-4018, USA; email: bzhou@cdc.gov

Microsporidial Keratoconjunctivitis Caused by *Vittaforma corneae*, Sea of Galilee, Israel, 2022–2024

Asaf Friehmann, Irit Lubitz, Fidaa El Zhalka, Sharon Amit

We describe a multiannual outbreak of keratoconjunctivitis caused by the microsporidium *Vittaforma corneae* in the Sea of Galilee, Israel. Patients had multifocal punctate corneal infiltrates and reduced visual acuity, confirmed by locally-developed pathogen-specific real-time PCR. Topical chlorhexidine, rather than traditional antimicrobial drugs, proved an effective and safe primary treatment.

Microsporidial keratitis, caused by spore-forming unicellular parasites now classified as fungi, has previously been recognized as a severe yet uncommon ocular infection, often associated with outbreaks worldwide (*1*,*2*). *Vittaforma corneae* (previously known as *Nosema corneum)* was first identified in a child from Sri Lanka in 1973 (*3*) and has emerged as a keratoconjunctivitis pathogen, especially in water-related outbreaks. *V. corneae* is characterized by small spores (3–4-μm long and 1–1.5-μm wide), has unique ultrastructural features, and exhibits a specific affinity for ocular tissues.

The natural reservoir of *V. corneae* remains unknown, yet it has been detected in various mammals and invertebrates, suggesting a broad host range. Of note, humans are not considered natural hosts of *V. corneae*. Environmental sources, particularly aquatic environments, are believed to play a crucial role in *V. corneae* transmission and persistence. Studies have identified *V. corneae* spores in both fresh and marine water samples, indicating its ability to survive in diverse aquatic settings (*1*,*2*).

In this article, we describe a multiannual outbreak of *V. corneae* keratoconjunctivitis associated with exposure to the Sea of Galilee in northern Israel. This outbreak is noteworthy for its prolonged duration and specific geographic association, which has not been previously reported for *V. corneae* infections. Our PCR-confirmed cases of *V. corneae* keratoconjunctivitis represent dozens of instances nationwide. This study was approved by the Meir Medical Center Internal Review Board (approval no. 0001-24-MMC).

The Study

During 2022–2024, we detected 12 PCR-confirmed patients, 6–51 years of age (median age 15.3 years; mean ± SD age 22.29 ± 19.76 years); 5 were female and 7 were male. All reported recent exposure to the Sea of Galilee before symptom onset, with a median duration of 14 days (range 10–18 days) and an average of 13.75 days (SD ± 2.33 days) between exposure and symptoms. Similar to other nationwide reported cases, no other epidemiologic links were identified (Appendix, https://wwwnc.cdc.gov/EID/article/31/8/24-1941-App1.pdf).

Patients reported eye symptoms of redness, watering, irritation, and a foreign-body sensation. Visual acuity when seeking care averaged 0.60 ± 0.34 decimal (normal vision ≥1.0 decimal). Slit-lamp examination revealed coarse, multifocal, punctate epithelial lesions (<1 mm) on the cornea, often accompanied by nonpurulent conjunctivitis with a mixed follicular-papillary reaction (Figure). Those findings were uniform across the patient cohort and consistent with previous descriptions of *V. corneae* infections.

During the early months of the outbreak, the causative organism was unidentified. The ophthalmologic findings matched those of previously reported microsporidial infections and were supported by microscopy of corneal scraping specimens. We found numerous oval spores 3–5 μm long and 1–2 μm wide (*4*; https://www.cdc.gov/dpdx/microsporidiosis/index.html) by using fluorescent calcofluor staining. We used a pan-microsporidial PCR targeting the small subunit rRNA of most microsporidia (ss18f, 5′-caccaggttgattctgcc-3′; ss1492r, 5′-ggttaccttgttacgactt-3′) (*5*), but it failed to identify any specific pathogen, likely

Author affiliations: Meir Medical Center, Kfar Sava, Israel (A. Friehmann, F. El Zhalka); Tel-Aviv University, Tel-Aviv, Israel (A. Friehmann, S. Amit); Sheba Medical Center, Ramat-Gan, Israel (I. Lubitz, S. Amit).

DOI: https://doi.org/10.3201/eid3108.241941

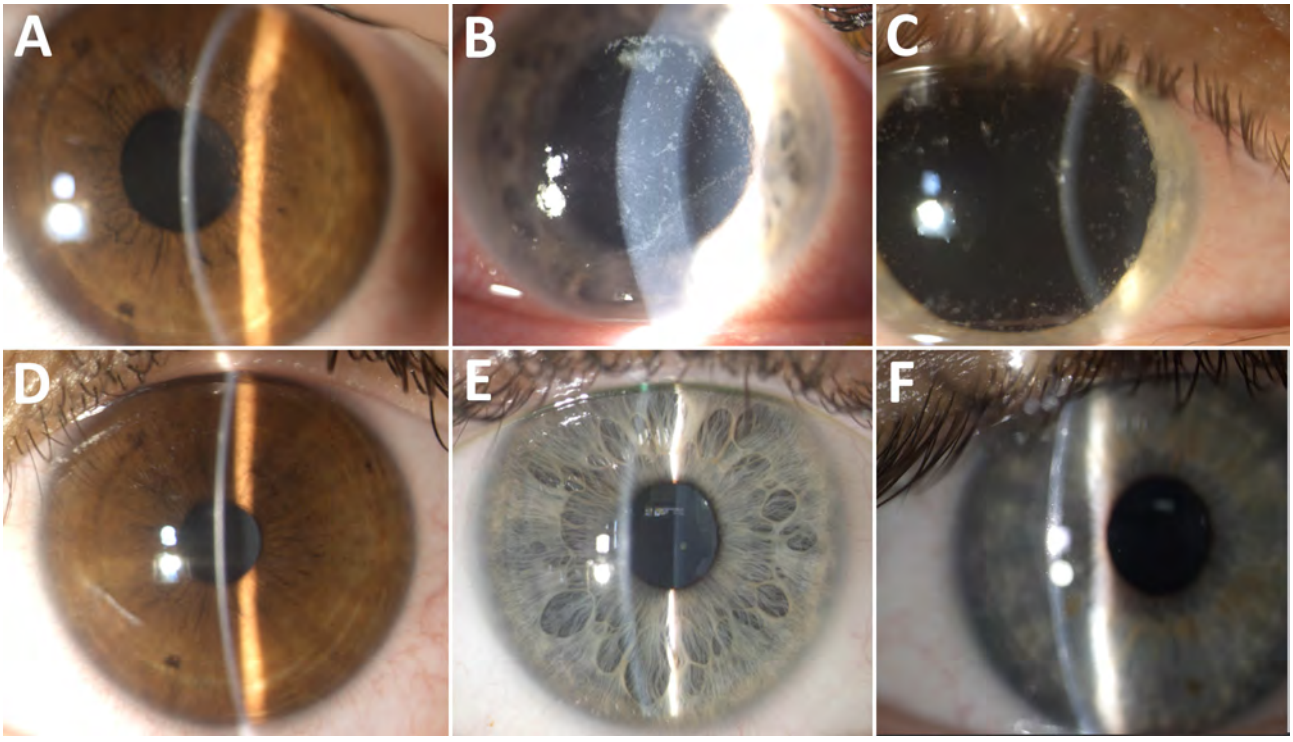

Figure. Slit-lamp photos of 3 patients before and after treatment of microsporidial keratoconjunctivitis caused by *Vittaforma corneae*, Sea of Galilee, Israel, 2022–2024. A) Patient 1 before treatment, visual acuity 0.8 decimal. B) Patient 2 before treatment, visual acuity 0.3 decimal. C) Patient 3 before treatment, visual acuity 0.3 decimal. D) Patient 1 after treatment, visual acuity 1 decimal. E) Patient 2 after treatment, visual acuity 1 decimal. F) Patient 3 after treatment, visual acuity 1 decimal. Clinical manifestations in all 3 patients included corneal epithelial microsporidial infiltrates and conjunctival irritation. After treatment with 0.02% topical chlorhexidine, the infiltrates resolved without scarring or other complications.

because of limited corneal scraping material and other technical limitations, such as primer mismatches with the target species. Next, we performed a shotgun metagenomic sequencing on pooled corneal scrapings by using a Nextera XT library and Illumina MiSeq platform (Illumina, https://www.illumina.com), yielding >7 million reads. Despite a predominance of host-derived sequences, species-specific reads mapping to the *V. corneae* small subunit rRNA gene verified the presence of *V. corneae*. To confirm this result, we developed a SYBR Green–based real-time PCR assay for *V. corneae*, following the methodology outlined previously (*6*). The assay used the primer sequences corn-F 5′-ctaccaagacagtgacggttga-3′ and corn-R 5′-ggcatcttttactgctggaact-3′. We conducted Sanger sequencing on the amplicons, yielding 100% coverage and >95% identity with *V. corneae*.

Our key finding was the efficacy of topical chlorhexidine as a first-line treatment after corneal debridement, which was therapeutic and diagnostic. All patients were treated with 0.02% chlorhexidine 2–3 times daily, demonstrating excellent tolerability and outcomes. This regimen marks a shift from the combination therapies (sometimes including systemic drugs) typically used for microsporidial keratitis (*7*,*8*).

In contrast, only 3 patients in our study received either topical moxifloxacin or topical voriconazole (2–3 times daily), and 3 were treated with short courses of adjunctive topical steroids during follow-up (Appendix Table 1). Of note, no patients required hospitalization or additional interventions beyond topical therapy. Chlorhexidine was well tolerated, and no major corneal scarring or reported ocular discomfort related to its use was reported. Those findings support the potential of a simplified, topical-only approach to treatment.

Visual acuity improved in most patients, and the mean at the last follow-up (average 6.1 ± 4.2 months) reached 0.87 ± 0.21 decimal visual acuity. Although not statistically significant ($p = 0.1$) because of the small sample size, the improvement in visual acuity does indicate that topical chlorhexidine is effective in preserving visual function and preventing disease progression.

Conclusions

In this article, we present a large outbreak of PCR-confirmed *V. corneae* keratoconjunctivitis associated

with a single freshwater body, the Sea of Galilee, which has not previously been linked to a microsporidial outbreak. The multiannual nature of this outbreak, spanning >3 consecutive years, suggests the presence of a persistent environmental reservoir of *V. corneae* in this ecosystem, potentially influenced by unique ecologic conditions or anthropogenic factors. This outbreak is of public health interest given the widespread recreational use of the Sea of Galilee, which is the only major freshwater lake in Israel.

Our findings underscore the effectiveness and safety of topical chlorhexidine as a treatment for *V. corneae* keratoconjunctivitis. This simple, cost-effective regimen achieved favorable outcomes without the need for complex multidrug therapies or hospitalization. Although chlorhexidine avoids unnecessary exposure to systemic antimicrobial drugs and offers broad-spectrum coverage, this regimen may be insufficient in more complicated cases, such as contact lens–related infections involving *Pseudomonas* spp., other more complex pathogens, or immunocompromised hosts. Corneal scarring did not develop in any of our patients, suggesting chlorhexidine can preserve corneal integrity.

Early and accurate diagnosis was essential for guiding appropriate treatment. Because of the rarity of microsporidial infections in Israel, a species-specific real-time PCR enabled rapid, reliable detection of *V. corneae* from limited ocular samples. PCR proved especially useful in settings where microsporidial keratitis was not routinely suspected, enabling timely therapy.

The first limitation of this study is that, apart from 1 patient with untreated stable sarcoidosis, all patients were immunocompetent, limiting applicability to immunocompromised populations who may require more intensive treatment and prolonged follow-up and whose keratitis could be associated with systemic infection (*9*). Finally, the restriction of the outbreak to a single, ecologically unique body of water, the Sea of Galilee, limits the broader generalizability of these findings.

Further research is needed to clarify the ecologic and microbiological factors contributing to the persistence of *V. corneae* in the Sea of Galilee and to assess the potential for similar outbreaks elsewhere. This event also emphasizes the need for public health measures, including environmental monitoring and preventive recommendations, highlighting an emerging pattern in waterborne microsporidial infections, and the need for increased awareness among clinicians and microbiologists. PCR was essential for rapid and accurate pathogen identification, and the success of chlorhexidine 0.02% as a primary therapy offers a promising, simplified approach for managing such infections.

Acknowledgments

We thank the Genetic Laboratory and the Bioinformatics Unit at the Israel Institute for Biological Research for their invaluable support in performing the metagenomic sequencing and analysis.

About the Author

Dr. Friehmann is the director of the Cornea Service at Meir Medical Center, Kfar Sava. His research interests include corneal infections, trauma, and transplantation.

References

1. Sabhapandit S, Murthy SI, Garg P, Korwar V, Vemuganti GK, Sharma S. Microsporidial stromal keratitis: clinical features, unique diagnostic criteria, and treatment outcomes in a large case series. Cornea. 2016;35:1569–74. https://doi.org/10.1097/ICO.0000000000000939
2. Moshirfar M, Somani SN, Shmunes KM, Espandar L, Gokhale NS, Ronquillo YC, et al. A narrative review of microsporidial infections of the cornea. Ophthalmol Ther. 2020;9:265–78. https://doi.org/10.1007/s40123-020-00243-z
3. Ashton N, Wirasinha PA. Encephalitozoonosis (nosematosis) of the cornea. Br J Ophthalmol. 1973;57:669–74. https://doi.org/10.1136/bjo.57.9.669
4. Didier ES, Orenstein JM, Aldras A, Bertucci D, Rogers LB, Janney FA. Comparison of three staining methods for detecting microsporidia in fluids. J Clin Microbiol. 1995;33:3138–45. https://doi.org/10.1128/jcm.33.12.3138-3145.1995
5. Ghosh K, Weiss LM. Molecular diagnostic tests for microsporidia. Interdiscip Perspect Infect Dis. 2009;2009:926521. https://doi.org/10.1155/2009/926521
6. Jayahar Bharathi M, Murugan N, Ramesh Kumar G, Ramakrishnan R, Anitha V, Ramesh S. *Vittaforma corneae* keratitis in southern India: role of a novel duplex PCR. J Med Microbiol. 2013;62:553–9. https://doi.org/10.1099/jmm.0.051722-0
7. Ramatchandirane B, A MK, Marimuthu Y, Nicodemus DS, Yarra MC. Successful treatment of microsporidial keratoconjunctivitis (MKC) with a combination of topical voriconazole 1% and gatifloxacin 0.5%: a large case series of 29 patients. Cureus. 2023;15:e49247. https://doi.org/10.7759/cureus.49247
8. Coca M, Kim J, Shenoy S, Chévez-Barrios P, Kapur M. Microsporidial stromal keratitis: successful treatment with topical voriconazole and oral itraconazole. Cureus. 2016;8:e934. https://doi.org/10.7759/cureus.934
9. Yeh TC, Kuo YS, Wang LC, Tai TY, Lin PY. Chlorhexidine in the treatment of microsporidial stromal keratitis and the effect of host immunity: a case series and literature review. J Chin Med Assoc. 2022;85:532–6. https://doi.org/10.1097/JCMA.0000000000000661

Address for correspondence: Sharon Amit, Sheba Medical Center, Derech Sheba 2, Ramat-Gan, 5266202, Israel; email: sharon.amit@sheba.health.gov.ilw

Identification of Co-Circulating Dengue and South America–Origin Zika Viruses, Pakistan, 2021–2022

Najeeha T. Iqbal,[1] Kaitlin Sawatzki,[1] Kumail Ahmed, Jennifer Tisoncik-Go, Elise Smith, Kathleen Voss, John Cornelius, Lu Wang, Alicen B. Spaulding, Leonid Serebryannyy, Daniel C. Douek, Muhammad Asif Syed, Syed Faisal Mahmood, Erum Khan, Wesley C. Van Voorhis, Michael Gale, Jr.

We collected samples from febrile patients in Karachi, Pakistan, in 2021–2022. Sequencing, molecular, and serologic screens revealed dengue serotype 2 and Zika virus. The Zika lineage was inferred to be from Brazil in 2016, indicating unobserved circulation. We conclude that Zika virus contributes to perceived dengue outbreak burden in Pakistan.

Orthoflavivirus is a genus of arthropod-borne, positive-strand RNA viruses capable of causing serious disease outbreaks in humans (*1*). Dengue virus (DENV) and Zika virus (ZIKV) are clinically relevant species with widespread circulation in tropical and subtropical climates via *Aedes* spp. mosquitoes; ≈400 million persons are at risk for infection each year (*2*–*5*). In 2018, Rajasthan State in India reported the country's first known cases of ZIKV infection (*6*). In that report, researchers tested household contacts and unrelated febrile persons near a single index case using a quantitative real-time reverse transcription PCR (qRT-PCR). The authors found that 153 (7.48%) of 2,043 contacts were positive for ZIKV viral RNA. This result demonstrates that ZIKV can begin circulation in new regions without a specific outbreak event. We report evidence of co-circulation of dengue virus serotype 2 (DENV-2) and Brazil-origin ZIKV in Pakistan.

The Study

In November 2021, local news sources reported an unknown viral outbreak in Karachi, Pakistan, which was subsequently investigated by the Field Epidemiology Lab Training Program of the Health Department–Sindh (*7*–*9*). DENV is endemic to the region, and infection outbreaks are common. We selected 7 patients with symptoms consistent with arbovirus infection, including fever, chills, headache and myalgia, for metagenomic analysis. We also probed blood samples with a pan-virus oligo panel and sequenced the samples to identify possible causative pathogens (Appendix, Tables 4, 5; https://wwwnc.cdc.gov/EID/article/31/8/25-0342-App1.pdf). We identified several viruses, including pegivirus, DENV), and ZIKV (Appendix Table 6). Results confirmed 6 patients were positive for DENV-2 and 2 were positive for ZIKV, including 1 person (patient E) co-infected with both viruses. Those results were consistent with qRT-PCR, apart from a weakly positive DENV that we could not identify in patient F from metagenomic reads (Table 1).

We obtained 7 complete and 1 partial orthoflavivirus genomes from the 7 patient samples (Appendix). Phylogenetic analysis confirmed all observed DENV to be the cosmopolitan genotype of DENV-2 of recent East and Southeast Asia origin (Appendix Figure 7). However, the 2 ZIKV strains we observed were more closely related to ZIKV circulating in South America than to contemporaneous ZIKV in neighboring countries to Pakistan (Figure, panels A, B; Appendix Figure 8). Three ZIKV amino acid changes were unique to the Pakistan viruses, and their inferred

Author affiliations: The Aga Khan University, Karachi, Pakistan (N.T. Iqbal, K. Ahmed, S.F. Mahmood, E. Khan); University of Washington, Seattle, Washington, USA (K. Sawatzki, J. Tisoncik-Go, E. Smith, K. Voss, J. Cornelius, W.C. Van Voorhis); National Institutes of Health, National Institute of Allergy and Infectious Diseases, Bethesda, Maryland, USA (L. Wang, A.B. Spaulding, L. Serebryannyy, D.C. Douek); Pakistan Field Epidemiology Laboratory Training Program, Karachi, (M.A. Syed); University of Minnesota, Minneapolis, Minnesota, USA (M. Gale, Jr.)

DOI: http://doi.org/10.3201/eid3108.250342

[1]These first authors contributed equally to this article.

Table 1. Real time qRT-PCR results for DENV and ZIKV in metagenomics analysis groups for co-circulation of dengue and South America–origin Zika viruses, Pakistan, 2021–2022*

Patient	DENV (Ct<40)	ZIKV (Ct<40)	ZIKV (Ct<38.5)	ZIKV (Ct<38.5)
A	**20.3**	Negative	Not done	Not done
B	**39.74**	Negative	Not done	Not done
C	**26.91**	Negative	Not done	Not done
D	**31.74**	Negative	Not done	Not done
E	**37.77**	**38.73**	Not done	Not done
F	**39.35**	Negative	**37.33**	39.05
G	Not done	Not done	Not done	Not done

*Bold text represents positive assay values. Ct, cycle threshold; DENV, dengue virus; qRT-PCR, quantitative reverse transcription PCR; ZIKV, Zika virus.

closest ancestor was most closely comparable to the Brazil ZIKV subclade (Figure, panel C). We observed 2 changes in prM, T74A and S109P. S109P is located in the prM region, which maps to the binding interface with Env, and both changes straddle the prM host cleavage site. We noted the third amino acid change, K587R, located at the 3′ end of the NS3-coding region, adjacent to NS4A. We identified a final change at the 3′ end of the NS1-coding region encoding M349V that distinguishes the subclade among other viruses circulating in Brazil and other regions of South America (Appendix Figure 9).

In 2022, we collected samples from a different cohort of 13 patients with evidence of ZIKV antibodies. Those patients demonstrated symptoms characteristic of arbovirus infection, including fever, rash, arthralgia, and thrombocytopenia (Appendix Table 7). We collected blood samples on day 1 (n = 4) and day 28 (n = 12) after hospital admission and assayed for evidence of recent DENV and ZIKV infection by ELISA and Meso Scale discovery (MSD) immunoassays (Table 2; Appendix). We tested patients with ≥1 positive or equivocal Zika IgG ELISA result by qRT-PCR for evidence of active infection. All 4

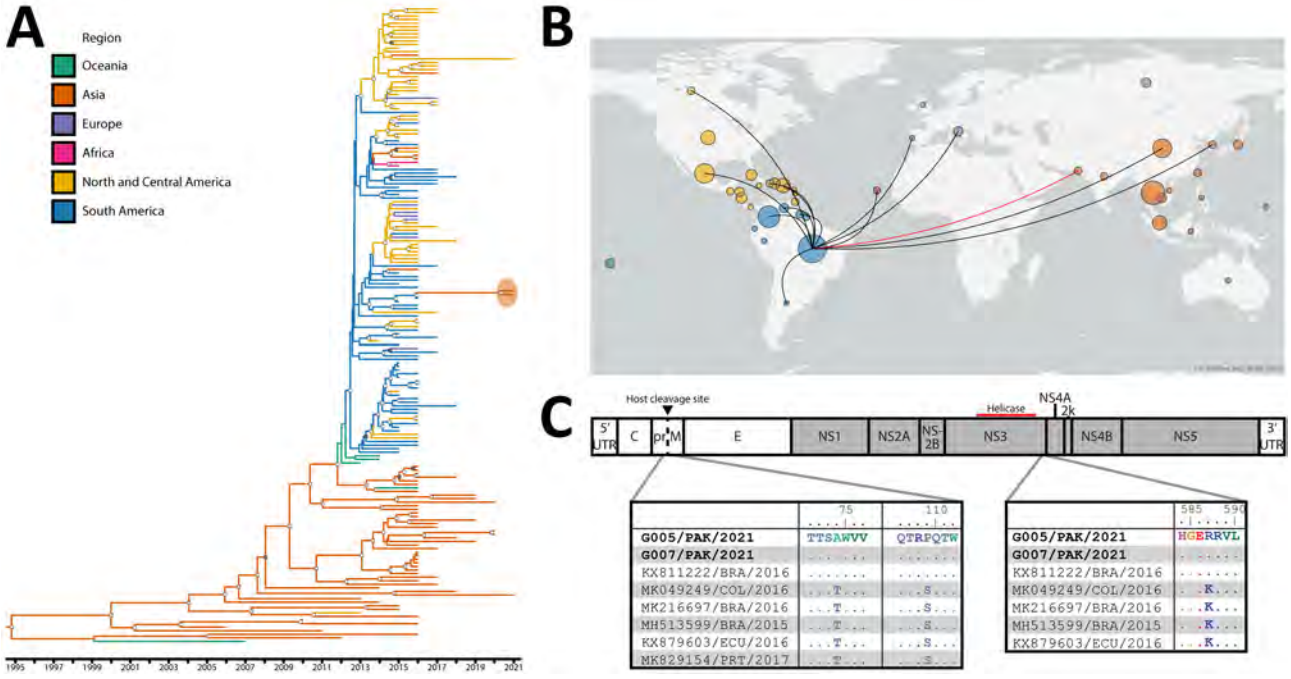

Figure. Phylogenetic analysis of Zika viruses (ZIKV) identified in a study of co-circulation of dengue and South American–origin Zika viruses, Pakistan, 2021–2022. A) BEAST (https://beast.community/index.html) time-aware maximum clade credibility tree describing inferred genetic lineage of global Asian-lineage ZIKV, colored by observed and estimated geographic origin. Branch backbones are colored when called with >80% confidence by Augur. Two newly described viruses from Pakistan are circled in orange, with the closest observed ancestors derived from circulating South American ZIKV. Open circles indicate posterior probability >0.9, solid dots 0.8–0.9. B) Phylogeographic map illustrating inferred international ZIKV transmission events originating in Brazil from viruses included in panel A. Map was visualized by inferred origin and transmission using Auspice (https://docs.nextstrain.org/projects/auspice/en/stable/index.html). Circle size is relative to the number of included viruses from the country and colored by continent. Red line highlights the inferred Brazil to Pakistan incursion. C) ZIKV sequences selected from the same clade and subclade as Pakistan-origin viruses aligned to G005/PAK/2021. Identical amino acid residues are shown as dots. We identified 2 changes in prM, T74A and S109P (left), and 1 in NS3, K587R (right). G005/PAK/2021 corresponds to patient E; G007/PAK/2021 corresponds to patient F. NS, nonstructural; UTR, untranslated region.

Table 2. Real time qRT-PCR and serologic assay results for DENV and ZIKV infection determination in study of co-circulation of dengue and South America–origin Zika viruses, Pakistan, 2021–2022*

Patient	Day	DENV (Ct<40)	ZIKV (Ct<40)	ZIKV (Ct<38.5)	ZIKV (Ct<38.5)	Zika IgG ELISA (OD)	MSD Assay IgG, ECL (ZIKV/DENV)
1	1	**24.88**	Not done	Negative	**37.57**	**0.2269**	5,572/9,031 (0.6×)
2	1	**32.95**	Not done	Negative	Negative	0.1356 (eq)	46,364/69,634 (0.6×)
3	1	**38.59**	Negative	**34.72**	**37.46**	0.1855 (eq)	35,809/57,433 (0.6×)
4	1	**37.64**	Negative	Negative	**37.21**	**1.9765**	**42,482/5,103 (8×)**
5	28	Negative	Not done	Negative	Negative	**2.1297**	103,454/378,372 (0.2×)
6	28	Negative	Not done	Negative	Negative	**1.1431**	25,304/111,319 (0.2×)
2	28	Negative	Not done	**33.36**	Negative	**2.3136**	167,354/644,477 (0.2×)
7	28	Negative	Not done	Negative	Negative	**1.192**	24,500/115,362 (0.2×)
8	28	**39.23**	Not done	Negative	Negative	**0.2008**	**14,599/5,609 (2.6×)**
9	28	**39.50**	Not done	Negative	Negative	**0.8356**	36,655/1,098,636 (0.03×)
3	28	Negative	Negative	**38.44**	38.93	**1.5498**	**30,842/5,012 (6×)**
4	28	Negative	Negative	Not done	Not done	−0.0012	8,975/319,294 (0.03×)
10	28	Negative	Not done	Negative	Negative	**0.2963**	22,245/413,868 (0.05×)
11	28	Negative	Not done	Negative	Negative	0.1616 (eq)	9,915/462,840 (0.02×)
12	28	Negative	Not done	Negative	39.04	**0.2974**	75,115/194,188 (0.4×)
13	28	44.26	Not done	**36.47**	Negative	**1.3555**	53,643/161,184 (0.3×)

*Bold text represents positive assay values. Ct, cycle threshold; DENV, dengue virus; ECL, electrochemiluminescence; eq, equivocal; MSD, Meso Scale Discovery; OD, optical density; qRT-PCR, quantitative reverse transcription PCR; ZIKV, Zika virus.

patient samples from day 1 tested positive for DENV by qRT-PCR; 1 patient (patient 3) tested positive for ZIKV infection by duplex qRT-PCR. By day 28, two of the 12 patient samples we collected were positive for DENV and none were positive for ZIKV by qRT-PCR. Three patients were antibody positive for ZIKV by both ELISA and MSD, which strictly controls for cross-reactivity between DENV-2 and ZIKV nonstructural (NS) 1 proteins.

Among the 2022 cohort of patients we sampled, 2 patients had longitudinal samples consistent with DENV and ZIKV co-infection. The first (patient 3) was symptomatic for 7 days upon admission. He initially sought treatment for respiratory symptoms, and tests revealed an elevated total leukocyte count (22.8×10^9 cells/L; reference range $5.0–10.0 \times 10^9$ cells/L), with neutrophils comprising 88% (reference range 50–80%) and lymphocytes 7% (reference range 20–40%). On day 1 of inpatient treatment, he tested positive by qRT-PCR for DENV (cycle threshold [Ct] 38.59) and ZIKV (Cts 34.72, 37.46) co-infection and was equivocal for ZIKV antibodies (Table 2). By day 28, he had ZIKV NS1 IgG as measured by ELISA (optical density [OD] 1.5498) and MSD, which showed a 6-fold higher ZIKV signal in the ZIKV/DENV-2 NS1 IgG ratio (electrochemiluminescence [ECL] 30,842/5,012).

The second co-infected patient (patient 4) had been symptomatic for 3 days before hospital admission. His symptoms were consistent with dengue fever, including a low platelet count (38×10^9/L; reference range $150–400 \times 10^9$/L) and a high lymphocyte percentage (47.9%; reference range 20–40%). On day 1 of inpatient treatment, he tested positive by both ELISA (OD 1.9765) and MSD (ECL 42,482/5,103, 8-fold) for ZIKV antibodies. qRT-PCR of this patient's sample was initially positive for DENV and equivocal for ZIKV (1/2 positive amplicons). By day 28, there was a major peak in the DENV-2 NS1 IgG response measured by MSD assay, with a corresponding decline in ZIKV IgG (ECL 8,975/319,294, 0.03-fold). Those results are suggestive of an initial, symptomatically mild ZIKV infection followed by emergent DENV co-infection. Both co-infected patients, as well as patient E, from whom we assembled both viral genomes, represent 3 cases of probable ZIKV-DENV co-infection.

Conclusions

Identifying and characterizing etiologic agents associated with infections of unknown etiology in Pakistan is critical to understanding the consequences of new or re-emerging viruses in the region. We identified unexpected ZIKV in Pakistan using a panviral metagenomics approach and were able to confirm it in additional samples using a real time qRT-PCR. Antibody testing further revealed co-circulation contemporaneous with dengue virus, with high seroconversion.

Metagenomic sequencing further revealed ZIKV as an arbovirus importation into the region. Rather than originating from bordering or nearby countries, the most closely related available ZIKV sequences originate from Brazil in 2016. This distinct clade of Asian-genotype ZIKV emerged in Brazil in 2015 and rapidly spread across the Americas. Brazil-origin ZIKV from the same time period was exported to many other countries, including Italy, South Korea, and Cabo Verde (Figure, panel C). Although many of those events are self-limiting, favorable ecologic conditions can establish new

areas of virus circulation, now making ZIKV a pathogen that should be part of both public health guidelines and private practice diagnostic considerations in Pakistan.

In summary, the evidence revealed from our investigation indicates that Brazil-origin ZIKV has spread to local *Aedes* spp. mosquitoes and is endemically circulating in Pakistan. ZIKV and DENV overlap in host mosquito species (*Ae. aegypti* and *Ae. albopictus*); therefore, incorporating ZIKV screening and surveillance in DENV management programs would make sense. As new arboviruses are discovered, outbreaks across diverse, international geographic areas will prompt the need to interrogate acute and convalescent samples to identify causative agents and develop specific diagnostic and therapeutic strategies for use in outbreak responses.

Acknowledgments

We thank Zack Lindbloom-Brown for information technology infrastructure support.

This study was funded in part by National Institute for Allergy and Infectious Diseases, National Institutes of Health, Centers for Research in Emerging Infectious Disease (program grant no. AI151698) establishing the United World Antiviral Research Network (grant nos. AI183793 and AI179722 to M.G.), and the Intramural Research Program of National Institute for Allergy and Infectious Diseases, National Institutes of Health.

About the Author

Dr. Iqbal is an associate professor and vice chair in the Department of Paediatrics and Child Health and an associate professor in the Department of Biological and Biomedical Sciences at Aga Khan University Medical College in Karachi. Her research is in infectious disease, primarily tuberculosis and enteric diseases.

References

1. Postler TS, Beer M, Blitvich BJ, Bukh J, de Lamballerie X, Drexler JF, et al. Renaming of the genus *Flavivirus* to *Orthoflavivirus* and extension of binomial species names within the family Flaviviridae. Arch Virol. 2023;168:224. https://doi.org/10.1007/s00705-023-05835-1
2. Yang X, Quam MBM, Zhang T, Sang S. Global burden for dengue and the evolving pattern in the past 30 years. J Travel Med. 2021;28:taab146. https://doi.org/10.1093/jtm/taab146
3. Waggoner JJ, Gresh L, Vargas MJ, Ballesteros G, Tellez Y, Soda KJ, et al. Viremia and clinical presentation in Nicaraguan patients infected with Zika virus, Chikungunya virus, and dengue virus. Clin Infect Dis. 2016;63:1584–90. https://doi.org/10.1093/cid/ciw589
4. Bhatt S, Gething PW, Brady OJ, Messina JP, Farlow AW, Moyes CL, et al. The global distribution and burden of dengue. Nature. 2013;496:504–7. https://doi.org/10.1038/nature12060
5. Brady OJ, Gething PW, Bhatt S, Messina JP, Brownstein JS, Hoen AG, et al. Refining the global spatial limits of dengue virus transmission by evidence-based consensus. PLoS Negl Trop Dis. 2012;6:e1760. https://doi.org/10.1371/journal.pntd.0001760
6. Malhotra B, Gupta V, Sharma P, Singh R, Sharma H, Vyas M, et al. Clinico-epidemiological and genomic profile of first Zika Virus outbreak in India at Jaipur city of Rajasthan state. J Infect Public Health. 2020;13:1920–6. https://doi.org/10.1016/j.jiph.2020.10.006
7. Centers for Disease Control and Prevention Center for Global Health. Division of Public Health Systems and Workforce Development. Pakistan FELTP. 2010 [cited 2024 Nov 1] https://stacks.cdc.gov/view/cdc/28158
8. Merchant HA. A dengue-like outbreak of unknown aetiology in Pakistan. Trop Med Health. 2022;50:35. https://doi.org/10.1186/s41182-022-00426-3
9. Waseem S, Ahmed SH, Shaikh TG, Qadar LT, Khalid S, Nimavat N, et al. Mysterious dengue-like virus: a case report from Pakistan. Clin Case Rep. 2022;10:e6107. https://doi.org/10.1002/ccr3.6107

Address for correspondence: Michael Gale, Jr., University of Minnesota, Department of Microbiology and Immunology, 689 23rd Ave SE, Minneapolis, MN 55455, USA; email: mgale@umn.edu

Genomic Surveillance Detection of SARS-CoV-1–Like Viruses in Rhinolophidae Bats, Bandarban Region, Bangladesh

Christopher Bradburne,[1] Ausraful Islam,[1] Ian Bird, Elliott Abbott, Sarah Harrison, Morgan Chunn, Diana Radune, Md Rakib Hasan, Brian Janes, Sean Lovett, John Lagergren, Timothy O'Hanlon, Konad Debnath, Clifton McKee, Mohammad Enayet Hossain, Molly Gallagher, Daniel Jacobson, Mohammed Ziaur Rahman, Katie Caviness, Raina K. Plowright, Emily S. Gurley

We sequenced sarbecovirus from *Rhinolophus* spp. bats in Bandarban District, Bangladesh, in a genomic surveillance campaign during 2022–2023. Sequences shared identity with SARS-CoV-1 Tor2, which caused an outbreak of human illnesses in 2003. Describing the genetic diversity and zoonotic potential of reservoir pathogens can aid in identifying sources of future spillovers.

Zoonotic disease risk is influenced by various factors, including reservoir host density and distribution, pathogen prevalence, pathogen release, host/human proximity, and ability to infect and spread through spillover between species (*1*). Bats are well-known coronavirus reservoirs in Southeast Asia and are candidates for genomic surveillance for potential zoonotic transmission. In other ecosystems, climate and abiotic stressors can cause proximal shifts in bat roost sites, bringing bats into contact with domestic animals where virus spillover, including Hendra virus spillover, can occur (*2*,*3*; J. Lagergren et al., unpub. data, https://www.biorxiv.org/content/10.1101/2023.12.01.569640v1). Therefore, surveillance among bats colocated with bridging hosts are critical for defining spillover risk in any given region. We report preliminary results from genomic surveillance efforts focused on *Rhinolophus* spp. bat colonies at roost sites within the region of Bandarban, Bangladesh (Figure 1). We obtained study approval from the Bangladesh Forest Department and the Research Review Committee and Animal Experimentation Ethics Committee of the icddr,b (research protocol no. PR-20058, bat capture permit no. 22.01.0000.101.23.136.21.1088).

The Study

As part of our overall field campaign, we collected fecal samples from 240 *Rhinolophus pusillus* bats, 20 each month, during May 2022–April 2023. We captured only *Rhinolophus* spp. bats and released other bat species immediately after capture. A trained veterinarian collected all the samples after anesthetizing the bats, and all the bats were released at the site of capture within 2–5 hours of capture.

We assessed sex, weight, and health of individual bats before collecting a fecal sample and, in some cases, a blood sample from the radial vein/wing vein for immunological cell counts. For our sequencing studies, we selected fecal samples from a mix of female, male, juvenile, and adult bats with different

Author affiliations: Johns Hopkins Applied Physics Laboratory, Laurel, Maryland, USA (C. Bradburne, I. Bird, S. Harrison, M. Chunn, T. O'Hanlon, M. Gallagher); icddr,b, Dhaka, Bangladesh (A. Islam, M.R. Hasan, K. Debnath, M.E. Hossain, M.Z. Rahman); National Bioforensic Analysis Center, National Biodefense Analysis and Countermeasures Center, Fort Detrick, Maryland, USA (E. Abbott, D. Radune, B. Janes, S. Lovett, K. Caviness); Biosciences Division, Oak Ridge National Laboratory, Oak Ridge, Tennessee, USA (J. Lagergren, D. Jacobson); Johns Hopkins University Bloomberg School of Public Health, Baltimore, Maryland, USA (C. McKee, E.S. Gurley); College of Veterinary Medicine, Cornell University, Ithaca, New York, USA (R.K. Plowright)

DOI: https://doi.org/10.3201/eid3108.250071

[1]These first authors contributed equally to this article.

body condition scores, choosing bats with higher leukocyte counts if those data were available. We inactivated the fecal samples by using TRIzol (Thermo Fisher Scientific, https://www.thermofisher.com) and later selected a subset of 12 fecal samples from summer 2022 (Table), representing 2 roosting locations (sites 1 and 2) in Bandarban, for initial screening on an iSeq (Illumina, https://www.illumina.com). We then performed deep sequencing on those samples by using a NextSeq 500 (Illumina). We enriched libraries by using the Comprehensive Viral Research Panel (Twist Bioscience, https://www.twistbioscience.com) supplemented with a custom-designed Chiropteran virus enrichment panel containing 134,000 probes. All sequencing was performed in a US Biosafety Level 4 facility. We deposited data into the National Center for Biotechnology Information Sequence Read Archive (submission no. SUB15226189 and BioProject no. PRJNA1249517).

We identified coronavirus sequence reads in 3 samples: B3, B4, and B6. The strongest signal was in B4, which comprised 1.2% of total reads and 5.5% of classified reads in the entire B4 sample (Table; Appendix Figures 1–3, https://wwwnc.cdc.gov/EID/article/31/8/25-0071-App1.pdf). We characterized virome components by using KRAKEN2 (*4*) and RefSeq viral database version April 2023 (Illumina). The B4-derived coronavirus sequences initially had 76.7% BLASTn (https://blast.ncbi.nlm.nih.gov/Blast.cgi?PROGRAM=blastn&PAGE_TYPE=BlastSearch&LINK_LOC=blasthome) identity to SARS-CoV-1 Tor2 (Appendix Figure 4), which was isolated in 2003 from a patient who traveled from Hong Kong, China, to Toronto, Ontario, Canada, and who was hospitalized with febrile respiratory illness (*5*).

We further compared B4 to Tor2 and relatives by creating similarity plots in SimPlot++ version 1.3 (https://github.com/Stephane-S/Simplot_PlusPlus), and creating maximum-likelihood phylogenetic trees aligning the whole genome, RNA-dependent RNA polymerase, and spike sequences by using MAFFT version 7.508 (https://mafft.cbrc.jp/alignment/software) and IQ-TREE version 2.3.6 (http://iqtree.cibiv.univie.ac.at) (Appendix Figures 4, 5) (*6*–*11*). We found 2 notable dropouts in the alignment to SARS-CoV-1 Tor2: a 1-kb gap at nonstructural protein (NSP) 2 and a 2.1-kb gap over most of the spike receptor-binding domain (RBD) (Appendix Figure 4). To obtain complete genome coverage, we designed 2 primer pairs for each gap and used those primers to generate and sequence amplicons (Appendix Table 1). Initial amplicon analysis using BLASTn provided GenBank accession no. KY417143.1, bat SARS-like coronavirus isolate RS4081, which shared 85%–94% identity over a 99% query length. The main difference was the spike region (85% identity), which had no hits for 214 nt. A BLASTx (https://blast.ncbi.nlm.nih.gov/Blast.cgi?PROGRAM=blastx&PAGE_TYPE=BlastSearch&LINK_LOC=blasthome) query of the spike-specific amplicon indicated 76.2% identity (182 mismatches and 8 gaps) over a 97% query length to GenBank accession no. QVN46559.1, a spike glycoprotein from bat SARS-like coronavirus Khosta-1. A top BLASTx hit for the NSP2-specific amplicon was protein sequence NP_828861.2, an NSP2 of SARS-CoV-1 Tor2, which had 72.5% identity over a 99% query length. Further phylogenetic analysis of whole genomes, spike, and RNA-dependent RNA polymerase supported a novel virus with close spike homology to *Sarbecovirus* spp. (Appendix Figure 5).

We used AlphaFold modeling (European Molecular Biology Laboratory, European Bioinformatics Institute, https://alphafold.ebi.ac.uk) to compare the RBD of B4 with SARS-CoV-1 Tor2 RBD

Figure 1. Location of Bandarban Region, Bangladesh, where genomic surveillance for detection of SARS-CoV-1–like viruses in Rhinolophidae bats was conducted during 2022–2023.

Table. Subset of samples selected for enrichment next-generation sequencing from genomic surveillance detection of SARS-CoV-1–like viruses in Rhinolophidae bats, Bandarban Region, Bangladesh, 2022–2023*

ID no.	Sample date, 2022	Roost site	Life stage/sex	Weight, g	Leukocyte counts		Health	Sequence reads		
					Neutrophils	Lymphocytes		Total raw, $\times 10^6$	Viral classified, $\times 10^6$	Coronavirus classified
B1	May 19	1	Adult/M	6.01	NA	NA	Fair	22.42	4.28	0
B2	May 21	1	Adult/F	5.9	NA	NA	Fair	29.2	6.69	0
B3	Jul 20	2	Adult/M	13.82	NA	NA	Good	30.16	1.27	1,420
B4	Jul 21	2	Adult/F	11.95	7	4	Good	17.97	4.01	220,000
B5	Jul 23	2	Adult/M	11.58	3	1	Good	25.9	5.54	0
B6	Jul 23	2	Juvenile/F	5.3	15	6	Fair	26.56	5.91	1,400
B7	Aug 29	2	Juvenile/M	4.69	50	3	Fair	23.76	4.99	0
B8	Aug 29	2	Juvenile/M	5.66	6	7	Fair	24.41	3.86	0
B9	Aug 29	2	Adult/F	10.86	10	12	Good	25.2	2.07	0
B10	Aug 30	2	Adult/F	11.92	25	20	Good	25.04	5.71	0
B11	Aug 30	2	Juvenile/F	5.17	10	7	Fair	28.2	7.11	0
B12	Sep 19	2	Juvenile/F	5.06	9	5	Fair	23.86	5.2	0

*In addition to neutrophils and lymphocytes shown in the table, leukocyte counts included eosinophils, basophils, and monocytes; however, none had >2 counts for any individual bat. Health was assessed by palpation of pectoral muscle mass. Viral-classified reads were compared with a viral sequencing database. ID, identification; NA, not applicable.

(Appendix Figure 6). Folding indicated similar shape and functionality and exhibited nonsynonymous substitutions and insertions. Two insertions were asparagine dimers, located on an edge likely to interact with mammalian angiotensin converting enzyme 2 (ACE2), and 1 insertion was a threonine located on another edge, making the B4 RBD sample structurally close to a sample from a known zoonotic human outbreak.

The binding of virus RBD to the primary receptor ACE2 is necessary for spillover infection to occur. We used a synthetic Förster resonance energy transfer–based assay (*12*) to test the binding affinity of known RBDs and the B4-derived RBD from our

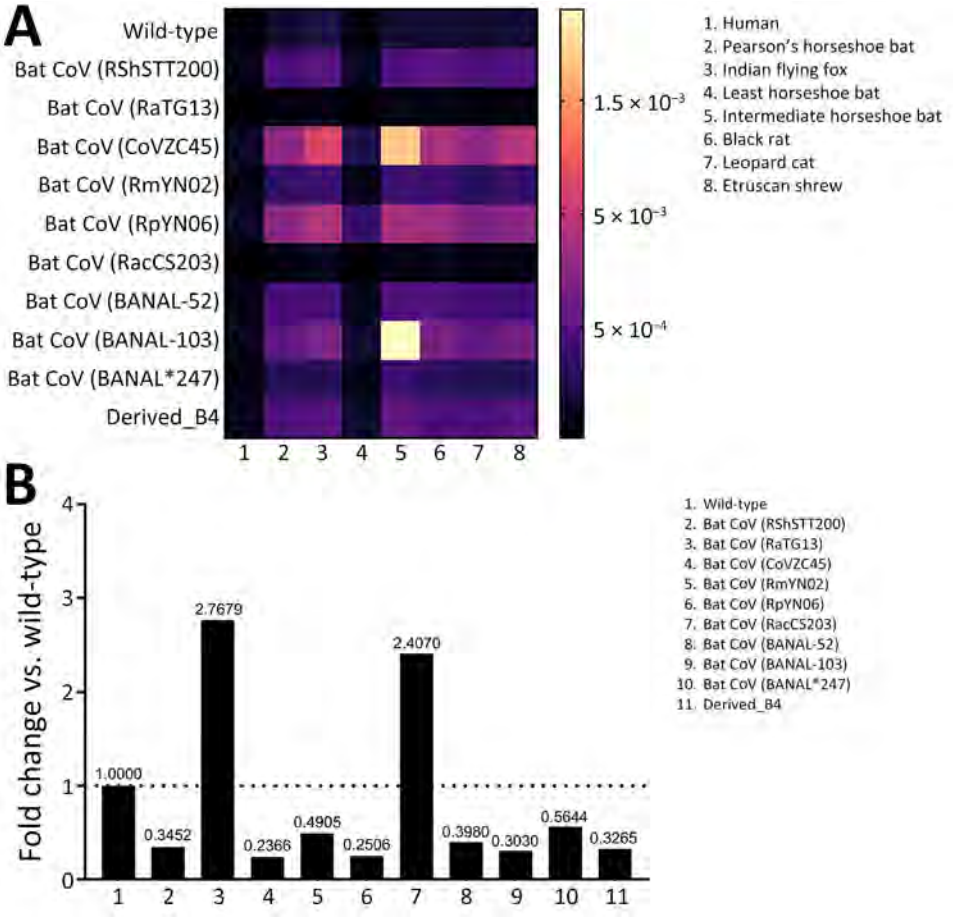

Figure 2. Binding efficiency and fold change of SARS-CoV-1–like viruses in Rhinolophidae bats, Bandarban Region, Bangladesh. A) Heatmap depicting the binding efficiency (Kd) of receptor-binding domain (RBD) sequences from the derived B4 sample and other known regional bat coronaviruses, with the angiotensin converting enzyme 2 (ACE2) sequences from regional bridging hosts. The map shows that derived B4 has low to moderate binding efficiency across hosts. B) Fold change of coronavirus RBDs including derived B4 to human ACE2, relative to wild-type virus (horizontal dotted line). B4, samples from bat 4; CoV, coronavirus.

genomic surveillance data (Appendix Figure 7). We used ACE2 receptors from a variety of sympatric mammals (Appendix Table 2), including species that might reside near our bat sampling sites, such as *Rattus* spp. rats, Leopard cats (*Prionailurus bengalensis*), and humans (*13*). We chose ACE2 of the Etruscan shrew (*Suncus etruscus*) , which had sequence available for protein derivation, as a representative *Suncus* species for testing. That species has not specifically been observed yet in Bandarban, but its close relative, the *S. murinus* shrew, is widespread there and throughout Bangladesh. Dissociation constants for the novel B4 and 10 other bat coronavirus RBDs showed moderate binding of B4 to several native sympatric animals (Figure 2, panel A).

We were also interested in the potential of the Tor2 homologous B4-derived virus to infect humans. Therefore, we evaluated binding affinity relative to the 2019 wild-type SARS-CoV-2 RBD (Figure 2, panel B). The B4-derived RBD demonstrated approximately one third the binding efficiency of the wild-type strain, which was similar to results for other tested bat coronaviruses not yet detected in humans.

In 2019, a Tor2 analog was described in a bat reservoir in Korea (*14*), indicating the viral homologue may be regionally widespread from Bangladesh to southern China and the Korean Peninsula. Abiotic stress including human land use is known to stress bat health and drive them closer to potential transitional hosts, a process implicated in spillover of other viruses (*2*,*3*).

Conclusions

We report a coronavirus in bats in Bangladesh that has high similarity to SARS-CoV-1 Tor2, isolated in 2003 from a febrile patient who had secondary exposure to a person who contracted coronavirus from an environmental source in southern China (*5*). The virus detected in Bandarban, Bangladesh, and sequenced and analyzed in this study shares identity with Tor2, except in the NSP2 and RBD genomic regions. The synthetically expressed RBD shows moderate binding affinity to ACE2 receptors of nearby species, suggesting potential for infection of co-occurring taxa within the host range. Additional study is needed to elucidate what drives host viral shedding and if spillovers are occurring that pose a public health risk. Describing the genetic diversity and transmission potential of this and other potentially zoonotic pathogens can aid in identifying sources and risk of future emerging spillovers.

Acknowledgments

We thank April Manzella for Biosafety Level 4 laboratory support, Mike Lee for bioinformatics support, and Robert Bull for support and encouragement throughout this study. We also thank Emma Spence, Sara LaTrielle, Manuel Ruiz-Aravena, Agnieszka Rynda-Apple, and Monica Hall for administrative and logistic support.

C.M., R.K.P., and E.S.G. were supported by the Defense Advanced Research Projects Agency's PREventing EMerging Pathogenic Threats program (cooperative agreement no. D18AC00031). R.K.P. (grant no. DEB-1716698) and J.L., D.J., and R.K.P. (grant nos. EF-2133763 and EF-2231624) were supported by the National Science Foundation. This work was funded in part under agreement no. HSHQDC-15-C-00064 awarded to Battelle National Biodefense Institute by the US Department of Homeland Security (DHS) Science and Technology Directorate for the management and operation of the National Biodefense Analysis and Countermeasures Center, a federally funded research and development center.

The views and conclusions contained in this document are those of the authors and should not be interpreted as necessarily representing the official policies, either expressed or implied, of DHS or the US government. DHS does not endorse any products or commercial services mentioned in this presentation. In no event shall DHS, Battelle National Biodefense Institute, or National Biodefense Analysis and Countermeasures Center have any responsibility or liability for any use, misuse, inability to use, or reliance upon the information contained herein. In addition, no warranty of fitness for a particular purpose, merchantability, accuracy, or adequacy is provided regarding the contents of this document.

This manuscript has been coauthored by UT-Battelle, LLC, under contract no. DE-AC05-00OR22725 with the US Department of Energy (DOE). The publisher, by accepting the article for publication, acknowledges that the US government retains a nonexclusive, paid-up, irrevocable, worldwide license to publish or reproduce the published form of this manuscript, or allow others to do so, for US government purposes. DOE will provide public access to these results of federally sponsored research in accordance with the DOE Public Access Plan (http://energy.gov/downloads/doe-public-access-plan).

About the Author

Dr. Bradburne is a biologist and project manager at The Johns Hopkins University Applied Physics Laboratory. His research interests include applying sequencing and

bioinformatics to viral and bacterial detection and diagnostics. Dr. Islam is a veterinarian working at the Infectious Diseases Division of the icddh,b. His research interests include zoonotic diseases.

References

1. Plowright RK, Parrish CR, McCallum H, Hudson PJ, Ko AI, Graham AL, et al. Pathways to zoonotic spillover. Nat Rev Microbiol. 2017;15:592–10. https://doi.org/10.1038/nrmicro.2017.45
2. Eby P, Peel AJ, Hoegh A, Madden W, Giles JR, Hudson PJ, et al. Pathogen spillover driven by rapid changes in bat ecology. Nature. 2023;613:340–4. https://doi.org/10.1038/s41586-022-05506-2
3. Cashman M, Vergara VGM, Lagergren JH, Lane M, Merlet J, Atkinson M, et al. Longitudinal effects on plant species involved in agriculture and pandemic emergence undergoing changes in abiotic stress. In: Proceedings of the Platform for Advanced Scientific Computing conference; 2023 Jun 26–28; Davos, Switzerland. New York: ACM; 2023.
4. Wood DE, Lu J, Langmead B. Improved metagenomic analysis with Kraken 2. Genome Biol. 2019;20:257. https://doi.org/10.1186/s13059-019-1891-0
5. Marra MA, Jones SJM, Astell CR, Holt RA, Brooks-Wilson A, Butterfield YS, et al. The genome sequence of the SARS-associated coronavirus. Science. 2003;300:1399–404. https://doi.org/10.1126/science.1085953
6. Katoh K, Misawa K, Kuma K, Miyata T. MAFFT: a novel method for rapid multiple sequence alignment based on fast Fourier transform. Nucleic Acids Res. 2002;30:3059–66. https://doi.org/10.1093/nar/gkf436
7. Minh BQ, Schmidt HA, Chernomor O, Schrempf D, Woodhams MD, von Haeseler A, et al. IQ-TREE 2: new models and efficient methods for phylogenetic inference in the genomic era. Mol Biol Evol. 2020;37:1530–4. https://doi.org/10.1093/molbev/msaa015
8. Kalyaanamoorthy S, Minh BQ, Wong TKF, von Haeseler A, Jermiin LS. ModelFinder: fast model selection for accurate phylogenetic estimates. Nat Methods. 2017;14:587–9. https://doi.org/10.1038/nmeth.4285
9. Hoang DT, Chernomor O, von Haeseler A, Minh BQ, Vinh LS. UFBoot2: improving the ultrafast bootstrap approximation. Mol Biol Evol. 2018;35:518–22. https://doi.org/10.1093/molbev/msx281
10. Samson S, Lord É, Makarenkov V. SimPlot++: a Python application for representing sequence similarity and detecting recombination. Bioinformatics. 2022;38:3118–20. https://doi.org/10.1093/bioinformatics/btac287
11. Ruan YJ, Wei CL, Ee AL, Vega VB, Thoreau H, Su ST, et al. Comparative full-length genome sequence analysis of 14 SARS coronavirus isolates and common mutations associated with putative origins of infection. Lancet. 2003;361:1779–85. https://doi.org/10.1016/S0140-6736(03)13414-9
12. Song Y, Rodgers VGJ, Schultz JS, Liao J. Protein interaction affinity determination by quantitative FRET technology. Biotechnol Bioeng. 2012;109:2875–83. https://doi.org/10.1002/bit.24564
13. Akhter T, Khan MMH, Nath S, Hasan S, Ahmed T. Photographic evidences of Pygmy white-toothed shrew *Suncus etruscus* in Bangladesh. Bangladesh J Zool. 52:337–40. https://doi.org/10.3329/bjz.v52i3.80794
14. Kim Y, Son K, Kim Y-S, Lee S-Y, Jheong W, Oem J-K. Complete genome analysis of a SARS-like bat coronavirus identified in the Republic of Korea. Virus Genes. 2019;55:545–9. https://doi.org/10.1007/s11262-019-01668-w

Addresses for correspondence: Chris Bradburne, Johns Hopkins University Applied Physics Laboratory, 11100 Johns Hopkins Rd, Laurel, MD 20723-6099, USA; email: chris.bradburne@jhuapl.edu

Crimean-Congo Hemorrhagic Fever Virus among Goats, Southern Bhutan

Sangay Rinchen,[1] Yoshihiro Kaku,[1] Eunsil Park,[1] Puspa Maya Sharma, Dawa Tshering, Tenzinla Tenzin, Aya Matsuu, Akiko Okutani, Ken Maeda, Shigeru Morikawa

Author affiliations: National Centre for Animal Health, Serbithang, Bhutan (S. Rinchen, P.M. Sharma, D. Tschering, T. Tenzin); National Institute of Infectious Diseases, Shinjuku, Tokyo, Japan (Y. Kaku, E. Park, A. Matsuu, A. Okutani, K. Maeda, S. Morikawa)

DOI: http://doi.org/10.3201/eid3108.241989

We conducted serosurveillance for Crimean-Congo hemorrhagic fever virus (CCHFV) among goats in southern Bhutan. Testing serum samples from 472 goats for CCHFV-specific IgG using an indirect fluorescent antibody test and ELISA, we found CCHFV antibody–positive goats along the analyzed border region with India, indicating widespread distribution of CCHFV in this area.

Crimean-Congo hemorrhagic fever (CCHF) is an acute febrile zoonosis caused by CCHF virus (CCHFV). CCHFV belongs to the genus *Orthonairovirus* (family Nairoviridae, order Bunyavirales) (*1*). It is transmitted by ticks, particularly of the genus *Hyalomma*, and is widespread across Africa, Asia, and Europe. Symptoms associated with CCHFV include fever, headache, myalgia, back pain, and arthralgia, and infected patients demonstrate varying degrees of hemorrhage (petechiae to maculopapular) in severe cases. Ticks play a crucial role in the CCHFV infection cycle, maintaining the virus through transstadial and transovarial transmission, and the virus persists in a tick–vertebrate–tick enzootic cycle. Human infection can result from tick bites or direct contact with asymptomatic animals, and CCHF occurs most frequently among livestock workers, slaughterhouse workers, and veterinarians. To mitigate the infection risk in humans, a One Health approach, including proactive surveillance of animals and ticks, is crucial.

In India, researchers described the first reported human case of CCHF in Gujarat in 2011; subsequent reports documented sporadic outbreaks (*2*–*4*). Since those initial reports, investigators have conducted CCHFV infection surveys in livestock and ticks in various locations in India, noting the virus' widespread distribution (*5*–*7*).

Bhutan shares a long and porous border with India, providing many opportunities for animal and human movement between countries. Continuous surveillance of various zoonotic agents in this area is therefore critical in assessing the risk for infection to animals and humans. To investigate CCHFV, a research team conducted a pilot serosurvey in 2015 using livestock sera collected in the southern region of Bhutan (*8*). They collected 81 goat samples from Sarpang district and 92 bovine samples from Trashigang and Samtse districts and tested them for CCHFV-specific IgG using an in-house ELISA kit (National Institute of Virology, Pune, India). Unfortunately, the results of this pilot survey did not fully elucidate the seroprevalence of CCHFV in southern Bhutan because of the limited sample size and study area.

To obtain more detailed information on the geographic range of CCHFV antibody-positive animals in southern Bhutan, we focused our study on goats in the southern border region, particularly the western and central areas along the border, where multiple cross-border animal trade hubs exist. We analyzed a total of 472 goat serum samples, collected in 2015 and 2022 from those border areas, using a combination of 2 testing methods: a different in-house ELISA kit (National Institute of Infectious Diseases, Tokyo, Japan) and an indirect fluorescent antibody test (Appendix, https://wwwnc.cdc.gov/EID/article/31/8/24-1989-App1.pdf). We employed this dual analytical approach to improve specificity against CCHFV antibodies, considering the possibility that multiple *Orthonairovirus* species co-circulate.

We charted seroprevalence of CCHFV in each district (Table), noting the presence of CCHFV antibody–positive goats in all surveyed districts from the central to western parts of Bhutan's southern border region. Our results confirmed the widespread seropositivity of CCHFV in this region, also revealing substantial regional variation in antibody positivity, ranging from high-positive (Sarpang, Samtse, and Chukha) to low-positive (Dagana and Tsirang). The 3 districts with high seropositivity rates are among the key formal entry points from India to Bhutan, characterized by numerous cross-border settlements, robust trade activities, and fluid cross-border movement of humans and animals. Considering both sides of the border as the same epidemiologic unit, the detection of seropositive animals in multiple districts suggested that CCHFV circulates in this region.

Our initial plan for this study entailed collecting samples in a much shorter timeframe; however, budget constraints and the COVID-19 outbreak resulted in a longer time lag between collection years.

[1]These authors contributed equally to this article.

Table. Comparison of viral seroprevalence among goats in southern border region in study of Crimean-Congo hemorrhagic fever virus among goats, southern Bhutan

District	No. tested samples	No. positive samples	Seroprevalence, %	Year of sample collection
Samtse	153	67	43.8	2015
Sarpang	81	49	65.1	2015
Chukha	123	39	31.7	2022
Dagana	74	6	8.1	2022
Tsirang	41	2	4.9	2022

Nonetheless, considering the frequent cross-border movement of animals and humans and the lack of comprehensive tick control measures in southern Bhutan, we postulated that the seroprevalence in goats did not change considerably during or after the sampling period. A better understanding of the spatial and temporal patterns of viral distribution of CCHFV in this region of Bhutan will require a longitudinal study targeting a larger sample size of animals and ticks.

Our findings document widespread seropositivity to CCHFV in goats in the western and central regions along Bhutan's southern border. In a previous serologic study (*8*), CCHFV-specific IgG was not detected in bovine samples from Samtse and Trashigang districts, which might have been a result of the limited sample size and study area. Cattle are known to be susceptible to CCHFV infection, so further testing of additional bovine samples is necessary to investigate CCHFV infection among cattle in Bhutan. More research is also needed to collect and analyze ticks to investigate their viral infection status. By obtaining viral genetic information from ticks in this region of Bhutan, researchers can confirm the genotypes of CCHFV prevalent in this area, providing potential insight into virus circulation. Because human CCHF cases might be underreported in Bhutan, conducting antibody testing of livestock workers in the country's southern region might inform both prevalence data and public health initiatives to educate workers on preventive measures to protect against CCHFV infection.

Acknowledgments

We thank Edanz (https://jp.edanz.com/ac) for editing a draft of this manuscript.

This research was approved by the Livestock Technical Advisory Committee of the Department of Livestock, Ministry of Agriculture and Livestock, Bhutan (approval no. DoL/GEN-03/2020-2021/108).

This work was supported by the Japan Agency for Medical Research and Development (grant no. 23fk0108683j1701) and the Japan Society for the Promotion of Science KAKENHI (grant no. 17H04489).

About the Author

Dr. Rinchen is an officiating program director at the National Centre for Animal Health, Serbithang, Bhutan. His primary research interest is the epidemiology of animal and zoonotic diseases.

References

1. Celina SS, Italiya J, Tekkara AO, Černý J. Crimean-Congo haemorrhagic fever virus in ticks, domestic, and wild animals. Front Vet Sci. 2025;11:1513123. https://doi.org/10.3389/fvets.2024.1513123
2. Mourya DT, Yadav PD, Shete AM, Gurav YK, Raut CG, Jadi RS, et al. Detection, isolation and confirmation of Crimean-Congo hemorrhagic fever virus in human, ticks and animals in Ahmadabad, India, 2010–2011. PLoS Negl Trop Dis. 2012;6:e1653. https://doi.org/10.1371/journal.pntd.0001653
3. Yadav PD, Patil DY, Shete AM, Kokate P, Goyal P, Jadhav S, et al. Nosocomial infection of CCHF among health care workers in Rajasthan, India. BMC Infect Dis. 2016;16:624. https://doi.org/10.1186/s12879-016-1971-7
4. Sahay RR, Shete AM, Yadav PD, Patil S, Majumdar T, Jain R, et al. Sequential determination of viral load, humoral responses and phylogenetic analysis in fatal and non-fatal cases of Crimean-Congo hemorrhagic fever patients from Gujarat, India, 2019. PLoS Negl Trop Dis. 2021;15:e0009718. https://doi.org/10.1371/journal.pntd.0009718
5. Mourya DT, Yadav PD, Shete AM, Sathe PS, Sarkale PC, Pattnaik B, et al. Cross-sectional serosurvey of Crimean-Congo hemorrhagic fever virus IgG in livestock, India, 2013-2014. Emerg Infect Dis. 2015;21:1837–9. https://doi.org/10.3201/eid2110.141961
6. Sahay RR, Dhandore S, Yadav PD, Chauhan A, Bhatt L, Garg V, et al. Detection of African genotype in *Hyalomma* tick pools during Crimean Congo hemorrhagic fever outbreak, Rajasthan, India, 2019. Virus Res. 2020;286:198046. https://doi.org/10.1016/j.virusres.2020.198046
7. Sarangi LN, Mulpuri H, Rana SK, Prasad A, Muthappa PN. Seroprevalence of Crimean-Congo haemorrhagic fever in Indian cattle and buffaloes. J Vector Borne Dis. 2023;60:259–64. https://doi.org/10.4103/0972-9062.364722
8. Wangchuk S, Pelden S, Dorji T, Tenzin S, Thapa B, Zangmo S, et al. Crimean-Congo hemorrhagic fever virus IgG in goats, Bhutan. Emerg Infect Dis. 2016;22:919–20. https://doi.org/10.3201/eid2205.151777

Address for correspondence: Shigeru Morikawa, Department of Veterinary Science, National Institute of Infectious Diseases, Japan Institute for Health Security, 1-23-1 Toyama, Shinjuku-ku, Tokyo 162-8640, Japan; email: morikawa@niid.go.jp

Molecular Characterization of *Echinococcus vogeli* from Human Case, Colombia, 2024

Jorge Alfredo Morcillo Muñoz, Diego Andrés Rodríguez-Lugo, Javier Hernández Moreno, María Helena Astorquiza, Luz Helena Patiño, Tatiana Marcela Cáceres, Angie Lorena Ramírez, Juan David Ramírez, Álvaro A. Faccini-Martínez

Author affiliations: Universidad Nacional de Colombia, Bogotá, Colombia (J.A. Morcillo Muñoz, D.A. Rodríguez-Lugo); Hospital Militar Central, Bogotá (J. Hernández Moreno, M.H. Astorquiza, Á.A. Faccini-Martínez); Universidad del Rosario, Bogotá (L.H. Patiño, T.M. Cáceres, A.L. Ramírez, J.D. Ramírez); University of South Florida, Tampa, Florida, USA (J.D. Ramírez); Universidad Militar Nueva Granada, Bogotá (Á.A. Faccini-Martínez)

DOI: https://doi.org/10.3201/eid3108.250361

In Colombia, 35 confirmed cases of neotropical polycystic echinococcosis were reported during 1978–2018. In most cases, *Echinococcus vogeli* was identified by means of morphologic identification. We describe a case of *E. vogeli* echinococcosis in a woman, diagnosed through PCR, mitochondrial DNA sequencing, and molecular characterization

Human echinococcosis (also known as hydatidosis) is a zoonotic neglected disease caused by infection of cestode larval form of *Echinococcus* spp. tapeworms (*1*,*2*). At least 4 *Echinococcus* species are recognized as causes of human disease and have relevance in public health: *E. granulosus* causes cystic echinococcosis and is a cosmopolitan species; *E. multilocularis* produces alveolar echinococcosis and predominates in the northern hemisphere; and *E. vogeli* causes neotropical polycystic and *E. oligarthus* unicystic echinococcosis, both confined to tropical zones in Central and South America (*1*,*2*). Neotropical polycystic echinococcosis (NPE) affects mostly persons living in rural and sylvatic regions where the cycle of the *E. vogeli* tapeworm involves the paca (*Cuniculus paca*) as the intermediate host and the bush dog (*Speothus venaticus*) as the natural final host (*2*,*3*). Nevertheless, a proposed domiciliary transmission cycle posits that human infection occurs incidentally through fecal contamination by domestic hunting dogs (alternative final host) after they fed on paca viscera (*2*,*4*).

In Colombia, 35 confirmed cases of NPE were reported during 1978–2018 (*2*,*5*–*7*). In most of them, *Echinococcus* spp. infection was identified by means of morphologic identification (*2*,*5*,*6*); in 1 case, the 2018 report, molecular detection identified the *E. vogeli* cytochrome c oxidase subunit 1 (*cox1*) mitochondrial gene without molecular characterization (*7*). Here, we present a case of *E. vogeli* echinococcosis in a woman in Colombia diagnosed through PCR, sequencing mitochondrial DNA, and molecular characterization. We obtained written consent from the patient to report on her case.

An otherwise healthy 50-year-old woman sought care at the emergency department of the Hospital Militar Central (Bogotá, Colombia) on September 23, 2024, after 8 days of epigastric and right hypochondrium pain; she did not have jaundice or other symptoms. As a child, she had lived in a rural region of Cesar Department (Colombian Caribbean region); she saw pacas often and always had kept domestic hunting dogs.

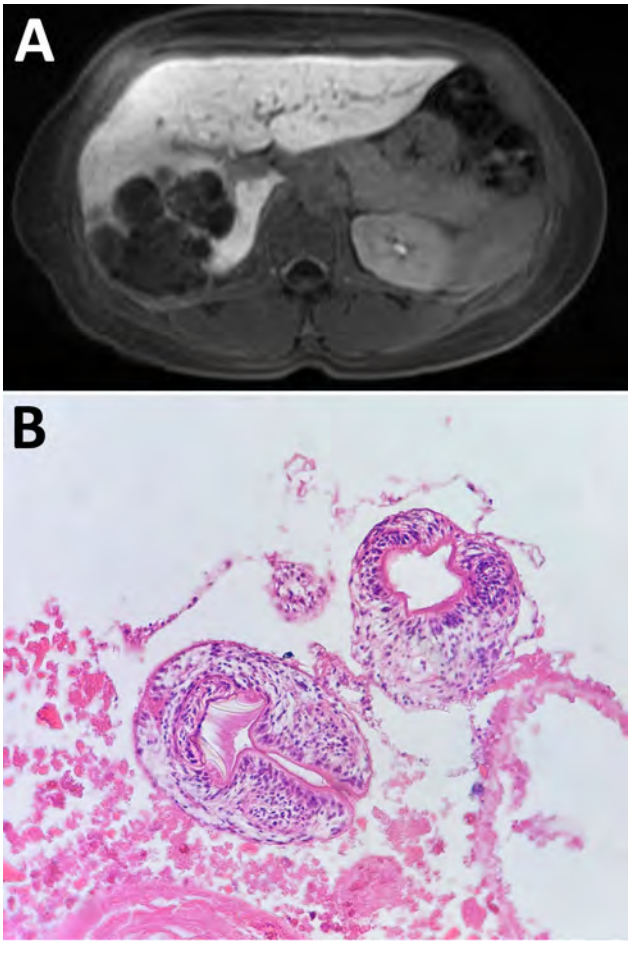

Figure 1. Neotropical polycystic echinococcosis in a woman, Colombia, 2024. A) Abdominal MRI scan showed hypodense, round polycystic vesicles, replacing right liver parenchyma with predominant peripheral calcifications and fat content. B) Protoscoleces of *Echinococcus* tapeworms with rostellar hooks. Hematoxylin & eosin staining; original magnification ×4.

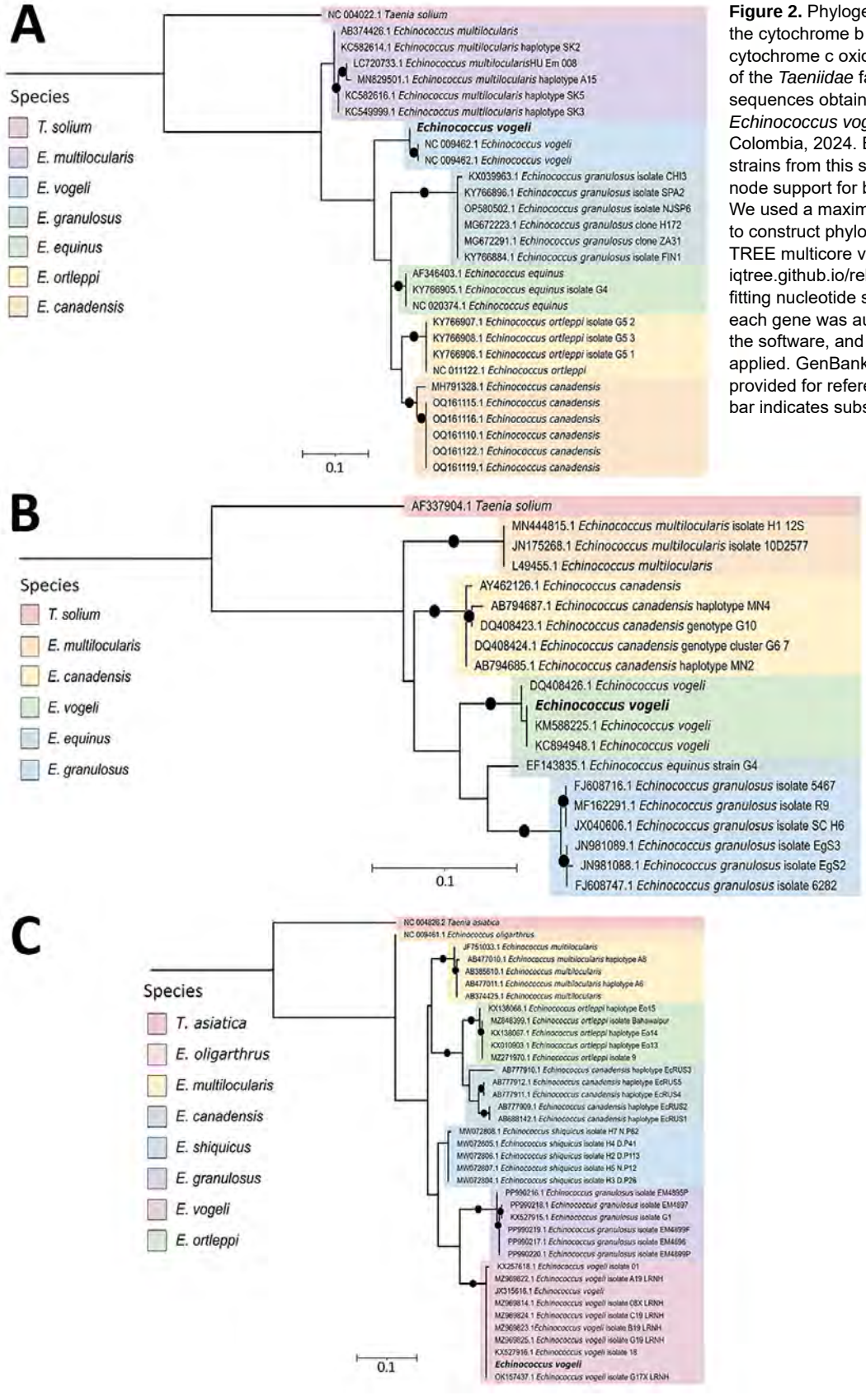

Figure 2. Phylogenetic reconstruction of the cytochrome b (A), 12S rRNA (B) and cytochrome c oxidase subunit 1 (C) genes of the *Taeniidae* family from consensus sequences obtained in study of *Echinococcus vogeli* infection in a human, Colombia, 2024. Bold text indicates strains from this study. Black dots indicate node support for bootstrap values >80. We used a maximum-likelihood approach to construct phylogenetic trees using IQ-TREE multicore version 1.6.12 (https://iqtree.github.io/release/v1.6.12). The best-fitting nucleotide substitution model for each gene was automatically selected by the software, and default parameters were applied. GenBank accession numbers are provided for reference sequences. Scale bar indicates substitutions per site.

Physical examination revealed a mild tenderness in right hypochondrium without peritoneal irritation signs. Serum liver function tests were without abnormality. Abdominal magnetic resonance imaging showed hypodense, round polycystic vesicles, replacing right liver parenchyma with predominant peripheral calcifications and fat content (Figure 1, panel A). Differential diagnoses were mucinous cystic neoplasm, hepatic liposarcoma, and hydatid cysts. We performed a total right segmental liver resection and cholecystectomy. The histopathological results of surgical liver specimen showed multiple cysts with *Echinococcus* protoscoleces (Figure 1, panel B). The patient received albendazole (200 mg 2×/d) for 1 month and was discharged.

We performed PCR on the liver histopathological sample, targeting the cytochrome b (Cob), 12S rRNA, and *cox1* genes, confirming the presence of *Echinococcus* sp. We sequenced the amplicons using Oxford Nanopore MinION (Oxford Nanopore Technologies, https://nanoporetech.com) and used those sequences for phylogenetic reconstruction. Phylogenetic analysis showed that the sequences we obtained of the 3 genes clustered with *E. vogeli* sequences downloaded from GenBank (Figure 2). Sequences from this study were deposited in GenBank (accession nos. PV243336, PV243987, and SUB15312175).

The clinical characteristics of NPE in patients depend on the location of the metacestode as well as the extent of invasion of tissues (*2*). The liver is the most frequently affected organ (*2*). Metacestodes could be found in the liver alone or with vesicles situated in the abdomen, in the liver and the lungs or pleural cavities, or only as calcified vesicles in the liver (*2*). Other organs involved included the diaphragm, spleen, pancreas, omentum, mesenteries, rectovesical pouch, ovaries, uterus, abdominal wall, psoas muscle, and vertebra (*2*). Before surgery, patients often receive misdiagnosis with a variety of disorders, including hepatic tumor, abscess, cirrhosis or cholecystitis, gall bladder cancer, mesenteric tumor, and costal chondrosarcoma (*2*).

Geographic origin of the patients is a crucial diagnostic clue for *E. vogeli* echinococcosis (*2*). They are typically born in or have lived for prolonged periods in rural tropical areas of Central or South America, particularly in regions with abundant wildlife (*2*). Familiarity with pacas and whether domestic dogs were fed viscera of pacas are characteristics that contribute to a correct diagnosis (*2*). Ultrasound fine-needle aspiration and histopathologic examination of surgical specimens can permit taxonomic identification through larval morphologic clues (protoscoleces, hook shape and size, proportions of small and long blades) and are considered the standard, but definitive diagnosis is difficult when the hooks are absent (*1*–*3*). Since 2017, in Brazil, using molecular characterization of *E. vogeli* through *cox1* mitochondrial gene in samples from humans, domestic dogs, and pacas has suggested the presence of shared haplotypes among different populations of this cestode, reflecting the retention of ancestral polymorphisms (*8*–*10*).

In summary, our report highlights the value of molecular characterization of *E. vogeli* from histopathologic samples. Consistent with previous reports (*2*), we recommend that NPE be considered not as a medical curiosity but as a possible diagnosis of polycystic masses in humans from tropical zones in Central or South America.

The authors declare that they have no known competing financial interests or personal relationships that could have appeared to influence the work reported in this paper.

About the Author

Dr. Morcillo Muñoz is an infectious diseases fellow at Universidad Nacional de Colombia in Bogotá, Colombia. His research interests primarily focus on neglected infectious diseases.

References

1. Wen H, Vuitton L, Tuxun T, Li J, Vuitton DA, Zhang W, et al. Echinococcosis: advances in the 21st century. Clin Microbiol Rev. 2019;32:e00075–18. https://doi.org/10.1128/CMR.00075-18
2. D'Alessandro A, Rausch RL. New aspects of neotropical polycystic (*Echinococcus vogeli*) and unicystic (*Echinococcus oligarthrus*) echinococcosis. Clin Microbiol Rev. 2008;21:380–401. https://doi.org/10.1128/CMR.00050-07
3. Tappe D, Stich A, Frosch M. Emergence of polycystic neotropical echinococcosis. Emerg Infect Dis. 2008;14:292–7. https://doi.org/10.3201/eid1402.070742
4. D'Alessandro A, Rausch RL, Morales GA, Collet S, Angel D. *Echinococcus* infections in Colombian animals. Am J Trop Med Hyg. 1981;30:1263–76. https://doi.org/10.4269/ajtmh.1981.30.1263
5. D'Alessandro A, Rausch RL, Cuello C, Aristizabal N. *Echinococcus vogeli* in man, with a review of polycystic hydatid disease in Colombia and neighboring countries. Am J Trop Med Hyg. 1979;28:303–17. https://doi.org/10.4269/ajtmh.1979.28.303
6. Botero D, Restrepo MI, Restrepo A. Report of four cases of neotropical polycystic equinococcosis caused by *Echinococcus vogeli* in Colombia. Curr Trop Med Rep. 2016;3:173–5. https://doi.org/10.1007/s40475-016-0090-2
7. Mondragon-Cardona A, Duran-Gutierrez LF, Yucuma-Gutierrez S, Bolaños F, Vizcaychipi K, Alzate-Carvajal V, et al. Neotropical echinococcosis caused by *Echinococcus vogeli* in rural Huila, Colombia: report of two last cases in the last 35 years. Int J Infect Dis. 2018;73:306–7. https://doi.org/10.1016/j.ijid.2018.04.4112

8. das Neves LB, Teixeira PEF, Silva S, de Oliveira FB, Garcia DD, de Almeida FB, et al. First molecular identification of *Echinococcus vogeli* and *Echinococcus granulosus* (sensu stricto) G1 revealed in feces of domestic dogs (*Canis familiaris*) from Acre, Brazil. Parasit Vectors. 2017;10:28. https://doi.org/10.1186/s13071-016-1952-0
9. Bittencourt-Oliveira F, Teixeira P, Alencar A, Menezes R, Corrêa C, Neves L, et al. First parasitological, histopathological and molecular characterization of *Echinococcus vogeli* Rausch and Bernstein, 1972 from *Cuniculus paca* Linnaeus, 1766 in the Cerrado biome (Mato Grosso do Sul, Brazil). Vet Parasitol. 2018;250:35–9. https://doi.org/10.1016/j.vetpar.2017.12.003
10. Daipert-Garcia D, Pavan MG, Neves LBD, Almeida FB, Siqueira NG, Santos GBD, et al. Genetic diversity of *Echinococcus vogeli* in the western Brazilian Amazon. Mem Inst Oswaldo Cruz. 2019;114:e190149. https://doi.org/10.1590/0074-02760190149

Address for correspondence: Álvaro A. Faccini-Martínez, Servicio de Infectología, Hospital Militar Central, Tv. 3C No. 49–02, Bogotá, Colombia; email: afaccini@gmail.com

Seroprevalence of Rift Valley and Crimean-Congo Hemorrhagic Fever Viruses, Benin, 2022–2023

Nadine Olk, Anges Yadouleton, Olga Quenum, Stephane Sohou, Aime Goundote, Grace Aho Glele Rodrigue, Blaise Guezo-Mevo, Sonia Bedie, Michael Nagel, Petra Emmerich, Benjamin Hounkpatin, Jan Felix Drexler

Author affiliations: Charité-Universitätsmedizin Berlin, corporate member of Freie Universität Berlin, Humboldt-Universität of Berlin, Institute of Virology, Berlin, Germany (N. Olk, J.F. Drexler); Ecole Normale Supérieure de Natitingou, Université Nationale des Sciences, Technologies, Ingénierie et Mathématiques, Cotonou, Benin (A. Yadouleton); Laboratoire des Fièvres Hémorragiques Virales, Ministry of Health, Cotonou (A. Yadouleton, O. Quenum, S. Sohou, A. Goundote, G.A.G. Rodrique, B. Guezo-Mevo, S. Bedie, B. Hounkpatin); Deutsche Gesellschaft für Internationale Zusammenarbeit, Bonn, Germany (M. Nagel); Bernhard Nocht Institute of Tropical Medicine, Hamburg, Germany (P. Emmerich); Center of Internal Medicine, University Medicine Rostock, Rostock, Germany (P. Emmerich); German Centre for Infection Research, associated partner Charité-Universitätsmedizin, Berlin (J.F. Drexler)

DOI: https://doi.org/10.3201/eid3108.250020

We screened 650 febrile patients from Benin for Rift Valley fever and Crimean-Congo hemorrhagic fever viruses during 2022–2023. None were positive by reverse transcription PCR; 1.1% and 0.3%, respectively, had virus-specific IgG. False-positive results from malaria-associated antibodies likely reacting with histidine-tagged viral antigens mandate careful validation of serologic tests in malaria-endemic regions.

Rift Valley fever virus (RVFV; family Phenuiviridae) and Crimean-Congo hemorrhagic fever virus (CCHFV; family Nairoviridae) are arthropodborne viruses endemic to Africa and the Arabian Peninsula (*1*,*2*) and high-priority pathogens that can cause lethal hemorrhagic fever (*2*–*4*) (https://www.who.int/publications/m/item/WHO-BS-2023-2449). In West Africa, RVFV and CCHFV are considered endemic in Senegal and Mauritania (*1*,*2*); regional circulation seems likely in Guinea, Burkina Faso, Ghana, and Nigeria (*2*). In Benin, CCHFV antibodies were reported in humans in 1981, but RVFV and CCHFV epidemiology remains unknown (*1*,*2*). Both RVFV and CCHFV infect diverse animals reared as livestock (*3*). Benin has been undergoing changes in traditional cattle farming, including increased herd sizes and sedentarization (*5*), which may intensify RVFV and CCHFV circulation. We collected serum samples for routine diagnostic examinations for RVFV and CCHFV in 7 hospitals located across ≈700 km and 3 ecozones in Benin (Appendix Table, Figure, https://wwwnc.cdc.gov/EID/article/31/8/25-0020-App1.pdf).

We investigated serum samples from 650 febrile patients (mean age 26.7 [interquartile range 18–34] years; 70.3% female, 29.7% male) who were seen during December 2022–January 2023. We analyzed samples for acute RVFV and CCHFV infection using PCR-based methods and had no positive results (Appendix). However, we detected IgG by using commercially available ELISA kits (RVFV, competitive ELISA; ID.Vet, https://bioadvance.life/en/id-vet-2; CCHFV, indirect ELISA; Euroimmun, https://www.euroimmun.com) with viral nucleoproteins as antigens. We confirmed CCHFV ELISA results by using a CCHFV immune complex capture IgG ELISA (Panadea Diagnostics, https://www.panadea-diagnostics.com) and RVFV and CCHFV ELISA results by indirect IgG immunofluorescence assays (IFAs).

The competitive RVFV IgG ELISA was positive in 10 (1.5%, 95% CI 0.6%–2.5%) samples; 7 were positive by RVFV IFA with high endpoint titers of 1:1,000–12,500 serum dilution (Figure 1, panel A; Figure 2, panel A; Appendix Table). Differential test sensitivity might cause discordant ELISA and IFA results, but ELISA reactivity was not weaker in IFA-negative samples compared with IFA-positive samples ($p = 0.83$ by Mann-Whitney U test). By indirect ELISA, 40 (6.1%, 95% CI 4.3%–8.0%) samples were positive for CCHFV, but only 5 samples tested positive by immune capture ELISA (Figure 2, panels B, C). Of those 5 samples, we confirmed 2 by CCHFV IFA, with low endpoint titers of 1:20–1:80 (Figure 1, panel B; Appendix Table). IFA-negative samples showed low reactivity in the immune capture ELISA, suggesting differential sensitivity or need to adjust ELISA positivity thresholds (Figure 2, panel C).

Discrepancies among detection rates of the 2 CCHFV ELISA tests and IFA were surprising. Unspecific ELISA reactivity can occur; for example, malaria or herpes virus infection might cause unspecific B-cell stimulation (*6*,*7*). Antibodies against *Plasmodium falciparum* parasites' histidine-rich proteins occur in ≈25% of people in malaria-endemic areas and decrease sensitivity of rapid diagnostic tests (*8*). During in vitro antigen production for serologic tests, ≤6 histidine residues are frequently added to expression constructs for protein purification (*9*). Increasing externally added histidine concentrations led to significantly decreased CCHFV indirect ELISA reactivity in potentially false-positive samples ($\rho = 0.41$; $p = 0.0015$) (Figure 2, panel D). In contrast, reactivities of likely true-positive samples (i.e., confirmed by IFA or immune capture ELISA) and likely true-negative samples were not affected by incremental histidine concentrations. Those data substantiated that antibodies potentially elicited by previous or acute *Plasmodium* infections targeting histidine-rich epitopes might have interacted

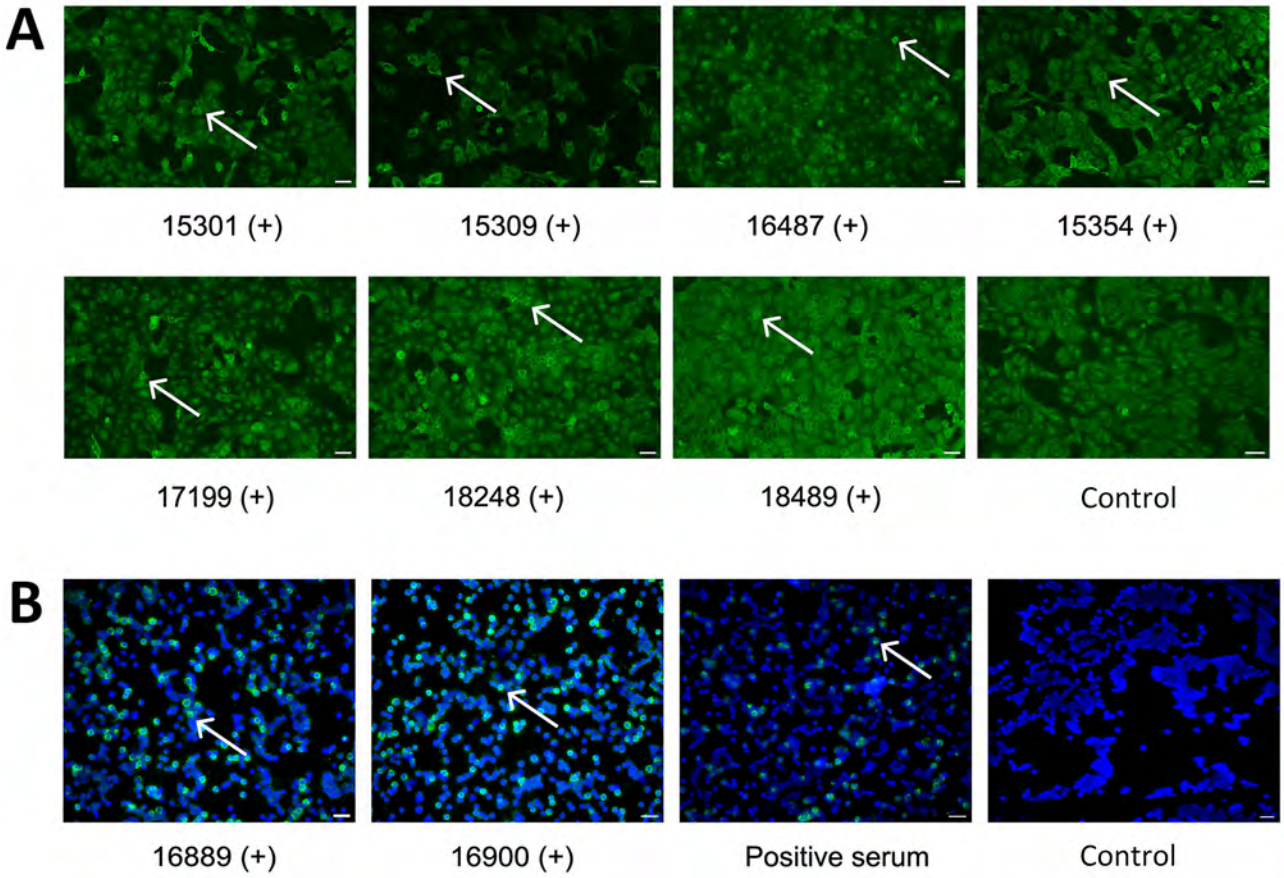

Figure 1. IFA for IgG against Rift Valley and Crimean-Congo hemorrhagic fever viruses, Benin, 2022–2023. A) Serum samples were tested using a commercial IFA (Euroimmun, https://www.euroimmun.com) with Rift Valley fever virus–infected Vero cells. Positive samples are shown at 1:100 dilution; white arrows mark infected cells. B) Serum samples were tested using in-house IFA with Crimean-Congo hemorrhagic fever virus–infected Vero cells (Appendix, https://wwwnc.cdc.gov/EID/article/31/8/25-0020-App1.pdf). Positive samples are shown at 1:10 dilution; white arrows mark infected cells. Titers are provided for the individual samples (Appendix Table). Noninfected controls are shown. Scale bars indicate 20 μm. +, positive serum sample; IFA, immunofluorescence assay.

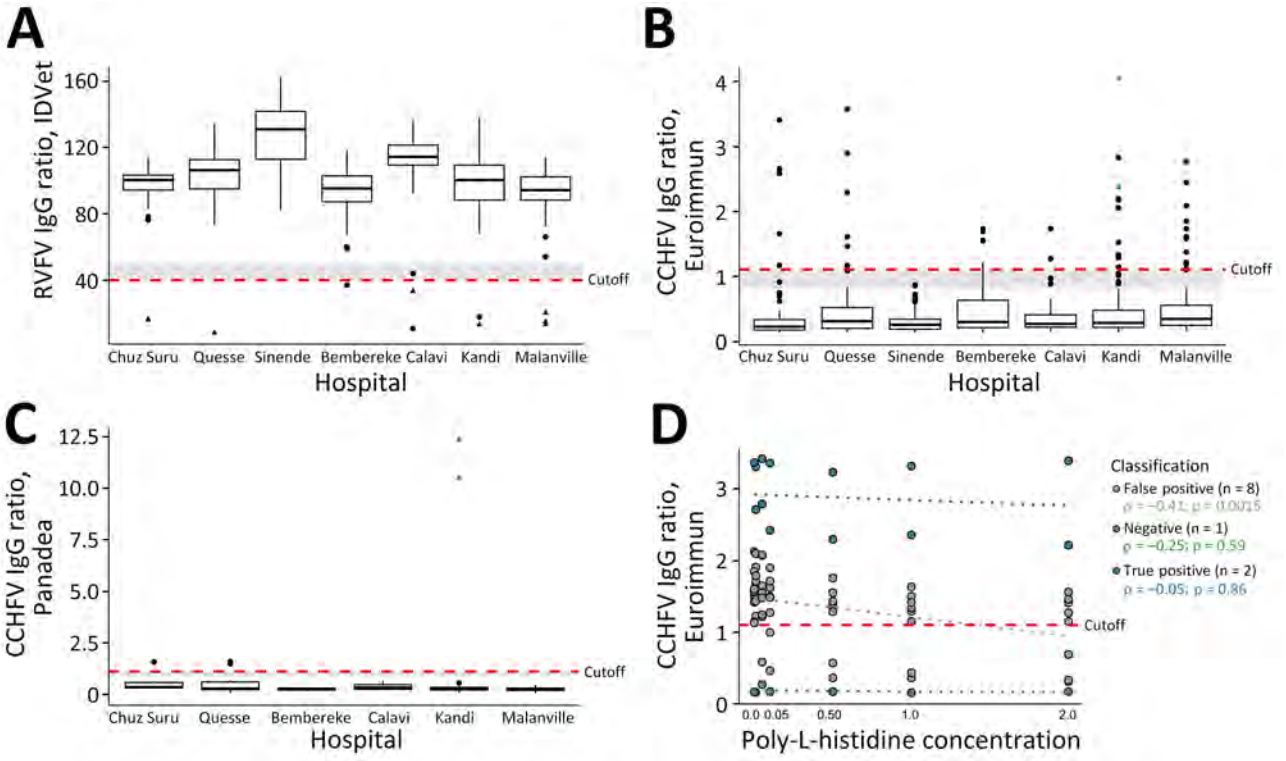

Figure 2. ELISA reactivity for Rift Valley and Crimean-Congo hemorrhagic fever viruses, Benin, 2022–2023. IgG ELISA (ID.Vet, https://bioadvance.life/en/id-vet-2) for RVFV for which a sample/negative percentage ≤40.0 is considered positive. IgG ELISAs (Euroimmun, https://www.euroimmun.com; Panadea Diagnostics, https://www.panadea-diagnostics.com) for CCHFV for which ratios >1.1 are considered positive according to the manufacturer. A) RVFV competitive ELISA (ID.Vet) using nucleoprotein as antigen. Positive samples, n = 10/650. B) CCHFV indirect ELISA (Euroimmun) using nucleoprotein as antigen. Positive samples, n = 40/650. C) CCHFV immune complex capture ELISA (Panadea) using nucleoprotein as antigen. Positive samples, n = 5/92. D) Reduced indirect IgG ELISA reactivity of CCHFV (Euroimmun) with poly-L-histidine concentrations of 0.01, 0.05, 0.10, 0.50, 1.00, and 2.00 mg/mL. Box plots show sample distribution, displaying medians (thick lines within boxes) and interquartile ranges (box top and bottom edges); whiskers indicate 1.5× interquartile range. Red lines show cutoff levels for ELISAs; gray shading shows the area for borderline results; black triangles show samples positive by RVFV immunofluorescence assay; blue triangles show samples positive by CCHFV immunofluorescence assay. The Spearman correlation was performed in R, and boxplots for RVFV and CCHFV were plotted using the ggplot2 package in R (https://www.r-project.org). Because of the low detection rates of RVFV-specific and CCHFV-specific IgG, negative reverse transcription PCR results, and low serum volumes, we did not perform IgM analyses. CCHFV, Crimean-Congo hemorrhagic fever virus; RVFV, Rift Valley fever virus.

with likely histidine-tagged indirect ELISA antigens to cause the observed reactivity pattern, including multiple likely false-positive test results. Other histidine-rich immunogens might also have elicited potentially cross-reactive antibodies, yet malaria-associated immune responses remain the most plausible explanation because of the abundance of malaria in sub-Saharan Africa and a similar rate of potentially false-positive COVID-19 results in a previous serologic study (*6*). Although the competitive RVFV ELISA and immune complex capture–based CCHFV ELISA might be more specific than indirect ELISA formats, we only considered IFA-positive results for conservative assessment of the RVFV antibody detection rate of 1.1% (95% CI 0.3%–1.9%; n = 7/650) and of the CCHFV antibody detection rate of 0.3% (95% CI −0.1% to 0.7%; n = 2/650) (Appendix Table).

Our serologic data thus substantiated circulation of RVFV and CCHFV in Benin (Appendix Table), albeit at relatively low rates that are largely comparable to neighboring countries (*1*,*2*). Livestock rearing in Benin is transitioning to partly sedentary systems with larger cattle herds (*5*), which highlights the need to continuously monitor RVFV and CCHFV circulation in humans and cattle (*10*) and support with robust serologic tests validated for specificity in malaria-endemic regions and direct detection of pathogens in arthropod vectors, such as *Culex* and *Aedes* mosquitoes for RVFV and *Hyalomma* ticks for CCHFV.

The main limitation of our study is that it is a nonrepresentative sample. However, including febrile patients from 7 hospitals across 3 ecozones provides broad geographic and ecologic coverage (*1*).

Beyond surveillance, strategies for future vaccination of livestock and humans will benefit from robust epidemiologic data on RVFV and CCHFV to efficiently use resources across sub-Saharan Africa. Serologic tests relying on tag-free protein production, alternative tags, and careful validation of histidine-tagged antigens for specificity are mandatory for use of antibody tests in malaria-endemic regions.

Acknowledgments

We thank Dominik Lehman and Marta Piche-Ovares for technical support.

This study was approved by the Charité–Universitätsmedizin Berlin (ethical permit no. EA2/251/23) and the Institute of Applied Biological Science in Benin (reference no. 184).

This study was supported by the German Federal Ministry of Economic Cooperation and Development via the Deutsche Gesellschaft für Internationale Zusammenarbeit GmbH (project no. 81305758).

About the Author

Ms. Olk is a researcher at the Institute of Virology, Charité Universitätsmedizin Berlin. Her research interests include the epidemiology of emerging viruses.

References

1. Tinto B, Quellec J, Cêtre-Sossah C, Dicko A, Salinas S, Simonin Y. Rift Valley fever in West Africa: a zoonotic disease with multiple socio-economic consequences. One Health. 2023;17:100583. https://doi.org/10.1016/j.onehlt.2023.100583
2. Temur AI, Kuhn JH, Pecor DB, Apanaskevich DA, Keshtkar-Jahromi M. Epidemiology of Crimean-Congo hemorrhagic fever (CCHF) in Africa—underestimated for decades. Am J Trop Med Hyg. 2021;104:1978–90. https://doi.org/10.4269/ajtmh.20-1413
3. Hawman DW, Feldmann H. Crimean-Congo haemorrhagic fever virus. Nat Rev Microbiol. 2023;21:463–77. https://doi.org/10.1038/s41579-023-00871-9
4. Petrova V, Kristiansen P, Norheim G, Yimer SA. Rift valley fever: diagnostic challenges and investment needs for vaccine development. BMJ Glob Health. 2020;5:e002694. https://doi.org/10.1136/bmjgh-2020-002694
5. Houessou SO, Dossa LH, Diogo RVC, Houinato M, Buerkert A, Schlecht E. Change and continuity in traditional cattle farming systems of West African Coast countries: a case study from Benin. Agric Syst. 2019;168:112–22. https://doi.org/10.1016/j.agsy.2018.11.003
6. Yadouleton A, Sander AL, Moreira-Soto A, Tchibozo C, Hounkanrin G, Badou Y, et al. Limited specificity of serologic tests for SARS-CoV-2 antibody detection, Benin. Emerg Infect Dis. 2021;27:233–7. https://doi.org/10.3201/eid2701.203281
7. Piche-Ovares M, García MP, Moreira-Soto A, Figueroa-Romero MD, Merino-Sarmiento NS, Marcelo-Ñique AI, et al. Rio Mamore hantavirus endemicity, Peruvian Amazon, 2020. Emerg Infect Dis. 2024;30:2532–43. https://doi.org/10.3201/eid3012.240249
8. Ho MF, Baker J, Lee N, Luchavez J, Ariey F, Nhem S, et al. Circulating antibodies against *Plasmodium falciparum* histidine-rich proteins 2 interfere with antigen detection by rapid diagnostic tests. Malar J. 2014;13:480. https://doi.org/10.1186/1475-2875-13-480
9. Debeljak N, Feldman L, Davis KL, Komel R, Sytkowski AJ. Variability in the immunodetection of His-tagged recombinant proteins. Anal Biochem. 2006;359:216–23. https://doi.org/10.1016/j.ab.2006.09.017
10. Boko KC, Ibrahim AI, Akpo Y, Alladassi ME, Aguidissou NO, Zoclanclounon AR, et al. Sero-prevalence of Rift Valley fever and brucellosis in cattle of northern Benin, West Africa. Am J Anim Vet Sci. 2022;17:267–73. https://doi.org/10.3844/ajavsp.2022.267.273

Address for correspondence: Jan Felix Drexler, Institute of Virology, Charitéplatz 1, 10117 Berlin, Germany; email: felix.drexler@charite.de

Complete Genome Analysis of African Swine Fever Virus Isolated from Wild Boar, India, 2021

Dhanapal Senthilkumar,[1] Katherukamem Rajukumar,[1] Govindarajulu Venkatesh, Fateh Singh, Gopal Sarkar, Jaswant Patel, Suman Mishra, Rohit Sahu, Nourin Khan, C. Neihthangpuii, Esther Lalzolian, Vijendra Pal Singh, Aniket Sanyal

Author affiliations: ICAR, National Institute of High Security Animal Diseases, Bhopal, India (D. Senthilkumar, K. Rajukumar, G. Venkatesh, F. Singh, G. Sarkar, J. Patel, S. Mishra, R. Sahu, N. Khan, V.P. Singh, A. Sanyal); Government of Mizoram, Aizawl, India (C. Neihthangpuii, E. Lalzoliani)

DOI: https://doi.org/10.3201/eid3108.250083

Complete genome analysis of African swine fever virus isolated from a wild boar in Mizoram, India, revealed ≈99% nucleotide identity with those of domestic pig origin but with unique mutations. A One Health approach toward food security necessitates awareness among veterinary and public health professionals on virus evolution and domestic–wild pig transmission.

[1]These authors contributed equally to this article.

African swine fever (ASF) is a devastating disease affecting pigs, with death rates reaching 100%. Wild boars (*Sus scrofa*), warthogs (*Phacochoerus aethiopicus*), and bushpigs (*Potamochoerus porcus*) can act as asymptomatic carriers, contributing to virus persistence in a sylvatic cycle (*1*). Soft ticks of the genus *Ornithodoros* further complicate ASF epidemiology. The disease is caused by ASF virus (ASFV), a large, double-stranded DNA virus belonging to the genus *Asfivirus* in the Asfarviridae family. The ASFV genome range is 171–193 kb, featuring inverted terminal repeats (ITRs) at both ends. Different ASFV genotypes are based on the 3′ end of the *B646L* gene; genotype II predominates in Asia, Europe, Oceania, and the Americas. Recent emergence of novel recombinant genotype I/II strains in China and Vietnam (*2*,*3*) is of great concern.

ASF was first reported in India in 2020 after outbreaks in domestic pigs in northeastern states (*4*). Outbreaks in wild boars have been documented in Assam, Karnataka, and Tamilnadu states (*5*,*6*). ASFVs circulating in India belong to genotype II and intergenic region (IGR) subcluster II. Complete genome sequencing of Indian ASFV isolates of domestic pig origin revealed unique mutations in the *MGF 360–11L, MGF 505–4R, K205R*, and *B263R* genes (*7*). We analyzed the complete genome of ASFVs isolated after ASF outbreaks affecting domestic pigs and wild boars in Mizoram, India, in August 2021.

We collected 40 samples from dead domestic pigs and those suspected of having ASF (Appendix Figure 1, https://wwwnc.cdc.gov/EID/article/31/8/25-0083-App1.pdf); 38 of those samples and a dead wild boar tested positive for ASF genome by quantitative PCR and were confirmed by virus isolation. We grew, processed for viral enrichment, and sequenced 1 ASFV isolate (MZ/21/PO-324) of wild boar origin and 1 isolate (MZ/21/PO-314) of domestic pig origin. We submitted nucleotide sequences to GenBank (accession nos. PV023909 and PV023910) (Appendix).

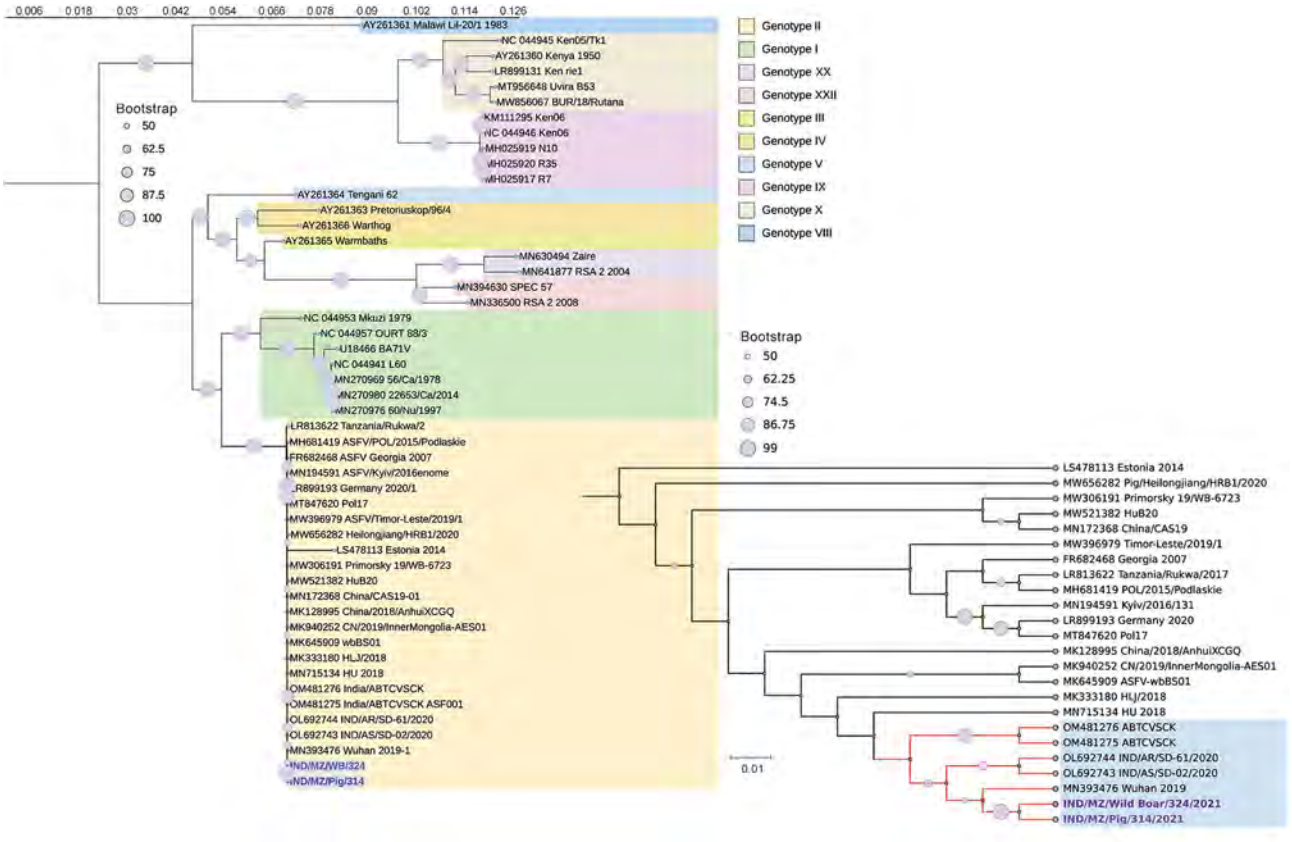

Figure 1. Phylogenetic tree generated from complete genome analysis of ASFV isolated from wild boar and domestic pig, India, 2021. The maximum-likelihood tree was MAFFT aligned (https://mafft.cbrc.jp/alignment/software) by using a general time-reversible plus gamma model in RAxMLGUI version 2.0 (https://sourceforge.net/projects/raxmlgui) and shows the relationship between ASFVs from India and other ASFVs including p72 genotype II. Enlarged area at bottom right shows detail of isolates from this study (bold text) and close reference sequences. GenBank accession numbers are provided. Scale bar indicates the number of expected substitutions per site (tree rooted at mid-point). ASFV, African swine fever virus.

Figure 2. Complete genome analysis of ASFV isolated from wild boar and domestic pig, India, 2021. A 50-nt deletion is observed in the *MGF-360–21R* gene of the ASFV isolate obtained from a wild boar in Mizoram, India, compared with ASFV isolates derived from domestic pigs in India. Bold isolates are from this study. GenBank accession numbers are provided. ASFV, African swine fever virus.

The wild boar ASFV genome comprised 190,489 bp with ITRs at the 5′ end (1,597 bp) and 3′ end (1,122 bp), whereas the ASFV genome from domestic pig measured 189,390 bp and had a 5′ end ITR of 422 bp and 3′ end ITR of 1,150 bp. Comparative analysis showed 99.93% nucleotide identity between those isolates (Appendix Figure 2). Phylogenetic analysis placed the ASFV in India within genotype II clade 2.2.2, alongside genotype II viruses reported during 2007–2023 across diverse regions. Within p72 genotype II viruses, isolates from India formed a distinct cluster with isolate ASFV/Wuhan/2019 (Figure 1). *EP402R* gene–based serogrouping confirmed isolates from India as part of serogroup 8, consistent with hemadsorption-positive viruses (Appendix Figure 3). There was an insertion of an additional tandem repeat sequence in the extragenic region between *I73R* and *I329L* (Appendix Figure 4), aligning with intergenic region II cluster isolates of genotype II. Central variable region analysis of the *B602L* gene indicated similarity to the Georgia 2007/1 central variable region I variant (*8*).

We observed multiple nucleotide insertions and deletions (Appendix Table 1) in the genome sequence of the wild boar isolate compared with isolate ASFV-Georgia/2007, leading to frame shift mutations in *DP60R* and *ASFV-GACD 190* genes, amino acid additions in *ASFV GACD-00300* and *ASFV GACD-00350* genes, and protein truncations in immune-modulatory genes, *MGF 110–7L, MGF 110–10L, MGF 110–14L, MGF 110–13Lb, I196L, B475L,* and *MGF 360–21R*, of which the last 3 mutations were unique to the wild boar isolate (Appendix). A 50-nt deletion in the *MGF 360–21R* gene resulted in a truncated protein of 327 aa. We did not observe that deletion in the ASFV isolate of domestic pig origin, and the deletion was unique to the wild boar isolate reported in this study. Further analyses and multiple sequence alignment of *MGF-360–21R* gene of ASFV isolates obtained from wild boar, warthog, and domestic pigs across different countries revealed that the gene is particularly susceptible to mutations during replication in wild boars compared with domestic pigs (Figure 2) and causes truncations at the carboxyl terminus of the encoded protein. Those observations reflect the role of the *MGF-360–21R* gene in evolutionary adaptations of ASFV in wild boar populations.

A comparative analysis of genotype II ASFV revealed 20 single-nucleotide polymorphisms comprising 16 nonsynonymous and 4 synonymous mutations across 18 open reading frames (Appendix Figure 5). Key nonsynonymous mutations included K32E in *ASFV GACD 300*, P406L in *EP1242L,* R188K in K205R, and Q104H in *E199L*. The proteins encoded by *K205R* and *E199L* genes are noted to interact with host proteins, potentially activating cellular responses such as unfolded protein response and autophagy (*9*,*10*).

In conclusion, ASFV sequences from both hosts showed ≈99% identity and highlighted transmission between domestic and wild pigs. However, we identified unique genetic variations in ASFVs isolated from wild boar, which may influence viral interactions with host cellular machinery. Our findings highlight the critical role of wild boars in ASF epidemiology and underscore the need for veterinary, wildlife and public health authorities to be aware of transmission dynamics between domestic and wild pigs and viral evolution, with implications for viral survival, immune modulation, and control strategies.

Acknowledgments

We thank the Indian Council of Agricultural Research, New Delhi, and the Director, Indian Council of Agricultural Research–National Institute of High Security Animal Diseases, Bhopal, for providing necessary facilities to carry out this work.

We received funding from the Indian Council of Agricultural Research, New Delhi, and the Department of Animal Husbandry, Dairying and Fisheries, Ministry of Agriculture and Farmers Welfare, Government of India under a Central Disease Diagnostic Laboratory grant.

About the Author

Dr. Senthilkumar is a senior scientist at the ICAR–National Institute of High Security Animal Diseases, Bhopal, India. His research focuses on surveillance, diagnostic and vaccine development, molecular epidemiology, and the pathogenesis of emerging swine diseases, particularly African swine fever and porcine reproductive and respiratory syndrome.

References

1. Lubisi BA, Bastos AD, Dwarka RM, Vosloo W. Molecular epidemiology of African swine fever in East Africa. Arch Virol. 2005;150:2439–52. https://doi.org/10.1007/s00705-005-0602-1
2. Zhao D, Sun E, Huang L, Ding L, Zhu Y, Zhang J, et al. Highly lethal genotype I and II recombinant African swine fever viruses detected in pigs. Nat Commun. 2023;14:3096. https://doi.org/10.1038/s41467-023-38868-w
3. Lee K, Vu TTH, Yeom M, Nguyen VD, Than TT, Nguyen VT, et al. Molecular characterization of emerging recombinant African swine fever virus of genotype I and II in Vietnam, 2023. Emerg Microbes Infect. 2024;13:2404156. https://doi.org/10.1080/22221751.2024.2404156
4. Rajukumar K, Senthilkumar D, Venkatesh G, Singh F, Patil VP, Kombiah S, et al. Genetic characterization of African swine fever virus from domestic pigs in India. Transbound Emerg Dis. 2021;68:2687–92. https://doi.org/10.1111/tbed.13986
5. Buragohain L, Barman NN, Sen S, Bharali A, Dutta B, Choudhury B, et al. Transmission of African swine fever virus to the wild boars of Northeast India. Vet Q. 2023;43:1–10. https://doi.org/10.1080/01652176.2023.2178689
6. Sai Balaji KG, Karikalan M, Saravanan S, Mahajan S, Rajeshkumar K, Vaseem M, et al. High mortality in free-ranging wild boars associated with African swine fever virus in India. Arch Virol. 2024;169:137. https://doi.org/10.1007/s00705-024-06065-9
7. Senthilkumar D, Rajukumar K, Venkatesh G, Singh F, Tosh C, Kombiah S, et al. Complete genome analysis of African swine fever virus isolated from domestic pigs during the first ASF outbreaks in India. Transbound Emerg Dis. 2022;69:e2020–7. https://doi.org/10.1111/tbed.14536
8. Gallardo C, Casado N, Soler A, Djadjovski I, Krivko L, Madueño E, et al. A multi gene-approach genotyping method identifies 24 genetic clusters within the genotype II-European African swine fever viruses circulating from 2007 to 2022. Front Vet Sci. 2023;10:1112850. https://doi.org/10.3389/fvets.2023.1112850
9. Chen S, Zhang X, Nie Y, Li H, Chen W, Lin W, et al. African swine fever virus protein E199L promotes cell autophagy through the interaction of PYCR2. Virol Sin. 2021;36:196–206. https://doi.org/10.1007/s12250-021-00375-x
10. Wang Q, Zhou L, Wang J, Su D, Li D, Du Y, et al. African swine fever virus K205r induces ER stress and consequently activates autophagy and the NF-κB signaling pathway. Viruses. 2022;14:394. https://doi.org/10.3390/v14020394

Address for correspondence: Dhanapal Senthilkumar, ICAR–National Institute of High Security Animal Diseases, Anand Nagar, Bhopal 462022, India; email: senvetpath@gmail.com

Influenza D Virus in Domestic and Stray Cats, Northern China, 2024

Mingshuai Shen,[1] Xinkun Zhao,[1] Jian Zhang,[1] Cun Liu, Chengyi Qi, Ruohan Wang, Jieshi Yu,[2] Kezhou Wang,[2] Zhao Wang[2]

Author affiliations: Shandong First Medical University, Jinan, China (M. Shen, X. Zhao, J. Zhang, C. Qi, R. Wang, K. Wang, Z. Wang); Shandong Provincial Center for Animal Disease, Jinan (C. Liu); Guangdong Academy of Agricultural Sciences, Guangzhou, China (J. Yu)

DOI: http://doi.org/10.3201/eid3108.250042

Influenza D virus infects primarily cattle, but infrequent reports of infections in cats occur. We detected influenza D virus antibodies in 8 of 360 cats in northern China. Domestic cats showed higher susceptibility than strays. Our results suggest a previously overlooked aspect of epidemiology of this virus in companion animals.

Influenza D virus (IDV) is a single-stranded, negative-sense RNA virus belonging to the genus *Deltainfluenzavirus*, family Orthomyxoviridae, and was first isolated from pigs in 2011 (*1*,*2*). IDV infects primarily cattle, but studies have documented the virus globally in a diverse range of animals, including small

[1]These authors contributed equally to this article.

[2]These authors contributed equally to this article.

ruminants (e.g., sheep), domestic animals (pigs, horses, camels), and wild ungulates (wild boars) (*3*,*4*). Although there is no direct evidence that IDV can infect humans, an increasing number of studies have indicated that IDV has the potential for causing zoonotic infections (*5*). One recent study in the Puglia region of Italy identified 14 positive IDV antibody samples from 426 dogs sampled in 2016–2023, indicating that companion animals can be exposed to IDV (*6*). Our study aimed to investigate whether cats, a popular companion animal, are susceptible to IDV.

We collected 360 serum samples from cats in northern China in 2024, comprising 181 samples from routine health checks at pet hospitals and 179 samples from pet rescue stations. We stored all samples at −80°C for subsequent analysis. Prior to testing them, we treated all samples with receptor-destroying enzyme to remove nonspecific inhibitors (*7*). We briefly mixed the samples with receptor-destroying enzyme in a 1:3 ratio, incubated them at 37°C overnight (18–20 h), then heat-inactivated them at 56°C for 30–60 minutes before hemagglutination inhibition (HI) testing. We performed screening by HI assay to identify antibodies against influenza A virus (A/China/SWL1304/2023 [H1N1]), influenza B virus (B/Guangdong/266/2021), and IDV (D/bovine/CHN/JY3002/2022), considering HI titers ≥10 to be positive (*8*). To confirm specificity, we further subjected HI-positive samples to virus neutralization assays using 100 $TCID_{50}$ (50% tissue culture infectious dose) of IDV propagated in Madin-Darby canine kidney cells. We deemed neutralization titers ≥10 (highest serum dilution showing ≥50% cytopathic effect reduction) to be confirmatory (*9*).

Serological analysis revealed 6 (3.31%) of 181 of veterinary hospital samples to be HI positive for IDV antibodies, with 4 (66.7%) confirmed by virus neutralization assay (titers 10–20). Among rescue station samples, 2 (1.12%) of 179 were HI positive, with 2 (100%) confirmed by virus neutralization (titer 10) (odds ratio 4.12, 95% CI 0.92–18.40; p = 0.027). All positive samples showed HI titers of 10–40, and none were reactive to influenza A virus or influenza B virus (Table).

Our findings demonstrated that, although overall IDV seroprevalence in cats in northern China was low (2.22%), domestic cats showed significantly higher exposure rates than strays. This difference might reflect increased human contact, potentially leading to viral exposure, considering stray cats' independent lifestyles potentially limit such transmission opportunities. As noted in similar studies of other species, the source of IDV infection in cats remains unclear. Potential transmission routes might include reverse zoonotic transmission or alternative pathways, such as raw milk exposure, as suggested by recent influenza A(H5N1) virus detections in cow's milk (*10*). Although our serologic data cannot confirm active transmission or clinical impacts, the observed higher seroprevalence in domestic cats suggests that close human–animal interaction could potentially increase exposure risk.

IDV is not currently a major zoonotic threat, but its detection in cats highlights the need for vigilance. Domestic cats may potentially serve as reservoirs for IDV, which could contribute to viral adaptation. Our study emphasizes the importance of monitoring IDV in companion animals, especially considering recent findings demonstrating the potential of influenza viruses for cross-species transmission via unconventional routes (i.e., H5N1 virus in bovine milk).

Future research should prioritize molecular confirmation of active infections and assess milkborne transmission risks. Proactive surveillance in pets and their food sources is critical to understanding IDV's evolving epidemiology and mitigating potential public health concerns.

Viral strains used in HI testing—influenza A(H1N1) virus (2009 pandemic lineage), influenza B virus (Victoria lineage), and IDV (D/Yama lineage)—were provided by Prof. Jieshi Yu.

Table. Hemagglutination inhibition and virus neutralization antibody titers against influenza D virus in feline serum samples from study of influenza D virus in domestic and stray cats, northern China, 2024*

	Influenza A virus, A/China/SWL1304/2023(H1N1)	Influenza B virus, B/Guangdong/266/2021	Influenza D virus, D/bovine/CHN/JY3002/2022	
Sample no.	HI	HI	HI	VN
A5	<10	<10	10, 10	10, 10
D5	<10	<10	20, 20	20, 20
D8	<10	<10	20, 20	10, 10
E3	<10	<10	10,10	<10
H1	<10	<10	40, 40	20, 20
I3	<10	<10	20, 20	10, 10
I6	<10	<10	10, 10	<10
L7	<10	<10	40, 40	20, 20

*Samples were tested against 3 strains: influenza A virus, influenza B virus, and influenza D virus. Titers below the detectable threshold (10) were indicated as <10 and considered negative. HI, hemagglutination inhibition; VN, virus neutralization.

This work was supported by National Natural Science Funds (32102750), Shandong Province Pig Industry Technology System (SDAIT-08-17), The Major Scientific and Technological Innovation Project (2023CXGC010705), and Innovation Project of Shandong Academy of Medical Sciences and Technology Bureau "20 Colleges and Universities" (2021GXRC011).

About the Author

Mr. Shen is a master's degree student in the College of Laboratory Animals at Shandong First Medical University. His main research interest is the study of influenza virus pathogenicity factors.

References

1. Hause BM, Collin EA, Liu R, Huang B, Sheng Z, Lu W, et al. Characterization of a novel influenza virus in cattle and swine: proposal for a new genus in the Orthomyxoviridae family. mBio. 2014;5:e00031–14.
2. Hause BM, Ducatez M, Collin EA, Ran Z, Liu R, Sheng Z, et al. Isolation of a novel swine influenza virus from Oklahoma in 2011 which is distantly related to human influenza C viruses. PLoS Pathog. 2013;9:e1003176.
3. Gaudino M, Moreno A, Snoeck CJ, Zohari S, Saegerman C, O'Donovan T, et al. Emerging influenza D virus infection in European livestock as determined in serology studies: are we underestimating its spread over the continent? Transbound Emerg Dis. 2021;68:1125–35.
4. Liu R, Sheng Z, Huang C, Wang D, Li F. Influenza D virus. Curr Opin Virol. 2020;44:154–61.
5. Yu J, Li F, Wang D. The first decade of research advances in influenza D virus. J Gen Virol. 2021;102:102.
6. Trombetta CM, Marchi S, Marotta MG, Moreno A, Chiapponi C, Montomoli E, et al. Detection of influenza D antibodies in dogs, Apulia region, Italy, 2016 and 2023. Emerg Infect Dis. 2024;30:1045–7.
7. Ehrengut W, Sarateanu DE, Rutter G. Influenza A antibodies in cervine animals. Infection. 1980;8:66–9.
8. Saegerman C, Salem E, Ait Lbacha H, Alali S, Zouagui Z, Meyer G, et al. Formal estimation of the seropositivity cut-off of the hemagglutination inhibition assay in field diagnosis of influenza D virus in cattle and estimation of the associated true prevalence in Morocco. Transbound Emerg Dis. 2021;68:1392–9.
9. Gauger PC, Vincent AL. Serum virus neutralization assay for detection and quantitation of serum neutralizing antibodies to influenza A virus in swine. Methods Mol Biol. 2020;2123:321–33.
10. Mostafa A, Naguib MM, Nogales A, Barre RS, Stewart JP, García-Sastre A, et al. Avian influenza A (H5N1) virus in dairy cattle: origin, evolution, and cross-species transmission. mBio. 2024;15:e0254224.

Address for correspondence: Zhao Wang, Shandong First Medical University No. 6699 Qingdao Rd, Jinan 250000, China; email: wangzhao@sdfmu.edu.cn

Nipah Virus Antibodies in Bats, the Philippines, 2013–2022

Yoshihiro Kaku, Shumpei Watanabe, Joseph S. Masangkay, Phillip Alviola, Satoshi Taniguchi, Edison Cosico, Yumi Une, Frances C. Recuenco, Satoko Sugimoto, Kentaro Kato, Shigeru Kyuwa, David Emmanuel M. General, Allen John F. Manalad, Sheryl A. Yap, Hironori Bando, Nanako Isobe, Yui Sakata, Shione Takeguchi, Hikaru Fujii, Masayuki Shimojima, Shigeru Morikawa, Ken Maeda, Tsutomu Omatsu

Author affiliations: National Institute of Infectious Diseases, Japan Institute for Health Security, Tokyo, Japan (Y. Kaku, S. Sugimoto, M. Shimojima, S. Morikawa, K. Maeda); Okayama University of Science, Imabari, Japan (S. Watanabe, Y. Une, N. Isobe, Y. Sakata, S. Takeguchi, H. Fujii, S. Morikawa); College of Veterinary Medicine, University of the Philippines Los Baños, Los Baños, the Philippines (J.S. Masangkay, A.J.F. Manalad); Museum of Natural History, University of the Philippines Los Baños, Los Baños (P. Alviola, E. Cosico, D.E.M. General, S.A. Yap); Graduate School of Medicine, University of Tokyo, Tokyo (S. Taniguchi); College of Science, De La Salle University, Manila, the Philippines (F.C. Recuenco); Graduate School of Agricultural and Life Sciences, University of Tokyo, Tokyo (S. Kyuwa); Tohoku University, Osaki, Japan (K. Kato, H. Bando); Center for Infectious Disease Epidemiology and Prevention Research, Faculty of Agriculture, Tokyo University of Agriculture and Technology, Tokyo (T. Omatsu)

DOI: https://doi.org/10.3201/eid3108.250210

In 2014, an outbreak of zoonotic Nipah virus (NiV) occurred on Mindanao Island, the Philippines. We investigated the prevalence of NiV in Philippine bats. Because neutralizing antibodies were detected in insectivorous bats on Siargao Island, public health officials should consider that the distribution range of NiV is not limited to Mindanao Island.

Nipah virus (NiV; family *Paramyxoviridae*, genus *Henipavirus*) was first discovered in 1998–1999. Officials in Malaysia and Singapore identified it as a causative virus of severe respiratory disease in pigs and highly fatal encephalitis or respiratory disease in humans (*1*). Subsequently, Bangladesh and India have reported sporadic outbreaks of the virus almost annually (*2*,*3*). Direct bat-to-human transmission is assumed in those outbreaks; however, human-to-human transmission through concentrated contact has also been reported (*3*).

In Southeast Asia, some frugivorous bat species (mainly of the genus *Pteropus*) and several insectivorous bat species (genera *Hipposideros*, *Scotophilus*, and *Rhinolophus*) are reservoirs of the virus, which has led to its widespread transmission (*4*–*6*). In 2014, in Sultan Kudarat Province, which is located in the southern part of Mindanao Island in the Philippines, 10 horses died, and serious infections occurred in 17 humans, mainly in those who had slaughtered horses or consumed horse meat (*7*). The humans who died had acute encephalitis syndrome, a severe influenza-like illness, or meningitis, and the etiology was diagnosed as henipavirus infection on the basis of neutralizing antibody detection in patient serum samples. One patient had a short 71-bp fragment sequence that was 99% homologous to the NiV strain from Malaysia, suggesting that NiV was the etiologic virus (*7*). The likely source of infection in horses is bats, which are a natural host of the virus.

Residual serum samples used in epidemiologic studies of bat-derived viruses conducted before 2019 were reused in this NiV epidemiologic study (*8*). In addition, we conducted new bat trapping at the end of 2022. In each study, we collected specimens from wild bats.

We attempted to detect NiV-neutralizing antibodies by using serum samples collected from bats in 6 regions of the Philippines, spanning from north to south (Figure). We determined the neutralization titer of each serum sample by using a surrogate assay without an infectious NiV, as previously established (*9*). Using vesicular stomatitis virus expressing secreted alkaline phosphatase pseudotyped with G and F proteins of the NiV strain from Malaysia (VSV-NiV-SEAP) (*9*), we determined the titer of the neutralizing antibody. Moreover, we performed detection of NiV RNA with reverse transcription PCR by using consensus primers that widely detect paramyxoviruses (PAR-F1, PAR-F2, and PAR-R) (Appendix, https://wwwnc.cdc.gov/EID/article/31/8/25-0210-App1.pdf) (*10*).

In total, we diluted 326 bat serum samples 80-fold and screened for VSV-NiV-SEAP (Table) (*9*). We subjected 4 serum samples that tested reactive in screening to serial dilution. We determined antibody titers as values of 16, 41, 47, and 141, which are shown as the reciprocal of the serum dilution factor at which SEAP activity was suppressed by ≥75% after VSV-NiV-SEAP entered the cells (*9*). We obtained positive samples from the insectivorous bat *Hipposideros diadema*, which was captured on Siargao Island j(Figure). We used a similar surrogate system to detect neutralizing antibodies against Hendra virus. The same 4 serum samples showed cell entry inhibition rates ranging from 35.2% to 63.1% against VSV pseudotyped with Hendra virus G and F proteins. Those results were weaker than those obtained for VSV-NiV-SEAP in the screening (Appendix Table). However, because of an insufficient volume of serum samples, we could not perform titration by serial dilution. In contrast, we did not detect any neutralizing antibodies in bats from Mindanao Island or elsewhere (Table). Moreover, we did not detect any viral RNA in reverse transcription PCR targeting paramyxoviruses (including NiV and Hendra virus) using RNA extracted from the 252 samples (collected from serum or spleen) (Table).

In this study, we investigated the prevalence of NiV with bat serum samples collected from 6 regions in the Philippines (Figure). We did not detect any antibodies on Mindanao Island, where the henipavirus outbreak occurred, which may be partially because

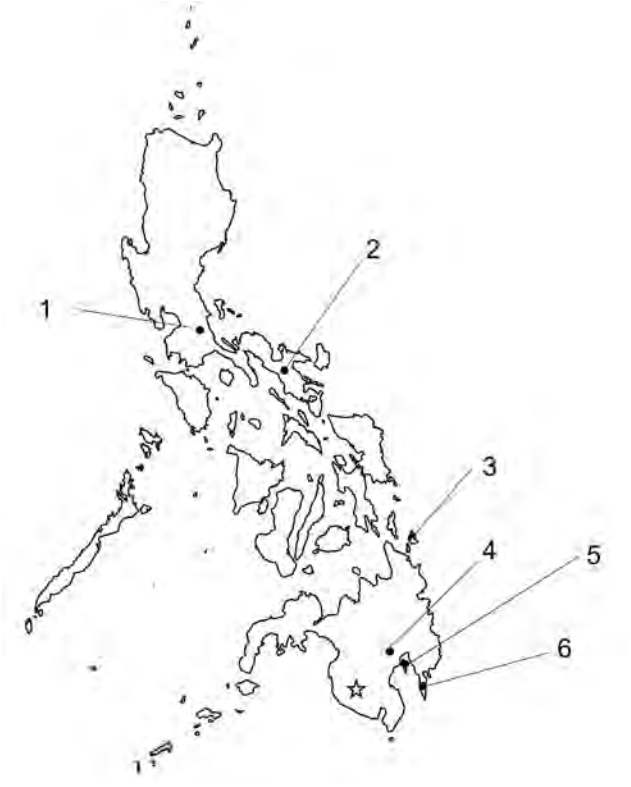

Figure. Locations of 6 bat collection sites for Nipah virus antibodies in bats, the Philippines, 2013–2022. 1, U.P. Laguna Quezon Land Grant, Siniloan, Laguna; 2, Naga, Camarines Sur; 3, Siargao Islands, Surigao del Norte; 4, Baguio District, Davao City, Mindanao; 5, Island Garden City of Samal and Talicud Island, Davao del Norte Province; 6, Lavigan, Governor Generoso, Davao Oriental, Mindanao. Star denotes area where Nipah virus outbreaks were reported in 2014.

Table. Neutralizing antibody titers in serum samples from 13 bat species for Nipah virus antibodies in bats, the Philippines, 2013–2022*

Bat species	No. positive/no. tested using pVSV-SNT						No. positive/no. tested using PaV RT-PCR					
	Site 1	Site 2	Site 3	Site 4	Site 5	Site 6	Site 1	Site 2	Site 3	Site 4	Site 5	Site 6
Cynopterus luzoniensis	0/41	0/25	0/22	NA	NA	NA	0/28	ND	0/17†	NA	NA	NA
Eonycteris spelaea	0/3	NA	0/2	NA	0/13	NA	0/3	NA	0/2†	NA	0/13	NA
Haplonycteris fischeri	0/1	NA	NA	NA	NA	NA	ND	NA	NA	NA	NA	NA
Macroglossus minimus	0/1	NA	0/9	0/1	NA	NA	ND	NA	0/6†	0/1	NA	NA
Ptenochirus jagori	0/63	0/22	0/17	NA	NA	NA	0/63	ND	0/12†	NA	NA	NA
Rousettus amplexicaudatus	0/5	NA	0/3	NA	0/44	0/19	0/5	NA	0/1†	NA	0/46	0/20
Hipposideros coronatus	NA	NA	ND	NA	NA	NA	NA	NA	0/1†	NA	NA	NA
Hipposideros diadema	NA	NA	4/23	NA	NA	NA	NA	NA	0/24†	NA	NA	NA
Hipposideros obscurus	NA	NA	ND	NA	NA	NA	NA	NA	0/9†	NA	NA	NA
Hipposideros pygmaeus	NA	NA	0/1	NA	NA	NA	NA	NA	ND	NA	NA	NA
Rhinolophus arcuatus	NA	NA	0/1	NA	NA	NA	NA	NA	0/1†	NA	NA	NA
Miniopterus eschscholtzii	NA	NA	0/3	NA	NA	NA	NA	NA	ND	NA	NA	NA
Scotophilus kuhlii	NA	0/7	NA	NA	NA	NA	NA	ND	NA	NA	NA	NA

*Site 1, Laguna 2022; site 2, Naga 2019; site 3, Siargao 2019; site 4, Baguio district 2013 (in Davao City); site 5, Samal and Talicud 2013; site 6, Lavigan 2013 (in Governor Generoso Municipality). NA, not applicable; ND, not done; PaV, paramyxovirus; pVSV-SNT, serum neutralizing test using vesicular stomatitis virus pseudovirus expressing the Nipah virus surface proteins (*9*); RT-PCR, reverse transcription PCR.
†RT-PCRs were performed by using RNAs extracted from spleen and not from serum samples.

we could not capture and study the primary reservoir, *Pteropus* bats, which fly and migrate at high altitudes. However, we detected NiV antibodies in 4 samples from 1 insectivorous bat species on Siargao Island (Table), which is geographically close, indicating that the distribution range of NiV is not limited to within Mindanao Island.

Antibodies have been reported from other *Hipposideros* bat species closely related to *H. diadema* (*5*). We also captured a species (*Scotophilus kuhlii*) other than *Pteropus* bats, for which antibodies were similarly detected in bats in previous reports (*5*), but we did not detect any antibodies. In contrast, we could not detect viral RNA in all samples because of the small number of samples. We consider it crucial to obtain more viral genetic information to understand the nature of the virus responsible for the henipavirus epidemic in the Philippines and to take countermeasures. More detailed surveys with larger sample sizes on Mindanao Island and surrounding areas are needed. Surveillance of NiV carriage in bats in the Philippines is necessary to characterize the virus, investigate risk factors for future outbreaks of henipavirus, and implement control measures.

Acknowledgments

We thank Momoko Ogata for assistance in this study. We thank Eduardo Eres, James D.V. Alvarez, Yuki Sugiura, and Roberto Puentespina Jr. for assistance in collecting samples. We also thank Editage (https://www.editage.com) for the English language editing.

Wild bats were captured under a permit issued by the Department of Environment and Natural Resources to the University of the Philippines Los Baños for this research purpose (Wildlife Gratuitous permit nos. RXI-2013-06, R13-2019-27, and R5-2019-105). Furthermore, for every scientific expedition undertaken by the authors to capture bats, a permit was issued by the Biodiversity Management Bureau. Each scientific expedition to capture bats was also covered by a permit granted by the local regional office of the Department of Environment and Natural Resources. The procedures for serum and spleen sample collection after euthanasia of the captured bats were carried out based on the guidance of the institutional animal care and use committee of the University of the Philippines Los Baños.

This study was supported by grants from the Takeda Science Foundation, Kanae Foundation for the Promotion of Medical Science, Japan Society for the Promotion of Science (JSPS KAKENHI, grant no. JP22K06016 and 19KK0242), Health Labour Sciences Research (grant no. 23HA2004), and the Japan Science and Technology Agency (JST SICORP e-ASIA, grant no. JPMJSC20U2).

About the Author

Dr. Kaku is a researcher at the National Institute of Infectious Diseases of Japan. His research interests include epidemiologic studies of henipavirus and rabies virus, analysis of viral pathogenicity mechanisms, and development of diagnostic systems.

References

1. Ang BSP, Lim TCC, Wang L. Nipah virus infection. J Clin Microbiol. 2018;56:e01875-17. https://doi.org/10.1128/JCM.01875-17
2. As AK, Sahay RR, Radhakrishnan C, P S, Kandath S, Patil DY, et al. Clinico-epidemiological presentations and management of Nipah virus infection during the outbreak in Kozhikode district, Kerala state, India 2023. J Med Virol.

2024;96:e29559. https://doi.org/10.1002/jmv.29559
3. Gurley ES, Montgomery JM, Hossain MJ, Bell M, Azad AK, Islam MR, et al. Person-to-person transmission of Nipah virus in a Bangladeshi community. Emerg Infect Dis. 2007;13:1031–7. https://doi.org/10.3201/eid1307.061128
4. Gokhale MD, Sreelekshmy M, Sudeep AB, Shete A, Jain R, Yadav PD, et al. Detection of possible Nipah virus infection in *Rousettus leschenaultii* and *Pipistrellus pipistrellus* bats in Maharashtra, India. J Infect Public Health. 2021;14:1010–2. https://doi.org/10.1016/j.jiph.2021.05.001
5. Plowright RK, Becker DJ, Crowley DE, Washburne AD, Huang T, Nameer PO, et al. Prioritizing surveillance of Nipah virus in India. PLoS Negl Trop Dis. 2019;13:e0007393. https://doi.org/10.1371/journal.pntd.0007393
6. Reynes JM, Counor D, Ong S, Faure C, Seng V, Molia S, et al. Nipah virus in Lyle's flying foxes, Cambodia. Emerg Infect Dis. 2005;11:1042–7. https://doi.org/10.3201/eid1107.041350
7. Ching PK, de los Reyes VC, Sucaldito MN, Tayag E, Columna-Vingno AB, Malbas FF Jr, et al. Outbreak of henipavirus infection, Philippines, 2014. Emerg Infect Dis. 2015;21:328–31. https://doi.org/10.3201/eid2102.141433
8. Taniguchi S, Maeda K, Horimoto T, Masangkay JS, Puentespina R Jr, Alvarez J, et al. First isolation and characterization of pteropine orthoreoviruses in fruit bats in the Philippines. Arch Virol. 2017;162:1529–39. https://doi.org/10.1007/s00705-017-3251-2
9. Kaku Y, Noguchi A, Marsh GA, Barr JA, Okutani A, Hotta K, et al. Second generation of pseudotype-based serum neutralization assay for Nipah virus antibodies: sensitive and high-throughput analysis utilizing secreted alkaline phosphatase. J Virol Methods. 2012;179:226–32. https://doi.org/10.1016/j.jviromet.2011.11.003
10. Tong S, Chern SW, Li Y, Pallansch MA, Anderson LJ. Sensitive and broadly reactive reverse transcription-PCR assays to detect novel paramyxoviruses. J Clin Microbiol. 2008;46:2652–8. https://doi.org/10.1128/JCM.00192-08

Address for correspondence: Shumpei Watanabe, Department of Microbiology, Faculty of Veterinary Medicine, Okayama University of Science, 1-3 Ikoinooka, Imabari, Ehime 794-8555, Japan; email: s-watanabe@ous.ac.jp

Crimean-Congo Hemorrhagic Fever Virus Africa 1 Lineage in *Hyalomma dromedarii* Ticks, Algeria, 2023

Marbouha Temani, Aissam Hachid, Rafik Garni, Amir Abderezzak Guessoum, Mohammed Hocine Benaissa, Ahmed Fayez Khardine, Abdelhakim Kimouche, Ahcéne Hakem, Idir Bitam, Kamal Eddine Benallal,[1] Ismail Lafri[1]

Author affiliations: Institut Pasteur d'Algérie, Algiers, Algeria (M. Temani, A. Hachid, R. Garni, A.A. Guessoum, A.F. Khardine, K.E. Benallal, I. Lafri); Université Alger 1 Faculté de Pharmacie, Algiers (A. Hachid); Centre de Recherche Scientifique Et Technique Sur Les Régions Arides, Touggourt, Algeria (M.H. Benaissa); Inspéction Vétérinaire, Direction des Services Agricoles de la Wilaya d'Illizi, Illizi, Algeria (A. Kimouche); Centre de Recherche en Agropastoralisme, Djelfa, Algeria (A. Hakem, I. Bitam); Université de Blida 1, Blida, Algeria (I. Lafri)

DOI: https://doi.org/10.3201/eid3108.250123

We conducted a Crimean-Congo hemorrhagic fever virus (CCHFV) survey of *Hyalomma* spp. ticks collected from camels in southeastern Algeria. Of 138 tick pools, 1 was CCHFV positive; the sequenced strain belonged to the Africa 1 genotype. Healthcare professionals in Algeria should be aware of this detection of a circulating pathogenic CCHFV genotype.

Infection with Crimean Congo hemorrhagic fever virus (CCHFV; *Orthonairovirus hemorrhagiae*; Nairoviridae: Bunyavirale) provokes fever and hemorrhagic manifestations in humans but results in asymptomatic infections in animals (*1*). CCHFV is maintained in nature through wild and domestic animals serving as amplification hosts and ticks as reservoirs. CCHFV is endemic to Africa, the Middle East, Asia, and Europe (*2*). However, knowledge of CCHFV in North Africa is limited to few serologic surveys and molecular characterization in ticks.

In Algeria, Agai virus (*Orthonairovirus parahemorrhagiae*), previously known as AP92-like CCHFV, has been detected in *Hyalomma aegyptium* ticks collected from tortoises (*3*). In addition, 2 seroprevalence studies of CCHFV conducted on dromedary camels (*Camelus dromedarius*) in different regions from southern Algeria showed a high rate of IgG against CCHFV (*2*,*4*). We aimed to detect CCHFV among ticks in southern Algeria, where serologic evidence of the virus was reported among camels.

[1]These authors contributed equally to this article.

During September–November 2023, we conducted surveillance for CCHFV in ticks collected from camels in the Wilayates (provinces) of Ouargla, Illizi, and Djanet, located in southeastern Algeria (Appendix, https://wwwnc.cdc.gov/EID/article/31/8/25-0123-App1.pdf). We morphologically identified ticks by using taxonomic keys and pooled specimens on the basis of species, sex, developmental stage, feeding status, and collection sites; we stored pools at −80°C until analysis. We cleaned ticks with 70% ethanol and then crushed them by using a Retsch MM 400 Mixer Mills (https://www.retsch.com). We extracted nucleic acid material (RNA and DNA) from supernatants by using NucleoSpin Virus kits (Macherey-Nagel, https://www.mn-net.com), according to the manufacturer's instructions. We screened tick extracts for CCHFV by using real-time reverse transcription PCR (RT-PCR) targeting the small (S) segment of CCHFV (*5*) and confirmed positive pools by using an endpoint RT-PCR targeting the S segment of the *Nairovirus* group (*6*), followed by Sanger sequencing. We molecularly confirmed positive pools by sequencing the mitochondrial cytochrome oxidase I gene (*7*). We constructed a maximum-likelihood tree with 1,000 bootstrap replicates using a Tamura 1992 with gamma distribution substitution model (*8*) using different CCHFV sequence genotypes (Figure). We deposited the sequence obtained in this study into GenBank (accession no. PQ246052).

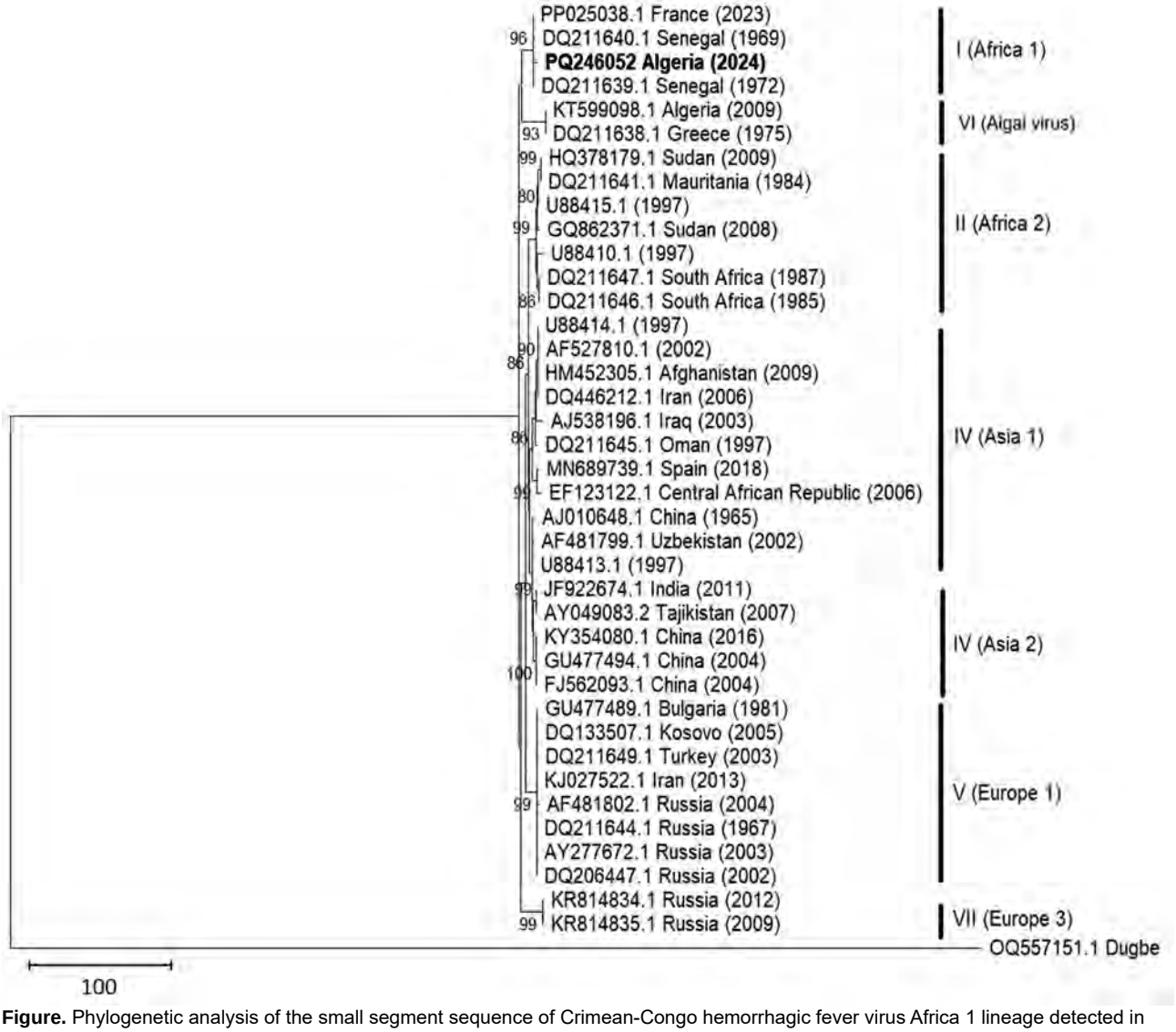

Figure. Phylogenetic analysis of the small segment sequence of Crimean-Congo hemorrhagic fever virus Africa 1 lineage detected in ticks collected from camels in southeastern Algeria, 2023. Bold indicates the strain detected in Algeria; other sequences are labeled by GenBank accession number, geographic origin, and sampling year. Only bootstrap values >80 are shown. Scale bar indicates substitutions per site.

Table. Description of CCHFV in tick pools collected from camels in southeastern Algeria, 2023*

Wilayates (province)	Tick species	No. pools	No. ticks/pool, by sex	Positive pool no./Ct/sex
Ouargla	*Hyalomma dromedarii*	45	20 M, 25 F	
	Hy. rufipes	2	1 M, 1 F	
Illizi	*Hy. dromedarii*	60	23 M, 37 F	13/39.04/M; 22/26.91/M
	Hy. rufipes	4	1 M, 3 F	
	Hy. impeltatum	6	1 M, 5 F	19/36.24/M
	Hy. impressum	2	2 F	
Djanet	*Hy. dromedarii*	13	4 M, 9 F	
	Hy. impeltatum	4	4 F	
	Hy. impressum	2	2 M	

*Pools of ticks were tested with quantitative reverse transcription PCR for the small segments of CCHFV RNA. A total of 138 pools, comprising 346 ticks collected from 103 camels, were tested for CCHFV. Only 3 pools of *Hy. dromedarii* ticks from Illizi were CCHFV positive; only the pool in bold, containing 5 male *Hy. dromedarii* ticks, generated a 465-bp fragment of the small segment using the endpoint RT-PCR. CCHFV, Crimean-Congo hemorrhagic fever virus; Ct, cycle threshold.

We grouped a total of 346 ticks collected from 103 camels into 138 pools. Tick species consisted of 290 (83.81%) *Hy. dromedarii*, 26 (7.51%) *Hy. rufipes*, 19 (5.49%) *Hy. impeltatum*, and 11 (3.17%) *Hy. impressum* (Table). Each pool contained 1–5 ticks grouped by feeding status, species, locality, and sex. Three pools tested positive for CCHFV by the first real-time RT-PCR: pool 22 (cycle threshold [Ct] value = 26.91), pool 19 (Ct = 36.24), and pool 13 (Ct = 39.04). Only pool 22, containing 5 male *Hy. dromedarii* ticks, generated a 465-bp fragment of the S segment using the endpoint RT-PCR. A maximum-likelihood tree showed that the Algeria sequence formed a monophyletic group or cluster with strains from Senegal and France belonging to the Africa 1 genotype (GenBank accession nos. DQ211639, DQ211639, and PP025038) with 95% bootstrap support (Figure). Molecular identification of ticks in positive pools using cytochrome oxidase I gene confirmed the presence of *Hy. dromedarii* and *Hy. impeltatum* ticks (Table), both species are known as competent vectors for CCHFV.

We detected and characterized a pathogenic strain of CCHFV in local tick populations collected from camels in southern Algeria, underscoring circulation of the virus in this region. Camels play a vital economic and cultural role in the region, especially through transhumance. However, movements between Algeria and endemic areas in neighboring countries through legal and illegal cross-border trade increase the likelihood of encountering viremic animals and tick vectors. Moreover, migratory birds from the Trans-Saharan Flyway carrying *Hyalomma* spp. ticks are likely a major source of CCHFV strains circulating between Africa and Europe, as reported in Morocco and France (*9*,*10*). Our findings suggest that the possible pathway of CCHFV dissemination to Algeria from endemic areas could involve migratory birds, considering that the CCHFV Africa 1 strain identified in this study is phylogenetically closely related to the strains previously reported in Corsica (France) and Senegal. The potential for the continuous spread of CCHFV across Algeria and North Africa is substantial. Indeed, Algeria's large territory harbors various tick species known for their CCHFV transmission competence, increasing the likelihood of CCHFV circulation among ticks and animals. This study, limited to 3 provinces in the Sahara, serves as a starting point for broader epidemiologic studies across the country; expanding surveillance to other regions, animals, humans, and tick vectors is crucial for informing policy-makers and enabling a comprehensive risk assessment of CCHFV exposure in Algeria. Using next-generation sequencing technologies for whole-genome sequencing of CCHFV will enable detailed genomic characterization and clarify spatiotemporal transmission dynamics.

In summary, our results document detection of a CCHFV pathogenic genotype among camels in Algeria, carried by *Hyalomma* spp. ticks. Healthcare professionals should be aware of CCHFV circulation in this region and the resulting potential for human infection.

Acknowledgments

We thank the local veterinary authorities for their technical and administrative supports and all camel breeders for their collaboration during sample collection.

This study was carried out under the auspices of the Ministry of Higher Education and Scientific Research of Algeria, as part of 2 approved research projects. Informed consents were obtained from all the camel owners at the time of tick sampling. The procedure for tick collection was performed by qualified entomologists of Institut Pasteur of Algeria. To ensure the well-being and safety of both the staff and the animals, appropriate physical restraint measures were taken before conducting tick collection.

This study was financially supported by the project LABEX-TA 2019 (EVARBO) and the project Programme

National de Recherche, supervised by I.L. and funded by the Ministry of Higher Education and Scientific Research of Algeria, The Directorate-General for Scientific Research and Technological Development, registered in 2021 and 2023.

About the Author

Dr. Temani is scientific microbiologist at Institut Pasteur d'Algérie, Algiers, Algeria. Her research interest are arboviruses and seroneutralization techniques.

References

1. Sánchez-Seco MP, Sierra MJ, Estrada-Peña A, Valcárcel F, Molina R, de Arellano ER, et al.; Group for CCHFv Research. Widespread detection of multiple strains of Crimean-Congo hemorrhagic fever virus in ticks, Spain. Emerg Infect Dis. 2021;28:394–402. https://doi.org/10.3201/eid2802.211308
2. Degui D, Hachid A, Derrar F, Messahel NE, Bia T, Mockbel Y, et al. A survey of the tick-borne disease Crimean-Congo hemorrhagic fever in southern Algeria: first serological evidence in the dromedary camel population. Vet Parasitol Reg Stud Reports. 2024;54:101089. https://doi.org/10.1016/j.vprsr.2024.101089
3. Kautman M, Tiar G, Papa A, Široký P. AP92-like Crimean-Congo hemorrhagic fever virus in *Hyalomma aegyptium* ticks, Algeria. Emerg Infect Dis. 2016;22:354–6. https://doi.org/10.3201/eid2202.151528
4. Guidoum KA, Carrera-Faja L, Espunyes J, Pailler-García L, Benallou B, Bouabdelli S, et al. Crimean-Congo hemorrhagic fever virus seropositivity among dromedary camels, Algeria, 2020–2021. Emerg Infect Dis. 2023;29:2546–8. https://doi.org/10.3201/eid2912.230587
5. Atkinson B, Chamberlain J, Logue CH, Cook N, Bruce C, Dowall SD, et al. Development of a real-time RT-PCR assay for the detection of Crimean-Congo hemorrhagic fever virus. Vector Borne Zoonotic Dis. 2012;12:786–93. https://doi.org/10.1089/vbz.2011.0770
6. Lambert AJ, Lanciotti RS. Consensus amplification and novel multiplex sequencing method for S segment species identification of 47 viruses of the *Orthobunyavirus*, *Phlebovirus*, and *Nairovirus* genera of the family *Bunyaviridae*. J Clin Microbiol. 2009;47:2398–404. https://doi.org/10.1128/JCM.00182-09
7. Folmer O, Black M, Hoeh W, Lutz R, Vrijenhoek R. DNA primers for amplification of mitochondrial cytochrome c oxidase subunit I from diverse metazoan invertebrates. Mol Mar Biol Biotechnol. 1994;3:294–9.
8. Tamura K, Stecher G, Kumar S. MEGA11: Molecular Evolutionary Genetics Analysis version 11. Mol Biol Evol. 2021;38:3022–7. https://doi.org/10.1093/molbev/msab120
9. Palomar AM, Portillo A, Santibáñez P, Mazuelas D, Arizaga J, Crespo A, et al. Crimean-Congo hemorrhagic fever virus in ticks from migratory birds, Morocco. Emerg Infect Dis. 2013;19:260–3. https://doi.org/10.3201/eid1902.121193
10. Kiwan P, Masse S, Piorkowski G, Ayhan N, Gasparine M, Vial L, et al. Crimean-Congo hemorrhagic fever virus in ticks collected from cattle, Corsica, France, 2023. Emerg Infect Dis. 2024;30:1036–9. https://doi.org/10.3201/eid3005.231742

Address for correspondence: Ismail Lafri, Institut Pasteur d'Algérie, Route du Petit Staoueli, Dely-Ibrahim, Algiers 16000, Algeria; email: lafrismail@gmail.com

Emergence of Novel Fluoroquinolone Resistance Mutations in *Mycoplasma bovis*, China, 2008–2023

Shimei Lan, Shuang Liu, Wenjing Cui, Zhangcheng Li, Huafang Hao, Ahmed Adel Baz, Jinjia Liang, Xiangrui Jin, Xinmin Yan, Pengcheng Gao, Fuying Zheng, Shengli Chen,[1] Yuefeng Chu[1]

Author affiliations: State Key Laboratory for Animal Disease Control and Prevention, College of Veterinary Medicine, Lanzhou University, Lanzhou Veterinary Research Institute, Chinese Academy of Agricultural Sciences, Lanzhou, China (S. Lan, S. Liu, W. Cui, Z. Li, H. Hao, A.A. Baz, J. Liang, X. Jin, X. Yan, P. Gao, F. Zheng, S. Chen, Y. Chu); Gansu Province Research Center for Basic Disciplines of Pathogen Biology, Lanzhou (S. Lan, S. Liu, Z. Li, H. Hao, A.A. Baz, J. Liang, X. Jin, X. Yan, P. Gao, F. Zheng, S. Chen, Y. Chu); Key Laboratory of Veterinary Etiological Biology, Key Laboratory of Ruminant Disease Prevention and Control (West), Ministry of Agricultural and Rural Affairs, Lanzhou (S. Lan, S. Liu, Z. Li, H. Hao, A.A. Baz, J. Liang, X. Jin, X. Yan, P. Gao, F. Zheng, S. Chen, Y. Chu)

DOI: https://doi.org/10.3201/eid3108.241137

We investigated quinolone resistance in *Mycoplasma bovis* samples isolated in China during 2008–2023. Sequence type 52 was the dominant genotype; GyrA (S83F/Y) and ParC (S80R) protein double mutations caused high resistance to fluoroquinolones. Increased vigilance and surveillance of *M. bovis* infections in cattle will be needed to prevent disease.

Diseases in cattle caused by *Mycoplasma bovis* include bronchopneumonia, mastitis, and arthritis (*1*,*2*). *M. bovis* was first isolated in 1961 (*3*) and, over the past >6 decades, it has become widespread worldwide. Bovine mycoplasmosis caused by *M. bovis* is an emerging disease in China. Since the first isolation of *M. bovis* strains in China's Hubei region in 2008, those strains have spread rapidly and extensively to most provinces in China (*4*–*6*). However, the epidemiologic features of *M. bovis* in China are unknown. Antimicrobial drugs are currently a critical means of controlling *M. bovis* infections (*7*,*8*). Fluoroquinolones have a substantial bactericidal effect against *Mycoplasma* spp.; however, their effectiveness has been gradually declining (*9*,*10*). Fluoroquinolone resistance in *Mycoplasma* spp. relies primarily on gene point mutations (*7*).

[1]These senior authors contributed equally to this article.

To elucidate molecular epidemiologic features of *M. bovis* in China, we performed a genetic evolutionary analysis of whole-genome sequences from 77 *M. bovis* isolates collected during 2008–2023 from 16 provinces in China; 34 isolates were identified in this study and 43 isolates were from GenBank (Appendix Table 1, https://wwwnc.cdc.gov/EID/article/31/8/24-1137-App1.pdf). We deposited sequence data for the *M. bovis* isolates from this study in the National Center for Biotechnology Information BioProject database (https://www.ncbi.nlm.nih.gov/bioproject; accession nos. PRJNA1124599–601).

We explored the contribution of genetic factors to fluoroquinolone resistance. We confirmed that sequence type (ST) 52, the primary genotype responsible for the *M. bovis* infection outbreak in 2008, was the most prevalent genotype in China; however, the topologic structure of the phylogenetic tree classified the 77 isolates into 5 distinct clusters (I–V) (Figure 1). Five of those isolates represented new multilocus sequence

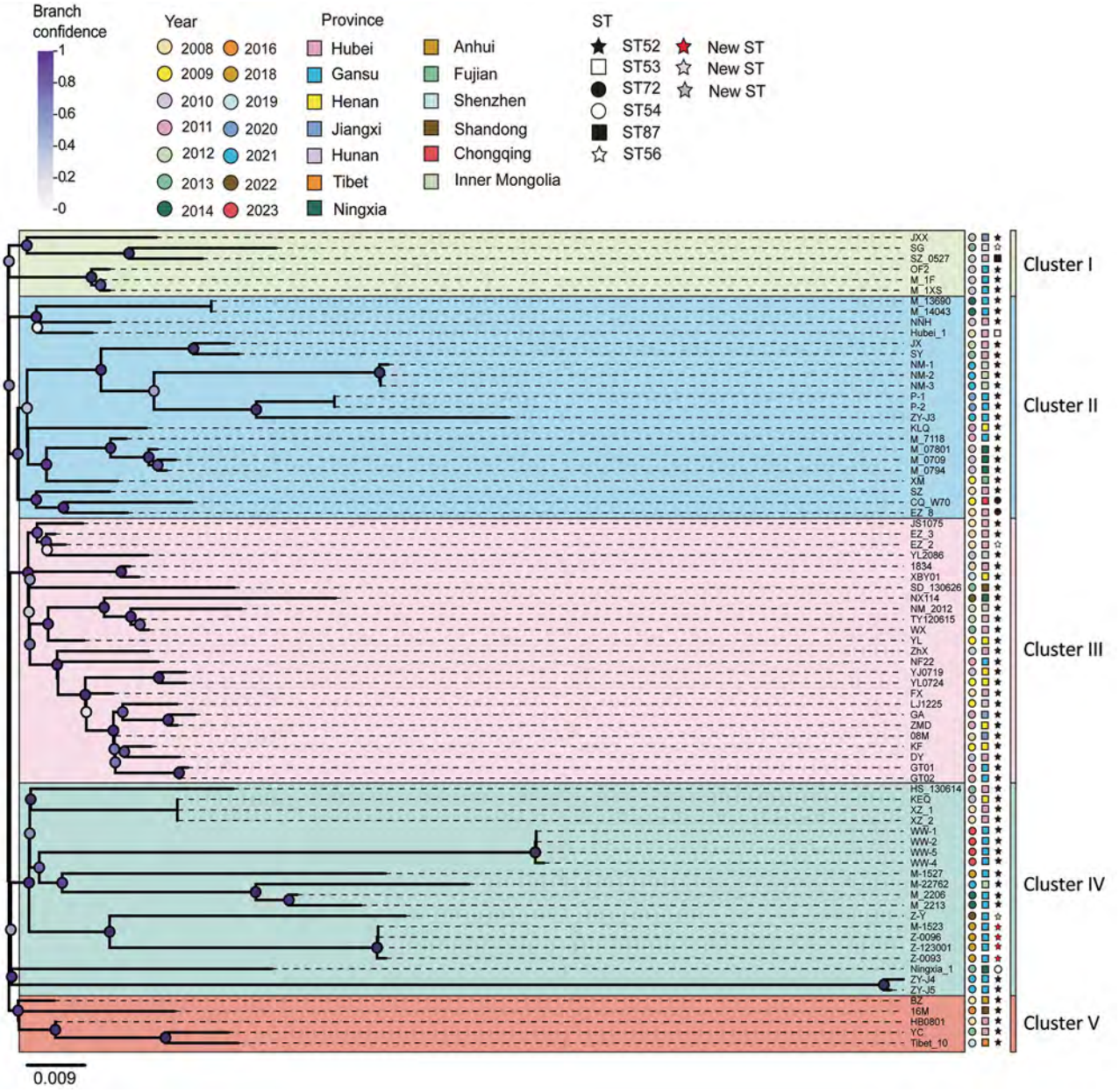

Figure 1. Phylogenetic analysis of *Mycoplasma bovis* in study of emergence of novel fluoroquinolone resistance mutations, China, 2008–2023. Maximum-likelihood tree shows 77 *M. bovis* isolates according to single-nucleotide polymorphisms identified by referencing the complete genome sequence of *M. bovis* strain HB0801. Name of isolate, year isolated, province, sequence type, and clustering are indicated. Scale bar indicates nucleotide substitutions per site.

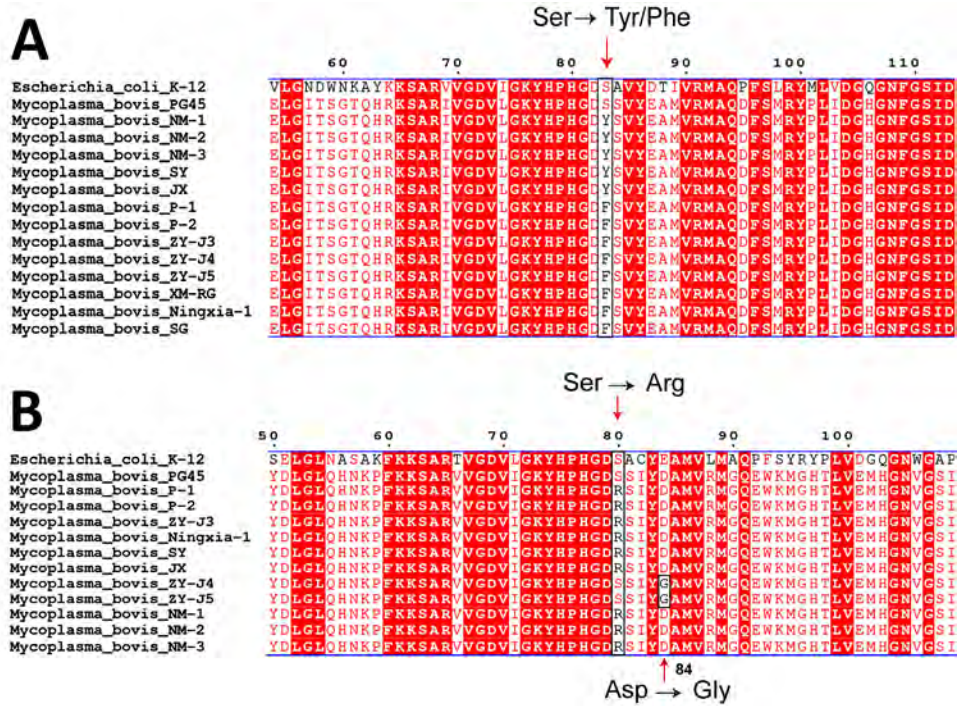

Figure 2. Amino acid sequence alignments of quinolone resistance-determining regions of *Mycoplasma bovis* isolates from China, 2008–2023. Multiple alignments of conserved GyrA (A) and ParC (B) protein sequences for *M. bovis* ParC protein–ciprofloxacin complex are shown. *Escherichia coli* K12 and *M. bovis* PG45 strains were used as controls. Red arrows and black rectangular borders indicate amino acid mutation sites.

typing (MLST) genotypes, which were primarily concentrated in cluster IV (which contained 4 MLST genotypes) (Figure 1; Appendix Figure 1), suggesting that isolates within cluster IV might have undergone rapid genetic changes. During the disease outbreak in 2008, ST53, ST56, and ST72 genotypes were also identified. Although those 3 genotypes were distributed sporadically, they have been isolated only in China and belong to the same clonal complex (CC) 52 as ST52 (Appendix Figure 1), exhibiting a high degree of genetic relatedness. That observation suggests that ST52 underwent genetic variation after spreading extensively in China. ST89 was isolated from cows with pneumonia and mastitis in China during 2018–2019 (Appendix Table 2); however, that genotype does not belong to CC52 (Appendix Figure 1). The isolation of only 3 ST89 strains suggested that strains with other genotypes might be infecting cattle in China.

We analyzed mutations within quinolone resistance–determining regions of the 77 isolated genomes from China. Mutations in those regions occurred primarily in *parC* and *gyrA* genes, leading to amino acid changes (Appendix Figure 2). Specifically, the GyrA protein contained S83Y and S83F mutations (Figure 2, panel A), and ParC contained S80R and D84G (Figure 2, panel B). The S80R mutation in ParC is uncommon in *M. bovis* and has not been reported in China. The binding energies of the GyrA S83F and S83Y and ParC S80R mutants with ciprofloxacin were higher than those for wild-type GyrA and ParC proteins. The mean ± SD binding energy increased from −46.115 ± 8.72 in wild-type GyrA to −10.242 ± 2.892 in the GyrA S83Y mutant (Appendix Table 3). The ParC S80R mutant had considerably higher binding energy than wild-type ParC, increasing from −19.973 ± 2.445 in wild-type protein to 26.861 ± 5.14 in the mutant. Those mutations led to a decreased and unstable binding capacity of GyrA and ParC with ciprofloxacin.

We investigated the effect of mutations on fluoroquinolone susceptibility of *M. bovis*. Clinical isolates with the GyrA S83Y/F and ParC S80R double mutations exhibited lower susceptibility to fluoroquinolones than strains that had the GyrA S83F and ParC D84G double mutations (Appendix Table 4, Figure 3), suggesting that S83Y/F in GyrA combined with S80R in ParC conferred high resistance to fluoroquinolones; the S80R ParC mutation appeared to be the main reason for increased fluoroquinolone resistance. Molecular dynamic simulations revealed that residue S80 of *M. bovis* ParC interacts with enrofloxacin through van der Waals forces (Appendix Figure 4). Strains with GyrA and ParC mutations were mainly

concentrated in cluster II (Figure 1), suggesting that cluster II strains are more prone to developing genetic features that confer resistance to fluoroquinolones.

In conclusion, we report that ST52 is the dominant *M. bovis* genotype circulating in China; however, ST52 strains gradually formed 2 subgroups with dominant genetic variation and fluoroquinolone resistance through widespread dissemination. The double mutation, S83F in GyrA and S80R in ParC, appears to be the current widespread mutation combination in China, and the emergence of high resistance to fluoroquinolones is driven by the ParC S80R mutation. Widespread resistance to fluoroquinolones poses a substantial challenge to the prevention and treatment of infections caused by *Mycoplasma* species; thus, increased vigilance and surveillance of *M. bovis* infections in cattle will be needed to prevent disease spread.

This work was supported by grants from the Key Program of the Natural Science Foundation of Gansu Province (grant no. 22JR5RA409), National Natural Science Foundation of China (grant no. 32373019), and Chinese Academy of Agricultural Science and Technology Innovation Project (grant no. CAAS-ASTIP-JBGS-20210701).

About the Author

Dr. Lan is a postdoctoral research scientist at the Mycoplasma Research Group in Bacterial Disease Team, State Key Laboratory for Animal Disease Control and Prevention and Lanzhou Veterinary Research Institute, Chinese Academy of Agricultural Sciences. Her research interests focus on the pathogenesis, prevention, and control of pathogenic *Mycoplasma* spp. in animals and *M. pneumoniae* in humans.

References

1. Kinnear A, Waldner M, McAllister TA, Zaheer R, Register K, Jelinski M. Application of four genotyping methods to *Mycoplasma bovis* isolates derived from western Canadian feedlot cattle. J Clin Microbiol. 2021;59:e0004421. https://doi.org/10.1128/JCM.00044-21
2. Nicholas RAJ, Ayling RD. *Mycoplasma bovis*: disease, diagnosis, and control. Res Vet Sci. 2003;74:105–12. https://doi.org/10.1016/S0034-5288(02)00155-8
3. Hale HH, Helmboldt CF, Plastridge WN, Stula EF. Bovine mastitis caused by a *Mycoplasma* species. Cornell Vet. 1962;52:582–91. PubMed
4. Qi J, Guo A, Cui P, Chen Y, Mustafa R, Ba X, et al. Comparative geno-plasticity analysis of *Mycoplasma bovis* HB0801 (Chinese isolate). PLoS One. 2012;7:e38239. https://doi.org/10.1371/journal.pone.0038239
5. Niu J, Li K, Pan H, Gao X, Li J, Wang D, et al. Epidemiological survey of *Mycoplasma bovis* in yaks on the Qinghai Tibetan Plateau, China. BioMed Res Int. 2021;2021:6646664. PubMed https://doi.org/10.1155/2021/6646664
6. Guo Y, Luo H, Guo S, Lei Y, Li Y, He S. Multi-locus sequence typing of *Mycoplasma bovis* to assess its genetic diversity from 2009 to 2018 in Ningxia Hui Autonomous Region, China. BMC Vet Res. 2020;16:454. https://doi.org/10.1186/s12917-020-02668-x
7. Gautier-Bouchardon AV. Antimicrobial resistance in *Mycoplasma* spp. Microbiol Spectr. 2018;6:10.1128/microbiolspec.arba-0030-2018. https://doi.org/10.1128/microbiolspec.ARBA-0030-2018
8. Lysnyansky I, Ayling RD. *Mycoplasma bovis*: mechanisms of resistance and trends in antimicrobial susceptibility. Front Microbiol. 2016;7:595. https://doi.org/10.3389/fmicb.2016.00595
9. Gautier-Bouchardon AV, Ferré S, Le Grand D, Paoli A, Gay E, Poumarat F. Overall decrease in the susceptibility of *Mycoplasma bovis* to antimicrobials over the past 30 years in France. PLoS One. 2014;9:e87672. https://doi.org/10.1371/journal.pone.0087672
10. Niu J, Yan M, Xu J, Xu Y, Chang Z, Sizhu S. The resistance mechanism of *Mycoplasma bovis* from yaks in Tibet to fluoroquinolones and aminoglycosides. Front Vet Sci. 2022;9:840981. https://doi.org/10.3389/fvets.2022.840981

Address for correspondence: Shengli Chen and Yuefeng Chu, State Key Laboratory for Animal Disease Control and Prevention, College of Veterinary Medicine, Lanzhou University, Lanzhou Veterinary Research Institute, Chinese Academy of Agricultural Sciences, No. 1, Xujiaping, Chengguan District, Lanzhou Gansu Province, 730046, China; email: chenshengli@caas.cn and chuyuefeng@caas.cn

Severe Fever with Thrombocytopenia Syndrome Acquired through Dog Bite, South Korea

Uh Jin Kim,[1] Hae Seong Jeong,[1] Keon Kim,[1] Ahrang Lee, Minji Kim, Sarah Kim, Sung Un Shin, Seung-Ji Kang, Sook In Jung, Hyungjun Kwak, Woong-Bin Ro, Choon-Mee Kim, Dong-Min Kim,[2] Kyung-Hwa Park[2]

Author affiliations: Chonnam National University Hospital, Gwangju, South Korea (U.J. Kim, H.S. Jeong, A. Lee, M. Kim, S. Kim, S.U. Shin, S.-J. Kang, S.I. Jung, K.-H. Park); Chonnam National University Medical School, Gwangju (U.J. Kim, S.-J. Kang, S.I. Jung, K.-H. Park); Chonnam National University College of Veterinary Medicine, Gwangju (K. Kim, W.-B. Ro); Gwangsan-gu Public Health Center, Gwangju (H. Kwak); Chosun University College of Medicine Gwangju (C.-M. Kim, D.-M. Kim); Chosun University Hospital, Gwangju (D.-M. Kim)

DOI: https://doi.org/10.3201/eid3108.250090

A veterinary technician in South Korea contracted severe fever with thrombocytopenia syndrome virus from a dog bite. Molecular evidence, including PCR sequencing, supports dog-to-human transmission. The case underscores the zoonotic risks posed by companion animals and highlights the importance of preventive measures.

Severe fever with thrombocytopenia syndrome (SFTS) is a zoonotic infectious disease caused by SFTS virus (*Dabie bandavirus*), primarily transmitted through tick bites (*1*). SFTS continues to spread across East Asia and poses a substantial public health threat; fatality rate in humans is ≈20% (*1*). Interspecies acquisition involving companion animals remains poorly understood; some reports suggest virus transmission from infected cats or dogs, but most lack definitive evidence such as documented bites (*2*–*4*). In South Korea, several canine SFTS cases have been reported (*5*). We describe a case of probable dog-to-human transmission of SFTSV through a bite, supported by molecular evidence.

A 23-year-old veterinary technician was transferred to Chonnam National University Hospital, a tertiary hospital in Gwangju, South Korea, after 6 days of fever. Laboratory findings showed leukopenia, thrombocytopenia, low C-reactive protein, and elevated liver enzymes and ferritin. The patient disclosed that a sick dog had bitten her right thumb 10 days before hospital admission; she had fed the dog wearing a mask but not gloves. The 7-mm wound had begun to heal after initial bleeding. The wound was rinsed under running water for <5 minutes before she arrived; hospital staff later applied antiseptic and administered a tetanus vaccine. Although the patient had no history of outdoor activity or known tick exposure, SFTS was suspected and subsequently confirmed by blood PCR. Her condition worsened on hospital day 2; we performed plasmapheresis on days 3 and 6 in the intensive care unit, leading to improvement.

The suspected source was a 4-year-old neutered male Pomeranian experiencing high fever, leukopenia, and thrombocytopenia, admitted to an animal hospital 10 days before the patient's hospital admission. According to its owner, the dog had experienced 4 days of fever and anorexia; lethargy was first noted ≈22 days before hospital admission. After 2 weeks of supportive care, the dog fully recovered.

To investigate potential dog-to-human transmission of SFTSV, we tested samples from the patient and the dog by reverse transcription PCR and immunofluorescent assay as previously described (*5*,*6*). To confirm the quantitative PCR results targeting the small segment by using the careGENE SFTS Virus RT-PCR kit (Wells Bio, https://www.wells-bio.net), we performed nested PCR. The dog's saliva (collected on patient's hospital day 4) showed a low level of SFTSV RNA (cycle threshold value 36.44), although no band was visible on nested PCR (Table). Sequencing of the nested PCR amplicon from blood samples revealed 99.6% identity in the medium segment and 100% in the large segment (Figure). Virus culture and sequencing of the small segment were unsuccessful.

Although the dog lived in an urban area, it was walked daily in nearby parks with dense vegetation. In the epidemiologic investigation, no ticks were found directly on the dog. We collected a total of 11 ticks from a suspected tick exposure site, a 94 m–high trail (34°58′15″N, 127°33′51″E) the dog and its owner frequently visited. The collected ticks included 6 adult female, 3 adult male, and 1 nymph *Haemaphysalis longicornis* ticks and 1 *Ixodes granulatus* nymph. All collected ticks tested negative for SFTSV.

A total of 43 persons, 3 household members with direct exposure to its saliva or bodily fluids and 40 veterinary staff, had contact with the dog. The Korea Disease Control and Prevention Agency recommended 2 weeks of symptom monitoring and PCR

[1]These first authors contributed equally to this article.

[2]These senior authors contributed equally to this article.

Table. Characteristics of samples infected with severe fever with thrombocytopenia syndrome virus, South Korea*

Source	Day	Specimen	Nested PCR			qPCR	IFA†	
			S seg, 346 bp	M seg, 540 bp	L seg, 860 bp	S seg, 71 bp	IgG	IgM
Human	HD 2	Blood	Positive	Positive	Positive	26.76	<1:32	<1:32
Dog	HD 0	Blood	Weak positive	Positive	Positive	32.99	ND	ND
	HD 2	Blood	Negative	Negative	Negative	38.32	>1:1,024	ND
	HD 4	Urine	Negative	Negative	Negative	32.18	1:32	ND
	HD 4	Saliva	Negative	Negative	Negative	36.44	ND	ND

*HD, hospital day. IFA, indirect immunofluorescence assay; L, large; M, medium; ND, not done; qPCR, quantitative PCR; S, small; seg, segment.
†IFA was performed on serum samples for both the patient and the dog. For the dog, urine and saliva specimens collected on HD 4 (July 6) were also tested in an exploratory manner to assess potential antibody presence in nonserum body fluids.

testing for those with direct contact. No PCR-positive or symptomatic cases were identified. None of the patient's 31 hospital contacts experienced symptoms.

This case provides strong molecular evidence of dog-to-human SFTSV transmission from a bite. Unlike previous reports that relied solely on serologic findings (*2*,*7*), this case was supported by sequence identity and a documented bite. Although we could not isolate viable virus and the viral load in saliva was low, our findings suggest that canine saliva, particularly through dog bites, represents a potential transmission route, consistent with previous studies that detected SFTSV RNA in dog oral swab specimens (*8*) and isolated live virus at ≈10^6 RNA copies/mL concentration from cat saliva (*9*). A limitation of this study is the inability to culture the virus, likely caused by delays in specimen collection. In addition, the absence of early saliva samples limits definitive confirmation of bite-mediated transmission, although the epidemiologic and molecular findings strongly support this route. Serologic testing was not performed for contacts, and asymptomatic cases may have gone undetected.

This case underscores the importance of personal protective equipment and infection control in both veterinary and human healthcare settings to prevent zoonotic transmission. Prompt wound care after animal bite or scratches, including washing with soap and running water for ≥20 minutes, can reduce the risk for infections such as B virus or rabies (*10*). Although the effectiveness of this approach against SFTS is unproven, the same principle may reduce the risk for other viral infections transmitted through animal bites or saliva exposure.

In conclusion, this case emphasizes the risk for SFTSV transmission not only via tick bites but also directly through bites from infected dogs. Enhanced awareness and preventive strategies in both veterinary and human healthcare settings are critical to mitigating the risks of SFTS.

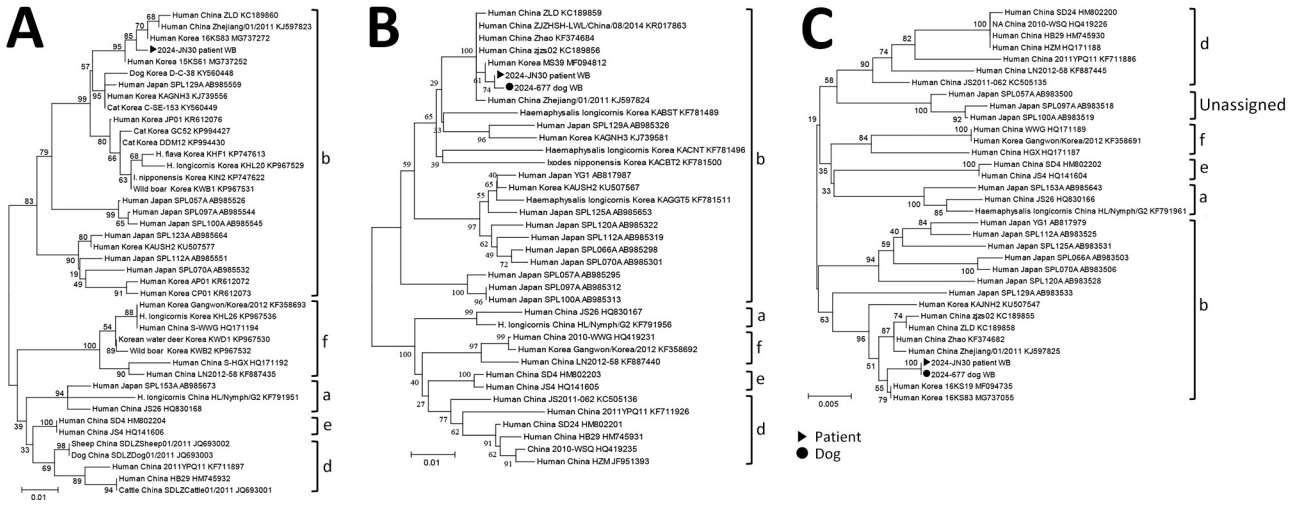

Figure. Phylogenetic analysis of SFTSV small (321 bp) (A), medium (477 bp) (B), and large (696 bp) (C) segments from human patient and dog, South Korea. Clustal X version 2.1 (http://www.clustal.org/clustal2) was used to construct the phylogenetic trees by using neighbor-joining with 1,000 bootstrap replicates. Genotypes of SFTSV are labeled (a, b, d, e, f). BLASTn (https://blast.ncbi.nlm.nih.gov) analysis revealed and nucleotide identity with reference SFTSV strain MF094812 of 99.44% (534/537) for the patient sample and 99.45% (541/544) for the dog sample; nucleotide identity with reference SFTSV strain MF094735 was 99.62% (785/788) for the patient sample and 99.63% (802/805) for the dog sample. The large segment nested PCR results showed 100% identity between the 2 samples. Scale bar indicates number of nucleotide substitutions per site. SFTSV, severe fever with thrombocytopenia syndrome virus.

Acknowledgments

We thank the patient and the animal hospital staff for granting permission to report their clinical symptoms and disease courses.

The patient provided written informed consent for publication. The Institutional Review Board of Chonnam National University granted ethics approval for this study (IRB no. CNUH-2022-032).

The Chonnam National University Hospital Biomedical Research Institute supported this study (grant no. BCR124055).

About the Author

Dr. Kim is an infectious disease specialist and an associate professor at Chonnam National University Hospital in Gwangju, South Korea. Her primary interests are zoonoses and hospital infection control.

References

1. Cui H, Shen S, Chen L, Fan Z, Wen Q, Xing Y, et al. Global epidemiology of severe fever with thrombocytopenia syndrome virus in human and animals: a systematic review and meta-analysis. Lancet Reg Health West Pac. 2024;48:101133. https://doi.org/10.1016/j.lanwpc.2024.101133
2. Oshima H, Okumura H, Maeda K, Ishijima K, Yoshikawa T, Kurosu T, et al. A patient with severe fever with thrombocytopenia syndrome (SFTS) infected from a sick dog with SFTS virus infection. Jpn J Infect Dis. 2022;75:423–6. https://doi.org/10.7883/yoken.JJID.2021.796
3. Yamanaka A, Kirino Y, Fujimoto S, Ueda N, Himeji D, Miura M, et al. Direct transmission of severe fever with thrombocytopenia syndrome virus from domestic cat to veterinary personnel. Emerg Infect Dis. 2020;26:2994–8. https://doi.org/10.3201/eid2612.191513
4. Kobayashi Y, Kato H, Yamagishi T, Shimada T, Matsui T, Yoshikawa T, et al.; SFTS Epidemiological Research Group Japan. Severe fever with thrombocytopenia syndrome, Japan, 2013–2017. Emerg Infect Dis. 2020;26:692–9. https://doi.org/10.3201/eid2604.191011
5. Han SW, Kang JG, Byeon AR, Cho YK, Choi KS, Chae JS. Severe fever with thrombocytopenia syndrome in canines from the Republic of Korea. Ticks Tick Borne Dis. 2020;11:101454. https://doi.org/10.1016/j.ttbdis.2020.101454
6. Kim CM, Han MA, Yun NR, Bang MS, Lee YM, Lee B, et al. Seroprevalence of severe fever with thrombocytopenia syndrome using specimens from the Korea National Health & Nutrition Examination Survey. PLoS Negl Trop Dis. 2023;17:e0011097. https://doi.org/10.1371/journal.pntd.0011097
7. Tsuru M, Suzuki T, Murakami T, Matsui K, Maeda Y, Yoshikawa T, et al. Pathological characteristics of a patient with severe fever with thrombocytopenia syndrome (SFTS) infected with SFTS virus through a sick cat's bite. Viruses. 2021;13:204. https://doi.org/10.3390/v13020204
8. Ishijima K, Tatemoto K, Park E, Kimura M, Fujita O, Taira M, et al. Lethal disease in dogs naturally infected with severe fever with thrombocytopenia syndrome virus. Viruses. 2022;14:1963. https://doi.org/10.3390/v14091963
9. Park ES, Shimojima M, Nagata N, Ami Y, Yoshikawa T, Iwata-Yoshikawa N, et al. Severe fever with thrombocytopenia syndrome phlebovirus causes lethal viral hemorrhagic fever in cats. Sci Rep. 2019;9:11990. https://doi.org/10.1038/s41598-019-48317-8
10. Centers for Disease Control and Prevention. CDC yellow book 2026: health information for international travel. Oxford: Oxford University Press; 2025.

Address for correspondence: Kyung-Hwa Park, Department of Infectious Diseases, Chonnam National University Medical School, 42 Jaebongro, Dong-gu, Gwangju 61469, South Korea; email: iammedkid@naver.com

Corrections

Vol. 31, No. 2

The name of author Alexis M. Siegler was incorrect in Contribution of Limited Molecular Testing to Low Ehrlichiosis Diagnosis in High Incidence Area, North Carolina, USA (A.M. Siegler et al.). The article has been corrected online (https://wwwnc.cdc.gov/eid/article/31/2/24-0281_article).

Vol. 31, No. 6

A category label was incorrect in Table 1 of High Prevalence of Artemisinin-Resistant Plasmodium falciparum, Southeastern Sudan (M. L'Episcopia et al.). The article has been corrected online (https://wwwnc.cdc.gov/eid/article/31/6/24-1810_article).

Vol. 31, No. 7

The name of author Evangelia Ouranou was incorrect in Spatiotemporal Distribution and Clinical Characteristics of Zoonotic Tuberculosis, Spain, 2018–2022 (Á. Roy et al.). The article has been corrected online (https://wwwnc.cdc.gov/eid/article/31/7/25-0031_article).

Henipavirus in Northern Short-Tailed Shrew, Alabama, USA

Viola C. Haring, Sandra Diederich, Martin Beer, Florian Pfaff

Author affiliation: Friedrich-Loeffler-Institut, Greifswald–Isle of Riems, Germany

DOI: https://doi.org/10.3201/eid3108.250401

To the Editor: The article "Henipavirus in northern short-tailed shrew, Alabama, USA," (*1*), describing the discovery of Camp Hill virus (family *Paramyxoviridae*) in the northern short-tailed shrew (*Blarina brevicauda*), sparked major media attention and raised concerns about zoonotic transmission and potential pandemic risk. However, it would be advisable to reevaluate this virus discovery within the broader context of related viruses. The increase in identified henipa-like viruses in various shrew species (*2*–*4*) led the International Committee on Taxonomy of Viruses to classify these henipa-like viruses into a distinct genus, *Parahenipavirus* (*5*), acknowledging their genetic difference from the highly pathogenic Hendra and Nipah virus.

Parahenipaviruses appear to be abundant in white- and red-toothed shrew species globally, but reports of infections in nonshrew species are limited so far, raising questions of their potential for spillover. Of note, no human infections with the Camp Hill virus have been reported to date, which aligns with the authors' statement. The only known related shrew virus, which was detected in febrile, hospitalized humans and later in Ussuri and Shantung white-toothed shrews, was Langya virus (LayV) in China (*4*). The relationship between Camp Hill virus and its supposed reservoir suggests a great evolutionary distance between LayV and the crocidurine shrews. Of note, Hasua virus, a virus discovered in a white-toothed shrew in Germany (*3*), is genetically much closer related to LayV, but there is currently no evidence of associated human infections.

Because of the limited understanding of parahenipaviruses and the lack of evidence for their zoonotic potential, we urge caution in assuming pandemic risks. The absence of viral isolates and serologic studies are major limitations, underscoring the need for future research to guide risk analysis and response strategies.

References

1. Parry RH, Yamada KYH, Hood WR, Zhao Y, Lu JY, Seluanov A, et al. Henipavirus in northern short-tailed shrew, Alabama, USA. Emerg Infect Dis. 2025;31:392–4. https://doi.org/10.3201/eid3102.241155
2. Horemans M, Van Bets J, Joly Maes T, Maes P, Vanmechelen B. Discovery and genome characterization of six new orthoparamyxoviruses in small Belgian mammals. Virus Evol. 2023;9:vead065. https://doi.org/10.1093/ve/vead065
3. Haring VC, Litz B, Jacob J, Brecht M, Bauswein M, Sehl-Ewert J, et al. Detection of novel orthoparamyxoviruses, orthonairoviruses and an orthohepevirus in European white-toothed shrews. Microb Genom. 2024;10:001275. https://doi.org/10.1099/mgen.0.001275
4. Zhang X-A, Li H, Jiang F-C, Zhu F, Zhang YF, Chen JJ, et al. A zoonotic henipavirus in febrile patients in China. N Engl J Med. 2022;387:470–2. https://doi.org/10.1056/NEJMc2202705
5. Simmonds P, Adriaenssens EM, Lefkowitz EJ, Oksanen HM, Siddell SG, Zerbini FM, et al. Changes to virus taxonomy and the ICTV Statutes ratified by the International Committee on Taxonomy of Viruses (2024). Arch Virol. 2024;169:236. https://doi.org/10.1007/s00705-024-06143-y

Address for correspondence: Viola C. Haring, Friedrich-Loeffler-Institut, Sueduefer 10, 17493 Greifswald–Isle of Riems, Germany; email: viola.haring@fli.de

Jean-Antoine Houdon (1741–1828), *Terre cuite marble bust of Honoré-Gabriel Riqueti*, comte de Mirabeau (1749–1791), élu du Tiers-État aux États-Généraux de 1789, 1791. Height, 0.537 m; length, 0.385 m; width, 0.347 m. Total height including polychrome marble pedestal, 0.67 m. Louvre-Lens, Galérie du Temps, Lens, France. Photograph by Andreas G. Nerlich.

The Pockmarked Face of the Comte de Mirabeau

Andreas G. Nerlich, Antonio Perciaccante, Simon T. Donell, Raffaella Bianucci

Honoré Gabriel Riqueti, Comte de Mirabeau (1749–1791 CE), was an accomplished French politician, writer, and orator and a distinguished figure in the National Assembly that governed France during the early phases of the French Revolution. Born a member of the prerevolutionary aristocracy, Mirabeau was a moderate and an advocate of constitutional monarchy. He died at age 42 before the revolution reached its radical climax. According to an autopsy, he died of purulent pericarditis and diffuse toxemia (*1*,*2*).

At age 3, Mirabeau suffered a smallpox infection (*1*,*2*). Supportive care was the treatment in that era, and Mirabeau did not develop severe complications, such as blindness (although he had eye problems in later life), cerebral involvement, or sepsis, which generally led to a high (20%–45%) case-fatality rate. He survived the infection but had high concentration of scars on his chin, cheeks, and nose. He was far from the only historical figure to contract smallpox; Mozart, Beethoven, Queen Elizabeth I, Mary Shelley, George Washington, Abraham Lincoln, Queen Mary II of England, Emperor Joseph I of Austria, and Tsar Peter II of Russia all had the disease (*3*).

The mean incubation period for smallpox is 10–12 days. The prodromal phase (2–3 days) is characterized

Author affiliations: Institute of Legal Medicine, Ludwig-Maximilians-University, Munich, Germany (A.G. Nerlich); Azienda Sanitaria Universitaria Giuliano Isontina Department of Medicine, "San Giovanni di Dio" Hospital, Gorizia, Italy (A. Perciaccante); Université Paris-Saclay, Montigny-le-Bretonneux, France (A. Perciaccante, R. Bianucci); Norwich Medical School, University of East Anglia, Norwich, UK (S.T. Donell)

DOI: https://doi.org/10.3201/eid3108.AC3108

by severe headache, backache, and fever, all beginning abruptly. Enanthema over the tongue, mouth, and oropharynx might precede the rash. The rash has a centrifugal distribution beginning as small, reddish macules, which become papules (2–3 mm) and then vesicles (2–5 mm). The lesions occur first on the face and extremities but gradually cover the body. Pustules (4–6 mm) develop ≈4–7 days after the onset of the rash and remain days to weeks, followed by umbilication and crusting. A second, less pronounced temperature spike might occur 5–8 days after the onset of the rash, especially if the patient has a secondary bacterial infection. The crusts begin separating by the second week of the eruption. Smallpox lesions have a peripheral or centrifugal distribution and are generally all at the same stage of development. Lesions on the palms and soles persist the longest. Death from smallpox is ascribed to sepsis, associated with immune complexes, and to hypotension (*4*,*5*).

Both variola virus (the cause of smallpox) and vaccinia virus (used in smallpox immunization) are associated with ocular complications, including eyelid and conjunctival infection, corneal ulceration, disciform keratitis, iritis, optic neuritis, and blindness (*6*). About 5%–9% smallpox patients developed ocular complications (*7*,*8*).

That Mirabeau had smallpox is confirmed by documentary sources (*1*), and further corroborated by the 1791 terre cuite marble bust by Jean Antoine Houdon (1741–1828) that appears on the cover of this issue of *Emerging Infectious Diseases*. Houdon meticulously reproduced the pockmarks while making the cast of Mirabeau's face on the day he died (April 3, 1791) (*1*,*2*). Pockmarks were also represented in a hard-paste biscuit porcelain bust by Claude-André Deseine (1740–1823), circa 1791–1792. However, no pockmarks were represented in a 1789 portrait by Louis XVI's pastellist, Joseph Boze (1745–1826) (Figure). This omission is not uncommon because facial smallpox undoubtedly posed an aesthetic challenge for both literati and painters or sculptors (*9*).

Smallpox was considered a doubly cruel disease, terrifying its victims and leaving survivors permanently disfigured, and was sometimes viewed as a providential collective sin (as written in several elegies) (*9*). Smallpox was not considered "a provisional sin but was historically seen and interpreted as punishment from God, attributed to sin and moral failings, particularly during periods of violent and widespread epidemics" (*9*). Therefore, artistic license was often used when public persons such as Mirabeau were represented (*9*). Although Boze did not represent Mirabeau's scars in his pastel, he did represent bilateral upper and lower lid ciliary madarosis (*10*,*11*), which manifests in several systemic illnesses, including endocrinopathies, infectious diseases, genetic abnormalities, and some autoimmune disorders (*10*,*11*).

During the 18th Century, ≈50,000–80,000 persons in France and 25,000–30,000 in England died from smallpox each year (*12*–*14*). Those figures also hold true for other countries and regions, which meant smallpox showed comparable mortality rates to plague, at least during outbreaks of the respective diseases (*12*–*14*).

Smallpox was the first infectious disease prevented by targeted (active) immunization, when Edward Jenner used a mild, benign cowpox in 1796 (*15*). However, cowpox might have been used to prevent smallpox in ancient India and, somewhat later, in China (*16*). In Europe, lay variolation was performed in England by Lady Mary Wortley Montague in 1727 (*17*) and by Johan Williamson, who administered smallpox inoculations for ≈3,000 patients during the late 18th Century (*18*); it was also practiced in Germany, in 1767, by Franz Heinrich Meinolf Wilhelm (*19*). However, variolation encountered initial resistance and skepticism from the population. The work of figures such as Voltaire and Catherine II of Russia mobilized the support of influential nobles to overcome hesitation (*20*). Variolation gained renewed popularity in Europe during the 1760s with the rise of the Sutton method (*21*), but that effort

Figure. Joseph Boze (1745–1826), Portrait of Honoré Mirabeau, 1789. Pastel on paper, 64.4 cm × 53.5 cm. Château de Versailles, Versailles, France. Photograph by Franck Raux.

came too late for the young Mirabeau, who contracted smallpox in 1751.

After Jenner's publication (*15*), vaccination was rapidly adopted globally. In France, vaccination was introduced in 1800. Rapid spread of vaccination programs throughout the world took place, and vaccination was strongly promoted in France by Napoleon Bonaparte, preventing troop losses in his army. In addition to massive vaccination campaigns in the 20th Century, development of a strategy involving surveillance and containment effectively led to the eradication of smallpox by 1980 (*22*). Without a natural reservoir, variola virus has since existed only in laboratories; indeed, the last case of smallpox resulted from infection acquired in a laboratory in the United Kingdom in 1978. Today, only the United States and Russia retain variola virus isolates (*23*,*24*).

Despite smallpox eradication, the threat from related viruses remains, and a very low probability of an accidental smallpox virus release exists; such an event could have serious consequences for modern populations, which largely lack immunity. The basic reproduction number (the average number of secondary infections generated by each infected person) for smallpox in contemporary populations has been estimated at 3–6 (*25*).

A further potential issue is the risk for outbreaks or pandemics caused by other orthopoxviruses that can be transmitted to humans, such as camelpox, cowpox, and monkeypox virus. The ongoing international outbreak of monkeypox virus has led to a declaration of a public health emergency by the World Health Organization (*26*). Continued global circulation poses a risk for spillover into new zoonotic reservoirs, which would make managing the virus more difficult. Strict global regulation and cooperation is needed to prevent and control such threats.

References

1. Hillemand P, Di Matteo J, Gilbrin E. La mort de Mirabeau (1749–1791). Hist Sci Med. 1977;4:211–9.
2. Charlier P, Froesch P, Tollefson M. Parry-Romberg syndrome on a major French revolution leader: Mirabeau, 1791. J Craniofac Surg. 2017;28:582. https://doi.org/10.1097/SCS.0000000000003091
3. Galassi FM, Varotto E. Smallpox in art: considerations on some of its medical and social aspects. J Eur Acad Dermatol Venereol. 2021;35:1612–3. https://doi.org/10.1111/jdv.17266
4. Breman JG, Henderson DA. Diagnosis and management of smallpox. N Engl J Med. 2002;346:1300–8. https://doi.org/10.1056/NEJMra020025
5. Moore ZS, Seward JF, Lane JM. Smallpox. Lancet. 2006;367:425–35. https://doi.org/10.1016/S0140-6736(06)68143-9
6. Semba RD. The ocular complications of smallpox and smallpox immunization. Arch Ophthalmol. 2003;121:715–9. https://doi.org/10.1001/archopht.121.5.715
7. Gambarotto G. Fenomeni oculari nel vaiuolo. Ann Ottal. 1896;25312–315.
8. Taconnet G. Ocular complications of smallpox [in French]. Echo Med Nord. 1904;8361–71.
9. Shuttleton DE. Smallpox and the literary imagination 1600–1820. Cambridge: Cambridge University Press; 2010.
10. Kumar A, Karthikeyan K. Madarosis: a marker of many maladies. Int J Trichology. 2012;4:3–18. https://doi.org/10.4103/0974-7753.96079
11. Nield LS, Keri JE, Kamat D. Alopecia in the general pediatric clinic: who to treat, who to refer. Clin Pediatr (Phila). 2006;45:605–12. https://doi.org/10.1177/0009922806291011
12. Darmon P. The beginnings of the distribution of the vaccine France (1800–1850) [in French]. Bull Acad Natl Med. 2001;185:767–76. https://doi.org/10.1016/S0001-4079(19)34520-0
13. Davenport R, Schwarz L, Boulton J. The decline of adult smallpox in eighteenth-century London. Econ Hist Rev. 2011;64:1289–314. https://doi.org/10.1111/j.1468-0289.2011.00599.x
14. Alfani G. Plague in seventeenth-century Europe and the decline of Italy: an epidemiological hypothesis. Eur Rev Econ Hist. 2013;17:408–30. https://doi.org/10.1093/ereh/het013
15. Morabia A. Edward Jenner's 1798 report of challenge experiments demonstrating the protective effects of cowpox against smallpox. J R Soc Med. 2018;111:255–7. https://doi.org/10.1177/0141076818783658
16. Mao D. Life of Wan Quan and some of his anecdotes [in Chinese]. Zhonghua Yi Shi Za Zhi. 1995;25:108–10.
17. Miller G. Putting Lady Mary in her place: a discussion of historical causation. Bull Hist Med. 1981;55:2–16.
18. Breedlove B. Unassisted by education, and unfettered by the rules of art. Emerg Infect Dis. 2023;29:1292–3. https://doi.org/10.3201/eid2906.AC2906
19. Sperling M. Specialization in medicine reflected in Würzburg's history [in German]. Wurzbg Medizinhist Mitt. 1985;3:153–84.
20. Chorba T, Esparza J. A head of state leading by example. Emerg Infect Dis. 2022;28:2141–3. https://doi.org/10.3201/eid2810.AC2810
21. Boylston A. Daniel Sutton, a forgotten 18th century clinician scientist. J R Soc Med. 2012;105:85–7. https://doi.org/10.1258/jrsm.2012.12k001
22. Simonsen KA, Snowden J. Smallpox. In: StatPearls. Treasure Island (FL): StatPearls Publishing; 2023.
23. Fenner F, Henderson DA, Arita I, Jezek Z, Ladnyi ID. Smallpox and its eradication. Geneva: World Health Organization; 1988.
24. Breman JG, Arita I. The confirmation and maintenance of smallpox eradication. N Engl J Med. 1980;303:1263–73. https://doi.org/10.1056/NEJM198011273032204
25. Gani R, Leach S. Transmission potential of smallpox in contemporary populations. Nature. 2001;414:748–51. https://doi.org/10.1038/414748a
26. World Health Organization. WHO Director-General declares the ongoing monkeypox outbreak a Public Health Emergency of International Concern [cited 2025 May 31]. https://www.who.int/europe/news/item/23-07-2022-who-director-general-declares-the-ongoing-monkeypox-outbreak-a-public-health-event-of-international-concern

Address for correspondence: Raffaella Bianucci, Laboratoire Anthropologie, Archéologie Biologie, Université Paris-Saclay, Montigny-le-Bretonneux, France; email: raffaella.bianucci@gmail.com

EMERGING INFECTIOUS DISEASES®

Upcoming Issue: Parasitic Infections

- Chagas Disease, an Endemic Disease in the United States
- Detection of Multiple Nosocomial *Trichosporon asahii* Transmission Events via Microsatellite Typing Assay, South America
- Epidemiology of *Sporothrix brasiliensis* in Felids at Border of Brazil—Treatment Failure without Initial Elevated Itraconazole MICs
- Drivers of Crimean-Congo Hemorrhagic Fever in Natural Host and Effects of Control Measures, Bulgaria
- Rickettsioses in Uganda as Underrecognized Cause of Hospitalization Due to Febrile Illness
- Differences in Lyme Disease Diagnosis among Medicaid and Medicare Beneficiaries, United States, 2016–2021
- Surge in Cumulative Incidence of *Candida auris* Skin Colonization Early in the COVID-19 Pandemic
- Severe Group A *Streptococcus* Infection among Children, France, 2022–2024
- New Insights into Infant Strongyloidiasis in Papua New Guinea
- Epidemiology of Chikungunya Hospitalizations, Brazil, 2014–2024
- *Theileria luwenshuni* and Novel *Babesia* spp. Infections in Humans, Yunnan Province, China
- CYP2D6 Genotype and Primaquine Treatment in Patients with Suspected Malaria, Venezuela
- Modeling Case Burden and Duration of Sudan Ebola Virus Disease Outbreak in Uganda, 2022
- Emergence of Autochthonous *Leishmania* (*Mundinia*) *martiniquensis* Infections in Horses, Czech Republic and Austria, 2019–2023
- Rapidly Progressing Melioidosis Outbreak in City Center Zoo, Hong Kong, 2024
- Melioidosis Cases with Highly Related *Burkholderia pseudomallei* Whole-Genome Sequences among 4 People with Unknown Exposure Source, Georgia, USA, 1983–2024
- Linezolid and Meropenem for *Nocardia otitidiscaviarum* Actinomycetoma
- New World Screwworm Infestation in Wild Mountain Tapirs, Central Andes Mountains, Colombia
- Clinical and Molecular Characterization of Emerging Human *Dirofilaria repens* Infections, Estonia, 2023
- Monkeypox Virus Clade IIa Infections, Liberia, 2023–2024
- Detection of Rat Lungworms in Invasive Mollusks, Georgia, USA, 2024
- Subarachnoid Neurocysticercosis Caused by Larval-Stage *Taenia crassiceps* Tapeworm, Slovenia
- Pediatric Case Report and Overview of Autochthonous Tick-Borne Encephalitis, Belgium

Complete list of articles in the September issue at https://wwwnc.cdc.gov/eid/#issue-325

Earning CME Credit

To obtain credit, you should first read the journal article. After reading the article, you should be able to answer the following, related, multiple-choice questions. To complete the questions (with a minimum 75% passing score) and earn continuing medical education (CME) credit, please go to http://www.medscape.org/journal/eid. Credit cannot be obtained for tests completed on paper, although you may use the worksheet below to keep a record of your answers.

You must be a registered user on http://www.medscape.org. If you are not registered on http://www.medscape.org, please click on the "Register" link on the right hand side of the website.

Only one answer is correct for each question. Once you successfully answer all post-test questions, you will be able to view and/or print your certificate. For questions regarding this activity, contact the accredited provider, CME@medscape.net. For technical assistance, contact CME@medscape.net. American Medical Association's Physician's Recognition Award (AMA PRA) credits are accepted in the US as evidence of participation in CME activities. For further information on this award, please go to https://www.ama-assn.org. The AMA has determined that physicians not licensed in the US who participate in this CME activity are eligible for AMA PRA Category 1 Credits™. Through agreements that the AMA has made with agencies in some countries, AMA PRA credit may be acceptable as evidence of participation in CME activities. If you are not licensed in the US, please complete the questions online, print the AMA PRA CME credit certificate, and present it to your national medical association for review.

Article Title

Emergence of Clade Ib Monkeypox Virus—Current State of Evidence

CME Questions

1. Which of the following clades of monkeypox virus (MPXV) resulted in the global outbreak noted in 2022 to 2023?

A. Clade I
B. Clade II
C. Clade III
D. Clade IV

2. Which of the following statements regarding comparisons between clade I and clade II of MPXV in the current study is most accurate?

A. Clade I is associated with lower case-fatality rates
B. Clade I is associated with less severe disease
C. Clade I is associated with infections among persons aged ≥50 years
D. Clade I is associated with greater nonsexual transmission among humans

3. Which of the following statements regarding vaccination against MPXV is most accurate?

A. Smallpox vaccines can no longer be applied to prevent mpox
B. Modified Vaccinia Ankara-Bavarian Nordic (MVA-BN) is >95% effective in the prevention of clade II mpox
C. Currently available vaccines require just 1 dose
D. MVA-BN is currently being employed in Africa to prevent clade I mpox

4. Which of the following statements regarding tecovirimat is most accurate?

A. It should not be combined with other antiviral agents
B. It has been associated with the development of resistance after prolonged treatment
C. It has been highly effective in resolving mpox due to clade I MPXV
D. It has been highly effective in resolving mpox due to clade IIb MPXV

Earning CME Credit

To obtain credit, you should first read the journal article. After reading the article, you should be able to answer the following, related, multiple-choice questions. To complete the questions (with a minimum 75% passing score) and earn continuing medical education (CME) credit, please go to http://www.medscape.org/journal/eid. Credit cannot be obtained for tests completed on paper, although you may use the worksheet below to keep a record of your answers.

You must be a registered user on http://www.medscape.org. If you are not registered on http://www.medscape.org, please click on the "Register" link on the right hand side of the website.

Only one answer is correct for each question. Once you successfully answer all post-test questions, you will be able to view and/or print your certificate. For questions regarding this activity, contact the accredited provider, CME@medscape.net. For technical assistance, contact CME@medscape.net. American Medical Association's Physician's Recognition Award (AMA PRA) credits are accepted in the US as evidence of participation in CME activities. For further information on this award, please go to https://www.ama-assn.org. The AMA has determined that physicians not licensed in the US who participate in this CME activity are eligible for AMA PRA Category 1 Credits™. Through agreements that the AMA has made with agencies in some countries, AMA PRA credit may be acceptable as evidence of participation in CME activities. If you are not licensed in the US, please complete the questions online, print the AMA PRA CME credit certificate, and present it to your national medical association for review.

Article Title

Scheffersomyces spartinae Fungemia among Pediatric Patients, Pakistan, 2020–2024

CME Questions

1. Which of the following statements regarding *Scheffersomyces spartinae* is the most accurate?

A. It is found in dry soil
B. It generally will die when temperatures drop below 10 °C
C. It only thrives in environments with pH below 7
D. It has not been considered an infectious agent among humans

2. What was the approximate median age of patients with positive cultures for *S. spartinae* in the current study?

A. 19 days
B. 4 months
C. 6 years
D. 16 years

3. *S. spartinae* demonstrated resistance to which of the following antifungal classes in the current study?

A. Amphotericin
B. Azoles
C. Echinocandins
D. None of the above

4. Which of the following statements regarding genetic studies of *S. spartinae* in the current study is the most accurate?

A. Only 1 clade was identified
B. There was a large degree of genetic variability among isolates
C. Isolates were diverse across time and geographic location
D. There was no co-circulation of independent lineages in particular locations

Emerging Infectious Diseases
Photo Quiz Articles

Volume 14, Number 9
September 2008

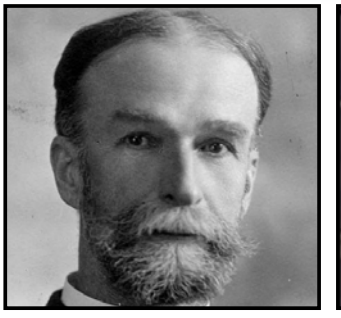

Volume 14, Number 12
December 2008

Volume 15, Number 9
September 2009

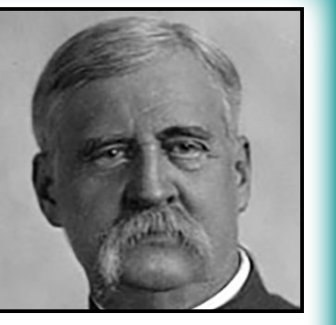

Volume 15, Number 10
October 2009

Volume 16, Number 6
June 2010

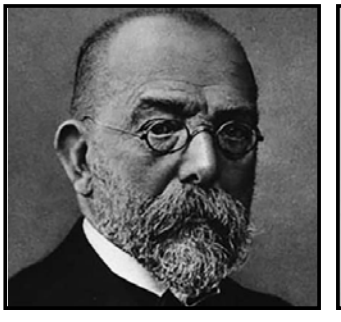

Volume 17, Number 3
March 2011

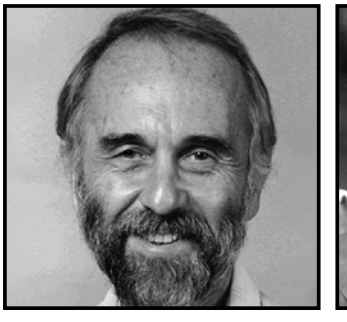

Volume 17, Number 12
December 2011

Volume 19, Number 4
April 2013

Volume 20, Number 5
May 2014

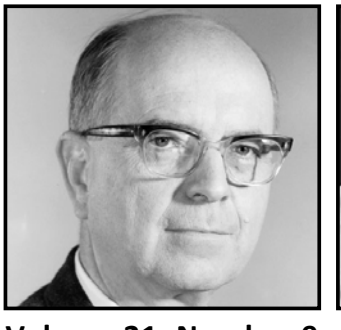

Volume 21, Number 9
September 2015

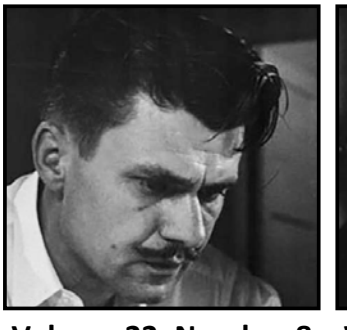

Volume 22, Number 8
August 2016

Volume 28, Number 3
March 2022

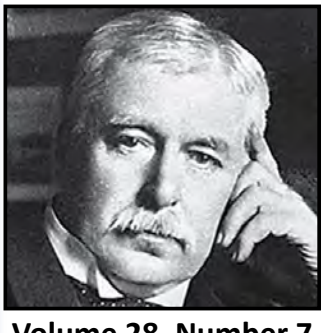

Volume 28, Number 7
July 2022

Click on the link below to read about the people behind the science.

https://bit.ly/3LN02tr

See requirements for submitting a photo quiz to EID.

https://bit.ly/3VUPqfj

EID Journal